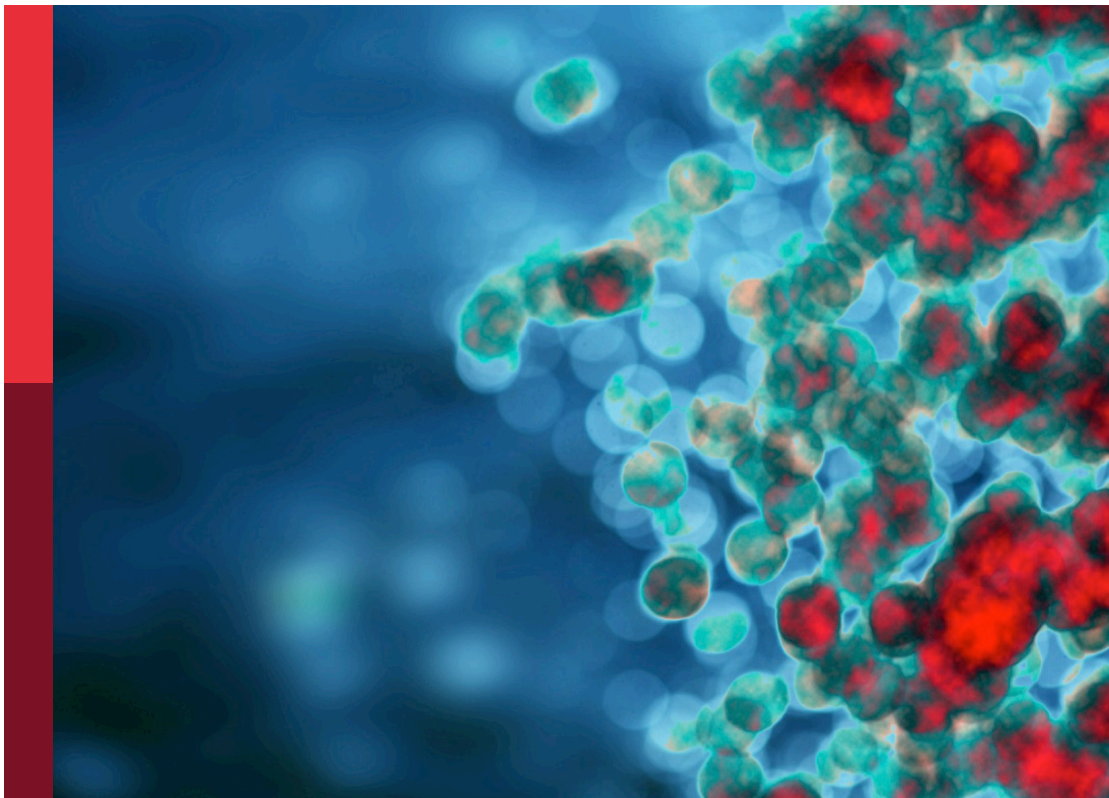
frontiers | Research Topics

Neuro-immune interaction in CNS injury and disease

Edited by
Bo Li, Guangzhi Ning and Ruiping Wang

Published in
Frontiers in Immunology



FRONTIERS EBOOK COPYRIGHT STATEMENT

The copyright in the text of individual articles in this ebook is the property of their respective authors or their respective institutions or funders. The copyright in graphics and images within each article may be subject to copyright of other parties. In both cases this is subject to a license granted to Frontiers.

The compilation of articles constituting this ebook is the property of Frontiers.

Each article within this ebook, and the ebook itself, are published under the most recent version of the Creative Commons CC-BY licence. The version current at the date of publication of this ebook is CC-BY 4.0. If the CC-BY licence is updated, the licence granted by Frontiers is automatically updated to the new version.

When exercising any right under the CC-BY licence, Frontiers must be attributed as the original publisher of the article or ebook, as applicable.

Authors have the responsibility of ensuring that any graphics or other materials which are the property of others may be included in the CC-BY licence, but this should be checked before relying on the CC-BY licence to reproduce those materials. Any copyright notices relating to those materials must be complied with.

Copyright and source acknowledgement notices may not be removed and must be displayed in any copy, derivative work or partial copy which includes the elements in question.

All copyright, and all rights therein, are protected by national and international copyright laws. The above represents a summary only. For further information please read Frontiers' Conditions for Website Use and Copyright Statement, and the applicable CC-BY licence.

ISSN 1664-8714
ISBN 978-2-8325-2998-0
DOI 10.3389/978-2-8325-2998-0

About Frontiers

Frontiers is more than just an open access publisher of scholarly articles: it is a pioneering approach to the world of academia, radically improving the way scholarly research is managed. The grand vision of Frontiers is a world where all people have an equal opportunity to seek, share and generate knowledge. Frontiers provides immediate and permanent online open access to all its publications, but this alone is not enough to realize our grand goals.

Frontiers journal series

The Frontiers journal series is a multi-tier and interdisciplinary set of open-access, online journals, promising a paradigm shift from the current review, selection and dissemination processes in academic publishing. All Frontiers journals are driven by researchers for researchers; therefore, they constitute a service to the scholarly community. At the same time, the *Frontiers journal series* operates on a revolutionary invention, the tiered publishing system, initially addressing specific communities of scholars, and gradually climbing up to broader public understanding, thus serving the interests of the lay society, too.

Dedication to quality

Each Frontiers article is a landmark of the highest quality, thanks to genuinely collaborative interactions between authors and review editors, who include some of the world's best academicians. Research must be certified by peers before entering a stream of knowledge that may eventually reach the public - and shape society; therefore, Frontiers only applies the most rigorous and unbiased reviews. Frontiers revolutionizes research publishing by freely delivering the most outstanding research, evaluated with no bias from both the academic and social point of view. By applying the most advanced information technologies, Frontiers is catapulting scholarly publishing into a new generation.

What are Frontiers Research Topics?

Frontiers Research Topics are very popular trademarks of the *Frontiers journals series*: they are collections of at least ten articles, all centered on a particular subject. With their unique mix of varied contributions from Original Research to Review Articles, Frontiers Research Topics unify the most influential researchers, the latest key findings and historical advances in a hot research area.

Find out more on how to host your own Frontiers Research Topic or contribute to one as an author by contacting the Frontiers editorial office: frontiersin.org/about/contact

Neuro-immune interaction in CNS injury and disease

Topic editors

Bo Li — Sun Yat-sen University, China

Guangzhi Ning — Tianjin Medical University General Hospital, China

Ruiping Wang — University of Texas MD Anderson Cancer Center, United States

Topic Coordinator

Niu Yu Chun — First People's Hospital of Foshan, China

Citation

Li, B., Ning, G., Wang, R., eds. (2023). *Neuro-immune interaction in CNS injury and disease*. Lausanne: Frontiers Media SA. doi: 10.3389/978-2-8325-2998-0

Table of contents

05 Cannabinoid receptor-2 attenuates neuroinflammation by promoting autophagy-mediated degradation of the NLRP3 inflammasome post spinal cord injury
Fan Jiang, Mingjie Xia, Yanan Zhang, Jie Chang, Jiang Cao, Zhongkai Zhang, Zhanyang Qian and Lei Yang

21 Microglia morphophysiological diversity and its implications for the CNS
Andrés Vidal-Itriago, Rowan A. W. Radford, Jason A. Aramideh, Cindy Maurel, Natalie M. Scherer, Emily K. Don, Albert Lee, Roger S. Chung, Manuel B. Graeber and Marco Morsch

37 Analysis of macular structure in age-related cataract patients with different antibody levels of severe acute respiratory syndrome coronavirus-2 vaccine
Xiaochun Li, Xiaoguang Cao, Zhongting Pan, Xinping Sun and Yongzhen Bao

45 CNS and CNS diseases in relation to their immune system
Jianhao Xu, Canyu Ma, Menglu Hua, Jiarui Li, Ze Xiang and Jian Wu

57 Screening the immune-related circRNAs and genes in mice of spinal cord injury by RNA sequencing
Yongjin Li, Baobao Wang, Wenzhi Sun, Chao Kong, Guowang Li, Xiaolong Chen and Shibao Lu

70 Neurotrophic and immunomodulatory effects of olfactory ensheathing cells as a strategy for neuroprotection and regeneration
Simona Denaro, Simona D'Aprile, Cristiana Alberghina, Anna Maria Pavone, Filippo Torrisi, Sebastiano Giallongo, Lucia Longhitano, Giuliana Mannino, Debora Lo Furno, Agata Zappalà, Rosario Giuffrida, Daniele Tibullo, Giovanni Li Volti, Nunzio Vicario and Rosalba Parenti

81 A single-cell atlas reveals the heterogeneity of meningeal immunity in a mouse model of Methyl CpG binding protein 2 deficiency
Huiping Li, Meixin Hu, Zhuxi Huang, Yi Wang, Ying Xu, Jingxin Deng, Ming Zhu, Weijun Feng and Xiu Xu

95 Review: The role of HMGB1 in spinal cord injury
Yizhang Mo and Kebing Chen

108 Combination of single-cell and bulk RNA seq reveals the immune infiltration landscape and targeted therapeutic drugs in spinal cord injury
Qing Zhang, Beibei Yu, Yongfeng Zhang, Yunze Tian, Shijie Yang, Yongfeng Chen and Haining Wu

121 Biomaterials delivery strategies to repair degenerated intervertebral discs by regulating the inflammatory microenvironment
Yuanliang Xia, Hengyi Wang, Ruohan Yang, Yulin Hou, Yuehong Li, Jianshu Zhu and Changfeng Fu

139 The mechanism of microglia-mediated immune inflammation in ischemic stroke and the role of natural botanical components in regulating microglia: A review
Jinsong Zeng, Tingting Bao, Kailin Yang, Xiaofei Zhu, Shanshan Wang, Wang Xiang, Anqi Ge, Liuting Zeng and Jinwen Ge

168 Integrated single-cell multiomics reveals novel immune candidate markers for post-traumatic coagulopathy
Ping Zheng, Ning Zhang, Dabin Ren, Cong Yu, Bin Zhao, Qingke Bai, Yisong Zhang and Wanju Sun

181 Meningoencephalitis associated with GAD65 autoimmunity
Zuying Kuang, José Fidel Baizabal-Carvallo, Mohammad Mofatteh, Sifen Xie, Mengqiu Pan, Jinlong Ye, Lihua Zhou, Shuiquang Yang, Zhanhang Wang, Yimin Chen and Yaqin Li

187 CD28-signaling can be partially compensated in CD28-knockout mice but is essential for virus elimination in a murine model of multiple sclerosis
Kirsten Hülskötter, Fred Lühder, Eva Leitzen, Alexander Flügel and Wolfgang Baumgärtner

frontiers | Frontiers in Immunology

TYPE Original Research
PUBLISHED 26 September 2022
DOI 10.3389/fimmu.2022.993168

Check for updates

OPEN ACCESS

EDITED BY
Bo Li,
Sun Yat-sen University, China

REVIEWED BY
Shiqing Feng,
Tianjin Medical University General Hospital, China
Valerio Chiurchiù,
National Research Council (CNR), Italy

*CORRESPONDENCE
Lei Yang
leiyang@njmu.edu.cn
Zhanyang Qian
spineqzy@126.com
Zhongkai Zhang
zhangzhongkai@sdfmu.edu.cn

†These authors have contributed equally to this work

SPECIALTY SECTION
This article was submitted to Multiple Sclerosis and Neuroimmunology, a section of the journal Frontiers in Immunology

RECEIVED 13 July 2022
ACCEPTED 06 September 2022
PUBLISHED 26 September 2022

CITATION
Jiang F, Xia M, Zhang Y, Chang J, Cao J, Zhang Z, Qian Z and Yang L (2022) Cannabinoid receptor-2 attenuates neuroinflammation by promoting autophagy-mediated degradation of the NLRP3 inflammasome post spinal cord injury. *Front. Immunol.* 13:993168. doi: 10.3389/fimmu.2022.993168

COPYRIGHT
© 2022 Jiang, Xia, Zhang, Chang, Cao, Zhang, Qian and Yang. This is an open-access article distributed under the terms of the Creative Commons Attribution License (CC BY). The use, distribution or reproduction in other forums is permitted, provided the original author(s) and the copyright owner(s) are credited and that the original publication in this journal is cited, in accordance with accepted academic practice. No use, distribution or reproduction is permitted which does not comply with these terms.

Cannabinoid receptor-2 attenuates neuroinflammation by promoting autophagy-mediated degradation of the NLRP3 inflammasome post spinal cord injury

Fan Jiang[1†], Mingjie Xia[2†], Yanan Zhang[1,3†], Jie Chang[4], Jiang Cao[4], Zhongkai Zhang[5*], Zhanyang Qian[6*] and Lei Yang[1,7*]

[1]Department of Orthopedics, Taizhou People's Hospital, Nanjing Medical University, Taizhou, China, [2]Department of Orthopedics, Nanjing First Hospital, Nanjing Medical University, Nanjing, China, [3]Postgraduate School, Dalian Medical University, Dalian, China, [4]Department of Orthopedics, Affiliated First Hospital of Nanjing Medical University, Nanjing, China, [5]Department of Orthopedics, Shandong Provincial Hospital Affiliated to Shandong First Medical University, Jinan, China, [6]Department of Orthopedics, Zhongda Hospital, Nanjing, China, [7]School of Bioinformatics Engineering, Nanjing Medical University, Nanjing, China

Background: Neuroinflammation following spinal cord injury (SCI) results in prolonged neurological damage and locomotor dysfunction. Polarization of microglia is vital to regulation of neuroinflammation, although the underlying mechanisms have not yet been elucidated. Endocannabinoid receptor subtype 2 (CB2R) is reported to ameliorate neurodegeneration *via* immunomodulation activities. However, the underlying machinery in the context of SCI remains unclear.

Methods: A lipopolysaccharide-induced microglia inflammation model and a mouse model of SCI were employed to investigate the regulatory role of CB2R in the polarization of microglia in response to excess neuroinflammation. Markers of inflammation and autophagy were measured by Western blot analysis, immunofluorescence, flow cytometry, and enzyme-linked immunosorbent assays. Histological staining with hematoxylin and eosin, Nissl, and Luxol® fast blue was conducted using commercial kits. The locomotor function of the hindlimbs of the experimental mice was evaluated with the Basso Mouse Scale, Louisville Swim Scale, and footprint assay.

Results: The results showed that CB2R promoted M2 differentiation, increased interleukin (IL)-10 expression, and inhibited M1 differentiation with decreased expression of IL-1β and IL-6. CB2R activation also increased ubiquitination of the NLRP3 inflammasome and interacted with the autophagy-related proteins p62 and microtubule-associated proteins 1B light chain 3. Treatment with the CB2R activator JWH-133 reduced loss of myelin, apoptosis of neurons, and

glial scarring, leading to improved functional recovery of the hindlimbs, while the CB2R antagonist AM630 produced opposite results.

Conclusion: Taken together, these results suggested that CB2R activation attenuated neuroinflammation targeting microglial polarization by promoting NLRP3 clearance, thereby facilitating functional recovery post-SCI.

KEYWORDS

cannabinoid receptor-2, neuroinflammation, NLRP3, autophagy, spinal cord injury

Introduction

Spinal cord injury (SCI) is a deteriorative neuropathy that results in irreversible neurological dysfunction and severe physio-psychological damage to the patient (1, 2). However, the pathogenesis of SCI remains unclear, as available reports have mostly focused on either the induction of neuroinflammation, accumulation of reactive oxygen species (ROS), or development of neurotoxicity (3). Microglia are indispensable components of pathological events (4). Damage to the spinal cord initiates various inflammatory responses *via* immunoregulation of microglial injury and subsequent activation of damage-associated molecular patterns, which promote activation of microglia in the resting state *via* multiple molecular signaling pathways, leading to increased differentiation of M1 microglia that release destructive pro-inflammatory mediators and induce ROS generation and a lack of M2 microglia, thereby limiting excess inflammation, but fueling neuroinflammation (5–7). The cross-kingdom efficacy of microglial polarization as an immune-inflammatory junction suggests a potential target as a defensive mechanism, although the specific components remain unclear.

The NLRP3 (NOD-, LRR-, and pyrin domain-containing 3) inflammasome, an intracellular signaling multiprotein complex, is reported to be activated in M1 microglia. It promotes production of numerous inflammatory amplifiers and has been implicated in the pathogenesis of various non-infectious diseases (8–10). As the most characteristic inflammatory sensor molecule, NLRP3 triggers activation of capase-1 and maturation of interleukin (IL)-1β and IL-18 (11, 12). Moreover, autophagy is a scavenging mechanism that delivers damaged organelles as well as excess proteins to lysosomes. Multiple lines of evidence show that accumulation of the NLRP3 inflammasome induces autophagosome formation, which limits inflammasome activity (13–15). However, the therapeutic effect of the destruction of the NLRP3 inflammasome *via* regulation of autophagy to alleviate secondary injury post-SCI remains unclear.

Previous studies have suggested that activated microglia produce endocannabinoids and express cannabinoid receptor subtypes that suppress neuroinflammation (16). In addition, endocannabinoids were reported to be an effective adjuvant to inhibit activation of NLRP3 inflammasome (17). The endocannabinoid system is mainly composed of endocannabinoid receptor subtype 1 (CB1R), endocannabinoid receptor subtype 2 (CB2R), and endocannabinoids like 2-arachidonoyl glycerol, anandamide, and other structurally related lipids, as well as related enzymes for transportation, synthesis, and degradation, which are involved in a variety of physiological functions and pathological processes (18–20). Of interest, activation of CB2R in the central nervous system plays a protective role against neurodegenerative diseases attributed to immune regulation (21–25). Previous reports suggest that targeting CB2R manipulates M1/M2 transition of macrophages in response to inflammation and regulates autophagy-related signaling (26, 27). However, the unique mechanisms underlying regulation of neuroinflammation post-SCI *via* CB2R and autophagy remain elusive.

In the present study, a model of lipopolysaccharide (LPS)-induced inflammation of microglia and a mouse model of contusion-induced SCI were employed to explore the role of CB2R in SCI-induced neuroinflammation *in vitro* and *in vivo*, respectively. The results showed that activation of CB2R facilitated phenotype transition of microglia to the M2 state, rather than M1, restrained neuronal apoptosis, and protected neurological functions, suggesting that CB2R attenuated SCI-induced neuroinflammation by promoting ubiquitination and clearance of NLRP3 through autophagy in microglia.

Materials and methods

Study approval

The animal study protocol was approved by the Institutional Animal Care and Use Committee of Nanjing Medical University

(Nanjing, China) and conducted in accordance with the guidelines described in "Animal Research: Reporting of *In Vivo* Experiments".

Antibodies

The antibodies (Abs) mentioned in this study are listed in Table 1.

Cell culture

BV2 microglia and human embryonic kidney (HEK)-293T cells were obtained from the Institute of Cell Research, Chinese Academy of Medical Sciences (Shanghai, China) and cultured in Dulbecco's modified Eagle medium (KGM12800-500; Nanjing KeyGen Biotech. Co. Ltd., Nanjing, China) supplemented with 10% fetal bovine serum (Gibco, Grand Island, NY, USA). At 80% confluence, the microglia and HEK-293T cells were pretreated for 24 h with the CB2R activator JWH-133 (10 nM; B7941; APExBIO Technology LLC, Houston, TX, USA) or antagonist AM630 (40 nM; A3168; APExBIO Technology LLC) dissolved in 0.1% dimethyl sulfoxide (KGT5131; Nanjing KeyGen Biotech. Co. Ltd.). Inflammation was stimulated by treatment with 1 μg/ml of LPS (Sigma-Aldrich, St. Louis, MO, USA) for 24 h.

Establishment of a mouse model of SCI

Male C57BL/6J mice, aged 8 weeks, were obtained from the Experimental Animal Center of Nanjing Medical University and randomly assigned to one of the following four groups: sham group (laminectomy and daily intraperitoneal [i.p.] administration of a vehicle solution composed of 5% ethanol, 5% dimethyl sulfoxide, 5% Tween 20, and 85% normal saline),

TABLE 1 The information of Abs

Antibody Name #Cat.	Source	Species	Application	Dilution rate
CNR2 Recombinant Rabbit Monoclonal Antibody # 703485	Invitrogen	Rb	WB/IF	1:500
NLRP3 Rabbit mAb #49012	Signalway Antibody	Rb	WB/IF/IP	1:1,000/1:200/1:30
Phospho-AMPKα (Thr172) (D4D6D) Rabbit mAb #50081	CST	Rb	WB	1:1,000
AMPKα (D63G4) Rabbit mAb #5832	CST	Rb	WB	1:1,000
Phospho-ULK1 (Ser757) (D7O6U) Rabbit mAb #14202	CST	Rb	WB	1:1,000
ULK1 (D8H5) Rabbit mAb #8054	CST	Rb	WB	1:1,000
LC3A Mouse Monoclonal Antibody(5G10) #44176	Signalway Antibody	Ms	WB	1:1,000
Anti-Ubiquitin (linkage-specific K48) antibody [EP8589] #ab140601	Abcam	Rb	WB	1:1,000
LC3B Polyclonal Antibody #29075	Signalway Antibody	Rb	WB/IF	1:1,000/1:100
Phospho-NF-κB p65 (Ser536) (93H1) Rabbit mAb #3033	CST	Rb	WB/IF	1:1,000
NF-κB p65 (D14E12) XP® Rabbit mAb #8242	CST	Rb	WB/IF	1:1,000/1:500
SQSTM1/p62 (D6M5X) Rabbit mAb (Rodent Specific) #23214	CST	Rb	WB	1:1,000
HRP-conjugated GAPDH Monoclonal antibody # HRP-60004	Proteintech	Ms	WB	1:10,000
Goat Anti-Rabbit IgG Secondary antibody (H+L), HRP #YFSA02	YIFEIXUE BioTech	Goat	WB	1:10,000
Goat Anti-Mouse IgG Secondary antibody (H+L), HRP # YFSA01	YIFEIXUE BioTech	Goat	WB	1:10,000
Anti-iNOS antibody #ab15323	Abcam	Rb	IF	1:100
Arginase-1 (D4E3M™) XP® Rabbit mAb #93668	CST	Rb	IF	1:50
Anti-Iba1 antibody [EPR16588] #ab178846	Abcam	Rb	IF	1:500
GFAP (GA5) Mouse mAb #3670	CST	Ms	IF	1:600
Neurofilament-H (RMdO 20) Mouse mAb #2836	CST	Ms	IF	1:400
Myelin Basic Protein (D8X4Q) XP® Rabbit mAb #78896	CST	Ms	IF	1:50
Anti-NeuN Antibody, clone A60 #MAB377	Millipore	Ms	IF	1:100
Anti-Annexin V/ANXA5 Antibody [EPR3980] #ab108194	Abcam	Rb	IF	1/50
Alexa Fluor® 594 AffiniPure Fab Fragment Goat Anti-Rabbit IgG (H+L) #111587003	Jackson ImmunoResearch	Goat	IF	1:500
Alexa Fluor® 488 AffiniPure Fab Fragment Goat Anti-Rabbit IgG (H+L) #111547003	Jackson ImmunoResearch	Goat	IF	1:500
Alexa Fluor® 594 AffiniPure F(ab')$_2$ Fragment Goat Anti-Mouse IgG (H+L) #115586003	Jackson ImmunoResearch	Goat	IF	1:500
Alexa Fluor® 488 AffiniPure F(ab')$_2$ Fragment Goat Anti-Mouse IgG (H+L) #115546003	Jackson ImmunoResearch	Goat	IF	1:500
BD Pharmingen™ PE Rat Anti-Mouse F4/80 #565410	BD Biosciences	Rat	FCA	1:500
BD Transduction Laboratories™ FITC Mouse Anti-iNOS/NOS Type II #610330	BD Biosciences	Ms	FCA	1:500
CD206 (MMR) Monoclonal Antibody (MR6F3), APC, eBioscience™#17-2061-82	Invitrogen	Rat	FCA	1:500

SCI group (SCI and i.p. administration of the vehicle solution), SCI+J group (SCI and i.p. administration of JWH-133 at 2 mg/kg per day), or SCI+A group (SCI and i.p. administration of AM630 at 2 mg/kg per day). JWH-133 and AM630 were initially administered 30 min prior to SCI and continued for 3 days. For SCI modeling, mice were anesthetized with ketamine (80 mg/kg) and xylazine (4 mg/kg) prior to laminectomy. A moderate contusion to the spinal cord at T10 was created with a 5-g impactor dropped from a height of 5 cm (28). The bladder of all mice with SCI was manually emptied once per day until the development of incontinence.

Western blot analysis

Proteins were extracted from cells and tissues using a total protein extraction kit (KGP2100; Nanjing KeyGen Biotech. Co. Ltd.) in accordance with the manufacturer's protocol. Following quantification using an enhanced bicinchoninic acid kit (P0010; Beyotime Institute of Biotechnology, Shanghai, China), equal amounts of protein from each group were separated by sodium dodecyl sulfate polyacrylamide gel electrophoresis and then transferred to polyvinylidene fluoride membranes (thickness, 0.45 μm; EMD Millipore Corporation, Billerica, MA, USA), which were blocked with 5% skim milk diluted in tris-buffered saline-Tween-20 for 1 h at room temperature and then incubated with primary Abs overnight at 4°C, followed by secondary Abs for 1 h at room temperature. Afterward, the membrane was visualized using a chemiluminescence system (4600; Tanon Science and Technology Co., Ltd., Shanghai, China) and analyzed with ImageJ software (https://imagej.nih.gov/ij/).

Enzyme-linked immunosorbent assay

The supernatant of the cell culture of each group was collected by centrifugation at 3,000 rpm for 10 min and stored at −80°C. Expression levels of inflammatory markers (IL-1β, IL-6, and IL-10) were measured using appropriate ELISA kits [EK201B, EK206, EK210; Multisciences (Lianke) Biotech Co., Ltd., Hangzhou, China] in accordance with the manufacturer's protocols. Absorbance was determined at 550 nm using a multifunctional microplate reader (Synergy™ HT; BioTek Instruments, Winooski, VT, USA).

Flow cytometry

Polarization of microglia was induced by incubation with phycoerythrin (PE)-conjugated F4/80 Ab plus fluorescein isothiocyanate-conjugated Ab against inducible nitric oxide synthase (iNOS) or PE-conjugated F4/80 Ab plus allophycocyanin-conjugated Ab against CD206 at 4°C for 30 min. Then, the proportions of polarized microglia in each group were determined using a BD FACSVerse™ flow cytometer (BD Biosciences, Franklin Lakes, NJ, USA). The generated dataset was analyzed using FlowJo software (version 8.0; https://www.flowjo.com/).

Terminal-deoxynucleotidyl transferase mediated nick end labeling assay

Cell death in injured spinal cord tissue was determined using a one-step terminal-deoxynucleotidyl transferase mediated nick end labeling (TUNEL) apoptosis kit (KGA7062; Nanjing KeyGen Biotech. Co. Ltd.) in accordance with the manufacturer's instructions. Briefly, tissue sections were incubated with a working buffer containing proteinase K at 37°C for 30 min, then washed three times with PBS for 5 min and incubated in DNase I solution at 37°C for 30 min. Afterward, the tissue sections were probed with an enzyme working buffer at 37°C for 1 h, then labeled with tetramethylrhodamine-conjugated streptavidin in the dark at 37°C for 30 min. The nuclei were counterstained with Fluoromount-G®, a water-soluble compound containing 4′,6-diamidino-2-phenylindole (0100; SouthernBiotech, Birmingham, AL, USA). The tissue sections were imaged with a fluorescence microscope (BX51; Olympus Corporation, Tokyo, Japan).

Immunoprecipitation

BV2 and HEK-293T cells were lysed with protein lysis buffer on ice for 30 min and centrifugated at 12,000 × *g* and 4°C for 10 min. Then, 50 μl of the supernatant containing protein was collected as the "input" group, while the remaining supernatant was probed with Protein G Sepharose® 4 Fast Flow beads (GE Healthcare Sverige AB, Stockholm, Sweden) coated with an Ab against NLRP3 at 60 rpm and 4°C overnight using a rotary table. The beads were boiled twice in 2× loading buffer at 100°C for 5 min and then washed at 120 rpm and 4°C.

Immunofluorescence staining

Microglia were deparaffinated, rehydrated, and fixed with 4% paraformaldehyde (P0099; Beyotime Institute of Biotechnology) for 15 min for antigen retrieval and blocked using Immunol Staining Blocking Buffer (P0102; Beyotime Institute of Biotechnology) at room temperature for 1 h. The samples were probed with primary Abs overnight at 4°C,

followed by secondary fluorescent Abs at room temperature for 1 h. The nuclei were counterstained with Fluoromount-G® and the samples were observed using a fluorescence microscope.

Histological staining

Histological staining with hematoxylin and eosin (H&E), Nissl, and Luxol® fast blue (LFB) was conducted using commercial kits (G1120, G1436, G3240; Beijing Solarbio Science and Technology Co., Ltd., Beijing, China) in accordance with the manufacturer's protocols. Sections were mounted with neutral balsam (G8590; Beijing Solarbio Science and Technology Co., Ltd.) and then photographed using a fluorescence microscope.

Behavioral assessment

Locomotor function of the hindlimbs of the experimental mice was evaluated by two blinded researchers in accordance with the Basso Mouse Scale, the Louisville Swim Scale, and a footprint assay as previously described (29, 30).

Statistical analysis

Statistical analysis was performed with Prism 8.3.0 software (GraphPad Software, Inc., San Diego, CA, USA) and the data are presented as the mean ± standard deviation. Comparisons between two groups were conducted using the unpaired *t*-test and among three or more groups using one-way or two-way analysis of variance followed by Tukey's *post hoc* test. A probability (*p*) value < 0.05 was considered statistically significant.

Results

Expression patterns of CB2R in cord tissue post-SCI

CB2R protein expression was measured from day 3 to week 6 post-SCI (Figure 1A). Post-SCI, CB2R protein expression significantly increased and peaked by 1 week, then gradually decreased to week 6 (Figure 1B), which was consistent with the IF staining results (Figure 1C). Furthermore, IF staining on day 7 post-SCI showed that the distribution of CB2R expression largely overlapped with the neuron-specific marker NeuN and microglia-specific marker IBA-1 in both the uninjured and injured mice. In contrast, astrocytes positive for expression of glial fibrillary acidic protein (GFAP) had expressed relatively low levels of CB2R (Figures 1D, E). Hence, microglia were selected for further studies.

CB2R regulates inflammation-mediated polarization of microglia

The CB2R activator JWH-133 and antagonist AM630 were employed to determine whether CB2R participates in regulation of the immunophenotype of LPS-treated microglia (31, 32). Specifically, the expression patterns of the M1 subtype marker iNOS and M2 subtype marker ARG-1 were determined by IF staining (Figure 2A). The results showed that LPS markedly increased expression of iNOS, but reduced that of ARG-1 in microglia. Subsequent treatment with JWH-133 decreased LPS-stimulated upregulated expression of iNOS, but rescued pull-down of ARG-1, while treatment with AM630 aggravated LPS-stimulated upregulation of iNOS and inhibited expression of ARG-1 (Figures 2B, C). In addition, the proportion of polarized cells was determined by flow cytometry. The results showed that the proportion of iNOS+ M1 microglia was significantly increased after LPS stimulation, and activation of CB2R by JWH-133 remarkably reduced such increase, while inhibition of CB2R by AM630 further intensified this effect (Figures 2D, E). In contrast, LPS stimulation remarkably reduced the proportion of CD206+ M2 microglia, which was further decreased by treatment with AM630 but increased by treatment with JWH-133 (Figures 2F, G). LPS stimulation increased expression of IL-1β, IL-6, and IL-10, whereas JWH-133 decreased expression of IL-1β and IL-6, but increased that of IL-10. In contrast, AM630 increased expression of IL-1β and IL-6, but decreased that of IL-10 (Figures 2H–J).

CB2R promoted ubiquitination and autophagy-induced degradation of NLRP3 *via* the adenosine monophosphate-activated protein kinase/unc-51-like autophagy activating kinase signaling pathway

To elucidate the specific mechanism underlying CB2R-regulated polarization of microglia, the relationship between NLRP3 and CB2R was determined by IF staining. As shown in Figure 3A, stimulation with LPS increased expression of CB2R and NLRP3, while treatment with JWH-133 increased expression of CB2R, but decreased that of NLRP3, and treatment with AM630 had opposite effects (Figures 3B, C). Furthermore, the expression levels of the autophagy-related proteins adenosine monophosphate-activated protein kinase (AMPK), unc-51-like autophagy activating kinase 1 (ULK1), and microtubule-associated proteins 1A/1B light chain 3 (LC3A/

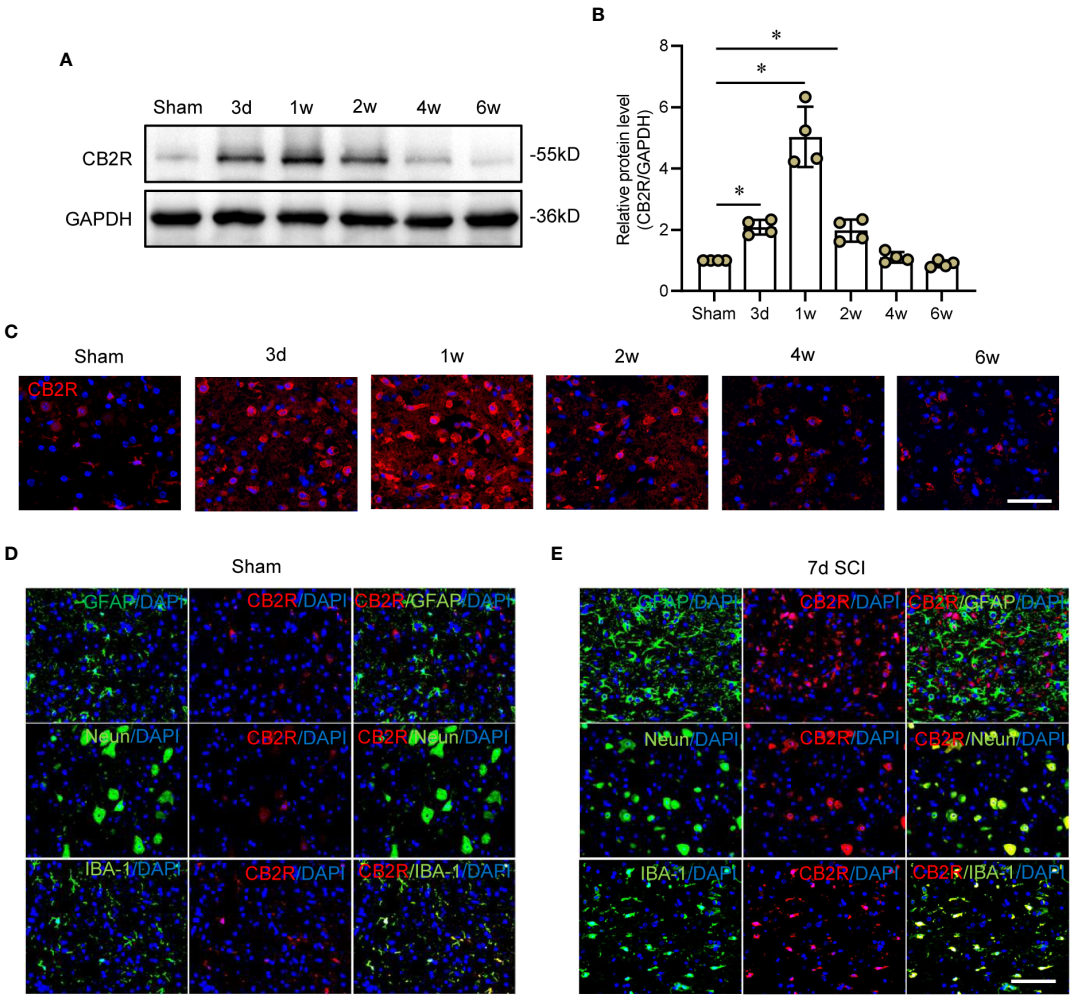


FIGURE 1
Expression patterns of CB2R in cord tissues post-SCI. **(A)** Representative protein band of CB2R on day 3 and weeks 1, 2, 4, and 6 post-SCI. **(B)** Quantitative analysis showing that CB2R expression was significantly increased on day 3 and weeks 1 and 2 post-SCI. **(C)** IF staining showing that CB2R (red) in cords of mice within 6W post-SCI. **(D)** IF staining of CB2R (red) with GFAP, Neun, or IBA-1 (green) in cords of sham mice. **(E)** IF staining of CB2R (red) with GFAP, Neun, or IBA-1 (green) in SCI mice on day 7 post-SCI. Scale bar = 100 μm. *$p < 0.05$.

B) were determined by WB analysis. The results showed that treatment with JWH-133 promoted phosphorylation of AMPK and ULK-1, leading to significantly increased expression of LC3B, which was reversed following CB2R inhibition by AM630 (Figures 3D–G). Moreover, activation of CB2R by JWH-133 decreased LPS-induced upregulation of NLRP3 and significantly reduced expression of p62, while treatment with AM630 had opposite effects (Figures 3H, J, K). Moreover, activation of CB2R inhibited phosphorylation of p65, while inhibition of CB2R fueled phosphorylation and nuclear expression of p65 (Figures 3H, I, L). The results of IP analysis showed that p62 was pulled down by NLRP3, indicating a direct interaction between NLRP3 and p62 (Figure 3M). Furthermore, in LPS-stimulated HEK-293T cells, treatment with JWH-133 increased binding of ubiquitin linkage-specific K48 to NLRP3, while treatment with AM630 had opposite effects (Figure 3N). These findings indicated that CB2R might also regulate ubiquitination of NLRP3 in LPS-stimulated microglia.

CB2R alleviated inflammation by promoting NLRP3-autophagosome formation in injured cords post-SCI

In vivo, the microglial polarization markers iNOS and ARG-1 with IBA-1 were measured. IF staining showed that the proportion of iNOS+ microglia was increased, while that of ARG-1+ microglia was decreased post-SCI. However, administration of JWH-133 markedly reduced the proportion of M1 microglia and increased that of the M2 subtype, while

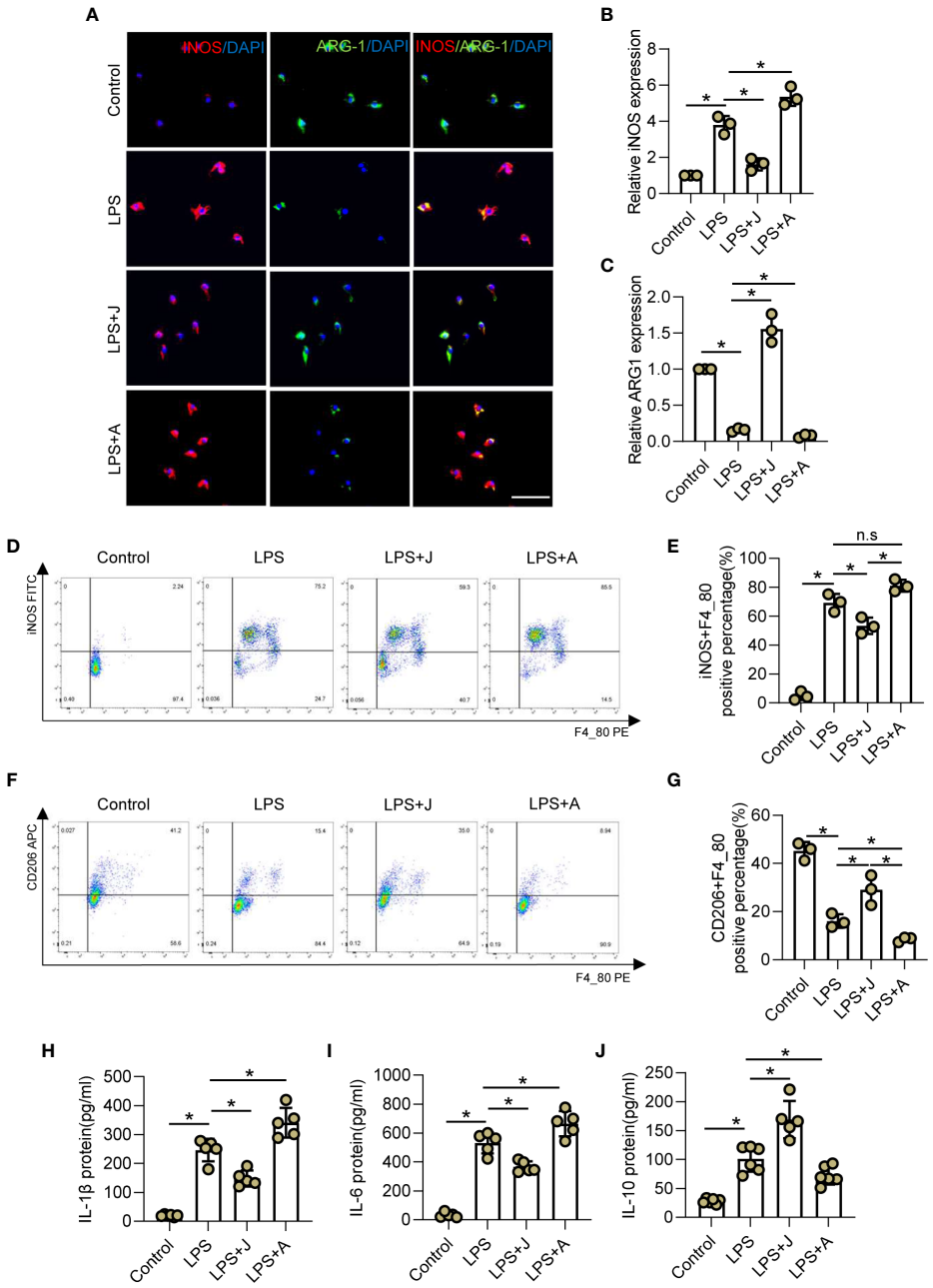


FIGURE 2
CB2R regulates inflammation-mediated polarization of microglia. **(A)** IF staining of iNOS (red) and ARG-1 (green) in BV2 microglia after LPS insult for 24 h with CB2R activation by JWH-133 (J) or inactivation by AM630 **(A)**. Scale bar = 50 μm. **(B)** Quantitative analysis indicating that CB2R significantly altered expression of the M1 marker iNOS during inflammation. **(C)** Quantitative analysis indicating that CB2R significantly altered expression of the M2 marker ARG-1 after LPS stimulation. **(D)** Flow cytometry results showing the relative proportion of M1 microglia (red) after LPS insult with and without CB2R activation or inactivation. **(E)** Quantitative analysis of M1 microglia. **(F)** Flow cytometry results showing the relative proportion of M2 microglia (red) after LPS insult with and without CB2R activation or inactivation. **(G)** Quantitative analysis of M2 microglia. ELISA results of IL-1β **(H)**, IL-6 **(I)**, and IL-10 **(J)** in the control, LPS, LPS+J (JWH-133), and LPS+A (AM630) groups. *$p < 0.05$. n.s means no significance.

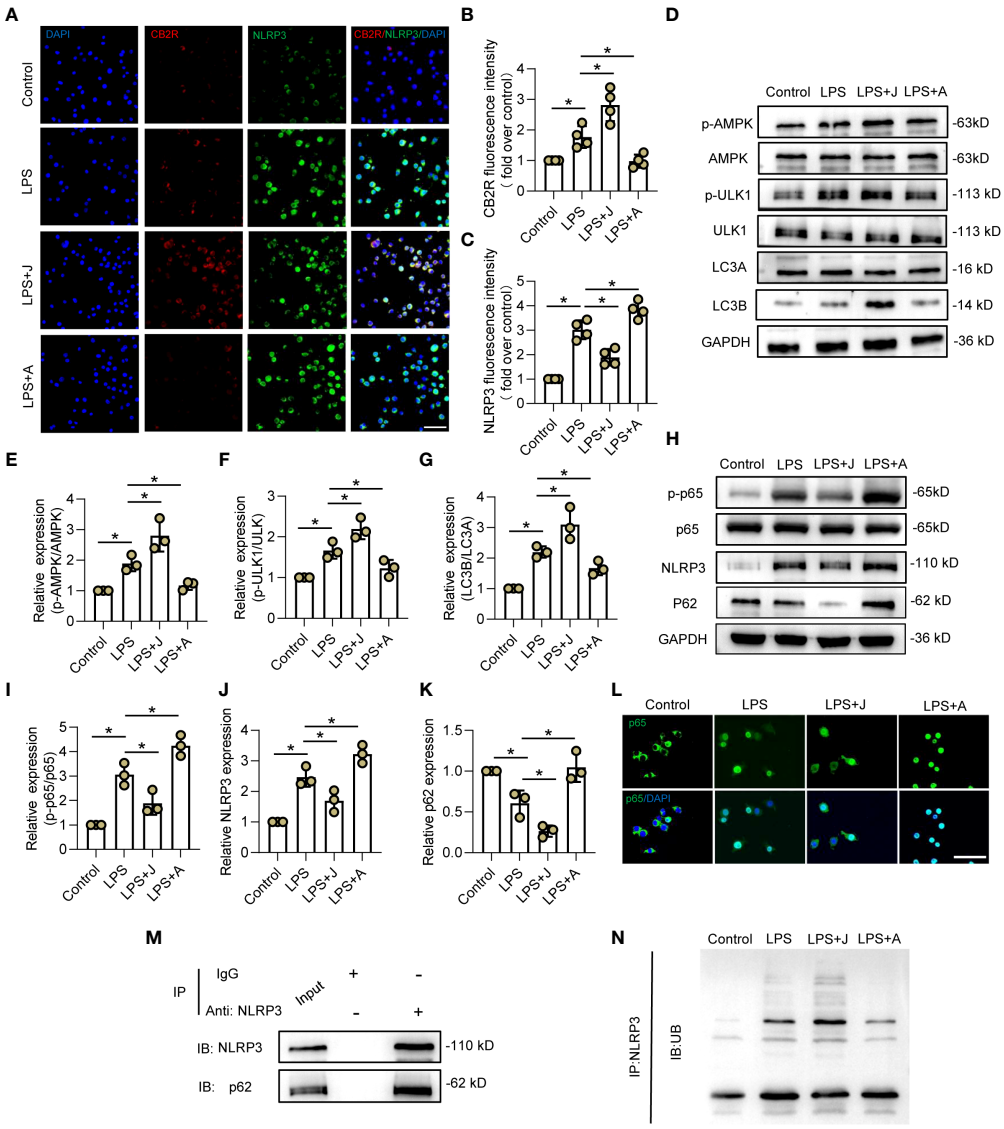


FIGURE 3
CB2R promoted ubiquitination and autophagy-induced degradation of NLRP3 *via* the AMPK/ULK signaling pathway. **(A)** IF staining of CB2R (red) and NLRP3 (green) after LPS stimuli for 24 h with CB2R activation by JWH-133 **(J)** or inactivation by AM630 **(A)**. Scale bar = 50 μm. **(B)** Quantitative analysis of CB2R. **(C)** Quantitative analysis of NLRP3. **(D)** Representative protein bands of p-AMPK, AMPK, p-ULK1, ULK1, LC3A, and LC3B in each group after 24 h of LPS insult. **(E)** Quantitative analysis of the p-AMPK/AMPK ratio. **(F)** Quantitative analysis of the p-ULK1/ULK1 ratio. **(G)** Quantitative analysis of the LC3B/LC3A ratio. **(H)** Representative protein bands of p-p65, p65, NLRP3, and p62 after 24 h of LPS stimulation. **(I)** Quantitative analysis of the p-p65/p65 ratio. **(J)** Quantitative analysis of NLRP3. **(K)** Quantitative analysis of p62. **(L)** IF staining of CB2R (red) and NLRP3 (green) after LPS stimulation for 24 h with CB2R activation by JWH-133 or CB2R inactivation by AM630. Scale bar = 50 μm. **(M)** Representative protein bands of NLRP3 and p62 in BV2 microglia after IP assay using an Ab against NLRP3. **(N)** Representative protein bands of ubiquitin linkage-specific K48 bound to NLRP3. *$p < 0.05$.

treatment with AM630 had opposite effects (Figures 4A–D). The WB results showed that JWH-133 treatment significantly increased phosphorylation of APMK and ULK1 as well as the LC3B/LC3A ratio, but markedly decreased NLRP3 expression, while treatment with AM630 had opposite effects (Supplementary Figures 2A–E). In addition, increased NLRP3 expression was mitigated by JWH-133-induced increased LC3B expression on day 3 post-SCI, while treatment with AM630 increased expression of NLRP3 and LC3B (Figure 4E). These results suggested that activated CB2R might protect against neuroinflammation by promoting the formation of the NLRP3-autophagosome.

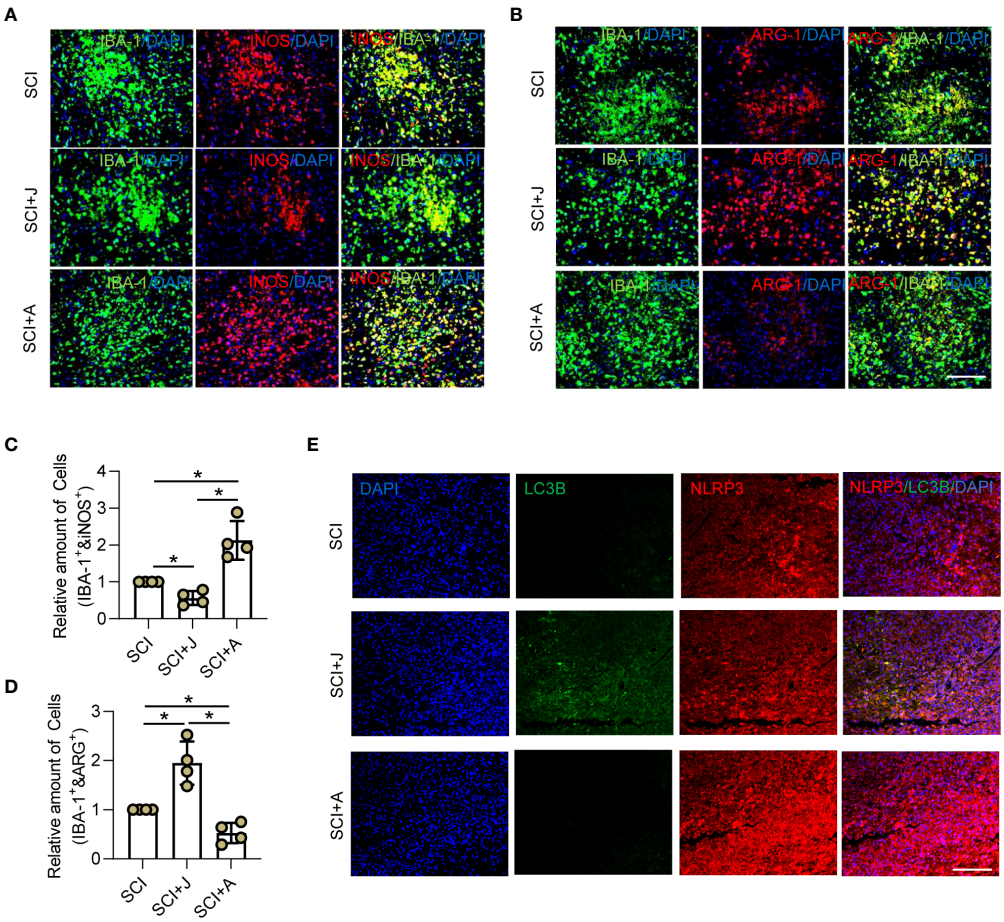


FIGURE 4
CB2R alleviated inflammation by promoting NLRP3-autophagosome formation in injured cords post-SCI. On day 3 post-SCI with CB2R activation by JWH-133 or inactivation by AM630, **(A)** IF staining of iNOS (red) and IBA-1 (green); **(B)** IF staining of ARG-1 (red) and IBA-1 (green). Scale bar = 100 μm. **(C)** Quantitative analysis of the number of iNOS$^+$ microglia. **(D)** Quantitative analysis of the number of ARG-1$^+$ microglia. **(E)** IF staining of NLRP3 (red) and LC3B (green) on day 3 post-SCI. Scale bar = 100 μm. *$p < 0.05$.

CB2R ameliorated secondary neuronal apoptosis and demyelination post-SCI

Given that CB2R was found to play a protective role in secondary injury, the LFB staining profiles of the injured spinal cord on day 7 post-SCI were compared among the groups. The results showed that treatment with JWH-133 resulted in a larger area of myelin as compared to the SCI mice, while treatment with AM630 caused significant myelin loss (Figures 5A, B), which was consistent with IF staining of myelin basic protein (Figures 5C, E). IF staining showed that treatment with JWH-133 increased the amount of neurofilaments, while treatment with AM630 further aggravated loss of neurofilaments as compared to the SCI mice (Figures 5C, D). TUNEL staining revealed that treatment with JWH-133 significantly reduced the amount of dead cells, while treatment with AM630 significantly increased cell death, as compared to the SCI mice (Figures 5F, G). Moreover, the number of apoptotic neurons was determined by staining with Annexin V, a marker of early apoptosis, IF analysis, and Nissl staining. The results showed that, as compared to the SCI mice, administration of JWH-133 resulted in fewer apoptotic neurons and a larger number of viable neurons, while treatment with AM630 produced opposite effects (Figures 5H–K).

CB2R mitigated expansion of neuronal damage and formation of glial scarring post-SCI

Since glial scarring was initiated on day 7 and completed on day 28 post-SCI, IF staining of the injured foci on days 7 and 28 post-SCI was compared. IF staining on day 7 post-SCI showed that JWH-133 administration significantly reduced the extent of

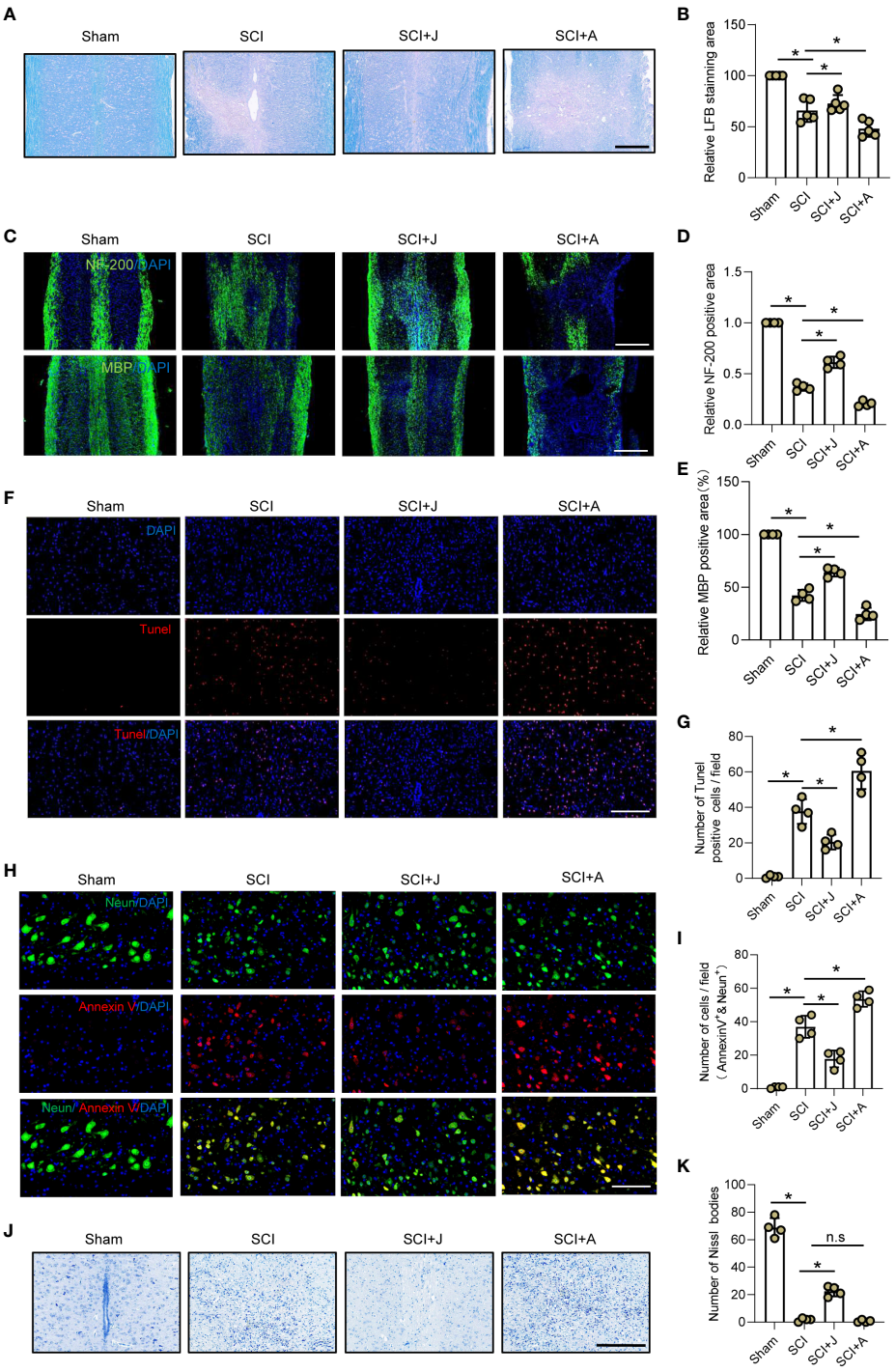


FIGURE 5
CB2R ameliorated secondary neuronal apoptosis and demyelination post-SCI. **(A)** LFB staining of spinal cords on day 7 post-SCI. Scale bar = 200 μm. **(B)** Quantitative analysis of LFB-labeled area. **(C)** IF staining of NF200 or myelin basic protein (green) on day 7 post-SCI. Scale bar = 500 μm. **(D)** Quantitative analysis of NF200. **(E)** Quantitative analysis of myelin basic protein. **(F)** TUNEL staining of spinal cords on day 7 post-SCI. Scale bar = 100 μm. **(G)** Quantitative analysis of TUNEL-positive cells. **(H)** IF staining of Neun (green) and Annexin V (red) on day 7 post-SCI. Scale bar = 100 μm. **(I)** Quantitative analysis of Annexin V-positive neurons. **(J)** Nissl staining of spinal cords on day 7 post-SCI. Scale bar = 200 μm. **(K)** Quantitative analysis of the number of neurons. *$p < 0.05$. n.s means no significance.

neuronal damage in areas occupied by microglia and astrocytes, as compared to the SCI mice, while administration of AM630 had opposite effects (Figures 6A–D). Assessment of these indices showed consistent trends on days 7 and 28 post-SCI during the period of spontaneous healing (Figures 6E–H).

CB2R attenuated histological and functional damage post-SCI

H&E staining showed that as compared to the SCI group on day 3 post-SCI, administration of JWH-133 reduced the areas of hemorrhage and damage of the injured cord tissues, while administration of AM630 increased the areas of hemorrhage and significantly increased the damaged areas (Figures 7A, B; Supplementary Figure 1A). Furthermore, H&E staining on day 28 post-SCI showed that treatment with JWH-133 prevented further histological damage to the injured foci, while treatment with AM630 exacerbated tissue damage, as compared to the SCI mice (Figures 7C, D; Supplementary Figure 1B). The results of the footprint assay showed that treatment with JWH-133 lowered the frequency of dorsiflexion of the hindlimbs with longer stride length and width, while treatment with AM630 was associated with lower crawling indices, as compared to the SCI mice (Figures 7E–G). The results of the swimming test showed that JWH-133-treated mice exhibited a smaller angle ranging from the trunk to the water surface with a higher frequency of hindlimb movements, while AM630-treated mice seldom exhibited any evident difference, as compared to the SCI mice on day 28 post-SCI (Figure 7H). Therefore, the Louisville Swim Scale scores of the JWH-133-treated mice were higher than those of the SCI mice and AM630-treated mice beginning on day 14 post-SCI (Figure 7I). The Basso Mouse Scale scores also showed that, as compared to the SCI mice, treatment with JWH-133 significantly improved locomotion, while treatment with AM630 significantly decreased locomotion beginning on day 7 post-SCI (Figure 7J).

Discussion

The findings of the present study suggested that the neuroprotective effects of CB2R activation in SCI were partly regulated by two main mechanisms: (i) attenuation of neuroinflammatory responses and reversed microglial polarization through inactivation of NLRP3 *via* AMPK/ULK1 signaling-induced autophagy and (ii) CB2R mitigation of neuroinflammation-mediated secondary neuropathology due to myelin loss, neuron apoptosis, and glial scar accumulation post-SCI.

LPS provokes inflammatory responses in multiple immune cells, including macrophages, T cells, and microglia (33, 34). Hence, LPS is often used to establish *in vitro* aseptic inflammatory models to mimic the pathogenesis of various neuro-immune diseases, such as autoimmune encephalomyelitis, multiple sclerosis, and depression (35–37). Of note, LPS is also widely used to induce microglial inflammation in mimetic models of SCI (38–40). LPS binds to Toll-like receptor 4 and promotes activation of p65, which then translocates to the nucleus and triggers the transcription of pro-inflammatory molecules (41, 42). The results of the current study confirmed that CB2R expression was significantly increased both in the cord tissues of SCI mice and in LPS-stimulated microglia, which then inhibited activation of p65, leading to decreased translocation to the nucleus. A previous report also suggested that CB2R activation could mitigate LPS-induced neuroinflammation (43), but the underlying molecular mechanism regulated by CB2R has not yet been elucidated. The results of the current study showed that pharmacological activation of CB2R by JWH-133 inhibited LPS-induced proinflammatory transition of the M1 subtype and increased the proportion of immunoregulatory M2 microglia *in vitro*, which was reversed by treatment with the CB2R antagonist AM630. These findings indicated that inhibition of neuroinflammation *via* CB2R potentially occurred through unidentified signaling pathways related to immunoregulation.

NLRP3, a classic biomarker of inflammation, responds to trauma *via* regulating activation of caspase-1 and maturation of IL-1β, thereby promoting inflammation-dominated neuropathology post-SCI (44, 45). Accumulating evidence indicates that either suppression of NLRP3 expression or promotion of cell autophagy ameliorates neuroinflammation-induced neurological injury, although the underlying mechanisms remain unclear. Numerous mechanisms have been proposed to explain the interactions between the NLRP3 inflammasome and autophagy, including autophagy activation by inflammatory signaling *via* limited IL-1β production and targeting ubiquitinated inflammasomes (13). In neurological diseases, non-coding RNA, bio-enzymes, and small molecular compounds have been implicated in the interplay between ubiquitination and autophagy of NLRP3 (46–48). In LPS-stimulated microglia, CB2R activation decreased NLRP3 expression associated with formation of autophagosomes, resulting in accumulation of LC3B and exhaustion of p62. Consistently, Shao et al. (49) demonstrated that alleviation of experimental autoimmune encephalomyelitis by CB2R activation was linked to activation of autophagosomes and inhibition of the NLRP3 inflammasome. In contrast, the results of the present study suggest that CB2R regulates NLRP3 ubiquitination by ubiquitin linkage-specific K48 and promotes binding of NLRP3 with p62, an autophagy substrate, and LC3B, an autophagy activator. K48-linked polyubiquitination of NLRP3 mediates self-degradation and reduces cellular NLRP3 levels, which are essential for inactivation of the NLRP3 inflammasome (50) and p62-dependent selective autophagy also inhibited the capacity of

10.3389/fimmu.2022.993168

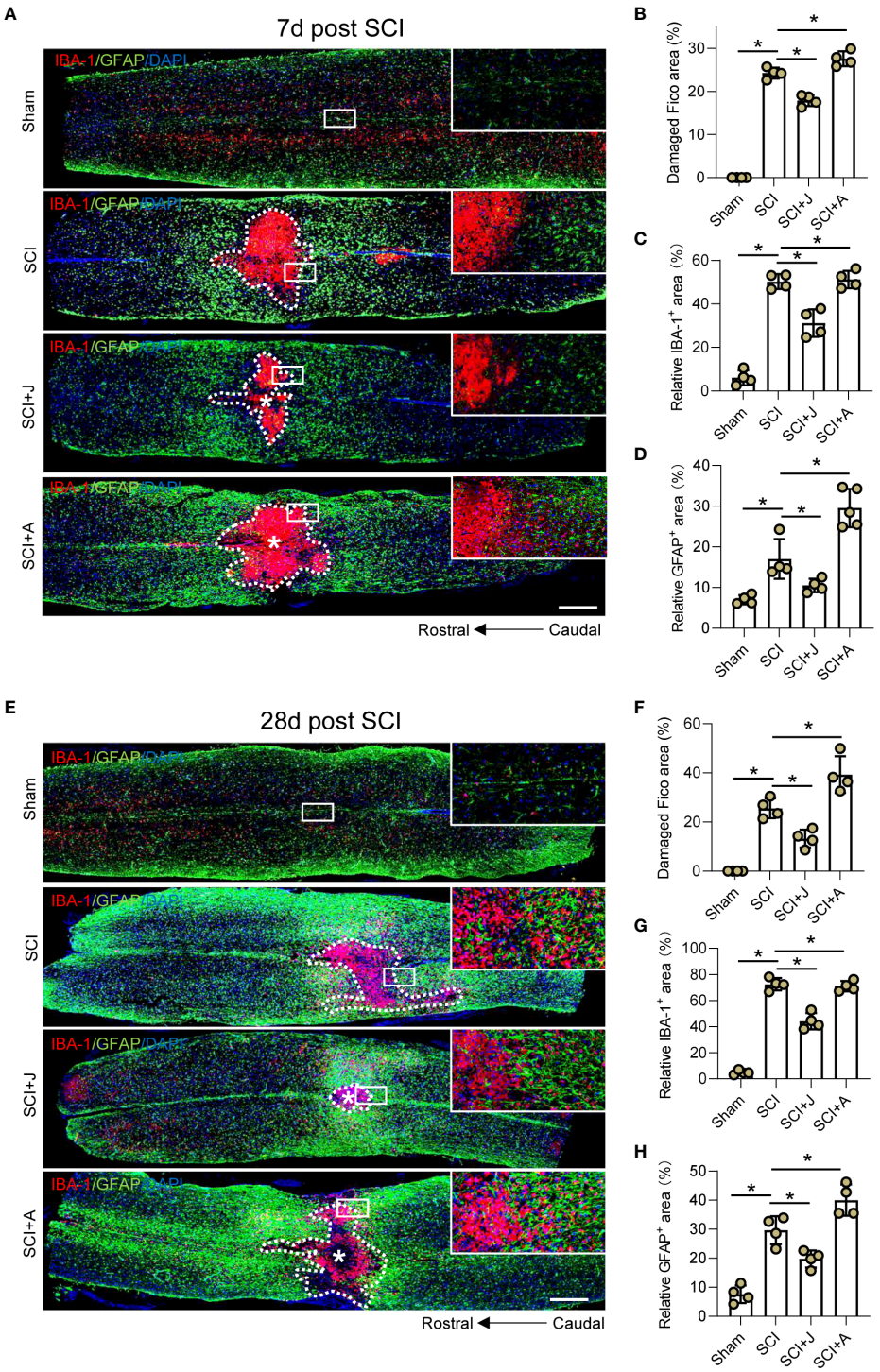


FIGURE 6
CB2R mitigated expansion of neuronal damage and formation of glial scarring post-SCI. **(A)** IF staining of GFAP (green) and IBA-1 (red) on day 7 post-SCI. Scale bar = 500 μm. Quantitative analysis of the area of injured foci inside the white dotted line **(B)**, microglia-occupied area, **(C)** and astrocyte-occupied area **(D)** on day 7 post-SCI. **(E)** IF staining of GFAP (green) and IBA-1 (red) on day 28 post-SCI. Scale bar = 500 μm. Quantitative analysis of the area of injured foci inside the white dotted line **(F)**, microglia-occupied area, **(G)** and astrocyte-occupied area **(H)** on day 28 post-SCI. *$p < 0.05$.

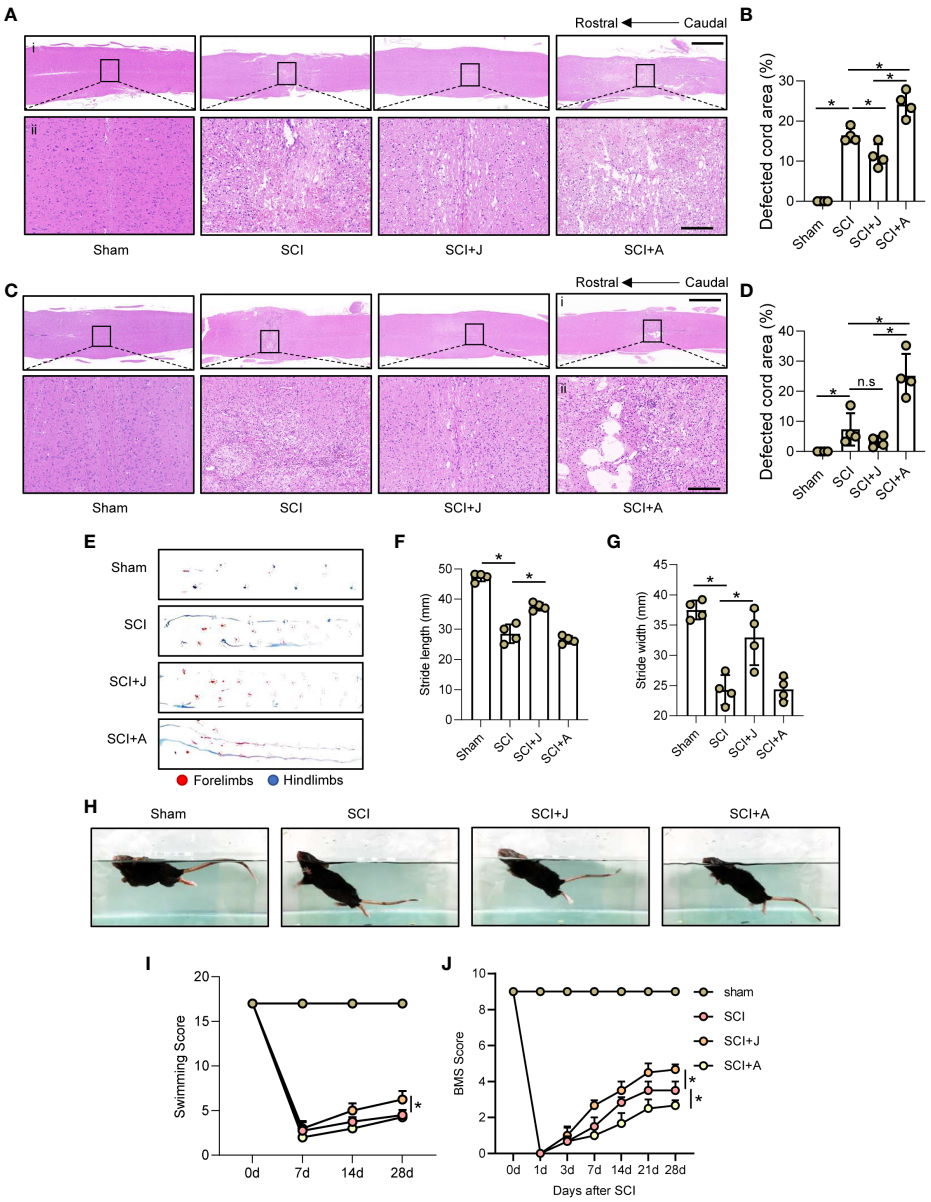


FIGURE 7
CB2R attenuated histological and functional damage post-SCI. **(A)** Representative images of H&E staining of spinal cords on day 3 post-SCI (injured cords in black frames). Scale bar **(i)** = 600 μm **(ii)** = 100 μm. **(B)** Quantitative analysis of defected area by H&E staining. **(C)** H&E staining of spinal cords on day 3 post-SCI (injured cords in black frames). Scale bar: **(i)** = 600 μm, **(ii)** = 100 μm. **(D)** Quantitative analysis of defected area by H&E staining. **(E)** Mouse footprint assay on day 28 post-SCI. Quantitative analysis of stride length **(F)** and width **(G)** of the hindlimbs of mice post-SCI. **(H)** Representative images of a mouse swimming on day 28 post-SCI. Statistical analysis of the Louisville Swim Scale score **(I)** and Basso Mouse Scale **(J)** over a 28-day period. *$p < 0.05$. n.s means no significance.

NLRP3 inflammasome-related proteins to attenuate inflammation-related pathology (51, 52). These findings confirmed that CB2R activation indeed mitigated neuroinflammation targeting polarization of microglia by regulating autophagy- and ubiquitination-mediated degradation of the NLRP3 inflammasome. AMPK, a nutrient and energy sensor that controls mitochondrial homeostasis, is activated by multiple physio-pathological insults, resulting in inflammation (53, 54), and subsequent phosphorylation of ULK1, resulting in activation of autophagosomes (55). Strikingly, CB2R has been implicated in upregulation of AMPK expression in models of aging, inflammation, and hyperglycemia (55–57), implying that CB2R might also participate in the regulation of autophagy. Interestingly, the

results of the present study showed that activation of CB2R increased AMPK/ULK1 phosphorylation, leading to increased expression of LC3B, indicating that CB2R activation in a state of neuroinflammation facilitated autophagy *via* activation of the AMPK/ULK1 axis.

An increase in the proportion of pro-inflammatory M1 microglia that express iNOS with a decrease in the proportion of anti-inflammatory M2 microglia expressing ARG-1 in the early stage of SCI plays a crucial role in neuroinflammation (58, 59). Therefore, upregulation of iNOS and downregulation of ARG-1 promote deteriorative secondary neuropathy and more intense neuroinflammation in the injured cord tissues post-SCI. The results of the *in vivo* experiments found that pro-inflammatory M1 microglia predominantly expressing iNOS and penuriously expressing ARG-1 had accumulated in the vicinity of the injured cord, while CB2R activation *via* administration of JWH-133 resulted in increased expression of ARG-1 with reduced levels of iNOS in microglia around the injury. In contrast, treatment with the CB2R antagonist AM630 promoted the formation of M1, rather than M2, microglia, suggesting that CB2R activation limited inflammation by manipulating polarization of microglia in the injured spinal cord. Accordingly, CB2R activation reduced secondary pathology like neuron loss, demyelination, and glial scarring, thereby improving functional recovery. However, these corrections were neutralized in AM630-treated mice, suggesting that CB2R may play a potent neuroprotective role in addition to anti-inflammatory activities. In summary, CB2R attenuated inflammatory responses *via* targeting microglial differentiation by facilitating autophagy- and ubiquitination-induced degradation of the NLRP3 inflammasome. CB2R expression in SCI mice reduced the area of glial scarring, rescued the deficiency of neurons and myelin, and improved recovery of locomotor function, in part, by inhibiting neuroinflammation.

These preliminary findings verified the role of CB2R in post-SCI neuroinflammation and subsequent neuropathology. Hence, further research is warranted to explore therapeutic strategies targeting CB2R and other functions of CB2R in neurons to reveal their potential immunotherapeutic value for SCI.

Data availability statement

The original contributions presented in the study are included in the article/Supplementary Material. Further inquiries can be directed to the corresponding authors.

Ethics statement

This study was reviewed and approved by the Institutional Animal Care and Use Committee of Nanjing Medical University.

Author contributions

FJ and ZZ conceived and designed the experiments. FJ performed the cell experiments. MX and YZ performed the animal experiments. JCh and JCa analyzed the data. ZQ wrote the paper. LY funded and supervised the research. All authors contributed to the article and approved the submitted version.

Funding

This study was supproted by 2022 Lifting Project for Young Scientific and Technological Talents Funded by Jiangsu Association of Science and Technology (To LY Grant No#:TJ-2022-033).

Acknowledgments

We thank the Key Laboratory of Taizhou People's Hospital for technological support and the use of equipment.

Conflict of interest

The authors declare that the research was conducted in the absence of any commercial or financial relationships that could be construed as a potential conflict of interest.

Publisher's note

All claims expressed in this article are solely those of the authors and do not necessarily represent those of their affiliated organizations, or those of the publisher, the editors and the reviewers. Any product that may be evaluated in this article, or claim that may be made by its manufacturer, is not guaranteed or endorsed by the publisher.

Supplementary material

The Supplementary Material for this article can be found online at: https://www.frontiersin.org/articles/10.3389/fimmu.2022.993168/full#supplementary-material

SUPPLEMENTARY FIGURE 1
Photos of 4% paraformaldehyde-fixed spinal cords on days 3 (**A**) and 28 (**B**) post-SCI in each group.

SUPPLEMENTARY FIGURE 2
(**A**) Representative protein bands including of p-AMPK, AMPK, p-ULK1, ULK1, LC3A, LC3B, and NLPR3 in each group 3 days after SCI. (**B**) Quantitative analysis of ratio of the p-AMPK/AMPK ratio. (**C**) Quantitative analysis of the p-ULK1/ULK1 ratio. (**D**) Quantitative analysis of the LC3B/LC3A ratio. (**E**) Quantitative analysis of NLRP3 expression.

References

1. Zipser CM, Cragg JJ, Guest JD, Fehlings MG, Jutzeler CR, Anderson AJ, et al. Cell-based and stem-cell-based treatments for spinal cord injury: Evidence from clinical trials. *Lancet Neurol* (2022) 21(7):659–70. doi: 10.1016/S1474-4422(21)00464-6

2. Slater PG, Dominguez-Romero ME, Villarreal M, Eisner V, Larrain J. Mitochondrial function in spinal cord injury and regeneration. *Cell Mol Life Sci* (2022) 79:239. doi: 10.1007/s00018-022-04261-x

3. Li Y, Ritzel RM, He J, Cao T, Sabirzhanov B, Li H, et al. The voltage-gated proton channel Hv1 plays a detrimental role in contusion spinal cord injury *via* extracellular acidosis-mediated neuroinflammation. *Brain Behav Immun* (2021) 91:267–83. doi: 10.1016/j.bbi.2020.10.005

4. Tan W, Su PP, Leff J, Gao X, Chen J, Guan AK, et al. Distinct phases of adult microglia proliferation: A myc-mediated early phase and a Tnfaip3-mediated late phase. *Cell Discovery* (2022) 8:34. doi: 10.1038/s41421-022-00377-3

5. Xu GY, Xu S, Zhang YX, Yu ZY, Zou F, Ma XS, et al. Cell-free extracts from human fat tissue with a hyaluronan-based hydrogel attenuate inflammation in a spinal cord injury model through M2 microglia/microphage polarization. *Small* (2022) 18:e2107838. doi: 10.1002/smll.202107838

6. Zhai X, Chen K, Yang H, Li B, Zhou T, Wang H, et al. Extracellular vesicles derived from CD73 modified human umbilical cord mesenchymal stem cells ameliorate inflammation after spinal cord injury. *J Nanobiotechnology* (2021) 19:274. doi: 10.1186/s12951-021-01022-z

7. Wang C, Xu T, Lachance BB, Zhong X, Shen G, Xu T, et al. Critical roles of sphingosine kinase 1 in the regulation of neuroinflammation and neuronal injury after spinal cord injury. *J Neuroinflamm* (2021) 18:50. doi: 10.1186/s12974-021-02092-4

8. Coll RC, Schroder K, Pelegrin P. NLRP3 and pyroptosis blockers for treating inflammatory diseases. *Trends Pharmacol Sci* (2022) 43(8):653–68. doi: 10.1016/j.tips.2022.04.003

9. Gangopadhyay A, Devi S, Tenguria S, Carriere J, Nguyen H, Jager E, et al. NLRP3 licenses NLRP11 for inflammasome activation in human macrophages. *Nat Immunol* (2022) 23(6):892–903. doi: 10.1038/s41590-022-01220-3

10. Xu Z, Li D, Qu W, Yin Y, Qiao S, Zhu Y, et al. Card9 protects sepsis by regulating Ripk2-mediated activation of NLRP3 inflammasome in macrophages. *Cell Death Dis* (2022) 13:502. doi: 10.1038/s41419-022-04938-y

11. Zhang Z, Guo P, Huang S, Jia Z, Chen T, Liu X, et al. Inhibiting microglia-derived NLRP3 alleviates subependymal edema and cognitive dysfunction in posthemorrhagic hydrocephalus after intracerebral hemorrhage *via* AMPK/Beclin-1 pathway. *Oxid Med Cell Longev* (2022) 2022:4177317. doi: 10.1155/2022/4177317

12. Zhang H, Wang J, Ruan C, Gao Z, Zhu Q, Li S. Co-Exposure of chronic stress and alumina nanoparticles aggravates hippocampal microglia pyroptosis by activating cathepsin B/NLRP3 signaling pathway. *J Hazard Mater* (2022) 436:129093. doi: 10.1016/j.jhazmat.2022.129093

13. Shi CS, Shenderov K, Huang NN, Kabat J, Abu-Asab M, Fitzgerald KA, et al. Activation of autophagy by inflammatory signals limits IL-1beta production by targeting ubiquitinated inflammasomes for destruction. *Nat Immunol* (2012) 13:255–63. doi: 10.1038/ni.2215

14. Lin Q, Li S, Jiang N, Shao X, Zhang M, Jin H, et al. PINK1-parkin pathway of mitophagy protects against contrast-induced acute kidney injury *via* decreasing mitochondrial ROS and NLRP3 inflammasome activation. *Redox Biol* (2019) 26:101254. doi: 10.1016/j.redox.2019.101254

15. Cai B, Zhao J, Zhang Y, Liu Y, Ma C, Yi F, et al. USP5 attenuates NLRP3 inflammasome activation by promoting autophagic degradation of NLRP3. *Autophagy* (2021), 18(5):990–1004. doi: 10.1080/15548627.2021.1965426

16. Young AP, Denovan-Wright EM. Synthetic cannabinoids reduce the inflammatory activity of microglia and subsequently improve neuronal survival. *vitro. Brain Behav Immun* (2022) 105:29–43. doi: 10.1016/j.bbi.2022.06.011

17. Johnson CT, Bradshaw HB. Modulatory potential of cannabidiol on the opioid-induced inflammatory response. *Cannabis Cannabinoid Res* (2021) 6:211–20. doi: 10.1089/can.2020.0181

18. Cristino L, Bisogno T, Di Marzo V. Cannabinoids and the expanded endocannabinoid system in neurological disorders. *Nat Rev Neurol* (2020) 16:9–29. doi: 10.1038/s41582-019-0284-z

19. Chiurchiu V, Maccarrone M. Bioactive lipids as modulators of immunity, inflammation and emotions. *Curr Opin Pharmacol* (2016) 29:54–62. doi: 10.1016/j.coph.2016.06.005

20. Moreno E, Cavic M, Canela EI. Functional fine-tuning of metabolic pathways by the endocannabinoid system-implications for health and disease. *Int J Mol Sci* (2021) 22(7):3661. doi: 10.3390/ijms22073661

21. Galve-Roperh I, Chiurchiu V, Diaz-Alonso J, Bari M, Guzman M, Maccarrone M. Cannabinoid receptor signaling in progenitor/stem cell proliferation and differentiation. *Prog Lipid Res* (2013) 52:633–50. doi: 10.1016/j.plipres.2013.05.004

22. Chiurchiu V, Leuti A, Maccarrone M. Cannabinoid signaling and neuroinflammatory diseases: A melting pot for the regulation of brain immune responses. *J Neuroimmune Pharmacol* (2015) 10:268–80. doi: 10.1007/s11481-015-9584-2

23. Bisogno T, Oddi S, Piccoli A, Fazio D, Maccarrone M. Type-2 cannabinoid receptors in neurodegeneration. *Pharmacol Res* (2016) 111:721–30. doi: 10.1016/j.phrs.2016.07.021

24. Chiurchiu V, van der Stelt M, Centonze D, Maccarrone M. The endocannabinoid system and its therapeutic exploitation in multiple sclerosis: Clues for other neuroinflammatory diseases. *Prog Neurobiol* (2018) 160:82–100. doi: 10.1016/j.pneurobio.2017.10.007

25. Tiberi M, Evron T, Saracini S, Boffa L, Mercuri NB, Chintalacharuvu SR, et al. Potent T cell-mediated anti-inflammatory role of the selective CB2 agonist lenabasum in multiple sclerosis. *Neuropathol Appl Neurobiol* (2022) 48:e12768. doi: 10.1111/nan.12768

26. Zhou H, Du R, Li G, Bai Z, Ma J, Mao C, et al. Cannabinoid receptor 2 promotes the intracellular degradation of HMGB1 *via* the autophagy-lysosome pathway in macrophage. *Int Immunopharmacol* (2020) 78:106007. doi: 10.1016/j.intimp.2019.106007

27. Luo XQ, Li A, Yang X, Xiao X, Hu R, Wang TW, et al. Paeoniflorin exerts neuroprotective effects by modulating the M1/M2 subset polarization of microglia/macrophages in the hippocampal CA1 region of vascular dementia rats *via* cannabinoid receptor 2. *Chin Med* (2018) 13:14. doi: 10.1186/s13020-018-0173-1

28. Qian Z, Chen H, Xia M, Chang J, Li X, Ye S, et al. Activation of glucagon-like peptide-1 receptor in microglia attenuates neuroinflammation-induced glial scarring *via* rescuing arf and rho GAP adapter protein 3 expressions after nerve injury. *Int J Biol Sci* (2022) 18:1328–46. doi: 10.7150/ijbs.68974

29. Basso DM, Fisher LC, Anderson AJ, Jakeman LB, McTigue DM, Popovich PG. Basso mouse scale for locomotion detects differences in recovery after spinal cord injury in five common mouse strains. *J Neurotrauma* (2006) 23:635–59. doi: 10.1089/neu.2006.23.635

30. Smith RR, Burke DA, Baldini AD, Shum-Siu A, Baltzley R, Bunger M, et al. The Louisville swim scale: A novel assessment of hindlimb function following spinal cord injury in adult rats. *J Neurotrauma* (2006) 23:1654–70. doi: 10.1089/neu.2006.23.1654

31. Ghosh K, Zhang GF, Chen H, Chen SR, Pan HL. Cannabinoid CB2 receptors are upregulated *via* bivalent histone modifications and control primary afferent input to the spinal cord in neuropathic pain. *J Biol Chem* (2022), 298(6):101999. doi: 10.1016/j.jbc.2022.101999

32. Sophocleous A, Yiallourides M, Zeng F, Pantelas P, Stylianou E, Li B, et al. Association of cannabinoid receptor modulation with normal and abnormal skeletal remodelling: A systematic review and meta-analysis of *in vitro*, *in vivo* and human studies. *Pharmacol Res* (2022) 175:105928. doi: 10.1016/j.phrs.2021.105928

33. Fan H, Chen Z, Tang HB, Shan LQ, Chen ZY, Wang XH, et al. Exosomes derived from olfactory ensheathing cells provided neuroprotection for spinal cord injury by switching the phenotype of macrophages/microglia. *Bioeng Transl Med* (2022) 7:e10287. doi: 10.1002/btm2.10287

34. Wang C, Xiao Y, Yu L, Tian F, Zhao J, Zhang H, et al. Protective effects of different bacteroides vulgatus strains against lipopolysaccharide-induced acute intestinal injury, and their underlying functional genes. *J Adv Res* (2022) 36:27–37. doi: 10.1016/j.jare.2021.06.012

35. Arioz BI, Tastan B, Tarakcioglu E, Tufekci KU, Olcum M, Ersoy N, et al. Melatonin attenuates LPS-induced acute depressive-like behaviors and microglial NLRP3 inflammasome activation through the SIRT1/Nrf2 pathway. *Front Immunol* (2019) 10:1511. doi: 10.3389/fimmu.2019.01511

36. Al-Ghezi ZZ, Busbee PB, Alghetaa H, Nagarkatti PS, Nagarkatti M. Combination of cannabinoids, delta-9-tetrahydrocannabinol (THC) and cannabidiol (CBD), mitigates experimental autoimmune encephalomyelitis (EAE) by altering the gut microbiome. *Brain Behav Immun* (2019) 82:25–35. doi: 10.1016/j.bbi.2019.07.028

37. Li Y, Zhou D, Ren Y, Zhang Z, Guo X, Ma M, et al. Mir223 restrains autophagy and promotes CNS inflammation by targeting ATG16L1. *Autophagy* (2019) 15:478–92. doi: 10.1080/15548627.2018.1522467

38. Xu S, Wang J, Zhong J, Shao M, Jiang J, Song J, et al. CD73 alleviates GSDMD-mediated microglia pyroptosis in spinal cord injury through PI3K/AKT/Foxo1 signaling. *Clin Transl Med* (2021) 11:e269. doi: 10.1002/ctm2.269

39. Liu Z, Yao X, Sun B, Jiang W, Liao C, Dai X, et al. Pretreatment with kaempferol attenuates microglia-mediate neuroinflammation by inhibiting MAPKs-NF-kappaB signaling pathway and pyroptosis after secondary spinal cord injury. *Free Radic Biol Med* (2021) 168:142–54. doi: 10.1016/j.freeradbiomed.2021.03.037

40. Zhang L, Zhuang X, Kotitalo P, Keller T, Krzyczmonik A, Haaparanta-Solin M, et al. Intravenous transplantation of olfactory ensheathing cells reduces neuroinflammation after spinal cord injury *via* interleukin-1 receptor antagonist. *Theranostics* (2021) 11:1147–61. doi: 10.7150/thno.52197

41. Li T, Sun H, Li Y, Su L, Jiang J, Liu Y, et al. Downregulation of macrophage migration inhibitory factor attenuates NLRP3 inflammasome mediated pyroptosis in sepsis-induced AKI. *Cell Death Discovery* (2022) 8:61. doi: 10.1038/s41420-022-00859-z

42. Yang D, Dai X, Xing Y, Tang X, Yang G, Harrison AG, et al. Intrinsic cardiac adrenergic cells contribute to LPS-induced myocardial dysfunction. *Commun Biol* (2022) 5:96. doi: 10.1038/s42003-022-03007-6

43. Sahu P, Mudgal J, Arora D, Kinra M, Mallik SB, Rao CM, et al. Cannabinoid receptor 2 activation mitigates lipopolysaccharide-induced neuroinflammation and sickness behavior in mice. *Psychopharmacol (Berl)* (2019) 236:1829–38. doi: 10.1007/s00213-019-5166-y

44. Xue S, Cao ZX, Wang JN, Zhao QX, Han J, Yang WJ, et al. Receptor-interacting protein kinase 3 inhibition relieves mechanical allodynia and suppresses NLRP3 inflammasome and NF-kappaB in a rat model of spinal cord injury. *Front Mol Neurosci* (2022) 15:861312. doi: 10.3389/fnmol.2022.861312

45. Mi J, Yang Y, Yao H, Huan Z, Xu C, Ren Z, et al. Inhibition of heat shock protein family a member 8 attenuates spinal cord ischemia-reperfusion injury *via* astrocyte NF-kappaB/NLRP3 inflammasome pathway: HSPA8 inhibition protects spinal ischemia-reperfusion injury. *J Neuroinflamm* (2021) 18:170. doi: 10.1186/s12974-021-02220-0

46. Xue Z, Zhang Z, Liu H, Li W, Guo X, Zhang Z, et al. lincRNA-Cox2 regulates NLRP3 inflammasome and autophagy mediated neuroinflammation. *Cell Death Differ* (2019) 26:130–45. doi: 10.1038/s41418-018-0105-8

47. Han X, Sun S, Sun Y, Song Q, Zhu J, Song N, et al. Small molecule-driven NLRP3 inflammation inhibition *via* interplay between ubiquitination and autophagy: Implications for Parkinson disease. *Autophagy* (2019) 15:1860–81. doi: 10.1080/15548627.2019.1596481

48. Chang P, Li H, Hu H, Li Y, Wang T. The role of HDAC6 in autophagy and NLRP3 inflammasome. *Front Immunol* (2021) 12:763831. doi: 10.3389/fimmu.2021.763831

49. Shao BZ, Wei W, Ke P, Xu ZQ, Zhou JX, Liu C. Activating cannabinoid receptor 2 alleviates pathogenesis of experimental autoimmune encephalomyelitis *via* activation of autophagy and inhibiting NLRP3 inflammasome. *CNS Neurosci Ther* (2014) 20:1021–8. doi: 10.1111/cns.12349

50. Song H, Zhao C, Yu Z, Li Q, Yan R, Qin Y, et al. UAF1 deubiquitinase complexes facilitate NLRP3 inflammasome activation by promoting NLRP3 expression. *Nat Commun* (2020) 11:6042. doi: 10.1038/s41467-020-19939-8

51. Cheng Y, Pan X, Wang J, Li X, Yang S, Yin R, et al. Fucoidan inhibits NLRP3 inflammasome activation by enhancing p62/SQSTM1-dependent selective autophagy to alleviate atherosclerosis. *Oxid Med Cell Longev* (2020) 2020:3186306. doi: 10.1155/2020/3186306

52. Su SH, Wu YF, Lin Q, Wang DP, Hai J. URB597 protects against NLRP3 inflammasome activation by inhibiting autophagy dysfunction in a rat model of chronic cerebral hypoperfusion. *J Neuroinflamm* (2019) 16:260. doi: 10.1186/s12974-019-1668-0

53. Herzig S, Shaw RJ. AMPK: Guardian of metabolism and mitochondrial homeostasis. *Nat Rev Mol Cell Biol* (2018) 19:121–35. doi: 10.1038/nrm.2017.95

54. Garcia D, Shaw RJ. AMPK: Mechanisms of cellular energy sensing and restoration of metabolic balance. *Mol Cell* (2017) 66:789–800. doi: 10.1016/j.molcel.2017.05.032

55. Du J, Xu M, Kong F, Zhu P, Mao Y, Liu Y, et al. CB2R attenuates intervertebral disc degeneration by delaying nucleus pulposus cell senescence through AMPK/GSK3beta pathway. *Aging Dis* (2022) 13:552–67. doi: 10.1016/j.molcel.2017.05.032

56. Choi IY, Ju C, Anthony JA, Lee DI, Prather PL, Kim WK. Activation of cannabinoid CB2 receptor-mediated AMPK/CREB pathway reduces cerebral ischemic injury. *Am J Pathol* (2013) 182:928–39. doi: 10.1016/j.ajpath.2012.11.024

57. Wu A, Hu P, Lin J, Xia W, Zhang R. Activating cannabinoid receptor 2 protects against diabetic cardiomyopathy through autophagy induction. *Front Pharmacol* (2018) 9:1292. doi: 10.3389/fphar.2018.01292

58. Hernandez J, Francos-Quijorna I, Redondo-Castro E, Lopez-Vales R, Navarro X. Microglia stimulation by protein extract of injured rat spinal cord. A novel *in vitro* model for studying activated microglia. *Front Mol Neurosci* (2021) 14:582497. doi: 10.3389/fnmol.2021.582497

59. Han D, Yu Z, Liu W, Yin D, Pu Y, Feng J, et al. Plasma hemopexin ameliorates murine spinal cord injury by switching microglia from the M1 state to the M2 state. *Cell Death Dis* (2018) 9:181. doi: 10.1038/s41419-017-0236-8

frontiers | Frontiers in Immunology

TYPE Review
PUBLISHED 19 October 2022
DOI 10.3389/fimmu.2022.997786

Check for updates

OPEN ACCESS

EDITED BY
Guangzhi Ning,
Tianjin Medical University General Hospital, China

REVIEWED BY
Jorge Tolivia,
University of Oviedo, Spain
Jinming Han,
Capital Medical University, China
Jessica M. Rosin,
University of British Columbia, Canada

*CORRESPONDENCE
Andrés Vidal-Itriago
andres.vidal-itriago@hdr.mq.edu.au
Marco Morsch
marco.morsch@mq.edu.au

SPECIALTY SECTION
This article was submitted to Multiple Sclerosis and Neuroimmunology, a section of the journal Frontiers in Immunology

RECEIVED 19 July 2022
ACCEPTED 20 September 2022
PUBLISHED 19 October 2022

CITATION
Vidal-Itriago A, Radford RAW, Aramideh JA, Maurel C, Scherer NM, Don EK, Lee A, Chung RS, Graeber MB and Morsch M (2022) Microglia morphophysiological diversity and its implications for the CNS.
Front. Immunol. 13:997786.
doi: 10.3389/fimmu.2022.997786

COPYRIGHT
© 2022 Vidal-Itriago, Radford, Aramideh, Maurel, Scherer, Don, Lee, Chung, Graeber and Morsch. This is an open-access article distributed under the terms of the Creative Commons Attribution License (CC BY). The use, distribution or reproduction in other forums is permitted, provided the original author(s) and the copyright owner(s) are credited and that the original publication in this journal is cited, in accordance with accepted academic practice. No use, distribution or reproduction is permitted which does not comply with these terms.

Microglia morphophysiological diversity and its implications for the CNS

Andrés Vidal-Itriago[1*], Rowan A. W. Radford[1], Jason A. Aramideh[2], Cindy Maurel[1], Natalie M. Scherer[1], Emily K. Don[1], Albert Lee[1], Roger S. Chung[1], Manuel B. Graeber[2] and Marco Morsch[1*]

[1]Faculty of Medicine, Health and Human Sciences, Macquarie Medical School, Macquarie University, Sydney, NSW, Australia, [2]Brain and Mind Centre, Faculty of Medicine and Health, The University of Sydney, Sydney, NSW, Australia

Microglia are mononuclear phagocytes of mesodermal origin that migrate to the central nervous system (CNS) during the early stages of embryonic development. After colonizing the CNS, they proliferate and remain able to self-renew throughout life, maintaining the number of microglia around 5-12% of the cells in the CNS parenchyma. They are considered to play key roles in development, homeostasis and innate immunity of the CNS. Microglia are exceptionally diverse in their morphological characteristics, actively modifying the shape of their processes and soma in response to different stimuli. This broad morphological spectrum of microglia responses is considered to be closely correlated to their diverse range of functions in health and disease. However, the morphophysiological attributes of microglia, and the structural and functional features of microglia-neuron interactions, remain largely unknown. Here, we assess the current knowledge of the diverse microglial morphologies, with a focus on the correlation between microglial shape and function. We also outline some of the current challenges, opportunities, and future directions that will help us to tackle unanswered questions about microglia, and to continue unravelling the mysteries of microglia, in all its shapes.

KEYWORDS

microglia, microglial morphology, microglia-neuron interactions, microglia diversity, microglia activation

1 Introduction

In the first descriptions of microglia by Pío del Río-Hortega in 1919, microglial activation was depicted as the transition from a ramified morphology (Figure 1A) in the 'resting' state to an amoeboid morphology (Figure 1B) in the'activated' state (1). Now it is widely accepted that ramified microglia actively screen the CNS, establish contacts with neurons and other cells, and monitor and influence neuronal activity (2–4). However, our understanding of microglial physiology in relation to its morphology is still very limited, and a lack of ramification is generally considered an indicator of microglial activation. New genetic, molecular and pharmacological interventions, combined with novel *in vivo* and *ex vivo* models, have begun to describe new morphological features of microglia physiology and its interactions with other cells, supporting the idea that microglial morphology is highly dynamic and complex (5–7). These studies of microglial morphophysiological heterogeneity provide further evidence that microglia activation cannot simply be reduced to a structural transition from a ramified to an amoeboid shape.

Understanding the relationship between microglial morphology and their precise physiological roles provides critical insights into the spatiotemporal dynamics of microglial responses. In turn, this will lead to a greater understanding of how microglia maintain CNS homeostasis or, on the contrary, contribute to disease etiology. We are now aware of the crucial involvement of microglia in synaptogenesis, synaptic plasticity, axonal regeneration, neuronal survival and regulation of neuronal activity, not only during development but throughout adult life (8–15). These additional functional roles of microglia highlight their importance far beyond their well-known roles in CNS immunity and debris elimination.

This review summarizes the current knowledge regarding the correlation of microglia morphology and function from the early stages of embryonic development throughout the adult life, in health, aging and disease. We highlight some of the specific microglial morphological features that we consider important

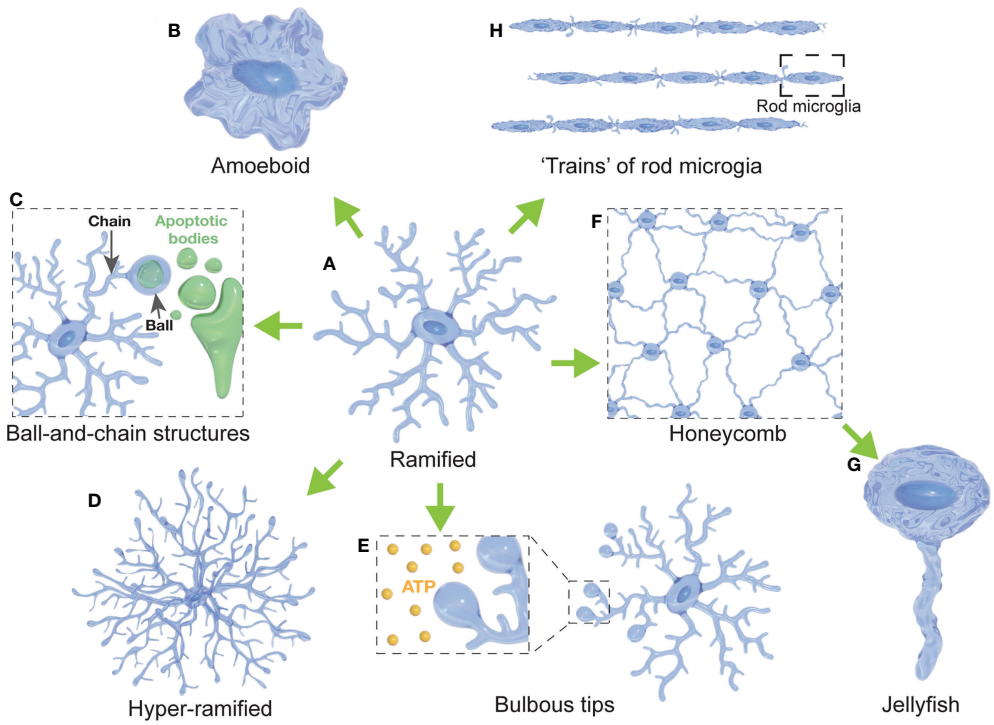


FIGURE 1
Diversity of microglial morphologies. **(A)** Ramified microglia are highly branched with multiple primary and secondary processes (often considered surveillant). **(B)** Amoeboid microglia present with a highly rounded morphology compared to their ramified states (often with a high phagocytic and migratory capacity). **(C)** Microglia can form ball-and-chain structures at the tip of their processes to phagocytose small amounts of material (such as synapses or apoptotic bodies). **(D)** Hyper-ramified microglia present with increased branching of their processes (often observed in acute and chronic stress models). **(E)** Microglia display bulbous budding at the end of some of their processes (considered to be important for ATP sensing). **(F)** Several microglial cells form a network resembling a honeycomb (reported in response to BBB leakage). **(G)** Jellyfish morphologies have been reported as a morphological transition of honeycomb microglia after extensive astrocytic death in the glia limitans (in response to TBI). **(H)** Rod microglia are characterized by an elongated, narrowed soma without planar processes that can form trains of rod microglial cells (in response to injury).

for their functional spectrum and future classifications. We further discuss the importance of investigating microglial dynamics using *in vivo* and *ex vivo* approaches to better understand the spatiotemporal changes microglia undergo in certain conditions and throughout life.

2 Microglial biology

Microglia are myeloid phagocytes and the only innate immune cells permanently residing in the central nervous system (CNS). Microglia comprise between 5% and 12% of all the cells in the murine CNS, with variable densities depending on the CNS region studied (16). Microglia have been historically considered as phagocytes and immune cells that react to neuronal insult and pathological events in the CNS. However, it has become apparent that microglia serve more functions besides phagocytosis and the production of inflammatory cytokines (17, 18). Many studies have provided clear evidence that microglia play crucial physiological roles in the healthy brain; being involved in the development of the CNS connectivity, synaptic plasticity, monitoring of neuronal activity, and maintaining CNS homeostasis into adult life (2, 19–21). To perform such a diverse range of functions, microglia must sense different cues in their immediate microenvironment and adapt their morphology to different stimuli, displaying a plethora of cellular shapes (Figure 1). Whether microglia achieve their functional diversity by means of their phenotypic plasticity or through an early diversification into a heterogeneous population of cells is still unknown. The literature states many examples that indicate a correlation between the morphology and function of microglia, i.e. that amoeboid microglia are associated with phagocytosis of cellular debris (2, 22–25). However, the lack of a standard classification of microglia morphophysiology makes it often difficult to compare such associations between studies. It remains unclear whether a certain function is linked to a specific morphology, and/or whether microglia with a certain shape are limited to a particular role.

2.1 Microglial ontology

Unlike neurons and other glial cells (oligodendrocytes and astrocytes), microglia are not of neuroectodermal origin. Instead, they are myeloid cells of hematopoietic origin (2). Microglia arise from erythromyeloid precursors generated in the yolk sac, from where they migrate *via* the blood stream to the CNS in the early stages of embryonic development (26–29). After colonizing the CNS, the microglial precursors complete their differentiation and microglia remain a stable CNS-resident population, maintaining their numbers through self-renewal (30, 31), where the signaling of the colony-stimulating factor-1 receptor (CSF1R) is crucial for the proliferation, differentiation and survival of mononuclear phagocytes such as macrophages, osteoclasts and microglia (32). For instance, in the human cortex, microglia have a median age of 4.2 years, replacing 28% of the population every year (33). In the murine cortex, microglia have a median lifetime of more than 15 months with approximately 50% of these cells surviving the entire lifespan of the mouse (34). Some studies have shown that circulating monocytes can enter the CNS during inflammation and pathological incidents, where the blood-brain barrier (BBB) permeability is compromised. However, these cells are classified into a differentiated subset of cells, not contributing to the microglial cell pool and without self-renewal capacity (35–38).

Other types of macrophages are located at the CNS interface, such as meningeal macrophages, perivascular macrophages and choroid plexus macrophages (39–41). For decades these macrophages were believed to be derived from blood-borne monocytes, however new evidence suggests that at least some of them also arise from yolk sac precursors, being closer to microglia than to monocytes in their ontogeny (39). Nevertheless, microglia and these non-parenchymal macrophages remain distinct cell populations, with different locations, functions and morphologies (39).

2.2 Microglial functional diversity

Microglia possess a remarkable plasticity that allow them to perform a plethora of functions in the CNS during development, health and disease. As immune effectors of the CNS, microglia are well known to play crucial roles in response to injury and infection (42). Microglia express pattern recognition receptors (PRR) that allow them to recognize molecular patterns associated with pathogens and tissue damage (43). Upon PRR activation, microglia undergo a morphological- and physiological- transformation that leads to the release of pro-inflammatory cytokines, and the phagocytosis of pathogens and cell debris (44, 45). Conventional descriptors of 'microglial activation' include a change in functional behavior, as well as the migration to the site of injury, retraction of processes, and 'compacting' the cell body into an amoeboid morphology (23, 24, 46). Many of the microglial functions and morphological changes during the innate immune response, and in the diseased CNS, are extensively discussed in the literature (47–52).

In addition, microglia play crucial roles during the embryonic and postnatal development of the CNS. In rodents, microglia display an amoeboid morphology, typical of a phagocytic phenotype (53, 54). Accordingly, it has been shown that microglia control cortical neuron populations through phagocytosis of neural precursor cells (NPC) in rats and primates (55). Also, it has been described *in vivo* that microglia actively engage in phagocytosis of apoptotic cell

bodies in the developing optic tectum and spinal cord of zebrafish (56, 57). In mice, *in utero* depletion of microglia during gestation, through CSF1R inhibition, led to the accumulation of dead cells in the hypothalamus and a significant increase in cell death throughout the developing hypothalamus, probably due to the lack of microglia-mediated elimination of apoptotic and dead cells (58). Interestingly, manipulating microglial activation had direct effects upon both the precursor cells population and the postnatal neuronal population. Microglial activation enhancement led to a decreased number of NPCs, while microglial deactivation increased the NPCs pool of cells (55). Microglia-mediated phagocytosis of synaptic material, known as synaptic pruning [reviewed in (59)], is crucial for the formation of neuronal pathways and the refining of neuronal circuits during development (60–63), ultimately affecting axonal growth, neuronal positioning and CNS cytoarchitecture (64).

Microglia have also been described to play key roles in the hypothalamus, were they influence the circuitry and signaling of the melanocortin system, responsible for the control of body weight and food intake (58, 65, 66). Administering PLX5622, a CSF1R-inhibitor, to pregnant mice achieved the *in utero* depletion of embryonic microglia (58), having postnatal effects upon energy balance. At postnatal day 4 (P4), pups from females treated with PLX5622 during pregnancy showed a reduction of 45% in the number of POMC neurons (58), neurons involved in the hypothalamic regulation of food intake through the release of anorexigenic peptides (67). The reduction of POMC neurons in PLX5622-exposed pups was accompanied by a significant increase in body weight gain from P5 to P15, when compared to pups from control females (58). These results show that depletion of microglia during gestation can affect the development of hypothalamic satiety circuits and have lasting effects upon body weight gain after birth (58). Embryonic microglia in the hypothalamus have also been shown to respond to different stimuli during gestation (68–71). *In utero* electroporation (IUE) is a procedure used to introduce plasmid DNA into the murine embryonic CNS (72). It has been shown that IUE induces morphological and gene expression changes in hypothalamic microglia, concomitant with an increased cell death in the developing hypothalamus (68). Furthermore, embryonic microglia interaction with radial glial cells (RGC) in the hypothalamus after IUE led to microglia-mediated degeneration and phagocytosis of RGC (69). Further evidence of the role of embryonic microglia during gestation has been shown in response to maternal stressors in a gestational cold stress model (70). In this study, cold exposure of pregnant mice led to an increase in the secretion of CCL3 and CCL4 by a subset of hypothalamic microglia, adjacent to neural stem cells (NSC), in the pups (70). Interestingly, this effect was only seen in male pups and was coincident with a decrease in the number of oxytocin neurons in the paraventricular nucleus of the hypothalamus (70). This effect seems to be CCL3 and CCL4-dependent, since these molecules also affected the proliferation and differentiation of hypothalamic NSC *in vitro* (70). Embryonic microglia have also been shown to be affected by gestational exposure to bisphenol A (BPA) (71). Exposing pregnant mice to BPA led to an increase of microglia numbers in the hypothalamus and changes in the morphology of microglial cells of the pups, showing higher ramification and higher number of phagocytic cups (71). These studies highlight the responsiveness of embryonic microglia to environmental factors, with lasting effects into the postnatal stages. The importance of hypothalamic microglia upon energy balance has also been shown in adults, where the microglia-specific disruption of leptin signaling caused hyperphagia and accelerated body weight gain, with concomitant loss of POMC neurons (66).

The microglial role during development goes beyond its phagocytic capacity, being able to secrete neurotrophic factors to promote neuronal survival, neurogenesis and oligodendrogenesis during early postnatal development (73, 74). In mice, it has been shown that microglia directly contribute to the survival of layer V cortical neurons through the secretion of the trophic factor insulin-like growth factor 1 (IGF-1) during postnatal development (74). In rats, microglia enhanced neurogenesis and oligodendrogenesis in the subventricular zone through the secretion of pro-inflammatory cytokines such as IL-1β, IL-6, TNF-α and IFN-γ (73). These studies highlight the importance of microglia during different stages of CNS development and maturation, not only being involved in the differentiation of other cell types but also refining the neuronal circuitry and CNS organization.

Microglial effects upon neuronal connectivity are also not limited to the developmental stage. In the adult CNS, microglia have been shown to engulf synaptic material in both the healthy brain and in neurodegenerative conditions (13, 75–77). Early ultrastructural studies described microglia-mediated displacement of synaptic terminals, suggesting that microglia actively participate in synaptic plasticity (78–80). More recently, microglia have been related to the elimination of synapses during adulthood and ageing across different regions of the CNS (13, 14, 81, 82). These functions suggest a key role of microglia in the modifications to the neuronal network in response to stress (81), memory maintenance (77), or in experience-dependent behavioral adaptation through synaptic plasticity (13). Interestingly, microglial ablation in adult mice led to a robust increase of the synaptic density in the hippocampus (83). Furthermore, it has been shown that blocking microglial BDNF (brain-derived neurotrophic factor) secretion, leads to a reduction in the formation of cortical dendritic spines associated with deficits in learning. This strongly suggests that microglia are not only involved in synaptic eliminations but also in synaptogenesis, with direct implications for learning-dependent plasticity (84). Altogether, this data show that microglia are involved in synaptic remodeling *via* both

synaptogenesis and elimination, directly influencing neural plasticity.

3 Morphophysiological traits of microglia

3.1 The classic (and outdated) two-state paradigm

The morphological plasticity of microglial cells was already acknowledged by Río-Hortega in his 1919 series of papers about microglia [reviewed in (1)]. He described the morphological changes experienced by microglia after neuronal insult as: *"The first phenomenon observed in microglia that evidences their distress in brain pathological processes is an increase in volume which mainly affects their dendrites ["processes"]. Hypertrophy ["increased cell size"] of microglial cell bodies is observed in some cases, and a more or less active hyperplasia ["increased cell density"] can also be observed"* (1). Río-Hortega also referred to the gain of migratory and phagocytic characteristics in neurodegenerative processes: *"The nomadic character of microglia is best observed in neurodegenerative processes, during which the apparent rest that they enjoyed in the normal state turns into migratory and phagocytic activity"* (1). This led to the assumption that microglia exist in two different states: i) 'Resting', characterized by a highly ramified morphology and limited phagocytic and migratory activity, and ii) 'Activated', characterized by amoeboid shape, high motility, with phagocytic and proliferative capacities. For most of the last century this 'two-state paradigm' has been widely adopted, contributing to the misconception that microglia in the healthy brain were functionally quiescent or dormant (85, 86). Equally, the ramified-to-amoeboid transition observed in microglia during infection, trauma or pathological processes was inferred as the key criteria for microglial activation (87). Morphometric parameters such as sphericity, volume, cell body area, number of processes, length of processes, number of endpoints, number of nodes or microglial process area have been extensively used in the assessment of microglial morphology (56, 88, 89). Often these parameters are used to measure how ramified or amoeboid a microglial cell presents itself, using these as an indication of its activation state.

It is now well accepted that microglia undergo a morphological and functional transformation upon neuronal insult. Microglia do indeed migrate to the site of lesion, perform their phagocytic capacity to clear debris or eliminate pathogens and adopt an amoeboid morphology (22, 90). However, it has become evident that microglia are not dormant or quiescent in the so-called 'resting' state. *In vivo* studies have demonstrated that ramified microglia are quite dynamic, and their processes are continuously moving to survey the CNS parenchyma (91, 92). It has been convincingly demonstrated that microglia are very active in the healthy brain, beyond their direct immunological response patterns, playing important roles in synaptic plasticity, neurotrophic support, myelin remodeling, and maintaining homeostasis in the CNS (2, 4, 7). Hence, the morphological changes that were considered for many years as the key indicator of microglial 'activation' rather correspond to a morphophysiological transition that reflects a change in function. Further indication that the two-state paradigm fails to accurately reflect the spectrum of microglial phenotypes is the introduction of diverse categories of microglia functions in the literature, including surveillant microglia, proliferating microglia, pruning/neuromodulatory microglia, phagocytic microglia, and inflammatory microglia (93).

3.2 Factors determining the morphophysiological diversity of microglia

Microglia have been historically considered a homogenous population of cells. However, the regional, functional and morphological diversity of neurons, as well as the highly specialized organization of the CNS, suggest that microglial characteristics might reflect a similar heterogeneity (16, 88). Over the last 20 years, it has become more and more apparent that microglia show region-specific characteristics that are also affected by age and sex in the developing and adult CNS, as discussed below.

3.2.1 Region

Early studies in adult mice showed variations in cell density throughout the brain that were accompanied by diverse morphologies of microglia depending on brain regions; with radially orientated arborized cells found abundantly throughout the grey matter, longitudinally branched elongated cells in the white matter, and compact amoeboid cells found around the circumventricular organs (16). Recent studies have also demonstrated region-specific differences in lysosome content and membrane properties of microglia throughout the brain (94, 95). Transcriptomic profiling of different peripheral macrophage populations also demonstrated inter-region variability (96). Further studies using RNA sequencing of microglia have also highlighted strong regional differences. For instance, it has been shown that the expression of genes related to the phagocytic capacity of microglia differ between different regions in mice. Using microglia-specific mRNA extraction, Ayata and colleagues showed that expression of cell-clearance genes was significantly more prominent in cerebellar microglia when compared to striatal or cortical cells (97). The fact that the cerebellum shows higher levels of neuronal loss compared to the striatum or cortex, suggests that microglial phenotypes may be

greatly determined by the surrounding microenvironment. Another study in mice used single-cell RNA sequencing (scRNA-seq) to investigate the regional differences of microglia at different developmental stages (6). Interestingly, Li and colleagues showed that early postnatal microglia located in highly proliferative regions showed a similar gene signature to that of degenerative disease-associated microglia. Furthermore, the authors found that the transcriptome of microglia expressing homeostatic genes in the adult mice was very similar regardless of the brain region, suggesting that the regional differences may change among different developmental stages, and that age is also a factor relevant for microglial phenotypic differences (6).

3.2.2 Age

Microglia migrate to the CNS at the very early stages of embryonic development and remain resident in the CNS parenchyma with self-renewal capacity throughout life. Hence, microglia are present during the developmental, adult, and aging stages of the CNS, presumably playing important roles by adapting to the different processes at different stages. The intense phagocytic activity observed during development correlates with the typical amoeboid morphology of phagocytic microglia (53, 54). On the other hand, microglia in the adult CNS show ramified morphology that is often considered an indication of microglial maturation (12, 98). Nonetheless, this loss of amoeboid morphology in adult microglia does not necessarily correlate with a loss of phagocytic activity, as many studies have described that microglia are phagocytically active even in the ramified state (11, 62). Furthermore, a recent study investigating microglial heterogeneity in mice at different ages using scRNA-seq showed that microglia display a higher transcriptomic diversity in the developing, aged, and diseased brain, compared to the adult microglial population (5).

3.2.3 Sex

The CNS presents a series of sex-specific characteristics regarding its anatomy, physiology, morphology, and epigenome (99–101). Sex-specific differences in the density, morphology and phagocytic activity have been described during development and in the adult mice (102), probably due to differential hormonal surges throughout life. This sex dimorphism not only comprises neuronal traits but also entails differences in non-neuronal cells. One of the first studies describing sex-specific differences in the microglial population reported that female mice showed an increase in microglia number, of at least 30% in the hippocampus compared to male littermates at three different ages (103). Another study highlighted that microglia number and morphology are affected by sex, age, and brain region (53). Male rats showed more deramification of microglia, the retraction of microglial processes and microglia adopting an amoeboid shape at early postnatal stages while females showed an increased number of deramified cells in juvenile and adult individuals. These differences in microglial number and morphology were also accompanied by differences in the gene expression of cytokines. These data suggest that microglial morphology, and likely their physiological state, are modulated by sex at different ages and regions. Subsequent studies suggested that microglia might have a relevant role in repressing the feminization of the brain, a process characterized by changes that sexual receptivity and maternal behavior (104). Specifically, one study described an increase in the number of microglia present in the preoptic area (POA) of neonatal male rats, showing a significant role of microglia in the synaptic patterning of the POA, crucial for masculinization of the brain and behavior (105). Interestingly, they also reported differences in the morphology of microglial cells in the POA, where neonatal males had twice as many amoeboid microglia compared to female littermates.

Some studies have also reported sex-specific traits in pain modulation directly related to microglia. For example, male mice were reported to show a TLR4-dependent activation of microglia during inflammation and neuropathic hypersensitivity (106). Another study assessing sciatic nerve hypersensitivity found that microglia were responsible for mediating hypersensitivity in male mice, while the response in females was mediated *via* T-cells (107). This difference was deemed mainly due to hormonal differences, as castrated males lacking testosterone lost the microglial response, while hypersensitivity was blocked by targeting microglia in females lacking T-cells and treated with testosterone (107). Differences in microglia-mediated pain hypersensitivity were also reported in rats, where inhibition of the P2X4R pathway in microglia resulted in the elimination of hypersensitivity in male rats but not in females, despite both displaying reactive microgliosis (108). Pharmacological modulation of neuropathic pain was also achieved with metformin, an antidiabetic drug, eliminating pain and microglial 'activation', determined by the activation marker Iba-1, in the spinal cord of male but not female mice (109). Dimorphic effects of morphine between female and male rats might also be related to sex-specific microglia differences. It has been reported that the increased number of deramified microglia in the periaqueductal gray is responsible for the attenuated effects of morphine seen in female rats (110). Interestingly, this was reversed through microglial modulation by blocking TLR4 in females. Altogether, these studies demonstrate that microglia might play a key role in pain modulation and that this is greatly influenced by sex-specific differences.

3.3 Microglia morphophysiological diversity

Although most studies use the ramified-amoeboid spectrum (Figure 2) to classify the morphology of microglial cells and generally directly correlate the phenotypic appearance with the

physiological response, several studies have identified alternative morphologies (Table 1). Importantly, these studies did not find a clear correlation between increased expression of pro- or anti-inflammatory markers with such morphologies. This suggests that microglia are capable of modifying and adapting their morphology in response to stimuli unrelated to their activation or immunological status.

3.3.1 Microglia fulfill important roles in their ramified state

Deramification (the transition to an amoeboid state) has been considered an indication of microglial activation for many decades. However, many studies have shown that microglia in the so-called 'resting' state, characterized by a highly ramified morphology (Figure 1A), are actually extremely dynamic and active. Early evidence was provided in studies using microglia-reporter mice and two-photon microscopy, allowing the observation of microglia and their processes *in vivo* (91, 92). Those studies revealed that while the soma remained relatively static with few signs of migratory behavior; microglial processes were in constant motion, establishing transient contacts with neurons, astrocytes and blood vessels (92). This constant and rapid extension-contraction of the microglial processes is thought to be part of a continuous surveillance of the CNS microenvironment, allowing the CNS parenchyma to be monitored every few hours (7, 92). Surface receptors allow microglia to detect changes in the environment (82, 132) and to monitor neuronal activity through transient contacts with synaptic structures (7, 13). As we discuss below, the role of ramified microglia is not limited to surveillance. It has been shown that microglia can present with bulbous processes, forming ball-and-chain structures (Figure 1C), which are believed to be an indicator of phagocytosis of small amounts of debris or tissue without transitioning to an amoeboid shape (11). This suggests that such microglial phagocytosis of synapses and apoptotic material might not require the loss of ramified

TABLE 1 Microglial morphologies and their reported functions.

Morphology	Functional characteristics	Model	References
Ramified	Classically considered a 'resting' state.	Human, mouse, rat, zebrafish	(7, 13, 57, 88, 91, 92, 111, 112)
	Frequent extension/contraction of microglial processes.		
	Surveillance of CNS parenchyma and neuronal activity.		
	Neuroprotective role during excitotoxicity.		
Amoeboid	Classically considered an 'activated' state.	Human, mouse, rat, zebrafish	(16, 23, 24, 46, 53, 56, 57, 59, 113)
	Transformation to amoeboid morphology in response to infection, injury and/or pathological processes.		
	Phagocytically active.		
	Key roles in the healthy brain, eliminating debris and apoptotic cells.		
Bulbous endings of microglial processes	Transient formation of bulbous structures in the apex of microglial processes.	Mouse, zebrafish	(91, 114–116)
	Involved in the chemotactic response to neuron-released ATP gradients.		
	Also involved in monitorization and control of neuronal activity.		
Ball-and-chain structures	Present in immunologically unchallenged microglia.	Mouse, rat, macaque, zebrafish	(11, 55, 117–121)
	Phagocytically active.		
	Involved in the phagocytosis of apoptotic cells, neural precursors and myelin sheaths.		
Hyper-ramified	Hyper-ramification of processes in response to acute and chronic stress.	Mouse, rat	(122–125)
	Possible role in stress-related synaptic modifications.		
Honeycomb	Formed in response to BBB leakage after compression-TBI.	Mouse	(126)
	Several microglia cells retract most processes, except 3-4 to form a contiguous network.		
Jellyfish	Formed in response to astrocytic death after compression-TBI.	Mouse	(126)
	Microglia extends a single non branching process.		
	Phagocytically active.		
Rod microglia	Elongated and narrowed soma.	Human, mouse, rat	(127–131)
	Thin polar processes.		
	Can form multicellular 'trains' of several rod microglia.		
	Rod microglia align adjacent to injured neurons.		
	Described in several pathological processes.		

morphology, contrasting with observations in pathological conditions, where phagocytosis is generally performed by amoeboid microglia (59). Some studies have further described ramified or hyper-ramified microglial phenotypes (Figure 1D) that are actively engaged in other scenarios, such as the physiological response to stress and excitotoxicity. For instance, chronic stress resulted in a higher expression of Iba-1 and the hyper-ramification of microglia in the prefrontal cortex of rats, correlating with an enhanced activation of neurons in that region and impaired spatial working memory (122). Another study used mouse organotypic hippocampal slice cultures and showed that ramified microglia exert neuroprotective effects upon neurons during NMDA-induced excitotoxicity (111). Vinet and colleagues demonstrated that some neurons in the CA3 and DG regions of the hippocampus were resistant to excitotoxicity. This resistance was lost after ablation of ramified microglia, severely affecting the viability of neurons, while replenishment of microglia-free slices restored the resistance in those regions (111). Interestingly, the results in this study suggest not only that ramified microglia are able to exert neuroprotective roles in pathologic processes, but also that this function might be region-specific as other hippocampal regions showed different responses.

3.3.2 Alternative microglial morphologies and their function

3.3.2.1 Bulbous endings of microglial processes

As early as 2005, in one of the first *in vivo* studies describing the dynamic nature of microglial processes, the authors described that microglia extended their processes in response to local brain injury in mice (91). Interestingly, this response was mimicked by local ATP injections and characterized by bulbous endings of microglial processes (Figure 1E). These observations were confirmed in later studies where the outgrowth of microglial processes was associated with a chemotactic response to gradients of neuron-released ATP, through NMDA receptors on the surface of microglial processes (114, 115). Both studies reported that the formation of these bulbous endings was transient and was reversed when ATP application was terminated. The role of ATP in inducing the formation of bulbous structures in microglial processes was also described *in vivo* in zebrafish (116). The authors revealed that these bulbous microglia-neuron interactions were dependent on neuronal Pannexin-1 hemichannel, permeable to ATP, and ATP/P2 receptors in microglia. Interestingly, they showed that microglia were more prone to form bulbous contacts with neurons depending on their activity, as microglial processes preferentially moved towards neurons showing higher frequencies of Ca2+ activity. Most importantly, they showed that ramified microglia were able to downregulate the activity of those neurons contacted with such bulbous structures. These results suggest that ATP plays an essential role in signaling between neurons and microglia, that microglia are capable of sensing neuronal activity, and that this activity can be modulated *via* microglial bulbous processes.

3.3.2.2 Ball-and-chain structures

After the initial *in vivo* observation that 'resting' microglia actively and constantly modify the length of their processes to monitor the CNS parenchyma (91, 92), another study showed in the adult murine CNS that immunologically unchallenged ramified microglia are able to phagocytose apoptotic cells (11). The authors described a novel phenomenon in hippocampal sections of 1 month-old mice, where some microglial processes adopted a so-called ball-and-chain structure, in which a spherical phagocytic pouch (ball) was formed at the tip of a microglial terminal branch (chain) during apoptotic clearance (Figure 1C). Other studies also described this morphological type of interaction during early development. In the postnatal (P13) mouse subventricular zone (SVZ), microglia engulfed apoptotic dividing cells by forming phagocytic cups at the tip of the processes (117). In macaque, microglia phagocytosed neural precursor cells in the developing neocortex (E80), through enveloping the cell with a phagocytic structure formed in the distal portion of one of its processes, forming a ball-and-chain structure (55). More recently, a study in rats described that ball-and-chain structures were prominent in early post-developmental SVZ (P10) (118). Interestingly, these structures were also abundant in later stages (P40) in rats exposed to neonatal hypoxia-ischemia surgery, suggesting that they might also be implicated in the response to long-lasting effects of perinatal neuronal challenges. Ball-and-chain structures were also observed in ramified microglia in the developing cerebellar cortex of rats (119). Even though the authors do not explicitly use the ball-and-chain terminology, a recent *in vivo* study found that microglia phagocytose myelin sheaths during the development of the optic tectum and spinal cord of juvenile zebrafish, in a fashion that resembles the ball-and-chain structure (120). They reported that phagocytic events, identified through calcium signaling, led to the phagocytosis of portions of myelin sheaths. Interestingly their images show elongated microglia with short processes that in some cases showed a phagocytic pouch at their tips, resembling the ball-and-chain morphology. This process was regulated by neuronal activity, with microglia engulfing more myelin when neuronal activity was reduced or suppressed (120). Microglial phagocytosis through ball-and-chain structures has also been shown to be involved in the masculinization of social behavior in juvenile rats (121). Microglia in the developing amygdala of male rats have been shown to have an increased phagocytic activity compared to female juveniles during the first postnatal week (121). The microglia formed ball-and-chain structures that consequently engulfed and phagocytose newborn astrocytes, a process that was testosterone-induced and dependent on endocannabinoid signaling (121). Moreover, phagocytosis of

the newborn astrocytes by ball-and-chain structures was complement-dependent, since blocking complement receptor 3 (CR3) signaling increased astrocytic survival and prevented social masculinization (121).

3.3.2.3 Hyper-ramified microglia

Ramified morphology of microglia (Figure 1A) has been considered for many decades as an indication of quiescence or a 'resting' state. However, recent studies in rodents have described a process of microglial hyper-ramification (Figure 1D) in response to acute and chronic stress. A study in rats described a non-injury-related hyper-ramification of microglia in the medial prefrontal cortex in response to chronic stress (122, 123). The authors reported that after chronic restraint stress, microglia presented higher ramification through an increase in the branching points of its processes. This hyper-ramification was accompanied by an upregulation of β1integrin, a protein that has been implicated in promoting microglial ramification. This effect was rescued after the administration of minocycline, a microglial inhibitor. Another study, using the chronic despair model (CDM) to induce stress-related depressive-like behavior in mice, observed a change in microglial morphology characterized by longer processes and increased branching in wild-type mice (124). Interestingly, CX3CR1-deficient mice showed enhanced resistance to the effects of CDM in regard to microglial morphology, and the administration of the anti-depressant venlafaxine reversed the hyper-ramification of microglia in the wild-type mice. These results suggest that the fractalkine-CX3CR1 axis might be involved in the neuron-microglia signaling during stress-induced depression. Furthermore, the authors reported that the administration of venlafaxine increased the expression of synaptic plasticity marker Arc/Arg 3.1 in wild-type mice but not in CX3CR1-deficient mice, suggesting that potential synaptic modifications are happening in response to stress. A recent study using a mouse model of post-traumatic stress disorder (PTSD) reported long-lasting fear response, decreased locomotor activity, and impaired behavior accompanied by an increased number of hyper-ramified microglia and loss of dendritic spines in a region-specific manner (125). Overall, these results suggest that microglial hyper-ramification can be a stress/depression-specific response that might also be implicated in synaptic modifications.

3.3.2.4 Honeycomb and jellyfish microglia

Other microglia morphologies have been reported in response to neuronal injury and glia limitans rupture after traumatic brain injury (TBI) in mice (126). The glia limitans is a layer of astrocytes endfeet processes that separate the CNS parenchyma and the perivascular space, just beneath the BBB (133). After thinning of the murine skull, a model of compression-mediated TBI, the authors reported leakage from the BBB through to the CNS parenchyma, mainly due to astrocytic death in the glia limitans (126) In response to this phenomenon, microglia retracted most of their processes except for two or three, forming a contiguous and highly connected network resembling a honeycomb structure (Figure 1F). Interestingly, this seemed to be a coordinated response of several microglial cells that surrounded surviving astrocytes to prevent further disruption of the glia limitans. The same study also reported a morphological transformation of honeycomb microglia into a shape that resembled a jellyfish, by the extension of a single, non-branching process (126) (Figure 1G). This transition from honeycomb to jellyfish-shaped microglia was observed in response to astrocytic death, likely suggesting the formation of a phagocytic cup. These structures were directly related to ATP-mediated microglial activation through the P2RY12 pathway. When the astrocytic release of ATP was inhibited with carbenoxolone, honeycomb and jellyfish structures were inhibited, and microglia remained ramified. These findings may suggest that honeycomb and jellyfish microglia are contributing to maintenance of the BBB integrity after TBI. A role of microglia in BBB integrity after brain injury was also demonstrated in mice, where photoablation of microglia and the inhibition of P2RY12 both resulted in the impairment of BBB closure (134). Inhibition of microglia through P2RY6 antagonism likewise resulted in increased parenchymal cell death 12 hours after compression injury (126).

3.3.2.5 Rod microglia

Until recent years, ramified and amoeboid morphologies have been the predominant morphological descriptors of microglia. However, already in 1899 Franz Nissl described cells with rod-like shape ("Stäbchenzellen") in the post-mortem brain of patients with general paresis of the insane. These cells are now recognized to be a differentiated morphology of 'activated' microglia, commonly referred to as rod microglia (127, 128, 135) (Figure 1H). Later studies from Ramón y Cajal, Río-Hortega, Achúcarro and Alzheimer helped to establish rod microglia as a neuropathological marker of general paresis, cerebral atrophy and multiple sclerosis (128, 135). Further post-mortem studies during the first half of the 20th century showed rod microglia in the cortex of patients with malaria, Alzheimer's disease, multiple sclerosis, epilepsy, and encephalitis (135). More recent studies defined rod microglia as cells with elongated and narrowed soma, with polarized thin processes mainly in the apical and basal ends of the cell due to the retraction of planar processes (128, 129). The authors observed the morphological transition of microglia adopting a rod-like shape after diffuse brain injury in rats, starting at 1-day post-injury and being prominent at 7 days post-injury (128). Similar results were observed after optic nerve transection in rats, where the presence of rod microglia was prevalent in the retina starting

at 7 days after injury and becoming more evident between 14 and 21 days after the nerve transection, with more than 80% of the retinal microglia displaying a rod-like shape (130).

A study of human post-mortem brain samples revealed a correlation between age and the presence of rod microglia in the hippocampus and cerebral cortex (131), suggesting age as a possible factor. The authors also found an increased number of rod microglia in the parietal cortex of samples from patients with Alzheimer's disease. Interestingly, no correlation was found between the history of traumatic brain injury and the presence of rod microglia, suggesting that the appearance of rod microglia after an acute brain injury might resolve after an undetermined period of time (131). Rod microglia have been usually described to adopt specific orientations and being adjacent to dendrites and axons of injured neurons (22, 128–130), suggesting a possible neuroprotective role by creating a barrier to protect uninjured neurons (129). Furthermore, it has been described that rod microglia align to each other after brain injury and optic nerve transection, forming structures resembling trains of rod microglia (Figure 1H) (128–130), suggesting a coordinated response of multiple rod microglial cells.

4 Discussion

It is remarkable that Pío del Río-Hortega's conclusions about the dynamic nature of microglia are still valid today considering his observations were based on static examinations of the CNS (1). In 1919, Río-Hortega already mentioned the mesodermal origin of microglia and the correlation existing between morphology and microglial function, noting the ability of these cells to change their shape in response to different stimuli. However, being the only phagocyte resident in the CNS parenchyma, microglia were almost exclusively labeled to be responsible for the initiation and resolution of 'neuroinflammatory' reactions. Thus, it is not surprising that other roles of microglia, especially in the healthy CNS, were overlooked. Microglial dynamics have generated significant interest in the field of neurological research, arguably due to technological advances that, for example, allowed *in vivo* visualizations of 'resting' microglia under minimally invasive condition (91, 92). Under near-physiological conditions, these *in vivo* observations transformed the field by demonstrating the dynamic nature of unchallenged microglia that were considered dormant or quiescent for many years. These observations helped to understand that microglia are not only active in response to pathological changes in the CNS when they adopt an amoeboid shape and increase their phagocytic activity, but that ramified microglia also play very important roles in maintaining CNS homeostasis without losing their ramified morphology.

The use of post-mortem human tissue from brain donors has been especially useful in studying microglial function in neuropathology, including different psychiatric and neurodegenerative disorders (93, 136–139). Post-mortem studies provide a unique opportunity to correlate a characteristic microglial morphology to different disease stages, neuropathological hallmarks and other clinical parameters such as disease severity and duration (140). However, variations of clinical and autopsy-related parameters between cases can impact microglial morphology for histological studies, potentially complicating some interpretation of the results. Also, studying the implications of microglia in non-diseased brains and during the onset and early stages of diseases has been difficult, mainly due to the scarce availability of such tissue (140). Post-mortem studies in animal models have likewise contributed to our understanding of processes such as microgliosis, the proliferation of reactive microglia in response to acute CNS injury and aging (141), or microglia-mediated synaptic modifications (78, 87). For instance, studies using rats undergoing facial nerve axotomy were crucial to reveal the role of microglia in synaptic plasticity through a process called synaptic stripping (78, 113), where microglia have been shown to selectively displace synapses from injured neurons (142). This led to a renewed interest in microglial function, which has since become a highly debated topic in glial biology and neuroscience because of its important implications in CNS homeostasis, disease outcomes, and even potential therapeutic interventions (1).

In vivo studies of microglial responses have revealed unprecedented insights into the behavior, physiology, and spectrum of these cells. It has become apparent that such visualization models can be instrumental in deciphering the diverse spectrum of microglia phenotypes and physiology. In recent years, many studies have investigated the dynamic nature of microglial physiology in both the healthy and diseased brain, from the early stages of embryonic development throughout the adult brain and aging, using *in vivo* and *ex vivo* animal models (111, 143–145). These approaches have, for instance, clarified the ontogeny of microglia in mice (26) and zebrafish (29), revealed the role of microglia in eliminating apoptotic cells in zebrafish during development (146) and in the developed CNS (56), identified microglia-mediated synaptic modifications in mice (7, 147), or the microglial proliferation in animal models of disease and aging (34, 148). More recently, the appearance of new molecular techniques, and in particular single-cell RNA sequencing, has made it possible to define new roles and new subpopulations of microglia, such as a recovery-related subpopulation in a mouse model of nerve injury (149), and microglial subpopulations expressing different transcriptional profiles in mice depending on the region, age, or disease state (5).

Many of these findings have illustrated various forms of interactions between microglia and other cells, interactions that differ from the classic ramified/amoeboid paradigm. These studies not only describe unique microglial morphologies, but also demonstrate that the classical associations ('ramified'

equating 'resting' microglia; 'amoeboid' equating 'active' microglia) are not appropriate in many cases (Figure 1). One of the first *in vivo* studies of microglia in mice already described the formation of a unique type of bulbous structures at the tips of microglial processes (Figure 1E) in response to neuronal damage and injections of ATP (91). This was later confirmed by other studies in mice (114, 115) and zebrafish (116). These structures appear to be closely related to the chemotactic attraction of microglia by ATP and, as observed in zebrafish, might be also involved in the regulation of neuronal activity (116). Other studies have also highlighted that branched microglia can be phagocytically active. One of the most observed microglia morphologies under physiological conditions is the ball-and-chain structure (Figure 1C), first described *ex vivo* in adult mice hippocampal sections (11). These structures have also been observed in the developing hippocampus of mice (117), the developing cerebral cortex of macaques (55), in the developing cerebellum in the rat (119), after neonatal hypoxia-ischemia also in rats (118), and remodeling myelin sheaths in zebrafish (120). Several features of these ball-and-chain structures remain unknown, for example whether this phagocytic structure arises exclusively when microglia are immunologically 'inactive' (i.e., in the absence of pathogens in the CNS or BBB disruption), or whether the volume of the phagocytosed material is a contributing factor. Another example where branched microglia are phagocytically active is the process of trogocytosis, where tiny pouches form on the surface of microglial processes to eliminate presynaptic structures in mice (147). The retraction of microglial processes has often been considered as indicative of microglial activation. However, some studies have described that microglia can adopt a hyper-ramified morphology in response to stress (122, 123). Other studies of murine models of chronic stress and PTSD correlated microglial hyper-ramification with long-lasting behavioral and motor impairment accompanied by synaptic modifications (124, 125).

Some studies have not only observed unique microglial morphologies but have also described that microglia can form multicellular networks with a very well-defined structure. Such is the case for the trains of rod-shaped microglia (Figure 1H) formed in close relationship with neuronal structures after diffuse brain injury in rats (128), or the arrangement of microglial cells forming a structure reminiscent of a honeycomb (Figure 1F) after TBI in mice (126). This suggests that microglia can orchestrate a joint and coordinated response to CNS insults. It will be interesting to see future studies further unravel our understanding of inter-glia and inter-cellular communication in the CNS, such as the microglia-mediated activation of astrocytes and neuronal degeneration (150). Identifying the molecules and signaling pathways that trigger such inter-cellular responses or intra-cellular morphophysiological transformations will undoubtedly help us to understand the cues leading to microglial differentiation (morphologically and functionally).

Thus, it seems clear that the extraordinary heterogeneity and diversity of microglial cells requires the reconsideration of the outdated dogma of their different activation states being linked to one particular morphology. The classical paradigm of microglia depicts their morphology and activation as correlated and on a linear spectrum — with ramified microglia being non-activated on one end and the amoeboid morphology reflecting activated microglia on the other end (Figure 2A). This paradigm does not account for the great variety of microglia morphologies seen in the CNS and does not encompass the emerging evidence of much more diverse morphophysiological correlations. Certainly, microglial responses are extremely complex and diverse, making it difficult to establish exact correlations between microglial functions and specific morphologies. It is therefore important for researchers to assess microglial dynamics, taking into account the spatiotemporal changes of both microglial morphology and function.

Species-specific traits of microglia are also important when accounting for variation between microglia morphophysiologies. Despite sharing a highly conserved transcriptome, several studies have already highlighted gene expression differences between human and murine microglia (151–153). Another example is the expression of a surface lectin in microglia, Siglec-11, that seems to be unique to the human brain (154). Torres-Platas and colleagues performed a morphometric analysis of cortical microglia in both humans and mice (88). The most evident differences between mice and human microglia arise from the proportion of the different morphologies described and the shape of the cell bodies. Mouse cortex showed a higher proportion of ramified microglia (≥90%) with microglial somata being highly heterogeneous in their shape, while in human cortex ramified microglia represented 43% of all cells and the cell bodies were classified either as rounded or amoeboid (88). Specifically, ramified, amoeboid and rod morphologies have been described in multiple species, including humans and mice, and highlighted in this review (Table 1). Notably, these are considered classical microglial morphologies, all being described in the first half of the 20th century. It will be interesting to study human microglia by taking into account more recently described morphologies and avoiding the ramified-amoeboid linear spectrum, allowing a more accurate comparison between different species in the future.

For future studies, we suggest the usage of a continuous multi-spectrum (Figure 2B) for microglia morphologies and functions. Such a spectrum accounts for the variety of functional states for each microglia morphology and emphasizes their capacity to alter their 'activation' status, independently of their morphological pattern (e.g. it is not clear whether microglia can be 'locked in' in a morphological or functional state). Overall, it seems sensible for the field to develop context-specific ways to investigate microglial

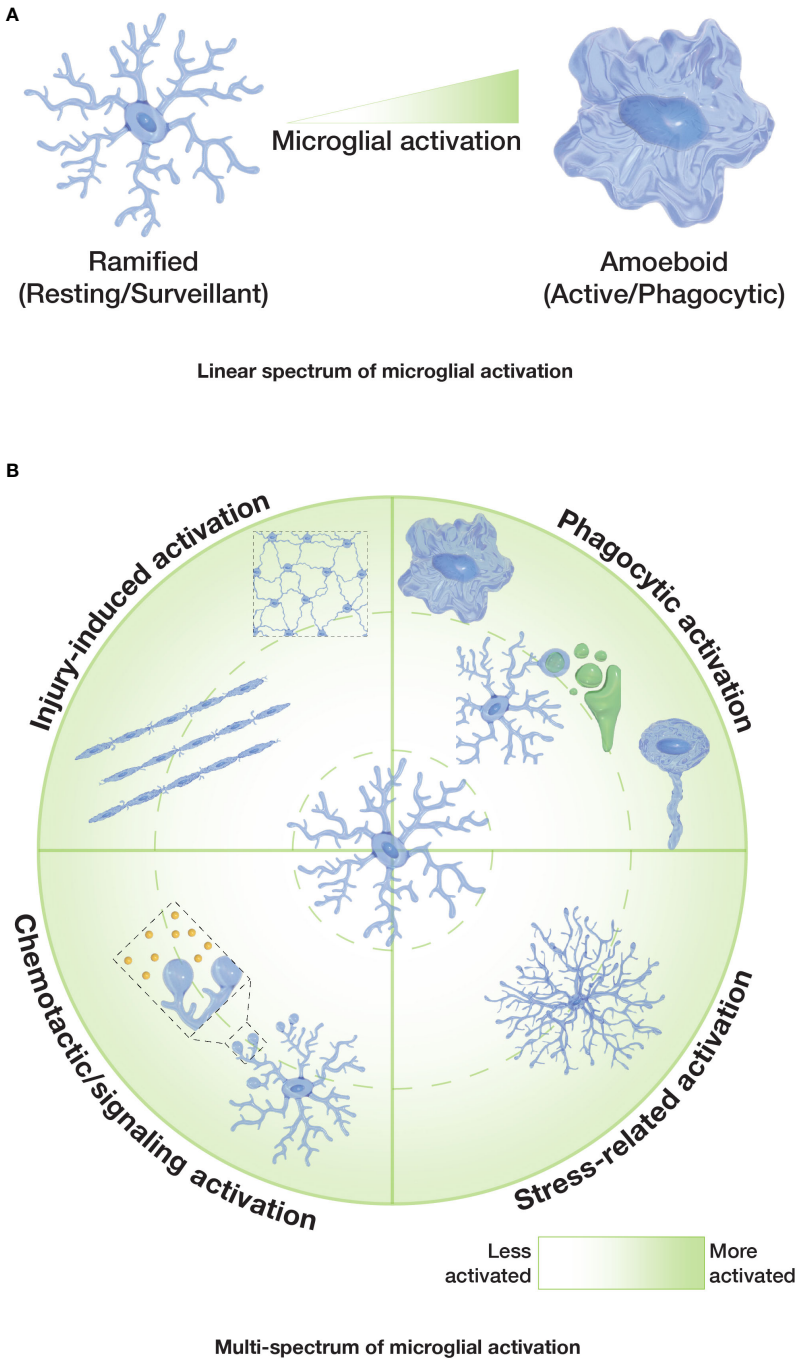


FIGURE 2
Spectrums of microglial activation. **(A)** Classical or 'linear spectrum' of microglial activation where ramified microglia are considered non-activated/resting, and amoeboid microglia are considered fully activated. Other microglial morphologies would reflect an intermediate state. **(B)** Proposed 'multi-spectrum' that reflects changes in microglial morphologies and function in a radial pattern, with context-dependent microglial activation.

activation, beyond simply quantifying the ramification or sphericity of these cells. More standardized ways of describing the shapes that microglia can adopt and clearly associate them to particular functions will facilitate the comparison of different microglial responses in different settings and scenarios. *In vivo* studies of microglial dynamics may help to better define the morphological transitions of microglia and their interactions with other cells in the future.

Author contributions

Conceptualization: AV-I and MM; data curation: AV-I and MM; writing—original draft preparation: AV-I, RR, CM, MM; writing—review and editing: all authors; visualization: AV-I and MM; supervision: AL, RC, ED, MG, and MM; funding acquisition: AL, CM, RC, MG, and MM. All authors have read and agreed to the final version of the manuscript.

Funding

This work was supported by Australian Research Council (ARC) grants (DP150104472 and DP210103469), a Snow Foundation Fellowship (towards MM), and donations made towards MND research at Macquarie University.

Acknowledgments

We wish to thank the Snow Foundation for their generous support towards establishing the transgenic zebrafish facility at Macquarie University and continued support of the researchers. We also wish to thank the zebrafish facility staff (past and present) for assistance in zebrafish care.

Conflict of interest

The authors declare that the research was conducted in the absence of any commercial or financial relationships that could be construed as a potential conflict of interest.

Publisher's note

All claims expressed in this article are solely those of the authors and do not necessarily represent those of their affiliated organizations, or those of the publisher, the editors and the reviewers. Any product that may be evaluated in this article, or claim that may be made by its manufacturer, is not guaranteed or endorsed by the publisher.

References

1. Sierra A, de Castro F, del Río-Hortega J, Rafael Iglesias-Rozas J, Garrosa M, Kettenmann H. The "Big-bang" for modern glial biology: Translation and comments on pío del río-hortega 1919 series of papers on microglia. *Glia* (2016) 64:1801–40. doi: 10.1002/glia.23046

2. Li Q, Barres BA. Microglia and macrophages in brain homeostasis and disease. *Nat Rev Immunol* (2018) 18:225–42. doi: 10.1038/nri.2017.125

3. Nimmerjahn A, Kirchhoff F, Helmchen F. Resting microglial cells are highly dynamic surveillants of brain parenchyma *in vivo*. *Science* (2005) 308:1314–8. doi: 10.1126/science.1110647

4. Tremblay ME, Stevens B, Sierra A, Wake H, Bessis A, Nimmerjahn A. The role of microglia in the healthy brain. *J Neurosci* (2011) 31:16064–9. doi: 10.1523/JNEUROSCI.4158-11.2011

5. Hammond TR, Dufort C, Dissing-Olesen L, Giera S, Young A, Wysoker A, et al. Single-cell RNA sequencing of microglia throughout the mouse lifespan and in the injured brain reveals complex cell-state changes. *Immunity* (2019) 50:253–71. doi: 10.1016/j.immuni.2018.11.004

6. Li Q, Cheng Z, Zhou L, Darmanis S, Neff NF, Okamoto J, et al. Developmental heterogeneity of microglia and brain myeloid cells revealed by deep single-cell RNA sequencing. *Neuron* (2019) 101:207–23. doi: 10.1016/j.neuron.2018.12.006

7. Wake H, Moorhouse AJ, Jinno S, Kohsaka S, Nabekura J. Resting microglia directly monitor the functional state of synapses *In vivo* and determine the fate of ischemic terminals. *J Neurosci* (2009) 29:3974–80. doi: 10.1523/JNEUROSCI.4363-08.2009

8. Akiyoshi R, Wake H, Kato D, Horiuchi H, Ono R, Ikegami A, et al. Microglia enhance synapse activity to promote local network synchronization. *eneuro* (2018) 5:0088–18. doi: 10.1523/ENEURO.0088-18.2018

9. Chen Z, Jalabi W, Hu W, Park HJ, Gale JT, Kidd GJ, et al. Microglial displacement of inhibitory synapses provides neuroprotection in the adult brain. *Nat Commun* (2014) 5: 1–12. doi: 10.1038/NCOMMS5486

10. Rodríguez-Iglesias N, Sierra A, Valero J. Rewiring of memory circuits: Connecting adult newborn neurons with the help of microglia. *Front Cell Dev Biol* (2019) 7:24. doi: 10.3389/fcell.2019.00024

11. Sierra A, Encinas JM, Deudero JJ, Chancey JH, Enikolopov G, Overstreet-Wadiche LS, et al. Microglia shape adult hippocampal neurogenesis through apoptosis-coupled phagocytosis. *Cell Stem Cell* (2010) 7:483–95. doi: 10.1016/j.stem.2010.08.014

12. Tay TL, Savage JC, Hui CW, Bisht K, Tremblay ME. Microglia across the lifespan: from origin to function in brain development, plasticity and cognition. *J Physiol* (2017) 595:1929–45. doi: 10.1113/JP272134

13. Tremblay ME, Lowery RL, Majewska AK. Microglial interactions with synapses are modulated by visual experience. *PloS Biol* (2010) 8:e1000527. doi: 10.1371/journal.pbio.1000527

14. Tremblay ME, Zettel ML, Ison JR, Allen PD, Majewska AK. Effects of aging and sensory loss on glial cells in mouse visual and auditory cortices. *Glia* (2012) 60:541–58. doi: 10.1002/glia.22287

15. Ziv Y, Avidan H, Pluchino S, Martino G, Schwartz M. Synergy between immune cells and adult neural stem/progenitor cells promotes functional recovery from spinal cord injury. *Proc Natl Acad Sci* (2006) 103:13174–9. doi: 10.1073/pnas.0603747103

16. Lawson L, Perry V, Dri P, Gordon S. Heterogeneity in the distribution and morphology of microglia in the normal adult mouse brain. *Neuroscience* (1990) 39:151–70. doi: 10.1016/0306-4522(90)90229-W

17. Smith JA, Das A, Ray SK, Banik NL. Role of pro-inflammatory cytokines released from microglia in neurodegenerative diseases. *Brain Res Bull* (2012) 87:10–20. doi: 10.1016/j.brainresbull.2011.10.004

18. Fu R, Shen Q, Xu P, Luo JJ, Tang Y. Phagocytosis of microglia in the central nervous system diseases. *Molecular neurobiology* (2014) 49:1422–34. doi: 10.1007/s12035-013-8620-6

19. Colonna M, Butovsky O. Microglia function in the central nervous system during health and neurodegeneration. *Annu Rev Immunol* (2017) 35:441–68. doi: 10.1146/annurev-immunol-051116-052358

20. Cserép C, Pósfai B, Lénárt N, Fekete R, László ZI, Lele Z, et al. Microglia monitor and protect neuronal function through specialized somatic purinergic junctions. *Science* (2020) 367:528–37. doi: 10.1126/science.aax6752

21. Pósfai B, Cserép C, Orsolits B, Dénes Á. New insights into microglia–neuron interactions: A neuron's perspective. *Neuroscience* (2019) 405:103–17. doi: 10.1016/j.neuroscience.2018.04.046

22. Graeber MB. Changing face of microglia. *Science* (2010) 330:783–8. doi: 10.1126/science.1190929

23. Kettenmann H, Hanisch UK, Noda M, Verkhratsky A. Physiology of microglia. *Physiol Rev* (2011) 91:461–553. doi: 10.1152/physrev.00011.2010

24. Kreutzberg GW. Microglia: a sensor for pathological events in the CNS. *Trends Neurosci* (1996) 19:312–8. doi: 10.1016/0166-2236(96)10049-7

25. Neumann H, Kotter MR, Franklin RJM. Debris clearance by microglia: an essential link between degeneration and regeneration. *Brain* (2008) :288–295. doi: 10.1093/brain/awn109

26. Ginhoux F, Greter M, Leboeuf M, Nandi S, See P, Gokhan S, et al. Fate mapping analysis reveals that adult microglia derive from primitive macrophages. *Science* (2010) 330:841–5. doi: 10.1126/science.1194637

27. Hoeffel G, Ginhoux F. Ontogeny of tissue-resident macrophages. *Front Immunol* (2015) 6:486(2015). doi: 10.3389/fimmu.2015.00486

28. Prinz M, Erny D, Hagemeyer N. Ontogeny and homeostasis of CNS myeloid cells. *Nat Immunol* (2017) 18:385–92. doi: 10.1038/ni.3703

29. Xu J, Wang T, Wu Y, Jin W, Wen Z. Microglia colonization of developing zebrafish midbrain is promoted by apoptotic neuron and lysophosphatidylcholine. *Dev Cell* (2016) 38:214–22. doi: 10.1016/j.devcel.2016.06.018

30. Ginhoux F, Lim S, Hoeffel G, Low D, Huber T. Origin and differentiation of microglia. *Front Cell Neurosci* (2013) 7:45(2013). doi: 10.3389/fncel.2013.00045

31. Hashimoto D, Chow A, Noizat C, Teo P, Beasley M, Leboeuf M, et al. Tissue-resident macrophages self-maintain locally throughout adult life with minimal contribution from circulating monocytes. *Immunity* (2013) 38:792–804. doi: 10.1016/j.immuni.2013.04.004

32. Li J, Chen K, Zhu L, Pollard JW. Conditional deletion of the colony stimulating factor-1 receptor (c-fms proto-oncogene) in mice. *Genesis (New York N Y. 2000)* (2006) 44:328–35. doi: 10.1002/DVG.20219

33. Réu P, Khosravi A, Bernard S, Mold JE, Salehpour M, Alkass K, et al. The lifespan and turnover of microglia in the human brain. *Cell Rep* (2017) 20:779–84. doi: 10.1016/j.celrep.2017.07.004

34. Füger P, Hefendehl JK, Veeraraghavalu K, Wendeln AC, Schlosser C, Obermüller U, et al. Microglia turnover with aging and in an alzheimer's model *via* long-term *in vivo* single-cell imaging. *Nat Neurosci* (2017) 20:1371–6. doi: 10.1038/nn.4631

35. Ajami B, Bennett JL, Krieger C, McNagny KM, Rossi FMV. Infiltrating monocytes trigger EAE progression, but do not contribute to the resident microglia pool. *Nat Neurosci* (2011) 14:1142–9. doi: 10.1038/nn.2887

36. Sevenich L. Brain-resident microglia and blood-borne macrophages orchestrate central nervous system inflammation in neurodegenerative disorders and brain cancer. *Front Immunol* (2018) 9:697(2018). doi: 10.3389/fimmu.2018.00697

37. Stranahan AM, Hao S, Dey A, Yu X, Baban B. Blood–brain barrier breakdown promotes macrophage infiltration and cognitive impairment in leptin receptor-deficient mice. *J Cereb Blood Flow Metab* (2016) 36:2108–21. doi: 10.1177/0271678X16642233

38. Varvel NH, Neher JJ, Bosch A, Wang W, Ransohoff RM, Miller RJ, et al. Infiltrating monocytes promote brain inflammation and exacerbate neuronal damage after status epilepticus. *Proc Natl Acad Sci* (2016) 113:E5665–74. doi: 10.1073/pnas.1604263113

39. Goldmann T, Wieghofer P, Jordão MJC, Prutek F, Hagemeyer N, Frenzel K, et al. Origin, fate and dynamics of macrophages at CNS interfaces. *Nat Immunol* (2016) 17:797. doi: 10.1038/NI.3423

40. Sato T, Konishi H, Tamada H, Nishiwaki K, Kiyama H. Morphology, localization, and postnatal development of dural macrophages. *Cell Tissue Res* (2021) 384:49–58. doi: 10.1007/S00441-020-03346-Y/FIGURES/7

41. Lee E, Eo JC, Lee C, Yu JW. Distinct features of brain-resident macrophages: Microglia and non-parenchymal brain macrophages. *Mol Cells* (2021) 44:281. doi: 10.14348/molcells.2021.0060

42. Aloisi F. Immune function of microglia. *Glia* (2001) 36:165–79. doi: 10.1002/glia.1106

43. Kigerl KA, de Rivero Vaccari JP, Dietrich WD, Popovich PG, Keane RW. Pattern recognition receptors and central nervous system repair. *Exp Neurol* (2014) 258:5–16. doi: 10.1016/j.expneurol.2014.01.001

44. Glezer I, Simard A, Rivest S. Neuroprotective role of the innate immune system by microglia. *Neuroscience* (2007) 147:867–83. doi: 10.1016/j.neuroscience.2007.02.055

45. Ransohoff RM, Brown MA. Innate immunity in the central nervous system. *J Clin Invest* (2012) 122:1164–71. doi: 10.1172/JCI58644

46. Stence N, Waite M, Dailey ME. Dynamics of microglial activation: A confocal time-lapse analysis in hippocampal slices. *Glia* (2001) 33:256–66. doi: 10.1002/1098-1136

47. Bachiller S, Jiménez-Ferrer I, Paulus A, Yang Y, Swanberg M, Deierborg T, et al. Microglia in neurological diseases: A road map to brain-disease dependent-inflammatory response. *Front Cell Neurosci* (2018) 12:488(2018). doi: 10.3389/fncel.2018.00488

48. Cartier N, Lewis CA, Zhang R, Rossi FMV. The role of microglia in human disease: therapeutic tool or target? *Acta Neuropathol* (2014) 128:363–80. doi: 10.1007/s00401-014-1330-y

49. Perry VH, Nicoll JAR, Holmes C. Microglia in neurodegenerative disease. *Nat Rev Neurol* (2010) 6:193–201. doi: 10.1038/nrneurol.2010.17

50. Radford RA, Morsch M, Rayner SL, Cole NJ, Pountney DL, Chung RS. The established and emerging roles of astrocytes and microglia in amyotrophic lateral sclerosis and frontotemporal dementia. *Front Cell Neurosci* (2015) 9:414. doi: 10.3389/fncel.2015.00414

51. Radford RAW, Vidal-Itriago A, Scherer NM, Lee A, Graeber M, Chung RS, et al. *Evidence for a growing involvement of glia in amyotrophic lateral sclerosis*. Spectrums Amyotrophic Lateral Sclerosis (Wiley) (2021), 123–42. doi: 10.1002/9781119745532.ch7

52. Wolf SA, Boddeke H, Kettenmann H. Microglia in physiology and disease. *Annu Rev Physiol* (2017) 79:619–43. doi: 10.1146/annurev-physiol-022516-034406

53. Schwarz JM, Sholar PW, Bilbo SD. Sex differences in microglial colonization of the developing rat brain. *J Neurochem* (2012) 120(6): 948–963. doi: 10.1111/j.1471-4159.2011.07630.x

54. Zusso M, Methot L, Lo R, Greenhalgh AD, David S, Stifani S. Regulation of postnatal forebrain amoeboid microglial cell proliferation and development by the transcription factor Runx1. *J Neurosci* (2012) 32:11285–98. doi: 10.1523/JNEUROSCI.6182-11.2012

55. Cunningham CL, Martinez-Cerdeno V, Noctor SC. Microglia regulate the number of neural precursor cells in the developing cerebral cortex. *J Neurosci* (2013) 33:4216–33. doi: 10.1523/JNEUROSCI.3441-12.2013

56. Morsch M, Radford R, Lee A, Don EK, Badrock AP, Hall TE, et al. *In vivo* characterization of microglial engulfment of dying neurons in the zebrafish spinal cord. *Front Cell Neurosci* (2015) 9:321. doi: 10.3389/fncel.2015.00321

57. Svahn AJ, Graeber MB, Ellett F, Lieschke GJ, Rinkwitz S, Bennett MR, et al. Development of ramified microglia from early macrophages in the zebrafish optic tectum. *Dev Neurobiol* (2013) 73:60–71. doi: 10.1002/dneu.22039

58. Rosin JM, Vora SR, Kurrasch DM. Depletion of embryonic microglia using the CSF1R inhibitor PLX5622 has adverse sex-specific effects on mice, including accelerated weight gain, hyperactivity and anxiolytic-like behaviour. *Brain behavior Immun* (2018) 73:682–97. doi: 10.1016/j.bbi.2018.07.023

59. Kettenmann H, Kirchhoff F, Verkhratsky A. Microglia: New roles for the synaptic stripper. *Neuron* (2013) 77:10–8. doi: 10.1016/j.neuron.2012.12.023

60. Hoshiko M, Arnoux I, Avignone E, Yamamoto N, Audinat E. Deficiency of the microglial receptor CX3CR1 impairs postnatal functional development of thalamocortical synapses in the barrel cortex. *J Neurosci* (2012) 32:15106–11. doi: 10.1523/JNEUROSCI.1167-12.2012

61. Paolicelli RC, Bolasco G, Pagani F, Maggi L, Scianni M, Panzanelli P, et al. Synaptic pruning by microglia is necessary for normal brain development. *Science* (2011) 333:1456–8. doi: 10.1126/science.1202529

62. Schafer D, Lehrman E, Kautzman A, Koyama R, Mardinly A, Yamasaki R, et al. Microglia sculpt postnatal neural circuits in an activity and complement-dependent manner. *Neuron* (2012) 74:691–705. doi: 10.1016/j.neuron.2012.03.026

63. Zhan Y, Paolicelli RC, Sforazzini F, Weinhard L, Bolasco G, Pagani F, et al. Deficient neuron-microglia signaling results in impaired functional brain connectivity and social behavior. *Nat Neurosci* (2014) 17:400–6. doi: 10.1038/nn.3641

64. Squarzoni P, Oller G, Hoeffel G, Pont-Lezica L, Rostaing P, Low D, et al. Microglia modulate wiring of the embryonic forebrain. *Cell Rep* (2014) 8:1271–9. doi: 10.1016/j.celrep.2014.07.042

65. Gao Y, Vidal-Itriago A, Kalsbeek MJ, Layritz C, Garcia-Caceres C, Tom RZ, et al. Lipoprotein lipase maintains microglial innate immunity in obesity. *Cell Rep* (2017) 20:3034–42. doi: 10.1016/j.celrep.2017.09.008

66. Gao Y, Vidal-Itriago A, Milanova I, Korpel NL, Kalsbeek MJ, Tom RZ, et al. Deficiency of leptin receptor in myeloid cells disrupts hypothalamic metabolic circuits and causes body weight increase. *Mol Metab* (2018) 7:155–60. doi: 10.1016/j.molmet.2017.11.003

67. Ramirez S, Gomez-Valades AG, Schneeberger M, Varela L, Haddad-Tovolli R, Altirriba J, et al. Mitochondrial dynamics mediated by mitofusin 1 is required for POMC neuron glucose-sensing and insulin release control. *Cell Metab* (2017) 25:1390–9. doi: 10.1016/j.cmet.2017.05.010

68. Rosin JM, Kurrasch DM. *In utero* electroporation induces cell death and alters embryonic microglia morphology and expression signatures in the developing hypothalamus. *J Neuroinflamm* (2018) 15:1–15. doi: 10.1186/S12974-018-1213-6/FIGURES/7

69. Rosin JM, Marsters CM, Malik F, Far R, Adnani L, Schuurmans C, et al. Embryonic microglia interact with hypothalamic radial glia during development and upregulate the TAM receptors MERTK and AXL following an insult. *Cell Rep* (2021) 34:16. doi: 10.1016/J.CELREP.2020.108587

70. Rosin JM, Sinha S, Biernaskie J, Kurrasch DM. A subpopulation of embryonic microglia respond to maternal stress and influence nearby neural progenitors. *Dev Cell* (2021) 56:1326–45. doi: 10.1016/j.devcel.2021.03.018

71. Rosin JM, Tretiakov N, Hanniman E, Hampton K, Kurrasch DM. Gestational bisphenol a exposure impacts embryonic hypothalamic microglia numbers, ramification, and phagocytic cups. *Front Neurosci* (2022) 16:100. doi: 10.3389/fnins.2022.830399

72. Dixit R, Lu F, Cantrup R, Gruenig N, Langevin LM, Kurrasch DM, et al. Efficient gene delivery into multiple CNS territories using in utero electroporation. journal of visualized experiments. *JoVE* (2011) (52). doi: 10.3791/2957

73. Shigemoto-Mogami Y, Hoshikawa K, Goldman JE, Sekino Y, Sato K. Microglia enhance neurogenesis and oligodendrogenesis in the early postnatal subventricular zone. *J Neurosci* (2014) 34:2231–43. doi: 10.1523/JNEUROSCI.1619-13.2014

74. Ueno M, Fujita Y, Tanaka T, Nakamura Y, Kikuta J, Ishii M, et al. Layer V cortical neurons require microglial support for survival during postnatal development. *Nat Neurosci* (2013) 16:543–51. doi: 10.1038/nn.3358

75. Aramideh JA, Vidal-Itriago A, Morsch M, Graeber MB. Cytokine signalling at the microglial penta-partite synapse. *Int J Mol Sci* (2021) 22:13186. doi: 10.3390/ijms222413186

76. Hong S, Beja-Glasser VF, Nfonoyim BM, Frouin A, Li S, Ramakrishnan S, et al. Complement and microglia mediate early synapse loss in Alzheimer mouse models. *Science* (2016) 352:712–6. doi: 10.1126/science.aad8373

77. Wang C, Yue H, Hu Z, Shen Y, Ma J, Li J, et al. Microglia mediate forgetting *via* complement-dependent synaptic elimination. *Science* (2020) 367:688–94. doi: 10.1126/science.aaz2288

78. Blinzinger K, Kreutzberg G. Displacement of synaptic terminals from regenerating motoneurons by microglial cells. *Z fur Zellforschung und Mikroskopische Anatomie* (1968) 85:145–57. doi: 10.1007/BF00325030

79. Chen DH. Qualitative and quantitative study of synaptic displacement in chromatolyzed spinal motoneurons of the cat. *J Comp Neurol* (1978) 177:635–63. doi: 10.1002/cne.901770407

80. Sumner B. A quantitative study of subsurface cisterns and their relationships in normal and axotomized hypoglossal neurones. *Exp Brain Res* (1975) 22: 175–183. doi: 10.1007/BF00237687

81. Milior G, Lecours C, Samson L, Bisht K, Poggini S, Pagani F, et al. Fractalkine receptor deficiency impairs microglial and neuronal responsiveness to chronic stress. *Brain Behavior Immun* (2016) 55:114–25. doi: 10.1016/j.bbi.2015.07.024

82. Paolicelli RC, Bisht K, Tremblay ME. Fractalkine regulation of microglial physiology and consequences on the brain and behavior. *Front Cell Neurosci* (2014) 8:129. doi: 10.3389/fncel.2014.00129

83. Rice RA, Spangenberg EE, Yamate-Morgan H, Lee RJ, Arora RPS, Hernandez MX, et al. Elimination of microglia improves functional outcomes following extensive neuronal loss in the hippocampus. *J Neurosci* (2015) 35:9977–89. doi: 10.1523/JNEUROSCI.0336-15.2015

84. Parkhurst C, Yang G, Ninan I, Savas J, Yates J, Lafaille J, et al. Microglia promote learning-dependent synapse formation through brain-derived neurotrophic factor. *Cell* (2013) 155:1596–609. doi: 10.1016/j.cell.2013.11.030

85. Giulian D, Baker T. Characterization of ameboid microglia isolated from developing mammalian brain. *J Neurosci* (1986) 6:2163–78. doi: 10.1523/JNEUROSCI.06-08-02163.1986

86. Jordan FL, Eric Thomas W. Brain macrophages: Questions of origin and interrelationship. *Brain Res Rev* (1988) 13:165–78. doi: 10.1016/0165-0173(88)90019-7

87. Streit WJ, Graeber MB, Kreutzberg GW. Functional plasticity of microglia: A review. *Glia* (1988) 1:301–7. doi: 10.1002/glia.440010502

88. Torres-Platas SG, Comeau S, Rachalski A, Bo GD, Cruceanu C, Turecki G, et al. Morphometric characterization of microglial phenotypes in human cerebral cortex. *J Neuroinflamm* (2014) 11:12. doi: 10.1186/1742-2094-11-12

89. Zhou K, Han J, Lund H, Boggavarapu NR, Lauschke VM, Goto S, et al. An overlooked subset of Cx3cr1 wt/wt microglia in the Cx3cr1 CreER-eyfp/wt mouse has a repopulation advantage over Cx3cr1 CreER-eyfp/wt microglia following microglial depletion. *J Neuroinflamm* (2022) 19:1–18. doi: 10.1186/S12974-022-02381-6/FIGURES/5

90. Garden GA, Möller T. Microglia biology in health and disease. *J Neuroimmune Pharmacol* (2006) 1:127–37. doi: 10.1007/s11481-006-9015-5

91. Davalos D, Grutzendler J, Yang G, Kim JV, Zuo Y, Jung S, et al. ATP mediates rapid microglial response to local brain injury *in vivo*. *Nat Neurosci* (2005) 8:752–8. doi: 10.1038/nn1472

92. Nimmerjahn A, Kirchhoff F, Helmchen F. Resting microglial cells are highly dynamic surveillants of brain parenchyma *in vivo*. *Science* (2005) 308:1314–8. doi: 10.1126/science.1110647

93. Gomez-Nicola D, Boche D. Post-mortem analysis of neuroinflammatory changes in human alzheimer's disease. *Alzheimer's Res Ther* (2015) 7:42. doi: 10.1186/s13195-015-0126-1

94. De Biase LM, Schuebel KE, Fusfeld ZH, Jair K, Hawes IA, Cimbro R, et al. Local cues establish and maintain region-specific phenotypes of basal ganglia microglia. *Neuron* (2017) 95:341–56. doi: 10.1016/j.neuron.2017.06.020

95. De Biase LM, Bonci A. Region-Specific Phenotypes of Microglia: The Role of Local Regulatory Cues. *The Neuroscientist* (2019) :314–333. doi: 10.1177/1073858418800996

96. Grabert K, Michoel T, Karavolos MH, Clohisey S, Baillie JK, Stevens MP, et al. Microglial brain region–dependent diversity and selective regional sensitivities to aging. *Nat Neurosci* (2016) 19:504–16. doi: 10.1038/nn.4222

97. Ayata P, Badimon A, Strasburger HJ, Duff MK, Montgomery SE, Loh YHE, et al. Epigenetic regulation of brain region-specific microglia clearance activity. *Nat Neurosci* (2018) 21:1049–60. doi: 10.1038/s41593-018-0192-3

98. Villa A, Vegeto E, Poletti A, Maggi A. Estrogens, neuroinflammation, and neurodegeneration. *Endocrine Rev* (2016) 37:372–402. doi: 10.1210/er.2016-1007

99. Lenz KM, McCarthy MM. A starring role for microglia in brain sex differences. *Neurosci* (2015) 21:306–21. doi: 10.1177/1073858414536468

100. McCarthy MM, Auger AP, Bale TL, De Vries GJ, Dunn GA, Forger NG, et al. The epigenetics of sex differences in the brain. *J Neurosci* (2009) 29:12815–23. doi: 10.1523/JNEUROSCI.3331-09.2009

101. McCarthy MM, Nugent BM, Lenz KM. Neuroimmunology and neuroepigenetics in the establishment of sex differences in the brain. *Nat Rev Neurosci* (2017) 18:471–84. doi: 10.1038/nrn.2017.61

102. Han J, Fan Y, Zhou K, Blomgren K, Harris RA. Uncovering sex differences of rodent microglia. *J Neuroinflamm* (2021) 18:1–11. doi: 10.1186/S12974-021-02124-Z/TABLES/2

103. Mouton PR, Long JM, Lei DL, Howard V, Jucker M, Calhoun ME, et al. Age and gender effects on microglia and astrocyte numbers in brains of mice. *Brain Res* (2002) 956:30–5. doi: 10.1016/S0006-8993(02)03475-3

104. Schwarz JM, McCarthy MM. Steroid-induced sexual differentiation of the developing brain: multiple pathways, one goal. *J Neurochem* (2008) 105:1561–72. doi: 10.1111/j.1471-4159.2008.05384.x

105. Lenz KM, Nugent BM, Haliyur R, McCarthy MM. Microglia are essential to masculinization of brain and behavior. *J Neurosci* (2013) 33:2761–72. doi: 10.1523/JNEUROSCI.1268-12.2013

106. Sorge RE, LaCroix-Fralish ML, Tuttle AH, Sotocinal SG, Austin JS, Ritchie J, et al. Spinal cord toll-like receptor 4 mediates inflammatory and neuropathic hypersensitivity in Male but not female mice. *J Neurosci* (2011) 31:15450–4. doi: 10.1523/JNEUROSCI.3859-11.2011

107. Sorge RE, Mapplebeck JCS, Rosen S, Beggs S, Taves S, Alexander JK, et al. Different immune cells mediate mechanical pain hypersensitivity in male and female mice. *Nat Neurosci* (2015) 18:1081–3. doi: 10.1038/nn.4053

108. Mapplebeck JC, Dalgarno R, Tu Y, Moriarty O, Beggs S, Kwok CH, et al. Microglial P2X4R-evoked pain hypersensitivity is sexually dimorphic in rats. *Pain* (2018) 159:1752–63. doi: 10.1097/j.pain.0000000000001265

109. Inyang KE, Szabo-Pardi T, Wentworth E, McDougal TA, Dussor G, Burton MD, et al. The antidiabetic drug metformin prevents and reverses neuropathic pain and spinal cord microglial activation in male but not female mice. *Pharmacol Res* (2019) 139:1–16. doi: 10.1016/j.phrs.2018.10.027

110. Doyle HH, Eidson LN, Sinkiewicz DM, Murphy AZ. Sex differences in microglia activity within the periaqueductal Gray of the rat: A potential mechanism driving the dimorphic effects of morphine. *J Neurosci* (2017) 37:3202–14. doi: 10.1523/JNEUROSCI.2906-16.2017

111. Vinet J, van Weering HR, Heinrich A, Kälin RE, Wegner A, Brouwer N, et al. Neuroprotective function for ramified microglia in hippocampal excitotoxicity. *J Neuroinflamm* (2012) 9:27. doi: 10.1186/1742-2094-9-27

112. Wake H, Moorhouse AJ, Miyamoto A, Nabekura J. Microglia: actively surveying and shaping neuronal circuit structure and function. *Trends Neurosci* (2013) 36:209–17. doi: 10.1016/j.tins.2012.11.007

113. Moran LB, Graeber MB. The facial nerve axotomy model. *Brain Res Rev* (2004) 44:154–78. doi: 10.1016/j.brainresrev.2003.11.004

114. Bernier LP, Bohlen CJ, York EM, Choi HB, Kamyabi A, Dissing-Olesen L, et al. Nanoscale surveillance of the brain by microglia *via* cAMP-regulated filopodia. *Cell Rep* (2019) 27:2895–908. doi: 10.1016/j.celrep.2019.05.010

115. Dissing-Olesen L, LeDue JM, Rungta RL, Hefendehl JK, Choi HB, MacVicar BA. Activation of neuronal NMDA receptors triggers transient ATP-mediated microglial process outgrowth. *J Neurosci* (2014) 34:10511–27. doi: 10.1523/JNEUROSCI.0405-14.2014

116. Li Y, Xf Du, Cs L, Zl W, Jl Du. Reciprocal regulation between resting microglial dynamics and neuronal activity *In vivo*. *Dev Cell* (2012) 23:1189–202. doi: 10.1016/j.devcel.2012.10.027

117. Frost JL, Schafer DP. Microglia: Architects of the developing nervous system. *Trends Cell Biol* (2016) 26:587–97. doi: 10.1016/j.tcb.2016.02.006

118. Fisch U, Brégère C, Geier F, Chicha L, Guzman R. Neonatal hypoxia-ischemia in rat elicits a region-specific neurotrophic response in SVZ microglia. *J Neuroinflamm* (2020) 17:26. doi: 10.1186/s12974-020-1706-y

119. Perez-Pouchoulen M, VanRyzin JW, McCarthy MM. Morphological and phagocytic profile of microglia in the developing rat cerebellum. *eneuro* (2015) 2:0036–15. doi: 10.1523/ENEURO.0036-15.2015

120. Hughes AN, Appel B. Microglia phagocytose myelin sheaths to modify developmental myelination. *Nat Neurosci* (2020) 23:1055–66. doi: 10.1038/s41593-020-0654-2

121. VanRyzin JW, Marquardt AE, Argue KJ, Vecchiarelli HA, Ashton SE, Arambula SE, et al. Microglial phagocytosis of newborn cells is induced by endocannabinoids and sculpts sex differences in juvenile rat social play. *Neuron* (2019) 102:435–49. doi: 10.1016/j.neuron.2019.02.006

122. Hinwood M, Morandini J, Day TA, Walker FR. Evidence that microglia mediate the neurobiological effects of chronic psychological stress on the medial prefrontal cortex. *Cereb Cortex* (2012) 22:1442–54. doi: 10.1093/cercor/bhr229

123. Hinwood M, Tynan RJ, Charnley JL, Beynon SB, Day TA, Walker FR. Chronic stress induced remodeling of the prefrontal cortex: Structural re-organization of microglia and the inhibitory effect of minocycline. *Cereb Cortex* (2013) 23:1784–97. doi: 10.1093/cercor/bhs151

124. Hellwig S, Brioschi S, Dieni S, Frings L, Masuch A, Blank T, et al. Altered microglia morphology and higher resilience to stress-induced depression-like behavior in CX3CR1-deficient mice. *Brain Behavior Immun* (2016) 55:126–37. doi: 10.1016/j.bbi.2015.11.008

125. Smith KL, Kassem MS, Clarke DJ, Kuligowski MP, Bedoya-Pérez MA, Todd SM, et al. Microglial cell hyper-ramification and neuronal dendritic spine loss in the hippocampus and medial prefrontal cortex in a mouse model of PTSD. *Brain Behavior Immun* (2019) 80:889–99. doi: 10.1016/j.bbi.2019.05.042

126. Roth TL, Nayak D, Atanasijevic T, Koretsky AP, Latour LL, McGavern DB. Transcranial amelioration of inflammation and cell death after brain injury. *Nature* (2014) 505:223–8. doi: 10.1038/NATURE12808

127. Holloway OG, Canty AJ, King AE, Ziebell JM. Rod microglia and their role in neurological diseases. *Semin Cell Dev Biol* (2019) 94:96–103. doi: 10.1016/j.semcdb.2019.02.005

128. Ziebell JM, Taylor SE, Cao T, Harrison JL, Lifshitz J. Rod microglia: Elongation, alignment, and coupling to form trains across the somatosensory cortex after experimental diffuse brain injury. *J Neuroinflamm* (2012) 9:1–11. doi: 10.1186/1742-2094-9-247/FIGURES/6

129. Taylor SE, Morganti-Kossmann C, Lifshitz J, Ziebell JM. Rod microglia: A morphological definition. *PloS One* (2014) 9:e97096. doi: 10.1371/journal.pone.0097096

130. Yuan TF, Liang YX, Peng B, Lin B, So KF. Local proliferation is the main source of rod microglia after optic nerve transection. *Sci Rep* (2015) 5:10788. doi: 10.1038/srep10788

131. Bachstetter AD, Ighodaro ET, Hassoun Y, Aldeiri D, Neltner JH, Patel E, et al. Rod-shaped microglia morphology is associated with aging in 2 human autopsy series. *Neurobiol Aging* (2017) 52:98–105. doi: 10.1016/j.neurobiolaging.2016.12.028

132. Haynes SE, Hollopeter G, Yang G, Kurpius D, Dailey ME, Gan WB, et al. The P2Y12 receptor regulates microglial activation by extracellular nucleotides. *Nat Neurosci* (2006) 9:1512–9. doi: 10.1038/nn1805

133. Quintana FJ. Astrocytes to the rescue! glia limitans astrocytic endfeet control CNS inflammation. *J Clin Invest* (2017) 127:2897–9. doi: 10.1172/JCI95769

134. Lou N, Takano T, Pei Y, Xavier AL, Goldman SA, Nedergaard M. Purinergic receptor P2RY12-dependent microglial closure of the injured blood–brain barrier. *Proc Natl Acad Sci* (2016) 113:1074–9. doi: 10.1073/pnas.1520398113

135. Giordano KR, Denman CR, Dubisch PS, Akhter M, Lifshitz J. An update on the rod microglia variant in experimental and clinical brain injury and disease. *Brain Commun* (2021) 3:12. doi: 10.1093/braincomms/fcaa227

136. Bayer TA, Buslei R, Havas L, Falkai P. Evidence for activation of microglia in patients with psychiatric illnesses. *Neurosci Lett* (1999) 271:126–8. doi: 10.1016/S0304-3940(99)00545-5

137. Hirsch EC, Vyas S, Hunot S. Neuroinflammation in parkinson's disease. *Parkinsonism Related Disord* (2012) 18:S210–2. doi: 10.1016/S1353-8020(11)70065-7

138. Hopperton KE, Mohammad D, Trépanier MO, Giuliano V, Bazinet RP. Markers of microglia in post-mortem brain samples from patients with alzheimer's disease: a systematic review. *Mol Psychiatry* (2018) 23:177–98. doi: 10.1038/mp.2017.246

139. Silvestroni A, Faull RL, Strand AD, Möller T. Distinct neuroinflammatory profile in post-mortem human huntington's disease. *NeuroReport* (2009) 20:1098–103. doi: 10.1097/WNR.0b013e32832e34ee

140. Luchetti S, Fransen NL, van Eden CG, Ramaglia V, Mason M, Huitinga I. Progressive multiple sclerosis patients show substantial lesion activity that correlates with clinical disease severity and sex: A retrospective autopsy cohort analysis. *Acta Neuropathol* (2018) 135:511–28. doi: 10.1007/s00401-018-1818-y

141. Streit WJ, Walter SA, Pennell NA. Reactive microgliosis. *Prog Neurobiol* (1999) 57:563–81. doi: 10.1016/S0301-0082(98)00069-0

142. Hamberger A, Hansson HA, Sjoüstrand J. SURFACE STRUCTURE OF ISOLATED NEURONS. *J Cell Biol* (1970) 47:319–31. doi: 10.1083/jcb.47.2.319

143. Eme-Scolan E, Dando SJ. Tools and approaches for studying microglia *In vivo*. *Front Immunol* (2020) 11:583647/BIBTEX. doi: 10.3389/FIMMU.2020.583647/BIBTEX

144. Hierro-Bujalance C, Bacskai BJ, Garcia-Alloza M. *In vivo* imaging of microglia with multiphoton microscopy. *Front Aging Neurosci* (2018) 10:218. doi: 10.3389/fnagi.2018.00218

145. Swinnen N, Smolders S, Avila A, Notelaers K, Paesen R, Ameloot M, et al. Complex invasion pattern of the cerebral cortex bymicroglial cells during development of the mouse embryo. *Glia* (2013) 61:150–63. doi: 10.1002/glia.22421

146. Casano A, Albert M, Peri F. Developmental apoptosis mediates entry and positioning of microglia in the zebrafish brain. *Cell Rep* (2016) 16:897–906. doi: 10.1016/j.celrep.2016.06.033

147. Weinhard L, di Bartolomei G, Bolasco G, Machado P, Schieber NL, Neniskyte U, et al. Microglia remodel synapses by presynaptic trogocytosis and spine head filopodia induction. *Nat Commun* (2018) 9:1228. doi: 10.1038/s41467-018-03566-5

148. Svahn AJ, Don EK, Badrock AP, Cole NJ, Graeber MB, Yerbury JJ, et al. Nucleo-cytoplasmic transport of TDP-43 studied in real time: Impaired microglia function leads to axonal spreading of TDP-43 in degenerating motor neurons. *Acta Neuropathol* (2018) 136:445–59. doi: 10.1007/s00401-018-1875-2

149. Tay TL, Dautzenberg J, Grün D, Prinz M. Unique microglia recovery population revealed by single-cell RNAseq following neurodegeneration. *Acta Neuropathol Commun* (2018) 6:87. doi: 10.1186/s40478-018-0584-3

150. Liddelow SA, Guttenplan KA, Clarke LE, Bennett FC, Bohlen CJ, Schirmer L, et al. Neurotoxic reactive astrocytes are induced by activated microglia. *Nature* (2017) 541:7638:481–7. doi: 10.1038/nature21029

151. Abels ER, Nieland L, Hickman S, Broekman ML, Khoury JE, Maas SL. Comparative analysis identifies similarities between the human and murine microglial sensomes. *Int J Mol Sci* (2021) 22:1–15. doi: 10.3390/IJMS22031495

152. Galatro TF, Holtman IR, Lerario AM, Vainchtein ID, Brouwer N, Sola PR, et al. Transcriptomic analysis of purified human cortical microglia reveals age-associated changes. *Nat Neurosci* (2017) 20:1162–71. doi: 10.1038/nn.4597

153. Gosselin D, Skola D, Coufal NG, Holtman IR, Schlachetzki JC, Sajti E, et al. An environment-dependent transcriptional network specifies human microglia identity. *Science* (2017) 356:1248–59. doi: 10.1126/SCIENCE.AAL3222

154. Hane M, Chen DY, Varki A. Human-specific microglial siglec-11 transcript variant has the potential to affect polysialic acid-mediated brain functions at a distance. *Glycobiology* (2021) 31:231–42. doi: 10.1093/glycob/cwaa082

frontiers | Frontiers in Immunology

TYPE Original Research
PUBLISHED 09 November 2022
DOI 10.3389/fimmu.2022.1024124

Check for updates

OPEN ACCESS

EDITED BY
Bo Li,
Department of Orthopedics, Sun Yat-sen University, China

REVIEWED BY
Tejabhiram Yadavalli,
University of Illinois at Chicago, United States
Zongshi Qin,
The University of Hong Kong, Hong Kong SAR, China

*CORRESPONDENCE
Yongzhen Bao
drbaoyz@sina.com

†These authors have contributed equally to this work and share first authorship

SPECIALTY SECTION
This article was submitted to Multiple Sclerosis and Neuroimmunology, a section of the journal Frontiers in Immunology

RECEIVED 21 August 2022
ACCEPTED 18 October 2022
PUBLISHED 09 November 2022

CITATION
Li X, Cao X, Pan Z, Sun X and Bao Y (2022) Analysis of macular structure in age-related cataract patients with different antibody levels of severe acute respiratory syndrome coronavirus-2 vaccine.
Front. Immunol. 13:1024124.
doi: 10.3389/fimmu.2022.1024124

COPYRIGHT
© 2022 Li, Cao, Pan, Sun and Bao. This is an open-access article distributed under the terms of the Creative Commons Attribution License (CC BY). The use, distribution or reproduction in other forums is permitted, provided the original author(s) and the copyright owner(s) are credited and that the original publication in this journal is cited, in accordance with accepted academic practice. No use, distribution or reproduction is permitted which does not comply with these terms.

Analysis of macular structure in age-related cataract patients with different antibody levels of severe acute respiratory syndrome coronavirus-2 vaccine

Xiaochun Li[1,2†], Xiaoguang Cao[1†], Zhongting Pan[2], Xinping Sun[3] and Yongzhen Bao[1*]

[1]Department of Ophthalmology, Peking University People's Hospital, Eye Diseases and Optometry Institute, Beijing Key Laboratory of Diagnosis and Therapy of Retinal and Choroid Diseases, College of Optometry, Peking University Health Science Center, Beijing, China, [2]Department of Ophthalmology, Peking University International Hospital, Beijing, China, [3]Clinical Laboratory, Peking University International Hospital, Beijing, China

Objective: To analyze the macular structure of age-related cataract (ARC) patients with different antibody levels after COVID-19 vaccine injection, in order to obtain the effect of COVID-19 vaccine on the macular structure, and speculate whether the COVID-19 vaccine has adverse effects on the macular structure.

Methods: This retrospective study is conducted to analysis on the status of COVID-19 vaccine and the thickness of different layers at different positions in the macular area of ARC patients. In the age, sex and eye axial length matched population, in the un-injection, no-antibody, IgM and IgG positive groups after vaccination, the choroid, ganglion cell complex, nerve fiber layer and retinal thickness at different positions of ETDRS zoning in the macular area were discussed.

Results: A total of 164 patients (164 eyes) were included in the analysis. There were 63 males and 101 females. The average age was 65.99 ± 8.43 years. There was no significant difference in age and sex among the groups ($p>0.05$). The average axial length of 164 eyes was 23.56 ± 1.46mm, and no significant difference between the groups ($p>0.05$). Non parametric test and ANOVA test for the thickness of choroid, retina, ganglion cell complex and retinal nerve fiber layer in each division of ETDRS showed no significant difference in the four groups of un-injection, no-antibody, IgM and IgG ($p>0.05$). There was no correlation between the antibody concentration and the thickness of macular structure ($p>0.05$).

Conclusion: There was no significant difference in the thickness of choroid, retina, ganglion cell complex and retinal fiber layer in different macular areas after COVID-19 vaccine injection. There was no linear correlation between the

10.3389/fimmu.2022.1024124

thickness of choroid, retina, ganglion cell complex and retinal fiber layer and the antibody concentration produced after COVID-19 vaccine injection. It suggests that the injection of COVID-19 vaccine might have no significant effect on the macular structure of eye.

KEYWORDS

COVID-19 vaccine, antibody, macula, ETDRS zoning, retina

Background

Novel coronavirus disease 2019 (COVID-19) is a global health disaster and a great challenge for mankind. The prevalence of COVID-19 has greatly impacted the global health system, disrupted the worldwide economy and caused incalculable losses (1). In the face of serious epidemic situation, in addition to avoiding contact with infectious sources as much as possible, the COVID-19 vaccination has brought new hope for the alleviation of epidemic. China is currently using five vaccine development technologies to develop and produce COVID-19 vaccines: whole virus inactivated vaccine, adenovirus vector vaccine, recombinant subunit vaccine, mRNA vaccine and attenuated influenza virus vector vaccine. Several studies have shown the effectiveness of different COVID-19 vaccines in inhibiting COVID-19. A meta-analysis by Zeng et al. evaluated the effectiveness of eleven COVID-19 vaccines against different variants of severe acute respiratory syndrome coronavirus 2 (SARS-CoV-2) (2). Another study reported that the efficacy of nine COVID-19 vaccines against symptomatic COVID-19 exceeded 50% (3).

COVID-19 is characterized by fever, fatigue and muscle soreness. As the disease progresses, dyspnea, respiratory failure, shock and multiple organ dysfunction may occur (4). Although ocular tissues are relatively less involved, some studies have reported ocular manifestations in patients with COVID-19 (5–9). Some studies found RNA of SARS-Cov-2 in the human ocular tissues (10–12). At present, conjunctivitis is the earliest ocular disorder caused by COVID-19 reported in the literature (13–15). COVID-19 conjunctivitis is similar to other viral conjunctivitis. At present, there is no case report of conjunctivitis affecting vision. However, the greater threat to vision is the vitreoretinopathy associated with COVID-19 infection, such as the manifestation of cotton wool spots and bleeding spots (16), flaming hemorrhage and ischemic lesions (cotton wool spots and retinal fan pallor) (17), retinal vein occlusion and retinal artery occlusion (18), resulting in macular lesions or change of thickness (16, 19–22).

COVID-19 vaccine is of great significance for the epidemic control, but its safety cannot be ignored. Some studies have reported the effects of COVID-19 vaccine on the eyes, mainly involving the posterior segment of the eyeball. The uvea, choroid and retinal vessels are most frequently affected. The median time of ocular pathological manifestations was 4 days after vaccine injected (23). The main manifestations are uveitis, white spot syndrome, central serous chorioretinopathy, retinal vein occlusion, acute macular neuroretinopathy and acute paracentric middle-level maculopathy. Other ocular manifestations include eyelid edema and rash, optic neuritis, oculomotor paralysis, etc (23). However, the causal relationship between the appearance of ocular pathology and the COVID-19 vaccine has not been confirmed by large sample and multi center research data. This study intends to analyze the macular structure of age-related cataract (ARC) patients with different antibody levels after COVID-19 vaccine injection, so as to obtain the effect of COVID-19 vaccine on the macular structure, and speculate whether the COVID-19 vaccine has adverse effects on the macular structure.

Methods

Recruitment of patients, and inclusion and exclusion criteria

This retrospective study is conducted in the Peking University International Hospital (PUIH), Beijing, China. The study is approved by the local ethical review board in accordance with the Declaration of Helsinki, and all patients provided the informed consent. In this study, ARC patients who were admitted to PUIH for ARC surgery, who were examined by optical coherence tomography (OCT) in the macula area and detected by COVID-19 antibody before surgery, were included. The vaccine is inactivated vaccine, which is inoculated according to personal wishes before they came to PUIH. According to whether the COVID-19 vaccine was injected or not and the antibody production after the COVID-19 vaccine injection, the differences in the macular structure of different groups were analyzed to obtain the effect of COVID-19 vaccine on the macular structure. Inclusion criteria: patients who were

hospitalized in PUIH, planned to undergo ARC surgery, and who underwent macular OCT and novel coronavirus antibody detection before surgery. Exclusion criteria: Patients with severe lens opacity and unable to clearly display macular structure by OCT were excluded. Patients with severe lens opacity and unable to accurately measure the ocular axial length were excluded. Patients with anterior and posterior segment diseases such as uveitis, exudative senile macular degeneration, anterior macular membrane and glaucoma were excluded. To avoid the influence of abnormal macular structure, patients with pathological myopia were excluded. In order to reduce the possible influence of systemic diseases on the macular structure, patients with diabetes were excluded. Exclude patients with hepatitis B, hepatitis C and other vaccines in the past half year. Patients who could not obtain COVID-19 vaccination information were excluded.

Clinical observations

Clinical history and routine clinical examination were performed by slit-lamp microscopy, indirect ophthalmoscopy, uncorrected (UCVA) and best-corrected visual acuity (BCVA) logMAR were tested, besides intraocular pressure (IOP). IOP was measured by noncontact tonometer (Canon TX-10/TX-F, Tokyo, Japan), slit lamp examination (Topcon SL-1E, Tokyo, Japan), and fundus examination (90 Dioptre, Volk Optical, Mentor, OH) with undilated pupil. All tests were performed in the outpatient of eye clinic.

OCT measurement

Macular thickness is measured with DRI OCT Trion (Topcon Corp., Tokyo, Japan), and the radiation scanning mode is adopted for the macular area. Before the examination, the patient was dripped with tropicamide eye drops to dilate the pupils. OCT can display the thickness of choroid (CHO), retina, ganglion cell complex (inner plexiform layer + ganglion cell layer, GCL+, GCLp), retinal nerve fiber layer (RNFL) in layers. The image of the structural thickness of each layer in the macular region is represented by ETDRS partitions, which include the central region (1mm in diameter, marked with C), the inner ring region (3mm in diameter, marked with I), and the outer ring region (6mm in diameter, marked with O). The inner and outer circles are respectively divided into superior, inferior, nasal and temporal regions, which are marked as S, I, N and T. For example, ChoC as the thickness for the central region of choroid, ChoIT, ChoIS, ChoIN and ChoII as the thickness for the inner temporal, superior, nasal and inferior ring region of choroid, ChoOT, ChoOS, ChoON and ChoOI as the thickness for the outer temporal, superior, nasal and inferior ring region of choroid, and ChoT as the thickness for the total choroid.

Detection of novel coronavirus antibody

The detection of SARS-Cov-2 antibody in this study uses the novel coronavirus (2019-nCoV) IgM antibody detection kit and novel coronavirus (2019-nCoV) IgG antibody detection kit provided by Maccura Biotechnology Co., Ltd. The determination method is micro magnetic particle chemiluminescence immunoassay. The blood sample is mixed with the micro magnetic particle coated with the mouse anti human IgM/IgG monoclonal antibody. The antibody in the sample forms an immune complex with the mouse anti human antibody. After washing, the acridine ester labeled novel coronavirus antigen is added. After washing again, the substrate solution was added to generate a chemiluminescence reaction, and the luminescence signal value was measured to obtain the antibody content.

Grouping

IgM antibody positive (IgG positive or negative) after injection of COVID-19 vaccine was defined as IgM group. IgG group was defined as IgG antibody positive (IgM negative) after injection of COVID-19 vaccine; The patients with negative antibody after injection of COVID-19 vaccine were defined as no-antibody group. Those who did not receive the COVID-19 vaccine were defined as the un-injection group.

Statistical analysis

SPSS statistical software (SPSS version 20.0, Armonk, New York, USA) was used for statistical analysis. In this study, except for gender and eye, the data are expressed as mean ± IQR or mean ± SD. Chi square analysis was used to compare the gender data. Kolmogorov–Smirnov test and Shapiro-Wilk test were used to test the normality of the thickness data for each layer in the macular area. Nonparametric test and ANOVA were used to compare the differences between groups. $P < 0.05$ means that the difference is statistically significant.

Results

General information

A total of 190 patients and 338 eyes were included in this study, who had the cataract operation in May 1st 2021 to May 31st 2022. Among them, 81 were male and 109 were female. The average age was 65.45 ± 9.39 years. To avoid research errors, only the data of right eye for all patients were taken for statistical analysis.

A total of 164 patients with 164 eyes were included as the right eye. There were 63 males and 101 females. The average age was 65.99 ± 8.43 years. Among them, 39 were in the un-injection group, 14 were male and 25 were female, with an average age of 66.26 ± 7.74 years. There were 35 in the no-antibody group, 17 males and 18 females, with an average age of 66.89 ± 6.54 years. IgM group has 12 patients, 3 males and 9 females, with an average age of 67.25 ± 9.51 years; The IgG group consisted of 78 persons, 29 males and 49 females, with an average age of 65.27 ± 9.38 years. There was no significant difference in age and gender among the groups (p=0.739 and p=0.459). See Table 1 for age and gender distribution information of patients in each group.

Axial length (AL)

Previous studies have shown that AL may affect the structure of the macular area (24). Therefore, we made statistical analysis and comparison on AL of each group. The average AL of 164 eyes was 23.56 ± 1.46mm. Among them, AL of the un-injection group was 23.41 ± 1.14mm, of the no-antibody group was 23.65 ± 1.30mm, of the IgM group was 23.52 ± 2.42mm, and of the IgG group was 23.60 ± 1.60mm. There was no significant difference in AL between the groups (p=0.894).

Analysis of macular structure

We tested the normal distribution of the macular structure data obtained by OCT. As some data are skew distribution, the nonparametric test is used for data statistical analysis. However, in order to avoid the false negative errors in statistics, one-way ANOVA was used for verification.

The choroidal thickness of the un-injection, no-antibody, IgM and IgG group in each division of the ETDRS table is shown in Table 2. The nonparametric test and ANOVA test of the thickness of each partition between these four groups showed no statistical significance (P > 0.05).

See Table 3 for the retinal thickness of the un-injection, no-antibody, IgM and IgG group in each division of the ETDRS table. Nonparametric test and ANOVA test showed no significant difference between these four groups. (P > 0.05). Table 4 shows the thickness of ganglion cell complex in each division of ETDRS in the un-injection, no-antibody, IgM and IgG groups. Nonparametric test and ANOVA test showed no significant difference between these four groups. (P > 0.05). Table 5 shows the thickness of retinal nerve fiber layer of un-injection, no-antibody, IgM and IgG groups in each division of ETDRS table. Nonparametric test and ANOVA test showed no significant difference between these four groups. (P > 0.05).

TABLE 1 General information for the included age-related cataract patients.

Groups	Un-injection	No-antibody	IgM	IgG	p
Included number	39	35	12	78	
Age (years)	66.26 ± 7.74	66.89 ± 6.54	67.25 ± 9.51	65.27 ± 9.38	0.739
Male (persons)	14	17	3	29	0.459
Female (persons)	25	18	9	49	

p values for ages (one-way ANOVA) and gender (Chi square analysis).

TABLE 2 Analysis of choroidal thickness in the age-related cataract patients with different COVID-19 antibody statues (median ± IQR, μm).

Group	Un-injection	No-antibody	IgM	IgG	P^a	P^b
ChoC	161.10 ± 108.12	189.07 ± 126.26	144.84 ± 79.85	182.14 ± 83.10	0.799	0.683
ChoIT	146.53 ± 117.91	173.50 ± 103.96	144.27 ± 107.03	172.16 ± 81.40	0.592	0.675
ChoIS	204.63 ± 124.36	199.72 ± 129.28	144.23 ± 112.89	175.76 ± 91.06	0.478	0.512
ChoIN	141.81 ± 131.05	182.12 ± 125.56	165.38 ± 114.64	165.47 ± 100.02	0.480	0.655
ChoII	168.44 ± 143.09	163.11 ± 130.50	135.93 ± 112.67	170.59 ± 117.31	0.544	0.540
ChoOT	158.73 ± 110.44	169.41 ± 113.04	117.95 ± 101.08	160.65 ± 76.42	0.388	0.318
ChoOS	184.38 ± 107.99	168.06 ± 109.08	145.73 ± 92.99	162.34 ± 82.69	0.523	0.788
ChoON	113.42 ± 96.13	126.43 ± 115.19	123.42 ± 109.54	124.03 ± 101.37	0.607	0.810
ChoOI	147.11 ± 101.76	141.14 ± 81.68	138.09 ± 89.75	160.66 ± 115.27	0.590	0.635
ChoT	158.03 ± 107.06	168.69 ± 109.76	136.72 ± 82.42	156.15 ± 96.16	0.754	0.723

ChoC as the thickness for the central region of choroid, ChoIT, ChoIS, ChoIN and ChoII as the thickness for the inner temporal, superior, nasal and inferior ring region of choroid, ChoOT, ChoOS, ChoON and ChoOI as the thickness for the outer temporal, superior, nasal and inferior ring region of choroid, and ChoT as the thickness for the total choroid. Unit of thickness: μm. P^a: p > 0.05 as nonparametric test. P^b: p > 0.05 as one-way ANOVA test.

TABLE 3 Analysis of retinal thickness in the age-related cataract patients with different COVID-19 antibody statues (median ± IQR, μm).

Group	Un-injection	No-antibody	IgM	IgG	P^a	P^b
RetinaC	229.16 ± 28.23	218.32 ± 35.12	219.45 ± 36.53	223.56 ± 36.16	0.879	0.665
RetinaIT	285.66 ± 17.66	287.17 ± 27.43	289.19 ± 31.51	284.07 ± 28.31	0.815	0.815
RetinaIS	300.16 ± 16.51	299.21 ± 20.81	299.74 ± 30.50	299.71 ± 24.44	0.551	0.365
RetinaIN	303.16 ± 16.75	296.52 ± 25.17	298.72 ± 41.50	301.41 ± 27.13	0.635	0.191
RetinaII	296.73 ± 24.02	294.77 ± 24.28	293.54 ± 32.50	296.54 ± 27.67	0.637	0.726
RetinaOT	251.04 ± 14.86	248.96 ± 25.12	254.74 ± 25.01	247.45 ± 27.09	0.303	0.886
RetinaOS	267.76 ± 19.43	263.02 ± 24.52	257.56 ± 19.81	266.28 ± 17.90	0.470	0.522
RetinaON	283.28 ± 22.65	273.61 ± 33.27	274.37 ± 21.10	278.17 ± 23.51	0.341	0.658
RetinaOI	256.45 ± 20.23	248.92 ± 23.70	255.62 ± 18.43	253.70 ± 24.25	0.636	0.534
RetinaT	270.24 ± 16.46	264.02 ± 24.17	268.60 ± 20.61	268.23 ± 22.43	0.658	0.447

RetinaC as the thickness for the central region of retina, RetinaIT, RetinaIS, RetinaIN and RetinaII as the thickness for the inner temporal, superior, nasal and inferior ring region of retina, RetinaOT, RetinaOS, RetinaON and RetinaOI as the thickness for the outer temporal, superior, nasal and inferior ring region of retina, and RetinaT as the thickness for the total retina. Unit of thickness: μm. P^a: $p > 0.05$ as nonparametric test. P^b: $p > 0.05$ as one-way ANOVA test.

The correlation analysis between the antibody concentration after COVID-19 vaccine injection and the thickness of each layer in the macular region was performed on 90 patients (90 eyes) in the antibody group (IgM group + IgG group), 12 patients (12 eyes) in IgM group, and 78 patients (78 eyes) in the IgG group. The results showed that there was no correlation between the antibody concentration of IgM group, IgG group or antibody group and the thickness of each layer for the macular structure ($P > 0.05$).

Discussion

In 2019, novel coronavirus pneumonia (COVID-19) began to rage. With the variation of sars-cov-2 virus strain, the severity of the disease and the immune escape ability of the virus are also constantly changing. In the face of the serious epidemic situation, in addition to avoiding contact with infectious sources as much as possible, COVID-19 vaccination has brought new hope for the alleviation of the epidemic situation (2, 25). At present, China is using five vaccine development technologies to develop and produce COVID-19 vaccine: whole virus inactivated vaccine, adenovirus vector vaccine, recombinant subunit vaccine, mRNA vaccine and attenuated influenza virus vector vaccine.

Inactivated vaccines are most widely used in China, accounting for more than 85%. Among them, two vaccine manufacturers, BBIBP-CorV and CoronaVac, are the most widely used vaccines (26). A retrospective cohort study showed that the resistance rate to infection was 51%, the resistance rate to COVID-19 pneumonia was 61%, and the resistance rate to severe COVID-19 was 82% (26). Completing two doses of inactivated vaccine can reduce the risk of COVID-19 from mild to moderate to severe by 74%. The efficacy of BBIBP-CorV and CoronaVac vaccines was similar. 164 right eye patients were included in our study, of which 39 had no history

TABLE 4 Analysis of ganglion cell complex thickness in the age-related cataract patients with different COVID-19 antibody statues (median ± IQR, μm).

Group	Un-injection	No-antibody	IgM	IgG	P^a	P^b
GCLC	38.37 ± 10.47	38.00 ± 14.95	36.28 ± 14.76	38.73 ± 15.52	0.959	0.836
GCLIT	74.76 ± 14.73	78.18 ± 25.43	74.49 ± 28.57	77.72 ± 28.94	0.921	0.747
GCLIS	83.93 ± 12.98	85.79 ± 17.20	86.02 ± 13.60	86.25 ± 17.50	0.672	0.926
GCLIN	84.54 ± 15.41	85.71 ± 17.17	81.22 ± 36.07	84.67 ± 20.44	0.474	0.277
GCLII	82.54 ± 18.48	86.67 ± 17.68	79.52 ± 31.37	85.55 ± 18.52	0.887	0.797
GCLOT	67.47 ± 17.70	62.01 ± 18.30	62.60 ± 11.49	65.65 ± 23.06	0.487	0.900
GCLOS	61.86 ± 8.02	64.60 ± 9.64	63.64 ± 10.95	61.48 ± 13.04	0.651	0.962
GCLON	66.04 ± 12.79	64.93 ± 12.84	68.74 ± 20.89	62.93 ± 14.79	0.165	0.436
GCLOI	59.09 ± 11.00	57.55 ± 12.63	59.59 ± 13.75	58.69 ± 12.65	0.623	0.927
GCLT	67.38 ± 10.45	65.86 ± 16.07	66.45 ± 14.82	66.78 ± 15.89	0.600	0.847

GCL ganglion cell complex. GCLC as the thickness for the central region of GCL, GCLIT, GCLIS, GCLIN and GCLII as the thickness for the inner temporal, superior, nasal and inferior ring region of GCL, GCLOT, GCLOS, GCLON and GCLOI as the thickness for the outer temporal, superior, nasal and inferior ring region of GCL, and GCLT as the thickness for the total GCL. Unit of thickness: μm. P^a: $p > 0.05$ as nonparametric test. P^b: $p > 0.05$ as one-way ANOVA test.

TABLE 5 Analysis of retinal nerve fiber layer thickness in age-related cataract patients with different COVID-19 antibody statues (median ± IQR, μm).

Group	Un-injection	No-antibody	IgM	IgG	P^a	P^b
RNFLC	6.17 ± 6.02	5.25 ± 5.45	5.22 ± 5.69	5.04 ± 4.58	0.167	0.499
RNFLIT	21.26 ± 9.62	21.32 ± 13.97	20.85 ± 18.89	20.18 ± 14.05	0.731	0.744
RNFLIS	25.98 ± 9.11	27.82 ± 8.71	26.02 ± 5.76	26.52 ± 7.56	0.750	0.493
RNFLIN	23.50 ± 7.97	22.81 ± 7.31	22.44 ± 8.89	23.82 ± 7.66	0.692	0.476
RNFLII	27.16 ± 8.41	28.08 ± 10.20	24.03 ± 9.97	26.34 ± 7.18	0.329	0.752
RNFLOT	23.61 ± 6.82	24.58 ± 13.41	26.96 ± 15.99	23.10 ± 12.10	0.659	0.666
RNFLOS	41.45 ± 14.13	39.76 ± 13.92	37.20 ± 11.64	40.66 ± 11.20	0.338	0.778
RNFLON	49.53 ± 15.83	50.85 ± 16.02	44.80 ± 13.88	49.24 ± 15.38	0.652	0.667
RNFLOI	42.01 ± 11.64	40.73 ± 14.07	39.74 ± 16.55	41.12 ± 10.29	0.452	0.796
RNFLT	36.01 ± 9.07	36.71 ± 9.77	35.87 ± 10.79	35.39 ± 8.77	0.426	0.442

RNFL retinal nerve fiber layer. RNFLC as the thickness for the central region of RNFL, RNFLIT, RNFLIS, RNFLIN and RNFLII as the thickness for the inner temporal, superior, nasal and inferior ring region of RNFL, RNFLOT, RNFLOS, RNFLON and RNFLOI as the thickness for the outer temporal, superior, nasal and inferior ring region of RNFL, and RNFLT as the thickness for the total RNFL. Unit of thickness: μm. P^a: $p > 0.05$ as nonparametric test. P^b: $p > 0.05$ as one-way ANOVA test.

of vaccine injection, and 125 had been injected with COVID-19 vaccine, with an injection rate of 76.2%. Although the samples are only from age-related cataract diseases in one hospital in Beijing, the proportion of vaccine injection in the samples also indicates that the current vaccine injection in China has reached a certain proportion, which provides a certain basis for epidemic control.

IgM is mainly produced in the primary immune response to infectious factors or antigens, as IgG mainly produced in the secondary. Studies have shown that SARS specific antibodies are produced in the second week of infection and last for a long time, while IgM is transiently expression (27). IgM is an antibody in the acute phase, which generally appears 3-5 days after the onset of the disease, remains positive for about one month, and then gradually decreases. IgG is a kind of recovery antibody and the main component of neutralizing antibody. The detection time of IgG is generally several days later than that of IgM, and it reaches the peak several weeks after the onset, and it can last for months or even years (28). Some studies analyzed the coronavirus antibody in the serum of patients with COVID-19. It was found that IgM antibody and IgG antibody appeared one after another in the first to second weeks after sars-cov-2 infection. After 3 weeks, IgM antibody of some individuals gradually disappeared and IgG antibody continued to exist (28). The kit of gold immunochromatography say (GICA) (Innovita Biotechnology Co., Ltd. Tangshan, China) was used in this study.

Among the 164 patients included in our study, 125 had a previous history of COVID-19 vaccine injection, including 12 (9.6%) patients with IgM antibody positive, 78 (62.4%) patients with IgG antibody positive, and 35 (28%) patients with negative antibody test. The total antibody positive rate was 72%, suggesting that COVID-19 vaccine can induce the immune response against sars-cov-2 virus antigen *in vivo*. However, it is worth noting that the antibodies measured by the clinical antibody kit are not neutralizing antibodies to sars-cov-2. Therefore, the negative antibody does not mean that the body has no immunity to sars-cov-2. Currently, inactivated vaccines are the main COVID-19 vaccines in China, accounting for more than 85%. The inactivated vaccine might need to be injected with booster injections before it can produce sufficient immune effect. It is speculated that some of the vaccine antibody negative patients may be related to not receiving intensive injection therapy. However, due to the age of the included patients, it is difficult to collect information such as vaccine injection time and injections. This study did not obtain enough information to verify this hypothesis.

Although COVID-19 vaccine injection is of great significance for epidemic control, its safety cannot be ignored. According to the report of the US vaccine adverse event reporting system, after 1893360 doses of bnt162b2 vaccine, the risk of allergic reaction was 11.1 cases/million doses, of which 71% occurred within 15 minutes after vaccination (29). The European Drug Administration recommends that the signs and symptoms of thrombosis and thrombocytopenia caused by the vaccine should be vigilant, such as shortness of breath, chest pain, leg swelling, persistent abdominal pain, neurological symptoms and minor bleeding spots under the skin outside the injection site (25).

Some studies have reported the effects of COVID-19 vaccine on the eyes. Although most of the studies are from case reports, the causal relationship between adverse reactions and COVID-19 vaccine injection events has not been determined. However, with the widespread popularity of vaccine injection, it is important to understand the effects of the vaccine on the eyes (30). At present, the ocular manifestations after COVID-19 vaccine injection mainly involve the posterior segment of the eyeball. The uvea, choroid and retinal vessels are most frequently affected. The median time of ocular adverse reactions was 4 days after the vaccine injection, and the main manifestations were

uveitis, white spot syndrome, central serous chorioretinopathy, retinal vein occlusion, acute macular Neuroretinopathy and acute paracentric middle maculopathy. Other ocular manifestations include eyelid edema and rash, optic neuritis, oculomotor paralysis, etc (23). It is speculated that the possible pathogenesis includes molecular simulation of vaccine components and host ocular tissues, antigen-specific cells and antibody mediated hypersensitivity to viral antigens and adjuvants present in the vaccine (23). The causal relationship between ocular signs and symptoms and COVID-19 vaccine has not been determined, and long-term observation and analysis of large sample multicenter data are still needed.

Our study found that after matching gender, age, and axial length, there was no statistical difference in the thickness of each layer in macular structure between vaccinated and unvaccinated patients. Whether the vaccine produces antibodies or not seems to have no effect on the structure and thickness of each layer in the macula. There was no significant difference between IgM group (short time after vaccine injection) and IgG group (long time after vaccine injection) in the thickness of macular structure. No inter group differences were observed even in the choroid, which was most susceptible to immune responses. Previous studies reported that the ocular complications caused by COVID-19 vaccine mostly occurred in the short term after the vaccine injection, with a median time of 4 days. However, our study found that the thickness of each layer in the macular region of IgM positive patients did not change. In antibody positive patients, there was no correlation between the concentration of antibody and the thickness of macular structure. It is suggested that the antibody production induced by the immune response of COVID-19 vaccine could not cause changes in the thickness of the macular layer structure. However, our study could not complete the observation of macular structure changes at the cellular and molecular level, and not analyze whether the macular supermicro structure has no change after COVID-19 vaccine injection. This is the limitation of this study, and we hope that pathological studies can further confirm it.

Most of the previous reports about the effects of COVID-19 vaccine on the eyes were case reports. Our study first analyzed the effects of COVID-19 vaccine on the macular structure from the perspective of different antibody statues after COVID-19 vaccine injection in age-related cataract patients. But our study also has some limitations. First of all, our enrolled patients were all age-related cataract patients and were older, so there was a certain selection bias. Secondly, our research has not been able to analyze the changes of macular structure from the cytological level. We hope that there will be more advanced research in the future to achieve this goal. Thirdly, our sample size is still small, and domestic COVID-19 vaccines are mainly inactivated vaccines, which cannot represent the effects of all COVID-19 vaccines. Therefore, further and more advanced research is needed.

Data availability statement

The original contributions presented in the study are included in the article/supplementary material. Further inquiries can be directed to the corresponding author.

Ethics statement

The studies involving human participants were reviewed and approved by Peking University International Hospital. The patients/participants provided their written informed consent to participate in this study.

Author contributions

XL and XC wrote the main manuscript text, and prepared figures and tables. ZP and XS provided the part of data. YB supervised the writing. All authors reviewed the manuscript.

Funding

This study was supported by the National Natural Science Foundation of China (NSFC, No. 21173012) and National Key R&D Program of China, No.2020YFC2008200.

Conflict of interest

The authors declare that the research was conducted in the absence of any commercial or financial relationships that could be construed as a potential conflict of interest.

Publisher's note

All claims expressed in this article are solely those of the authors and do not necessarily represent those of their affiliated organizations, or those of the publisher, the editors and the reviewers. Any product that may be evaluated in this article, or claim that may be made by its manufacturer, is not guaranteed or endorsed by the publisher.

References

1. Brandão-de-Resende C, Diniz-Filho A, de Almeida Brito F, Vasconcelos-Santos D. SARS-CoV-2 and COVID-19 for the ophthalmologist. *Clin Exp Ophthalmol* (2021) 49:70–80. doi: 10.1111/ceo.13877

2. Zeng B, Gao L, Zhou Q, Yu K, Sun F. Effectiveness of COVID-19 vaccines against SARS-CoV-2 variants of concern: a systematic review and meta-analysis. *BMC Med* (2022) 20:200. doi: 10.1186/s12916-022-02397-y

3. Hadj Hassine I. Covid-19 vaccines and variants of concern: A review. *Rev Med Virol* (2022) 32:e2313. doi: 10.1002/rmv.2313

4. Zhang H, Du F, Cao X, Feng X, Zhang H, Wu Z, et al. Clinical characteristics of coronavirus disease 2019 (COVID-19) in patients out of wuhan from China: a case control study. *BMC Infect Dis* (2021) 21:207. doi: 10.1186/s12879-021-05897-z

5. Galassi G, Rispoli V, Iori E, Ariatti A, Marchioni A. Coincidental onset of ocular myasthenia gravis following ChAdOx1 n-CoV-19 vaccine against severe acute respiratory syndrome coronavirus 2 (SARS-CoV-2). *Israel Med Assoc J: IMAJ* (2022) 24:9–10.

6. Mazzotta C, Giancipoli E. Anterior acute uveitis report in a SARS-CoV-2 patient managed with adjunctive topical antiseptic prophylaxis preventing 2019-nCoV spread through the ocular surface route. *Int Med Case Rep J* (2020) 13:513–20. doi: 10.2147/IMCRJ.S260252

7. Yener A. COVID-19 and the eye: Ocular manifestations, treatment and protection measures. *Ocular Immunol Inflammation* (2021) 29:1225–33. doi: 10.1080/09273948.2021.1977829

8. Shemer A, Einan-Lifshitz A, Itah A, Dubinsky-Pertzov B, Pras E, Hecht I. Ocular involvement in coronavirus disease 2019 (COVID-19): a clinical and molecular analysis. *Int Ophthalmol* (2021) 41:433–40. doi: 10.1007/s10792-020-01592-1

9. Douglas K, Douglas V, Moschos M. Ocular manifestations of COVID-19 (SARS-CoV-2): A critical review of current literature. *In Vivo* (2020) 34:1619–28. doi: 10.21873/invivo.11952

10. Dutescu R, Banasik P, Schildgen O, Schrage N, Uthoff D. Detection of coronavirus in tear samples of hospitalized patients with confirmed SARS-CoV-2 from oropharyngeal swabs. *Cornea* (2021) 40:348–50. doi: 10.1097/ICO.0000000000002562

11. Gasparini M, Dos Santos L, Hamade A, Gross L, Favarato A, de Vasconcellos J, et al. Identification of SARS-CoV-2 on the ocular surface in a cohort of COVID-19 patients from Brazil. *Exp Biol Med* (2021) 246:2495–501. doi: 10.1177/15353702211024651

12. Reinhold A, Tzankov A, Matter M, Mihic-Probst D, Scholl H, Meyer P. Ocular pathology and occasionally detectable intraocular severe acute respiratory syndrome coronavirus-2 RNA in five fatal coronavirus disease-19 cases. *Ophthal Res* (2021) 64:785–92. doi: 10.1159/000514573

13. Sirakaya E, Sahiner M, Aslan Sirakaya H. A patient with bilateral conjunctivitis positive for SARS-CoV-2 RNA in a conjunctival sample. *Cornea* (2021) 40:383–6. doi: 10.1097/ICO.0000000000002485

14. Ozturker Z. Conjunctivitis as sole symptom of COVID-19: A case report and review of literature. *Eur J Ophthalmol* (2021) 31:NP161–6. doi: 10.1177/1120672120946287

15. Lim L, Tan G, Yong V, Anderson D, Lye D, Young B, et al. Acute onset of bilateral follicular conjunctivitis in two patients with confirmed SARS-CoV-2 infections. *Ocular Immunol Inflammation* (2020) 28:1280–4. doi: 10.1080/09273948.2020.1821901

16. Marinho P, Marcos A, Romano A, Nascimento H, Belfort R. Retinal findings in patients with COVID-19. *Lancet* (2020) 395:1610. doi: 10.1016/S0140-6736(20)31014-X

17. Pereira L, Soares L, Nascimento P, Cirillo L, Sakuma H, Veiga G, et al. Retinal findings in hospitalised patients with severe COVID-19. *Br J Ophthalmol* (2022) 106:102–5. doi: 10.1136/bjophthalmol-2020-317576

18. Fonollosa A, Hernández-Rodríguez J, Cuadros C, Giralt L, Sacristán C, Artaraz J, et al. CHARACTERIZING COVID-19-RELATED RETINAL VASCULAR OCCLUSIONS: A case series and review of the literature. *Retina* (2022) 42:465–75. doi: 10.1097/IAE.0000000000003327

19. Vavvas D, Sarraf D, Sadda S, Eliott D, Ehlers J, Waheed N, et al. Concerns about the interpretation of OCT and fundus findings in COVID-19 patients in recent lancet publication. *Eye* (2020) 34:2153–4. doi: 10.1038/s41433-020-1084-9

20. Oren B, Aksoy Aydemır G, Aydemır E, Atesoglu H, Goker Y, Kızıltoprak H, et al. Quantitative assessment of retinal changes in COVID-19 patients. *Clin Exp optometry* (2021) 104:717–22. doi: 10.1080/08164622.2021.1916389

21. Patel S, Yonekawa Y. ACUTE MACULAR NEURORETINOPATHY AFTER SARS-COV-2 VACCINATION. *Retinal cases Brief Rep* (2022) 16:5–8. doi: 10.1097/ICB.0000000000001195

22. Burgos-Blasco B, Güemes-Villahoz N, Vidal-Villegas B, Martinez-de-la-Casa J, Donate-Lopez J, Martín-Sánchez F, et al. Optic nerve and macular optical coherence tomography in recovered COVID-19 patients. *Eur J Ophthalmol* (2022) 32:628–36. doi: 10.1177/11206721211001019

23. Sen M, Honavar S. After the storm: Ophthalmic manifestations of COVID-19 vaccines. *Indian J Ophthalmol* (2021) 69:3398–420. doi: 10.4103/ijo.IJO_2824_21

24. Zhang Q, Yang L, Xu X, Lan X, Wang Z, Sun Y, et al. The association of axial length with macular microvascular changes in Chinese diabetic retinopathy patients. *Int J Gen Med* (2022) 15:3895–902. doi: 10.2147/IJGM.S364790

25. Lai C, Chen I, Chao C, Lee P, Ko W, Hsueh P. COVID-19 vaccines: concerns beyond protective efficacy and safety. *Expert Rev Vaccines* (2021) 20:1013–25. doi: 10.1080/14760584.2021.1949293

26. Wu D, Zhang Y, Tang L, Wang F, Ye Y, Ma C, et al. Effectiveness of inactivated COVID-19 vaccines against symptomatic, pneumonia, and severe disease caused by the delta variant: Real world study and evidence - China, 2021. *China CDC weekly* (2022) 4:57–65. doi: 10.46234/ccdcw2022.009

27. Zhu M. SARS immunity and vaccination. *Cell Mol Immunol* (2004) 1:193–8.

28. Li Y, He Q, Yu R, Jiang H, Wang W, Feng D, et al. Highlighted prospects of an IgM/IgG antibodies test in identifying individuals with asymptomatic severe acute respiratory syndrome coronavirus 2 (SARS-CoV-2) infection. *Arch Pathol Lab Med* (2021) 145:39–45. doi: 10.5858/arpa.2020-0310-SA

29. CDC COVID-19 Response Team, Food and Drug Administration, MMWR Morb Mortal Wkly Rep. *Allergic reactions including anaphylaxis after receipt of the first dose of pfizer-BioNTech COVID-19 vaccine - United States, Food and Drug Administration*. (2021) 70(2):46–51. doi: 10.15585/mmwr.mm7002e1

30. Montano D. Frequency and associations of adverse reactions of COVID-19 vaccines reported to pharmacovigilance systems in the European union and the United States. *Front Public Health* (2021) 9:756633. doi: 10.3389/fpubh.2021.756633

frontiers | Frontiers in Immunology

TYPE Review
PUBLISHED 16 November 2022
DOI 10.3389/fimmu.2022.1063928

Check for updates

OPEN ACCESS

EDITED BY
Bo Li,
Department of Orthopedics,
Sun Yat-sen University, China

REVIEWED BY
Gang Chen,
Tongji University School of Medicine, China
Yuzhen Xu,
Tongji University, China

*CORRESPONDENCE
Jian Wu
wujianglinxing@163.com

†These authors have contributed equally to this work

SPECIALTY SECTION
This article was submitted to Multiple Sclerosis and Neuroimmunology, a section of the journal Frontiers in Immunology

RECEIVED 07 October 2022
ACCEPTED 31 October 2022
PUBLISHED 16 November 2022

CITATION
Xu J, Ma C, Hua M, Li J, Xiang Z and Wu J (2022) CNS and CNS diseases in relation to their immune system. *Front. Immunol.* 13:1063928. doi: 10.3389/fimmu.2022.1063928

COPYRIGHT
© 2022 Xu, Ma, Hua, Li, Xiang and Wu. This is an open-access article distributed under the terms of the Creative Commons Attribution License (CC BY). The use, distribution or reproduction in other forums is permitted, provided the original author(s) and the copyright owner(s) are credited and that the original publication in this journal is cited, in accordance with accepted academic practice. No use, distribution or reproduction is permitted which does not comply with these terms.

CNS and CNS diseases in relation to their immune system

Jianhao Xu[1†], Canyu Ma[2†], Menglu Hua[2†], Jiarui Li[2], Ze Xiang[2] and Jian Wu[3*]

[1]Department of Laboratory Medicine, The Yangzhou University Jianhu Clinical College, Jianhu, China, [2]Zhejiang University School of Medicine, Hangzhou, Zhejiang, China, [3]Department of Clinical Laboratory, The Affiliated Suzhou Hospital of Nanjing Medical University, Suzhou Municipal Hospital, Gusu School, Nanjing Medical University, Suzhou, Jiangsu, China

The central nervous system is the most important nervous system in vertebrates, which is responsible for transmitting information to the peripheral nervous system and controlling the body's activities. It mainly consists of the brain and spinal cord, which contains rich of neurons, the precision of the neural structures susceptible to damage from the outside world and from the internal factors of inflammation infection, leading to a series of central nervous system diseases, such as traumatic brain injury, nerve inflammation, etc., these diseases may cause irreversible damage on the central nervous or lead to subsequent chronic lesions. After disease or injury, the immune system of the central nervous system will play a role, releasing cytokines to recruit immune cells to enter, and the immune cells will differentiate according to the location and degree of the lesion, and become specific immune cells with different functions, recognize and phagocytose inflammatory factors, and repair the damaged neural structure. However, if the response of these immune cells is not suppressed, the overexpression of some genes can cause further damage to the central nervous system. There is a need to understand the molecular mechanisms by which these immune cells work, and this information may lead to immunotherapies that target certain diseases and avoid over-activation of immune cells. In this review, we summarized several immune cells that mainly play a role in the central nervous system and their roles, and also explained the response process of the immune system in the process of some common neurological diseases, which may provide new insights into the central nervous system.

KEYWORDS

central nervous system (CNS) injury, immunocytes, immune system, neuro-immune interaction, role

Introduction

The immune processes involved in these two types of immunity and the therapeutic regulation of disease and injury by immune cells are not unidirectional in their effects on the CNS, for the reason that the wrong activation or over-response can cause damage to the central nervous system. The developed nervous system of vertebrates is an important sign of high evolution (1, 2). Central Nervous System (CNS) is the main component of the human nervous system, including the brain, which is located in the skull cavity, and the spinal cord, which is located in the spinal canal. CNS can accept incoming information from all over the body, integrate and process it, and finally control the body through outgoing signals (3), or use this information to complete memory and learning, so that the organism can carry out a series of thinking activities.

Because the CNS is the most important vertebrate nervous system, and the brain and spinal cord, the two main components of the CNS, have been shown to be non-renewable (4). Therefore, CNS injury and disease and the subsequent repair of immune responses are crucial for the CNS. Like the immune system of most other tissues, the immune system of CNS is composed of the innate immune system and the specific immune system (5, 6). The innate immune system is mainly composed of congenital macrophages. The main process of specific immunity is the specific immune response produced by the specific combination of antigens and antibodies. The immune process involved in these two immune modes and the therapeutic regulation of immune cells on diseases and injuries have a non-unidirectional effect on the CNS —— incorrect activation or excessive response may cause damage to the central nervous system (7).

At present, there is a relatively clear understanding of the birth and differentiation of immune cells, and more understanding of the possible functions of most immune cells after differentiation. Studies on CNS immunity from 2020 to the present have mainly focused on the molecular mechanism of immune cells entering the CNS and promoting CNS inflammation, and on this basis, how to regulate the response degree of immune cells. For some immune cells, the researchers found other types of differentiation and other effects. Other studies have attempted to explain the link between CNS immunity and other diseases, and have attempted to use CNS immunotherapy as a clinical treatment (8, 9).

In this review, we illustrated the immune components of CNS and their roles, observe the performance of these immune components in different neurological diseases, and judged whether they are beneficial or harmful for CNS diseases. Based on this information, we may find ideas and methods of immunotherapy for these diseases.

Central nervous system

Composition of CNS

The central nervous system of the human body consists of the brain and the spinal cord (Figure 1). The spinal cord is the lowest level of motor center, and it is also the basic reflex center to complete the movement of the organism, under the control of the brain, through the neural circuit signal conduction, so as to achieve motor regulation. The spinal cord is composed of gray and white matter and contains nerve cell bodies and their ascending and descending conduction tracts (10). Classical studies of spinal cord function have focused on well-defined neural pathways that are thought to mediate automatic functions of stereotyping, such as stretch and flexion reflexes, and allocate inputs from sensory and descending fibers to appropriate targets (11).

Brain, generally refers to three parts which are: cerebellum, brainstem, diencephalon. The brainstem is an important part of the brain responsible for sensing injury and processing pain signals, and transmits and processes signals between the brain, cerebellum and spinal. The conventional wisdom about the cerebellum is that it is essential for motor function and contributes little to cognitive function (12). However, multiple studies by Middleton FA et al. showed that cerebellar output targets involved multiple cortical regions, including not only primary motor cortex (13, 14), but also oculomotor nerve (15, 16), prefrontal lobe and inferior temporal region (17, 18), which indicates that cerebellum plays a role in both motor and cognitive function.

Working mechanism of CNS

The sensory organs with receptors establish communication with the central nervous system through the afferent nerves, so as to realize the regulation of the central nervous system. Peripheral nerve tissue is composed of afferent sensory fibers and efferent motor fibers. When receptors such as the skin are stimulated by the outside world, they will produce nerve impulses. Nerve synapses release neurotransmitters, which are received by cells, and the resting potential is converted into action potential (19). After receiving the neurotransmitter, the receiver may process it and react on the afferent nerve synapse (20), and intercellular conduction and closed interaction of nerve electrical signals are realized. The electrical signal is transmitted to the CNS along the sensory fibers, and the CNS processes the signal and transmits it along the motor fibers to control the body movement (21). In this way, the CNS is connected to the rest of the nervous system.

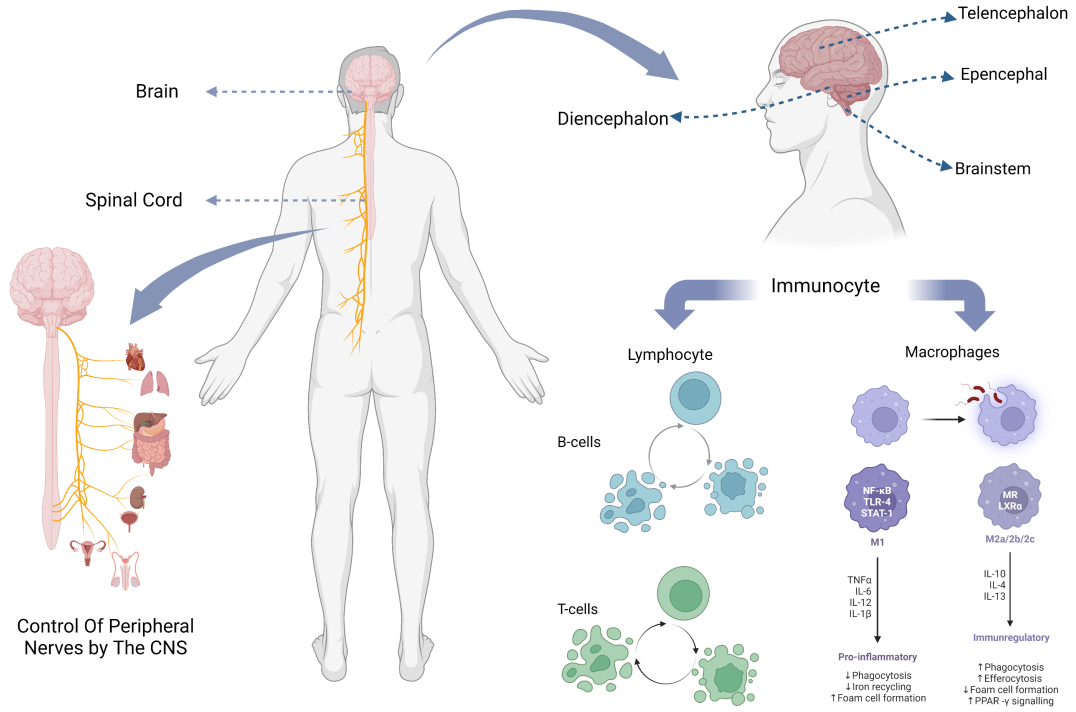


FIGURE 1
The composition of the CNS, the location of its parts, and the major immune cells it contains.

Take, for example, the mechanism of regulation of renal afferent sensory nerves in the central nervous system. Kidney is an important sensory organ with abundant baroreceptors and chemoreceptors, as well as a large number of afferent nerves. Renal afferents can directly project to areas of the central nervous system, such as the lateral thalamic area and the paraventricular nucleus (PVN), and indirectly project to other areas of the hypothalamus (22). During stimulation of the afferent renal nerve, the firing frequency of the large-cell neurons in the PVN increased (23). Renal afferents activate the central nervous system and enhance sympathetic activity (24).

In simple terms, the peripheral nervous system gives information to the CNS in the form of electrical stimulation through the afferent nerve, which is processed by the CNS to realize the regulation of the body.

Immune cells and immune system in the CNS

Immune cells

Among all immune cells in the central nervous system, macrophages and glial cells derived from them, as well as lymphocytes including T cells, B cells and self-killing immune cells, play a major role (Table 1).

Microglia are the main cellular component of the innate immune system of the brain. They are distributed in the whole brain at different densities, accounting for 5%-20% of the total brain cells, and are developed from primitive macrophages (25, 26). Microglia are activated and polarized after being exposed to external stimuli (42), which will present two phenotypes M1/M2 with different functional status and markers (27). The M1 phenotype produced by the general activation pathway can exert pro-inflammatory and neurotoxic effects, while the M2 phenotype produced by the selective activation pathway can exert anti-inflammatory and neuroprotective effects (28, 29), promoting medullary regeneration by inhibiting cell differentiation (34). Such a classification of microglia was originally proposed by Mills et al. (30). However, this classification method based on stimuli does not reflect the range and function of phenotypes well, and Mills himself has also shown that the main existence should be a continuous intermediate of M1 and M2 (43), so this once widely used classification method has been questioned by many people (44, 45). Later, Devanney et al. proposed a function-based classification method (27). For the function of microglia, there has been a high similarity between microglia and macrophages due to their structural characteristics (46), researchers have long thought that its function is mainly an immune response, like macrophages, to recognize and take up pathogens and other

TABLE 1 The distribution, roles, types and relationships of immune cells in the CNS.

Authors	Immunocyte	Role	Content	References
Alliot et al.	Microglia	Microglia arise from the yolk sac and emerge during embryonic development, increasing in number during gestation and steadily increasing in number during the first two weeks postpartum, when about 95% of microglia are born	The origin and proliferation of microglia	(25)
Lawson et al.	Microglia	Microglia are abundant in the brain, but their distribution is not uniform. They are more distributed in hippocampus, olfactory skull, basal ganglia and substantia nigra, and less distributed in fiber tracts, cerebellum and most brain stem	Morphology and distribution of microglia	(26)
Devanney et al.	Microglia and macrophage	The M2 phenotype of macrophages is age-dependent and can play an anti-inflammatory role, and the M1 phenotype is enhanced phagocytosis, but the M1M2 classification has limitations	The role of immune metabolism in neurotrauma	(27)
Gensel et al.	Macrophage	M1, M2a, M2b, and M2c macrophages were sequentially activated during the healing phase, but the duration of this phase was prolonged after the onset of injury inflammation	Role of macrophages in spinal cord injury	(28)
Tang et al.	Microglia	M1 microglia dominate the injury site at the end stage of the disease. At this time, the immunolysis and repair process of M2 microglia are inhibited, and endogenous stimulation may continue to activate M1 proinflammatory response, eventually leading to irreversible neuronal loss	Microglia can be classified into two phenotypes, M1/M2, and this classification has important roles in neurological diseases	(29)
Mills et al.	Macrophage	Lymphocyte Activation Macrophage Activation	The division of two phenotypes and paradigms of macrophages and their association	(30)
Wright-Jin et al.	Microglia	Microglia differentiate and remove brain inflammation to maintain CNS homeostasis	Role of microglia in CNS homeostasis	(31)
Takahashi et al.	NK	NK cells may actively inhibit potentially pathogenic autoimmune T cells that may mediate CNS inflammation	Role of NK in multiple sclerosis	(32)
Nimmerjahn et al.	Microglia	Microglia are highly active in their putative resting state, continuously investigate their microenvironment, and have extremely strong motility processes and protrusions	Highly dynamic monitoring of brain parenchyma by microglia *in vivo*	(33)
Miron et al.	M2 Microglia	The dominant response of microglia and peripheral macrophages changed from M1- to M2. M2 cell density is increased in lesions in aged mice	M2 cell polarization is essential for effective myelin regeneration and contributes to the treatment of multiple cell sclerosis	(34)
Boudreau et al.	NK	NK cells achieve structural diversity through mutation, making them specific and adaptive to different immune environments	Diversity in NK cell reactive capacities driven by NK education protect some individuals against a variety of infections and diseases	(35)
Bluestone et al.	T cells	Cytokines are important factors driving the differentiation of CD4 effector T cells	CD4 T cells are divided into functional subsets with different immune functions	(36)
Engelhardt et al.	T cells	Leukocytes cross the CNS barrier in response to chemokines and activators	During inflammation, T cells migrate across the CNS barrier and transport signals	(37)
Constant et al.	B cells	In the experiments designed to determine the ability of splenic dendritic cells (DCs) and B lymphocytes to take up peptide or protein Ags *in vivo*, Ags were taken up preferentially by DCs, whereas proteins were taken up by Ag-specific B cells *in vivo*	By presenting antigens to T cells, B cells cause T cells to perform protein antigens	(38)
Finkelman et al.	B cells	By activating B cells and presenting B cell antigens, anti-IGD antibodies induce T cell activation and tolerance	The antigen presentation of B cells is required to produce T-cell dependent antibody responses *in vivo*, and the antigen presentation of repetitive B cells to T cells is a necessary condition for the expansion of B cells.	(39)
Pistoia et al.	B cells	B cells can not only produce antibodies, but also present antigens to T cells	B cell function and its relevance to disease	(40)
Kipnis et al.	T cells	Autoimmune T cells can produce neurotrophic factors when activated by relevant antigens, and T cells can also activate non-immune cell colonization and participate in homeostasis restoration regulation	T cells and the immune system in schizophrenia	(41)

CNS, Central Nervous System.

substances, and analyze their environment (33). However, many subsequent experiments have shown that, especially when there is no need for immunity, the role of microglia is mainly to carry out sensing, information processing and nerve protection in the central nervous system (25), and maintain the homeostasis of the central nervous system (31, 47). It promotes neural development over a period of time (48) and can affect nerve impulses in the adult brain (49).

Lymphocytes are the main cells of the body's immune response, which are produced by lymphoid organs and can respond to signals such as foreign pathogens or inflammatory stimuli. T cells, B cells and natural killer cells play a significant role in central nervous system immunity. The main reason for the suppression of immune action in the CNS is the blockage of the blood-brain barrier (50, 51). Only a small number of lymphocytes can enter the CNS through the blood-brain barrier, blood-meningeal barrier, and blood-cerebrospinal fluid barrier during brain health and injury, and play an immune function or promote neuroinflammation (52–54).

T cells and B cells together constitute acquired immunity. They can all differentiate into different subtypes (55), release different cytokines or perform different functions, which greatly contributes to their immune specificity (36, 40, 56–58).

B cells travel from the skull to the meninges through blood vessels (59, 60), and their main role is to produce antibodies (61). After receiving antigen presentation, B cells can differentiate into plasma cells and memory cells. The former will produce specific antibodies that bind to the antigen and destroy it[98][99]. B cells can also act as antigen-presenting cells (APCs), processing antigens and presenting them to antigen-specific T cells (38, 39, 62), and promote the development of pro-inflammatory T cells (63). In the treatment of CNS autoimmune diseases, by depleting activated B cells, B cells as APC can be stimulated to target T cells, so that they can differentiate and develop, thus enhancing the immune effect (64, 65).

T lymphocytes, the sentinels of the adaptive immune system, respond to antigen-specific signals by bursting, proliferating, and differentiating into effector subsets to recognize and eliminate threats to the host (66, 67). In addition to the previously mentioned antigen presentation and immune role with B cells, T cells also have the function of promoting cognitive learning in the brain (41, 68, 69), as well as a certain role in maintaining CNS homeostasis. A large number of T cells are used for immune monitoring of the brain barrier (37).

Natural killer immune cell (NK) is a kind of large granular hematopoietic cell derived from bone marrow (70), and its function varies in different individuals due to different genes (35). Like T and B cells, NK also has a variety of subtypes (71), among which the CD56 bright NK cells are the main ones present in CD56 bright NK cells (72). It has been suggested that NK may play a regulatory role in central nervous system diseases (32). NK can repair nerves after CNS damage, coordinate immune responses, and inhibit the development of inflammation (73, 74). It is able to regulate the neurological diseases such as Parkinson disease, and can play a neuroprotective role by killing T cells that promote neurotoxicity (75). In some neuroinflammation, such as autoimmune encephalomyelitis (EAE), the cytotoxicity is reduced and the memory EAE is inhibited (76, 77). In addition, NK can also work with other lymphocytes (78) to cooperate in immune action in neurological diseases such as Alzheimer's disease (79).

Recent studies have shown that astrocytes play an important role in CNS immunity by associating with other immune cells. For example, the recognition of astrocytes depends on microglia, and the subsequent release of caspases induced by astrocytes promotes apoptosis and reduces cellular inflammation. IF-33 released by astrocytes can recruit twice as many T cells and promote the repair of CNS diseases such as neurodegenerative diseases and spinal cord injuries (80).

Immune system

The CNS immune system is divided into innate immunity and specific immunity, which make different immune responses in different situations. Some autoimmunity can lead to diseases, but the immune effect after injury helps to recover from injury (81).

After CNS injury, a series of subsequent immune responses are triggered, first innate immunity and then specific immunity. Both types of immunity can expand their number by releasing cytokines and regulating genes from immune cells (82–84). The innate immune system is the first line of defense to help the central nervous system resist foreign pathogens, and the specific immune response is slow, which will gather and play a role after inflammation or injury occurs (85, 86). A correct understanding of the immune system in different CNS diseases at different stages of development can help us find appropriate immunotherapy methods.

Due to the particularity of the CNS, the BBB still acts as a barrier, making the CNS an immune privileged organ. Its carrier and receptor proteins are the only way for outside proteins to enter the CNS, ensuring precise regulation of what enters the brain (87). This barrier creates an important difference between CNS immunity and peripheral nervous system immunity. There are only a small number of protoimmune cells in the CNS. These immune cells and some immune progenitors release chemokines and cytokines to recruit peripheral immune cells after brain injury, thus amplifying the immune effect (88). For example, fatty acids can activate peripheral macrophages through TLR4-mediated mechanism. Such recruitment needs to be carefully regulated, and the process will be discussed later (89).

However, the CNS has connections to all surrounding organs (90). There is an external barrier to immune cells, but the immune system of CNS is not isolated. Cerebrospinal fluid is used as the medium to exchange immune cells with the outside world through the meninges. Compartmentalized immune cells are recruited to cross the blood-brain barrier when the brain needs immune repair (91). These barriers used to be thought to insulate the CNS from its immune system, but recent research suggests that these barriers facilitate communication between the CNS and the outside world. Some of them also act as immune hubs, such as the dura mater, which associates with

the brain through the lymphatic system, metabolizing waste and maintaining brain homeostasis (92).

CNS disease and the association with immune system

Central nervous system diseases include central neurodegenerative diseases, nervous system infections, brain tumors and other types of diseases, including brain injury, spinal cord injury and peripheral nerve injury from the point of view of injury and disease location. These diseases are related to the immune system to some extent. Here we focus on central neurodegenerative neurological diseases, CNS tumors, traumatic brain injury, and spinal cord injury.

CNS neoplasms

Brain tumors are generally divided into two categories, namely those from external sources, also known as metastases, and those arising from the central nervous system, such as gliomas (93). We focus on tumors arising spontaneously in the central nervous system. When tumors occur, tumor associated macrophages (TAMs) are the main immune cells in the tumor microenvironment (TME) in the CNS. Studies have shown that the incidence of some primary tumors is very low after immunosuppression (94, 95), which indicates that TAM targeted inhibition plays an important role in tumor therapy (96). Take glioma as an example, it is a tumor developed by glial cells, among which glioblastoma (GBM) is the most common glial tumor and one of the highest mortality among all cancers (97). The average overall survival time is not more than 15 years, and only seven percent of patients can be cured (98, 99). Some other subgroups of low-grade gliomas have molecular features similar to glioblastoma, with an invasive process (100). Glial cells will release CSF-1 and other cytokines and recruit TAM (101). Studies have shown that TAM can promote the growth rate and morphological size of glioma cells (102, 103), and a small number of TAMs and microglia will lead to a larger volume of tumors (104). In fact, in GBM, the number of TAMs is positively correlated with tumor severity, and there are very few in patients who do not relapse after recovery (105). According to this characteristic of TAM, the development of tumor therapy targeting TAM has become a new direction for brain tumor treatment (106, 107).

CNS tumor immune process after the basic follow - tumor immune system cycle, this is Chen et al. Applied to inducing tumor immune response rule (108), after the tumor cells results in the release, antigen precursor release activating factor to activate T cells, as effector cells infiltrating tumor, T cell contact and identify the antibody, to destroy, then the immune cells apoptosis (109). T cells can track and eliminate cancer by recognizing specific exogenous factors to track and damage host cells (79). In fact, the development of tumor immunotherapy based on this principle has been widely carried out and achieved remarkable results (110, 111), and the application in brain tumors is also an example to follow.

Degenerative neurological diseases

In 2019, there were about 50 million people living with neurodegenerative diseases worldwide, and this number is expected to rise to 152 million by 2060 (112). In his study, Richard Armstrong listed a series of factors that lead to degenerative neurological diseases and pointed out that age is the most important risk factor (113). The two diseases with the highest incidence of degenerative neurological diseases are Alzheimer's disease (AD) (114) and Parkinson's disease (PD) (115, 116), which are also a hot research topic in CNS diseases.

An important component of neurodegenerative diseases is the triggering of innate immune mechanisms. Microglia and other cell types in the brain can be activated by misfolded proteins or abnormally localized nucleic acids. This detents microglia from their physiological and beneficial functions and leads to a sustained release of their proinflammatory mediators (25). In the process of Parkinson's disease, for example, after the activation of microglia as the main cells of immune function, may cause nerve nutrition through compound, such as brain derived neurotrophic factor, nerve protective effect, but there are also likely to produce neurotoxicity of proinflammatory cytokines (such as tumor necrosis factor (TNF), interleukins) (117, 118). For these two functions, which are almost opposite to the development of the disease, the current view is that at the beginning, the cytokines of activated microglia may have neuroprotective effects, but then the activated microglia undergo toxic degeneration, leading to the progression of Parkinson's disease to neurotoxicity (119). Sawada showed in his experimental studies that activated microglia may be neuroprotective in neonatal mice but neurotoxic in aged mice. This conclusion is consistent with the fact that age is a major risk factor in the pathogenesis of degenerative neurological diseases, because the performance of two subsets of activated microglia (with toxic and neuroprotective functions, respectively) is strongly correlated with age.

Spinal cord injury

Spinal cord injury (SCI) refers to the injury of the spinal cord and the pathological changes such as sensory and motor disorders after the body encounters direct or indirect external interference. Spinal cord injury may lead to loss of limb

perception, incontinence and even complete paralysis, which may not recover for a lifetime or even be life-threatening (120).

After SCI, to ensure the regeneration of damaged axons (121), the CNS begins to recruit peripheral neutrophils into the CNS (122) and begins to clear axons and myelin debris nerve remnants (123), within the first hour after injury, playing a major clearing role. Subsequently, the recruited neutrophils begin to apoptosis and release attractant factors that attract and recruit monocytes, and at the same time can also recruit certain macrophages. After reaching the injury site, monocytes differentiate into macrophages according to the chemokines at the injury site (124–126), and the macrophages produced at this time will phagocytize the apoptotic neutrophils and other tissue debris (127). Similarly, microglia are also involved in injury repair (128). So similar to the white blood cells, neutrophils and other related immune cells in the spinal cord damage happens after apoptosis, part of the nerve ending structure will be destroyed in the process of damage (120). Experiments have shown that there are many repair factors in the central nervous system that promote regeneration of biological factors in nerve and immune cells (Ramer, Ramer et al., 2005), but regeneration does not represent full functional recovery. Therefore, after the immune system deals with spinal cord injury, the body will have reduced immunity and be prone to infection (129). Moreover, although the immune system responds to traumatic stimuli, it drastically changes as the injury worsens, which may exacerbate the injury and inflammation (130, 131).

Traumatic brain injury

Traumatic brain injury (TBI) is an injury to the brain caused by external forces or external shocks, which may lead to a reduction or change in the state of consciousness and easily cause biochemical cascade damage, so it may be accompanied by long-term sequelae (132). After the occurrence of TBI, symptoms such as intracranial hemorrhage, brain contusion, concussion, and damage to nerve synapses are first caused (133), and a cascade of damage occurs within minutes to months. TBI has a high incidence among both military personnel and the general public (134).

Neuroinflammation and peripheral neuropathy are easily triggered after TBI (135). There are many factors that cause this situation, such as purines, heat shock proteins, and receptors of pathogen associated endogenous molecules (PAMPs) and damage associated endogenous molecules (DAMPs), which may promote inflammation (136–138). The latter can combine with proteins to form inflammasomes, release and infiltrate microglia, astrocytes and other cell populations, and produce proinflammatory factors after activation (139). Proinflammatory factors can further lead to neuroinflammation, and more severe inflammation can even transform TBI into chronic neurological diseases (140).

Similar to other neurological diseases, in TBI, immune cells can both promote recovery and aggravate injury (141). TBI can instantly induce cell death, after which the damaged cells release DAMPs, signal to immune cells, recruit microglia, astrocytes, etc. After they are activated, they will further recruit peripheral immune cells to pass through the damaged blood-brain barrier (142). Microglia respond immediately after injury and accumulate in large numbers in the injured area (33, 143), removing cell debris through phagocytosis (44). It can also release trophic factors to protect nerves (133) and is involved in remodeling injured nerves (144). However, microglial activation will produce excessive inflammatory mediators, recruit peripheral immune cells, produce a large number of pro-inflammatory factors and cytotoxic substances, hinder the repair of the central nervous system, and even lead to cell death and neuronal dysfunction (145, 146). Similarly, although neutrophils can participate in the immune regulation of TBI, they will also release some acute inflammatory cytokines to aggravate brain injury. The protective and injury effects largely depend on the location, type and stage of injury (147). Which more complicated is that the immune function and immune effect after TBI are related to gender (148) and age (149). Therefore, studying the relationship between these influencing factors and immune effect is an important entry point for the treatment of TBI (Table 2).

Now the treatment of some kinds of new ideas are mainly concentrated in cell therapy (151), because the immune cells such as macrophages have different phenotypes, their functions have significant difference, so can adjust the balance between different phenotypes, as far as possible avoid inflammation cause of neurodegenerative diseases, lower immune cell toxicity effect (152). In a study of the effects of Anakinra, a recombinant human IL-1 receptor antagonist, the treatment group had a higher cure rate than the control group (153). In addition, some small particles, such as zinc ions, have also been shown to be involved in neuroprotection and nerve recovery after injury (150). TBI ZnT3-KO mice were more severely injured when compared with juvenile wild-type mice.

In each of these diseases, the brain is damaged to a degree that releases specific substances that activate the innate immune system, which in turn activates and recruits the peripheral immune system. The immune system plays an important role in the anti-inflammatory response to disease injury and subsequent damage repair, but some immune responses also lead to the deterioration of the disease, so it is believed that CNS diseases and CNS immune system have an important relationship (Figure 2).

Conclusion and future prospects

Although some immune cells in the CNS have been discovered and their functions have been relatively obvious, a

TABLE 2 Studies on the role of different immune cells in TBI.

Authors	Immunocyte	Role	The research methods	References
Roth et al.	Microglia, astrocytes	The skull is permeable to small molecular weight compounds and uses this delivery route to modulate inflammation and therapeutically ameliorate brain injury through transcranial administration of the ROS scavor glutathione	Traumatic Head Injury Neuroimaging Classification (THINC)	(133)
Davalos et al.	Microglia	ATP is an important signaling molecule that mediates interactions between various cell types in the brain, and glial and endothelial cells may contribute to microglial responses by releasing large amounts of ATP upon injury	Microglia were imaged *in vivo* using a two-photon microscope	(137)
Liu et al.	Microglia, astrocytes	The innate immune system engages in a series of PRRS to detect "danger" signals, such as PAMPs or DAMPs, to defend against infection or injury. NLR recognizes many PAMPs as well as various DAMPs to activate the assembly of inflammasomes that trigger the maturation of proinflammatory cytokines, such as IL-1β and IL-18	Western blot analysis	(139)
Liu et al.	Neutrophils	Neutrophils are an important component of the innate immune system, and their inappropriate or excessive activation may lead to tissue damage.	Drug blockade, etc.	(147)
Damani et al.	Microglia	Most microglia are long-lived cells that have a long residence time in the CNS and are therefore susceptible to the *in situ* aging effects that occur during the normal lifespan of the animal	*In vitro* imaging of the explant retina	(149)
Doering et al.	Zinc-rich (ZEN) neurons	Zn ions are protective against TBI effects	Diseased mice were treated with DEDTC or selenite	(150)
Loane et al.	Microglia	In injured brains, microglia produce neuroprotective factors that remove cellular debris and coordinate the process of nerve repair	Drug therapy, gene blocking, etc	(142)
Griffin et al.	Microglia-directed neurons	Traumatic brain injury, mild and severe, open and closed, leads to immune suppression and infection	Autologous reinfusion of WBCs (adoptive immune therapy)	(132)
Jassam et al.	Microglia, astrocytes	TBI induces an immune response composed of locally and peripherally derived participants that begins within minutes of the onset of TBI if the injury does not resolve or causes chronic diseases such as chronic traumatic encephalopathy	Inhibitors block immune cell activation	(44)
Edwards et al.	Steroids	Refutes any substantial reduction in corticosteroid mortality or severe disability within 6 months after traumatic brain injury	MRC CRASH: A randomized controlled trial of the effects of corticosteroids	(141)

TBI, Traumatic brain injury.

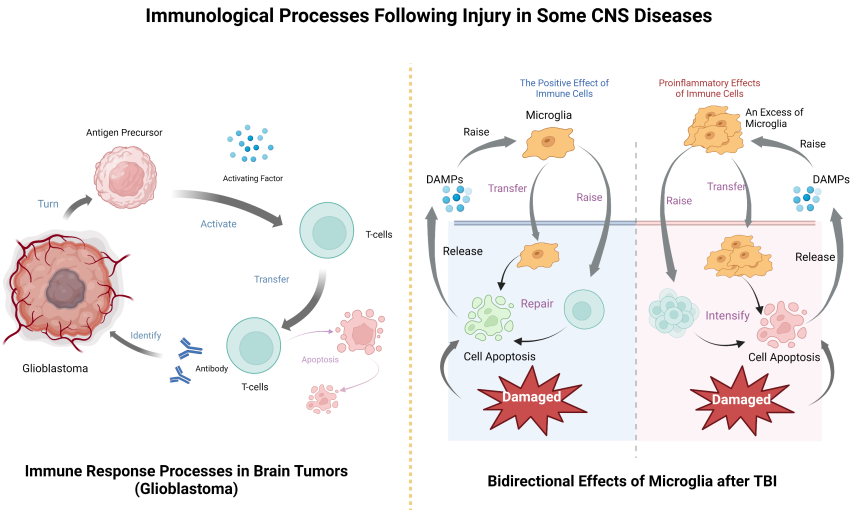


FIGURE 2
The processes by which immune cells exert their effects after CNS tumors and TBI, including their bidirectional effects on the disease.

large part of the CNS is still unknown. Previous studies have shown that the molecular pattern and molecular reason for these apparent phenomena are still unclear after addressing the expression role of the immune system. For example, do NK cells maintain or regulate repair functions in the central nervous system and how do they do it? What is the mechanism of macrophage phagocytosis and foam cell formation after SCI? How do macrophages recognize and internalize specific molecules in apoptotic neutrophils? All these problems now seem difficult to solve (154, 155).

In addition, some immune cells were surprisingly found to be present in specific disease contexts, which could not be explained by current understanding. Some CNS diseases currently have no suitable treatment (156, 157), and some therapies that appear to be effective have substantial limitations. For example, although checkpoint inhibitors have been relatively successful in many solid tumor types, they have been difficult to succeed in CNS tumors. Even some serious CNS diseases have not received enough attention (158).

In the future studies, more neurological diseases will be taken into account, and the immune connection between the CNS and the peripheral nervous system may become an important consideration of immune effects.

Author contributions

JX and CM had the idea for the article. MH and JL performed the literature search and data analysis. JW and ZX drafted and critically revised the work. All authors contributed to the article and approved the submitted version.

Conflict of interest

The authors declare that the research was conducted in the absence of any commercial or financial relationships that could be construed as a potential conflict of interest.

Publisher's note

All claims expressed in this article are solely those of the authors and do not necessarily represent those of their affiliated organizations, or those of the publisher, the editors and the reviewers. Any product that may be evaluated in this article, or claim that may be made by its manufacturer, is not guaranteed or endorsed by the publisher.

References

1. Albuixech-Crespo B, Herrera-Úbeda C, Marfany G, Irimia M, Garcia-Fernàndez J. Origin and evolution of the chordate central nervous system: Insights from amphioxus genoarchitecture. *Int J Dev Biol* (2017) 61(10-11-12):655–64. doi: 10.1387/ijdb.170258jg

2. Albuixech-Crespo B, López-Blanch L, Burguera D, Maeso I, Sánchez-Arrones L, Moreno-Bravo JA, et al. Molecular regionalization of the developing amphioxus neural tube challenges major partitions of the vertebrate brain. *PloS Biol* (2017) 15 (4):e2001573. doi: 10.1371/journal.pbio.2001573

3. Osadchiy V, Martin CR, Mayer EA. Gut microbiome and modulation of cns function. *Compr Physiol* (2019) 10(1):57–72. doi: 10.1002/cphy.c180031

4. Shinozaki M, Nagoshi N, Nakamura M, Okano H. Mechanisms of stem cell therapy in spinal cord injuries. *Cells* (2021) 10(10):2676. doi: 10.3390/cells10102676

5. Wubben R, Efstathiou C, Stevenson NJ. The interplay between the immune system and viruses. *Vitam Horm* (2021) 117:1–15. doi: 10.1016/bs.vh.2021.06.011

6. Colgan TJ, Moran PA, Archer LC, Wynne R, Hutton SA, McGinnity P, et al. Evolution and expression of the immune system of a facultatively anadromous salmonid. *Front Immunol* (2021) 12:568729. doi: 10.3389/fimmu.2021.568729

7. Hagan N, Kane JL, Grover D, Woodworth L, Madore C, Saleh J, et al. Csf1r signaling is a regulator of pathogenesis in progressive Ms. *Cell Death Dis* (2020) 11 (10):904. doi: 10.1038/s41419-020-03084-7

8. Stepp MA, Menko AS. Immune responses to injury and their links to eye disease. *Transl Res* (2021) 236:52–71. doi: 10.1016/j.trsl.2021.05.005

9. Lebrun A, Kean RB, Hooper DC. Brain tissue-resident immune memory cells are required for long-term protection against cns infection with rabies virus. *Future Virol* (2020) 15(11):755–61. doi: 10.2217/fvl-2020-0132

10. Fan B, Wei Z, Yao X, Shi G, Cheng X, Zhou X, et al. Microenvironment imbalance of spinal cord injury. *Cell Transplant* (2018) 27(6):853–66. doi: 10.1177/0963689718755778

11. Boyce VS, Mendell LM. Neurotrophins and spinal circuit function. *Front Neural Circuits* (2014) 8:59. doi: 10.3389/fncir.2014.00059

12. Baizer JS. Unique features of the human brainstem and cerebellum. *Front Hum Neurosci* (2014) 8:202. doi: 10.3389/fnhum.2014.00202

13. Middleton FA, Strick PL. Anatomical evidence for cerebellar and basal ganglia involvement in higher cognitive function. *Science* (1994) 266(5184):458–61. doi: 10.1126/science.7939688

14. Middleton FA, Strick PL. Basal ganglia and cerebellar loops: Motor and cognitive circuits. *Brain Res Brain Res Rev* (2000) 31(2-3):236–50. doi: 10.1016/s0165-0173(99)00040-5

15. Middleton FA, Strick PL. Basal ganglia and cerebellar output influences non-motor function. *Mol Psychiatry* (1996) 1(6):429–33.

16. Middleton FA, Strick PL. Cerebellar output channels. *Int Rev Neurobiol* (1997) 41:61–82. doi: 10.1016/s0074-7742(08)60347-5

17. Middleton FA, Strick PL. Dentate output channels: Motor and cognitive components. *Prog Brain Res* (1997) 114:553–66. doi: 10.1016/s0079-6123(08)63386-5

18. Middleton FA, Strick PL. Cerebellar output: Motor and cognitive channels. *Trends Cognit Sci* (1998) 2(9):348–54. doi: 10.1016/s1364-6613(98)01220-0

19. Sulkowski G, Dąbrowska-Bouta B, Salińska E, Strużyńska L. Modulation of glutamate transport and receptor binding by glutamate receptor antagonists in eae rat brain. *PloS One* (2014) 9(11):e113954. doi: 10.1371/journal.pone.0113954

20. Shen J, Rothman DL, Behar KL, Xu S. Determination of the glutamate-glutamine cycling flux using two-compartment dynamic metabolic modeling is sensitive to astroglial dilution. *J Cereb Blood Flow Metab* (2009) 29(1):108–18. doi: 10.1038/jcbfm.2008.102

21. Catala M, Kubis N. Gross anatomy and development of the peripheral nervous system. *Handb Clin Neurol* (2013) 115:29–41. doi: 10.1016/b978-0-444-52902-2.00003-5

22. Calaresu FR, Ciriello J. Renal afferent nerves affect discharge rate of medullary and hypothalamic single units in the cat. *J Auton Nerv Syst* (1981) 3 (2-4):311–20. doi: 10.1016/0165-1838(81)90072-2

23. Ciriello J. Afferent renal inputs to paraventricular nucleus vasopressin and oxytocin neurosecretory neurons. *Am J Physiol* (1998) 275(6):R1745–54. doi: 10.1152/ajpregu.1998.275.6.R1745

24. Wang Y, Liu S, Liu Q, Lv Y. The interaction of central nervous system and acute kidney injury: Pathophysiology and clinical perspectives. *Front Physiol* (2022) 13:826686. doi: 10.3389/fphys.2022.826686

25. Alliot F, Godin I, Pessac B. Microglia derive from progenitors, originating from the yolk sac, and which proliferate in the brain. *Brain Res Dev Brain Res* (1999) 117(2):145–52. doi: 10.1016/s0165-3806(99)00113-3

26. Lawson LJ, Perry VH, Dri P, Gordon S. Heterogeneity in the distribution and morphology of microglia in the normal adult mouse brain. *Neuroscience* (1990) 39(1):151–70. doi: 10.1016/0306-4522(90)90229-w

27. Devanney NA, Stewart AN, Gensel JC. Microglia and macrophage metabolism in cns injury and disease: The role of immunometabolism in neurodegeneration and neurotrauma. *Exp Neurol* (2020) 329:113310. doi: 10.1016/j.expneurol.2020.113310

28. Gensel JC, Zhang B. Macrophage activation and its role in repair and pathology after spinal cord injury. *Brain Res* (2015) 1619:1–11. doi: 10.1016/j.brainres.2014.12.045

29. Tang Y, Le W. Differential roles of M1 and M2 microglia in neurodegenerative diseases. *Mol Neurobiol* (2016) 53(2):1181–94. doi: 10.1007/s12035-014-9070-5

30. Mills CD, Kincaid K, Alt JM, Heilman MJ, Hill AM. M-1/M-2 macrophages and the Th1/Th2 paradigm. *J Immunol* (2000) 164(12):6166–73. doi: 10.4049/jimmunol.164.12.6166

31. Wright-Jin EC, Gutmann DH. Microglia as dynamic cellular mediators of brain function. *Trends Mol Med* (2019) 25(11):967–79. doi: 10.1016/j.molmed.2019.08.013

32. Takahashi K, Aranami T, Endoh M, Miyake S, Yamamura T. The regulatory role of natural killer cells in multiple sclerosis. *Brain* (2004) 127(Pt 9):1917–27. doi: 10.1093/brain/awh219

33. Nimmerjahn A, Kirchhoff F, Helmchen F. Resting microglial cells are highly dynamic surveillants of brain parenchyma in vivo. *Science* (2005) 308(5726):1314–8. doi: 10.1126/science.1110647

34. Miron VE, Boyd A, Zhao JW, Yuen TJ, Ruckh JM, Shadrach JL, et al. M2 microglia and macrophages drive oligodendrocyte differentiation during cns remyelination. *Nat Neurosci* (2013) 16(9):1211–8. doi: 10.1038/nn.3469

35. Boudreau JE, Hsu KC. Natural killer cell education and the response to infection and cancer therapy: Stay tuned. *Trends Immunol* (2018) 39(3):222–39. doi: 10.1016/j.it.2017.12.001

36. Bluestone JA, Mackay CR, O'Shea JJ, Stockinger B. The functional plasticity of T cell subsets. *Nat Rev Immunol* (2009) 9(11):811–6. doi: 10.1038/nri2654

37. Engelhardt B, Ransohoff RM. The ins and outs of T-lymphocyte trafficking to the cns: Anatomical sites and molecular mechanisms. *Trends Immunol* (2005) 26(9):485–95. doi: 10.1016/j.it.2005.07.004

38. Constant S, Schweitzer N, West J, Ranney P, Bottomly K. B lymphocytes can be competent antigen-presenting cells for priming Cd4+ T cells to protein antigens in vivo. *J Immunol* (1995) 155(8):3734–41.

39. Finkelman FD, Lees A, Morris SC. Antigen presentation by b lymphocytes to Cd4+ T lymphocytes in vivo: Importance for b lymphocyte and T lymphocyte activation. *Semin Immunol* (1992) 4(4):247–55.

40. Pistoia V. Production of cytokines by human b cells in health and disease. *Immunol Today* (1997) 18(7):343–50. doi: 10.1016/s0167-5699(97)01080-3

41. Kipnis J, Cohen H, Cardon M, Ziv Y, Schwartz M. T Cell deficiency leads to cognitive dysfunction: Implications for therapeutic vaccination for schizophrenia and other psychiatric conditions. *Proc Natl Acad Sci U.S.A.* (2004) 101(21):8180–5. doi: 10.1073/pnas.0402268101

42. Hu X, Leak RK, Shi Y, Suenaga J, Gao Y, Zheng P, et al. Microglial and macrophage polarization–new prospects for brain repair. *Nat Rev Neurol* (2015) 11(1):56–64. doi: 10.1038/nrneurol.2014.207

43. Martinez FO, Gordon S. The M1 and M2 paradigm of macrophage activation: Time for reassessment. *F1000Prime Rep* (2014) 6:13. doi: 10.12703/p6-13

44. Jassam YN, Izzy S, Whalen M, McGavern DB, El Khoury J. Neuroimmunology of traumatic brain injury: Time for a paradigm shift. *Neuron* (2017) 95(6):1246–65. doi: 10.1016/j.neuron.2017.07.010

45. Morganti JM, Riparip LK, Rosi S. Call off the Dog(Ma): M1/M2 polarization is concurrent following traumatic brain injury. *PloS One* (2016) 11(1):e0148001. doi: 10.1371/journal.pone.0148001

46. Li Q, Barres BA. Microglia and macrophages in brain homeostasis and disease. *Nat Rev Immunol* (2018) 18(4):225–42. doi: 10.1038/nri.2017.125

47. Bohlen CJ, Friedman BA, Dejanovic B, Sheng M. Microglia in brain development, homeostasis, and neurodegeneration. *Annu Rev Genet* (2019) 53:263–88. doi: 10.1146/annurev-genet-112618-043515

48. Frost JL, Schafer DP. Microglia: Architects of the developing nervous system. *Trends Cell Biol* (2016) 26(8):587–97. doi: 10.1016/j.tcb.2016.02.006

49. Heneka MT, Kummer MP, Latz E. Innate immune activation in neurodegenerative disease. *Nat Rev Immunol* (2014) 14(7):463–77. doi: 10.1038/nri3705

50. Hickey WF. Leukocyte traffic in the central nervous system: The participants and their roles. *Semin Immunol* (1999) 11(2):125–37. doi: 10.1006/smim.1999.0168

51. Pachter JS, de Vries HE, Fabry Z. The blood-brain barrier and its role in immune privilege in the central nervous system. *J Neuropathol Exp Neurol* (2003) 62(6):593–604. doi: 10.1093/jnen/62.6.593

52. Kunis G, Baruch K, Rosenzweig N, Kertser A, Miller O, Berkutzki T, et al. Ifn-Γ-Dependent activation of the brain's choroid plexus for cns immune surveillance and repair. *Brain* (2013) 136(Pt 11):3427–40. doi: 10.1093/brain/awt259

53. Louveau A, Plog BA, Antila S, Alitalo K, Nedergaard M, Kipnis J. Understanding the functions and relationships of the glymphatic system and meningeal lymphatics. *J Clin Invest* (2017) 127(9):3210–9. doi: 10.1172/jci90603

54. Raper D, Louveau A, Kipnis J. How do meningeal lymphatic vessels drain the cns? *Trends Neurosci* (2016) 39(9):581–6. doi: 10.1016/j.tins.2016.07.001

55. Harris DP, Haynes L, Sayles PC, Duso DK, Eaton SM, Lepak NM, et al. Reciprocal regulation of polarized cytokine production by effector b and T cells. *Nat Immunol* (2000) 1(6):475–82. doi: 10.1038/82717

56. Ware CF, VanArsdale TL, Crowe PD, Browning JL. The ligands and receptors of the lymphotoxin system. *Curr Top Microbiol Immunol* (1995) 198:175–218. doi: 10.1007/978-3-642-79414-8_11

57. Cui D, Tang Y, Jiang Q, Jiang D, Zhang Y, Lv Y, et al. Follicular helper T cells in the immunopathogenesis of sars-Cov-2 infection. *Front Immunol* (2021) 12:731100.. doi: 10.3389/fimmu.2021.731100

58. Wang G, Xiang Z, Wang W, Chen Z. Seasonal coronaviruses and sars-Cov-2: Effects of preexisting immunity during the covid-19 pandemic. *J Zhejiang University-Sci B* (2022) 23(6):451–60. doi: 10.1631/jzus.B2200049

59. Brioschi S, Wang WL, Peng V, Wang M, Shchukina I, Greenberg ZJ, et al. Heterogeneity of meningeal b cells reveals a lymphopoietic niche at the cns borders. *Science* (2021) 373(6553). doi: 10.1126/science.abf9277

60. Schafflick D, Wolbert J, Heming M, Thomas C, Hartlehnert M, Börsch AL, et al. Single-cell profiling of cns border compartment leukocytes reveals that b cells and their progenitors reside in non-diseased meninges. *Nat Neurosci* (2021) 24(9):1225–34. doi: 10.1038/s41593-021-00880-y

61. Ankeny DP, Popovich PG. B cells and autoantibodies: Complex roles in cns injury. *Trends Immunol* (2010) 31(9):332–8. doi: 10.1016/j.it.2010.06.006

62. Weber MS, Prod'homme T, Patarroyo JC, Molnarfi N, Karnezis T, Lehmann-Horn K, et al. B-cell activation influences T-cell polarization and outcome of anti-Cd20 b-cell depletion in central nervous system autoimmunity. *Ann Neurol* (2010) 68(3):369–83. doi: 10.1002/ana.22081

63. Cervenak L, Magyar A, Boja R, László G. Differential expression of Gl7 activation antigen on bone marrow b cell subpopulations and peripheral b cells. *Immunol Lett* (2001) 78(2):89–96. doi: 10.1016/s0165-2478(01)00239-5

64. Lehmann-Horn K, Schleich E, Hertzenberg D, Hapfelmeier A, Kümpfel T, von Bubnoff N, et al. Anti-Cd20 b-cell depletion enhances monocyte reactivity in neuroimmunological disorders. *J Neuroinflamm* (2011) 8:146. doi: 10.1186/1742-2094-8-146

65. Martinez-Pasamar S, Abad E, Moreno B, Velez de Mendizabal N, Martinez-Forero I, Garcia-Ojalvo J, et al. Dynamic cross-regulation of antigen-specific effector and regulatory T cell subpopulations and microglia in brain autoimmunity. *BMC Syst Biol* (2013) 7:34. doi: 10.1186/1752-0509-7-34

66. Cantrell D. Signaling in lymphocyte activation. *Cold Spring Harb Perspect Biol* (2015) 7(6). doi: 10.1101/cshperspect.a018788

67. Pearce EL, Poffenberger MC, Chang CH, Jones RG. Fueling immunity: Insights into metabolism and lymphocyte function. *Science* (2013) 342(6155):1242454. doi: 10.1126/science.1242454

68. Brynskikh A, Warren T, Zhu J, Kipnis J. Adaptive immunity affects learning behavior in mice. *Brain Behav Immun* (2008) 22(6):861–9. doi: 10.1016/j.bbi.2007.12.008

69. Derecki NC, Cardani AN, Yang CH, Quinnies KM, Crihfield A, Lynch KR, et al. Regulation of learning and memory by meningeal immunity: A key role for il-4. *J Exp Med* (2010) 207(5):1067–80. doi: 10.1084/jem.20091419

70. Hazenberg MD, Spits H. Human innate lymphoid cells. *Blood* (2014) 124(5):700–9. doi: 10.1182/blood-2013-11-427781

71. Vivier E, Tomasello E, Baratin M, Walzer T, Ugolini S. Functions of natural killer cells. *Nat Immunol* (2008) 9(5):503–10. doi: 10.1038/ni1582

72. Han S, Lin YC, Wu T, Salgado AD, Mexhitaj I, Wuest SC, et al. Comprehensive immunophenotyping of cerebrospinal fluid cells in patients with neuroimmunological diseases. *J Immunol* (2014) 192(6):2551–63. doi: 10.4049/jimmunol.1302884

73. Liu Q, Sanai N, Jin WN, La Cava A, Van Kaer L, Shi FD. Neural stem cells sustain natural killer cells that dictate recovery from brain inflammation. *Nat Neurosci* (2016) 19(2):243–52. doi: 10.1038/nn.4211

74. Zhang L, Zhang Y, Fan D. Pathological role of natural killer cells in parkinson's disease: A systematic review. *Front Aging Neurosci* (2022) 14:890816. doi: 10.3389/fnagi.2022.890816

75. Earls RH, Lee JK. The role of natural killer cells in parkinson's disease. *Exp Mol Med* (2020) 52(9):1517–25. doi: 10.1038/s12276-020-00505-7

76. Antel J, Owens T. Multiple sclerosis and immune regulatory cells. *Brain* (2004) 127(Pt 9):1915–6. doi: 10.1093/brain/awh272

77. Matsumoto Y, Kohyama K, Aikawa Y, Shin T, Kawazoe Y, Suzuki Y, et al. Role of natural killer cells and tcr gamma delta T cells in acute autoimmune encephalomyelitis. *Eur J Immunol* (1998) 28(5):1681–8. doi: 10.1002/(SICI)1521-4141(199805)28:05<1681::AID-IMMU1681>3.0.CO;2-T

78. Campagnolo DI, Dixon D, Schwartz J, Bartlett JA, Keller SE. Altered innate immunity following spinal cord injury. *Spinal Cord* (2008) 46(7):477–81. doi: 10.1038/sc.2008.4

79. Uddin I, Joshi K, Oakes T, Heather JM, Swanton C, Chain B. An economical, quantitative, and robust protocol for high-throughput T cell receptor sequencing from tumor or blood. *Methods Mol Biol* (2019) 1884:15–42. doi: 10.1007/978-1-4939-8885-3_2

80. Han RT, Kim RD, Molofsky AV, Liddelow SA. Astrocyte-immune cell interactions in physiology and pathology. *Immunity* (2021) 54(2):211–24. doi: 10.1016/j.immuni.2021.01.013

81. Schwartz M, Raposo C. Protective autoimmunity: A unifying model for the immune network involved in cns repair. *Neuroscientist* (2014) 20(4):343–58. doi: 10.1177/1073858413516799

82. Buck MD, O'Sullivan D, Pearce EL. T Cell metabolism drives immunity. *J Exp Med* (2015) 212(9):1345–60. doi: 10.1084/jem.20151159

83. Wu J, Guo Y, Lu X, Huang F, Lv F, Wei D, et al. Th1/Th2 cells and associated cytokines in acute hepatitis e and related acute liver failure. *J Immunol Res* (2020) 2020. doi: 10.1155/2020/6027361

84. Li P, Zhang Y, Xu Y, Cao H, Li L. Characteristics of Cd8+ and Cd4+ tissue-resident memory lymphocytes in the gastrointestinal tract. *Adv Gut Microbiome Res* (2022) 2022. doi: 10.1155/2022/9157455

85. Baruch K, Ron-Harel N, Gal H, Deczkowska A, Shifrut E, Ndifon W, et al. Cns-specific immunity at the choroid plexus shifts toward destructive Th2 inflammation in brain aging. *Proc Natl Acad Sci U.S.A.* (2013) 110(6):2264–9. doi: 10.1073/pnas.1211270110

86. Zorzella-Pezavento SF, Chiuso-Minicucci F, França TG, Ishikawa LL, da Rosa LC, Colavite PM, et al. Downmodulation of peripheral mog-specific immunity by Pvaxhsp65 treatment during eae does not reach the cns. *J Neuroimmunol* (2014) 268(1-2):35–42. doi: 10.1016/j.jneuroim.2013.12.015

87. Huang X, Hussain B, Chang J. Peripheral inflammation and blood-brain barrier disruption: Effects and mechanisms. *CNS Neurosci Ther* (2021) 27(1):36–47. doi: 10.1111/cns.13569

88. Ramaglia V, Florescu A, Zuo M, Sheikh-Mohamed S, Gommerman JL. Stromal cell-mediated coordination of immune cell recruitment, retention, and function in brain-adjacent regions. *J Immunol* (2021) 206(2):282–91. doi: 10.4049/jimmunol.2000833

89. Avraham O, Feng R, Ewan EE, Rustenhoven J, Zhao G, Cavalli V. Profiling sensory neuron microenvironment after peripheral and central axon injury reveals key pathways for neural repair. *Elife* (2021) 10. doi: 10.7554/eLife.68457

90. Ludwig PE, Reddy V, Varacallo M. Neuroanatomy, central nervous system (Cns). In: *Statpearls*. Treasure Island (FL: StatPearls Publishing Copyright © 2022, StatPearls Publishing LLC (2022).

91. Croese T, Castellani G, Schwartz M. Immune cell compartmentalization for brain surveillance and protection. *Nat Immunol* (2021) 22(9):1083–92. doi: 10.1038/s41590-021-00994-2

92. Chen Z, Liu P, Xia X, Wang L, Li X. Living on the border of the cns: Dural immune cells in health and disease. *Cell Immunol* (2022) 377:104545. doi: 10.1016/j.cellimm.2022.104545

93. Friebel E, Kapolou K, Unger S, Núñez NG, Utz S, Rushing EJ, et al. Single-cell mapping of human brain cancer reveals tumor-specific instruction of tissue-invading leukocytes. *Cell* (2020) 181(7):1626–42.e20. doi: 10.1016/j.cell.2020.04.055

94. Coté TR, Manns A, Hardy CR, Yellin FJ, Hartge P. Epidemiology of brain lymphoma among people with or without acquired immunodeficiency syndrome. *Aids/Cancer Study Group J Natl Cancer Inst* (1996) 88(10):675–9. doi: 10.1093/jnci/88.10.675

95. Gandhi MK, Hoang T, Law SC, Brosda S, O'Rourke K, Tobin JWD, et al. Ebv-associated primary cns lymphoma occurring after immunosuppression is a distinct immunobiological entity. *Blood* (2021) 137(11):1468–77. doi: 10.1182/blood.2020008520

96. Zhai H, Heppner FL, Tsirka SE. Microglia/Macrophages promote glioma progression. *Glia* (2011) 59(3):472–85. doi: 10.1002/glia.21117

97. Lukas RV, Wainwright DA, Ladomersky E, Sachdev S, Sonabend AM, Stupp R. Newly diagnosed glioblastoma: A review on clinical management. *Oncol (Williston Park)* (2019) 33(3):91–100.

98. Molinaro AM, Taylor JW, Wiencke JK, Wrensch MR. Genetic and molecular epidemiology of adult diffuse glioma. *Nat Rev Neurol* (2019) 15(7):405–17. doi: 10.1038/s41582-019-0220-2

99. Vargas López AJ. Glioblastoma in adults: A society for neuro-oncology (Sno) and European society of neuro-oncology (Eano) consensus review on current management and future directions. *Neuro Oncol* (2021) 23(3):502–3. doi: 10.1093/neuonc/noaa287

100. Brat DJ, Aldape K, Colman H, Holland EC, Louis DN, Jenkins RB, et al. Cimpact-now update 3: Recommended diagnostic criteria for "Diffuse astrocytic glioma, idh-wildtype, with molecular features of glioblastoma, who grade iv". *Acta Neuropathol* (2018) 136(5):805–10. doi: 10.1007/s00401-018-1913-0

101. Badie B, Schartner J, Klaver J, Vorpahl J. *In vitro* modulation of microglia motility by glioma cells is mediated by hepatocyte growth Factor/Scatter factor. *Neurosurgery* (1999) 44(5):1077–82. doi: 10.1097/00006123-199905000-00075

102. Bettinger I, Thanos S, Paulus W. Microglia promote glioma migration. *Acta Neuropathol* (2002) 103(4):351–5. doi: 10.1007/s00401-001-0472-x

103. Carvalho da Fonseca AC, Wang H, Fan H, Chen X, Zhang I, Zhang L, et al. Increased expression of stress inducible protein 1 in glioma-associated Microglia/Macrophages. *J Neuroimmunol* (2014) 274(1-2):71–7. doi: 10.1016/j.jneuroim.2014.06.021

104. Wei J, Gabrusiewicz K, Heimberger A. The controversial role of microglia in malignant gliomas. *Clin Dev Immunol* (2013) 2013:285246. doi: 10.1155/2013/285246

105. Dorward IG, Luo J, Perry A, Gutmann DH, Mansur DB, Rubin JB, et al. Postoperative imaging surveillance in pediatric pilocytic astrocytomas. *J Neurosurg Pediatr* (2010) 6(4):346–52. doi: 10.3171/2010.7.Peds10129

106. Aldape K, Brindle KM, Chesler L, Chopra R, Gajjar A, Gilbert MR, et al. Challenges to curing primary brain tumours. *Nat Rev Clin Oncol* (2019) 16(8):509–20. doi: 10.1038/s41571-019-0177-5

107. Lu-Emerson C, Snuderl M, Kirkpatrick ND, Goveia J, Davidson C, Huang Y, et al. Increase in tumor-associated macrophages after antiangiogenic therapy is associated with poor survival among patients with recurrent glioblastoma. *Neuro Oncol* (2013) 15(8):1079–87. doi: 10.1093/neuonc/not082

108. Chen DS, Mellman I. Oncology meets immunology: The cancer-immunity cycle. *Immunity* (2013) 39(1):1–10. doi: 10.1016/j.immuni.2013.07.012

109. Tesniere A, Panaretakis T, Kepp O, Apetoh L, Ghiringhelli F, Zitvogel L, et al. Molecular characteristics of immunogenic cancer cell death. *Cell Death Differ* (2008) 15(1):3–12. doi: 10.1038/sj.cdd.4402269

110. Robert C, Long GV, Brady B, Dutriaux C, Maio M, Mortier L, et al. Nivolumab in previously untreated melanoma without braf mutation. *N Engl J Med* (2015) 372(4):320–30. doi: 10.1056/NEJMoa1412082

111. Wolchok JD, Kluger H, Callahan MK, Postow MA, Rizvi NA, Lesokhin AM, et al. Nivolumab plus ipilimumab in advanced melanoma. *N Engl J Med* (2013) 369(2):122–33. doi: 10.1056/NEJMoa1302369

112. Jia RX, Liang JH, Xu Y, Wang YQ. Effects of physical activity and exercise on the cognitive function of patients with Alzheimer disease: A meta-analysis. *BMC Geriatr* (2019) 19(1):181. doi: 10.1186/s12877-019-1175-2

113. Armstrong R. What causes neurodegenerative disease? *Folia Neuropathol* (2020) 58(2):93–112. doi: 10.5114/fn.2020.96707

114. Ownby RL. Quetiapine and rivastigmine for agitation in alzheimer's disease. *Curr Psychiatry Rep* (2006) 8(1):10. doi: 10.1007/s11920-006-0075-2

115. Hirsch L, Jette N, Frolkis A, Steeves T, Pringsheim T. The incidence of parkinson's disease: A systematic review and meta-analysis. *Neuroepidemiology* (2016) 46(4):292–300. doi: 10.1159/000445751

116. Vinters HV. Emerging concepts in alzheimer's disease. *Annu Rev Pathol* (2015) 10:291–319. doi: 10.1146/annurev-pathol-020712-163927

117. Sawada M, Sawada H, Nagatsu T. Effects of aging on neuroprotective and neurotoxic properties of microglia in neurodegenerative diseases. *Neurodegener Dis* (2008) 5(3-4):254–6. doi: 10.1159/000113717

118. Wu J, Lu WY, Cui LL. Clinical significance of Stat3 and mapk phosphorylation, and the protein expression of cyclin D1 in skin squamous cell carcinoma tissues. *Mol Med Rep* (2015) 12(6):8129–34. doi: 10.3892/mmr.2015.4460

119. Sawada M, Imamura K, Nagatsu T. Role of cytokines in inflammatory process in parkinson's disease. *J Neural Transm Suppl* (2006) 70):373–81. doi: 10.1007/978-3-211-45295-0_57

120. Popovich P, McTigue D. Damage control in the nervous system: Beware the immune system in spinal cord injury. *Nat Med* (2009) 15(7):736–7. doi: 10.1038/nm0709-736

121. Vargas ME, Barres BA. Why is wallerian degeneration in the cns so slow? *Annu Rev Neurosci* (2007) 30:153–79. doi: 10.1146/annurev.neuro.30.051606.094354

122. Hsu JY, McKeon R, Goussev S, Werb Z, Lee JU, Trivedi A, et al. Matrix metalloproteinase-2 facilitates wound healing events that promote functional recovery after spinal cord injury. *J Neurosci* (2006) 26(39):9841–50. doi: 10.1523/jneurosci.1993-06.2006

123. Lindborg JA, Mack M, Zigmond RE. Neutrophils are critical for myelin removal in a peripheral nerve injury model of wallerian degeneration. *J Neurosci* (2017) 37(43):10258–77. doi: 10.1523/jneurosci.2085-17.2017

124. Alexander JK, Popovich PG. Neuroinflammation in spinal cord injury: Therapeutic targets for neuroprotection and regeneration. *Prog Brain Res* (2009) 175:125–37. doi: 10.1016/s0079-6123(09)17508-8

125. Hawthorne AL, Popovich PG. Emerging concepts in myeloid cell biology after spinal cord injury. *Neurotherapeutics* (2011) 8(2):252–61. doi: 10.1007/s13311-011-0032-6

126. Wang X, Cao K, Sun X, Chen Y, Duan Z, Sun L, et al. Macrophages in spinal cord injury: Phenotypic and functional change from exposure to myelin debris. *Glia* (2015) 63(4):635–51. doi: 10.1002/glia.22774

127. Milich LM, Ryan CB, Lee JK. The origin, fate, and contribution of macrophages to spinal cord injury pathology. *Acta Neuropathol* (2019) 137 (5):785–97. doi: 10.1007/s00401-019-01992-3

128. Donnelly DJ, Longbrake EE, Shawler TM, Kigerl KA, Lai W, Tovar CA, et al. Deficient Cx3cr1 signaling promotes recovery after mouse spinal cord injury by limiting the recruitment and activation of Ly6clo/Inos+ macrophages. *J Neurosci* (2011) 31(27):9910–22. doi: 10.1523/jneurosci.2114-11.2011

129. García-Alías G, Barkhuysen S, Buckle M, Fawcett JW. Chondroitinase abc treatment opens a window of opportunity for task-specific rehabilitation. *Nat Neurosci* (2009) 12(9):1145–51. doi: 10.1038/nn.2377

130. Campagnolo DI, Bartlett JA, Keller SE, Sanchez W, Oza R. Impaired phagocytosis of staphylococcus aureus in complete tetraplegics. *Am J Phys Med Rehabil* (1997) 76(4):276–80. doi: 10.1097/00002060-199707000-00005

131. Campagnolo DI, Keller SE, DeLisa JA, Glick TJ, Sipski ML, Schleifer SJ. Alteration of immune system function in tetraplegics. a pilot study. *Am J Phys Med Rehabil* (1994) 73(6):387–93. doi: 10.1097/00002060-199411000-00003

132. Griffin GD. The injured brain: Tbi, mtbi, the immune system, and infection: Connecting the dots. *Mil Med* (2011) 176(4):364–8. doi: 10.7205/milmed-d-10-00021

133. Roth TL, Nayak D, Atanasijevic T, Koretsky AP, Latour LL, McGavern DB. Transcranial amelioration of inflammation and cell death after brain injury. *Nature* (2014) 505(7482):223–8. doi: 10.1038/nature12808

134. Maas AI, Stocchetti N, Bullock R. Moderate and severe traumatic brain injury in adults. *Lancet Neurol* (2008) 7(8):728–41. doi: 10.1016/s1474-4422(08)70164-9

135. Lu J, Goh SJ, Tng PY, Deng YY, Ling EA, Moochhala S. Systemic inflammatory response following acute traumatic brain injury. *Front Biosci (Landmark Ed)* (2009) 14(10):3795–813. doi: 10.2741/3489

136. Binder RJ. Functions of heat shock proteins in pathways of the innate and adaptive immune system. *J Immunol* (2014) 193(12):5765–71. doi: 10.4049/jimmunol.1401417

137. Davalos D, Grutzendler J, Yang G, Kim JV, Zuo Y, Jung S, et al. Atp mediates rapid microglial response to local brain injury in vivo. *Nat Neurosci* (2005) 8(6):752–8. doi: 10.1038/nn1472

138. Gold M, El Khoury J. β-amyloid, microglia, and the inflammasome in alzheimer's disease. *Semin Immunopathol* (2015) 37(6):607–11. doi: 10.1007/s00281-015-0518-0

139. Liu HD, Li W, Chen ZR, Hu YC, Zhang DD, Shen W, et al. Expression of the Nlrp3 inflammasome in cerebral cortex after traumatic brain injury in a rat model. *Neurochem Res* (2013) 38(10):2072–83. doi: 10.1007/s11064-013-1115-z

140. VanItallie TB. Traumatic brain injury (Tbi) in collision sports: Possible mechanisms of transformation into chronic traumatic encephalopathy (Cte). *Metabolism* (2019) 100s:153943. doi: 10.1016/j.metabol.2019.07.007

141. Edwards P, Arango M, Balica L, Cottingham R, El-Sayed H, Farrell B, et al. Final results of mrc crash, a randomised placebo-controlled trial of intravenous corticosteroid in adults with head injury-outcomes at 6 months. *Lancet* (2005) 365 (9475):1957–9. doi: 10.1016/s0140-6736(05)66552-x

142. Loane DJ, Kumar A. Microglia in the tbi brain: The good, the bad, and the dysregulated. *Exp Neurol* (2016) 275 Pt 3(03):316–27. doi: 10.1016/j.expneurol.2015.08.018

143. Acosta SA, Tajiri N, Shinozuka K, Ishikawa H, Grimmig B, Diamond DM, et al. Long-term upregulation of inflammation and suppression of cell proliferation in the brain of adult rats exposed to traumatic brain injury using the controlled cortical impact model. *PloS One* (2013) 8(1):e53376. doi: 10.1371/journal.pone.0053376

144. Elkabes S, DiCicco-Bloom EM, Black IB. Brain Microglia/Macrophages express neurotrophins that selectively regulate microglial proliferation and function. *J Neurosci* (1996) 16(8):2508–21. doi: 10.1523/jneurosci.16-08-02508.1996

145. David S, Kroner A. Repertoire of microglial and macrophage responses after spinal cord injury. *Nat Rev Neurosci* (2011) 12(7):388–99. doi: 10.1038/nrn3053

146. Shlosberg D, Benifla M, Kaufer D, Friedman A. Blood-brain barrier breakdown as a therapeutic target in traumatic brain injury. *Nat Rev Neurol* (2010) 6(7):393–403. doi: 10.1038/nrneurol.2010.74

147. Liu YW, Li S, Dai SS. Neutrophils in traumatic brain injury (Tbi): Friend or foe? *J Neuroinflamm* (2018) 15(1):146. doi: 10.1186/s12974-018-1173-x

148. Caplan HW, Cox CS, Bedi SS. Do microglia play a role in sex differences in tbi? *J Neurosci Res* (2017) 95(1-2):509–17. doi: 10.1002/jnr.23854

149. Damani MR, Zhao L, Fontainhas AM, Amaral J, Fariss RN, Wong WT. Age-related alterations in the dynamic behavior of microglia. *Aging Cell* (2011) 10 (2):263–76. doi: 10.1111/j.1474-9726.2010.00660.x

150. Doering P, Stoltenberg M, Penkowa M, Rungby J, Larsen A, Danscher G. Chemical blocking of zinc ions in cns increases neuronal damage following traumatic brain injury (Tbi) in mice. *PloS One* (2010) 5(4):e10131. doi: 10.1371/journal.pone.0010131

151. Aertker BM, Bedi S, Cox CSJr. Strategies for cns repair following tbi. *Exp Neurol* (2016) 275 Pt 3:411–26. doi: 10.1016/j.expneurol.2015.01.008

152. Ma SF, Chen YJ, Zhang JX, Shen L, Wang R, Zhou JS, et al. Adoptive transfer of M2 macrophages promotes locomotor recovery in adult rats after spinal cord injury. *Brain Behav Immun* (2015) 45:157–70. doi: 10.1016/j.bbi.2014.11.007

153. Nuki G, Bresnihan B, Bear MB, McCabe D. Long-term safety and maintenance of clinical improvement following treatment with anakinra (Recombinant human interleukin-1 receptor antagonist) in patients with rheumatoid arthritis: Extension phase of a randomized, double-blind, placebo-controlled trial. *Arthritis Rheum* (2002) 46(11):2838–46. doi: 10.1002/art.10578

154. Barker RA, Widner H. Immune problems in central nervous system cell therapy. *NeuroRx* (2004) 1(4):472–81. doi: 10.1602/neurorx.1.4.472

155. Michel-Monigadon D, Brachet P, Neveu I, Naveilhan P. Immunoregulatory properties of neural stem cells. *Immunotherapy* (2011) 3(4 Suppl):39–41. doi: 10.2217/imt.11.49

156. Goyal M, Avery JA. Paroxysmal disorders and the autonomic nervous system in pediatrics. *Am J Electroneurodiagn Technol* (2005) 45(4):240–7. doi: 10.1080/1086508X.2005.11079541

157. Popugaev KA, Lubnin AY, Zabelin MV, Samoylov AS. Autonomic nervous system and its imbalance in neuro intensive care unit. *Anesteziol Reanimatol* (2016) 61(2):137–42.

158. Lafaille FG, Pessach IM, Zhang SY, Ciancanelli MJ, Herman M, Abhyankar A, et al. Impaired intrinsic immunity to hsv-1 in human ipsc-derived Tlr3-deficient cns cells. *Nature* (2012) 491(7426):769–73. doi: 10.1038/nature11583

frontiers | Frontiers in Immunology

TYPE Original Research
PUBLISHED 21 November 2022
DOI 10.3389/fimmu.2022.1060290

Check for updates

OPEN ACCESS

EDITED BY
Bo Li,
Department of Orthopedics, Sun Yat-sen University, China

REVIEWED BY
Cailiang Shen,
First Affiliated Hospital of Anhui Medical University, China
Xiangyang Wang,
The Second Affiliated Hospital and Yuying Children's Hospital of Wenzhou Medical University, China
Desi Shang,
Harbin Medical University, Harbin, China

*CORRESPONDENCE
Xiaolong Chen
chensmalldragon@163.com
Shibao Lu
spinelu@163.com

SPECIALTY SECTION
This article was submitted to Multiple Sclerosis and Neuroimmunology, a section of the journal Frontiers in Immunology

RECEIVED 03 October 2022
ACCEPTED 28 October 2022
PUBLISHED 21 November 2022

CITATION
Li Y, Wang B, Sun W, Kong C, Li G, Chen X and Lu S (2022) Screening the immune-related circRNAs and genes in mice of spinal cord injury by RNA sequencing. *Front. Immunol.* 13:1060290. doi: 10.3389/fimmu.2022.1060290

COPYRIGHT
© 2022 Li, Wang, Sun, Kong, Li, Chen and Lu. This is an open-access article distributed under the terms of the Creative Commons Attribution License (CC BY). The use, distribution or reproduction in other forums is permitted, provided the original author(s) and the copyright owner(s) are credited and that the original publication in this journal is cited, in accordance with accepted academic practice. No use, distribution or reproduction is permitted which does not comply with these terms.

Screening the immune-related circRNAs and genes in mice of spinal cord injury by RNA sequencing

Yongjin Li[1], Baobao Wang[1], Wenzhi Sun[1], Chao Kong[1], Guowang Li[2], Xiaolong Chen[1]* and Shibao Lu[1]*

[1]Department of Orthopedics, Xuanwu Hospital, Capital Medical University, Beijing, China, [2]Graduate School, Tianjin Medical University, Tianjin, China

Spinal cord injury (SCI) is a pathological condition that leading to serious nerve damage, disability and even death. Increasing evidence have revealed that circular RNAs (circRNAs) and mRNA are widely involved in the regulation of the pathological process of neurological diseases by sponging microRNAs (miRNAs). Nevertheless, the potential biological functions and regulatory mechanisms of circRNAs in the subacute stage of SCI remain unclear. We analyzed the expression and regulatory patterns of circRNAs and mRNAs in SCI mice models using RNA-sequencing and bioinformatics analysis. A total of 24 circRNAs and 372 mRNAs were identified to be differentially expressed. Then we identifying the immune-related genes (IRGs) from them. The protein-protein interaction network were constructed based on the STRING database and Cytoscape software. Furthermore, Go and KEGG enrichment analysis were conducted to predict the functions of the IRGs and host genes of DECs. These findings will contribute to elucidate the pathophysiology of SCI and provide effective therapeutic targets for SCI patients.

KEYWORDS

spinal cord injury, RNA-sequencing, circular RNA, immune, inflammation

Introduction

Spinal cord injury (SCI) is a life-shattering central nervous system injury with high disability rate and mortality rate, which is known to bring serious social-economic burden around the world (1, 2). It has been reported that the annual incidence of SCI in different countries ranges from 11.5 to 57.8 cases per million people (3, 4), and these patients face a heavy economic burden and a significantly reduced quality of life because SCI is often accompanied by permanent neurological impairment and various complications (1, 5). At

present, the etiological classification of SCI is roughly divided into two categories: traumatic and nontraumatic injuries (2). The traffic and sports accident, violence and falls are the predominant causes of traumatic SCI (2, 3), while nontraumatic injuries is mainly caused by infection and tumor (2, 6). Some scholars have divided the pathophysiology of SCI into primary mechanism and secondary mechanism. SCI often start with primary mechanical injury, the structural integrity of the spinal cord is damaged under severe impact or continuous compression, which is usually the most important factor to determine the severity of SCI; then gradually progress into secondary SCI with a series of endogenous molecular pathological processes, such as the abnormally elevated inflammatory response, oxidative stress, and immune response (7–9). Secondary SCI can be divided into acute, subacute, and chronic stages, with the subacute stage lasting 2 days to 2 weeks after SCI (10, 11). The subacute stage of SCI is a potentially critical time point for further study of SCI repair, which may play a significant role in the secondary SCI (10, 11). Current treatments are limited and cannot completely recover the function of the spinal cord (12, 13), and the effective therapeutic strategies to avoid secondary SCI are still lacking. Therefore, it is very necessary to comprehensively and deeply understand the molecular pathological mechanisms following secondary SCI (especially in the subacute stage) to explore new therapeutic methods that promote the functional recovery of spinal cord.

Non-coding RNAs (ncRNAs) are a group of RNAs that regulate messenger RNAs (mRNAs), and its family includes circular RNAs (circRNAs), long-chain ncRNAs (lncRNAs), and microRNAs (miRNAs), most of which cannot encode proteins and can regulate cellular physiology and functions (14). CircRNA is a major regulatory single-stranded ncRNA and an important post-transcriptional regulatory element without 5' to 3' polarity and polyadenylated tail, its 5' and 3' ends are linked together to form a covalently closed circular structure, this special structure endows it with high stability and is not easily degraded by exonuclease, which can serve as novel diagnostic and prognostic biomarkers in many diseases (15–17). Accumulating evidence have suggested that miRNAs can accelerate target gene mRNAs degradation prevent its translation and reducing its expression by directly binding to the 3' untranslated region (3'UTR) of mRNAs in the cytoplasm (18, 19). As competing endogenous RNA (ceRNA), circRNAs were reported to be widely involved in regulating the pathological process after SCI by targeting miRNAs-mRNA pathway, such as inflammatory response, oxidative stress, cell death, autophagy, neuronal migration, and adhesion (20–28). Wang et al. (21) verified that the circPlek/miR-135b-5p/TGF-βR1 signaling axis is involved in the activation of fibroblasts and fibrous scar formation in the subacute stage of SCI. Nevertheless, the potential biological functions and regulatory mechanisms of circRNAs in the subacute stage of SCI remain unclear.

In this study, we construct a contusion SCI mouse model. High-throughput RNA-sequencing (RNA-seq) technology was utilized to measure the circRNAs and mRNAs expression profile on 4th day after SCI in mice. We identified 24 differentially expressed circRNAs (DECs) and 372 differentially expressed genes (DEGs). Then we identifying the immune-related genes (IRGs) from them. In addition, we conducted Go and KEGG enrichment analysis to predict the functions of the IRGs and host genes of DECs.

Material and methods

Construction of mouse SCI model

We purchased six C57BL/6 male mice (8 weeks, weights 20-25g) from the Institute of Radiation Medicine, Chinese Academy of Medical Sciences. They were randomly divided into 2 groups, namely control (n = 3) and SCI group (n = 3). The mice were anesthetized through intraperitoneal injection of 90 mg/kg ketamine and 10 mg/kg xylazine. Three control mice underwent a laminectomy at the T10 level without injury to the spinal cord, the other three experimental mice were placed on the NYU IMPACTOR MODEL-II spinal cord hitter platform after laminectomy at the T10 level, and the T10 spinal cord was hit with a hitting head weighing 10 grams to construct a SCI model. All the six mice were killed on the 4th day after surgery, and the spinal cord tissue about 4 cm long around the T10 level were collected for high-throughput RNA-sequencing. All mice procedures were in consistent with international and national animal care and ethical guidelines and have been approved by the institutional animal welfare committee.

Construction of sequencing library

The TRlzol kit (B511311, Sangon, China) was used to extract total RNAs from spinal cord tissues. Then we added RNase-free DNase I to remove genomic DNA. The ribosomal RNA was removed from total RNA with Ribo-off rRNA depletion kit (Nanjing, China). To measure RNA quality and purity, we used NanoPhotometer® spectrophotometer (IMPLEN, CA, USA) and an Agilent 2100 bioanalyzer (Agilent Technologies, CA, USA) for detection. Subsequently, VAHTSTM mRNA-seq V2 Library Prep Kit for Illumina® was used to construct sequencing libraries according to manufacturer's suggestions. High-quality RNA was further purified by a RNeasy mini kit (QIAGEN, GmBH, Germany). Finally, a HiSeq Xen sequencer (Illumina, San Diego, CA) was used for pair-end sequencing of the libraries.

Analysis of circRNAs and mRNAs expression profile

RNA sequencing program were conducted by Sangon Biotechnology Company (Shanghai, China). The quality of the

sequencing raw data was assessed by FastQC, and we then performed mass clipping using Trimmomatic to get relatively accurate valid data. The data were aligned to the reference genome using bwa, and circRNAs were then identified by CIRI2. The origination of circRNAs were determined based on their location information and known gene annotations using BEDtools. The expression of circRNAs was calculated by the reads per kilobase of transcript per million mapped reads (RPKM) formula based on BSJ reads. The expression of mRNAs was calculated by the transcripts per kilobase of exon model per million mapped reads (TKM) formula. The data processing were conducted using the R software package. The differentially expressed circRNAs (DECs) and differentially expressed mRNAs (DEMs) were analyzed using DESeq2 software. The screening criteria for DECs was $|\log_2$ fold-change (FC)$| > 2$ and P value < 0.05; and the screening criteria for DEMs was $|\log_2$ FC$| > 5$ and P.adj value < 0.01. Hierarchical Clustering and volcano plot were conducted to display the distinguishable circRNAs and mRNAs expression pattern among samples.

Identifying the IRGs related to SCI

We obtained the IRGs from the online immunology database and analysis portal (immport, https://www.immport.org/home) (29). Venn analysis was performed to select IRGs related to SCI through merging the DEGs and IRGs.

The pathway enrichment analysis

Gene Ontology (GO) functional annotations and Kyoto Encyclopedia of Genes and Genomes (KEGG) pathway enrichment analysis were conducted to predict the potential roles of the host genes of DECs. Briefly, GO analysis was applied to elucidate genetic regulatory networks of interest by forming hierarchical categories according to the BP, CC, and MF aspects of the differentially expressed genes (http://www.geneontology.org). Pathway analysis was performed to explore the significant pathways of the host genes of DECs according to KEGG (http://www.genome.jp/kegg/). The analytical results were visualized by clusterProfiler package in R (30). A value of p <0:05 was set as a statistically significant difference.

Construction protein-protein interaction network and identification of hub genes

The Search Tool for the Retrieval of Interacting Genes (STRING) database (https://cn.string-db.org/) was used to evaluate PPIs in functional protein association networks (31). Then we imported the DEGs into the multiple protein section of STRING database and set the organisms as "Mus musculus" to generate the PPI network data. The "required score" was set at > 0.4. Subsequently, the PPI data was imported into Cytoscape (https://cytoscape.org/) software to obtain the top 10 genes as hub genes using the Maximal Clique Centrality (MCC) method of the cytoHubba plugin (32) in Cytoscape.

Results

Determining the reasonable for the samples selection and grouping

This study collected 6 spinal cord tissues from normal and SCI mice for circRNA-sequencing. In order to ensure more reliable results of the bioinformatics analysis of the sequencing results, we carried out the correlation analysis of expression levels between samples, which is an important indicator to detect the reliability of the experiment and whether the sample selection is reasonable. As shown in Figures 1A–F, the pearson correlation coefficient among samples is close to 1, indicating that the expression patterns among samples are similar. The inter-sample correlation analysis Heatmap (Figure 1G) and the heatmap of distance between samples (Figure 1H) further revealed the high similarity among samples. Moreover, There was a greater differences between intra-group and inter-group, suggesting this grouping is meaningful (Figure 1I). Principal Component Analysis (PCA) can be used to reflect the difference and distance between samples. The closer the distance in the PCA diagram, the more similar the sample composition. Figure 1J presented that there was a relatively consistent similarity between samples and the grouping is reasonable. In addition, the uniformity of each group of repeated samples is good, and the following difference analysis can be carried out (Figure 1J). Taken together, these results unveiled that the samples selection and grouping meet experimental requirements.

The characteristics and expression profiles of circRNA in the subacute stage after SCI in mice

We found a total of 6341 circRNAs by circRNA sequencing. The length distribution and GC content distribution of them was shown in Figures 2A, B. Among them, circRNAs with 600-800 and more than 3800 base pairs and 45 GC content accounted for the largest proportion. Then, we evaluated the proportion of circRNAs derived from exons, introns, and intergenic regions in the identified circRNAs, Figure 2C displayed that the vast majority of circRNAs were derived from gene exons regions,

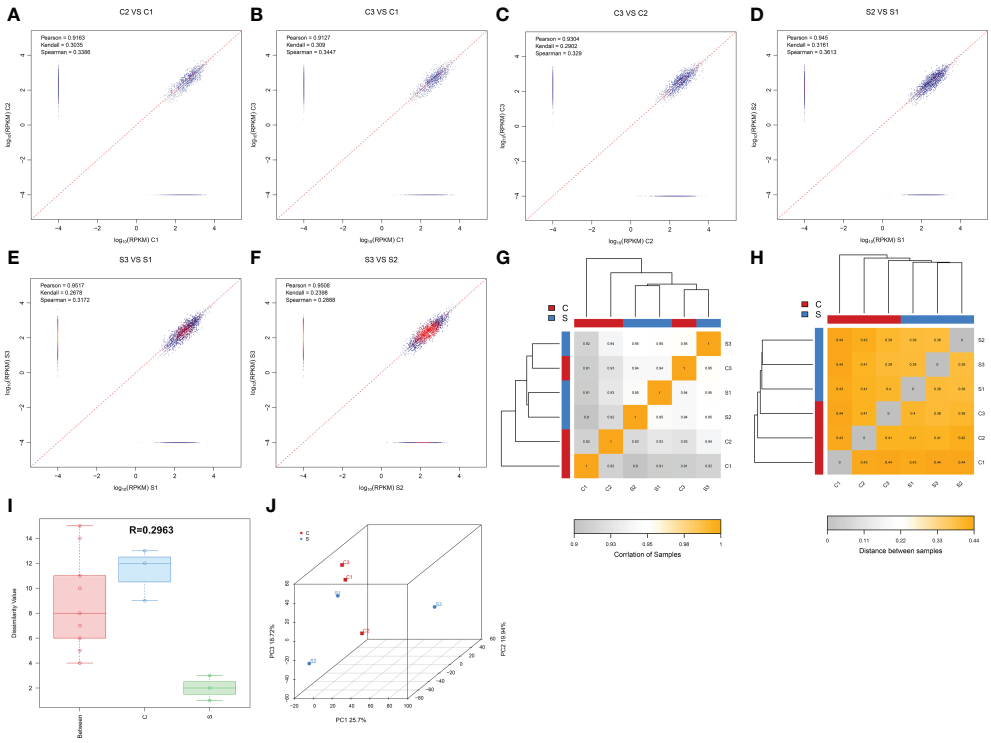


FIGURE 1
Determining the reasonable for the samples selection. **(A–F)** Duplicate correlation check scatter plot. The horizontal and vertical coordinates are the $\log_{10}$ (RPKM) values for the two samples, respectively. Three correlation indices are calculated in the figure: pearson, kendall, and spearman. The more similar the samples are, the closer the similarity index is to 1, and most of the points will be concentrated near the diagonal. **(G)** Inter-sample correlation analysis Heatmap. The color block represents the correlation index value. The grayer the color, the lower the correlation index among samples. The yellower the color, the higher the correlation index. **(H)** Heatmap of distance between samples. The color block represents the distance value. The grayer the color, the closer the distance between samples and the higher the similarity. The yellower the color, the farther the distance is. **(I)**: Anosim between-group similarity analysis boxplot. The boxes on the left refer to the between-group differences, and the middle and right boxes represent the within-group differences of the normal and SCI groups, respectively. The R value ranges from -1 to +1, with an R value closer to 1 indicating greater between-group differences than within-group differences. **(J)** Principal component analysis diagram, the horizontal and vertical coordinates reflect the relative distance between samples. Red points indicate control group, whereas green points indicate SCI group.

and a few circRNAs were derived from gene introns and intergenic regions. Most exonic circRNAs count were between 2-4 (Figure 2D). Interestingly, most exonic circRNAs were 4000 base pairs in length (Figure 2E). Zheng et al (33). reported that there was often a predominantly expressed circRNA isoform from one gene locus, our study also observed that most of the host genes produced one isoform (Figure 2F).

FPKM denoted the number of reads per kilobase length from a circRNA per million reads, which can be used to count the abundance of circRNA expression in different samples. RPKM method can eliminate the influence of circRNA length and sequencing quantity difference on the calculation of circRNA expression, and thus FPKM value represented the circRNA expression level. The circRNAs expression abundance in different samples were shown with density curve plot (Figure 2G) and violin plot (Figure 2H) using RPKM method, suggesting that the circRNAs were differential expression in the subacute phase after SCI in mice.

The circRNAs were differentially expressed in the subacute stage after SCI in mice

To compare differences in circRNA expression between the control group and the SCI group, we conducted circRNA differential expression analysis. The significance threshold was set as $|\log2\ (\text{fold-change})| > 2$ and P value < 0.05. Through the analysis of the sequencing results, we identified 24 DECs, of which 20 DECs were up-regulated and 4 DECs were down-regulated in the subacute stage after SCI in mice (Figure 3A). Hierarchical clustering analysis further unveiled the 24 DECs between normal

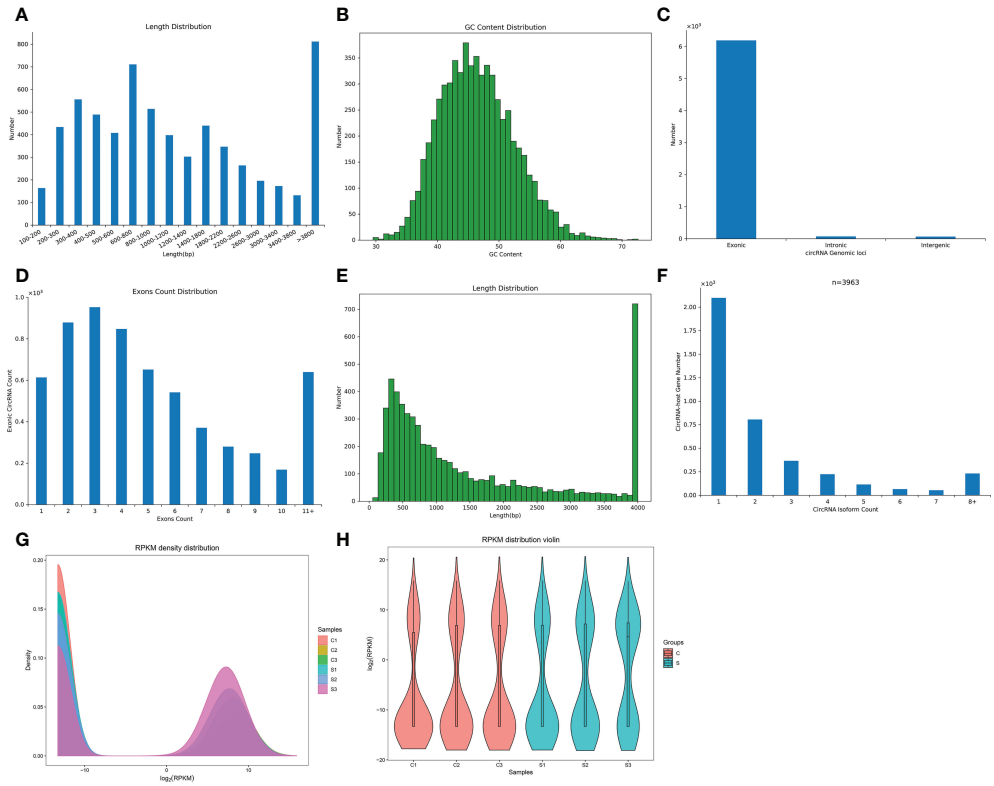


FIGURE 2
The characteristics and expression profiles of circRNA in the subacute stage after SCI in mice. **(A)** The length distribution of circRNAs. **(B)** The GC content distribution of circRNAs. **(C)** The statistical diagram of circRNAs sources. **(D)** The exons count distribution of circRNAs. **(E)**: The exons length distribution of circRNAs. **(F)** The distribution of circRNA host genes numbers and circRNA isoform count. **(G)** CircRNA expression density curve. The horizontal axis represent the log (RPKM) value, the higher the value, the higher the circRNA expression level; the vertical axis represent the corresponding relative density value, that is, the number of circRNAs on the horizontal axis/the total number of circRNAs. Each color represents a sample, the area of each region is 1, and the peak of the density curve represents the region with the most concentrated circRNA expression in the entire sample. **(H)** Violin plot of circRNA expression calculated using RPKM Reads. The horizontal axis represent the sample name, and the vertical axis represent the log (RPKM) value. The width of each violin reflects the number of circRNAs at that expression levels.

and SCI tissues (Figure 3B). According to the log2 (fold-change), the top 20 up-regulated and 4 down-regulated DECs in SCI tissues were visualized in Table 1 and Figure 3C, of which circRNA02778 and circRNA02370 were top up-regulated and circRNA05219 was top down-regulated DECs in SCI tissues. Furthermore, the specific expression of 24 DECs in 3 normal and 3 SCI tissues were further shown with ballon plot (Figure 3D). To explore the origin of these DECs, the distribution of DECs on chromosomes were analyzed. The results unveiled that these DECs were distributed on the human chromosomes 1-7, 9,11, and 14-19 (Figure 3E). To explore the interaction between circRNA and miRNA, miRanda database and the miRBase sequence of the mice are used to predict the target miRNA of circRNA. Venn diagram shown the mmu-miR-7056-5p, mmu-miR-5130, mmu-miR-2861, mmu-miR-6971-5p, mmu-miR-207, and mmu-miR-1956 were the downstream targets of circRNA02370 (Figure 3F).

The genes were differentially expressed in the subacute stage after SCI in mice

The expression of genes in the subacute stage after SCI was calculated by the TKM method. Based on this method, the genes expression abundance in different samples were displayed using density curve plot (Figure 4A) and violin plot (Figure 4B). Differential genes expression analysis uncovered that 372 DEGs after SCI, among which 274 DEGs were up-regulated and 98 DEGs were down-regulated based on the standard of $|\log2\ \text{fold-change}| > 5$ and P.adj value < 0.01 (Figure 4C). Moreover, the specific expression of top 10 up-regulated and down-regulated DEGs were presented with hierarchical clustering, ballon plot, and Bar plot (Figures 4D–F). The most significantly up- and down-regulated genes were Ctsd and Huwe1, respectively (Figures 4C–F).

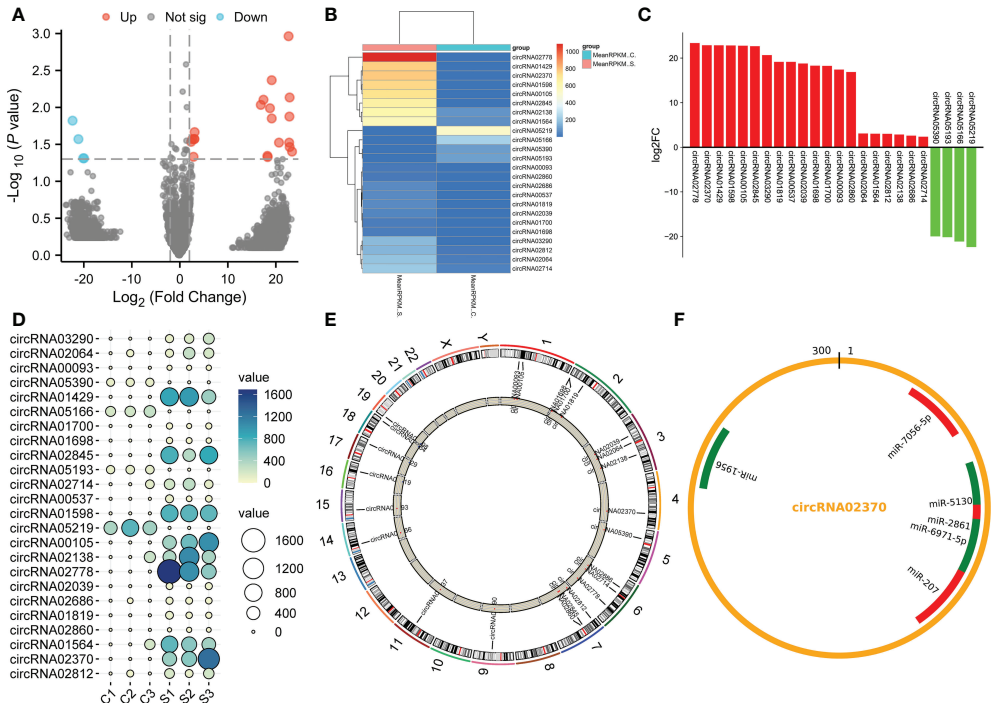


FIGURE 3
The circRNAs were differentially expressed in the subacute stage after SCI in mice. **(A)** Volcano plot. Green points indicate down-regulation (left side), gray points indicate undifferential expression (middle), and red points indicate up-regulation (right side). **(B)** Hierarchical clustering. with rows indicating DECs and columns indicating samples. **(C)** Bar plot shown the top 20 upregulated and 4 downregulated DECs in SCI tissues. The X-axis represents miRNA and the Y-axis represents log2 fold change. Red means up-regulation, above the X-axis; green means down-regulation, below the X-axis. **(D)** Ballon plot. The size of the circle shows the size of each value in the matrix, and the size of the value is represented by the shade of color. **(E)** The distribution of DECs on chromosomes. **(F)** CircRNA targeted miRNA distribution circle. The orange circle represents circRNA, and the red segment represents miRNA.

TABLE 1 The expression profile of DEC sin SCI tissue sin mice.

circRNA	log2FC	P Value	Expression
circRNA02778	23.378252	0.039683944	up
circRNA02370	22.88608881	0.034350749	up
circRNA01429	22.86905921	0.007337619	up
circRNA01598	22.8284641	0.01330039	up
circRNA00105	22.77940422	0.029959172	up
circRNA02845	22.65361058	0.001087619	up
circRNA03290	20.65823853	0.029959172	up
circRNA01819	19.14461664	0.014108052	up
circRNA00537	19.13661319	0.004282085	up
circRNA02039	18.77929156	0.010261397	up
circRNA01698	18.29319659	0.047053684	up
circRNA01700	18.24867342	0.045271645	up
circRNA00093	17.42548821	0.007869117	up
circRNA02860	16.8670717	0.009248431	up
circRNA02064	3.082454738	0.021587718	up
circRNA01564	3.032968379	0.02677553	up

(Continued)

TABLE 1 Continued

circRNA	log2FC	P Value	Expression
circRNA02812	3.013834348	0.026814454	up
circRNA02138	2.851016978	0.046616704	up
circRNA02686	2.589680564	0.026961922	up
circRNA02714	2.350170435	0.029230947	up
circRNA05390	-19.9568273	0.048811362	down
circRNA05193	-20.13556347	0.048811362	down
circRNA05166	-21.12786911	0.026879289	down
circRNA05219	-22.34705232	0.015115009	down

Identifying the IRGs related to SCI

Immune and neuroinflammation exert an important role after SCI (34). Thus, we selected the IRGs related to SCI *via* the intersection of DEGs and IRGs. A total of 73 DEGs were identified as IRGs (Figure 5A). To further identify the key hub genes, we constructed a PPI network of 73 DEGs using the STRING database. Then we used the MCC algorithms of the cytoHubba plugin in Cytoscape to obtain the top 10 genes as hub genes (Figures 5B, C). The top 10 genes were listed as

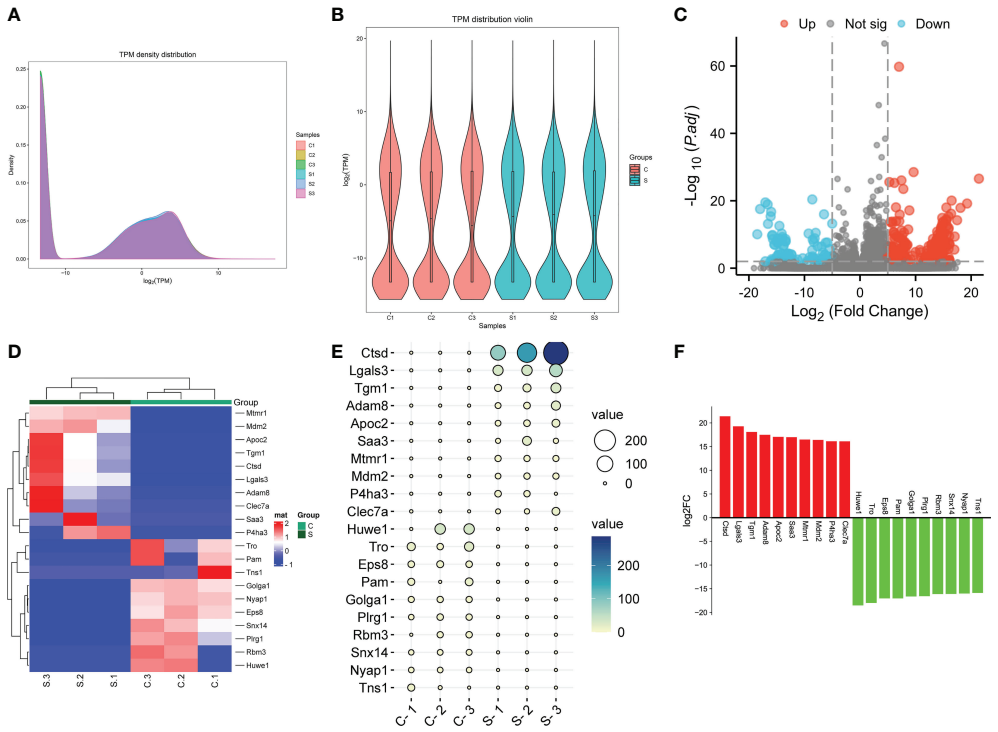


FIGURE 4
The genes were differentially expressed in the subacute stage after SCI in mice. **(A)** Gene expression density curve. The horizontal axis represent the log (TPM) value, the higher the value, the higher the gene expression level; the vertical axis represent the number of genes on the horizontal axis/the total number of genes. **(B)** Violin plot of gene expression calculated using TPM. The horizontal axis represent the sample name, and the vertical axis represent the log (TPM) value. The width of each violin reflects the number of genes at that expression levels. **(C)** Volcano plot. Green points indicate down-regulation (left side), gray points indicate undifferential expression (middle), and red points indicate up-regulation (right side). **(D)** Hierarchical clustering shown the top 10 upregulated and top 10 downregulated genes. with rows indicating DECs and columns indicating samples. **(E)** Ballon plot. The size of the circle shows the size of each value in the matrix, and the size of the value is represented by the shade of color. **(F)** Bar plot shown the top 10 upregulated and top 10 downregulated genes in SCI tissues. The X-axis represents gene and the Y-axis represents log2 fold change. Red means up-regulation, above the X-axis; green means down-regulation, below the X-axis.

follows: Ptprc, Fcgr2b, Ccl2, Tlr7, Cxcl10, Cd28, Ccr1, Il10ra, Cd68, and Tlr3 (Figure 5C). Interestingly, they all significantly upregulated after SCI (Figure 5D). Additionally, we used MCC, MNC, Degree, EPC, and Closeness algorithms to verify the obtaining 10 hub genes in Cytoscape software. A total of 9 overlapping genes (except Ccr1) were predicted *via* Venn diagram (Figure 5E), suggesting that Ptprc, Fcgr2b, Ccl2, Tlr7, Cxcl10, Cd28, Il10ra, Cd68, and Tlr3 were the key IRGs.

Go functional and KEGG pathway enrichment analysis of the host genes of DECs

In view of circRNAs are derived from precursor (pre)-mRNAs and formed by back-splicing, namely a downstream 5′ splice site is covalently binded with an upstream 3′ splice site (15–17, 35). Moreover, the abundance of circRNAs are negatively correlated with their linear host genes mRNAs because of there is a competition between circRNA biogenesis and pre-mRNA splicing (36). Thus, whether the host genes of DECs are involved in the regulation of SCI is a meaningful issue worth studying. Subsequently, Go functional and KEGG pathway enrichment analyses were conducted to investigate the potential biological functions of their host genes. GO function annotations included terms in the biological process (BP), molecular function (MF), and cellular component (CC) categories. The top 10 BP terms encompassed hair follicle maturation, regulation of synaptic transmission GABAergic, actin filament organization, regulation of protein ubiquitination, synapse organization, regulation of cell-substrate adhesion, synaptic transmission, GABAergic, regulation of protein modification by small protein conjugation or removal, positive regulation of protein localization to plasma membrane, and positive regulation of protein localization to cell periphery(Figures 6A, B). The enriched top 10 CC were actin filament, adherens junction, insulin-responsive compartment, actin cytoskeleton, postsynaptic actin cytoskeleton, filopodium tip, postsynaptic cytoskeleton, late endosome, presynaptic cytosol, and

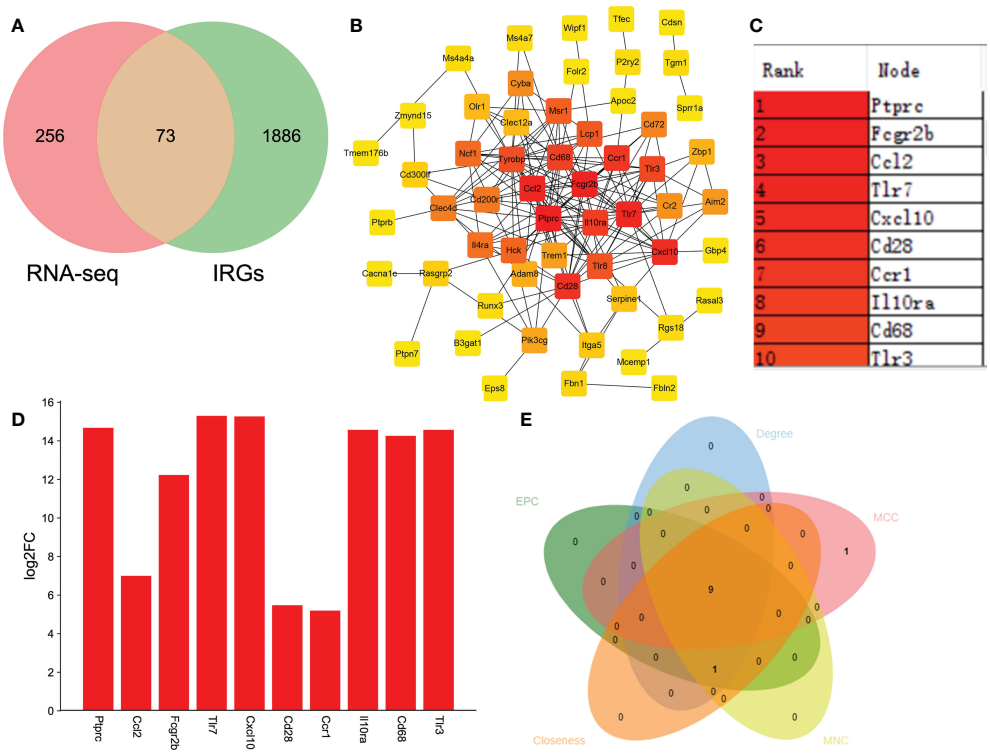


FIGURE 5
Identifying the IRGs related to SCI. **(A)** Venn analysis to select the overlapping genes between RNA-seq and immune-related genes (IRGs). **(B)** Identifying the key hub genes *via* constructing the protein-protein interaction network and further visualizing using Cytoscape software. **(C)** The top 10 hub genes from PPI network. **(D)** Bar plot shown the top 10 IRGs related to SCI. The X-axis represents gene and the Y-axis represents log2 fold change. Red means up-regulation, above the X-axis. **(E)** MCC, MNC, Degree, EPC, and Closeness algorithms were used to verify the obtaining 10 hub genes in Cytoscape software.

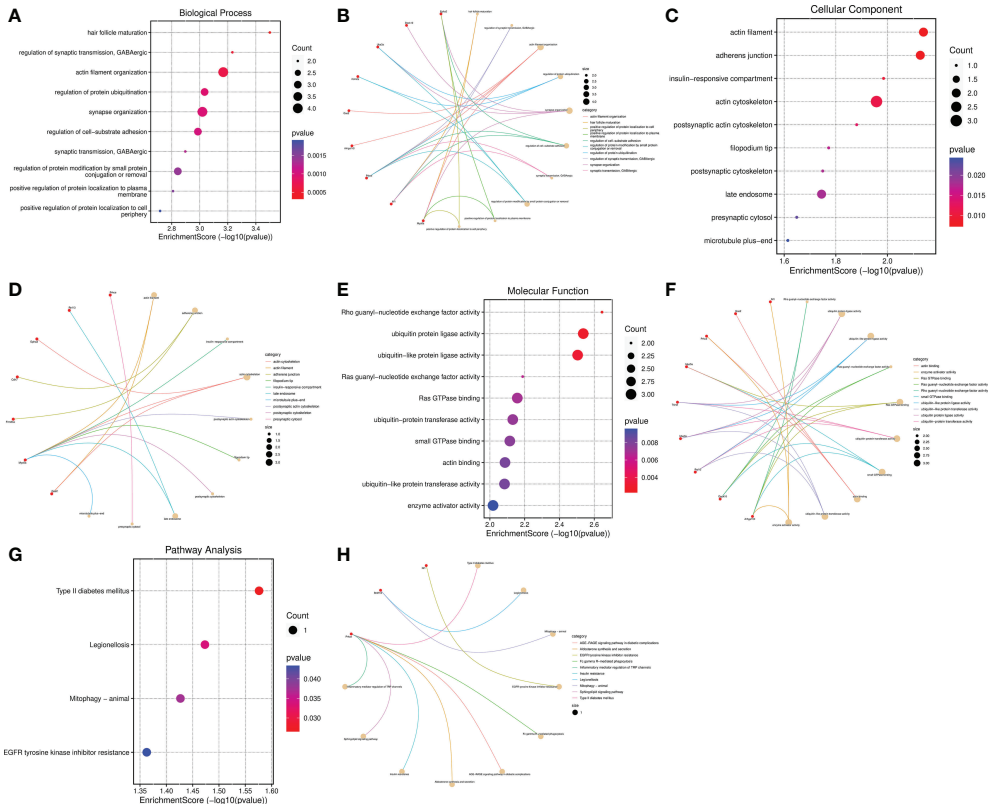


FIGURE 6
Functional and pathway enrichment analysis of the host genes of DECs. **(A–F)** Bubble diagram and cnetplot showing the host genes of DECs enriched in the different GO categories, including BP, CC, and MF. **(G, H)** KEGG pathway enrichment analysis of the host genes of DECs.

microtubule plus-end (Figures 6C, D). The MF analysis unveiled that the host genes of DECs were significantly enriched in the following terms: Rho guanyl-nucleotide exchange factor activity, ubiquitin protein ligase activity, ubiquitin-like protein ligase activity, Ras guanyl-nucleotide exchange factor activity, Ras GTPase binding, ubiquitin-protein transferase activity, small GTPase binding, actin binding, ubiquitin-like protein transferase activity, and enzyme activator activity (Figures 6E, F). The cneplots shown the enrichment of the host genes of DECs in each pathway (Figures 6B, D, F).

The enriched top 10 KEGG pathways included the Prkce-mediated Type II diabetes mellitus、Fc gamma R-mediated phagocytosis AGE-RAGE signaling pathway in diabetic complications Aldosterone synthesis and secretion、Insulin resistance、Sphingolipid signaling pathway and Inflammatory mediator regulation of TRP channels, Bcl2l13-mediated Legionellosis and Mitophagy, and Nf1-mediated EGFR tyrosinekinase inhibitor resistance (Figures 6G, H). Among them, the pathways of Type II diabetes mellitus, Legionellosis, Mitophagy, and EGFR tyrosinekinase inhibitor resistance were statistically significant (P value<0.05) (Figure 6G). Taken together, these results suggested that the host genes of DECs possibly regulate synapse function, inflammatory response, and mitophagy, etc.

Go functional and KEGG pathway enrichment analysis of the IRG-related DEGs

The top 10 BP terms including positive regulation of cytokine production, positive regulation of response to external stimulus, regulation of phagocytosis, positive regulation of cell adhesion, negative regulation of immune system process, myeloid leukocyte activation, positive regulation of tumor necrosis factor superfamily cytokine production, regulation of tumor necrosis factor superfamily cytokine production, tumor necrosis factor superfamily cytokine production, and phagocytosis (Figures 7A, B). The enriched CC were receptor complex, membrane microdomain, membrane region, focal adhesion, membrane raft, cell-substrate junction, NADPH oxidase complex, low-density lipoprotein particle, cytoplasmic side of membrane, and apical part of cell (Figures 7C, D). The MF were significantly enriched in the

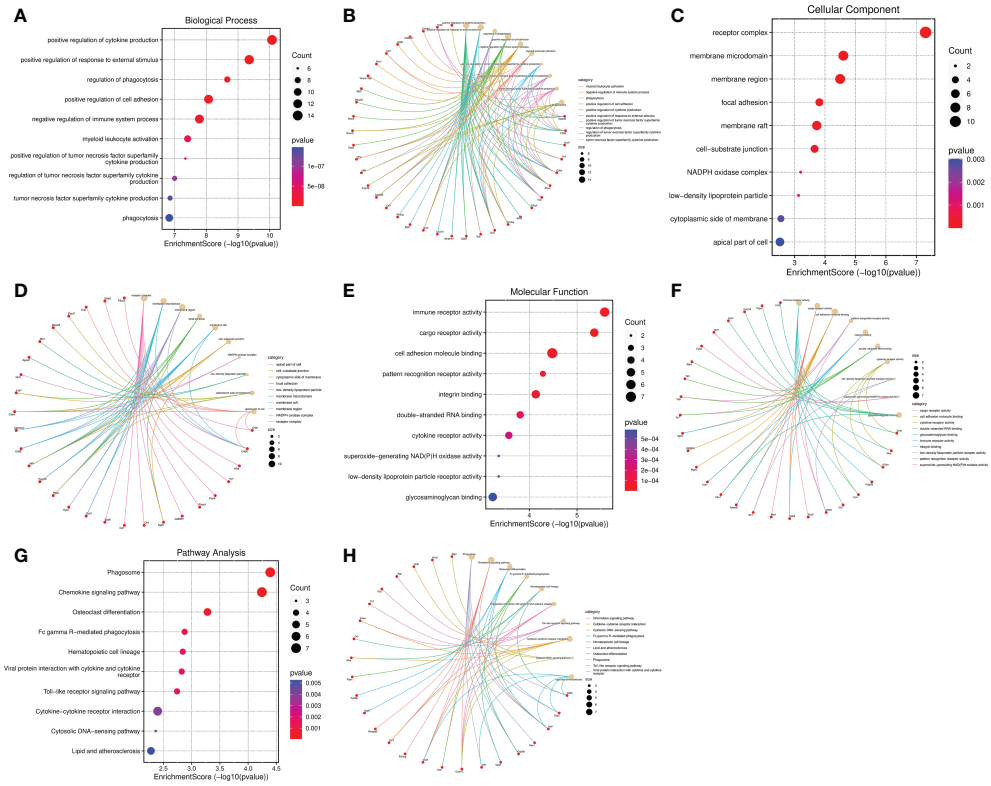


FIGURE 7
Functional and pathway enrichment analysis of the IRGs related to SCI. **(A–F)** Bubble diagram and cnetplot showing the host genes of DECs enriched in the different GO categories, including BP, CC, and MF. **(G, H)** KEGG pathway enrichment analysis of the host genes of DECs.

following terms: immune receptor activity, cargo receptor activity, cell adhesion molecule binding, pattern recognition receptor activity, integrin binding, double-stranded RNA binding, cytokine receptor activity, low-density lipoprotein particle receptor activity, superoxide-generating NAD(P)H oxidase activity, and glycosaminoglycan binding (Figures 7E, F). The cneplots shown the enrichment of the host genes of DECs in each pathway (Figures 7B, D, F). The KEGG enrichment analysis results were described as follows: Phagosome, Chemokine signaling pathway, Osteoclast differentiation, Fc gamma R-mediated phagocytosis, Hematopoietic cell lineage, Viral protein interaction with cytokine and cytokine receptor, Toll-like receptor signaling pathway, Cytokine-cytokine receptor interaction, Cytosolic DNA-sensing pathway, and Lipid and atherosclerosis (Figures 7G, H).

Discussion

In the past decade, genetic regulation of the occurrence and progression of diseases has received increasing attention. The occurrence of a large number of DECs and DEGs after SCI is the pathological features of SCI (20–28), but the mechanism by which circRNAs-mediated the pathological process in the subacute stage after SCI has not been reported yet. In the present study, the circRNAs and mRNAs expression profiles were sequenced by high-throughput sequencing technology in the mice model of the subacute stage after SCI, and the characteristics and expression levels of DECs and DEGs were analyzed. Through the bioinformatics analysis, we found 20 DECs and 274 DEGs were up-regulated as well as 4 DECs and 98 DEGs were down-regulated after SCI in mice. Among them, circRNA02778 and circRNA02370 were top up-regulated and circRNA05219 was top down-regulated DECs in SCI tissues. Furthermore, we predicted that mmu-miR-7056-5p, mmu-miR-5130, mmu-miR-2861, mmu-miR-6971-5p, mmu-miR-207, and mmu-miR-1956 were the downstream targets of circRNA02370. However, the study of circRNA02778, circRNA02370, and circRNA05219 in SCI remain a blank, whether they act as ceRNA to mediate the pathological process of SCI in a miRNA-dependent manner, which need further investigation.

Then we performed GO and KEGG function enrichment analysis on the host genes of DECs, and observed that Prkce (circRNA01429 host gene) and Nf1 (circRNA00537) were involved in the regulation of synaptic transmission,

GABAergic and enzyme activator activity; Dock10 (circRNA00105), Myo5a(circRNA03290), Ube3a (circRNA02860), and Epha3 (circRNA05219) were related to synapse organization; Bcl2l13(circRNA02778) linked to mitophagy; Myo5a associated with postsynaptic actin cytoskeleton and postsynaptic cytoskeleton; and Prkce linked to presynaptic cytosol and inflammatory mediator regulation of TRP channels. Consistent with our results, Shi et al (37). found that several DEGs participated in axon guidance, dopaminergic synapses, glutamatergic synapses, GABAergic synapses, and inflammatory signaling pathway in rats SCI model by RNA-sequencing. Furthermore, synaptic transmission, synapse remodeling, synapse reorganization and neuroinflammation have implicated in SCI (34, 38–40). Thus, we hypothesized that the DECs might be closely related to the pathological process of SCI.

Growing evidence have unveiled that neuronal inflammatory and immune responses are the pathomechanism of SCI (34, 39–43). Buzoianu-Anguiano and colleagues believed that the inflammatory and immune responses develop as follows: first is the immune cells such as neutrophils and macrophages secrete different cytokines and ROS, and followed by activating the chemokine CXCL10 and type II histocompatibility complex MCH-II, leading to a pro-inflammatory and immune microenvironment (40). Shi et al (37). identified that DEGs most enriched in immune response *via* Go analysis. Grassner et al (41). pointed to neutrophils and eosinophils were activated and infiltrated in SCI patients with infection, indicating that systemic immune imbalance after SCI can predict the risk of infection and the recovery of neurological function. Axon regeneration exerts a crucial role in promoting neurological recovery after SCI, and immune and inflammatory cells are involved in the regeneration of damaged neuronal axons (39, 42, 43). Horn et al (42). confirmed that the interactions between activated macrophages and injured neuronal axons play a central role in axonal retraction. Kurimoto et al (43). uncovered that neutrophils first respond in immune system after SCI, which can promote axonal regeneration induced by inflammation.

In this study, we identified top 9 IRGs (Ptprc, Fcgr2b, Ccl2, Tlr7, Cxcl10, Cd28, Il10ra, Cd68, and Tlr3) related to SCI and found they were significantly upregulated after SCI. Interestingly, Yan et al (44). also reported that the relative expression level of Ptprc and Fcgr2b were remarkably increased after SCI *via* PCR detection. Wang et al (45). demonstrated that CXCL10 was remarkably increased in SCI and had positive correlation with pro-inflammatory response. CXCL10 and CCL2 were reported to act as a predictors of increased infections after SCI (41). Toll-like receptors (TLRs) have the potential to modulate inflammatory and initiate immune responses (46, 47). Gucluler et al (47). reported that there was a toll like receptor-7 (TLR7) and TLR9-mediated innate immune dysfunction in SCI patients. TLR3 and TLR7 also promoted the secretion of the pro-inflammatory cytokines in the spinal cord, and contributing to inflammatory pain (46). Even though, the reason why the expression levels of the IRGs significantly increased and their functions in the subacute stage of SCI needs to be further identified. Furthermore, more experiments need to be performed to validate and understand how the IRGs mediated SCI *via* regulating neuronal inflammatory and immune responses.

Nevertheless, this study also has several limitations need to be taken seriously. First is the predictive results were mainly based on bioinformatics analysis, and the study samples were collected from rats rather than humans, so the relevant molecular biology and animal experiments were needed to further demonstrate the immunomodulatory effects and corresponding mechanisms of the key IRGs after SCI. Then there's the relatively small size of the sample that might affect the conclusions. Finally, the correlation of circRNA, miRNA, and mRNA, and whether they constitute the circRNA-miRNA-mRNA ceRNA signaling axis that plays a role in SCI, is also a topic worthy of investigation.

Conclusion

In summary, we screened 24 DECs and 372 DEGs by high-throughput RNA sequencing analysis, and found that circRNA02778, circRNA02370, and Ctsd were top up-regulated as well as circRNA05219 and Huwe1 were top down-regulated after SCI. Functional enrichment analysis shown that the functions of DECs are mainly focused on synaptic functions and inflammatory response. Meanwhile, we identified multiple IRGs (Ptprc, Fcgr2b, Ccl2, Tlr7, Cxcl10, Cd28, Il10ra, Cd68, and Tlr3) related to SCI and found they were significantly upregulated after SCI, but the specific mechanisms by which they regulate SCI by mediating neuronal inflammatory and immune responses need to be further explored. Findings of this study provide new direction and molecular basis for the diagnosis and treatment of SCI in the future.

Data availability statement

The data presented in the study are deposited in the GEO repository (https://www.ncbi.nlm.nih.gov/gds/), accession number GSE217797. We declare that the data supporting the findings of this study are available with in the article and from the corresponding author upon reasonable request.

Ethics statement

The animal study was reviewed and approved by Xuanwu Hospital ethics committee, Capital Medical University.

Author contributions

YL designed and wrote the manuscript. XC and SL critically reviewed and revised the manuscript. BW and WS performed the bioinformatics analysis. GL and CK collected samples for RNA-sequencing. All authors contributed to the article and approved the submitted version.

Funding

This research was funded by National key R&D plan (2020YFC2004905) R&D Program of Beijing Municipal Education Commission (KZ/KM/SZ/SM2022100250**), and Beijing Municipal Medical Science Institute-Public Welfare Development Reform Pilot Project (Capital Medical Research No. 2019-2).

Conflict of interest

The authors declare that the research was conducted in the absence of any commercial or financial relationships that could be construed as a potential conflict of interest.

Publisher's note

All claims expressed in this article are solely those of the authors and do not necessarily represent those of their affiliated organizations, or those of the publisher, the editors and the reviewers. Any product that may be evaluated in this article, or claim that may be made by its manufacturer, is not guaranteed or endorsed by the publisher.

References

1. Sweis R, Biller J. Systemic complications of spinal cord injury. *Curr Neurol Neurosci Rep* (2017) 17(2):8. doi: 10.1007/s11910-017-0715-4

2. Ge L, Arul K, Ikpeze T, Baldwin A, Nickels JL, Mesfin A. Traumatic and nontraumatic spinal cord injuries. *World Neurosurg* (2018) 111:e142–e8. doi: 10.1016/j.wneu.2017.12.008

3. Lee BS, Kim O, Ham D. Epidemiologic changes in nontraumatic spinal cord injury for the last 30 years (1990-2019) in south Korea. *Spinal cord* (2022) 60 (3):268–73. doi: 10.1038/s41393-021-00695-5

4. Ackery A, Tator C, Krassioukov A. A global perspective on spinal cord injury epidemiology. *J neurotrauma* (2004) 21(10):1355–70. doi: 10.1089/neu.2004.21.1355

5. Orr MB, Gensel JC. Spinal cord injury scarring and inflammation: Therapies targeting glial and inflammatory responses. *Neurotherapeutics* (2018) 15(3):541–53. doi: 10.1007/s13311-018-0631-6

6. Ge L, Arul K, Mesfin A. Spinal cord injury from spinal tumors: Prevalence, management, and outcomes. *World Neurosurg* (2019) 122:e1551–e6. doi: 10.1016/j.wneu.2018.11.099

7. Quadri SA, Farooqui M, Ikram A, Zafar A, Khan MA, Suriya SS, et al. Recent update on basic mechanisms of spinal cord injury. *Neurosurg Rev* (2020) 43 (2):425–41. doi: 10.1007/s10143-018-1008-3

8. Zhu LL, Li MQ, He F, Zhou SB, Jiang W. Mitochondria targeted peptide attenuates mitochondrial dysfunction, controls inflammation and protects against spinal cord injury-induced lung injury. *Cell Physiol Biochem* (2017) 44(1):388–400. doi: 10.1159/000484919

9. Tator CH. Update on the pathophysiology and pathology of acute spinal cord injury. *Brain Pathol (Zurich Switzerland)* (1995) 5(4):407–13. doi: 10.1111/j.1750-3639.1995.tb00619.x

10. Rowland JW, Hawryluk GW, Kwon B, Fehlings MG. Current status of acute spinal cord injury pathophysiology and emerging therapies: Promise on the horizon. *Neurosurg Focus* (2008) 25(5):E2. doi: 10.3171/foc.2008.25.11.E2

11. Syková E, Homola A, Mazanec R, Lachmann H, Konrádová SL, Kobylka P, et al. Autologous bone marrow transplantation in patients with subacute and chronic spinal cord injury. *Cell Transplant* (2006) 15(8-9):675–87. doi: 10.3727/000000006783464381

12. Martirosyan NL. Pharmacologic and cell-based therapies for acute spinal cord injury. *Neurosurg Clinics North America* (2021) 32(3):389–95. doi: 10.1016/j.nec.2021.03.010

13. Vismara I, Papa S, Rossi F, Forloni G, Veglianese P. Current options for cell therapy in spinal cord injury. *Trends Mol Med* (2017) 23(9):831–49. doi: 10.1016/j.molmed.2017.07.005

14. Panni S, Lovering RC, Porras P, Orchard S. Non-coding RNA regulatory networks. *Biochim Biophys Acta Gene Regul Mech* (2020) 1863(6):194417. doi: 10.1016/j.bbagrm.2019.194417

15. Patop IL, Wüst S, Kadener S. Past, present, and future of circRNAs. *EMBO J* (2019) 38(16):e100836. doi: 10.15252/embj.2018100836

16. Chen LL. The expanding regulatory mechanisms and cellular functions of circular RNAs. *Nat Rev Mol Cell Biol* (2020) 21(8):475–90. doi: 10.1038/s41580-020-0243-y

17. Kristensen LS, Andersen MS, Stagsted LVW, Ebbesen KK, Hansen TB, Kjems J. The biogenesis, biology and characterization of circular RNAs. *Nat Rev Genet* (2019) 20(11):675–91. doi: 10.1038/s41576-019-0158-7

18. Thomson DW, Dinger ME. Endogenous microRNA sponges: Evidence and controversy. *Nat Rev Genet* (2016) 17(5):272–83. doi: 10.1038/nrg.2016.20

19. Pasquinelli AE. MicroRNAs and their targets: Recognition, regulation and an emerging reciprocal relationship. *Nat Rev Genet* (2012) 13(4):271–82. doi: 10.1038/nrg3162

20. Bie F, Wang K, Xu T, Yuan J, Ding H, Lv B, et al. The potential roles of circular RNAs as modulators in traumatic spinal cord injury. *Biomed pharmacother* (2021) 141:111826. doi: 10.1016/j.biopha.2021.111826

21. Wang W, He D, Chen J, Zhang Z, Wang S, Jiang Y, et al. Circular RNA plek promotes fibrogenic activation by regulating the mir-135b-5p/Tgf-βr1 axis after spinal cord injury. *Aging* (2021) 13(9):13211–24. doi: 10.18632/aging.203002

22. Li X, Kang J, Lv H, Liu R, Chen J, Zhang Y, et al. Circprkcsh, a circular RNA, contributes to the polarization of microglia towards the M1 phenotype induced by spinal cord injury and acts *Via* the Jnk/P38 mapk pathway. *FASEB J* (2021) 35(12): e22014. doi: 10.1096/fj.202100993R

23. Chen JN, Zhang YN, Tian LG, Zhang Y, Li XY, Ning B. Down-regulating circular RNA prkcsh suppresses the inflammatory response after spinal cord injury. *Neural regen Res* (2022) 17(1):144–51. doi: 10.4103/1673-5374.314114

24. Sun Y, Zhou Y, Shi X, Ma X, Peng X, Xie Y, et al. Circtyw1 serves as a sponge for microRNA-380 in accelerating neurological recovery following spinal cord injury *Via* regulating Fgf9. *Cell Cycle (Georgetown Tex)* (2021) 20(18):1828–44. doi: 10.1080/15384101.2021.1962634

25. Qin C, Liu CB, Yang DG, Gao F, Zhang X, Zhang C, et al. Circular RNA expression alteration and bioinformatics analysis in rats after traumatic spinal cord injury. *Front Mol Neurosci* (2018) 11:497. doi: 10.3389/fnmol.2018.00497

26. Zhou ZB, Du D, Chen KZ, Deng LF, Niu YL, Zhu L. Differential expression profiles and functional predication of circular ribonucleic acid in traumatic spinal cord injury of rats. *J neurotrauma* (2019) 36(15):2287–97. doi: 10.1089/neu.2018.6366

27. Zhao J, Qi X, Bai J, Gao X, Cheng L. A circRNA derived from linear Hipk3 relieves the neuronal cell apoptosis in spinal cord injury *Via* cerna pattern. *Biochem Biophys Res Commun* (2020) 528(2):359–67. doi: 10.1016/j.bbrc.2020.02.108

28. Wang WZ, Li J, Liu L, Zhang ZD, Li MX, Li Q, et al. Role of circular RNA expression in the pathological progression after spinal cord injury. *Neural regen Res* (2021) 16(10):2048–55. doi: 10.4103/1673-5374.308100

29. Bhattacharya S, Dunn P, Thomas CG, Smith B, Schaefer H, Chen J, et al. Immport, toward repurposing of open access immunological assay data for translational and clinical research. *Sci Data* (2018) 5:180015. doi: 10.1038/sdata.2018.15

30. Yu G, Wang LG, Han Y, He QY. Clusterprofiler: An r package for comparing biological themes among gene clusters. *Omics* (2012) 16(5):284–7. doi: 10.1089/omi.2011.0118

31. Szklarczyk D, Gable AL, Lyon D, Junge A, Wyder S, Huerta-Cepas J, et al. String V11: Protein-protein association networks with increased coverage, supporting functional discovery in genome-wide experimental datasets. *Nucleic Acids Res* (2019) 47(D1):D607–d13. doi: 10.1093/nar/gky1131

32. Chin CH, Chen SH, Wu HH, Ho CW, Ko MT, Lin CY. Cytohubba: Identifying hub objects and Sub-networks from complex interactome. *BMC Syst Biol* (2014) 8 Suppl 4(Suppl 4):S11. doi: 10.1186/1752-0509-8-s4-s11

33. Zheng Q, Bao C, Guo W, Li S, Chen J, Chen B, et al. Circular RNA profiling reveals an abundant Circhipk3 that regulates cell growth by sponging multiple miRNAs. *Nat Commun* (2016) 7:11215. doi: 10.1038/ncomms11215

34. Chio JCT, Xu KJ, Popovich P, David S, Fehlings MG. Neuroimmunological therapies for treating spinal cord injury: Evidence and future perspectives. *Exp Neurol* (2021) 341:113704. doi: 10.1016/j.expneurol.2021.113704

35. Yang L, Wilusz JE, Chen LL. Biogenesis and regulatory roles of circular RNAs. *Annu Rev Cell Dev Biol* (2022) 38:263-289. doi: 10.1146/annurev-cellbio-120420-125117

36. Ashwal-Fluss R, Meyer M, Pamudurti NR, Ivanov A, Bartok O, Hanan M, et al. CircRNA biogenesis competes with pre-mRNA splicing. *Mol Cell* (2014) 56 (1):55–66. doi: 10.1016/j.molcel.2014.08.019

37. Shi LL, Zhang N, Xie XM, Chen YJ, Wang R, Shen L, et al. Transcriptome profile of rat genes in injured spinal cord at different stages by RNA-sequencing. *BMC Genomics* (2017) 18(1):173. doi: 10.1186/s12864-017-3532-x

38. Bunday KL, Perez MA. Motor recovery after spinal cord injury enhanced by strengthening corticospinal synaptic transmission. *Curr Biol* (2012) 22(24):2355–61. doi: 10.1016/j.cub.2012.10.046

39. O'Shea TM, Burda JE, Sofroniew MV. Cell biology of spinal cord injury and repair. *J Clin Invest* (2017) 127(9):3259–70. doi: 10.1172/jci90608

40. Buzoianu-Anguiano V, Torres-Llacsa M, Doncel-Pérez E. Role of aldynoglia cells in neuroinflammatory and neuroimmune responses after spinal cord injury. *Cells* (2021) 10(10):2783. doi: 10.3390/cells10102783

41. Grassner L, Klein B, Garcia-Ovejero D, Mach O, Scheiblhofer S, Weiss R, et al. Systemic immune profile predicts the development of infections in patients with spinal cord injuries. *J neurotrauma* (2022) 39:1-9. doi: 10.1089/neu.2021.0448

42. Horn KP, Busch SA, Hawthorne AL, van Rooijen N, Silver J. Another barrier to regeneration in the cns: Activated macrophages induce extensive retraction of dystrophic axons through direct physical interactions. *J Neurosci* (2008) 28(38):9330–41. doi: 10.1523/jneurosci.2488-08.2008

43. Kurimoto T, Yin Y, Habboub G, Gilbert HY, Li Y, Nakao S, et al. Neutrophils express oncomodulin and promote optic nerve regeneration. *J Neurosci* (2013) 33(37):14816–24. doi: 10.1523/jneurosci.5511-12.2013

44. Yan L, Fu J, Dong X, Chen B, Hong H, Cui Z. Identification of hub genes in the subacute spinal cord injury in rats. *BMC Neurosci* (2022) 23(1):51. doi: 10.1186/s12868-022-00737-5

45. Wang Q, Liu L, Cao J, Abula M, Yimingjiang Y, Feng S. Weighted gene Co-expression network analysis reveals that Cxcl10, Irf7, Mx1, Rsad2, and Stat1 are related to the chronic stage of spinal cord injury. *Ann Trans Med* (2021) 9 (15):1248. doi: 10.21037/atm-21-3586

46. Liu T, Gao YJ, Ji RR. Emerging role of toll-like receptors in the control of pain and itch. *Neurosci Bull* (2012) 28(2):131–44. doi: 10.1007/s12264-012-1219-5

47. Gucluler G, Adiguzel E, Gungor B, Kahraman T, Gursel M, Yilmaz B, et al. Impaired toll like receptor-7 and 9 induced immune activation in chronic spinal cord injured patients contributes to immune dysfunction. *PloS One* (2017) 12(2): e0171003. doi: 10.1371/journal.pone.0171003

frontiers | Frontiers in Immunology

TYPE Review
PUBLISHED 19 December 2022
DOI 10.3389/fimmu.2022.1098212

Check for updates

OPEN ACCESS

EDITED BY
Guangzhi Ning,
Tianjin Medical University General Hospital, China

REVIEWED BY
Changfeng Fu,
The First Hospital of Jilin University, China
Qun Xue,
Affiliated Hospital of Nantong University, China

*CORRESPONDENCE
Nunzio Vicario
nunzio.vicario@unict.it
Rosalba Parenti
rosalba.parenti@unict.it

†These authors share first authorship

SPECIALTY SECTION
This article was submitted to Multiple Sclerosis and Neuroimmunology, a section of the journal Frontiers in Immunology

RECEIVED 14 November 2022
ACCEPTED 06 December 2022
PUBLISHED 19 December 2022

CITATION
Denaro S, D'Aprile S, Alberghina C, Pavone AM, Torrisi F, Giallongo S, Longhitano L, Mannino G, Lo Furno D, Zappalà A, Giuffrida R, Tibullo D, Li Volti G, Vicario N and Parenti R (2022) Neurotrophic and immunomodulatory effects of olfactory ensheathing cells as a strategy for neuroprotection and regeneration.
Front. Immunol. 13:1098212.
doi: 10.3389/fimmu.2022.1098212

COPYRIGHT
© 2022 Denaro, D'Aprile, Alberghina, Pavone, Torrisi, Giallongo, Longhitano, Mannino, Lo Furno, Zappalà, Giuffrida, Tibullo, Li Volti, Vicario and Parenti. This is an open-access article distributed under the terms of the Creative Commons Attribution License (CC BY). The use, distribution or reproduction in other forums is permitted, provided the original author(s) and the copyright owner(s) are credited and that the original publication in this journal is cited, in accordance with accepted academic practice. No use, distribution or reproduction is permitted which does not comply with these terms.

Neurotrophic and immunomodulatory effects of olfactory ensheathing cells as a strategy for neuroprotection and regeneration

Simona Denaro[1†], Simona D'Aprile[1†], Cristiana Alberghina[1], Anna Maria Pavone[1], Filippo Torrisi[1], Sebastiano Giallongo[2], Lucia Longhitano[2], Giuliana Mannino[3], Debora Lo Furno[1], Agata Zappalà[1], Rosario Giuffrida[1], Daniele Tibullo[2], Giovanni Li Volti[2], Nunzio Vicario[1*] and Rosalba Parenti[1*]

[1]Section of Physiology, Department of Biomedical and Biotechnological Sciences, University of Catania, Catania, Italy, [2]Section of Biochemistry, Department of Biomedical and Biotechnological Sciences, University of Catania, Catania, Italy, [3]Department of Chemical, Biological, Pharmaceutical and Environmental Sciences, University of Messina, Messina, Italy

Accumulating evidence sustains glial cells as critical players during central nervous system (CNS) development, homeostasis and disease. Olfactory ensheathing cells (OECs), a type of specialized glia cells sharing properties with both Schwann cells and astrocytes, are of critical importance in physiological condition during olfactory system development, supporting its regenerative potential throughout the adult life. These characteristics prompted research in the field of cell-based therapy to test OEC grafts in damaged CNS. Neuroprotective mechanisms exerted by OEC grafts are not limited to axonal regeneration and cell differentiation. Indeed, OEC immunomodulatory properties and their phagocytic potential encourage OEC-based approaches for tissue regeneration in case of CNS injury. Herein we reviewed recent advances on the immune role of OECs, their ability to modulate CNS microenvironment *via* bystander effects and the potential of OECs as a cell-based strategy for tissue regeneration.

KEYWORDS

OECs, immunomodulation, neurotrophic factors, intercellular communication, neuroregeneration

1 Introduction

During the last decades, increasing evidence support the hypothesis that glial cells are important players in crucial aspects of neurogenesis, neuronal functions and diseases (1, 2). Indeed, glial cells guide neuronal migration during development, participate in synaptic formation and plasticity, regulate vasculature and blood–brain barrier (BBB),

10.3389/fimmu.2022.1098212

modulate neuroimmunity, and support neural regeneration (1–3). The term *glia*, from the Greek "γλία", meaning "glue", was originally assigned assuming that these cells were responsible to keep neural cells together. In the adult central nervous system (CNS) three main types of glial cells can be distinguished: astrocytes and oligodendrocytes, deriving from neural crest, and microglia, which originate from the myeloid lineage. In the peripheral nervous system (PNS), Schwann cells represent the main class of glia. Olfactory ensheathing cells (OECs) are a type of specialized glia cells, restricted to the olfactory system, which play a crucial role in olfactory development and regeneration (4–6). Indeed, the olfactory system has a unique neurogenic niche where unlike most regions of the nervous system, olfactory sensory neurons retain a lifetime regeneration potential (4, 5). Since the olfactory neuroepithelium is in direct contact with the external environment, it has evolved a remarkable ability to recruit sensory neurons during normal cell turnover or after traumatic olfactory nerve injury (7, 8). This unique feature is now widely attributed to the presence of OECs, able to wrap olfactory axons and support olfactory receptor neurons turnover and axonal regeneration (9–11). OECs perform their axon growth-promoting properties and provide structural support by extending thin processes that envelop group of axons as an insulator (Figure 1) (12, 13). Moreover, when new olfactory sensory neurons are generated from stem cells in the olfactory epithelium, OECs establish functional connections along the olfactory neuroaxis (8, 14).

In contrast to neural crest-derived PNS glia and neural tube-derived CNS glia, OECs have generally been thought to originate from the olfactory placode (15). However, several studies show that the olfactory placode arises from ontogenetically heterogeneous sources of cells and OECs derive from neural crest, like Schwann cells (16–18). These cells are located in the lamina propria of the olfactory mucosa, as well as the outer layers of the olfactory bulbs, the inner and outer nerve fiber layers (Figure 1) (19).

OECs share many properties with Schwann cells and astrocytes. They express some typical markers such as the p75 neurotrophic receptor (p75NTR), the polysialylated form of neural cell adhesion molecule (PSA-NCAM), and, like astrocytes, they express the glial fibrillary acid protein (GFAP), and the S100 proteins (20, 21). Furthermore, OECs are able to secret high level of growth factors, such as nerve growth factor (NGF), basic fibroblast growth factors (bFBF), brain derived neurotrophic factor (BDNF), glial derived neurotrophic factor (GDNF), ciliary neurotrophic factor (CNTF), neurotrophins NT4, NT5 and neuregulins, which exhibit important functions as neuronal supporting elements (13, 22–24).

In recent years, significant advances have been made in cellular-based therapies, which focus on the restoration, regrowth or replacement of damaged or dysfunctional cells, tissues and organs, in order to treat neurodegenerative diseases (25) and CNS injuries (26–28). Moreover, cell-based approaches, including OEC grafts, have been reported to induce beneficial effects in spinal cord injury (SCI) models. In addition to neuroprotective mechanisms, axon regeneration and remyelination were observed, leading to significant sensory and locomotor functions amelioration (29–31). Thus, OEC transplantation is proposed as a potential therapeutic strategy for SCI, due to their unique characteristics, such as anti-

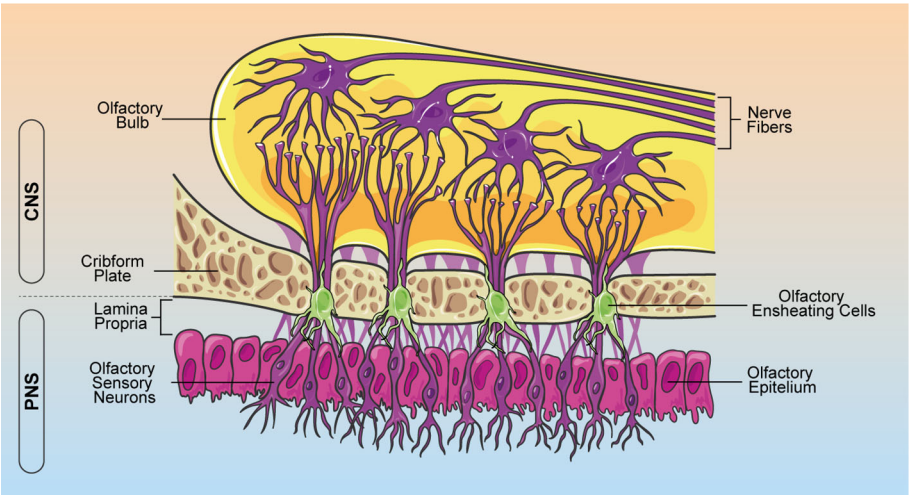


FIGURE 1
Schematic representation of OEC localization within the olfactory system. OECs ensheath bundles of olfactory receptor axons along their course through the lamina propria in the PNS. Olfactory nerves and their associated OECs cross through the cribform plate into the CNS, making connections with the olfactory bulb. OEC, olfactory ensheathing cells; CNS, central nervous system; PNS, peripheral nervous system.

neuroinflammation, growth-promoting factor secretion, and debris clearance activity. However, there is a lack of in-depth studies focusing on the phagocytic function of these cells, particularly the molecular and cellular mechanisms involved in this intricate process and on the synergistic effects with neural and mesenchymal stem cells (MSCs) in improving cell differentiation. Exploring these unique features will lead to a better understanding of the role of OECs in development and regeneration and will identify how the use of OECs can be optimized for neural regeneration therapies. These approaches may benefit from accumulating evidence pointing out a significant role of checkpoint therapy in inducing regeneration upon CNS injury (32). Herein we reviewed the current knowledge about the immunomodulatory and anti-inflammatory properties of OECs in neuroinflammation, neurodegeneration and during stem cell differentiation. Owing to the strong pro-regenerative properties of OECs, and their unique ability to promote stem cell differentiation, we explored the potential of OEC transplantation for tissue regeneration.

2 Immune role of OECs

The olfactory system is continuously exposed to various pathogens since the primary olfactory neurons are in direct contact with the external environment (7, 8). However, most cases of CNS infections do not occur through the olfactory system. In this scenario OECs play a crucial role in protecting CNS structures. Specifically, they participate in innate immune responses, secrete immunoregulatory molecules and exert their phagocytic activity thus maintaining microenvironmental homeostasis, supporting neuron survival and axonal growth (33–35).

2.1 Phagocytic activity of OECs

CNS lesions are characterized by neuronal degeneration and death, and by the persistence of cellular and myelinated debris that create an adverse environment for neural survival, germination of neurites and renewal of neurons (36, 37). Since olfactory receptor neurons renew themselves throughout lifetime, a large amount of apoptotic debris is generated continuously (35). Several studies support phagocytic functions of OECs throughout life (35, 38) especially following injury (38, 39). In fact, by switching from a resting state to a phagocytic phenotype to remove axonal debris and bacteria, they protect the olfactory nerve from microbial infections (35, 40, 41). A combination of morphological and phenotypic changes distinguishes reactive OECs from their resting state, including cytoskeletal hypertrophy and rearrangement (34, 42). However, the identification of specific molecular markers capable of discriminating between quiescent and reactive OECs could better elucidate the molecular mechanisms underlying their activation.

While Schwann cells participate in debris removal mainly by increasing the secretion of several pro-inflammatory molecules, thus recruiting professional phagocytes, including macrophages and neutrophils (43), OECs operate differently (38, 44). Wright et al. showed that OECs repel macrophages in co-culture, by expressing the macrophage migration inhibitory factor (MIF), which would explain the absence of macrophages in the olfactory nerve bundles (45).

In vitro studies reported that OECs possess several phagocytic-related receptors, including toll-like receptor 4 (TLR4), phosphatidylserine and mannose receptors (34, 46, 47). Particularly, during apoptosis, olfactory neurons display the "eat me" signal phosphatidylserine, recognized by OEC phosphatidylserine receptor, leading to the engulfment of apoptotic and necrotic cell debris (33, 44). Milk fat globule-EGF factor 8 (MFGE-8), which interacts with integrin receptors (48), is a bridging molecule that participates in several cell surface-mediated regulatory events. Li et al. demonstrated *in vitro* that OECs express MFGE-8 when apoptotic debris is added to the culture (49). Moreover, OECs have been reported to adopt a "microglia-like" phenotype showing high levels of CD11 expression after their transplantation into the X-irradiated spinal cord of female Sprague Dawley rats (50). However, *in vitro* immunolabelling of OECs has revealed that they do not express this microglial marker in physiological conditions (34). Interestingly, Nazareth et al. reported that OECs produce less pro-inflammatory cytokines, compared to Schwann cells and macrophages when exposed to necrotic bodies (37). Conversely, some anti-inflammatory cytokines, such as interleukin-10 (IL-10) and transforming growth factor beta (TGF-β) promote OEC phagocytic activity (49).

In summary, the phagocytic activity of OECs plays a crucial role in creating a favorable environment to promote neuronal turnover, aiding the overall process of neuronal regeneration. Hence, this peculiar feature of OECs may be particularly useful for neural repair therapies including their transplantation after SCI.

2.2 OEC-mediated effects during neuroinflammation

As abovementioned, OECs show several unique properties of inflammatory cells, allowing them to modulate immune responses and neuronal pro-regenerative processes. Overall, inflammation is thought to hinder cell differentiation and regeneration but, although OECs are able to secrete a range of pro-inflammatory cytokines and chemokines after injury or infections, they simultaneously promote nervous regeneration.

Following SCI, resident immune cells, including microglia and astrocytes, are activated by injured-released inflammatory

stimuli (51). Indeed, the microenvironment of lesioned CNS switch towards pro-apoptotic and anti-regenerative milieu. Particularly, inflammatory responses in SCI are mainly mediated by pro-inflammatory cytokines and chemokines secreted by reactive astrocytes and microglia. In this scenario, M1-polarized microglia induces astrocyte activation, resulting in chondroitin sulfate proteoglycan (CSPG) deposits and astrocytic scar formation, which limits the spread of inflammation but at the same time hampers axon regeneration (52). Concomitantly, glial cell activation causes the release of specific chemokines and pro-inflammatory cytokines, including IL-1, IL-6, and TNF. These cytokines, by activating their respective cascades, amplify inflammatory responses, alter the microenvironment and promote cell death, therefore blocking axonal regeneration (Figure 2) (53, 54). As a result, inflammatory response induces secondary tissue damage with detrimental consequences to neural tissue and its functions (55). In general terms, inflammatory response maintains a dynamic balance of pro-inflammatory and anti-inflammatory cytokine release; therefore, understanding the modulation of the inflammatory response mediated by OECs, could be a successful strategy to improve neuronal functional outcome after CNS injury.

OECs are reported to express chemokines/cytokines and their cognate receptors, such as chemokine (CXC motif) ligand 1 (CXCL1), a neurotrophic chemoattractant, which may have a role during embryogenesis or after OECs transplantation in the injured site, CXCL12, CXCL4, chemokine (CX3C motif) ligand 1 (CX3CL1) (56) that have been proven to play pivotal roles in neuroinflammation, acting as a signaling factor for the recruitment of neutrophilis and various leucocytes (57). The inflammatory monocyte chemotactic protein 1 (MCP-1), and its receptor CCR2 specifically mediates monocytes chemotaxis, which results in the recruitment of macrophages to the site of injury. Moreover, nuclear factor kappa B (NF-κB)-mediated signaling pathway, responsible for microglia and astrocytes activation after SCI, is activated by TROY, a member of the tumor necrosis factor (TNF) receptor superfamily, which has been detected *via in situ* hybridization and immunohistochemistry investigations in the olfactory system (58). OECs or OEC-released molecules are able to inhibit NF-κB activation, so exerting a neuroprotective role after CNS injury. OECs also release several signaling molecules, such as TNF and IL-1β, to recruit macrophages, thus modulating inflammation and neurodegeneration (14, 44, 59). In this context, OECs could modulate microglia-astrocyte responses by secreting anti-inflammatory cytokines such as IL-4, IL-10, IL-13 and TGF-β, capable to downregulate the pro-inflammatory factors IL-1β, TNF and IL-6 (Figure 2) (60–62). A recent study showed that IL-1α and IL-1β, which are significantly involved in inflammatory responses, were down-regulated after OEC transplantation at the injury site. This response is probably related to IL-1 receptor antagonist (IL-1Ra) mechanism, which is a competitive inhibitor of IL-1 by binding to its receptor (Figure 2). Therefore, OECs, reaching the site of the lesion, are subjected to pro-inflammatory factors released by the activated microglia, and secrete IL-1Ra in response, thus reducing microglial activation and pro-inflammatory factor production and limiting microglia-mediated pro-inflammatory cytokine release (63).

It is worth noticing that the abovementioned OEC-derived anti-inflammatory factors participate in modulating cell survival, proliferation and migration, thus reducing glial scar and promoting regeneration after SCI (64). IL-4 and TGF-β have a direct impact on neural survival given their modulatory effects on acute and chronic immune cell responses and on their

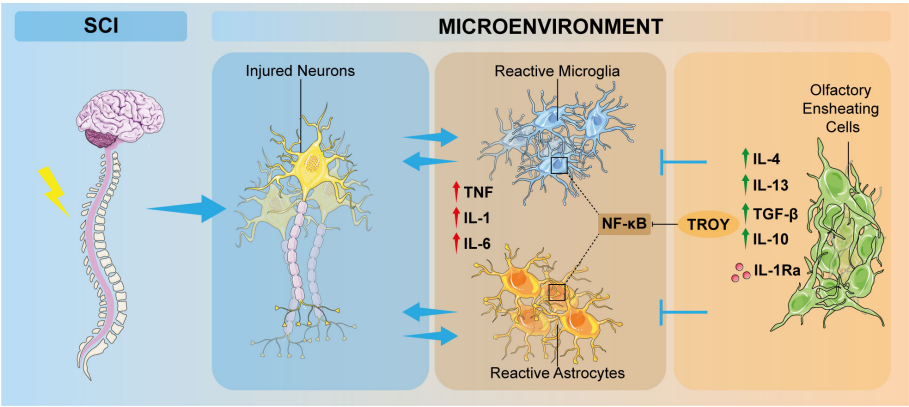


FIGURE 2
Schematic overview of the involvement of OECs in inflammation modulation after SCI. Neuronal damage induces pathological increasing of inflammatory responses, which promotes microglia polarization from a resting state to a M1-phenotype and astrocyte activation. OECs are able to modulate these inflammatory events by interacting directly or indirectly with microglia and astrocytes, thus ameliorating the detrimental condition of the altered microenvironment. OEC, olfactory ensheathing cell; SCI, spinal cord injury; TNF, tumor necrosis factor; IL, interleukin; TGF-β, transforming growth factor β, IL-1Ra: interleukin-1 receptor antagonist.

expression of detrimental molecules including nitric oxide (NO), reactive oxygen species (ROS), caspase and their secretion of neurotrophins (65).

Taken together these findings suggest that OECs delay the activation of microglia or macrophages and reduce the peak of the immune response, leading to neuroprotection against inflammatory damage.

3 OEC bystander effects on cell fate and differentiation

The ability of OECs in regulating neuroprotection is enhanced by the release of several protective factors in the microenvironment as OEC-conditioned medium (OEC-CM) promotes the differentiation of neural stem cells (NSCs) (66). Specifically, using OEC-CM, it has been shown that soluble factors larger than 30 kDa, which are secreted by OECs, promote migration, differentiation and maturation of NSCs within 7 days. By immunocytochemical analysis, it has been shown that NSCs in contact with OEC-CM, exhibited an up-regulation of neurofilament (NF), beta-III-tubulin (TUJ1), GFAP and a down-regulation of nestin, suggesting a differentiation of NSCs toward neuronal and astrocytic lineages. In addition, the presence in NSCs of synapsin-1, which is involved in the neurotransmitter release mechanism, has also been demonstrated, supporting the effect of OEC-CM in driving and/or stimulating neuronal differentiation. This study also claims that differentiation of NSCs, promoted by OECs, also occurs through indirect contact (67). OECs also exert their trophic effects directly through the secretion of factors involved in neurogenesis, neural differentiation and response, including both NGF and BDNF, small proteins including neurturin (NTN), CNTF, GDNF (68, 69), and heavier soluble factors including secreted protein acidic and cysteine rich (SPARC), sonic hedgehog protein (SHH), matrix metalloproteinase 2 (MMP 2), fibronectin, and laminin (70–72) (Table 1). Moreover, TGF-β3 secreted by OECs is involved in the regulation of neuronal differentiation, negatively regulating Yes-associated protein (YAP) (76). The potential of OECs to induce differentiation of NSCs into neurons has also been demonstrated by functional electrophysiological studies that showed that NSC-derived neurons exposed to OEC-CM acquire active electrophysiological properties, expressing sodium and potassium channels suitable for onset of action potentials similar to primary neuronal cells (66). *In vivo* studies demonstrated that OECs are able to promote NSC differentiation into dopaminergic neurons or cholinergic neurons, pointing out that OECs can induce NSC differentiation toward a specific neuron subtype (77, 78). OEC-induced effects would be exerted by influencing Wnt/beta-catenin signaling pathway, which is important in the proliferation and self-renewal of adult NSCs (79, 80). Indeed, it was shown that CM from Wnt-activated OECs (wOEC-CM) stimulates the proliferation and differentiation of NSCs, by increasing the percentage of Ki67/Sox2 double positive cells, maintaining Nestin expression under differentiation condition, but also stimulating NSC differentiation into Tuj1-positive neurons (81).

Many reports have shown that hypoxic preconditioned stem cells survive longer, exhibiting an efficient neuronal differentiation and showing enhanced paracrine effects (82, 83). Wang et al. demonstrated that CM from hyperthermia-conditioned OECs induces NSC neural differentiation more efficiently, thanks to the upregulation of HIF-1α, leading to synergistic effects that improve differentiation (84). By using OEC-CM under hypoxic condition, olfactory mucosa MSCs (OM-MSCs) are stimulated to differentiate into dopaminergic neurons. Specifically, OEC-CM under hypoxia upregulates transcriptional factors mediated by HIF-1α and it is involved in the development of dopaminergic neurons from OM-MSCs (85).

MSCs, including adipose tissue-derived MSCs (ASCs), are a type of non-hematopoietic stem cells which under appropriate conditions can give rise to several precursors (86–90). OEC-CM is also implicated in the differentiation ASCs toward a neuronal phenotype (91). ASCs treated with OEC-CM expressed markers

TABLE 1 OEC released factors involved in neural differentiation and neurogenesis.

Factors	Molecular weight	Functions	References
Brain Derived Neurotrophic Factor (BDNF)	26.7 kDa	Involved in the promotion of Schwann cell migration	(69)
Ciliary Neurotrophic Factor (CNTF)	22.9 kDa	Support neurogenesis	(67)
Fibronectin	440 kDa	Promote neural progenitor cell migration	(73)
Laminin	400 kDa	Involved in neural progenitor cell differentiation	(74)
Matrix Metalloproteinase 2 (MMP2)	67 kDa	Important for neural cell migration	(75)
Nerve Growth Factor (NGF)	26.7 kDa	Involved in the promotion of Schwann cell migration	(69)
Neurturin (NTN)	23.6 kDa	Support neurogenesis	(67)
Sonic Hedgehog protein (Shh)	67 kDa	Induce NSC differentiation into neurons	(72)
Secreted Protein Acidic and Cysteine Rich (SPARC)	43 kDa	Implicated in neural differentiation and in neurite extension	(70)

of progenitor and mature neurons, including Nestin, protein gene product 9.5 (PGP 9.5), and microtubule-associated protein 2 (MAP2) in a time-dependent manner and exhibited neuron like morphology, while they were negative for GFAP and A2B5, markers of astrocytes and oligodendrocytes, respectively (92). In addition, although a significant increase of Nestin, PGP 9.5, Synapsin I, and GFAP was reported, MAP2 was identified as the most representative, thus suggesting a greater tendency toward the neuronal phenotype (93). This result is confirmed by another study where a neural-like connexin expression was induced in ASCs after OEC-CM treatment (94–98). On the other hand, when ASCs were co-cultured with OECs using 3D collagen scaffolds, they differentiated into cells with OEC-like morphology and were reported to be p75NTR and Nestin positive and GFAP negative. These co-cultured ASCs also expressed various functional markers of mature OECs: BDNF, GDNF and the myelin proteolipid protein (PLP). Thus, these results demonstrate that using specific scaffolds, ASCs might differentiate into OEC-like cells *in vitro* (99). Altogether, it can be inferred that OECs play a key role in cell differentiation toward a neural type and are able to prompt MSC differentiation towards neural phenotype and even to mature OECs. As such, these intrinsic properties of OECs may be relevant for therapeutic approaches aiming at CNS tissue regeneration.

4 OECs for tissue regeneration and transplantation

In recent years, OECs have been investigated for their reparative ability following acute or chronic lesions that involve CNS. As already mentioned, it appears that OECs may play a crucial role in the treatment of SCI (100–103). Usually, SCI severely affects CNS microenvironment, leading to a series of deleterious processes such as inflammation and hypoxia, and progressive cell death (104). OECs exhibit several characteristics that enable them to have beneficial effects in neuro-repairing potential. They are able to reduce the inflammatory response following injury, thereby decreasing the size of the glial scar and promoting angiogenesis. In addition, they promote regrowth, plasticity and remyelination of axons (105–107). OECs can also interact with resident cell populations, particularly astrocytes and meningeal cells, either within the window of the glial scar formation or once the scar has already established (108, 109). Thus, in addition to penetrate glial tissue, OECs also produce extracellular matrix proteases and can reduce astrocytic reactivity. Overall, these properties may reduce glial scar formation and all consequential limitations, which strongly limit axonal regrowth and injury bridging (110). In SCI animal models, grafted OECs exhibit the ability to promote axon regrowth and propagation (30, 100, 111). In particular, OEC transplantation improves sensorimotor and autonomic nerve recovery, also reducing neuropathic pain due to SCI. OECs secrete a number of neurotrophic factors, which allow the establishment of a favorable microenvironment for the regrowth of damaged axons. Undoubtedly, it is crucial to have functional recovery in transplanted animals in order to consider OEC transplants a successful therapy for the treatment of SCI (107). A study of Ramon-Cueto et al., revealed that adult rats undergoing spinal cord resection and subsequent OEC transplantation, showed both functional and structural recovery. In particular, from 3 to 7 months after surgery, all transplanted animals improved locomotor functions and sensorimotor reflexes (103). To show actual recoveries in transplanted animals, electrophysiological studies were also carried out, demonstrating that animals with transplanted OECs not only exhibited functional recovery, but also showed recovery of action or evoked potentials (112, 113). Studies on OEC transplantation have also been carried out in human clinical in many countries around the world. Completed clinical trials have demonstrated the safety and efficacy of OEC transplantation, but recovery in patients is often highly variable. This variability may be related to a number of factors, such as difficulties in establishing master cell banks and working cell banks, cell purity, and transplantation techniques. Forty-four eligible trials, involving 1,266 SCI patients, investigated several cell-based treatments to improve functional independent misure (FIM) score. Among them, OEC transplantation proved to ameliorate the FIM score at 6 months, thus improving disease prognosis (114). However, a common consequence in these studies is the poor survival of transplanted cells, with survival rates ranging from 0.3 percent to 3 percent. This issue is probably related to the fact that when OECs are isolated, expanded *in vitro*, and then transplanted into the injury site, their therapeutic potential is reduced, probably due to bleeding, damaged tissue and anatomical structures and hostile microenvironment present in the lesioned area (115–117). Therefore, *in vitro* models challenging OECs, by mimicking the injured tissue microenvironment, are needed. For example, it has been found that preconditioned OECs showed increased migratory, phagocytic and immunomodulatory capacities. To improve their efficacy and yield upon graft, cells could be then exposed to a low oxygen level, or they could grow into three-dimensional scaffolds before being transplanted into the lesion (116).

Another effective strategy for SCI treatment is the co-transplantation of NSCs and OECs. Indeed, co-grafting of NSCs and OECs ameliorate SCI by inhibiting receptor-interacting protein kinase 3 (RIP3)/mixed lineage kinase domain-like protein (MLKL)-mediated necroptosis and stimulating NSC proliferation in the medulla. Evidence reports that OECs are able to increase NSCs

proliferation and differentiation and, importantly, co-grafts significantly support NSCs survival, opening the way for a potential stem cells-based regenerative approach. In this way, neural regeneration could be improved exploiting the synergistic effect of NSCs and OECs (118). In addition, a study by He Y. t al., showed that curcumin-activated OECs (aOECs) effectively improve neuronal differentiation of NSCs even under conditions of inflammation, and co-transplantation of aOECs and NSCs enhaces the neurological recovery of rats after SCI, providing a hopeful strategy for SCI repair by co-transplantation of aOECs and NSCs (119). Besides OEC transplantation, OECs-CM has also been shown to have therapeutic effects for SCI, enhancing functional recovery and axonal regeneration probably because of various factors previously secreted by OECs in their culture medium (120). In this context, exosomes derived from OECs (OEC-Exo) also promote neuronal survival and improve axon condition, facilitating functional recovery following SCI. OEC-Exo can be internalized by microglia/macrophages and are able to modulate their polarization. The main ability of OEC-Exo consists in an immunomodulatory function that shape immune microenvironment towards a pro-regenerative phenotype, supporting OEC-Exo as neuroprotective and regenerative strategy for CNS diseases (121). Furthermore, OECs secrete, *via* exosomes, alpha B-crystallin (CryAB), an anti-inflammatory protein, leading to an intercellular immune response. Thus, CryAB, together with other OEC-secreted factors, may ameliorate the hostile growth environment created by neurotoxic reactive astrocytes following CNS injury (122).

SCI microenvironment is characterized by a prevalence of M1-like pro-inflammatory macrophages over M2-like. This phenomenon results in a microenvironment that is unfavorable for cell differentiation and regeneration. Therefore, for a better potential regenerative strategy, a fundamental role is played by immune cell modulation (123, 124). Macrophages are a prominent population in SCI microenvironment, also able to alter the activity of transplanted OECs. However, the interaction appears to be reciprocal, as OECs express MIFs and can also lead to reduced macrophage recruitment *in vitro* (45). To enhance this interaction in favor of OECs by improving the cellular microenvironment at the injury level, a study of vascular endothelial growth factor (VEGF) and platelet-derived growth factor (PDGF) modulation in the SCI microenvironment was carried out. It was shown that CM from macrophages exposed to PDGF or combined VEGF and PDGF, under inflammatory conditions, increased OEC phagocytosis, also modulating the expression of genes related to nerve repair. Specifically, both PDGF and VEGF/PDGF reduced pro-inflammatory cytokines (i.e., TNF) by decreasing NF-κB translocation, promoting phagocytosis of myelin debris. For this reason, administering growth factors before OEC transplantation could improve transplant success and neural recovery (125).

5 Conclusions

Our knowledge of the properties, functions, and therapeutic potential of OECs is markedly increasing. OECs can be considered as a good candidate for cell-replacement and have shown remarkable capabilities to exert neuroprotective mechanisms. The uniqueness of OECs appears to collaborate with other recruited cell types to orchestrate the molecular signaling responsible for resolving the inflammatory state and creating a favorable environment for neural regeneration.

However, the development of human OEC transplants for clinical application in SCI still requires an in-depth understanding of the cellular and molecular biological characteristics of OECs. It seems now clear that OECs expanded *in vitro* and grafted back *in vivo* show limited therapeutic potential, probably due to the hostile microenvironment at the damaged tissue. In fact, a major issue limiting spinal cord regeneration is also the poor survival of transplanted cells (126). In order to describe the therapeutic potential of OECs it appears critical to characterize OEC gene expression aiming at identifying OEC-specific markers. Indeed, the most used marker to identify OECs, p75NTR, is also expressed *in vitro* by Schwann cells (10), astrocytes and lamina propria MSCs (127). The lack of a solid method for OECs identification, isolation and purification is among the main factors limiting reproducibility and reliability of transplantation studies. Furthermore, without a unique method for OEC identification, it is possible that their repair capacity is influenced by the presence of the various cells types co-existing alongside OECs.

One of the most effective approaches in transplantation of OECs is co-grafting with NSCs, achieving better therapeutic effects. Indeed OECs, by releasing trophic factors into the microenvironment, also play an important role in promoting the differentiation of NSCs, able to change their morphology, stimulating their differentiation towards mature neurons.

Despite the variability of results reported and limiting factors, OECs should be considered as valuable cell-based approach for SCI and a potential candidate to promote cell differentiation and regeneration. Finally, a deeper understanding of OEC anti-inflammatory properties and their interplay with other cells involved in neuro-repairing is crucial for the development of future therapies, using transplantation of OECs to treat neural injuries.

Author contributions

Conceptualization: SD, SD'A, NV, and RP; writing—original draft preparation: SD, SD'A, NV, and RP; writing—review and editing: all authors; visualization: SD, SD'A, CA, AP, and FT;

supervision: DLF, AZ, RG, DT, GLV, NV, and RP. All authors contributed to the article and approved the submitted version.

Funding

SD, CA, and AP were supported by the PhD program in Biotechnologies, Biometec, University of Catania. FT was supported by Fondazione Umberto Veronesi. NV was supported by the PON AIM R&I 2014-2020-E66C18001240007.

Acknowledgments

The authors thank Servier Medical Art (smart.servier.com, accessed on 13 November 2022)

Conflict of interest

The authors declare that the research was conducted in the absence of any commercial or financial relationships that could be construed as a potential conflict of interest.

Publisher's note

All claims expressed in this article are solely those of the authors and do not necessarily represent those of their affiliated organizations, or those of the publisher, the editors and the reviewers. Any product that may be evaluated in this article, or claim that may be made by its manufacturer, is not guaranteed or endorsed by the publisher.

References

1. Lobsiger CS, Cleveland DW. Glial cells as intrinsic components of non-cell-autonomous neurodegenerative disease. *Nat Neurosci* (2007) 10(11):1355–60. doi: 10.1038/nn1988

2. Barres BA. The mystery and magic of glia: A perspective on their roles in health and disease. *Neuron* (2008) 60(3):430–40. doi: 10.1016/j.neuron.2008.10.013

3. Wang X, Jiang C, Zhang Y, Chen Z, Fan H, Zhang Y, et al. The promoting effects of activated olfactory ensheathing cells on angiogenesis after spinal cord injury through the PI3K/Akt pathway. *Cell Biosci* (2022) 12(1):23. doi: 10.1186/s13578-022-00765-y

4. Graziadei GA, Graziadei PP. Neurogenesis and neuron regeneration in the olfactory system of mammals. II. Degeneration and reconstitution of the olfactory sensory neurons after axotomy. *J Neurocytol* (1979) 8(2):197–213. doi: 10.1007/BF01175561

5. Graziadei PP, Graziadei GA. Neurogenesis and neuron regeneration in the olfactory system of mammals. i. morphological aspects of differentiation and structural organization of the olfactory sensory neurons. *J Neurocytol* (1979) 8 (1):1–18. doi: 10.1007/BF01206454

6. Mackay-Sim A, Kittel P. Cell dynamics in the adult mouse olfactory epithelium: A quantitative autoradiographic study. *J Neurosci* (1991) 11(4):979–84. doi: 10.1523/JNEUROSCI.11-04-00979.1991

7. Schwob JE. Neural regeneration and the peripheral olfactory system. *Anat Rec* (2002) 269(1):33–49. doi: 10.1002/ar.10047

8. Leung CT, Coulombe PA, Reed RR. Contribution of olfactory neural stem cells to tissue maintenance and regeneration. *Nat Neurosci* (2007) 10(6):720–6. doi: 10.1038/nn1882

9. Doucette R. Glial influences on axonal growth in the primary olfactory system. *Glia* (1990) 3(6):433–49. doi: 10.1002/glia.440030602

10. Chen CR, Kachramanoglou C, Li D, Andrews P, Choi D. Anatomy and cellular constituents of the human olfactory mucosa: A review. *J Neurol Surg B Skull Base* (2014) 75(5):293–300. doi: 10.1055/s-0033-1361837

11. Schwob JE, Jang W, Holbrook EH, Lin B, Herrick DB, Peterson JN, et al. Stem and progenitor cells of the mammalian olfactory epithelium: Taking poietic license. *J Comp Neurol* (2017) 525(4):1034–54. doi: 10.1002/cne.24105

12. Rieger A, Deitmer JW, Lohr C. Axon-glia communication evokes calcium signaling in olfactory ensheathing cells of the developing olfactory bulb. *Glia* (2007) 55(4):352–9. doi: 10.1002/glia.20460

13. Ursavas S, Darici H, Karaoz E. Olfactory ensheathing cells: Unique glial cells promising for treatments of spinal cord injury. *J Neurosci Res* (2021) 99(6):1579–97. doi: 10.1002/jnr.24817

14. Roet KC, Verhaagen J. Understanding the neural repair-promoting properties of olfactory ensheathing cells. *Exp Neurol* (2014) 261:594–609. doi: 10.1016/j.expneurol.2014.05.007

15. Shields SD, Moore KD, Phelps PE, Basbaum AI. Olfactory ensheathing glia express aquaporin 1. *J Comp Neurol* (2010) 518(21):4329–41. doi: 10.1002/cne.22459

16. Barraud P, Seferiadis AA, Tyson LD, Zwart MF, Szabo-Rogers HL, Ruhrberg C, et al. Neural crest origin of olfactory ensheathing glia. *Proc Natl Acad Sci U S A* (2010) 107(49):21040–5. doi: 10.1073/pnas.1012248107

17. Forni PE, Taylor-Burds C, Melvin VS, Williams T, Wray S. Neural crest and ectodermal cells intermix in the nasal placode to give rise to GnRH-1 neurons, sensory neurons, and olfactory ensheathing cells. *J Neurosci* (2011) 31(18):6915–27. doi: 10.1523/JNEUROSCI.6087-10.2011

18. Katoh H, Shibata S, Fukuda K, Sato M, Satoh E, Nagoshi N, et al. The dual origin of the peripheral olfactory system: Placode and neural crest. *Mol Brain* (2011) 4:34. doi: 10.1186/1756-6606-4-34

19. Yao R, Murtaza M, Velasquez JT, Todorovic M, Rayfield A, Ekberg J, et al. Olfactory ensheathing cells for spinal cord injury: Sniffing out the issues. *Cell Transpl* (2018) 27(6):879–89. doi: 10.1177/0963689718779353

20. Pellitteri R, Spatuzza M, Stanzani S, Zaccheo D. Biomarkers expression in rat olfactory ensheathing cells. *Front Biosci (Schol Ed)* (2010) 2(1):289–98. doi: 10.2741/s64

21. Barton MJ, John JS, Clarke M, Wright A, Ekberg J. The glia response after peripheral nerve injury: A comparison between schwann cells and olfactory ensheathing cells and their uses for neural regenerative therapies. *Int J Mol Sci* (2017) 18(2):287–306. doi: 10.3390/ijms18020287

22. Boruch AV, Conners JJ, Pipitone M, Deadwyler G, Storer PD, Devries GH, et al. Neurotrophic and migratory properties of an olfactory ensheathing cell line. *Glia* (2001) 33(3):225–9. doi: 10.1002/1098-1136(200103)33:3<225::AID-GLIA1021>3.0.CO;2-Y

23. Stepanova OV, Voronova AD, Chadin AV, Fursa GA, Karsuntseva EK, Valikhov MP, et al. Neurotrophin-3 enhances the effectiveness of cell therapy in chronic spinal cord injuries. *Bull Exp Biol Med* (2022) 173(1):114–8. doi: 10.1007/s10517-022-05504-4

24. Russo C, Patane M, Russo A, Stanzani S, Pellitteri R. Effects of ghrelin on olfactory ensheathing cell viability and neural marker expression. *J Mol Neurosci* (2021) 71(5):963–71. doi: 10.1007/s12031-020-01716-3

25. Lo Furno D, Mannino G, Giuffrida R. Functional role of mesenchymal stem cells in the treatment of chronic neurodegenerative diseases. *J Cell Physiol* (2018) 233(5):3982–99. doi: 10.1002/jcp.26192

26. Golchin A, Shams F, Kangari P, Azari A, Hosseinzadeh S. Regenerative medicine: Injectable cell-based therapeutics and approved products. *Adv Exp Med Biol* (2020) 1237:75–95. doi: 10.1007/5584_2019_412

27. Mannino G, Russo C, Longo A, Anfuso CD, Lupo G, Lo Furno D, et al. Potential therapeutic applications of mesenchymal stem cells for the treatment of eye diseases. *World J Stem Cells* (2021) 13(6):632–44. doi: 10.4252/wjsc.v13.i6.632

28. Mannino G, Cristaldi M, Giurdanella G, Perrotta RE, Lo Furno D, Giuffrida R, et al. ARPE-19 conditioned medium promotes neural differentiation of adipose-derived mesenchymal stem cells. *World J Stem Cells* (2021) 13(11):1783–96. doi: 10.4252/wjsc.v13.i11.1783

29. Menezes K, Nascimento MA, Goncalves JP, Cruz AS, Lopes DV, Curzio B, et al. Human mesenchymal cells from adipose tissue deposit laminin and promote regeneration of injured spinal cord in rats. *PloS One* (2014) 9(5):e96020. doi: 10.1371/journal.pone.0096020

30. Lu J, Feron F, Mackay-Sim A, Waite PM. Olfactory ensheathing cells promote locomotor recovery after delayed transplantation into transected spinal cord. *Brain* (2002) 125(Pt 1):14–21. doi: 10.1093/brain/awf014

31. Pearse DD, Sanchez AR, Pereira FC, Andrade CM, Puzis R, Pressman Y, et al. Transplantation of schwann cells and/or olfactory ensheathing glia into the contused spinal cord: Survival, migration, axon association, and functional recovery. *Glia* (2007) 55(9):976–1000. doi: 10.1002/glia.20490

32. Taylor MJ, Thompson AM, Alhajlah S, Tuxworth RI, Ahmed Z. Inhibition of Chk2 promotes neuroprotection, axon regeneration, and functional recovery after CNS injury. *Sci Adv* (2022) 8(37):eabq2611. doi: 10.1126/sciadv.abq2611

33. He BR, Xie ST, Wu MM, Hao DJ, Yang H. Phagocytic removal of neuronal debris by olfactory ensheathing cells enhances neuronal survival and neurite outgrowth *via* p38MAPK activity. *Mol Neurobiol* (2014) 49(3):1501–12. doi: 10.1007/s12035-013-8588-2

34. Hao DJ, Liu C, Zhang L, Chen B, Zhang Q, Zhang R, et al. Lipopolysaccharide and curcumin Co-stimulation potentiates olfactory ensheathing cell phagocytosis *Via* enhancing their activation. *Neurotherapeutics* (2017) 14(2):502–18. doi: 10.1007/s13311-016-0485-8

35. Su Z, Chen J, Qiu Y, Yuan Y, Zhu F, Zhu Y, et al. Olfactory ensheathing cells: the primary innate immunocytes in the olfactory pathway to engulf apoptotic olfactory nerve debris. *Glia* (2013) 61(4):490–503. doi: 10.1002/glia.22450

36. Vargas ME, Barres BA. Why is wallerian degeneration in the CNS so slow? *Annu Rev Neurosci* (2007) 30:153–79. doi: 10.1146/annurev.neuro.30.051606.094354

37. Nazareth L, Shelper TB, Chacko A, Basu S, Delbaz A, Lee JYP, et al. Key differences between olfactory ensheathing cells and schwann cells regarding phagocytosis of necrotic cells: implications for transplantation therapies. *Sci Rep* (2020) 10(1):18936. doi: 10.1038/s41598-020-75850-8

38. Nazareth L, Lineburg KE, Chuah MI, Tello Velasquez J, Chehrehasa F, St John JA, et al. Olfactory ensheathing cells are the main phagocytic cells that remove axon debris during early development of the olfactory system. *J Comp Neurol* (2015) 523(3):479–94. doi: 10.1002/cne.23694

39. Wewetzer K, Kern N, Ebel C, Radtke C, Brandes G. Phagocytosis of O4+ axonal fragments *in vitro* by p75- neonatal rat olfactory ensheathing cells. *Glia* (2005) 49(4):577–87. doi: 10.1002/glia.20149

40. Panni P, Ferguson IA, Beacham I, Mackay-Sim A, Ekberg JA, St John JA. Phagocytosis of bacteria by olfactory ensheathing cells and schwann cells. *Neurosci Lett* (2013) 539:65–70. doi: 10.1016/j.neulet.2013.01.052

41. Jiang Y, Guo J, Tang X, Wang X, Hao D, Yang H. The immunological roles of olfactory ensheathing cells in the treatment of spinal cord injury. *Front Immunol* (2022) 13:881162. doi: 10.3389/fimmu.2022.881162

42. Li Y, Huo S, Fang Y, Zou T, Gu X, Tao Q, et al. ROCK inhibitor Y27632 induced morphological shift and enhanced neurite outgrowth-promoting property of olfactory ensheathing cells *via* YAP-dependent up-regulation of L1-CAM. *Front Cell Neurosci* (2018) 12:489. doi: 10.3389/fncel.2018.00489

43. Hartlehnert M, Derksen A, Hagenacker T, Kindermann D, Schafers M, Pawlak M, et al. Schwann cells promote post-traumatic nerve inflammation and neuropathic pain through MHC class II. *Sci Rep* (2017) 7(1):12518. doi: 10.1038/s41598-017-12744-2

44. Nazareth L, St John J, Murtaza M, Ekberg J. Phagocytosis by peripheral glia: Importance for nervous system functions and implications in injury and disease. *Front Cell Dev Biol* (2021) 9:660259. doi: 10.3389/fcell.2021.660259

45. Wright AA, Todorovic M, Murtaza M, St John JA, Ekberg JA. Macrophage migration inhibitory factor and its binding partner HTRA1 are expressed by olfactory ensheathing cells. *Mol Cell Neurosci* (2020) 102:103450. doi: 10.1016/j.mcn.2019.103450

46. Vincent AJ, Choi-Lundberg DL, Harris JA, West AK, Chuah MI. Bacteria and PAMPs activate nuclear factor kappaB and gro production in a subset of olfactory ensheathing cells and astrocytes but not in schwann cells. *Glia* (2007) 55 (9):905–16. doi: 10.1002/glia.20512

47. Carvalho LA, Nobrega AF, Soares ID, Carvalho SL, Allodi S, Baetas-da-Cruz W, et al. The mannose receptor is expressed by olfactory ensheathing cells in the rat olfactory bulb. *J Neurosci Res* (2013) 91(12):1572–80. doi: 10.1002/jnr.23285

48. Hanayama R, Tanaka M, Miwa K, Shinohara A, Iwamatsu A, Nagata S. Identification of a factor that links apoptotic cells to phagocytes. *Nature* (2002) 417 (6885):182–7. doi: 10.1038/417182a

49. Li Y, Zou T, Xue L, Yin ZQ, Huo S, Xu H. TGF-beta1 enhances phagocytic removal of neuron debris and neuronal survival by olfactory ensheathing cells *via* integrin/MFG-E8 signaling pathway. *Mol Cell Neurosci* (2017) 85:45–56. doi: 10.1016/j.mcn.2017.08.006

50. Lankford KL, Sasaki M, Radtke C, Kocsis JD. Olfactory ensheathing cells exhibit unique migratory, phagocytic, and myelinating properties in the X-irradiated spinal cord not shared by schwann cells. *Glia* (2008) 56(15):1664–78. doi: 10.1002/glia.20718

51. Orr MB, Gensel JC. Spinal cord injury scarring and inflammation: Therapies targeting glial and inflammatory responses. *Neurotherapeutics* (2018) 15(3):541–53. doi: 10.1007/s13311-018-0631-6

52. Yu SS, Li ZY, Xu XZ, Yao F, Luo Y, Liu YC, et al. M1-type microglia can induce astrocytes to deposit chondroitin sulfate proteoglycan after spinal cord injury. *Neural Regener Res* (2022) 17(5):1072–9. doi: 10.4103/1673-5374.324858

53. Ramesh G, MacLean AG, Philipp MT. Cytokines and chemokines at the crossroads of neuroinflammation, neurodegeneration, and neuropathic pain. *Mediators Inflamm* (2013) 2013:480739. doi: 10.1155/2013/480739

54. Jin X, Yamashita T. Microglia in central nervous system repair after injury. *J Biochem* (2016) 159(5):491–6. doi: 10.1093/jb/mvw009

55. David S, Kroner A. Repertoire of microglial and macrophage responses after spinal cord injury. *Nat Rev Neurosci* (2011) 12(7):388–99. doi: 10.1038/nrn3053

56. Yan Y, Su J, Zhang Z. The CXCL12/CXCR4/ACKR3 response axis in chronic neurodegenerative disorders of the central nervous system: Therapeutic target and biomarker. *Cell Mol Neurobiol* (2022) 42(7):2147–56. doi: 10.1007/s10571-021-01115-1

57. Vincent AJ, Taylor JM, Choi-Lundberg DL, West AK, Chuah MI. Genetic expression profile of olfactory ensheathing cells is distinct from that of schwann cells and astrocytes. *Glia* (2005) 51(2):132–47. doi: 10.1002/glia.20195

58. Hisaoka T, Morikawa Y, Kitamura T, Senba E. Expression of a member of tumor necrosis factor receptor superfamily, TROY, in the developing mouse brain. *Brain Res Dev Brain Res* (2003) 143(1):105–9. doi: 10.1016/S0165-3806(03)00101-9

59. Su Z, He C. Olfactory ensheathing cells: biology in neural development and regeneration. *Prog Neurobiol* (2010) 92(4):517–32. doi: 10.1016/j.pneurobio.2010.08.008

60. Donnelly DJ, Popovich PG. Inflammation and its role in neuroprotection, axonal regeneration and functional recovery after spinal cord injury. *Exp Neurol* (2008) 209(2):378–88. doi: 10.1016/j.expneurol.2007.06.009

61. Cataldi C, Mari NL, Lozovoy MAB, Martins LMM, Reiche EMV, Maes M, et al. Proinflammatory and anti-inflammatory cytokine profiles in psoriasis: use as laboratory biomarkers and disease predictors. *Inflammation Res* (2019) 68(7):557–67. doi: 10.1007/s00011-019-01238-8

62. Daines JM, Schellhardt L, Wood MD. The role of the IL-4 signaling pathway in traumatic nerve injuries. *Neurorehabil Neural Repair* (2021) 35(5):431–43. doi: 10.1177/15459683211001026

63. Zhang L, Zhuang X, Kotitalo P, Keller T, Krzyczmonik A, Haaparanta-Solin M, et al. Intravenous transplantation of olfactory ensheathing cells reduces neuroinflammation after spinal cord injury *via* interleukin-1 receptor antagonist. *Theranostics* (2021) 11(3):1147–61. doi: 10.7150/thno.52197

64. Park J, Decker JT, Margul DJ, Smith DR, Cummings BJ, Anderson AJ, et al. Local immunomodulation with anti-inflammatory cytokine-encoding lentivirus enhances functional recovery after spinal cord injury. *Mol Ther* (2018) 26(7):1756–70. doi: 10.1016/j.ymthe.2018.04.022

65. Khankan RR, Griffis KG, Haggerty-Skeans JR, Zhong H, Roy RR, Edgerton VR, et al. Olfactory ensheathing cell transplantation after a complete spinal cord transection mediates neuroprotective and immunomodulatory mechanisms to facilitate regeneration. *J Neurosci* (2016) 36(23):6269–86. doi: 10.1523/JNEUROSCI.0085-16.2016

66. Duan D, Rong M, Zeng Y, Teng X, Zhao Z, Liu B, et al. Electrophysiological characterization of NSCs after differentiation induced by OEC conditioned medium. *Acta Neurochir (Wien)* (2011) 153(10):2085–90. doi: 10.1007/s00701-011-0955-z

67. Sethi R, Sethi R, Redmond A, Lavik E. Olfactory ensheathing cells promote differentiation of neural stem cells and robust neurite extension. *Stem Cell Rev Rep* (2014) 10(6):772–85. doi: 10.1007/s12015-014-9539-7

68. Lipson AC, Widenfalk J, Lindqvist E, Ebendal T, Olson L. Neurotrophic properties of olfactory ensheathing glia. *Exp Neurol* (2003) 180(2):167–71. doi: 10.1016/S0014-4886(02)00058-4

69. Cao L, Zhu YL, Su Z, Lv B, Huang Z, Mu L, et al. Olfactory ensheathing cells promote migration of schwann cells by secreted nerve growth factor. *Glia* (2007) 55 (9):897–904. doi: 10.1002/glia.20511

70. Au E, Richter MW, Vincent AJ, Tetzlaff W, Aebersold R, Sage EH, et al. SPARC From olfactory ensheathing cells stimulates schwann cells to promote neurite outgrowth and enhances spinal cord repair. *J Neurosci* (2007) 27(27):7208–21. doi: 10.1523/JNEUROSCI.0509-07.2007

71. Higginson JR, Barnett SC. The culture of olfactory ensheathing cells (OECs)–a distinct glial cell type. *Exp Neurol* (2011) 229(1):2–9. doi: 10.1016/j.expneurol.2010.08.020

72. Zhang X, Klueber KM, Guo Z, Cai J, Lu C, Winstead WI, et al. Induction of neuronal differentiation of adult human olfactory neuroepithelial-derived progenitors. *Brain Res* (2006), 1073–1074:109–19. doi: 10.1016/j.brainres.2005.12.059

73. Kearns SM, Laywell ED, Kukekov VK, Steindler DA. Extracellular matrix effects on neurosphere cell motility. *Exp Neurol* (2003) 182(1):240–4. doi: 10.1016/S0014-4886(03)00124-9

74. Wilkinson AE, Kobelt LJ, Leipzig ND. Immobilized ECM molecules and the effects of concentration and surface type on the control of NSC differentiation. *J BioMed Mater Res A* (2014) 102(10):3419–28. doi: 10.1002/jbm.a.35001

75. Wang L, Zhang ZG, Zhang RL, Gregg SR, Hozeska-Solgot A, LeTourneau Y, et al. Matrix metalloproteinase 2 (MMP2) and MMP9 secreted by erythropoietin-activated endothelial cells promote neural progenitor cell migration. *J Neurosci* (2006) 26(22):5996–6003. doi: 10.1523/JNEUROSCI.5380-05.2006

76. Ge L, Zhang C, Xie H, Zhuo Y, Xun C, Chen P, et al. A phosphoproteomics study reveals a defined genetic program for neural lineage commitment of neural stem cells induced by olfactory ensheathing cell-conditioned medium. *Pharmacol Res* (2021) 172:105797. doi: 10.1016/j.phrs.2021.105797

77. Shukla S, Chaturvedi RK, Seth K, Roy NS, Agrawal AK. Enhanced survival and function of neural stem cells-derived dopaminergic neurons under influence of olfactory ensheathing cells in parkinsonian rats. *J Neurochem* (2009) 109(2):436–51. doi: 10.1111/j.1471-4159.2009.05983.x

78. Srivastava N, Seth K, Khanna VK, Ansari RW, Agrawal AK. Long-term functional restoration by neural progenitor cell transplantation in rat model of cognitive dysfunction: co-transplantation with olfactory ensheathing cells for neurotrophic factor support. *Int J Dev Neurosci* (2009) 27(1):103–10. doi: 10.1016/j.ijdevneu.2008.08.002

79. Qu Q, Sun G, Li W, Yang S, Ye P, Zhao C, et al. Orphan nuclear receptor TLX activates wnt/beta-catenin signalling to stimulate neural stem cell proliferation and self-renewal. *Nat Cell Biol* (2010) 12(1):31–40. doi: 10.1038/ncb2001

80. Mannino G, Russo C, Maugeri G, Musumeci G, Vicario N, Tibullo D, et al. Adult stem cell niches for tissue homeostasis. *J Cell Physiol* (2022) 237(1):239–57. doi: 10.1002/jcp.30562

81. Yue Y, Xue Q, Yang J, Li X, Mi Z, Zhao G, et al. Wnt-activated olfactory ensheathing cells stimulate neural stem cell proliferation and neuronal differentiation. *Brain Res* (2020) 1735:146726. doi: 10.1016/j.brainres.2020.146726

82. Peterson KM, Aly A, Lerman A, Lerman LO, Rodriguez-Porcel M. Improved survival of mesenchymal stromal cell after hypoxia preconditioning: role of oxidative stress. *Life Sci* (2011) 88(1-2):65–73. doi: 10.1016/j.lfs.2010.10.023

83. Stubbs SL, Hsiao ST, Peshavariya HM, Lim SY, Dusting GJ, Dilley RJ. Hypoxic preconditioning enhances survival of human adipose-derived stem cells and conditions endothelial cells *in vitro*. *Stem Cells Dev* (2012) 21(11):1887–96. doi: 10.1089/scd.2011.0289

84. Wang L, Jiang M, Duan D, Zhao Z, Ge L, Teng X, et al. Hyperthermia-conditioned OECs serum-free-conditioned medium induce NSC differentiation into neuron more efficiently by the upregulation of HIF-1 alpha and binding activity. *Transplantation* (2014) 97(12):1225–32. doi: 10.1097/TP.0000000000000118

85. Zhuo Y, Wang L, Ge L, Li X, Duan D, Teng X, et al. Hypoxic culture promotes dopaminergic-neuronal differentiation of nasal olfactory mucosa mesenchymal stem cells *via* upregulation of hypoxia-inducible factor-1alpha. *Cell Transpl* (2017) 26(8):1452–61. doi: 10.1177/0963689717720291

86. Calabrese G, Giuffrida R, Lo Furno D, Parrinello NL, Forte S, Gulino R, et al. Potential effect of CD271 on human mesenchymal stromal cell proliferation and differentiation. *Int J Mol Sci* (2015) 16(7):15609–24. doi: 10.3390/ijms160715609

87. Lo Furno D, Mannino G, Cardile V, Parenti R, Giuffrida R. Potential therapeutic applications of adipose-derived mesenchymal stem cells. *Stem Cells Dev* (2016) 25(21):1615–28. doi: 10.1089/scd.2016.0135

88. Mannino G, Longo A, Gennuso F, Anfuso CD, Lupo G, Giurdanella G, et al. Effects of high glucose concentration on pericyte-like differentiated human adipose-derived mesenchymal stem cells. *Int J Mol Sci* (2021) 22(9):4604–19. doi: 10.3390/ijms22094604

89. Lo Furno D, Graziano AC, Caggia S, Perrotta RE, Tarico MS, Giuffrida R, et al. Decrease of apoptosis markers during adipogenic differentiation of mesenchymal stem cells from human adipose tissue. *Apoptosis* (2013) 18(5):578–88. doi: 10.1007/s10495-013-0830-x

90. Musumeci G, Mobasheri A, Trovato FM, Szychlinska MA, Graziano AC, Lo Furno D, et al. Biosynthesis of collagen I, II, RUNX2 and lubricin at different time points of chondrogenic differentiation in a 3D *in vitro* model of human mesenchymal stem cells derived from adipose tissue. *Acta Histochem* (2014) 116(8):1407–17. doi: 10.1016/j.acthis.2014.09.008

91. Russo C, Mannino G, Patane M, Parrinello NL, Pellitteri R, Stanzani S, et al. Ghrelin peptide improves glial conditioned medium effects on neuronal differentiation of human adipose mesenchymal stem cells. *Histochem Cell Biol* (2021) 156(1):35–46. doi: 10.1007/s00418-021-01980-3

92. Lo Furno D, Pellitteri R, Graziano AC, Giuffrida R, Vancheri C, Gili E, et al. Differentiation of human adipose stem cells into neural phenotype by neuroblastoma- or olfactory ensheathing cells-conditioned medium. *J Cell Physiol* (2013) 228(11):2109–18. doi: 10.1002/jcp.24386

93. Lo Furno D, Mannino G, Giuffrida R, Gili E, Vancheri C, Tarico MS, et al. Neural differentiation of human adipose-derived mesenchymal stem cells induced by glial cell conditioned media. *J Cell Physiol* (2018) 233(10):7091–100. doi: 10.1002/jcp.26632

94. Lo Furno D, Mannino G, Pellitteri R, Zappala A, Parenti R, Gili E, et al. Conditioned media from glial cells promote a neural-like connexin expression in human adipose-derived mesenchymal stem cells. *Front Physiol* (2018) 9:1742. doi: 10.3389/fphys.2018.01742

95. Vicario N, Castrogiovanni P, Imbesi R, Giallongo S, Mannino G, Furno DL, et al. GJA1/CX43 high expression levels in the cervical spinal cord of ALS patients correlate to microglia-mediated neuroinflammatory profile. *Biomedicines* (2022) 10(9):2246–64. doi: 10.3390/biomedicines10092246

96. Vicario N, Parenti R. Connexins signatures of the neurovascular unit and their physio-pathological functions. *Int J Mol Sci* (2022) 23(17):9510–26. doi: 10.3390/ijms23179510

97. Vicario N, Turnaturi R, Spitale FM, Torrisi F, Zappala A, Gulino R, et al. Intercellular communication and ion channels in neuropathic pain chronicization. *Inflammation Res* (2020) 69(9):841–50. doi: 10.1007/s00011-020-01363-9

98. Mannino G, Vicario N, Parenti R, Giuffrida R, Lo Furno D. Connexin expression decreases during adipogenic differentiation of human adipose-derived mesenchymal stem cells. *Mol Biol Rep* (2020) 47(12):9951–8. doi: 10.1007/s11033-020-05950-1

99. Wang B, Han J, Gao Y, Xiao Z, Chen B, Wang X, et al. The differentiation of rat adipose-derived stem cells into OEC-like cells on collagen scaffolds by co-culturing with OECs. *Neurosci Lett* (2007) 421(3):191–6. doi: 10.1016/j.neulet.2007.04.081

100. Garcia-Alias G, Lopez-Vales R, Fores J, Navarro X, Verdu E. Acute transplantation of olfactory ensheathing cells or schwann cells promotes recovery after spinal cord injury in the rat. *J Neurosci Res* (2004) 75(5):632–41. doi: 10.1002/jnr.20029

101. Lopez-Vales R, Fores J, Verdu E, Navarro X. Acute and delayed transplantation of olfactory ensheathing cells promote partial recovery after complete transection of the spinal cord. *Neurobiol Dis* (2006) 21(1):57–68. doi: 10.1016/j.nbd.2005.06.011

102. Lopez-Vales R, Garcia-Alias G, Fores J, Navarro X, Verdu E. Increased expression of cyclo-oxygenase 2 and vascular endothelial growth factor in lesioned spinal cord by transplanted olfactory ensheathing cells. *J Neurotrauma* (2004) 21(8):1031–43. doi: 10.1089/0897715041651105

103. Ramon-Cueto A, Cordero MI, Santos-Benito FF, Avila J. Functional recovery of paraplegic rats and motor axon regeneration in their spinal cords by olfactory ensheathing glia. *Neuron* (2000) 25(2):425–35. doi: 10.1016/S0896-6273(00)80905-8

104. Rossignol S, Schwab M, Schwartz M, Fehlings MG. Spinal cord injury: time to move? *J Neurosci* (2007) 27(44):11782–92. doi: 10.1523/JNEUROSCI.3444-07.2007

105. Andrews MR, Stelzner DJ. Evaluation of olfactory ensheathing and schwann cells after implantation into a dorsal injury of adult rat spinal cord. *J Neurotrauma* (2007) 24(11):1773–92. doi: 10.1089/neu.2007.0353

106. Ramer LM, Au E, Richter MW, Liu J, Tetzlaff W, Roskams AJ. Peripheral olfactory ensheathing cells reduce scar and cavity formation and promote regeneration after spinal cord injury. *J Comp Neurol* (2004) 473(1):1–15. doi: 10.1002/cne.20049

107. Gomez RM, Sanchez MY, Portela-Lomba M, Ghotme K, Barreto GE, Sierra J, et al. Cell therapy for spinal cord injury with olfactory ensheathing glia cells (OECs). *Glia* (2018) 66(7):1267–301. doi: 10.1002/glia.23282

108. Li Y, Li D, Raisman G. Interaction of olfactory ensheathing cells with astrocytes may be the key to repair of tract injuries in the spinal cord: the 'pathway hypothesis'. *J Neurocytol* (2005) 34(3-5):343–51. doi: 10.1007/s11068-005-8361-1

109. Franssen EH, Roet KC, de Bree FM, Verhaagen J. Olfactory ensheathing glia and schwann cells exhibit a distinct interaction behavior with meningeal cells. *J Neurosci Res* (2009) 87(7):1556–64. doi: 10.1002/jnr.21979

110. Pastrana E, Moreno-Flores MT, Gurzov EN, Avila J, Wandosell F, Diaz-Nido J. Genes associated with adult axon regeneration promoted by olfactory ensheathing cells: a new role for matrix metalloproteinase 2. *J Neurosci* (2006) 26(20):5347–59. doi: 10.1523/JNEUROSCI.1111-06.2006

111. Chuah MI, Choi-Lundberg D, Weston S, Vincent AJ, Chung RS, Vickers JC, et al. Olfactory ensheathing cells promote collateral axonal branching in the injured adult rat spinal cord. *Exp Neurol* (2004) 185(1):15–25. doi: 10.1016/j.expneurol.2003.09.008

112. Imaizumi T, Lankford KL, Kocsis JD. Transplantation of olfactory ensheathing cells or schwann cells restores rapid and secure conduction across

the transected spinal cord. *Brain Res* (2000) 854(1-2):70–8. doi: 10.1016/S0006-8993(99)02285-4

113. Toft A, Scott DT, Barnett SC, Riddell JS. Electrophysiological evidence that olfactory cell transplants improve function after spinal cord injury. *Brain* (2007) 130(Pt 4):970–84. doi: 10.1093/brain/awm040

114. Xu X, Liang Z, Lin Y, Rao J, Lin F, Yang Z, et al. Comparing the efficacy and safety of cell transplantation for spinal cord injury: A systematic review and Bayesian network meta-analysis. *Front Cell Neurosci* (2022) 16:860131. doi: 10.3389/fncel.2022.860131

115. Kawaja MD, Boyd JG, Smithson LJ, Jahed A, Doucette R. Technical strategies to isolate olfactory ensheathing cells for intraspinal implantation. *J Neurotrauma* (2009) 26(2):155–77. doi: 10.1089/neu.2008.0709

116. Murtaza M, Mohanty L, Ekberg JAK, St John JA. Designing olfactory ensheathing cell transplantation therapies: Influence of cell microenvironment. *Cell Transpl* (2022) 31:9636897221125685. doi: 10.1177/09636897221125685

117. Miah M, Ferretti P, Choi D. Considering the cellular composition of olfactory ensheathing cell transplants for spinal cord injury repair: A review of the literature. *Front Cell Neurosci* (2021) 15:781489. doi: 10.3389/fncel.2021.781489

118. Wang X, Kuang N, Chen Y, Liu G, Wang N, Kong F, et al. Transplantation of olfactory ensheathing cells promotes the therapeutic effect of neural stem cells on spinal cord injury by inhibiting necrioptosis. *Aging (Albany NY)* (2021) 13 (6):9056–70. doi: 10.18632/aging.202758

119. He Y, Jiang Y, Dong L, Jiang C, Zhang L, Zhang G, et al. The aOECs facilitate the neuronal differentiation of neural stem cells in the inflammatory microenvironment through up-regulation of bioactive factors and activation of Wnt3/beta-catenin pathway. *Mol Neurobiol* (2022). doi: 10.1007/s12035-022-03113-w

120. Gu M, Gao Z, Li X, Guo L, Lu T, Li Y, et al. Conditioned medium of olfactory ensheathing cells promotes the functional recovery and axonal regeneration after contusive spinal cord injury. *Brain Res* (2017) 1654(Pt A):43–54. doi: 10.1016/j.brainres.2016.10.023

121. Fan H, Chen Z, Tang HB, Shan LQ, Chen ZY, Wang XH, et al. Exosomes derived from olfactory ensheathing cells provided neuroprotection for spinal cord injury by switching the phenotype of macrophages/microglia. *Bioeng Transl Med* (2022) 7(2):e10287. doi: 10.1002/btm2.10287

122. Saglam A, Calof AL, Wray S. Novel factor in olfactory ensheathing cell-astrocyte crosstalk: Anti-inflammatory protein alpha-crystallin b. *Glia* (2021) 69 (4):1022–36. doi: 10.1002/glia.23946

123. Kigerl KA, Gensel JC, Ankeny DP, Alexander JK, Donnelly DJ, Popovich PG. Identification of two distinct macrophage subsets with divergent effects causing either neurotoxicity or regeneration in the injured mouse spinal cord. *J Neurosci* (2009) 29(43):13435–44. doi: 10.1523/JNEUROSCI.3257-09.2009

124. Kroner A, Greenhalgh AD, Zarruk JG, Passos Dos Santos R, Gaestel M, David S. TNF and increased intracellular iron alter macrophage polarization to a detrimental M1 phenotype in the injured spinal cord. *Neuron* (2014) 83(5):1098–116. doi: 10.1016/j.neuron.2014.07.027

125. Basu S, Choudhury IN, Lee JYP, Chacko A, Ekberg JAK, St John JA. Macrophages treated with VEGF and PDGF exert paracrine effects on olfactory ensheathing cell function. *Cells* (2022) 11(15):2408–28. doi: 10.3390/cells11152408

126. Reshamwala R, Shah M, St John J, Ekberg J. Survival and integration of transplanted olfactory ensheathing cells are crucial for spinal cord injury repair: Insights from the last 10 years of animal model studies. *Cell Transpl* (2019) 28 (1_suppl):132S–59S. doi: 10.1177/0963689719883823

127. Lindsay SL, Toft A, Griffin J, MME A, Barnett SC, Riddell JS. Human olfactory mesenchymal stromal cell transplants promote remyelination and earlier improvement in gait co-ordination after spinal cord injury. *Glia* (2017) 65(4):639–56. doi: 10.1002/glia.23117

frontiers | Frontiers in Immunology

TYPE Original Research
PUBLISHED 10 January 2023
DOI 10.3389/fimmu.2022.1056447

Check for updates

OPEN ACCESS

EDITED BY
Bo Li,
Department of Orthopedics, Sun Yat-sen University, China

REVIEWED BY
Yunzhong Cheng,
Department of Orthopedic Surgery, Capital Medical University, China
Jinming Han,
Capital Medical University, China

*CORRESPONDENCE
Huiping Li
lihuiping@fudan.edu.cn
Weijun Feng
fengweijun@fudan.edu.cn
Xiu Xu
xuxiu@fudan.edu.cn

SPECIALTY SECTION
This article was submitted to Multiple Sclerosis and Neuroimmunology, a section of the journal Frontiers in Immunology

RECEIVED 28 September 2022
ACCEPTED 23 December 2022
PUBLISHED 10 January 2023

CITATION
Li H, Hu M, Huang Z, Wang Y, Xu Y, Deng J, Zhu M, Feng W and Xu X (2023) A single-cell atlas reveals the heterogeneity of meningeal immunity in a mouse model of Methyl CpG binding protein 2 deficiency. *Front. Immunol.* 13:1056447. doi: 10.3389/fimmu.2022.1056447

COPYRIGHT
© 2023 Li, Hu, Huang, Wang, Xu, Deng, Zhu, Feng and Xu. This is an open-access article distributed under the terms of the Creative Commons Attribution License (CC BY). The use, distribution or reproduction in other forums is permitted, provided the original author(s) and the copyright owner(s) are credited and that the original publication in this journal is cited, in accordance with accepted academic practice. No use, distribution or reproduction is permitted which does not comply with these terms.

A single-cell atlas reveals the heterogeneity of meningeal immunity in a mouse model of Methyl CpG binding protein 2 deficiency

Huiping Li[1]*, Meixin Hu[1], Zhuxi Huang[2,3], Yi Wang[1], Ying Xu[2,3], Jingxin Deng[1], Ming Zhu[2,3], Weijun Feng[2,3]* and Xiu Xu[1]*

[1]Department of Child Health Care, Children's Hospital of Fudan University, National Children's Medical Center, Shanghai, China, [2]Institute of Pediatrics, Children's Hospital of Fudan University, Shanghai, China, [3]Shanghai Key Laboratory of Medical Epigenetics, International Co-laboratory of Medical Epigenetics and Metabolism, Institutes of Biomedical Sciences, Shanghai Medical College, Fudan University, Shanghai, China

Methyl CpG binding protein 2 (MeCP2) is a DNA methylation reader protein. Mutations in *MeCP2* are the major cause of Rett syndrome (RTT). Increasing evidence has shown that dysregulated immunity and chronic subclinical inflammation are linked to MeCP2 deficiency and contribute to RTT development and deterioration. The meninges surrounding the central nervous system (CNS) contain a wide repertoire of immune cells that participate in immune surveillance within the CNS and influence various brain functions; however, the characterization and role of meningeal immunity in CNS with MeCP2 deficiency remain poorly addressed. Here, we used single-cell sequencing to profile Mecp2-deficient meningeal immune cells from the dura mater, which has been reported to contain the most meningeal immune cells during homeostasis. Data showed that the meninges of *Mecp2*-null mice contained the same diverse immune cell populations as control mice and showed an up-regulation of immune-related processes. B cell populations were greater in *Mecp2*-null mice than in control mice, and the expression of genes encoding for immunoglobulins was remarkably higher. Mecp2-deficient meninges also contained more cytotoxic $CD8^+$ T cells than control meninges. With increased interferon-γ transcription in T and natural killer cells, meningeal macrophages showed decreased suppression and increased activity in Mecp2-deficienct mice. Together, these findings provide novel insights into meningeal immunity, which is a less studied aspect of neuroimmune interactions in *Mecp2*-mutated diseases, and offer an essential resource for comparative analyses and data exploration to better understand the functional role of meningeal immunity in RTT.

KEYWORDS

methyl CpG binding protein 2, Rett syndrome, meningeal immunity, mouse model, central nervous system, single-cell analysis

Introduction

Methyl CpG binding protein 2 (MeCP2) is a DNA methylation reader protein, which is able to recognize DNA and histone methylation marks and acts as a methylation-dependent transcriptional modulator within the context of chromatin (1). MeCP2 exerts both transcriptionally repressive and activating functions by interacting with various cofactors, thereby affecting a myriad of genes. *MeCP2* mutations account for 90-95% of classic Rett syndrome (RTT) cases and typically cause the deterioration of acquired psychomotor skills, including the regression of motor and communicative skills, repetitive hand movements, seizures, irregular breathing, ataxia, and autistic features (2).

Although the loss of functional MeCP2 in neurons is thought to cause the majority of symptoms associated with RTT, increasing evidence has shown that dysregulated immunity and chronic subclinical inflammation are also linked to MeCP2 deficiency (3). For instance, several studies have highlighted the role of microglia, which are the primary brain-resident macrophages, in RTT during brain development (4, 5). Additionally, MeCP2 can regulate T cells by influencing the expression of the Forkhead box P3 (Foxp3) transcription factors (6), and MeCP2 deficiency has been associated with enhanced NF-κB signaling in human peripheral blood mononuclear cells (PBMCs) and the human monocyte line THP1 (7).

The meninges surrounding the central nervous system (CNS) comprise a triple layer of membranes, including the pia mater, arachnoid mater, and dura mater. In recent years, the meninges have been found to not only physically protect the CNS, but to also contain a wide repertoire of immune cells that constitute meningeal immunity. Meningeal immune cells and the cytokines they produce participate in immune surveillance within the CNS; influence the response to CNS injury (8) and chronic neurodegenerative conditions; and regulate higher brain functions, such as cognition and social behavior (9). Notably, meningeal macrophages are lost during disease progression in *Mecp2*-null mice (10). Although macrophages are the major cell population in the meninges (11, 12), the characteristics and roles of meningeal immunity in the CNS with MeCP2 deficiency remain poorly understood.

Here, we applied a single-cell sequencing to profile Mecp2-deficient meningeal immune cells from the dura mater, which has been reported to have the most numerous meningeal immune cells in homeostasis (13).

Methods

2.1 Mice

Female B6.129P2(C)-Mecp2$^{tm1.1Bird}$/J (Heterozygous *Mecp2* knockout, Jax:003890) mice were purchased from the Jackson Laboratory (Bar Harbor, ME, USA) and maintained in laboratory on a C57BL/6 background. The mice were maintained and bred in-house under standard 12-h light-dark cycle conditions. They were provided with standard rodent chow and sterilized tap water ad libitum. Male B6.129P2(C)-Mecp2$^{tm1.1Bird}$/J mice (Hemizygote *Mecp2* knockout, *Mecp2*-null mice) at 4-8 weeks of age were used for the experiments, and age-matched wild-type (WT) mice were used as controls. All experiments were approved by the Institutional Animal Care and Use Committee of Fudan University (No. 2019-289).

2.2 Isolation of CD45-positive cells from whole dura matter

One-month-old mice were euthanized by an overdose of Avertin (2, 2, 2-Tribromoethanol, 20 mg/mL) and transcardially perfused with 20 mL ice-cold phosphate-buffered saline (PBS). The mice were immediately decapitated posterior to the occipital bone. After the removal of the overlying skin and muscles from the skull, the dorsal part of the skull was carefully removed to isolate the dura. Then, the dura was cut into small pieces in ice-cold RPMI 1640 medium (Gibco, Thermo Fisher Scientific, Waltham, MA, USA) and incubated with an enzyme mix (0.25% Trypsin and 10 U mL^{-1} collagenase type I) at 37°C for 15 min. The solution was gently passed through 70 mm nylon mesh cell strainers using a sterile plastic plunger to yield a single-cell suspension. The single-cell suspension was then centrifuged at 300 g for 10 min. After the supernatant was removed completely, the cell pellet was resuspended in FACS buffer (pH 7,4; 0.1 M PBS; 1 mM Ethylene-Diamine-Tetra-Acetic acid (EDTA); 1% bovine serum albumin (BSA)). CD45-positive cells were subjected to magnetic separation using CD45 MicroBeads (Miltenyi Biotec, Bergisch Gladbach, Germany) according to the manufacturer's instructions. The cells were placed on ice during all steps except during enzymatic digestion and were prepared for single-cell RNA sequencing (scRNA-seq) or flow cytometry.

2.3 ScRNA-seq using 10x Genomics platform

Single CD45^{+} immune cells were freshly isolated from the dura using the procedure described above. For *Mecp2*-null mice, dura from three individual mice were pooled and the experiments were repeated twice. For WT mice, the dura from two and three individual mice were pooled in two repeated experiments. Sequencing was performed by OE Biotech Co., Ltd. (Shanghai, China). Cellular suspensions were loaded onto a GemCode Single Cell Instrument (10x Genomics, Pleasanton,

CA, USA) to generate single-cell gel beads-in-emulsion (GEMs) and scRNA-seq libraries using Chromium Next GEM Single Cell 3′ Gel Beads and Library Kit v3.1 (10x Genomics) according to the manufacturer's instructions. RNA transcripts were uniquely barcoded within single cells and reverse-transcribed into barcoded cDNAs to generate a single multiplexed library. Indexed libraries were sequenced using a NovaSeq 6000 System (Illumina, San Diego, CA, USA) with 2 × 150 paired-end reads.

2.4 ScRNA-seq data processing

We processed the unique molecular identifier (UMI) count matrix using the Seurat R package (v3.1.1) (14). Cellular barcodes were demultiplexed using the Cell Ranger software pipeline (v5.0.0) provided by 10× Genomics. Cells with log10GenesPerUMI <0.7 were filtered out to remove low-quality cells and likely multiplet captures. Low-quality cells with >10% of the counts belonging to mitochondrial genes and >5% of the counts belonging to hemoglobin genes were discarded. DoubletFinder package (v2.0.2) was used to identify potential doublets (15). After applying these quality control criteria, 12,129 cells from *Mecp2*-null mice and 13,794 cells from WT mice were included in downstream analyses. Library size normalization was performed using the NormalizeData function in Seurat. Gene expression measurements for each cell were normalized to total expression using "LogNormalize", multiplied by a scaling factor (10,000 by default), and the results were log-transformed.

Cells were visualized using a two-dimensional Uniform Manifold Approximation and Projection (Umap) algorithm with the RunnUMAP function. The FindVariableGenes, FindClusters, and FindAllMarkers functions in Seurat were used to select variable genes, cluster cells, and identify marker genes, respectively. Differentially expressed genes (DEGs) were identified using the FindMarkers function. P value < 0.05 and | log2foldchange| > 0.58 were set as the thresholds for significant differential expression. Gene ontology (GO) enrichment, Kyoto encyclopedia of genes and genomes (KEGG) pathway enrichment analysis, gene set variation analysis (GSVA), single-cell rEgulatory network inference and clustering (SCENIC), cell-cell communication, and pseudotime analysis were performed as described in previous studies (16–20).

2.5 Intracisterna magna injection

For meningeal lymphatic drainage experiments, intracisterna magna (i.c.m.) injection was performed as described previously (21). After mice were anaesthetized by intraperitoneal injection with Avertin (250μL/10g), skin on the back of the neck was shaved and cleaned with 75% ethanol, and a 1 cm midline incision was made to expose the cisterna magna. Next, the cisterna magna was injected slowly with 2 μL of fluorescent beads (FluoSpheres Carboxylate-Modified Microspheres, yellow-green, 0.5μm, ThermoFisher) using micro-syringes (Figure 1F). After injection, the needle was left in place for 2 min to avoid cerebrospinal fluid (CSF) backflow. The mice were then sutured and allowed to recover on a heating pad. Deep cervical lymph nodes (dCLNs), which are the major meningeal lymphatic draining lymph nodes (21, 22), were harvested 2 h after i.c.m. injection for immunofluorescence staining.

2.6 Flow cytometry

CD45-positive cells isolated from the dura mater were stained for extracellular markers using rat anti-CD45 FITC-conjugated (11-0451-82; eBioscience), rat anti-CD3 PE-conjugated (12-0193-82; eBioscience), and rat anti-CD11b APC-conjugated (17-0112-82; eBioscience). Live/dead cells were selected using a Zombie Aqua Fixable Viability Kit (423101, BioLegend). Fluorescence data were collected using a FACSCelesta flow cytometer (BD Company) and analyzed using FlowJo software (v10). Cells were gated using the height, area, forward and side scatter, and live cells with negative Zombie Aqua staining. Cells were gated for the appropriate markers of cell types.

2.7 Immunofluorescence staining

After transcardial perfusion with ice-cold PBS and 4% paraformaldehyde (PFA), whole dura maters with the skullcap or dCLNs were dissected from one-month-old mice and post-fixed in 4% PFA at 4 °C. Dura maters were then peeled from the skullcap. The dCLNs were dehydrated using PBS containing 30% sucrose and sliced into 40 μm-thick sections onto gelatin-coated slides. For immunohistochemistry, dura maters or dCLNs sections were incubated in blocking buffer (PBS containing 1% BSA, 2% donkey serum, 0.2% Triton X-100, and 0.1% Tween 20) for 1 h at room temperature (RT). Then, dura maters or sections were moved to appropriate dilutions of the following primary antibodies in blocking buffer for overnight at 4°C: rat anti-CD3 eFluor 660-conjugated (1:200; 50-0032-82; eBioscience), rat anti-Lyve-1 AF488-conjugated (1:200; 53-0443-82; eBioscience), rat anti-Lyve-1 eFluor 570-conjugated (41-0443-82, eBioscience), rat anti-IFN-γ PE/Cyanine7-conjugated (1:200; 505826; BioLegend), and rabbit anti-MeCP2 (1:200; 3456; Cell Signaling). Goat anti-rabbit Alexa Fluor 594 secondary antibody (1:1000; A-11012; Invitrogen) were incubated 1 hour at RT in necessity. Before whole-mounted with Aqua-Mount (Lerner) under coverslips, dura maters or dCLNs sections were staining with 1:10000 DAPI (Sigma-Aldrich) and washed with PBST (PBS containing 0.2% Triton X-100 and 0.1% Tween 20) 3 times for 15 min at RT.

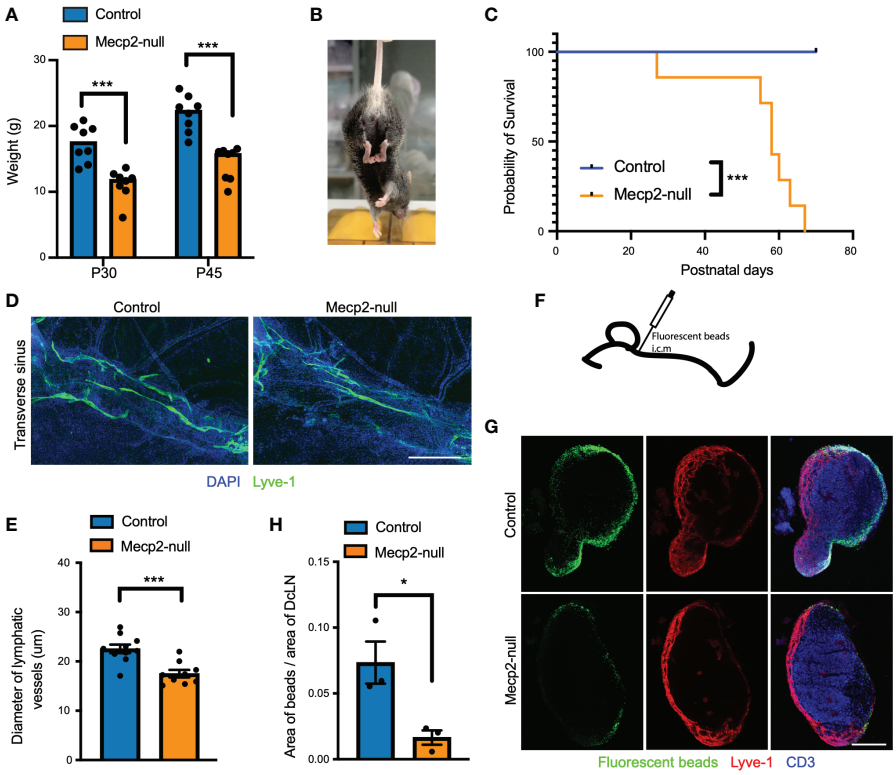


FIGURE 1
RTT-like phenotypes and deficiency of meningeal lymphatics in *Mecp2*-null mice. **(A)** Bar graph showing retarded growth of *Mecp2*-null mice compared to control at postnatal days 30 and 45 (n=8). *P*=0.0003 (P30) and *P*=0.00006 (P45), multiple t tests. **(B)** Representative images of hindlimb clasping in a *Mecp2*-null mouse at postnatal day 45. **(C)** Kaplan-Meier survival plot for control and *Mecp2*-null mice. (n=7 per group). *P*=0.0001 by the Log-rank test. **(D)** Representative images of the transverse sinus of dura maters with Lyve-1 (green) staining for 1-month-old control and *Mecp2*-null mice. Scale bars: 500µm. **(E)** Quantification of the diameter of Lyve-1$^+$ lymphatic vessels (n=10 for control mice; n=9 for *Mecp2*-null mice). Data represent the mean ± SEM. *P* = 0.0005, two-tailed unpaired *t* test. **(F)** Schematic of intracisterna magna injection with fluorescent beads. **(G)** Representative images showing dCLNs with fluorescent beads (green), Lyve-1 (red), and CD3 (blue) staining in control and *Mecp2*-null mice. Scale bars: 250µm. **(H)** Quantification of the percentage of fluorescent beads coverage of the dCLNs from control and *Mecp2*-null mice (n=3 per group). Data represent the mean ± SEM. *P* = 0.0281, two-tailed unpaired *t* test. *p < 0.05, ***p < 0.001.

Images were acquired using Leica TSC SP8 confocal system with a 10× (0.4 NA), 20× (0.75 NA), or 40× (0.85 NA) objectives. FIJI software (NIH) was used for image quantitative assessments. The diameter of lymphatic vessels was measured each 50 µm alongside the transverse sinus of dura mater, and the mean was calculated for each sample. Bead coverage in the dCLNs was quantified by dividing the area of GFP fluorescence over the area of the lymph node, as indicated by Lyve-1 and CD3 staining. The density of CD3-positive cells or IFN-γ was determined by dividing the number of CD3-labeled cells or the IFN-γ-positive area per section by the area of dura maters.

2.8 Statistical analysis

Statistical analysis was performed by GraphPad PRISM 8. Data were compared using two-tailed unpaired Student's *t*-tests, multiple t tests, and Kaplan-Meier survival plot. Statistical significance was defined as $p < 0.05$.

Results

3.1 RTT-like phenotypes and meningeal lymphatics in *Mecp2*-null mice

As reported previously (5, 23), *Mecp2*-null mice (male B6.129P2(C)-Mecp2$^{tm1.1Bird}$/J) displayed RTT-like phenotypes, including significantly retarded growth, hindlimb clasping, and short postnatal life expectancy (Figures 1A–C). In addition, we observed meningeal lymphatics deficiency in *Mecp2*-null mice, as indicated by a decrease in the diameter of meningeal lymphatic vessels (Figures 1D, E) and a decrease in the drainage of CSF fluorescent beads from the cisterna magna

into dCLNs (Figures 1G, H). Meningeal lymphatics play important roles in the development and recirculation of CNS immune cells (21, 24); hence, these observations suggest that meningeal immunity may be altered in *Mecp2*-null mice.

3.2 Meningeal immune cell diversity

To identify meningeal immune changes associated with Mecp2 deficiency, we generated 12,129 and 13,794 high-quality single-cell transcriptomes for meningeal immune cells ($CD45^+$ cells) from six *Mecp2*-null and five WT mice, respectively (Figure 2A). Cells from the various mice were also pooled into a single dataset, and color-coded Umap plots were generated to visualize the origin of each cell (Figure 2B). Immune cells formed 18 major clusters that expressed varying levels of *Ptprc*, a gene encoding CD45 (Supplementary Figure S1A, B). We classified the different cell types based on the expression levels of the most variable genes and the shared expression features of known marker genes (Figure 2C; Supplementary Figure S1C). Consistently with the results of previous studies on Mecp2 in immune system (6, 10), we found that meningeal immune cells expressed Mecp2 (Supplementary Figure S2).

The dura maters of both control and *Mecp2*-null mice contained diverse immune cell populations, including

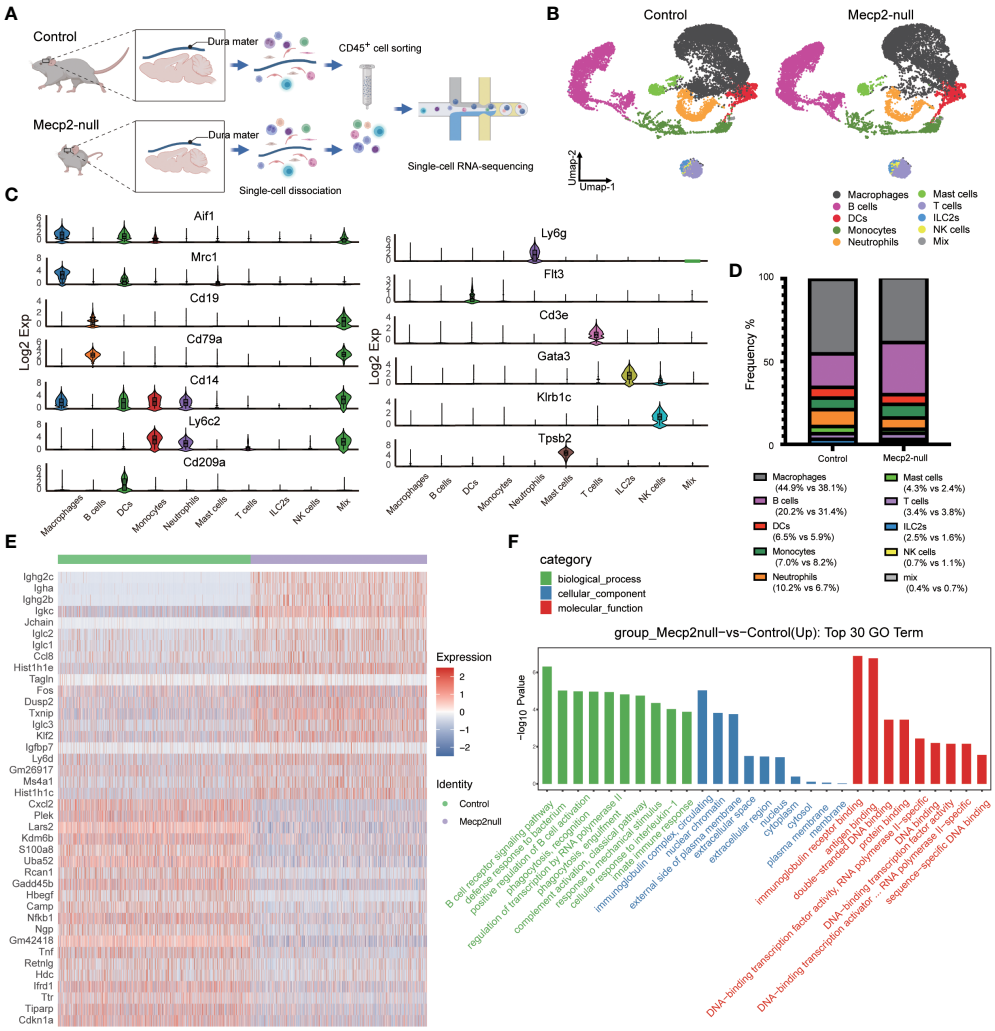


FIGURE 2
Single-cell transcriptomics survey of dura immune cells from WT and Mecp2-deficienct mice. **(A)** Schematic of the experimental approach (created with Biorender.com). 10x chromium scRNA-seq for $CD45^+$ immune cells isolated from dura maters of 1-month-old WT (control) and Mecp2-deficienct (*Mecp2*-null) mice. **(B)** Umap plot displaying 10 dura immune cell types from control and *Mecp2*-null mice. Colored show annotated cell types. **(C)** Violin plots showing the expression levels of 13 specific marker genes for different cell types. **(D)** Frequency of each cell type in control and *Mecp2*-null mice. **(E)** Heatmap of group-specific DEGs. Color indicates relative gene expression, with representative genes shown together. **(F)** The top 30 most enriched GO terms for DEGs in control and *Mecp2*-null group.

macrophages, B cells, dendritic cells (DCs), monocytes, neutrophils, mast cells, T cells, innate lymphoid cells-2 (ILC-2), and natural killer (NK) cells (Figure 2B). Obvious differences in the cell populations were observed between *Mecp2*-null mice and control mice, with a loss of macrophages and an increase in B cells (Figure 2D). According to previous studies (5, 10), Mecp2 deficiency causes the decline of macrophages and microglia, which are specific types of myeloid cells resident in the brain. Surprisingly, we found that the frequency of B cell populations was almost 1.5 times higher in *Mecp2*-null mice. The expression of genes encoding immunoglobulins, such as *Ighg2c, Igha, Ighg2b, Igkc, Iglc2, Iglc1*, and *Iglc3*, was also markedly higher in *Mecp2*-null mice than in control mice (Figure 2E). Other DEGs included CC chemokine (*Ccl8*), histones (*Hist1h1e, Hist1h1c*), transcription factor (*Fos*), protein phosphatase (*Dusp2*), and thioredoxin-binding protein (Txnip) (Figure 2E; Supplementary Data Sheet 1). GO enrichment analysis revealed the up-regulation of immune-related processes and regulation of transcription in *Mecp2*-null mice, including the B cell receptor signaling pathway, innate immune response, and DNA-transcription factor activity (Figure 2F).

3.3 Meningeal B cell activity

Although B cells accounted for the main changes observed in the meninges of *Mecp2*-null mice, little is known about their characteristics under homeostasis. We also observed an increase in the B cell population in the dura maters of *Mecp2*-null mice by flow cytometry (Figure 3A). The B cell population was then re-clustered into seven clusters (C1 to C7) on a single Umap space (Figure 3B). B cells from the *Mecp2*-null and control mice occupied overlapping territories; however, the frequencies of C2 and C3 were reversed between the two groups (Figure 3C). Consistent with previous studies by Wang et al. (25) and Brioschi et al. (26), the seven sub-clusters formed a consecutive development trajectory of B lineage cells (Figure 3D). Mature B cells (C1 and C3) expressed high levels of *Ighd, Ighm*, and *Ms4a1*. Meanwhile, immature B cells (C2) expressed high levels of *Ighm*, but not *Ighd*. In cycling pre-B cells (C4 and C5) the expression of *Top2a, H2afx*, and *Mki67* was upregulated. Pre-B cells (C6) expressed high levels of *Vpreb1, Vpreb3, Dntt, Lef1*, and *Rag1*, while plasma cells (C7) highly expressed *Prdm1* and *Il10*.

In *Mecp2*-null mice, the C3 cluster of mature B cells (Mature B_C2) expanded and strongly expressed B cell activation markers, such as *Cd83, Egr3, Fcer2a, Myc*, and *Cxcr5* (Figure 3E). Analysis of the regulon most highly associated with this subset revealed a high regulon specificity score for transcription factors *Kdm2b, Rel*, and *Crem* compared to the mature B_C1 cluster (C1) (Figure 3F). The regulon activity heatmap also showed increased activities for *Kdm2b* and *Rel* in *Mecp2*-null mice (Figure 3G).

In addition, we ranked the estimated pathway activities for individual B cells using GSVA. This approach revealed the strong enrichment of T cell activation involved in the immune response, positive regulation of Il-12 secretion, positive regulation of cytokine production involved in the inflammatory response, and B cell activation and proliferation (Figure 3H).

3.4 Cytotoxic activity of T lymphocytes

To better understand T cell activation in Mecp2-deficient mice, we re-clustered ILC2s, NK cells, and T cells into seven clusters (Figure 4A). The major cell types were identified by defining genes for $CD4^+$ T cells (C1) characterized by *Cd3e* and *Cd4* expression; $CD8^+$ T cells (C2) characterized by *Cd3e* and *Cd8* expression; ILC2s (C3) characterized by *Gata3* expression; NK cells (C4) characterized by *Nrc1* and *Klrd1* expression and without Cd3e expression; NKT cells (C5) characterized by *Cd3* and *Klrd1* expression; regulatory T cells (Treg, C6) characterized by *Cd3e, Cd4*, and *Foxp3* expression; and γ-δ T cells (C7) characterized by *Cd3e* and *Tcrg-C1* expression (Figure 4B). The frequencies of ILC2, NK cell, and T cell populations were affected by Mecp2 deficiency. *Mecp2*-null mice had higher frequencies of $CD4^+$ T cells, $CD8^+$ T cells, NK, and NKT cells. In contrast, the frequencies of ILC2s and γ-δ T cells were lower (Figure 4C). Immunofluorescence staining for CD3 also showed a higher density of CD3 positive cells in dura mater of *Mecp2*-null mice (Figures 4D, E).

$CD8^+$ T cells are a critical population of MHC I-restricted T cells that directly kill infected or damaged cells. Differential gene expression from the scRNA-seq data of $CD8^+$ T cells resolved the subsets and functional states into two subsets (Figure 4F). Subset 1 showed higher *Tcf7*, *Sell, CCr7*, and *Lef1* expression, which corresponded with the resting state of $CD8^+$ T cells (Figure 4G). Subset 2 showed increased expressions of *Ifng* (encoding interferon-γ; IFN-γ), *Ccl5, Gzmb*, and *Prf1*, which are associated with cytotoxicity and activation (Figure 4H). The distribution of subset 2 was more enriched in *Mecp2*-null mice than in the control group, suggesting that the cytotoxic activity of T lymphocytes was enhanced in *Mecp2*-null mice.

3.5 IFN-γ transcription and cell-cell interactions

$CD8^+$ T cells of *Mecp2*-null mice displayed increased expression of *Ifng*, which encodes IFN-γ. IFN-γ is the only member of the type II class of interferons and plays a critical role in both innate and adaptive immunity (27). Yang et al. reported that Mecp2 overexpression results in defective IFN-γ secretion and suggested that MeCP2 could be a regulatory factor in *Ifng* transcription (28). Here, compared to that in control mice, we found that *Mecp2*-null mice had higher *Ifng* expression in NK, $CD8^+$ T, $CD4^+$ T, and NKT cells (Figures 5A, B).

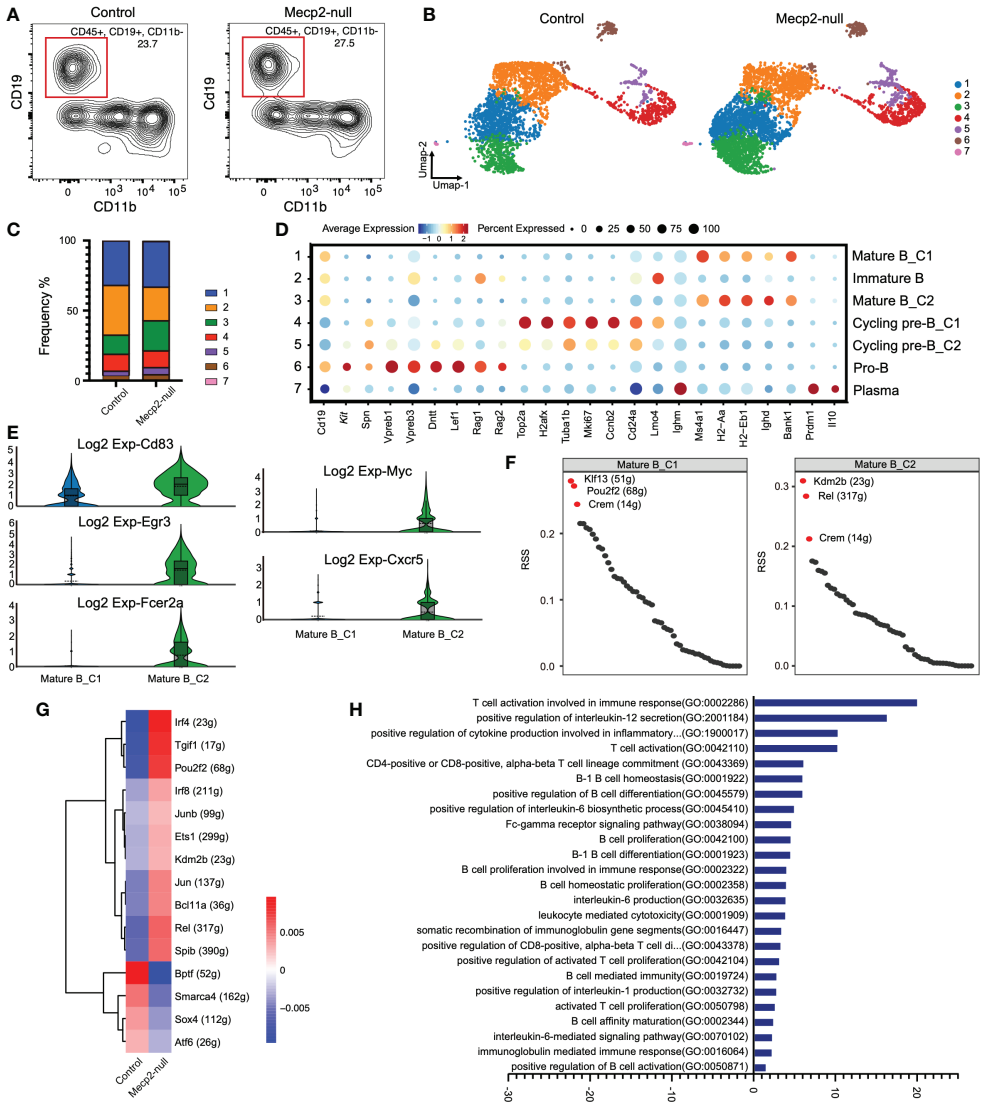


FIGURE 3
Gene expression and characterization of B cells compared to control and *Mecp2*-null mice. **(A)** Representative flow cytometry contour plot showing the proportion of B cells within the $CD45^+$ population in the dura of control and *Mecp2*-null mice. B cells were gated as $CD45^+CD19^+$ and $CD11b^-$. n=3 for each group. **(B)** Distribution of seven B cell clusters on the Umap plot for two groups. Clusters are rank-ordered by size. **(C)** Bar plots showing cell cluster distribution within different groups. **(D)** Dot plots displaying the relative expression of selected B cell marker genes (columns) across clusters (rows) in **(B)**. Dot size indicates the fraction of cells in the clusters that express a gene. Color indicates the Z-score of mean gene expression in the cluster (Z-score of average log2). **(E)** Violin plots of *Cd83, Egr3, Fcer2a, Myc,* and *Cxcr5* expression in control and *Mecp2*-null mice. **(F)** Rank for regulons in cluster1 and cluster2 of mature B cells (Mature B_C1 and Mature B_C2) based on regulon specificity score (RSS). **(G)** Heatmap of regulon activity score (RAS) in two groups. Rows represent different regulons and columns represent mouse groups. **(H)** Bar plot showing different enriched pathways comparing in *Mecp2*-null and control mice determined using GSVA. *T*-values > 0 represent up-regulated pathways.

Immunofluorescence staining further revealed that IFN-γ expression was higher in the dura maters of *Mecp2*-null mice (Figures 5C, D). However, the expression of the IFN-γ receptors, *Ifngr1* and *Ifngr2*, was not significantly affected by Mecp2 deficiency, with the exception of high *Ifngr2* expression in Treg cells (Figure 5E). CellChat was used to explore the differences in intercellular communication networks of the IFN-II signaling pathway between control and *Mecp2*-null mice, which were visualized using circle plots. *Mecp2*-null mice showed more complex intercellular communication in the IFN-II signaling pathway (Figures 5F, G).

3.6 Macrophages activated in response to IFN-γ in *Mecp2*-null mice

IFN-γ plays a key role in macrophage activation and reinforces the M1 phenotype (29). To stratify the activity of

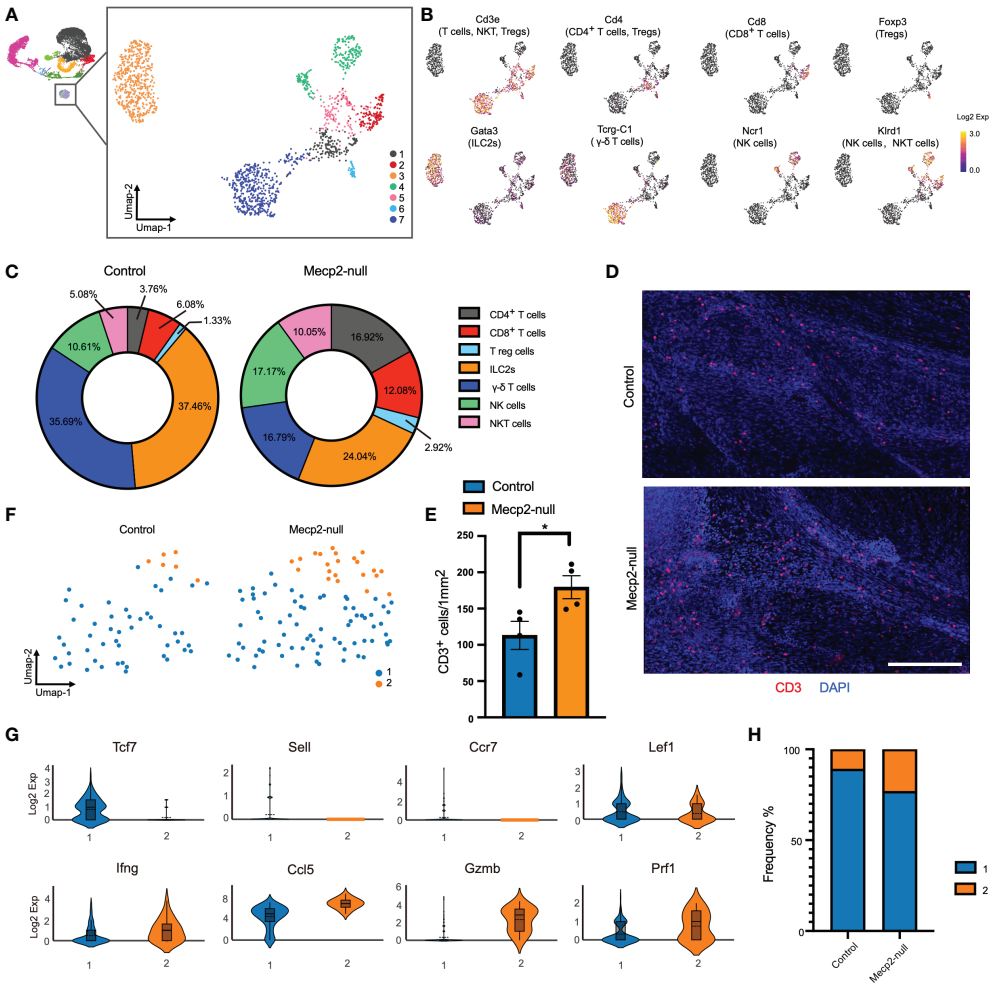


FIGURE 4
Increased T cell cytotoxicity in Mecp2-deficienct mice. **(A)** Umap plot showing the distributions of seven clusters for T cells, NK cells, and ILC2s. **(B)** Umap plots showing the expression of signature genes for $CD4^+$ T, $CD8^+$ T, Tregs, γ-δ T, ILC2s, NK, and NKT cells. **(C)** Percentages of each cell population among the total meningeal T cells, NK cells, and ILC2s in control and *Mecp2*-null mice. **(D)** Representative confocal images of CD3 (red)-positive cells in the dura maters of control and *Mecp2*-null mice. Scale bars: 250μm. **(E)** Quantification of the density of CD3-positive cells in the dura maters of control and *Mecp2*-null mice (n=4 per group). Data represent the mean ± SEM. *p < 0.05, *P* = 0.0371, two-tailed unpaired *t* test. **(F)** Umap plots indicating the two sub-clusters of $CD8^+$ T cells. **(G)** Violin plots representing the expression of resting state (top row) and cytotoxicity/activated (bottom row) related markers. **(H)** Frequency of two sub-clusters of $CD8^+$ T cells in control and *Mecp2*-null mice.

macrophages, we re-clustered the macrophage population into five subpopulations based on the expression level of signature genes (Figure 6A). Although Mecp2-deficient meningeal macrophages mainly overlapped with those in the control group, some obvious differences were observed, especially in subclusters 1 and 2 (Figure 6B). We examined the top 50 up-regulated genes in the macrophage subclusters. Subclusters 1, 2, and 5 fell into the MHC II low group (11), which exhibited high *Lyve1* and *Gas6* expression (Figure 6C), while subclusters 3 and 4 fell into the MHC II high group, which exhibited high *H2-Aa* and *Cd72* expression (Figure 6C). Subcluster 1 displayed increased expression of *Rcan1*, which encodes a small protein that inhibits calcineurin phosphatase activity and acts as a central negative regulator of inflammation (30).

Finally, we performed SCORPIUS trajectory inference on the macrophages. The macrophages were divided into seven states (Figure 6D). The cell trajectory patterns of Mecp2-deficient mice shifted from state 1 to state 7 (Figure 6E), with gene expression profiles changing dynamically along the trajectory. The most predictive genes were clustered into modules, which revealed the transcriptional gradients of genes that were lost or gained in pseudotime (Figure 6H). IFN-γ mediates the polarization of macrophages to an "M1-like" state by activating Janus kinase (Jak)-signal transducer and activator of transcription 1 (Stat1) (31). GO analyses indicated that the late pseudotime, which consisted mainly of state 7, was enriched for the genes involved in phagocytosis, recognition, engulfment, and the Jak1/2-Stat1 signaling pathway. Conversely, early pseudotime mainly consisted

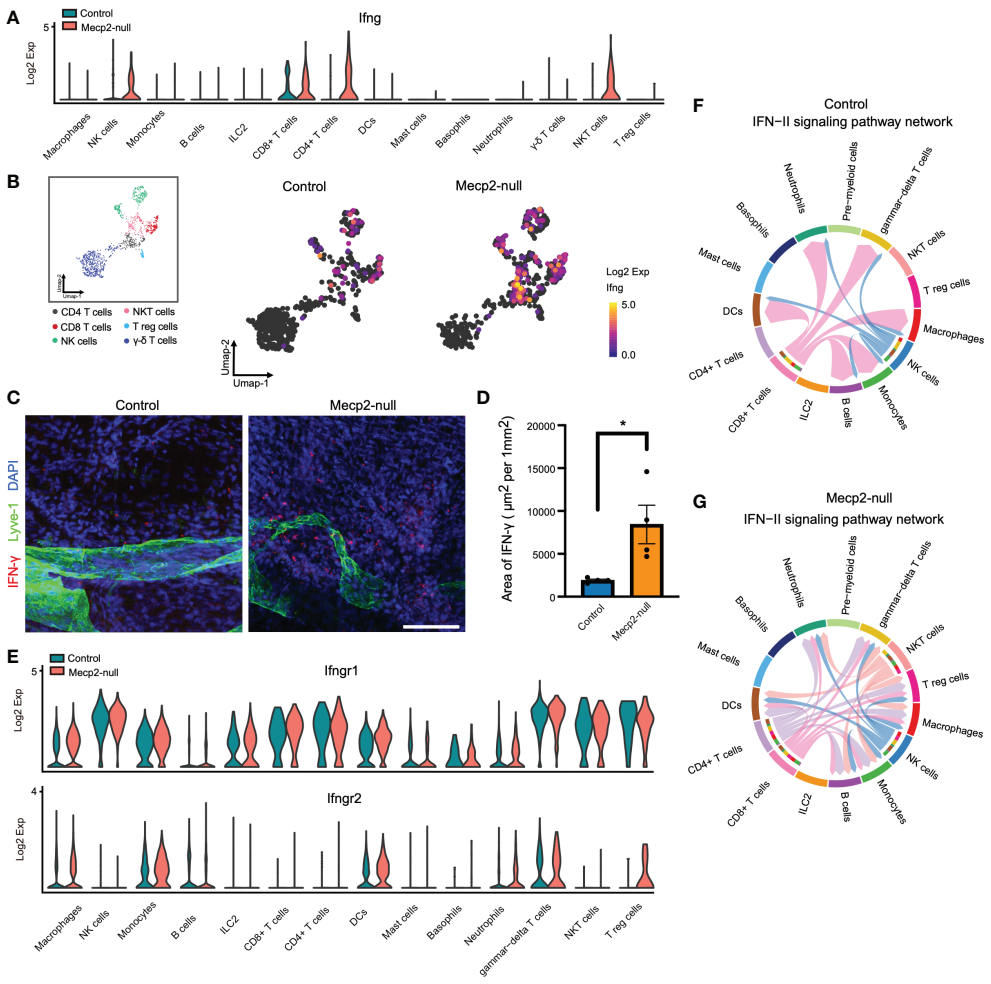


FIGURE 5
scRNA-seq analysis of IFN-II signaling pathway upregulation in multiple Mecp2-deficient cell populations. **(A)** Violin plots showing Ifng expression in different meningeal immune cells from control and *Mecp2*-null mice. **(B)** Umap plots depicting Ifng expression in the main producer cells. **(C)** Representative confocal images of IFN-γ (red) with lymphatic vessel endothelial receptor 1 (Lyve-1, Green) in the dura maters of control and *Mecp2*-null mice. Scale bars: 100μm. **(D)** Quantification of the area of IFN-γ in the dura maters of control and *Mecp2*-null mice (n=4 per group). Data represent the mean ± SEM. *p < 0.05, *P* = 0.0278, two-tailed unpaired *t* test. **(E)** Violin plots showing the expression of IFN-γ receptors (Ifngr1 and Ifngr2) in different meningeal immune cells in control and *Mecp2*-null mice. **(F)** Chord diagram visualizing cell-cell communication for the IFN-II signaling pathway in WT mice. **(G)** Chord diagram visualizing the cell-cell communication for IFN-II signaling pathway in *Mecp2*-null mice.

of state 1 and was enriched for genes in the Jak2-Stat5a and Jak1-Stat3 signaling pathways (Figure 6I). Taken together, these results indicate that macrophages are activated in response to IFN-γ in *Mecp2*-null mice.

Discussion

Due to the unique position and structural composition of the meninges, and the functional characteristics of meningeal immune cells, meningeal immunity plays an important role in maintaining the CNS under healthy and disease conditions (12, 32). MeCP2 is expressed in immune cells. Polymorphisms in MeCP2 have been linked to increased susceptibility to autoimmune diseases, and alterations in MeCP2 expression levels affect immune function and cytokine production (3, 33). However, little is known about changes in meningeal immunity in the absence of MeCP2 and the role of meningeal immunity in RTT progression. Using single-cell genomic analysis, we explored the meningeal immune niche of pre-phenotypic Mecp2-deficienct mice, which displayed mild symptoms but were less affected by systemic damage. The meninges of *Mecp2*-null mice contained diverse immune cell populations like control mice and showed an up-regulation of immune-related processes, including the B cell

10.3389/fimmu.2022.1056447

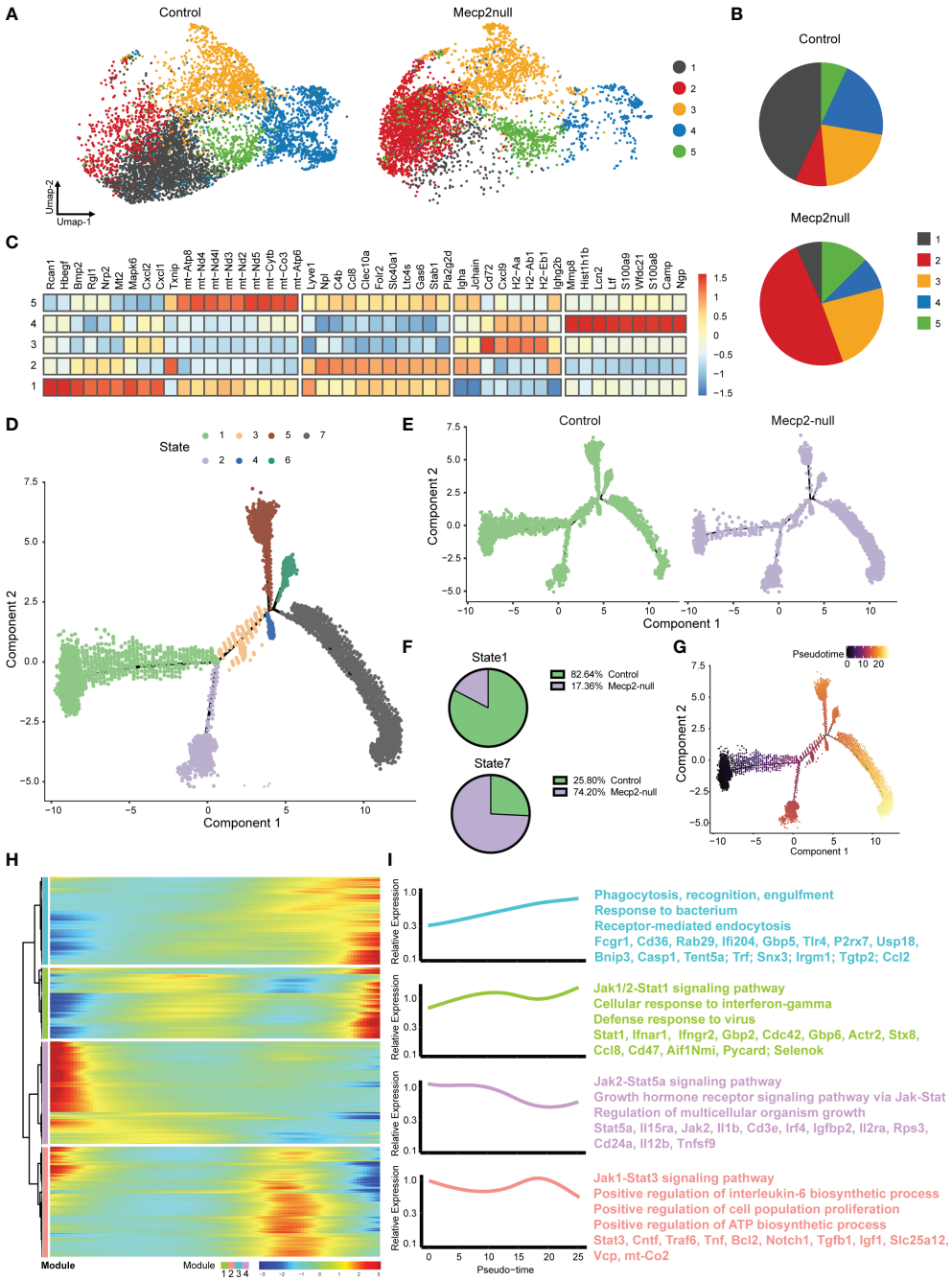


FIGURE 6
MeCP2 deficiency macrophages have increased response to IFN-γ. **(A)** Umap plots showing the clusters of WT and Mecp2-deficienct macrophages. **(B)** Pie chart showing the distribution of five clusters in WT and Mecp2-deficienct meningeal macrophages. **(C)** Heat map displaying the relative expression fold change (log2) of the top 50 up-regulated genes in macrophage clusters identified in **(A)**. **(D)** Visualization of the seven cell states predicted using the Monocle2 algorithm. **(E)** Trajectories for control and *Mecp2*-null mice. **(F)** Numbers expressed as percentages of control (green) and *Mecp2*-null (purple) macrophages in state 1 (top) and state 7 (bottom) cell populations, respectively. **(G)** Pseudotime of macrophages indicated by gradient color intensity from dark to bright, indicating the progression from the early to late pseudotime. **(H)** Heatmap displaying genes ordering during pseudotime. Color gradient from blue to red indicates low to high relative expression levels. **(I)** The GO and KEGG of enriched functions and pathways for the significantly differentially expressed (SDE) genes.

receptor signaling pathway, cytotoxic activities of T lymphocytes, and macrophage activities. Furthermore, Mecp2 deficiency increased IFN-γ transcription and cell-cell interactions mediated by the IFN-II signaling pathway.

Interestingly, our findings on meningeal immunity with Mecp2 deficiency have some similarities and differences compared to previous studies. Papini et al. (34) demonstrated that patients with RTT showed a consistent and highly significant increase in the serum IgM fraction and we found that the expression of immunoglobulin-family genes in Mecp2 deficient meningeal immune cells (*Ighg2c, Igha, Ighg2b, Igkc*, etc.) was abnormally high (Figure 1). Li et al. (6) found that Mecp2 is essential for maintaining stable Foxp3 expression and the lineage identity of mature Tregs during inflammation, but is dispensable for the initial induction of Foxp3 expression during Treg development. Consistently, we observed no loss in Foxp3 expression or decrease in the number of Tregs in our immune cell population with no inflammatory challenge (Figure 3B). Leoncini et al. (35) showed that significantly reduced plasma levels of IFN-γ in patients with *MeCP2*-mutated RTT; however, we observed enhanced IFN-γ transcription in MeCP2-deficient meningeal immune cells (Figure 4), indicating that meningeal immunity is unique.

IFN-γ is a dimerized soluble cytokine that was originally identified as a 'macrophage-activating factor' (31). IFN-γ concentrations in the brain are elevated in certain pathologies, including multiple sclerosis, cerebral ischemia, and neurotrauma (36). In this study, we found that *Mecp2*-null mice lost a population of meningeal macrophages with high Rcan1 expression, which suppresses macrophage activity and negatively regulates inflammation. SCORPIUS trajectory inference showed that the state enriched for phagocytosis, recognition, engulfment, and the Jak1/2-Stat1 signaling pathway (activated by the IFN-γ receptor) was enhanced in Mecp2-deficienct meningeal macrophages. Thus, the abnormally enhanced innate immune response observed in Mecp2-deficienct meningeal immunity may participate in the onset and progression of RTT by causing low-grade neuroinflammation, as reported by Pecorlli et al. (3). However, the cellular targets of IFN-γ extend beyond immune cells. Due to the exclusion system of cerebrospinal fluid, meningeal soluble mediators, such as cytokines, have limited ability to enter and affect the brain parenchyma under steady-state conditions (37). With the expression of IFN-γ receptors in the membranes of neurons (36), IFN-γ has been known to regulate dendrite morphology,

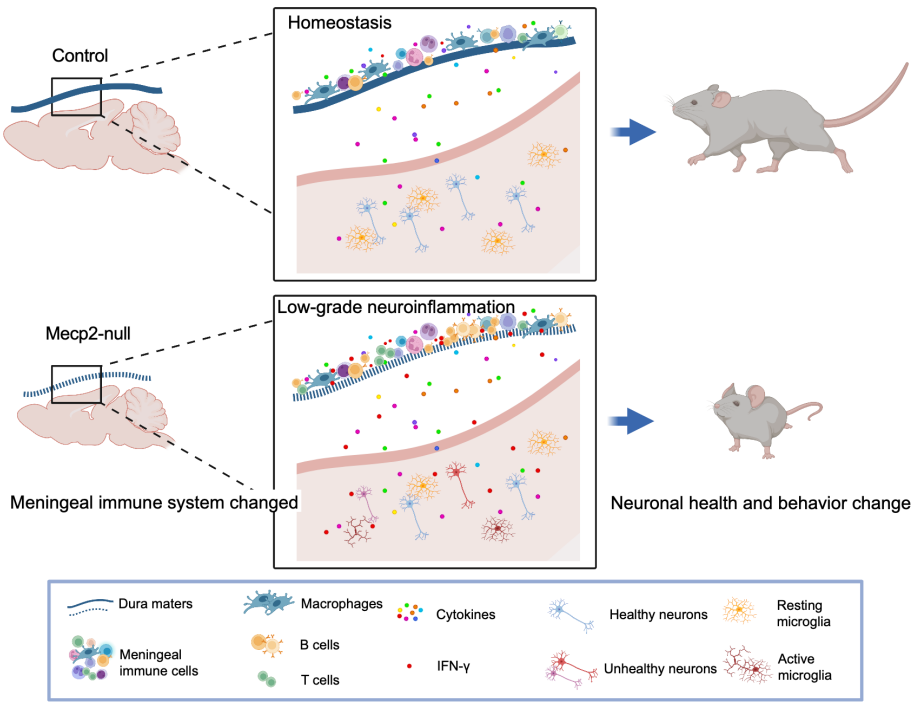


FIGURE 7
Model for the mechanisms of meningeal immunity in *Mecp2*-null mouse. Illustration of the hypothesis for the mechanisms of meningeal immunity with the progression of disease in *Mecp2*-null mice (created with Biorender.com). Meninges surrounding the brain have functional lymphatic system and abundant of immune cells which play important roles for maintaining the central nervous system in health. *Mecp2*-null mice show deficiency of meningeal lymphatics and activity status altered of immune cells in dura mater. The non-infectious inflammatory response can spread to the CNS parenchyma, causing low-grade neuroinflammation, and further impairing neuronal health and behavior change.

inhibit the formation of excitatory synapses in sympathetic neurons and the neocortex (38), and promote inhibitory currents in GABAergic neurons in the prefrontal cortex (39). Furthermore, studies have shown that reduced dendritic complexity, synaptic strength, and dysfunction of GABAergic neurons contribute towards RTT (40–42).

There is still much to understand regarding how meningeal immunity affects neuronal function. It remains unclear how the association of meningeal immunity changes with the progression of *MeCP2*-mutated diseases. Accumulating evidence has shown that meningeal immunity supports the brain function and may play potential roles in neurodegenerative diseases (9, 43, 44). Indeed, *Mecp2*-mutant rodents and humans have severely impaired brain function and progressive aggravation (45). Meningeal immunity is thought to support the brain function by secreting cytokines that could be carried by the CSF to corresponding receptors expressed in the brain parenchyma (32). Deficiency in meningeal-derived cytokines, such as IL-4, IL-13, and IL-17α, has been shown to impaired learning, memory, social, and anxiety-like behaviors (9, 43, 46). Based on our findings, we propose a model associating heterogeneity in meningeal immunity with the progression of disease in *Mecp2*-null mice (Figure 7). In *Mecp2*-null mice, immune-related processes including the B cell receptor signaling pathway, cytotoxic T lymphocyte activities, and macrophage activities are up-regulated. This heterogeneity of meningeal immune cells and activity status alters the secretion of cytokines (especially IFN-γ), which can enter the brain parenchyma through CSF and affect neuronal function. However, further research is required to confirm the role of meningeal immunity in RTT development.

In summary, our study provides novel insights into the pathology of *MeCP2*-mutated diseases. The meninges, which contain a wide repertoire of immune cells and participate in immune surveillance in the CNS, showed decreased suppression and increased activity for both innate and adaptive immunocytes in MeCP2-deficienct mice. Furthermore, we found that the overexpression of meningeal IFN-γ might not only modulate the status of immune cells in the meninges, but also affect brain function and contribute towards RTT development and deterioration.

Data availability statement

The datasets presented in this study can be found in online repositories. The name of the repository and accession number can be found below: NCBI Gene Expression Omnibus; GSE221361.

Ethics statement

The animal study was reviewed and approved by Institutional Animal Care and Use Committee of Fudan University.

Author contributions

Conceptualization, HL. Mouse genotyping, MH, ZH, YX, MZ. Meningeal dissection and dissociation, HL, MH, YW, JD. Data analysis, HL, MH. Investigation, HL, WF, and XX. Data curation, MZ. Writing-original draft, HL. Writing-review and editing, WF, and XX. Supervision, WF, and XX. All authors contributed to the article and approved the submitted version.

Funding

This work was supported by The National Natural Science Foundation of China (Grant No. 82171540), Key Subject Construction Project of Shanghai Municipal Health Commission (Grant No. shslczdzk02903), The "Thousand Talents Program" to WF, and the Young Clinical Scientist Program of Children's Hospital of Fudan University (Grant No. 2022LCKXJ03).

Acknowledgments

The authors would like to thank Yongbing Ba (Lu Ming Biotech Co., Ltd., Shanghai, China) for assistance with the bioinformatics analyses. We thank Prof. Ying Zhu and Shenbing Liu for editing the manuscript. We thank Prof. Wenhao Zhou for valuable exceptional support in this work.

Conflict of interest

The authors declare that the research was conducted in the absence of any commercial or financial relationships that could be construed as a potential conflict of interest.

Publisher's note

All claims expressed in this article are solely those of the authors and do not necessarily represent those of their affiliated organizations, or those of the publisher, the editors and the reviewers. Any product that may be evaluated in this article, or claim that may be made by its manufacturer, is not guaranteed or endorsed by the publisher.

Supplementary material

The Supplementary Material for this article can be found online at: https://www.frontiersin.org/articles/10.3389/fimmu.2022.1056447/full#supplementary-material

SUPPLEMENTARY FIGURE 1
Single-cell characterization of meningeal immune cells with typical signature marker genes. **(A)** Umap plot displays distributions of 18 major clusters of meningeal immune cells. **(B)** Log2 expression of *Ptprc* in individual cells on the Umap graph of **(A)**. **(C)** Violin plots showing the expression of signature genes for different immune cell types.

SUPPLEMENTARY FIGURE 2
Meningeal immune cells express Mecp2. **(A)** Representative confocal images of Mecp2 (red) and Lyve-1(green) staining in the dura mater of 1-month-old WT mice. Scale bars: 50μm. **(B)** Violin plots representing the Log2 expression of *Mecp2* in different meningeal immune cells from WT mice.

References

1. Good KV, Vincent JB, Ausio J. MeCP2: The genetic driver of rett syndrome epigenetics. *Front Genet* (2021) 12:620859. doi: 10.3389/fgene.2021.620859

2. Chahrour M, Zoghbi HY. The story of rett syndrome: from clinic to neurobiology. *Neuron* (2007) 56(3):422–37. doi: 10.1016/j.neuron.2007.10.001

3. Pecorelli A, Cervellati C, Cordone V, Hayek J, Valacchi G. Compromised immune/inflammatory responses in rett syndrome. *Free Radic Biol Med* (2020) 152:100–6. doi: 10.1016/j.freeradbiomed.2020.02.023

4. Maezawa I, Jin LW. Rett syndrome microglia damage dendrites and synapses by the elevated release of glutamate. *J Neurosci* (2010) 30(15):5346–56. doi: 10.1523/JNEUROSCI.5966-09.2010

5. Derecki NC, Cronk JC, Lu Z, Xu E, Abbott SB, Guyenet PG, et al. Wild-type microglia arrest pathology in a mouse model of rett syndrome. *Nature* (2012) 484 (7392):105–9. doi: 10.1038/nature10907

6. Li C, Jiang S, Liu SQ, Lykken E, Zhao LT, Sevilla J, et al. MeCP2 enforces Foxp3 expression to promote regulatory T cells' resilience to inflammation. *Proc Natl Acad Sci U.S.A.* (2014) 111(27):E2807–16. doi: 10.1073/pnas.1401505111

7. O'Driscoll CM, Lima MP, Kaufmann WE, Bressler JP. Methyl CpG binding protein 2 deficiency enhances expression of inflammatory cytokines by sustaining NF-kappaB signaling in myeloid derived cells. *J Neuroimmunol* (2015) 283:23–9. doi: 10.1016/j.jneuroim.2015.04.005

8. Gadani SP, Smirnov I, Wiltbank AT, Overall CC, Kipnis J. Characterization of meningeal type 2 innate lymphocytes and their response to CNS injury. *J Exp Med* (2017) 214(2):285–96. doi: 10.1084/jem.20161982

9. Alves de Lima K, Rustenhoven J, Da Mesquita S, Wall M, Salvador AF, Smirnov I, et al. Meningeal gammadelta T cells regulate anxiety-like behavior via IL-17a signaling in neurons. *Nat Immunol* (2020) 21(11):1421–9. doi: 10.1038/s41590-020-0776-4

10. Cronk JC, Derecki NC, Ji E, Xu Y, Lampano AE, Smirnov I, et al. Methyl-CpG binding protein 2 regulates microglia and macrophage gene expression in response to inflammatory stimuli. *Immunity* (2015) 42(4):679–91. doi: 10.1016/j.immuni.2015.03.013

11. Van Hove H, Martens L, Scheyltjens I, De Vlaminck K, Pombo Antunes AR, De Prijck S, et al. A single-cell atlas of mouse brain macrophages reveals unique transcriptional identities shaped by ontogeny and tissue environment. *Nat Neurosci* (2019) 22(6):1021–35. doi: 10.1038/s41593-019-0393-4

12. Alves de Lima K, Rustenhoven J, Kipnis J. Meningeal immunity and its function in maintenance of the central nervous system in health and disease. *Annu Rev Immunol* (2020) 38:597–620. doi: 10.1146/annurev-immunol-102319-103410

13. Di Marco Barros R, Fitzpatrick Z, Clatworthy MR. The gut-meningeal immune axis: Priming brain defense against the most likely invaders. *J Exp Med* (2022) 219(3):1-9. doi: 10.1084/jem.20211520

14. Butler A, Hoffman P, Smibert P, Papalexi E, Satija R. Integrating single-cell transcriptomic data across different conditions, technologies, and species. *Nat Biotechnol* (2018) 36(5):411–20. doi: 10.1038/nbt.4096

15. McGinnis CS, Murrow LM, Gartner ZJ. DoubletFinder: Doublet detection in single-cell RNA sequencing data using artificial nearest neighbors. *Cell Syst* (2019) 8(4):329–337 e4. doi: 10.1016/j.cels.2019.03.003

16. Hanzelmann S, Castelo R, Guinney J. GSVA: gene set variation analysis for microarray and RNA-seq data. *BMC Bioinf* (2013) 14:7. doi: 10.1186/1471-2105-14-7

17. Aibar S, Gonzalez-Blas CB, Moerman T, Huynh-Thu VA, Imrichova H, Hulselmans G, et al. SCENIC: single-cell regulatory network inference and clustering. *Nat Methods* (2017) 14(11):1083–6. doi: 10.1038/nmeth.4463

18. Suo S, Zhu Q, Saadatpour A, Fei L, Guo G, Yuan GC. Revealing the critical regulators of cell identity in the mouse cell atlas. *Cell Rep* (2018) 25(6):1436–1445 e3. doi: 10.1016/j.celrep.2018.10.045

19. Jin S, Guerrero-Juarez CF, Zhang L, Chang I, Ramos R, Kuan CH, et al. Inference and analysis of cell-cell communication using CellChat. *Nat Commun* (2021) 12(1):1088. doi: 10.1038/s41467-021-21246-9

20. Trapnell C, Cacchiarelli D, Grimsby J, Pokharel P, Li S, Morse M, et al. The dynamics and regulators of cell fate decisions are revealed by pseudotemporal ordering of single cells. *Nat Biotechnol* (2014) 32(4):381–6. doi: 10.1038/nbt.2859

21. Louveau A, Herz J, Alme MN, Salvador AF, Dong MQ, Viar KE, et al. CNS lymphatic drainage and neuroinflammation are regulated by meningeal lymphatic vasculature. *Nat Neurosci* (2018) 21(10):1380–91. doi: 10.1038/s41593-018-0227-9

22. Antila S, Karaman S, Nurmi H, Airavaara M, Voutilainen MH, Mathivet T, et al. Development and plasticity of meningeal lymphatic vessels. *J Exp Med* (2017) 214(12):3645–67. doi: 10.1084/jem.20170391

23. Guy J, Hendrich B, Holmes M, Martin JE, Bird A. A mouse Mecp2-null mutation causes neurological symptoms that mimic rett syndrome. *Nat Genet* (2001) 27(3):322–6. doi: 10.1038/85899

24. Rustenhoven J, Drieu A, Mamuladze T, de Lima KA, Dykstra T, Wall M, et al. Functional characterization of the dural sinuses as a neuroimmune interface. *Cell* (2021) 184:1–17. doi: 10.1016/j.cell.2020.12.040

25. Wang Y, Chen D, Xu D, Huang C, Xing R, He D, et al. Early developing b cells undergo negative selection by central nervous system-specific antigens in the meninges. *Immunity* (2021) 54(12):P2784–2794.E6. doi: 10.1016/j.immuni.2021.09.016

26. Brioschi S, Wang WL, Peng V, Wang M, Shchukina I, Greenberg ZJ, et al. Heterogeneity of meningeal b cells reveals a lymphopoietic niche at the CNS borders. *Science* (2021) 373(6553):1-14. doi: 10.1126/science.abf9277

27. Green DS, Young HA, Valencia JC. Current prospects of type II interferon gamma signaling and autoimmunity. *J Biol Chem* (2017) 292(34):13925–33. doi: 10.1074/jbc.R116.774745

28. Tianshu Yang MBR, Neul JL, Lu W, Roberts L, Knight J, Ward CS, et al. Overexpression of methyl-CpG binding protein 2 impairs TH1 responses. *Sci Trans Med* (2012) 4(163):163ra158. doi: 10.1126/scitranslmed.3004430

29. Wu C, Xue Y, Wang P, Lin L, Liu Q, Li N, et al. IFN-gamma primes macrophage activation by increasing phosphatase and tensin homolog via downregulation of miR-3473b. *J Immunol* (2014) 193(6):3036–44. doi: 10.4049/jimmunol.1302379

30. Junkins RD, MacNeil AJ, Wu Z, McCormick C, Lin TJ. Regulator of calcineurin 1 suppresses inflammation during respiratory tract infections. *J Immunol* (2013) 190(10):5178–86. doi: 10.4049/jimmunol.1203196

31. Ivashkiv LB. IFNgamma: signalling, epigenetics and roles in immunity, metabolism, disease and cancer immunotherapy. *Nat Rev Immunol* (2018) 18 (9):545–58. doi: 10.1038/s41577-018-0029-z

32. Ma T, Wang F, Xu S, Huang JH. Meningeal immunity: Structure, function and a potential therapeutic target of neurodegenerative diseases. *Brain Behav Immun* (2021) 93:264–76. doi: 10.1016/j.bbi.2021.01.028

33. Zalosnik MI, Fabio MC, Bertoldi ML, Castanares CN, Degano AL. MeCP2 deficiency exacerbates the neuroinflammatory setting and autoreactive response during an autoimmune challenge. *Sci Rep* (2021) 11(1):10997. doi: 10.1038/s41598-021-90517-8

34. Papini AM, Nuti F, Real-Fernandez F, Rossi G, Tiberi C, Sabatino G, et al. Immune dysfunction in rett syndrome patients revealed by high levels of serum anti-N(Glc) IgM antibody fraction. *J Immunol Res* (2014) 2014:260973. doi: 10.1155/2014/260973

35. Leoncini S, De Felice C, Signorini C, Zollo G, Cortelazzo A, Durand T, et al. Cytokine dysregulation in MECP2- and CDKL5-related rett syndrome: Relationships with aberrant redox homeostasis, inflammation, and omega-3 PUFAs. *Oxid Med Cell Longev* (2015) 2015:421624. doi: 10.1155/2015/421624

36. Janach GMS, Reetz O, Dohne N, Stadler K, Grosser S, Byvaltcev E, et al. Interferon-gamma acutely augments inhibition of neocortical layer 5 pyramidal neurons. *J Neuroinflamm* (2020) 17(1):69. doi: 10.1186/s12974-020-1722-y

37. Rua R, McGavern DB. Advances in meningeal immunity. *Trends Mol Med* (2018) 24(6):542–59. doi: 10.1016/j.molmed.2018.04.003

38. Andres DA, Shi GX, Bruun D, Barnhart C, Lein PJ. Rit signaling contributes to interferon-gamma-induced dendritic retraction via p38 mitogen-activated protein kinase activation. *J Neurochem* (2008) 107(5):1436–47. doi: 10.1111/j.1471-4159.2008.05708.x

39. Filiano AJ, Xu Y, Tustison NJ, Marsh RL, Baker W, Smirnov I, et al. Unexpected role of interferon-gamma in regulating neuronal connectivity and social behaviour. *Nature* (2016) 535(7612):425–9. doi: 10.1038/nature18626

40. Chao HT, Chen H, Samaco RC, Xue M, Chahrour M, Yoo J, et al. Dysfunction in GABA signalling mediates autism-like stereotypies and rett syndrome phenotypes. *Nature* (2010) 468(7321):263–9. doi: 10.1038/nature09582

41. Wang IT, Reyes AR, Zhou Z. Neuronal morphology in MeCP2 mouse models is intrinsically variable and depends on age, cell type, and Mecp2 mutation. *Neurobiol Dis* (2013) 58:3–12. doi: 10.1016/j.nbd.2013.04.020

42. Chao HT, Zoghbi HY, Rosenmund C. MeCP2 controls excitatory synaptic strength by regulating glutamatergic synapse number. *Neuron* (2007) 56(1):58–65. doi: 10.1016/j.neuron.2007.08.018

43. Herz J, Fu Z, Kim K, Dykstra T, Wall M, Li H, et al. GABAergic neuronal IL-4R mediates T cell effect on memory. *Neuron* (2021) 109(22):3609–3618 e9. doi: 10.1016/j.neuron.2021.10.022

44. Magliozzi R, Howell OW, Durrenberger P, Arico E, James R, Cruciani C, et al. Meningeal inflammation changes the balance of TNF signalling in cortical grey matter in multiple sclerosis. *J Neuroinflamm* (2019) 16(1):259. doi: 10.1186/s12974-019-1650-x

45. Ehinger Y, Matagne V, Villard L, Roux JC. Rett syndrome from bench to bedside: recent advances. *F1000Res* (2018) 7:398. doi: 10.12688/f1000research.14056.1

46. Brombacher TM, Nono JK, De Gouveia KS, Makena N, Darby M, Womersley J, et al. IL-13-Mediated regulation of learning and memory. *J Immunol* (2017) 198(7):2681–8. doi: 10.4049/jimmunol.1601546

frontiers | Frontiers in Immunology

TYPE Review
PUBLISHED 12 January 2023
DOI 10.3389/fimmu.2022.1094925

Check for updates

OPEN ACCESS

EDITED BY
Bo Li,
Department of Orthopedics,
Sun Yat-sen University, China

REVIEWED BY
Junqing Huang,
Jinan University, China
Xiaoli Wu,
Tianjin University, China

*CORRESPONDENCE
Kebing Chen
chkbing@mail.sysu.edu.cn

SPECIALTY SECTION
This article was submitted to Multiple Sclerosis and Neuroimmunology, a section of the journal Frontiers in Immunology

RECEIVED 10 November 2022
ACCEPTED 19 December 2022
PUBLISHED 12 January 2023

CITATION
Mo Y and Chen K (2023) Review: The role of HMGB1 in spinal cord injury.
Front. Immunol. 13:1094925.
doi: 10.3389/fimmu.2022.1094925

COPYRIGHT
© 2023 Mo and Chen. This is an open-access article distributed under the terms of the Creative Commons Attribution License (CC BY). The use, distribution or reproduction in other forums is permitted, provided the original author(s) and the copyright owner(s) are credited and that the original publication in this journal is cited, in accordance with accepted academic practice. No use, distribution or reproduction is permitted which does not comply with these terms.

Review: The role of HMGB1 in spinal cord injury

Yizhang Mo and Kebing Chen*

Department of Spine Surgery, The Sixth Affiliated Hospital of Sun Yat-sen University, Guangzhou, China

High mobility group box 1 (HMGB1) has dual functions as a nonhistone nucleoprotein and an extracellular inflammatory cytokine. In the resting state, HMGB1 is mainly located in the nucleus and regulates key nuclear activities. After spinal cord injury, HMGB1 is rapidly expressed by neurons, microglia and ependymal cells, and it is either actively or passively released into the extracellular matrix and blood circulation; furthermore, it also participates in the pathophysiological process of spinal cord injury. HMGB1 can regulate the activation of M1 microglia, exacerbate the inflammatory response, and regulate the expression of inflammatory factors through Rage and TLR2/4, resulting in neuronal death. However, some studies have shown that HMGB1 is beneficial for the survival, regeneration and differentiation of neurons and that it promotes the recovery of motor function. This article reviews the specific timing of secretion and translocation, the release mechanism and the role of HMGB1 in spinal cord injury. Furthermore, the role and mechanism of HMGB1 in spinal cord injury and, the challenges that still need to be addressed are identified, and this work will provide a basis for future studies.

KEYWORDS

HMGB1, spinal cord injury, inflammation, neuron, mechanism

1 Introduction

High mobility group box 1 (HMGB1), also known as amphotericin or HMG1, is a nonhistone chromatin binding protein first discovered in the 1960s. HMGB1 shows high electrophoretic mobility when run on polyacrylamide gels, hence its name (1, 2). HMGB1 is highly conserved in evolution, and the HMGB1 in rodents shares 99% homology with that in humans (3–5). HMGB1 is also expressed partially in the cytoplasm because it shuttles back and forth from the nucleus (6). HMGB1 has the dual functions of a nonhistone nucleoprotein and an extracellular inflammatory cytokine. HMGB1 binds extensively to DNA in the nucleus and participates in transcriptional regulation, DNA replication and repair, telomere maintenance and nucleosome assembly (7). Extracellular HMGB1 is passively released or actively secreted by necrotic tissue or stress cells. As a chemokine or cytokine, it binds to pattern recognition receptors (PRRs) to create a damage-associated molecular pattern (DAMP) (6–12). HMGB1 plays an important role

in many diseases, including traumatic shock, fatty liver disease, septicaemia, autoimmune diseases, and cancer (8, 11, 13–15).

In recent years, the role of HMGB1 in spinal cord injury (SCI) has attracted a great deal of attention. SCI is characterized by sensory, motor and autonomic nerve dysfunction (16) mediated by complex and diverse pathophysiological processes, including neuroinflammation, neuronal death, glial scar formation and axonal regeneration (17–20). The concentration of HMGB1 in the injured area increases rapidly and lasts for a long time (21–31), and it not only aggravates injury by playing the role of an inflammatory cytokine, but it also promotes the recovery of the injured spinal cord.

This article reviews the research progress of studies investigating the expression and release of HMGB1 after SCI, its effect on the injured spinal cord and its potential therapeutic mechanism.

2 Main text

2.1 The structure of HMGB1 and the lower function of the resting state

The HMGB1 protein is a highly conserved nuclear protein that consists of 215 amino acids and has a molecular weight of approximately 30 kDa. Structurally, HMGB1 is divided into the following three functional regions: the A-box, the B-box and the acidic C-terminus. The A-box and B-box are composed of 80-90 amino acid residues with similar amino acid repeat sequences and nonspecific DNA-binding sites, and the B-box is the functional structural region that causes inflammation (32, 33); however, the A-box has a certain antagonistic effect on the B-box (34). The acidic C-terminus containing aspartic acid and glutamate is mainly involved in regulating the binding of HMGB1 to DNA and mediating gene transcription and chromosome unwinding (35). The B-box domain has two key binding sites, Toll-like receptor 4 (TLR4) and a receptor for advanced glycation end (RAGE) products, which regulate the release of proinflammatory cytokines (36, 37). HMGB1 has two nuclear localization sequences (NLSs); one is in the A-box, the other is between the B-box and the C-terminal tail, and the nuclear export signal (NES) is contained in the DNA-binding domain (38).

During the resting state of HMGB1, it is located mainly in the nucleus and it regulates key nuclear activities, including transcription, replication, DNA repair and nucleosome formation, all of which are important for maintaining steady-state cellular function (7, 38).

Collectively, these results show that HMGB1 is a highly conserved protein with proinflammatory and anti-inflammatory potential. In the resting state, HMGB1 is located mainly in the nucleus and regulates physiological processes there; however, there are no related studies on the structural and functional changes to HMGB1 in the nucleus after SCI.

2.2 Expression of HMGB1 after SCI

After SCI, HMGB1 is expressed and released by neurons, microglia/macrophages, and ependymal cells (21–23). After injury, the expression of HMGB1 is rapidly upregulated and released into the extracellular matrix and circulating blood, which lasts for a long period of time. In a rat experiment, the expression of HMGB1 mRNA and HMGB1 protein was found to be upregulated 2-6 hours after SCI, the peak level was reached 1-3 days after injury, and this enhanced level lasted for 28 days after SCI (21, 23, 39, 40); however, the number of HMGB1 positive cells in the spinal cord of injured rats was the highest 48 hours after injury (41). In addition, Fan et al. found that the concentration of HMGB1 in serum increased significantly 3 days after SCI (42). In a model of SCI using neurons *in vitro*, we found that after injury, the concentration of HMGB1 in the culture medium immediately increased to 5 ng and 17 ng/ml at 6 and 12 hours, respectively, and reached 19 ng/ml HMGB1 at 24 hours (27). Interestingly, in addition to the increased expression of HMGB1 in the acute and subacute phases after SCI, the level of HMGB1 also increased significantly in the chronic phase. Papatheodorou et al. found that HMBG1 levels also increased significantly in patients 5 or more years after SCI (43). However, the findings of Fang et al. in zebrafish experiments suggested different expression patterns of HMGB1, and these results contradict the continuous increase in HMGB1 found by most studies. The level of HMGB1 mRNA increased twofold at 4 hours after SCI, decreased 12 hours and 11 days after injury, and increased again 21 days after injury (22).

Collectively, these results show that the expression of HMGB1 increases rapidly after SCI and lasts for a long time, even throughout the acute, subacute, and chronic stages, implying that HMGB1 may affect the severity of SCI and the process of recovery. In addition, the expression of HMGB1 was still upregulated in the chronic phase after injury, and its specific mechanism and effect still need to be explored. Moreover, the specific mechanism of the new model of HMGB1 expression remains to be further validated. Reguarding the role of HMGB1, we speculate that the first increase in HMGB1 expression is beneficial to protect injured neurons, then the decrease in

HMGB1 expression is beneficial to reduce inflammation and further reduce neuronal death, and then the continuous increase in expression helps promote nerve regeneration and recovery of the injured spinal cord.

2.3 Translocation time of HMGB1 after SCI

After SCI, the expression of HMGB1 increases rapidly, translocates from the nucleus to the cytoplasm; furthermore, it may be released into the extracellular matrix through cytoplasmic vacuoles. Two hours after SCI, the nuclear level of HMGB1 increased significantly, and HMGB1 in the nucleus was gradually released into the cytoplasm. Six hours after injury, the cytoplasmic level of HMGB1 increased significantly. HMGB1 is located mainly in the nucleus of neurons in the early stages after SCI, and then it translocates to the cytoplasm a few hours later (21, 27, 44). Interestingly, in a zebrafish SCI model, Fang et al. found that HMGB1 was in the cytoplasm of motoneurons 4 hours after injury; however, 12 hours after injury, the cytoplasmic HMGB1 level in motoneurons decreased. On the 21st day of SCI, the level of HMGB1 in the cytoplasm decreased, but HMGB1 was again detected in the nucleus. HMGB1 exists in the motoneuron nucleus and it translocates to the cytoplasm after injury; furthermore, its expression is downregulated in motoneurons (22). The most significant change in HMGB1 translocation after SCI in mice was in the macrophages at the lesion centre and near the lesion boundary. HMGB1 could not even be detected in the nucleus, while it was still found in small cytoplasmic vacuoles, implying that HMGB1 may be packaged in the cell to be secreted into the extracellular space (23).

Taken together, these results indicate that HMGB1 increased in the nucleus and was released from the nucleus to the cytoplasm and extracellular matrix; however, the specific time and node of translocation have not been clarified.

2.4 Possible mechanism of HMGB1 release after SCI

The mechanism of secretion and release of HMGB1 in SCI has not been specifically explained, but it is generally thought that HMGB1 mainly comes from the secretion of inflammatory cells and the release of dead neurons (21–23, 45, 46).

In SCI, HMGB1 may carry out nuclear and cytoplasmic transport through acetylation, phosphorylation and methylation of the nuclear localization sites (NLS). In a study of *T. thermophila* CU 427 and CU 428, two NLSs were found to control the nuclear localization of HMGB1 in the steady state (47). Posttranslational modifications of the NLS site, including acetylation, phosphorylation and methylation, regulate the ability of HMGB1 to be transported to the cytoplasm during cellular stress (48–51). In a study of mouse fibroblasts, HeLa cells and Saos-2 cells, it was found that excessive acetylation of lysine at the NLS site was essential for the translocation of HMGB1 from the nucleus to the cytoplasm in monocytes stimulated by LPS, TNF or IL-1. Inhibiting the peracetylation of the NLS, can inhibit the translocation of HMGB1 from the nucleus to the cytoplasm and block the translocation of HMGB1 from the cytoplasm to the nucleus (2, 48, 52). In addition, the NLS site of HMGB1 was found to be phosphorylated and translocated to the cytoplasm of mouse macrophages stimulated by TNF (53). In neutrophils, the methylation of the lysine site of HMGB1 NLS was found to weaken the DNA-binding activity of HMGB1, resulting in the passive diffusion of HMGB1 out of the nucleus (49).

In SCI, the mechanism of extracellular secretion of HMGB1 is related to inflammation. Inflammation can induce many kinds of cells to secrete HMGB1 (54, 55); however, HMGB1 cannot be actively secreted through the conventional endoplasmic reticulum-Golgi secretion pathway utilized by most soluble secretory proteins (56, 57). At present, scholars have proposed two forms of active release of HMGB1 (58). One is stimulation and activation of the target cells, causing HMGB1 to be secreted into the outer space of the cells (48, 59). The second is packaging HMGB1 into intracellular vesicles, and then releasing HMGB1 outside the cell after the vesicles fuse with the cell membrane (60, 61). The latter is consistent with HMGB1 being in cytoplasmic vacuoles in macrophages after SCI (23).

HMGB1 translocation and release during aseptic inflammation can be regulated by calcium-mediated signal transduction (50, 62, 63). Phosphorylation and release of HMGB1 are regulated by activation of calcium-mediated protein kinases, especially calmodulin-dependent protein kinases (CaMKKs) (64–67). Calcium signal inhibitors inhibit HMGB1 secretion and protect animals in various disease models (50, 68). In addition, heat shock protein family A (Hsp70) member 1A (HSPA 1A, also known as HSP72) can block HMGB1 secretion in macrophages by inhibiting the interaction between HMGB1 and XPO1 (69). In different inflammation and injury models, peroxisome proliferator activated receptor (PPAR) binds to specific ligands and activates the transcription of PPAR target genes. The secretion of HMGB1 in activated macrophages is negatively regulated by PPAR (70). In contrast, JAK-regulated STAT1 and STAT3 activation plays an active role in the expression, modification and/or release of HMGB1 (71–75), while extracellular HMGB1 can trigger the activation of the STAT1 and STAT3 pathways (74–78). In addition, MAPK family members and inflammatory bodies promote the release of HMGB1 in different inflammatory and injury models (79–82). Deficiency of complement 5a

receptor 2 (C5aR2) limits the activation of NLRP3 inflammatory bodies and the release of HMGB1 *in vitro* (83).

Expression of the inflammatory cytokines TNF and NF-κB were upregulated after SCI. TNF knockout or a TNF neutralization antibody directly inhibited TNF and partially inhibited HMGB1 release induced by IFN-γ and LPS in macrophages, indicating that the secretion of HMGB1 is partially mediated by a TNF-dependent mechanism (84). In addition, the NF-κB pathway is involved in the release of HMGB1, and the inhibition of the classical NF-κB pathway limits the secretion of HMGB1 in activated immune cells; however, the target gene of NF-κB that causes the secretion of HMGB1 is still unknown (85–87). Furthermore, the involvement of TNF (the classical NF-κB target gene) in the NF-κB dependent release of HMGB1 cannot be ruled out.

After SCI, HMGB1 can be passively released after various types of cell death in response to various stimuli or injuries. In addition, the release of many intracellular substances (cathepsin, antioxidant enzymes, DNase, caspases) after cell death can also promote the secretion of HMGB1 by inflammatory cells (81, 88–100).

In summary, although the secretion and release mechanism of HMGB1 in SCI has not been specifically described, the release mechanism of HMGB1 described in other fields if of great value. In SCI, HMGB1 may be actively released by inflammatory cells or passively released by necrotic neurons, and intracellular substances released by necrotic cells may further induce the active secretion of HMGB1 (Figure 1).

2.5 HMGB1 may regulate cell migration after SCI

Although the role of that HMGB1 plays in inducing cell migration in SCI has not been reported, in other diseases, HMGB1 has been found to induce cell migration by activating RAGE or activating the CXCR4 receptor through a heterologous complex with CXCL12. Many studies have shown that HMGB1, as a potential host cell-derived chemokine, promotes the migration of nerve processes and many cell types. These cells include smooth muscle cells, myoblasts, tumour cells, hepatic stellate cells, stem cells, endothelial cells, keratinocytes, monocytes, dendritic cells and neutrophils (101–117).

RAGE is necessary for HMGB1-mediated cell migration. HMGB1 triggers RAGE to induce the transcription of chemokine genes such as CCL3, CCL4 and CXCL12, while HMGB1-induced migration can quickly be blocked by anti-RAGE or anti-HMGB1 neutralizing antibodies, confirming the importance of RAGE in the process of migration (102, 118–121). Recent studies have shown that the triggering of RAGE by HMGB1 induces the transcription of chemokine genes such as CCL3, CCL4 and CXCL12, and subsequently it participates in

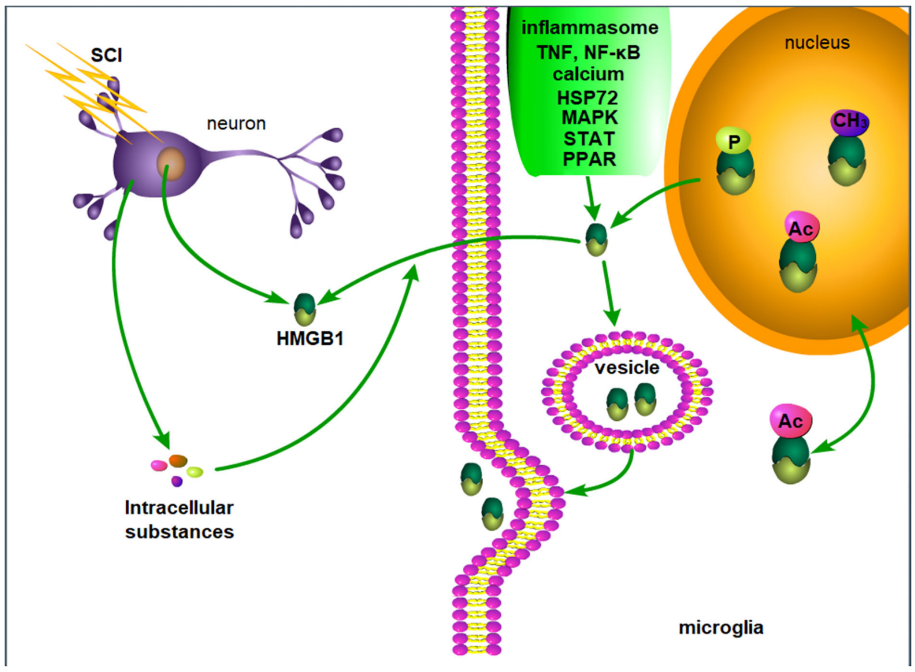


FIGURE 1
Possible mechanism of HMGB1 release after SCI. After SCI, injured neurons passively release HMGB1, and the intracellular substances released by necrotic neurons and inflammation lead to the active release of HMGB1 by microglia. P, phosphorylation. Ac, acetylation. CH3, methylation.

cell migration (118, 119, 121). In addition, HMGB1 can induce cell migration by forming heterocomplexes with CXCL12 is mediated by CXCR4 receptors, and the HMGB1-CXCL12 complex is more effective in inducing monocyte migration than CXCL12 alone (109, 122–124). By activating CXCR4 receptors, HMGB1-CXCL12 complexes recruit leukocytes from the circulation, and then induce leukocytes to activate and secrete cytokines and chemokines, thus promoting inflammation (125, 126). Interestingly, HMGB1 not only stimulates but also inhibits migration in some cells. For example, exogenous HMGB1 selectively inhibits VEGF-induced cell migration in pulmonary artery endothelial cells (HPAECs), but does not inhibit human umbilical vein endothelial cells (HUVECs). In addition, the IRF3-dependent TLR4 pathway is necessary for HMGB1-mediated inhibition of migration in HPAECs (115).

Collectively, these data show that HMGB1 can promote the migration of a variety of cells, including inflammatory cells and stem cells. Although the chemotaxis of HMGB1 has not been studied in SCI, it remains possible that HMGB1 could induce inflammatory cell migration to aggravate the inflammatory response or promote injury recovery by inducing stem cell migration following SCI.

2.6 HMGB1 induces an inflammatory response after SCI

HMGB1 aggravates the inflammatory response after SCI. We found that after SCI, HMGB1 and its receptors were significantly colocalized in the white matter of the injured rat spinal cord (21). After HMGB1 injection, the focus of activated microglia was obviously in the ventral horn of the spinal cord (23), but the lesion area of anti-HMGB1 mAb-treated mice was significantly smaller than the lesion area of untreated mice (127–129). HMGB1 is thought to aggravate SCI. To further investigate its specific mechanism, Nakajo et al. found that anti-HMGB1 mAb treatment could protect the BSCB from damage caused by SCI, reduce the level of AQP4 protein in the spinal cord, and inhibit the swelling of the injured spinal cord. Anti-HMGB1 mAb inhibits inflammation after SCI in the early acute phase and it can prevent BSCB destruction directly or indirectly by inhibiting the expression of inflammatory cytokines and MMP in SCI model mice. Anti-HMGB1 mAb can relieve SCI, oedema and demyelination, thus promoting the recovery of the spinal cord (27, 128).

After SCI, HMGB1 induces inflammation mainly by activating microglia rather than astrocytes. Colocalization of microglial activation and obvious neuronal loss occurs in the spinal cord of rats with HMGB1 injection (23). HMGB1 has been reported to induce inflammation by activating microglia/macrophages (21, 44). In addition, further studies found that HMGB1 contributes to the development of the neurotoxic inflammatory macrophages (M1) phenotype after SCI (23). The mRNA levels of TNF-α, iNOS and CD86 increased significantly in microglia treated with HMGB1, which provided direct evidence for the activation of microglia to the M1 phenotype by HMGB1. HMGB1 or RAGE inhibition can inhibit the activation of macrophages/microglia to the M1 phenotype and promote the activation of macrophages/microglia to the M2 phenotype after SCI (27, 42, 130). Moreover, recombinant HMGB1 promoted the migration of BV2 microglia, while the anti-HMGB1 polyclonal antibody weakened the migration of BV2 microglia. The secretion of HMGB1 after SCI has been reported to recruit microglia to participate in the inflammatory response (27); however, HMGB1 failed to activate the classical inflammatory signalling pathway of primary astrocytes, indicating that astrocytes may not be induced by HMGB1.

After SCI, HMGB1 regulates the expression of inflammatory factors and the inflammatory response through RAGE and TLR2/4. HMGB1,TNF-α and RAGE are expressed in the same apoptotic neurons after SCI (41). There was a significant correlation between the levels of HMGB1 and NF-κB and the expression of TLR4 and NF-κB protein after SCI (131). HMGB1, TNF-α and RAGE are expressed in the same apoptotic neurons, and the temporal expression patterns of RAGE and HMGB-1 are similar (21, 41). The expression of RAGE, TNF-α, NF-κB IFN-γ, IL-1α, IL-6 and IL-17 increased in microglia treated with HMGB1, while inhibition of HMGB1 decreased the levels of RAGE, TNF-α, NF-κB IFN-γ, IL-1α, IL-6 and IL-17 (27, 42). HMGB1 induced inflammation by activating TLR2/4 or RAGE, activating its downstream pathway and upregulating the levels of TNF-α and NF-κB (28, 132–136). Interestingly, Wang et al. found that the administration of recombinant HMGB1 did not increase the levels of inflammatory cytokines TNF-α and IL-1β, while blocking RAGE reduced the induction of cytokines induced by LPS. It has been proposed that HMGB1/RAGE does not directly increase proinflammatory cytokines, and the effect of RAGE on cytokines may be related to pathogen-related interactions (137).

Collectively, these results shown that the expression of HMGB1 is upregulated after SCI, the inflammatory response is aggravated by regulating the activation of microglia to the M1 phenotype, and the expression of inflammatory factors is regulated by RAGE and TLR2/4. However, the studies of Wang et al. indicate different possibilities, and the specific mechanism remains to be further validated. In addition, these studies investigated the role of HMGB1 in only acute and subacute SCI. However, as the expression of HMGB1 is still upregulated in the chronic phase of SCI, its specific role needs to be further explored. Finally, extracellular HMGB1 can aggravate the inflammatory response after SCI, but the specific changes in nuclear HMGB1 after SCI are not clear, and its specific role

needs to be understood.

2.7 Effect of HMGB1 on injured neurons after SCI

After SCI, HMGB1 promotes neuronal death by promoting nerve inflammation. After HMGB1 injection, focus of activated microglia and the area of neuronal loss were determined. Coculture of macrophages stimulated by HMGB1 with neurons showed a decrease in axonal growth (23). Inhibition of the HMGB1/TLR4/NF-κB signalling pathway can inhibit neuroinflammation and apoptosis in SCI, reduce the damage, oedema and demyelination, improve the survival rate of host neurons, and promote the recovery of the spinal cord (24, 27, 28, 127, 128, 138–140) Interestingly, Song et al. found that transplantation of HMGB1-preconditioned neural stem cells can promote neuronal survival after SCI in rats, promote the connection between relay neurons and motor neurons; furthermore, the newly formed neural circuits greatly improved motor recovery (25, 30). These findings are consistent with the findings of Wang et al. in cerebral ischemia-reperfusion injury. HMGB1 preconditioning can significantly reduce neurological deficits, infarct size, brain swelling, apoptosis and blood-brain barrier permeability in rats with cerebral ischemia-reperfusion injury (141). In addition, RAGE blockade was shown to not be conducive to neuronal survival after SCI (137), and consistent with the findings of Huttunen et al. HMGB1 can promote neuronal survival and axonal growth by activating RAGE and increasing the expression of the anti-apoptotic protein Bcl2 (142–145). HMGB1 is thought to be beneficial for the survival of injured spinal cord neurons.

In summary, numerous studies have shown that HMGB1 can exacerbate neuronal injury by aggravating neuroinflammation. Some studies have also suggested that HMGB1 is conducive to the survival and recovery of injured neurons. However, the specific mechanism by which HMGB1 protects injured neurons and promotes injury recovery is not clear, and this does not rule out the possibility that HMGB1 indirectly injures neurons by promoting the inflammatory response and protects neurons through direct action.

2.8 HMGB1 induces neuronal regeneration after SCI

After SCI, HMGB1 promotes the growth of neuronal axons and induces the differentiation of neural stem cells. Fang et al. found that HMGB1 increased significantly and the number of perivascular motoneurons increased significantly 6th days after SCI. After inhibition of HMGB1, the number of detected axons decreased significantly. HMGB1 is thought to participate in axonal regeneration and promote motor recovery (22). Further *in vitro* experiments showed that HMGB1, especially when close to the neuronal cell body, significantly increased neuronal axonal growth (23). In addition, HMGB1 can also promote neuronal differentiation. HMGB1 can induce the differentiation of neural stem cells through the ERK signalling pathway and the RAGE signalling pathway, while antagonism of these pathways can reduce the expression of marker molecules in mature neurons (25, 137). These results indicate that HMGB1 can induce the differentiation and maturation of neural stem cells through the ERK signalling pathway and the RAGE signalling pathway. Interestingly, Palumbo et al. found that HMGB1 can induce stem cells to migrate across the endothelial barrier *in vitro* and *in vivo* (104). Thus, the role of recruiting stem cells in the recovery of SCI remains to be explored.

Collectively, these results show that HMGB1 can promote the growth of neuronal axons and induce the differentiation of neural stem cells after SCI; although, the specific mechanism needs to be further explored. In addition, in the chronic stage of SCI, the upregulation of HMGB1 may be involved in regulating neuronal regeneration and promoting motor recovery.

2.9 HMGB1: A potential target for clinical treatment after SCI

After SCI, HMGB1 aggravates the damage by inducing inflammation, and after treatment with hyperbaric oxygen, shikorin, glycyrrhizin, Higenamine, ethyl pyruvate, glycyrrhizin, Catalpol, Dihydrotanshinone I, mir-34a, anti-HMGB1 mAb, etc., HMGB1 can reduce inflammation and reduce spinal cord oedema, protect spinal cord neurons and promote functional recovery after SCI by downregulating the expression of HMGB1 and NF-κB (24, 26, 30, 42, 127–129, 131, 146–153). Among these studies, Higenamine induced an increase in M2 macrophages and saw an enhanced the anti-inflammatory effect (147). miR-34a, miR-129-5p, Catalpol and shikonin-induced HMGB1 downregulate the NF-κB signalling pathway involved in the decreased expression of TLR4 (24, 131, 148, 149, 151). Dihydrotanshinone I was shown to protects against SCI *in vivo* through the HMGB1/TLR4/NOX4 pathway. Ethyl pyruvate or glycyrrhizin we shown to reduce spinal cord oedema by reducing the expression of AQP4 in the spinal cord of rats with SCI (129). Furthermore, glycyrrhizin reduced the area of the cystic cavity and glial scar formation (153). However, as mentioned earlier, HMGB1 does not only induce inflammation to aggravate SCI, but it also promotes neuronal regeneration. Transplantation of neural stem cells pre-treated with HMGB1 promotes neuronal survival after SCI in rats. The motor recovery of rats in the HMGB1 combination with neural stem cell group was better than the motor recovery of rats in the single transplantation group and in HMGB1 group (25) (Table 1).

TABLE 1 Summary of targeted HMGB1 treatment of SCI.

S.N.	Study Model	Intervention and Dosing Schedule	Observations	References
1	SCI model of adult SD rats established by Allen gravity drop method	HBO (8~10L/min, 2.5 ATA, Once or twice a day. Inhaling oxygen for 45 minutes at a time)	HMGB1 mRNA and protein expression water, NF-κB mRNA decreased averagely, and Basso, Beattie and Bresnahan scores increased significantly after HBO intervention.	(146)
2	SCI model of contusion in C57BL/6J WT male mice	Higenamine (10 mg/kg, i.p.)	HG decreased the expression of HMGB1, increased the expression of IL-4 and IL-10, promoted the production of HO-1 and the activation of macrophage M2, and increased the BMS score of mice.	(147)
3	SCI model of adult SD rats established by Allen gravity drop method	HBO (8~10L/min, 2.5 ATA, Once a day. Inhaling oxygen for 45 minutes at a time)	The production of HMGB1 mRNA, NF-κB mRNA, TLR4 protein and NF-κB mRNA decreased, and BBB score increased. HMGB1 mRNA and TLR4 mRNA were positively correlated with TLR4 protein.	(131)
4	SCI models of adult male Sprague-Dawley rats established by gravity drop method	1.5 μ L RAGE antibody (1 μ g/ml) injected into the affected area.	RAGE inhibition reduced the expression of Nestin in MAP-2, a marker of mature neurons, and did not improve the Basso, Beattie, and Bresnahan (BBB) scores after SCI.	(137)
5	SCI model of adult male S D rats established by Allen gravity drop method	Shikonin (10-100mg/kg, i.p.)	Shikonin decreased the expression of HMGB1, TLR4 and NF-κB, alleviated inflammatory reaction, spinal cord oedema and increased BBB score after SCI.	(148)
6	SCI model of male SD rats established by aneurysm clip compression	Dexmedetomidine intrathecal injection (1, 2, and 4μg/kg)	Dexmedetomidine pretreatment increased the expression of α 7nAChR and acetylcholine and activated PI 3 K/Akt, and increased the BBB score of mice after SCI.	(40)
7	SCI model of NOD-SCID female mice established by Infinite Horizon Impactor	anti-HMGB1 (2-16 mg/kg, i.p.)	After treatment with anti-HMGB1 antibody, the destruction of blood spinal screen and the formation of oedema were alleviated, the survival from neurons was increased, and the BMS score was increased, suggesting that the functional recovery was increased. The subsequent hiPSC-NSC transplantation greatly enhanced this recovery.	(127)
8	SCI model of adult female S D rats established by Allen gravity drop method	Ethyl pyruvate (50 mg/kg, i.p.) Glycyrrhizin (50 mg/kg, i.p.)	Both EP and GL could effectively inhibit the expression of HMGB1 in spinal cord and the level of serum HMGB1 in SCI rats, inhibit the activation of TLR4/MyD88/NF-κB signal pathway, reduce the overexpression of SCI-related GFAP and AQP4 in spinal cord, improve the motor function of SCI rats, reduce the water content of spinal cord and relieve spinal cord oedema.	(129)
9	SCI model of C57 BL/6 female mice established by Infinite Horizon impactor	Catalpol (60 mg/kg, i.g)	Catalpol treatment can reduce the expression of HMGB1/TLR4/NF-κB pathway protein, inhibit apoptosis, reduce inflammation and oxidation, and increase the BBB score of SCI mice.	(24)
10	SCI model of adult female S D rats established by Allen gravity drop method	Glycyrrhizin (100 mg/kg, i.p.)	Glycyrrhizin decreased the expression of GFAP, CSPG, HMGB1 and NF-κB in spinal cord, reduced the formation of glial scar and promoted the recovery of hindlimb motor function in rats.	(153)
11	SCI model of male SD rats established by modified Tetzlaf lateral spinal cord compression	Glycyrrhizin (100 mg/kg, i.p.) FPS-ZM1 (1 mg/kg, i.p.)	Inhibition of HMGB1 or RAGE effectively reduced the number of harmful proinflammatory macrophages/microglia and increased the number of anti-inflammatory cells after SCI. Inhibition of HMGB1 or RAGE significantly reduced neuronal loss and demyelination after SCI, and improved functional recovery after SCI.	(42)

(Continued)

TABLE 1 Continued

S.N.	Study Model	Intervention and Dosing Schedule	Observations	References
12	SCI model of male SD rats established by aneurysm clip compression	NSCs preconditioned with 1 ng/ml HMGB1 in 3 μl DMEM	NSCs pre-treated with HMGB1-increased the number of functional Nissl bodies in neurons, increased the number of βIII-tubulin$^+$ cells in the injured spinal cord of SCI rats, promoted the differentiation of NSCs into neurons and increased BBB score.	(25)
13	SCI model of adult SD rats established by Allen gravity drop method	Dihydrotanshinone I (2-4 mg/kg, p.o.)	DI treatment inhibited the levels of TLR4, MyD88, HMGB1, NOX 4, TNF-α, IL-1b, IL-6, iNOS and TOS, increased the level of TAS, alleviated the pathological injury caused by SCI and promoted the recovery of neurological function.	(26)
14	SCI model of C57BL/6 female mice prepared by clamp method	Electroacupuncture (1.5 Hz/7.5 Hz,1.0mA) was applied to "jiaji" (EXH-B2) for 10 minutes, once a day for 5-14 days, separately	After electroacupuncture treatment, the expression level of TLR4 protein, HMGB1 and Iba1 protein decreased significantly, the number of Iba1 positive cells and HMGB1/Iba1 copositive cells in spinal cord decreased significantly, and the morphology of microglia in spinal cord changed from overactivated state to resting state. BBB score increased significantly.	(152)
15	SCI model of male Wistar rats established by aneurysm clip compression	1 μM ATRA-treated BM-MSCs	ATRA-MSCs increased the levels of Beclin-1 and LC3-II, downregulated the levels of proteins related to HMGB1/NF-κB/NLRP3 pathway, inhibited proinflammatory cytokines, improved the motor activity of hindlimb, and contributed to the survival of neurons, showing a greater beneficial effect than MSCs.	(31)
16	SCI model of male SD rats established by aneurysm clip compression	Glycyrrhizic Acid (100 mg/kg, i.p.)	GA significantly decreased the expression of HMGB1 and inflammatory factors after SCI. GA decreased the phosphorylation of p38 and JunN-terminal kinase proteins, but did not decrease their expression levels.	(44)

In summary, HMGB1 plays a multifunctional role in SCI. Inhibition of HMGB1 inhibits nerve inflammation and protects the spinal cord; furthermore, HMGB1 can be used to protect neurons, promote neuronal regeneration and induce neuronal differentiation to promote the recovery of SCI. This information will provide new theoretical support and therapeutic targets for SCI; however, at present, research on treating SCI by targeting HMGB1 is not sufficient, and its specific application scheme still needs to be further explored.

3 Discussion

The HMGB1 protein is a highly conserved nonhistone binding nuclear protein. Structurally, HMGB1 is divided into the following three functional regions: the A-box, the B-box and the acidic C-terminus, with similar amino acid repeat sequences and nonspecific DNA-binding sites; the B-box is the functional structural region that causes inflammation, the A-box has a certain antagonistic effect on the B-box, and the C-terminal is involved mainly in regulating the binding affinity of HMGB1 and DNA, mediating gene transcription and chromosome unwinding. In the resting state, HMGB1 is located primarily in the nucleus and it regulates key nuclear activities, including transcription, replication, DNA repair and nucleosome formation, all of which are important for maintaining steady-state cellular function; however, there are no related studies on the structural and functional changes in HMGB1 after SCI.

After SCI, HMGB1 is expressed and released by neurons, microglia/macrophages and ependymal cells. After injury, the expression of HMGB1 is rapidly upregulated and released into the extracellular matrix and circulating blood, where it remains for a long time. Interestingly, in addition to the increased expression of HMGB1 in the acute and subacute phases after SCI, the level of HMGB1 also increased significantly in the chronic phases. The expression of HMGB1 increases after SCI, and it runs through the acute, subacute and chronic stages of SCI, indicating that HMGB1 may affect the severity and recovery process of SCI. In addition, the expression of HMGB1 is still upregulated in the chronic phase after injury, and its specific mechanism and effect still need to be explored. HMGB1 increased in the nucleus and it was then released from the nucleus to the cytoplasm and extracellular matrix; however, the specific time and node of translocation have not been clarified.

In SCI, the secretion and release mechanism of HMGB1 has not been specifically described, but it is generally thought that most HMGB1 comes from the secretion of inflammatory cells and the release of dead neurons. Inflammation can induce many kinds of cells to secrete HMGB1; however, HMGB1 cannot be actively secreted through the conventional endoplasmic reticulum-Golgi secretion pathway utilized by most soluble secretory proteins. Scholars have proposed two mechanisms for secretion. Among these, one mechanism hypothesizes that HMGB1 is packaged into intracellular vesicles, and then HMGB1 is released out of cells after the fusion of vesicles and

the cytoplasmic membrane, consistent with the cytoplasmic vacuoles of HMGB1 observed in macrophages after SCI.

After SCI, HMGB1 may promote the active release of inflammatory cells through calcium-mediated signal transduction in inflammation, HSPA1A inhibition of the interaction between HMGB1 and XPO1, MAPK family members, inflammatory bodies, activation of STAT1 and STAT3 regulated by JAK, and upregulated expression of TNF and NF-κB. HMGB1 may also be passively released by necrotic neurons, and the intracellular substances released by necrotic cells can also induce further active secretion of HMGB1.

HMGB1 that is secreted and released into the extracellular space can induce the migration of inflammatory cells, aggravate the inflammatory response by regulating the activation of microglia to the M1 phenotype, and regulate the expression of inflammatory factors through RAGE and TLR2/4. However, the studies of Wang et al. show different results, and the specific mechanism needs to be further explored. In addition, the above studies address the role of HMGB1 only in acute and subacute SCI; however, the expression of HMGB1 is still upregulated in the chronic stage of SCI. Its specific role needs to be further explored, and the possibility that HMGB1 promotes the recovery of SCI cannot be ruled out. Moreover, extracellular HMGB1 can aggravate the inflammatory response after SCI, but the specific changes in nuclear HMGB1 after SCI are not clear, and its specific role remains to be understood.

HMGB1 can aggravate neuronal inflammation and lead to neuronal death, and it is also beneficial to neuronal survival and recovery. However, the specific mechanism by which HMGB1 protects injured neurons and promotes injury recovery is not clear, and possibility that HMGB1 injures neurons indirectly by promoting the inflammatory response, while protecting neurons through direct action has not been excluded. In addition, further studies have found that HMGB1 can promote the growth of neuronal axons and induce the migration and differentiation of neural stem cells. The specific mechanism needs to be further explored. In the chronic stage of SCI, the upregulation of HMGB1 may be involved in regulating neuronal regeneration and promoting motor recovery.

HMGB1 plays a multifunctional role in SCI. Inhibiting HMGB1 inhibits nerve inflammation and protects the spinal cord; furthermore, it can be used to protect neurons, promote neuronal regeneration and induce neuronal differentiation to promote the recovery of SCI. These findings provide a new theoretical basis for studying SCI and new therapeutic targets for SCI treatment. However, at present, research into the treatment of SCI based on targeting HMGB1 is not sufficient, and its specific application scheme still needs to be further defined.

For future research, we suggest focusing on the different roles of HMGB1 in the nucleus and in the extracellular space after SCI, clarifying the specific secretion and release mechanism, and determining the spatiotemporal relationship of HMGB1 expression, the protective effect on neurons, and the mechanism of promoting differentiation.

In summary, HMGB1 plays a complex role in SCI, and its mechanism remains to be understood. Additional research will provide a new theoretical basis and therapeutic target for the treatment of SCI.

Author contributions

Conceptualization, data curation, writing-original draft preparation, writing-review and editing: all authors; supervision: KC. Funding acquisition: KC. All authors contributed to the article and approved the submitted version.

Funding

This work was supported by the National Natural Science Foundation of China (82072513 to KC), Science and Technology Programme of Guangzhou (202102080182 to KC).

Acknowledgments

We wish to thank the National Natural Science Foundation of China, the Science and Technology Programme of Guangzhou, for their generous support. We also wish to thank Guojun Qi for his guidance on this article and the relevant authors in the citations.

Conflict of interest

The authors declare that the research was conducted in the absence of any commercial or financial relationships that could be construed as a potential conflict of interest.

Publisher's note

All claims expressed in this article are solely those of the authors and do not necessarily represent those of their affiliated organizations, or those of the publisher, the editors and the reviewers. Any product that may be evaluated in this article, or claim that may be made by its manufacturer, is not guaranteed or endorsed by the publisher.

References

1. Einck L, Bustin M. The intracellular distribution and function of the high mobility group chromosomal proteins. *Exp Cell Res* (1985) 156(2):295–310. doi: 10.1016/0014-4827(85)90539-7

2. Chen L, Fischle W, Verdin E, Greene WC. Duration of nuclear NF-kappaB action regulated by reversible acetylation. *Science* (2001) 293(5535):1653–7. doi: 10.1126/science.1062374

3. Ferrari S, Ronfani L, Calogero S, Bianchi ME. The mouse gene coding for high mobility group 1 protein (HMG1). *J Biol Chem* (1994) 269(46):28803–8. doi: 10.1016/S0021-9258(19)61977-0

4. Gariboldi M, De Gregorio L, Ferrari S, Manenti G, Pierotti MA, Bianchi ME, et al. Mapping of the Hmg1 gene and of seven related sequences in the mouse. *Mamm Genome* (1995) 6(9):581–5. doi: 10.1007/BF00352361

5. Wen L, Huang JK, Johnson BH, Reeck GR. A human placental cDNA clone that encodes nonhistone chromosomal protein HMG-1. *Nucleic Acids Res* (1989) 17(3):1197–214. doi: 10.1093/nar/17.3.1197

6. Kang R, Chen R, Zhang Q, Hou W, Wu S, Cao L, et al. HMGB1 in health and disease. *Mol Aspects Med* (2014) 40:1–116. doi: 10.1016/j.mam.2014.05.001

7. Lotze MT, Tracey KJ. High-mobility group box 1 protein (HMGB1): nuclear weapon in the immune arsenal. *Nat Rev Immunol* (2005) 5(4):331–42. doi: 10.1038/nri1594

8. Andersson U, Yang H, Harris H. High-mobility group box 1 protein (HMGB1) operates as an alarmin outside as well as inside cells. *Semin Immunol* (2018) 38:40–8. doi: 10.1016/j.smim.2018.02.011

9. Sims GP, Rowe DC, Rietdijk ST, Herbst R, Coyle AJ. HMGB1 and RAGE in inflammation and cancer. *Annu Rev Immunol* (2010) 28:367–88. doi: 10.1146/annurev.immunol.021908.132603

10. Aucott H, Lundberg J, Salo H, Klevenvall L, Damberg P, Ottosson L, et al. Neuroinflammation in response to intracerebral injections of different HMGB1 redox isoforms. *J Innate Immun* (2018) 10(3):215–27. doi: 10.1159/000487056

11. Tang D, Kang R, Zeh HJ 3rd, Lotze MT. High-mobility group box 1, oxidative stress, and disease. *Antioxid Redox Signal* (2011) 14(7):1315–35. doi: 10.1089/ars.2010.3356

12. Klune JR, Dhupar R, Cardinal J, Billiar TR, Tsung A. HMGB1: endogenous danger signaling. *Mol Med* (2008) 14(7-8):476–84. doi: 10.2119/2008-00034.Klune

13. Yu Y, Tang D, Kang R. Oxidative stress-mediated HMGB1 biology. *Front Physiol* (2015) 6:93. doi: 10.3389/fphys.2015.00093

14. Okamoto K, Tamura T, Sawatsubashi Y. Sepsis and disseminated intravascular coagulation. *J Intensive Care* (2016) 4:23. doi: 10.1186/s40560-016-0149-0

15. Venereau E, De Leo F, Mezzapelle R, Careccia G, Musco G, Bianchi ME. HMGB1 as biomarker and drug target. *Pharmacol Res* (2016) 111:534–44. doi: 10.1016/j.phrs.2016.06.031

16. Quadri SA, Farooqui M, Ikram A, Zafar A, Khan MA, Suriya SS, et al. Recent update on basic mechanisms of spinal cord injury. *Neurosurgical Rev* (2018) 43(2):425–41. doi: 10.1007/s10143-018-1008-3

17. Ge MH, Tian H, Mao L, Li DY, Lin JQ, Hu HS, et al. Zinc attenuates ferroptosis and promotes functional recovery in contusion spinal cord injury by activating Nrf2/GPX4 defense pathway. *CNS Neurosci Ther* (2021) 27(9):1023–40. doi: 10.1111/cns.13657

18. Han B, Liang W, Hai Y, Liu Y, Chen Y, Ding H, et al. Elucidating the potential mechanisms underlying distraction spinal cord injury-associated neuroinflammation and apoptosis. *Front Cell Dev Biol* (2022) 10:839313. doi: 10.3389/fcell.2022.839313

19. Parker D. The functional properties of synapses made by regenerated axons across spinal cord lesion sites in lamprey. *Neural Regener Res* (2022) 17(10):2272–7. doi: 10.4103/1673-5374.335828

20. Zhou G, Wang Z, Han S, Chen X, Li Z, Hu X, et al. Multifaceted roles of cAMP signaling in the repair process of spinal cord injury and related combination treatments. *Front Mol Neurosci* (2022) 15:808510. doi: 10.3389/fnmol.2022.808510

21. Chen KB, Uchida K, Nakajima H, Yayama T, Hirai T, Rodriguez Guerrero A, et al. High-mobility group box-1 and its receptors contribute to proinflammatory response in the acute phase of spinal cord injury in rats. *Spine (Phila Pa 1976)* (2011) 36(25):2122–9. doi: 10.1097/BRS.0b013e318203941c

22. Fang P, Pan HC, Lin SL, Zhang WQ, Rauvala H, Schachner M, et al. HMGB1 contributes to regeneration after spinal cord injury in adult zebrafish. *Mol Neurobiol* (2014) 49(1):472–83. doi: 10.1007/s12035-013-8533-4

23. Kigerl KA, Kigerl KA, Lai W, Wallace LM, Yang H, Popovich PG.. High mobility group box-1 (HMGB1) is increased in injured mouse spinal cord and can elicit neurotoxic inflammation. *Brain Behav Immun* (2018) 72:22–33. doi: 10.1016/j.bbi.2017.11.018

24. Xia H, Wang D, Guo X, Wu K, Huang F, Feng Y. Catalpol protects against spinal cord injury in mice through regulating MicroRNA-142-Mediated HMGB1/TLR4/NF-kappaB signaling pathway. *Front Pharmacol* (2020) 11:630222. doi: 10.3389/fphar.2020.630222

25. Xue X, Zhang L, Yin X, Chen XX, Chen ZF, Wang CX, et al. Transplantation of neural stem cells preconditioned with highmobility group box 1 facilitates functional recovery after spinal cord injury in rats. *Mol Med Rep* (2020) 22(6):4725–33. doi: 10.3892/mmr.2020.11565

26. Yu L, Qian J. Dihydrotanshinone I alleviates spinal cord injury via suppressing inflammatory response, oxidative stress and apoptosis in rats. *Med Sci Monit* (2020) 26:e920738. doi: 10.12659/MSM.920738

27. Chen KB, Chang MM, Wang SL, Li YX, Wang YX, Xu ZG, et al. High mobility group box-1 serves a pathogenic role in spinal cord injury via the promotion of pro-inflammatory cytokines. *J Leukoc Biol* (2021) 110(6):1131–42. doi: 10.1002/JLB.3MA0721-007R

28. Niu F, Pan S. MicroRNA-488 inhibits neural inflammation and apoptosis in spinal cord injury through restraint on the HMGB1/TLR4/NF-kappaB signaling pathway. *Neuroreport* (2021) 32(12):1017–26. doi: 10.1097/WNR.0000000000001680

29. Song HH, Song TC, Yang T, Sun CS, He BQ, Li H, et al. High mobility group box 1 mediates inflammatory response of astrocytes via cyclooxygenase 2/prostaglandin E2 signaling following spinal cord injury. *Neural Regener Res* (2021) 16(9):1848–55. doi: 10.4103/1673-5374.303039

30. Zhu Y, Uezono N, Yasui T, Nakajo M, Nagai T, Wang D, et al. Combinatrial treatment of anti-high mobility group box-1 monoclonal antibody and epothilone b improves functional recovery after spinal cord contusion injury. *Neurosci Res* (2021) 172:13–25. doi: 10.1016/j.neures.2021.04.002

31. Gholaminejhad M, Jameie SB, Abdi M, Abolhassani F, Mohammed I, Hassanzadeh G. All-trans retinoic acid-preconditioned mesenchymal stem cells improve motor function and alleviate tissue damage after spinal cord injury by inhibition of HMGB1/NF-kappaB/NLRP3 pathway through autophagy activation. *J Mol Neurosci* (2022) 72(5):947–62. doi: 10.1007/s12031-022-01977-0

32. Stros M. HMGB proteins: interactions with DNA and chromatin. *Biochim Biophys Acta* (2010) 1799(1-2):101–13. doi: 10.1016/j.bbagrm.2009.09.008

33. Li J, Kokkola R, Tabibzadeh S, Yang R, Ochani M, Qiang X, et al. Structural basis for the proinflammatory cytokine activity of high mobility group box 1. *Mol Med* (2003) 9(1-2):37–45. doi: 10.1007/BF03402105

34. Ellerman JE, Brown CK, de Vera M, Zeh HJ, Billiar T, Rubartelli A, et al. Masquerader: high mobility group box-1 and cancer. *Clin Cancer Res* (2007) 13(10):2836–48. doi: 10.1158/1078-0432.CCR-06-1953

35. Ueda T, Chou H, Kawase T, Shirakawa H, Yoshida M. Acidic c-tail of HMGB1 is required for its target binding to nucleosome linker DNA and transcription stimulation. *Biochemistry* (2004) 43(30):9901–8. doi: 10.1021/bi035975l

36. Huttunen HJ, Fages C, Kuja-Panula J, Ridley AJ, Rauvala H. Receptor for advanced glycation end products-binding COOH-terminal motif of amphoterin inhibits invasive migration and metastasis. *Cancer Res* (2002) 62(16):4805–11.

37. Diener KR, Al-Dasooqi N, Lousberg EL, Hayball JD. The multifunctional alarmin HMGB1 with roles in the pathophysiology of sepsis and cancer. *Immunol Cell Biol* (2013) 91(7):443–50. doi: 10.1038/icb.2013.25

38. Xue J, Suarez JS, Minaai M, Li S, Gaudino G, Pass HI, et al. HMGB1 as a therapeutic target in disease. *J Cell Physiol* (2021) 236(5):3406–19. doi: 10.1002/jcp.30125

39. Didangelos A, Puglia M, Iberl M, Sanchez-Bellot C, Roschitzki B, Bradbury EJ. High-throughput proteomics reveal alarmins as amplifiers of tissue pathology and inflammation after spinal cord injury. *Sci Rep* (2016) 6:21607. doi: 10.1038/srep21607

40. Rong H, Zhao Z, Feng J, Lei Y, Wu H, Sun R, et al. The effects of dexmedetomidine pretreatment on the pro- and anti-inflammation systems after spinal cord injury in rats. *Brain Behav Immun* (2017) 64:195–207. doi: 10.1016/j.bbi.2017.03.006

41. Kawabata H, Setoguchi T, Yone K, Souda M, Yoshida H, et al. High mobility group box 1 is upregulated after spinal cord injury and is associated with neuronal cell apoptosis. *Spine (Phila Pa 1976)* (2010) 35(11):1109–15. doi: 10.1097/BRS.0b013e3181bd14b6

42. Fan H, Tang HB, Chen Z, Wang HQ, Zhang L, Jiang Y, et al. Inhibiting HMGB1-RAGE axis prevents pro-inflammatory macrophages/microglia polarization and affords neuroprotection after spinal cord injury. *J Neuroinflamm* (2020) 17(1):295. doi: 10.1186/s12974-020-01973-4

43. Papatheodorou A, Stein A, Bank M, Sison CP, Gibbs K, Davies P, et al. High-mobility group box 1 (HMGB1) is elevated systemically in persons with acute or chronic traumatic spinal cord injury. *J Neurotrauma* (2017) 34(3):746–54. doi: 10.1089/neu.2016.4596

44. Wu Z, Zhang Z, Wang Z, Zhu H, Li M. MiR-181a-5p alleviates the inflammatory response of PC12 cells by inhibiting high-mobility group box-1 protein expression. *World Neurosurg* (2022) 162:e427–35. doi: 10.1016/j.wneu.2022.03.025

45. Scaffidi P, Misteli T, Bianchi ME. Release of chromatin protein HMGB1 by necrotic cells triggers inflammation. *Nature* (2002) 418(6894):191–5. doi: 10.1038/nature00858

46. Rovere-Querini P, Capobianco A, Scaffidi P, Valentinis B, Catalanotti F, Giazzon M, et al. HMGB1 is an endogenous immune adjuvant released by necrotic cells. *EMBO Rep* (2004) 5(8):825–30. doi: 10.1038/sj.embor.7400205

47. Schulman IG, et al. Macronuclei and micronuclei in tetrahymena thermophila contain high-mobility-group-like chromosomal proteins containing a highly conserved eleven-amino-acid putative DNA-binding sequence. *Mol Cell Biol* (1991) 11(1):166–74. doi: 10.1128/mcb.11.1.166-174.1991

48. Bonaldi T, Talamo F, Scaffidi P, Ferrera D, Porto A, Bachi A, et al. Monocytic cells hyperacetylate chromatin protein HMGB1 to redirect it towards secretion. *EMBO J* (2003) 22(20):5551–60. doi: 10.1093/emboj/cdg516

49. Ito I, Fukazawa J, Yoshida M. Post-translational methylation of high mobility group box 1 (HMGB1) causes its cytoplasmic localization in neutrophils. *J Biol Chem* (2007) 282(22):16336–44. doi: 10.1074/jbc.M608467200

50. Zhang X, Wheeler D, Tang Y, Guo L, Shapiro RA, Ribar TJ, et al. Calcium/calmodulin-dependent protein kinase (CaMK) IV mediates nucleocytoplasmic shuttling and release of HMGB1 during lipopolysaccharide stimulation of macrophages. *J Immunol* (2008) 181(7):5015–23. doi: 10.4049/jimmunol.181.7.5015

51. Tang Y, Zhao X, Antoine D, Xiao X, Wang H, Andersson U, et al. Regulation of posttranslational modifications of HMGB1 during immune responses. *Antioxid Redox Signal* (2016) 24(12):620–34. doi: 10.1089/ars.2015.6409

52. Gu W, Roeder RG. Activation of p53 sequence-specific DNA binding by acetylation of the p53 c-terminal domain. *Cell* (1997) 90(4):595–606. doi: 10.1016/S0092-8674(00)80521-8

53. Youn JH, Shin JS. Nucleocytoplasmic shuttling of HMGB1 is regulated by phosphorylation that redirects it toward secretion. *J Immunol* (2006) 177 (11):7889–97. doi: 10.4049/jimmunol.177.11.7889

54. Wang H, Bloom O, Zhang M, Vishnubhakat JM, Ombrellino M, Che J, et al. HMG-1 as a late mediator of endotoxin lethality in mice. *Science* (1999) 285 (5425):248–51. doi: 10.1126/science.285.5425.248

55. Cai X, Biswas I, Panicker SR, Giri H, Rezaie AR. Activated protein c inhibits lipopolysaccharide-mediated acetylation and secretion of high-mobility group box 1 in endothelial cells. *J Thromb Haemost* (2019) 17(5):803–17. doi: 10.1111/jth.14425

56. Kwak MS, Kim HS, Lee B, Kim YH, Son M, Shin JS. Immunological significance of HMGB1 post-translational modification and redox biology. *Front Immunol* (2020) 11:1189. doi: 10.3389/fimmu.2020.01189

57. Palade G. Intracellular aspects of the process of protein synthesis. *Science* (1975) 189(4200):347–58. doi: 10.1126/science.1096303

58. Volchuk A, Ye A, Chi L, Steinberg BE, Goldenberg NM. Indirect regulation of HMGB1 release by gasdermin d. *Nat Commun* (2020) 11(1):4561. doi: 10.1038/s41467-020-18443-3

59. Lee WJ, Song SY, Roh H, Ahn HM, Na Y, Kim J, et al. Profibrogenic effect of high-mobility group box protein-1 in human dermal fibroblasts and its excess in keloid tissues. *Sci Rep* (2018) 8(1):8434. doi: 10.1038/s41598-018-26501-6

60. Lu B, Wang C, Wang M, Li W, Chen F, Tracey KJ, et al. Molecular mechanism and therapeutic modulation of high mobility group box 1 release and action: an updated review. *Expert Rev Clin Immunol* (2014) 10(6):713–27. doi: 10.1586/1744666X.2014.909730

61. Pisetsky DS. The expression of HMGB1 on microparticles released during cell activation and cell death in vitro and in vivo. *Mol Med* (2014) 20:158–63. doi: 10.2119/molmed.2014.00014

62. Peng HH, Liu YJ, Ojcius DM, Lee CM, Chen RH, Huang PR, et al. Mineral particles stimulate innate immunity through neutrophil extracellular traps containing HMGB1. *Sci Rep* (2017) 7(1):16628. doi: 10.1038/s41598-017-16778-4

63. Tian T, Yao D, Zheng L, Zhou Z, Duan Y, Liu B, et al. Sphingosine kinase 1 regulates HMGB1 translocation by directly interacting with calcium/calmodulin protein kinase II-delta in sepsis-associated liver injury. *Cell Death Dis* (2020) 11(12):1037. doi: 10.1038/s41419-020-03255-6

64. Zhao P, Ye T, Yan X, Hu X, Liu P, Wang X. HMGB1 release by H2O2-induced hepatocytes is regulated through calcium overload and 58-f interference. *Cell Death Discovery* (2017) 3:17008. doi: 10.1038/cddiscovery.2017.8

65. Chen S, Dong Z, Yang P, Wang X, Jin G, Yu H, et al. Hepatitis b virus X protein stimulates high mobility group box 1 secretion and enhances hepatocellular carcinoma metastasis. *Cancer Lett* (2017) 394:22–32. doi: 10.1016/j.canlet.2017.02.011

66. Quan H, Bae HB, Hur YH, Lee KH, Lee CH, Jang EA, et al. Stearoyl lysophosphatidylcholine inhibits LPS-induced extracellular release of HMGB1 through the G2A/calcium/CaMKKbeta/AMPK pathway. *Eur J Pharmacol* (2019) 852:125–33. doi: 10.1016/j.ejphar.2019.02.038

67. Li W, Deng M, Loughran PA, Yang M, Lin M, Yang C, et al. LPS induces active HMGB1 release from hepatocytes into exosomes through the coordinated activities of TLR4 and caspase-11/GSDMD signaling. *Front Immunol* (2020) 11:229. doi: 10.3389/fimmu.2020.00229

68. Shin JH, Kim ID, Kim SW, Lee HK, Jin Y, Park JH, et al. Ethyl pyruvate inhibits HMGB1 phosphorylation and release by chelating calcium. *Mol Med* (2015) 20:649–57. doi: 10.2119/molmed.2014.00039

69. Tang D, Kang R, Xiao W, Wang H, Calderwood SK, Xiao X.. The anti-inflammatory effects of heat shock protein 72 involve inhibition of high-mobility-group box 1 release and proinflammatory function in macrophages. *J Immunol* (2007) 179(2):1236–44. doi: 10.4049/jimmunol.179.2.1236

70. Hernandez-Quiles M, Broekema MF, Kalkhoven E. PPARgamma in metabolism, immunity, and cancer: Unified and diverse mechanisms of action. *Front Endocrinol (Lausanne)* (2021) 12:624112. doi: 10.3389/fendo.2021.624112

71. Zhou S, Lu H, Chen R, Tian Y, Jiang Y, Zhang S, et al. Angiotensin II enhances the acetylation and release of HMGB1 in RAW264.7 macrophage. *Cell Biol Int* (2018) 42(9):1160–9. doi: 10.1002/cbin.10984

72. Hao J, Zhang YJ, Lv X, Xu N, Liu QJ, Zhao S, et al. IFN-gamma induces lipogenesis in mouse mesangial cells via the JAK2/STAT1 pathway. *Am J Physiol Cell Physiol* (2013) 304(8):C760–7. doi: 10.1152/ajpcell.00352.2012

73. Park EJ, Kim YM, Kim HJ, Chang KC. Degradation of histone deacetylase 4 via the TLR4/JAK/STAT1 signaling pathway promotes the acetylation of high mobility group box 1 (HMGB1) in lipopolysaccharide-activated macrophages. *FEBS Open Bio* (2018) 8(7):1119–26. doi: 10.1002/2211-5463.12456

74. Imbaby S, Matsuda N, Tomita K, Hattori K, Palikhe S, Yokoo H, et al. Beneficial effect of STAT3 decoy oligodeoxynucleotide transfection on organ injury and mortality in mice with cecal ligation and puncture-induced sepsis. *Sci Rep* (2020) 10(1):15316. doi: 10.1038/s41598-020-72136-x

75. Wu Y, Xu J, Xu J, Zheng W, Chen Q, Jiao D. Study on the mechanism of JAK2/STAT3 signaling pathway-mediated inflammatory reaction after cerebral ischemia. *Mol Med Rep* (2018) 17(4):5007–12. doi: 10.3892/mmr.2018.8477

76. Wang G, Zhang J, Dui D, Ren H, Liu J. High mobility group box 1 induces the activation of the janus kinase 2 and signal transducer and activator of transcription 3 (JAK2/STAT3) signaling pathway in pancreatic acinar cells in rats, while AG490 and rapamycin inhibit their activation. *Bosn J Basic Med Sci* (2016) 16(4):307–12. doi: 10.17305/bjbms.2016.1442

77. Guo HF, Liu SX, Zhang YJ, Liu QJ, Hao J, Gao LX. High mobility group box 1 induces synoviocyte proliferation in rheumatoid arthritis by activating the signal transducer and activator transcription signal pathway. *Clin Exp Med* (2011) 11 (2):65–74. doi: 10.1007/s10238-010-0116-3

78. Conti L, Lanzardo S, Arigoni M, Antonazzo R, Radaelli E, Cantarella D. The noninflammatory role of high mobility group box 1/Toll-like receptor 2 axis in the self-renewal of mammary cancer stem cells. *FASEB J* (2013) 27(12):4731–44. doi: 10.1096/fj.13-230201

79. Ma Y, Zhang Z, Chen R, Shi R, Zeng P, Chen R. NRP1 regulates HMGB1 in vascular endothelial cells under high homocysteine condition. *Am J Physiol Heart Circ Physiol* (2019) 316(5):H1039–h1046. doi: 10.1152/ajpheart.00746.2018

80. Craven RR, Gao X, Allen IC, Gris D, Bubeck Wardenburg J, McElvania-Tekippe E. Staphylococcus aureus alpha-hemolysin activates the NLRP3-inflammasome in human and mouse monocytic cells. *PloS One* (2009) 4(10): e7446. doi: 10.1371/journal.pone.0007446

81. Lamkanfi M, Sarkar A, Vande Walle L, Vitari AC, Amer AO, Wewers MD, et al. Inflammasome-dependent release of the alarmin HMGB1 in endotoxemia. *J Immunol* (2010) 185(7):4385–92. doi: 10.4049/jimmunol.1000803

82. Barlan AU, Griffin TM, McGuire KA, Wiethoff CM. Adenovirus membrane penetration activates the NLRP3 inflammasome. *J Virol* (2011) 85(1):146–55. doi: 10.1128/JVI.01265-10

83. Yu S, Wang D, Huang L, Zhang Y, Luo R, Adah D, et al. The complement receptor C5aR2 promotes protein kinase r expression and contributes to NLRP3 inflammasome activation and HMGB1 release from macrophages. *J Biol Chem* (2019) 294(21):8384–94. doi: 10.1074/jbc.RA118.006508

84. Chen G, Li J, Ochani M, Rendon-Mitchell B, Qiang X, Susarla S, et al. Bacterial endotoxin stimulates macrophages to release HMGB1 partly through CD14- and TNF-dependent mechanisms. *J Leukoc Biol* (2004) 76(5):994–1001. doi: 10.1189/jlb.0404242

85. Lin F, Pei L, Zhang Q, Han W, Jiang S, Lin Y, et al. Ox-LDL induces endothelial cell apoptosis and macrophage migration by regulating caveolin-1 phosphorylation. *J Cell Physiol* (2018) 233(10):6683–92. doi: 10.1002/jcp.26468

86. Hiramoto S, Tsubota M, Yamaguchi K, Okazaki K, Sakaegi A, Toriyama Y, et al. Cystitis-related bladder pain involves ATP-dependent HMGB1 release from macrophages and its downstream H2S/Cav3.2 signaling in mice. *Cells* (2020) 9 (8):1748. doi: 10.3390/cells9081748

87. Wang CM, Jiang M, Wang HJ. Effect of NFkappaB inhibitor on highmobility group protein B1 expression in a COPD rat model. *Mol Med Rep* (2013) 7(2):499–502. doi: 10.3892/mmr.2012.1181

88. Castro RC, Gonçales RA, Zambuzi FA, Frantz FG. Notch signaling pathway in infectious diseases: role in the regulation of immune response. *Inflammation Res* (2021) 70(3):261–74. doi: 10.1007/s00011-021-01442-5

89. Khambu B, Huda N, Chen X, Antoine DJ, Li Y, et al. HMGB1 promotes ductular reaction and tumorigenesis in autophagy-deficient livers. *J Clin Invest* (2018) 128(6):2419–35. doi: 10.1172/JCI91814

90. Qin S, Wang H, Yuan R, Li H, Ochani M, Ochani K, et al. Role of HMGB1 in apoptosis-mediated sepsis lethality. *J Exp Med* (2006) 203(7):1637–42. doi: 10.1084/jem.20052203

91. Morinaga Y, Yanagihara K, Nakamura S, Hasegawa H, Seki M, Izumikawa K, et al. Legionella pneumophila induces cathepsin b-dependent necrotic cell death with releasing high mobility group box1 in macrophages. *Respir Res* (2010) 11:158. doi: 10.1186/1465-9921-11-158

92. Chen L, Zhao Y, Lai D, Zhang P, Yang Y, Li Y, et al. Neutrophil extracellular traps promote macrophage pyroptosis in sepsis. *Cell Death Dis* (2018) 9(6):597. doi: 10.1038/s41419-017-0090-8

93. Brambilla L, Martorana F, Guidotti G, Rossi D. Dysregulation of astrocytic HMGB1 signaling in amyotrophic lateral sclerosis. *Front Neurosci* (2018) 12:622. doi: 10.3389/fnins.2018.00622

94. Yon JM, Kim YB, Park D. The ethanol fraction of white rose petal extract abrogates excitotoxicity-induced neuronal damage in vivo and in vitro through inhibition of oxidative stress and proinflammation. *Nutrients* (2018) 10(10):1375. doi: 10.3390/nu10101375

95. Lo Coco D, Veglianese P, Allievi E, Bendotti C. Distribution and cellular localization of high mobility group box protein 1 (HMGB1) in the spinal cord of a transgenic mouse model of ALS. *Neurosci Lett* (2007) 412(1):73–7. doi: 10.1016/j.neulet.2006.10.063

96. Kang R, Livesey KM, Zeh HJ 3rd, Lotze MT, Tang D. HMGB1 as an autophagy sensor in oxidative stress. *Autophagy* (2011) 7(8):904–6. doi: 10.4161/auto.7.8.15704

97. Tang D, Kang R, Livesey KM, Zeh HJ 3rd, Lotze MT. High mobility group box 1 (HMGB1) activates an autophagic response to oxidative stress. *Antioxid Redox Signal* (2011) 15(8):2185–95. doi: 10.1089/ars.2010.3666

98. Shichita T, Hasegawa E, Kimura A, Morita R, Sakaguchi R, Takada I, et al. Peroxiredoxin family proteins are key initiators of post-ischemic inflammation in the brain. *Nat Med* (2012) 18(6):911–7. doi: 10.1038/nm.2749

99. Yamada Y, Fujii T, Ishijima R, Tachibana H, Yokoue N, Takasawa R, et al. The release of high mobility group box 1 in apoptosis is triggered by nucleosomal DNA fragmentation. *Arch Biochem Biophys* (2011) 506(2):188–93. doi: 10.1016/j.abb.2010.11.011

100. Yamada Y, Fujii T, Ishijima R, Tachibana H, Yokoue N, Takasawa R, et al. DR396, an apoptotic DNase gamma inhibitor, attenuates high mobility group box 1 release from apoptotic cells. *Bioorg Med Chem* (2011) 19(1):168–71. doi: 10.1016/j.bmc.2010.11.037

101. Fages C, Nolo R, Huttunen HJ, Eskelinen E, Rauvala H. Regulation of cell migration by amphoterin. *J Cell Sci* (2000) 113(Pt 4):611–20. doi: 10.1242/jcs.113.4.611

102. Degryse B, Bonaldi T, Scaffidi P, Müller S, Resnati M, Sanvito F, et al. The high mobility group (HMG) boxes of the nuclear protein HMG1 induce chemotaxis and cytoskeleton reorganization in rat smooth muscle cells. *J Cell Biol* (2001) 152(6):1197–206. doi: 10.1083/jcb.152.6.1197

103. Degryse B, de Virgilio M. The nuclear protein HMGB1, a new kind of chemokine? *FEBS Lett* (2003) 553(1-2):11–7. doi: 10.1016/S0014-5793(03)01027-5

104. Palumbo R, Bianchi ME. High mobility group box 1 protein, a cue for stem cell recruitment. *Biochem Pharmacol* (2004) 68(6):1165–70. doi: 10.1016/j.bcp.2004.03.048

105. Palumbo R, Sampaolesi M, De Marchis F, Tonlorenzi R, Colombetti S, Mondino A, et al. Extracellular HMGB1, a signal of tissue damage, induces mesoangioblast migration and proliferation. *J Cell Biol* (2004) 164(3):441–9. doi: 10.1083/jcb.200304135

106. Rouhiainen A, Kuja-Panula J, Wilkman E, Pakkanen J, Stenfors J, Tuominen RK, et al. Regulation of monocyte migration by amphoterin (HMGB1). *Blood* (2004) 104(4):1174–82. doi: 10.1182/blood-2003-10-3536

107. Dumitriu IE, Bianchi ME, Bacci M, Manfredi AA, Rovere-Querini P. The secretion of HMGB1 is required for the migration of maturing dendritic cells. *J Leukoc Biol* (2007) 81(1):84–91. doi: 10.1189/jlb.0306171

108. Orlova VV, Choi EY, Xie C, Chavakis E, Bierhaus A, Ihanus E, et al. A novel pathway of HMGB1-mediated inflammatory cell recruitment that requires mac-1-integrin. *EMBO J* (2007) 26(4):1129–39. doi: 10.1038/sj.emboj.7601552

109. Palumbo R, Galvez BG, Pusterla T, De Marchis F, Cossu G, Marcu KB, et al. Cells migrating to sites of tissue damage in response to the danger signal HMGB1 require NF-kappaB activation. *J Cell Biol* (2007) 179(1):33–40. doi: 10.1083/jcb.200704015

110. Pedrazzi M, Patrone M, Passalacqua M, Ranzato E, Colamassaro D, Sparatore B, et al. Selective proinflammatory activation of astrocytes by high-mobility group box 1 protein signaling. *J Immunol* (2007) 179(12):8525–32. doi: 10.4049/jimmunol.179.12.8525

111. Yang D, Chen Q, Yang H, Tracey KJ, Bustin M, Oppenheim JJ. High mobility group box-1 protein induces the migration and activation of human dendritic cells and acts as an alarmin. *J Leukoc Biol* (2007) 81(1):59–66. doi: 10.1189/jlb.0306180

112. Palumbo R, De Marchis F, Pusterla T, Conti A, Alessio M, Bianchi ME. Src family kinases are necessary for cell migration induced by extracellular HMGB1. *J Leukoc Biol* (2009) 86(3):617–23. doi: 10.1189/jlb.0908581

113. Ranzato E, Patrone M, Pedrazzi M, Burlando B. HMGb1 promotes scratch wound closure of HaCaT keratinocytes via ERK1/2 activation. *Mol Cell Biochem* (2009) 332(1-2):199–205. doi: 10.1007/s11010-009-0192-4

114. van Zoelen MA, Yang H, Florquin S, Meijers JC, Akira S, Arnold B, et al. Role of toll-like receptors 2 and 4, and the receptor for advanced glycation end products in high-mobility group box 1-induced inflammation in vivo. *Shock* (2009) 31(3):280–4. doi: 10.1097/SHK.0b013e318186262d

115. Bauer EM, Shapiro R, Billiar TR, Bauer PM. High mobility group box 1 inhibits human pulmonary artery endothelial cell migration via a toll-like receptor 4- and interferon response factor 3-dependent mechanism(s). *J Biol Chem* (2013) 288(2):1365–73. doi: 10.1074/jbc.M112.434142

116. Chen HG, Xie KL, Han HZ, Wang WN, Liu DQ, Wang GL, et al. Heme oxygenase-1 mediates the anti-inflammatory effect of molecular hydrogen in LPS-stimulated RAW 264.7 macrophages. *Int J Surg* (2013) 11(10):1060–6. doi: 10.1016/j.ijsu.2013.10.007

117. Rauvala H, Rouhiainen A. Physiological and pathophysiological outcomes of the interactions of HMGB1 with cell surface receptors. *Biochim Biophys Acta* (2010) 1799(1-2):164–70. doi: 10.1016/j.bbagrm.2009.11.012

118. Andersson U, Wang H, Palmblad K, Aveberger AC, Bloom O, Erlandsson-Harris H, et al. High mobility group 1 protein (HMG-1) stimulates proinflammatory cytokine synthesis in human monocytes. *J Exp Med* (2000) 192 (4):565–70. doi: 10.1084/jem.192.4.565

119. Taguchi A, Blood DC, del Toro G, Canet A, Lee DC, Qu W, et al. Blockade of RAGE-amphoterin signalling suppresses tumour growth and metastases. *Nature* (2000) 405(6784):354–60. doi: 10.1038/35012626

120. Andersson U, Harris HE. The role of HMGB1 in the pathogenesis of rheumatic disease. *Biochim Biophys Acta* (2010) 1799(1-2):141–8. doi: 10.1016/j.bbagrm.2009.11.003

121. Penzo M, Molteni R, Suda T, Samaniego S, Raucci A, Habiel DM, et al. Inhibitor of NF-kappa b kinases alpha and beta are both essential for high mobility group box 1-mediated chemotaxis [corrected]. *J Immunol* (2010) 184(8):4497–509. doi: 10.4049/jimmunol.0903131

122. Kew RR, Penzo M, Habiel DM, Marcu KB. The IKKalpha-dependent NF-kappaB p52/RelB noncanonical pathway is essential to sustain a CXCL12 autocrine loop in cells migrating in response to HMGB1. *J Immunol* (2012) 188(5):2380–6. doi: 10.4049/jimmunol.1102454

123. Schiraldi M, Raucci A, Muñoz LM, Livoti E, Celona B, Venereau E, et al. HMGB1 promotes recruitment of inflammatory cells to damaged tissues by forming a complex with CXCL12 and signaling via CXCR4. *J Exp Med* (2012) 209(3):551–63. doi: 10.1084/jem.20111739

124. Salanga CL, Handel TM. Chemokine oligomerization and interactions with receptors and glycosaminoglycans: the role of structural dynamics in function. *Exp Cell Res* (2011) 317(5):590–601. doi: 10.1016/j.yexcr.2011.01.004

125. Shakir M, Tang D, Zeh HJ, Tang SW, Anderson CJ, Bahary N, et al. The chemokine receptors CXCR4/CXCR7 and their primary heterodimeric ligands CXCL12 and CXCL12/high mobility group box 1 in pancreatic cancer growth and development: finding flow. *Pancreas* (2015) 44(4):528–34. doi: 10.1097/MPA.0000000000000298

126. Fiuza C, Bustin M, Talwar S, Tropea M, Gerstenberger E, Shelhamer JH, et al. Inflammation-promoting activity of HMGB1 on human microvascular endothelial cells. *Blood* (2003) 101(7):2652–60. doi: 10.1182/blood-2002-05-1300

127. Uezono N, Zhu Y, Fujimoto Y, Yasui T, Matsuda T, Nakajo M, et al. Prior treatment with anti-high mobility group box-1 antibody boosts human neural stem cell transplantation-mediated functional recovery after spinal cord injury. *Stem Cells* (2018) 36(5):737–50. doi: 10.1002/stem.2802

128. Nakajo M, Uezono N, Nakashima H, Wake H, Komiya S, Nishibori M, et al. Therapeutic time window of anti-high mobility group box-1 antibody

administration in mouse model of spinal cord injury. *Neurosci Res* (2019) 141:63–70. doi: 10.1016/j.neures.2018.03.004

129. Sun L, Li M, Ma X, Zhang L, Song J, Lv C, et al. Inhibiting high mobility group box-1 reduces early spinal cord edema and attenuates astrocyte activation and aquaporin-4 expression after spinal cord injury in rats. *J Neurotrauma* (2019) 36(3):421–35. doi: 10.1089/neu.2018.5642

130. Wu Z, Wang Z, Xie Z, Zhu H, Li C, Xie S, et al. Glycyrrhizic acid attenuates the inflammatory response after spinal cord injury by inhibiting high mobility group box-1 protein through the p38/Jun n-terminal kinase signaling pathway. *World Neurosurg* (2022) 158:e856–64. doi: 10.1016/j.wneu.2021.11.085

131. Kang N, Hai Y, Yang J, Liang F, Gao CJ. Hyperbaric oxygen intervention reduces secondary spinal cord injury in rats via regulation of HMGB1/TLR4/NF-κB signaling pathway. *Int J Clin Exp Pathol* (2015) 8(2):1141–53.

132. Park JS, Svetkauskaite D, He Q, Kim JY, Strassheim D, Ishizaka A, et al. Involvement of toll-like receptors 2 and 4 in cellular activation by high mobility group box 1 protein. *J Biol Chem* (2004) 279(9):7370–7. doi: 10.1074/jbc.M306793200

133. Paudel YN, Angelopoulou E, Piperi C, Balasubramaniam VRMT, Othman I, Shaikh MF. Enlightening the role of high mobility group box 1 (HMGB1) in inflammation: Updates on receptor signalling. *Eur J Pharmacol* (2019) 858:172487. doi: 10.1016/j.ejphar.2019.172487

134. van Beijnum JR, Buurman WA, Griffioen AW. Convergence and amplification of toll-like receptor (TLR) and receptor for advanced glycation end products (RAGE) signaling pathways via high mobility group B1 (HMGB1). *Angiogenesis* (2008) 11(1):91–9. doi: 10.1007/s10456-008-9093-5

135. Andersson U, Tracey KJ. HMGB1 is a therapeutic target for sterile inflammation and infection. *Annu Rev Immunol* (2011) 29:139–62. doi: 10.1146/annurev-immunol-030409-101323

136. Harris HE, Andersson U, Pisetsky DS. HMGB1: a multifunctional alarmin driving autoimmune and inflammatory disease. *Nat Rev Rheumatol* (2012) 8 (4):195–202. doi: 10.1038/nrrheum.2011.222

137. Wang H, Mei X, Cao Y, Liu C, Zhao Z, Guo Z, et al. HMGB1/Advanced glycation end products (RAGE) does not aggravate inflammation but promote endogenous neural stem cells differentiation in spinal cord injury. *Sci Rep* (2017) 7 (1):10332. doi: 10.1038/s41598-017-10611-8

138. Kim D, Murray M, Simansky KJ. The serotonergic 5-HT(2C) agonist m-chlorophenylpiperazine increases weight-supported locomotion without development of tolerance in rats with spinal transections. *Exp Neurol* (2001) 169 (2):496–500. doi: 10.1006/exnr.2001.7660

139. Nothias JM, Mitsui T, Shumsky JS, Fischer I, Antonacci MD, Murray M. Combined effects of neurotrophin secreting transplants, exercise, and serotonergic drug challenge improve function in spinal rats. *Neurorehabil Neural Repair* (2005) 19(4):296–312. doi: 10.1177/1545968305281209

140. Ghosh M, Pearse DD. The role of the serotonergic system in locomotor recovery after spinal cord injury. *Front Neural Circuits* (2014) 8:151. doi: 10.3389/fncir.2014.00151

141. Wang C, Liu XX, Huang KB, Yin SB, Wei JJ, Hu YF, et al. Preconditioning with recombinant high-mobility group box 1 induces ischemic tolerance in a rat model of focal cerebral ischemia-reperfusion. *J Neurochem* (2016) 137(4):576–88. doi: 10.1111/jnc.13611

142. Passalacqua M, Patrone M, Picotti GB, Del Rio M, Sparatore B, Melloni E, et al. Stimulated astrocytes release high-mobility group 1 protein, an inducer of LAN-5 neuroblastoma cell differentiation. *Neuroscience* (1998) 82(4):1021–8. doi: 10.1016/s0306-4522(97)00352-7

143. Huttunen HJ, Kuja-Panula J, Rauvala H. Receptor for advanced glycation end products (RAGE) signaling induces CREB-dependent chromogranin expression during neuronal differentiation. *J Biol Chem* (2002) 277(41):38635–46. doi: 10.1074/jbc.M202515200

144. Huttunen HJ, Kuja-Panula J, Sorci G, Agneletti AL, Donato R, Rauvala H. Coregulation of neurite outgrowth and cell survival by amphoterin and S100 proteins through receptor for advanced glycation end products (RAGE) activation. *J Biol Chem* (2000) 275(51):40096–105. doi: 10.1074/jbc.M006993200

145. Hayakawa K, Qiu J, Lo EH. Biphasic actions of HMGB1 signaling in inflammation and recovery after stroke. *Ann N Y Acad Sci* (2010) 1207:50–7. doi: 10.1111/j.1749-6632.2010.05728.x

146. Yang J, Liu X, Zhou Y, Wang G, Gao C, Su Q. Hyperbaric oxygen alleviates experimental (spinal cord) injury by downregulating HMGB1/NF-kappaB expression. *Spine (Phila Pa 1976)* (2013) 38(26):E1641–8. doi: 10.1097/BRS.0000000000000005

147. Zhang Z, Li M, Wang Y, Wu J, Li J. Higenamine promotes M2 macrophage activation and reduces Hmgb1 production through HO-1 induction in a murine model of spinal cord injury. *Int Immunopharmacol* (2014) 23(2):681–7. doi: 10.1016/j.intimp.2014.10.022

148. Bi Y, Zhu Y, Zhang M, Zhang K, Hua X, Fang Z, et al. Effect of shikonin on spinal cord injury in rats via regulation of HMGB1/TLR4/NF-kB signaling pathway. *Cell Physiol Biochem* (2017) 43(2):481–91. doi: 10.1159/000480474

149. Yang Y, Wang J, Yang Q, Wu S, Yang Z, Zhu H, et al. Shikonin inhibits the lipopolysaccharide-induced release of HMGB1 in RAW264.7 cells via IFN and NF-kappaB signaling pathways. *Int Immunopharmacol* (2014) 19(1):81–7. doi: 10.1016/j.intimp.2014.01.003

150. Zhou J, Shuang O, Li J, Cai Z, Wu C, Wang W. miR-34a alleviates spinal cord injury via TLR4 signaling by inhibiting HMGB-1. *Exp Ther Med* (2019) 17 (3):1912–8. doi: 10.3892/etm.2018.7102

151. Wan G, An Y, Tao J, Wang Y, Zhou Q, Yang R, et al. MicroRNA-129-5p alleviates spinal cord injury in mice via suppressing the apoptosis and inflammatory response through HMGB1/TLR4/NF-kappaB pathway. *Biosci Rep* (2020) 40(3):BSR20193315. doi: 10.1042/BSR20193315

152. Zhao HD, Huang SQ, Tang CL, Dai N, Dai P, Tan YL. [Influence of electroacupuncture on locomotor function and expression of spinal HMGB1 and TLR4 in mice with spinal cord injury]. *Zhen Ci Yan Jiu* (2021) 46(4):259–65. doi: 10.13702/j.1000-0607.200490

153. He Y, Sun L, Feng H, Li J, Zhang N, Wang Z. [Effect and mechanism of glycyrrhizin on glial scar formation after spinal cord injury in rats]. *Zhongguo Xiu Fu Chong Jian Wai Ke Za Zhi* (2020) 34(10):1298–304. doi: 10.7507/1002-1892.202002116

frontiers | Frontiers in Immunology

TYPE Original Research
PUBLISHED 19 January 2023
DOI 10.3389/fimmu.2023.1068359

Check for updates

OPEN ACCESS

EDITED BY
Guangzhi Ning,
Tianjin Medical University General Hospital, China

REVIEWED BY
Niels Hellings,
University of Hasselt, Belgium
Ruiqing Zheng,
Central South University, China

*CORRESPONDENCE
Yongfeng Chen
xjchenyongfeng@163.com
Haining Wu
hnwu@fmmu.edu.cn

†These authors have contributed equally to this work

SPECIALTY SECTION
This article was submitted to Multiple Sclerosis and Neuroimmunology, a section of the journal Frontiers in Immunology

RECEIVED 12 October 2022
ACCEPTED 03 January 2023
PUBLISHED 19 January 2023

CITATION
Zhang Q, Yu B, Zhang Y, Tian Y, Yang S, Chen Y and Wu H (2023) Combination of single-cell and bulk RNA seq reveals the immune infiltration landscape and targeted therapeutic drugs in spinal cord injury. *Front. Immunol.* 14:1068359. doi: 10.3389/fimmu.2023.1068359

COPYRIGHT
© 2023 Zhang, Yu, Zhang, Tian, Yang, Chen and Wu. This is an open-access article distributed under the terms of the Creative Commons Attribution License (CC BY). The use, distribution or reproduction in other forums is permitted, provided the original author(s) and the copyright owner(s) are credited and that the original publication in this journal is cited, in accordance with accepted academic practice. No use, distribution or reproduction is permitted which does not comply with these terms.

Combination of single-cell and bulk RNA seq reveals the immune infiltration landscape and targeted therapeutic drugs in spinal cord injury

Qing Zhang[1†], Beibei Yu[2†], Yongfeng Zhang[2†], Yunze Tian[2], Shijie Yang[2], Yongfeng Chen[3*] and Haining Wu[3,4*†]

[1]Key laboratory of Shaanxi Province for Craniofacial Precision Medicine Research, College of Stomatology, Xi'an Jiaotong University, Xi'an, China, [2]Department of Neurourgery, the Second Affiliated Hospital of Xi'an Jiao Tong University, Xi'an, China, [3]Department of Orthopaedics, Xijing Hospital, Fourth Military Medical University, Xi'an, China, [4]State Key Laboratory of Cancer Biology, Department of Biochemistry and Molecular Biology, Fourth Military Medical University, Xi'an, China

Background: In secondary spinal cord injury (SCI), the immune microenvironment of the injured spinal cord plays an important role in spinal regeneration. Among the immune microenvironment components, macrophages/microglia play a dual role of pro-inflammation and anti-inflammation in the subacute stage of SCI. Therefore, discovering the immune hub genes and targeted therapeutic drugs of macrophages/microglia after SCI has crucial implications in neuroregeneration. This study aimed to identify immune hub genes and targeted therapeutic drugs for the subacute phase of SCI.

Methods: Bulk RNA sequencing (bulk-RNA seq) datasets (GSE5296 and GSE47681) and single-cell RNA sequencing (scRNA-seq) dataset (GSE189070) were obtained from the Gene Expression Omnibus database. In the bulk RNA-seq, the R package 'limma,' 'WGCNA,' and 'CIBERSORT' were used to jointly screen key immune genes. Subsequently, the R package 'Seurat' and the R package 'celldex' were used to divide and annotate the cell clusters, respectively. After using the Autodock software to dock immune hub genes and drugs that may be combined, the effectiveness of the drug was verified using an *in vivo* experiment with the T9 SCI mouse model.

Results: In the bulk-RNA seq, *B2m*, *Itgb5*, and *Vav1* were identified as immune hub genes. Ten cell clusters were identified in scRNA-seq, and *B2m and Itgb5* were mainly located in the microglia, while *Vav1* was mainly located in macrophages. Molecular docking results showed that the proteins corresponding to these immune genes could accurately bind to decitabine. In decitabine-treated mice, the pro-inflammatory factor (TNF-α, IL-1β) levels were decreased while anti-inflammatory factor (IL-4, IL-10) levels were increased at 2 weeks post-SCI, and macrophages/microglia transformed from M1 to M2. At 6 weeks post-SCI, the neurological function score and electromyography of the decitabine treatment group were also improved.

Conclusion: In the subacute phase of SCI, *B2m, Itgb5, and Vav1* in macrophages/microglia may be key therapeutic targets to promote nerve regeneration. In addition, low-dose decitabine may promote spinal cord regeneration by regulating the polarization state of macrophages/microglia.

KEYWORDS

spinal cord injury, immune infiltration, macrophages/microglia, decitabine, ScRNA-seq

1 Introduction

Spinal cord injury (SCI) is commonly caused by external physical impact (e.g., traffic accidents, violence, or sports-related injury), and it has devastating physical and social consequences for patients and their families. The high complexity of the spinal cord and imbalanced inflammatory microenvironment following SCI hinder neural regeneration and functional recovery. SCI patients have multiple disabilities in motosensory function (1). However, despite its associated severe neurological dysfunction and poor prognosis, the clinical treatment for SCI mainly involves palliative surgical decompression and glucocorticoids (2, 3) These strategies fail to prevent inflammatory injury and neurodegeneration in the injured spinal cord. Thus, improved treatment modalities are a critical unmet need in SCI management.

SCI can be divided into three phases, namely, acute (<48 hours), subacute(>48 hours, <2 weeks), and intermediate and chronic phases (>2 weeks, <6 months) (4). In the subacute phase, neuronal loss and axon and myelin necrosis activate macrophages to release proinflammatory cytokines, which lead to an extensive inflammatory response in the SCI microenvironment (5, 6). Subsequently, the blood–spinal cord barrier is destroyed, resulting in immune microenvironment disorder and poor regeneration of the injured spinal cord (7). Macrophages/microglia plays an important role in maintaining the immune homeostasis of the CNS microenvironment. Homeostatic microglia could promote neuronal development, axonal regeneration and pruning of neuronal/synaptic side branches, and once it was activated or in the microenvironment of disease, microglia are transformed into disease-associated microglia (DAM) (8). In spinal cord injury, Milich et al. classified DAM as inflammatory, dividing, and migrating microglia based on the single-cell RNA sequencing (scRNA-seq) and flow cytometry. However, overall, macrophages/microglia play dual roles in the pathogenesis and prognosis of SCI, that is, anti-inflammatory and anti-inflammatory effects (9). As such, a deeper understanding of the heterogeneity of the immune microenvironment after SCI and targeting the macrophages/microglia may be helpful for establishing the optimal regeneration strategy after SCI.

RNA-seq high-throughput sequencing is currently widely used in biology owing to its convenience for discovering immune hub genes and distinguishing the heterogeneity of immune cells. This study aimed to identify immune hub genes and targeted therapeutic drugs for the subacute phase of SCI. Towards this goal, we screened the key immune genes in the subacute stage post-SCI through differential gene expression analysis, weighted gene coexpression network analysis (WGCNA), and immune infiltration analysis in the bulk RNA sequencing (bulk RNA-seq) datasets GSE5296 and GSE47681. Subsequently, in the scRNA-seq dataset GSE189070, the composition of cell clusters and cell clusters where these immune genes were located were identified. Finally, based on the key immune genes, we identified the drug that may promote the regeneration of SCI mice by switching the polarization state of macrophages/microglia and verified its effectiveness through *in vivo* experiments.

2 Materials and methods

2.1 Microarray datasets

Open-access microarray data were retrieved from the Gene Expression Omnibus database[1] at the National Center for Biotechnology Information. Three datasets, namely, GSE5296, GSE47681, and GSE189070, were selected according to the following inclusion criteria: (1) samples of the experimental group were collected from mice after SCI in the thoracic segment and without drug or other interventions and (2) microarray of the SCI sample was sequenced in the subacute phase (2–14 days). The bulk RNA-seq datasets (GSE5296 and GSE47681), all based on the GPL1261 platform and contained 10 samples (four control and six SCI) and 12 samples (four control and eight SCI) were sequenced at 3 days post-injury (dpi) and 7 dpi, respectively (10, 11). The GSE189070 dataset based on the GPL24247 platform containing single-cell RNA data from six mice in the uninjured group and 12 mice in the injured group were sequenced at 3 dpi and 7 dpi, which corresponds to the sequencing time of bulk RNA seq datasets (12). The study flow chart is shown in Figure 1.

2.2 Data processing and screening of key regulatory genes

R version 4.1.0 (R Foundation for Statistical Computing, Vienna, Austria) was used for all statistical analyses. Using the 'combat' function (in the 'sva' package), batch effects were removed after the combination of the bulk RNA-seq datasets (GSE5296 and GSE47681). To visualize the separation of the uninjured and injured group,

1 http://www.ncbi.nlm.nih.gov/geo/

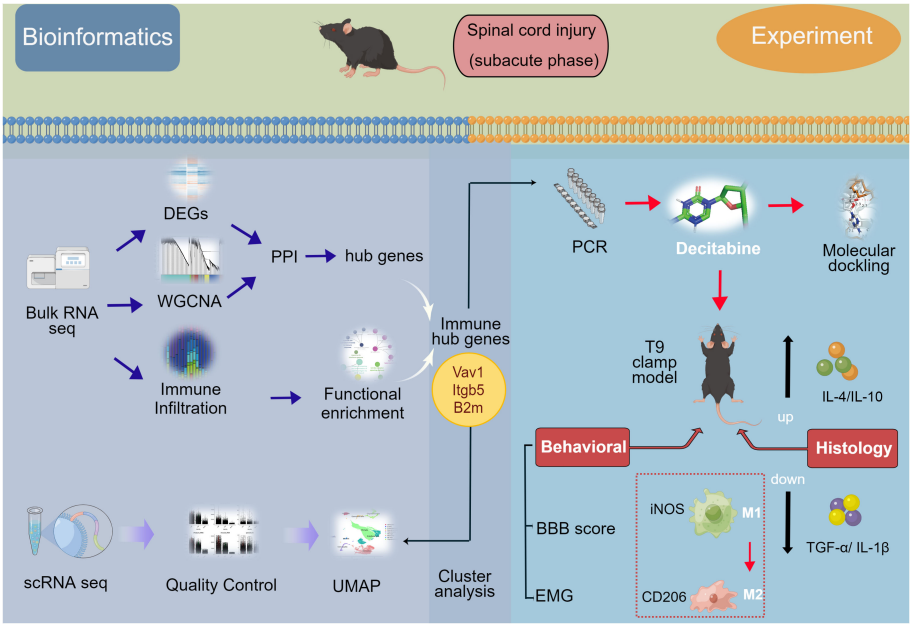


FIGURE 1
Flow-diagram for the study. SCI, spinal cord injury; DEGs, differentially expressed genes; PPI, protein-protein interaction; WGCNA, weighted gene coexpression network analysis (WGCNA); UMAP, uniform manifold approximation and projection; BBB score, Basso-Beattie-Bresnahan locomotion testing score; EMG, electromyography.

principal component analysis was performed using the 'factoextra' package. Under the filter of |log 2 (fold-change) (FC) | >1 and an adjusted p<0.05, differentially expressed genes (DEGs) were identified using the bioconductor package "limma."

WGCNA, which can identify gene modules with similar expression patterns, map regulatory networks between gene sets, and identify key regulatory genes (13), was used to perform module analysis. After selecting genes with variance greater than 25%, the power of 8 was determined by pickSoftThreshold function. Through average linkage hierarchical clustering, the genes with similar expression profiles were categorized to gene modules using the TOM-based dissimilarity measure. Ultimately, the correlation between each module and the sample trait (presence or absence of SCI) was assessed. Modules with the highest correlation were used to intersect with DEGs using the 'VennDiagram' package.

2.3 Analysis of key regulatory genes and immune infiltration

The protein–protein interaction network analysis was carried out by using Metascape and STRING database[2,3]. The most significant modules were identified using the MCODE plug of Cytoscape, with a cutoff score of 5. Gene Ontology and Kyoto Encyclopedia of Genes and Genomes enrichment analysis was performed by the ClueGO plug of Cytoscape software, with P<0.05 and gene counts ≥ 3 set as the cut-off criteria for enrichment items.

For immune infiltration analysis, CIBERSORT algorithm[4] was applied to compute immune cell abundance of the samples. The 'pheatmap' package was used to visualize the content of 22 kinds of immune cells in spinal cord tissues. Spearman's correlation analysis was then performed to detect the correlation coefficients between immune cells and gene expression levels. The criteria for selection of key immune genes related to SCI were as follows: >2 immune cell correlation, correlation coefficient >0.3, and p<0.05.

2.4 ScRNA-seq data processing and identification of cell types

For single-cell genomics analysis, the processed data were analyzed using the 'Seurat' package. For downstream analyses, we excluded cells with a total number of expressed genes exceeding 6,000, mitochondrial gene counts exceeding 15%, and genes expressed in more than three cells. Subsequently, the expression matrix was standardized using the log2 (CPM+1) values as input matrix. High variable genes were identified using the 'FindVariableGenes' function, and principal component analysis was performed. The dimension reduction method for single-cell visualization was uniform manifold approximation and projection (UMAP). Then, differential expression analysis was performed using 'FindAllMarkers' function with |log 2 (fold-change) |>0.3 and adjusted p<0.05. 'DimPlot' function was used to visualize the single-cell plot, and 'FeaturePlot' function was used to visualize the gene expression plot. Thereafter, the single-cell

2 http://metascape.org

3 https://cn.string-db.org

4 https://cibersort.stanford.edu

subgroups were annotated using the 'MouseRNAseqData' function in the 'celldex' package. Finally, the cellular crosstalk was calculated with "CellChat" package.

2.5 Molecular modeling analysis

We hypothesized that the FDA-approved drugs and experimental compounds may be combined with key immune targets using the DSigDB database[5]. The two-dimensional structures of selected compounds were downloaded from the Pubchem database[6]. The RCSB Protein Data Bank[7] was used to obtain the structures of the proteins. We specified three PDBQT files: proteins rigid, flexible, and ligands. The AutoDock 4 software was used in the flexible ligand docking simulations. Finally, PyMol software was used to represent these structures.

2.6 SCI model

All animal experiments were approved by the Intramural Animal Use and Care Committee of the Fourth Military Medical University and were conducted in accordance with institutional guidelines.

Adult female C57BL/6 mice (18–20 g, n=27) were randomly divided into three groups: (1) the uninjured group (9 mice); (2) the SCI + phosphate-buffered saline (PBS) group (9 mice); (3) the SCI + decitabine group (9 mice). Mice were first anesthetized with sodium pentobarbital, and then surgery for laminectomy was performed under a microscope at the level of the 10th thoracic vertebra. The T9-T10 segment of the spinal cord was fully exposed; subsequently, the mouse spinal cord was injured at the T9 segment using an arterial clamp for 1 minute, as previously reported (14). After clamp injury, the muscles and skin were closed. To restore spontaneous voiding, bladders were manually expressed twice daily for a week, and mice were treated with antibiotics (ceftriaxone 16 mg/kg) intraperitoneally twice a day for 5 days. In the drug-treated group, 15 μg/10 g decitabine (A10292, Adooq Bioscience, Nanjing, China) was administered intraperitoneally continuously for 7 days (once/day) postoperatively. The functional recovery of SCI mice was evaluated by 21-point Basso-Beattie-Bresnahan locomotion testing score (15). Treatment outcomes were evaluated once every 2 weeks (2w, 4w, 6w). At 6 weeks postoperative, motor evoked potentials (MEPs) of the hindlimb were assessed by electromyography. The samples of heart, kidney, liver, lung, stomach and spleen in SCI mice treated with decitabine for 6 weeks were stained with HE staining solution, and the HE staining characteristics were observed with an optical microscope.

5 http://dsigdb.tan-lab.org/DSigDBv1.0/

6 https://pubchem.ncbi.nlm.nih.gov/

7 https://www.pdbus.org/

2.7 Immunofluorescence staining and imaging and qRT-PCR

At 2 weeks post-injury, mice spinal cord tissues were fixed overnight in 4% paraformaldehyde. The samples were then permeabilized with 0.2% Triton X-100 (0.1%, Sigma-Aldrich) and blocked for 1h at 37°C in 1% BSA (6%, Bio-froxx, Germany) in 0.2% Triton X-100. After blocking, incubations were performed using specific primary antibodies (rabbit anti-CD206 [1:200, TD4149, Abmart], rabbit anti-iNOS [1:500, GB11119, Servicebio]) for 12 h followed by incubations with secondary antibodies for another 1 h. Images were captured using a fluorescence microscope (Olympus fluorescence microscope, Japan)

For quantitative real-time polymerase chain reaction, total mRNA was extracted from tissues (Life Technologies, USA) at 7dpi and 2 weeks post-injury using TRIzol-chloroform. cDNA was reversely transcribed with a PrimeScriptTM RT Master Mix (Takara, Dalian, China). PCR analysis was performed using a MiniOpticon Real-Time PCR system and Bio-Rad's CFX manager software version 1.5. Finally, fold change was calculated as 2 to the -ΔΔCt power (2 -ΔΔCt). The qRT-PCR primers are summarized in Table 1.

TABLE 1 The primers for Real-Time Quantitative PCR.

Gene	Sequence
Vav1	TGTGAGAAGTTCGGCCTCAAG (Forward) CAGAGCAGACAGGGTGTAGAT (Reverse)
Itgb5	GAAGTGCCACCTCGTGTGAA (Forward) GGACCGTGGATTGCCAAAGT (Reverse)
B2m	GGCCCATCTTGCATTCTAGGG (Forward) CAGGCAACGGCTCTATATTGAAG (Reverse)
TNF-α	TCAGCCTCTTCTCATTCCTGC (Forward) TTGGTGGTTTGCTACGACGTG (Reverse)
IL1β	CTCCATGAGCTTTGTACAAGG (Forward)
	GGGGTTGACCATGTAGTCGT (Reverse)
IL-4	GGTCTCAACCCCCAGCTAGT (Forward)
	GCCGATGATCTCTCTCAAGTGAT (Reverse)
IL-10	CTTACTGACTGGCATGAGGATCA (Forward) GCAGCTCTAGGAGCATGTGG(Reverse)
TGF-β	TCTGCATTGCACTTATGCTGA (Forward)
	AAAGGGCGATCTAGTGATGGA (Reverse)
GAPDH	TTGTCTCCTGCGACTTCAAC (Forward)
	GTCATACCAGGAAATGAGCTTG (Reverse)
iNOS	GGGTCTTGTTAGCCTAGTCA (Forward)
	TGTTGTTGGGCTGGGAATAG (Reverse)
Arg-1	CTCCAAGCCAAAGTCCTTAGAG (Forward)
	AGGAGCTGTCATTAGGGACATC (Reverse)

2.8 Statistical analysis

Data were presented as the mean ± standard deviation, and all statistical analyses were performed with one-way analysis of variance using the GraphPad Prism software (GraphPad Prism Software, San Diego, California). Differences with $p<0.05$ were considered statistically significant.

3 Results

3.1 Identification of key regulatory genes

Based on principal component analysis results of bulk RNA-seq datasets, the 22 sample characteristics of the SCI group (3 dpi and 7 dpi) were clearly distinguished from those of the sham group (Figure 2A). The heatmap and the volcano map indicated the presence of 1387 DEGs in these samples, including 947 upregulated genes and 440 downregulated genes (Figures 2B, C). All 22 samples in GSE5296 and GSE47681 met the condition of h <100 and were therefore included in the WGCNA analysis to search for key module genes of SCI (Figure 3A). In the analysis of these datasets, the smallest value (β=8) that resulted in a nearly scale-free network with a truncated scale-free fitting index of R2 = 0.80 (Figure 3B) was selected. Five modules with significant correlation with SCI were identified (Figures 3C, D), among which the yellow module was the most significant (module feature correlation=0.93). The heatmap of correlations between modules is shown in Figure 3E. Finally, the correlation coefficient between the 686 genes in the yellow module and the importance of SCI genes was 0.97 (Figure 3F).

3.2 Comprehensive analysis of key regulatory genes

In the Venn diagram, 452 genes were intersected between DEGs and yellow module genes (Figure 4A). Functional enrichment showed that these regulatory genes were mainly enriched in biological pathways such as negative regulation of lymphocyte activation, antigen processing and presentation of exogenous peptide antigen, and positive regulation of inflammatory response to antigenic stimulus (Figure 4B). Further immune pathway enrichment analysis showed that key regulatory genes involved in response to interferon-gamma, toll-like receptor signaling pathway (Figure 4C). Overall, 29 hub genes were selected in the protein–protein interaction through the MCODE application (Figures 4A, D). These hub genes were involved in the positive regulation of immunoglobulin production, ECM-receptor, endodermal cell differentiation (Figures 4E).

3.3 Analysis of immune cell infiltration

Considering the important role of changes in the immune microenvironment on post-SCI regeneration and the enrichment of key regulatory genes in immune-related pathways, we calculated the contents of 22 immune cells in the samples based on the CIBERSORT algorithm (Figure 5A). The heatmap of immune cell abundance in each sample is shown in Figure 5B. In addition, the correlation of immune cells in these samples was also analyzed (Figure 5C). Among them, M0 macrophages had the strongest positive correlation with activated NK cells (r=0.94), while M1 macrophages had the strongest negative correlation with M2 macrophages (r=-0.67). In addition, the levels of $CD8^+$ T cells, M2 macrophages, and resting dendritic cells were higher in the SCI group than in the sham group. Meanwhile, the levels of plasma cells, memory $CD4^+$ T cells, T follicular helper cells, activated NK cells, and M0 macrophages were lower in the SCI group than in the sham group (Figure 5D).

The expression matrix heatmap of 29 hub genes is shown in Figure 6A. Based on the screening criteria, six genes (*Vav1, Itgb5, B2m, Col1a2, Col4a5, Col6a2*) were identified as immune hub genes (Figure 6B). According to the results of lollipop plot (Figure 6C), *Itgb5* had the strongest positive correlation with resting dendritic cells

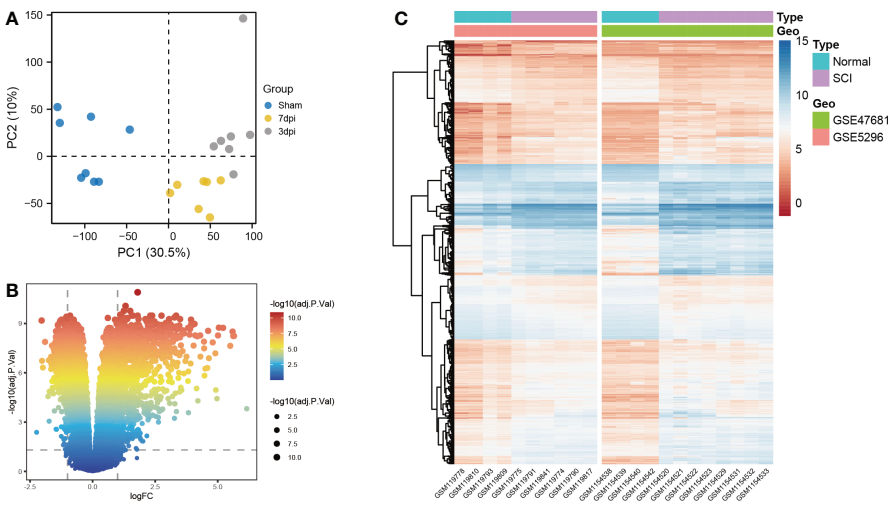


FIGURE 2
Screening for differentially expressed genes (DEGs) of bulk RNA-seq datasets. **(A)** Principal component analysis (PCA) analysis of GSE5296 and GSE47681. **(B)** Volcano plots of DEGs, screening criteria: |log 2 (fold-change) (FC)>1 and an adjusted $p<0.05$. **(C)** Heatmap of DEGs.

10.3389/fimmu.2023.1068359

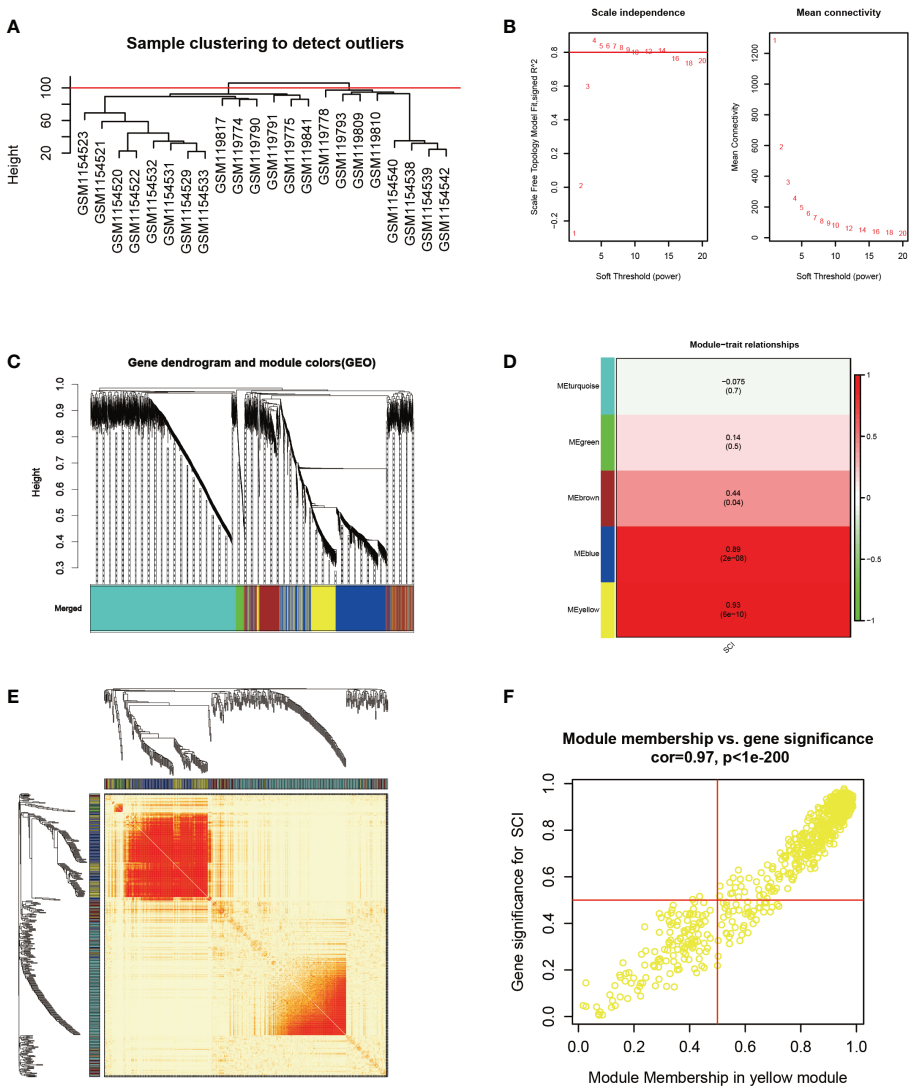


FIGURE 3
Identification of key modules genes of bulk RNA-seq datasets. **(A)** Outlier removal with "h > 100". **(B)** Soft threshold setting according to R2 = 0.80. **(C)** The gene set is divided into 5 different modules. **(D)** The correlation of modules with SCI occurrence. **(E)** The heatmap of correlations between modules. **(F)** The correlation between yellow module and SCI gene significance. Gene significance for SCI refers to compare the correlation between a gene and its corresponding traits (absence of SCI).

(r=0.83), and *Col6a2* had the strongest negative correlation with plasma cells (r=-0.80).

3.4 ScRNA-seq analysis

After integrating data from the sham group (10,227 cells), the 3-dpi group (12,783 cells), and the 7-dpi group (16,447 cells) in the GSE189070 dataset, a total of 39,457 cells were identified. Low-quality cells were filtered using an nFeature_RNA cutoff,400; nCount_RNA cutoff, 1000; and percent mitochondrial genes cutoff, 15%. Subsequently, 34,331 high-quality cells from the sham group (7,499 cells), the 3-dpi group (11,496 cells), and the 7-dpi group (15,336 cells) were screened for downstream analysis. After selecting the top 2000 highly variable genes, linear dimensionality reduction was performed to identify the available dimensions of the dataset. First 20 principal components were used to generate the UMAP visualization. Finally, 10 cell clusters were identified, and UMAP plots were visualized between different time points and different groups of cell clusters.

Ten cell clusters (astrocytes, B cells, endothelial cells, ependymal cells, granulocytes, microglia, macrophages, monocytes, NK cells, oligodendrocytes) were identified on the UMAP plot (Figure 7A). Neurons were not annotated because of their susceptibility to death during enzymatic dissociation. The results of functional enrichment analysis showed that the functions of DEGs of cell clusters were mainly enriched in regulation of lymphocyte proliferation, negative regulation of leukocyte activation, and microglial cell activation in immune pathway. (Figure 7B). The percentage of expression of immune hub genes in each cluster are is as violin plots and UMAP

10.3389/fimmu.2023.1068359

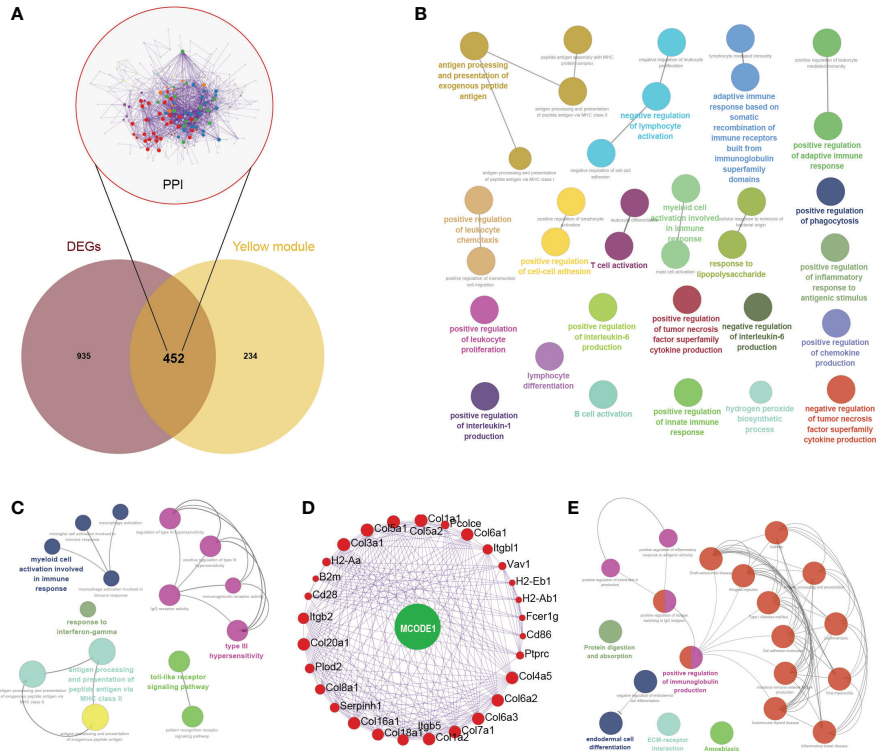


FIGURE 4
Comprehensive analysis of key regulatory genes. **(A)** Venn diagram of intersected genes between differentially expressed genes (DEGs) and yellow module genes. Protein-protein interaction network of 452 key regulatory genes were also displayed. **(B)** Biological pathways of these 452 key regulatory genes. **(C)** Immune pathway of key regulatory genes. **(D)** Hub genes were selected in the protein–protein interaction through the MCODE application. **(E)** Biological pathways of these 29 hub genes.

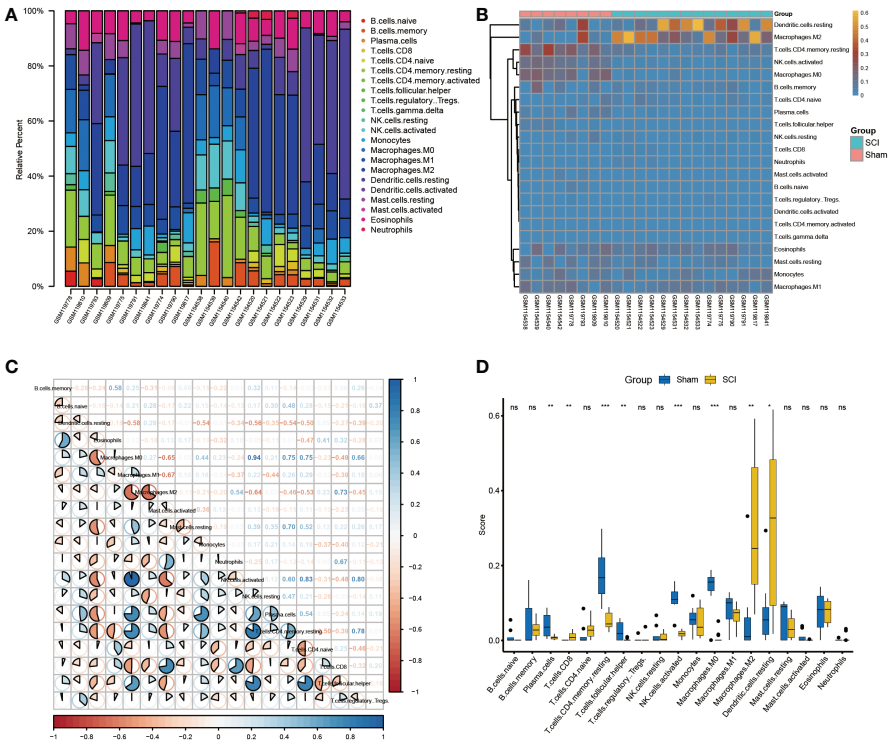


FIGURE 5
Immune infiltration analysis of bulk RNA-seq datasets. **(A)** Immune infiltration of the 22 immune cells in GSE5296 and GSE47681dataset. **(B)**Immune infiltration heatmap in GSE5296 and GSE47681dataset. **(C)** Correlation heatmap of immune cells. **(D)** The expression difference of 22 immune cells between SCI and uninjured samples. *P < 0.05, **P < 0.01, ***P < 0.001.

10.3389/fimmu.2023.1068359

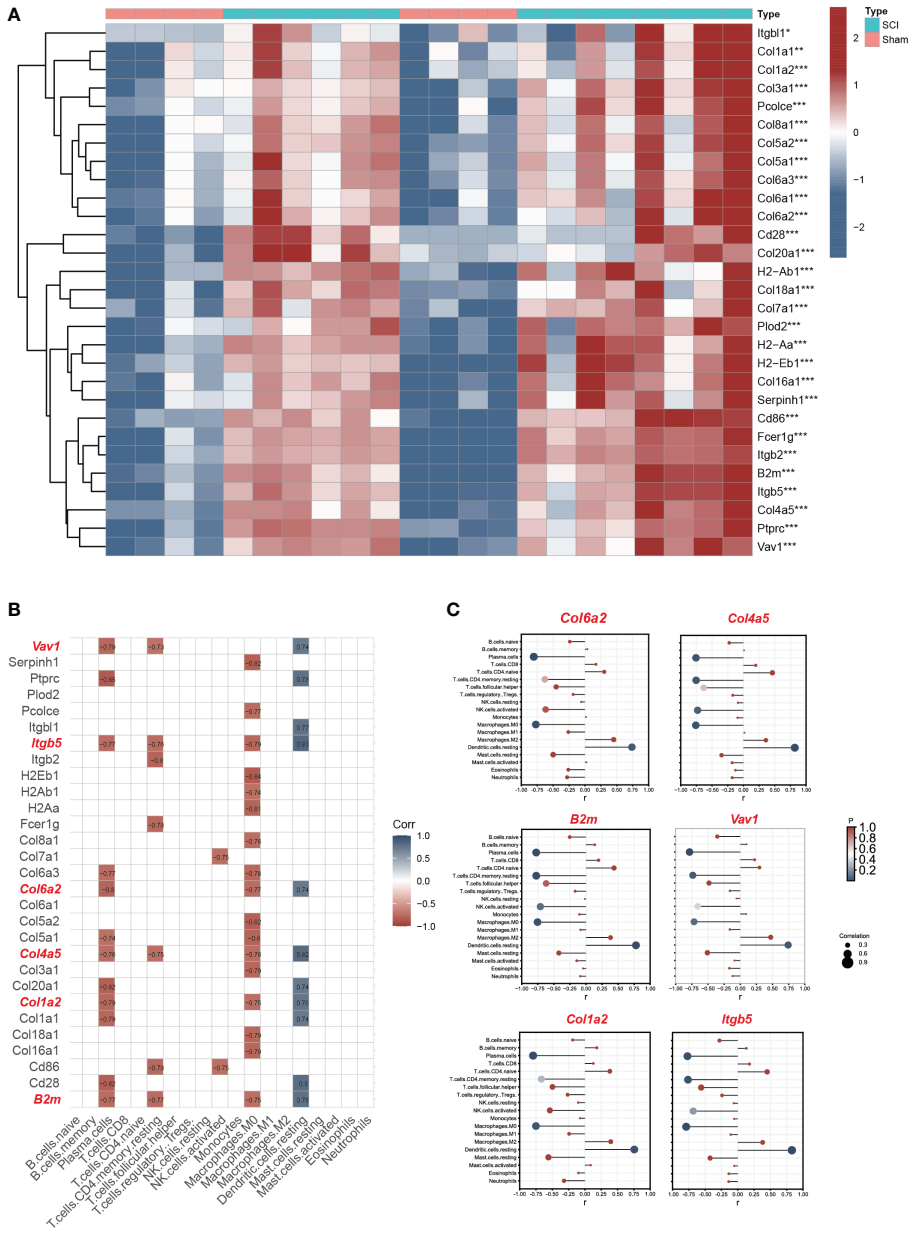


FIGURE 6
Screening immune hub genes based on bulk RNA seq datasets. **(A)** The expression matrix heatmap of 29 hub genes. **(B)**The correlation analyses between hub genes and immune characteristics between SCI and uninjured samples. The criteria for selection of key immune genes related to SCI were as follows: >2 immune cell correlation, correlation coefficient >0.3, and p<0.05. **(C)** The lollipop plot of six immune hub genes (*Vav1, Itgb5, B2m, Col1a2, Col4a5, Col6a2*). *P < 0.05, **P < 0.01, ***P < 0.001.

plots (Figures 7C, D). Among these immune hub genes, *Vav1* (Log FC=0.37), *Itgb5* (Log FC=0.75), and *B2m* (Log FC=0.75) are characteristic genes of microglia/macrophages (Figure 7E). We also found that *B2m* and *Itgb5* were mainly located in microglia (*Trem2*, *C1qa*, *Fcrls*), while *Vav1* was mainly located in macrophages (*Cx3cr1*, *Csf1r*, *Cst3*). The number and strength of interactions between 10 cell clusters are shown in Figure 7F. For immune cells, B cells were strongly associated with monocytes, macrophages with astrocytes, monocytes with endothelial cells, and NK cells with ganglion cells. It was worth noting that microglia have strong correlation with endothelial cells, astrocytes and oligodendrocytes.

3.5 Validation of immune hub genes and drug prediction

In the bulk RNA-seq datasets, *B2m, Itgb5, and Vav1* were all highly expressed in the SCI group (Figure 8A), consistent with the validation results of qRT-PCR in 7 dpi (Figure 8B). Based on the DSigDB database results, we speculate that decitabine (P=0.02) may be a small molecule compound that binds to these immune hub genes (Figure 8C). Finally, the possible binding sites of decitabine with *B2m, Itgb5*, and *Vav1* proteins were successfully predicted using AutoDock software (Figures 8D–F).

10.3389/fimmu.2023.1068359

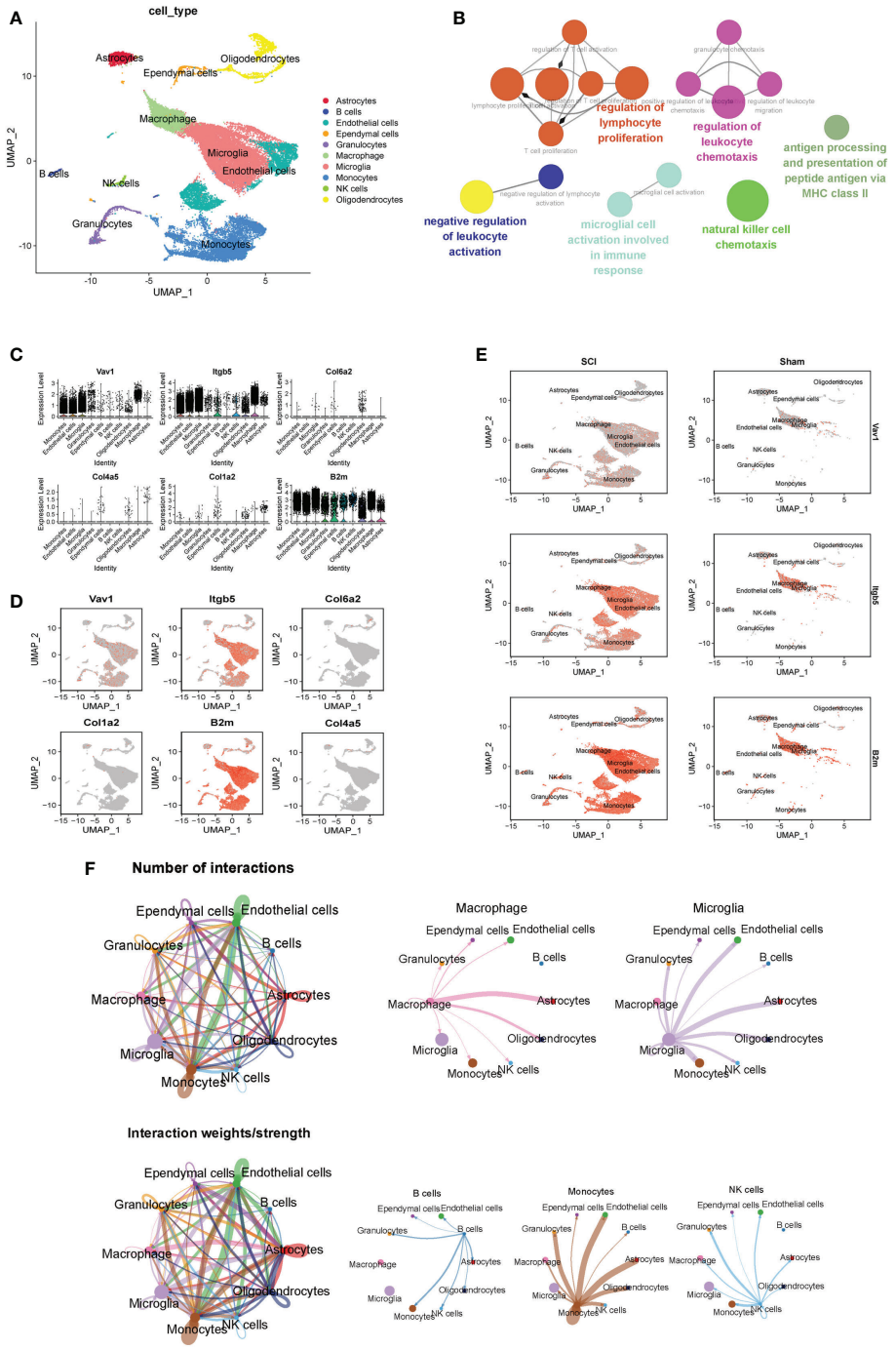


FIGURE 7
ScRNA-seq analysis of the subacute phase of spinal cord injury. **(A)** Nine cell clusters (astrocytes, B cells, endothelial cells, ependymal cells, granulocytes, microglia, monocytes, NK cells, oligodendrocytes) were identified on the UMAP plot. **(B)** The functional enrichment analysis of differentially expressed genes in different cell clusters. **(C)** The violin plots of six immune hub genes in each cluster. **(D)** The UMAP plots of six immune hub genes in each cluster. **(E)** Among these immune hub genes, *Vav1* (Log FC=0.37), *Itgb5* (Log FC=0.75), and *B2m* (Log FC=0.75) are characteristic genes of microglia/macrophages. **(F)** The number and strength of interactions between 10 cell clusters.

3.6 *In vivo* functional and histological assessment

After exposing the spinal cord of the T9 segment, we successfully made a T9 clamp SCI model (Figure 9A). Improved MEPs were observed at 6 weeks post-SCI in the decitabine group (Figure 9B). In addition, the Basso-Beattie-Bresnahan locomotion testing score was also improved 6 weeks post-SCI in the decitabine group, although the improvement in the decitabine group was not statistically significant in the first 4 weeks post-SCI (Figure 9C). Notably, HE staining of the heart, kidney, liver, lung, stomach and spleen did not show significant morphological changes in SCI mice treated with decitabine for 6 weeks (Figure 9D).Follow-up analysis of the tissue samples from each group at 2 weeks post-SCI showed that compared with the SCI + PBS group, the

10.3389/fimmu.2023.1068359

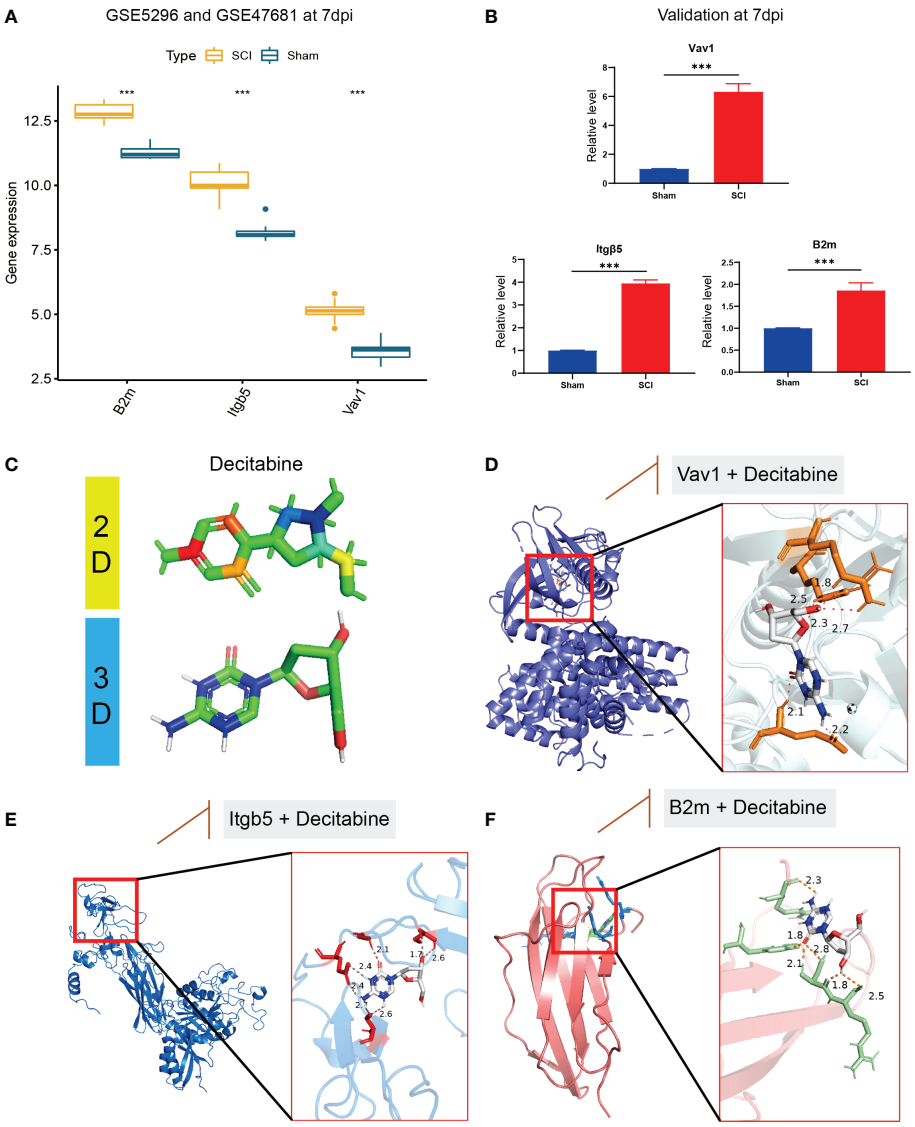


FIGURE 8
Validation of immune hub genes and drug prediction. **(A)** In the bulk RNA-seq datasets, *B2m, Itgb5, and Vav1* were all highly expressed in the SCI group, **(B)** consistent with the validation results of qRT-PCR in 7 dpi. **(C)** The two-dimensional and three-dimensional structure of decitabine. **(D–F)** the possible binding sites of decitabine with *B2m, Itgb5,* and *Vav1* proteins. &Statistically significant difference appeared on this day. ***$P < 0.001$.

decitabine group had higher levels of Arg-1, IL-4, and IL-10 ($P<0.05$) (Figure 9E). Meanwhile, the decitabine group showed lower levels of iNOS, TGF-α and IL-1β ($P<0.05$). Finally, under decitabine stimulation, CD206 showed stronger red fluorescence, while iNOS showed weak red fluorescence. All in all, these results all support the transition of macrophages/microglia from M1 type to M2 type (Figure 9F).

4 Discussion

SCI often leads to irreversible neurological impairment and also has a significant socioeconomic impact on both the patients and the healthcare system (16). The altered immune microenvironment after SCI hinders neural regeneration and repair, but related studies have been met with conflicting findings (17). Next-generation sequencing is a novel modality that enabled the discovery of the altered immune microenvironment after SCI (18). The current study was based on Bulk RNA-seq and scRNA-seq and explored the immune hub genes and immune cell composition in the subacute phase of SCI. Drugs to promote regeneration by regulating the polarization status of microglia were successfully identified. Importantly, the study shows that regulating the dual role of the immune microenvironment is a potential strategy in managing neuroinflammation during SCI.

Various immune cells, including neutrophils, macrophages, microglia, B lymphocytes, and T lymphocytes, have been shown to be involved in the inflammatory response after SCI (19). Concurrently, the composition and phenotype of immune cells are also altered with the stage of injury and the signals in the injury microenvironment. For example, microglia/macrophages, T cells, and B cells are capable of both pro-inflammatory and anti-inflammatory responses in the injured spinal cord, thereby regulating secondary injury after SCI. Microglia/macrophages start to accumulate at 3 days after SCI and peak at 7 dpi

10.3389/fimmu.2023.1068359

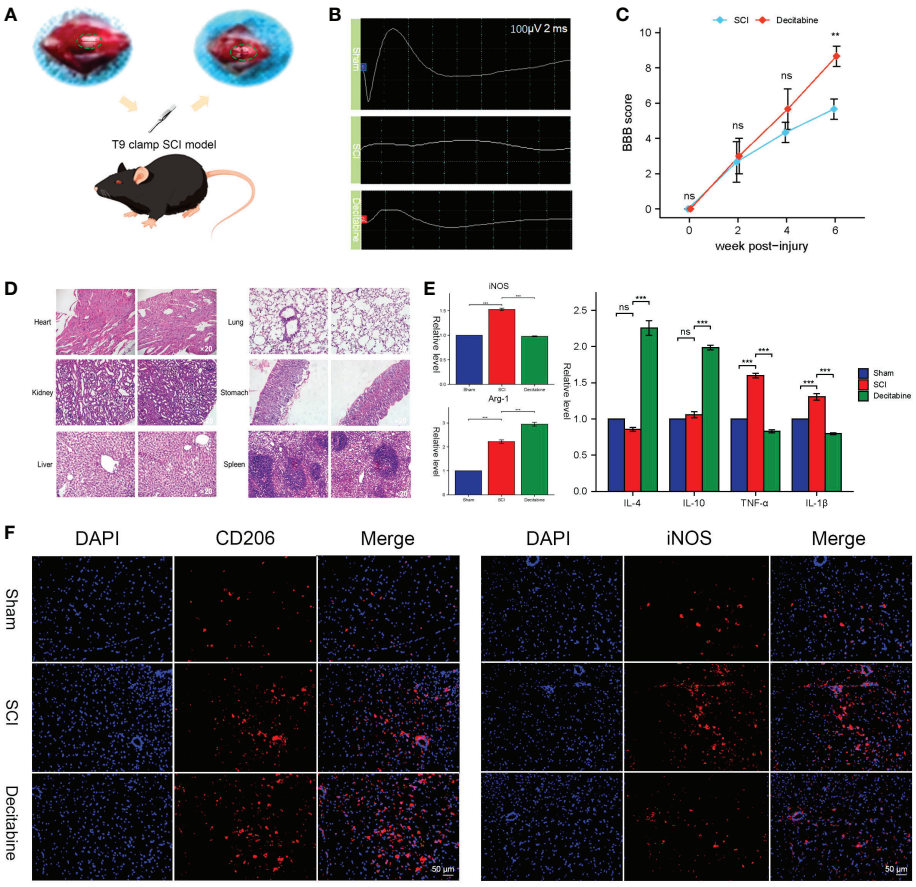


FIGURE 9
In vivo functional and histological assessment. **(A)** The spinal cord injury model of T9 by arterial clamp. **(B)** Electromyography was observed at 6 weeks post-SCI in uninjured group, the SCI + phosphate-buffered saline (PBS) group and the SCI + decitabine group. **(C)** The Basso-Beattie-Bresnahan locomotion testing score at 6 weeks post-SCI in the SCI + PBS group and the SCI + decitabine group (n = 6 in each group). **(D)** HE-stained sections of the heart, liver, spleen, lung and kidney of the mice at 6 weeks post-SCI in the SCI + decitabine group (magnification, ×200). **(E)** The expression level of iNOS, Arg, IL-4, IL-10, TGF-α, and IL-1β at 2 weeks in uninjured group, the SCI + PBS group and the SCI + decitabine group. **(F)**The immunofluorescence staining of CD206 and iNOS at 2 weeks post-SCI. &Statistically significant difference appeared on this day. $^{**}P < 0.01$, $^{***}P < 0.001$.

(20). Consistently, immune infiltration analysis in the current study showed that levels of M2 macrophages were higher in the SCI group than in the sham group. Interestingly, we also found changes in the immune microenvironment of some acquired immune cells (resting dendritic cells, plasma cells and activated NK cell), which is closely related to the destruction of the blood–spinal cord barrier.

By combining the screening of DEGs, WGCNA, and immune infiltration analysis, *B2m, Itgb5, and Vav1*, were identified as immune hub genes of SCI. Cartarozzi et al. reported that *B2m* knockout could lead to weakened neuronal axon regeneration after SCI by enhancing microglia activation (21). Another reptile-based study also showed that *Vav1* can regulate the inflammatory reaction mediated by the macrophage migration inhibitory factor to promote the regeneration of the nervous system (22). Although the immune invasion of *Itgb5* in gastric cancer and glioblastoma has been well demonstrated, its role in SCI still needs further research (23, 24).

Activated microglia and blood-infiltrating macrophages are indistinguishable after SCI, and both exacerbate inflammatory injury by releasing protein hydrolases, reactive oxygen species, and inflammatory factors (25). However, the heterogeneity of the microglia and macrophages prevents the in-depth study of post-SCI regeneration, which can be further identified by scRNA-seq. Wang et al. performed scRNA-seq on immune cells sorted by flow cytometry after SCI and divided microglia and macrophages into three clusters and seven clusters, respectively (18). Highly accurate differentiation of microglia identified that targeting Hif1α may contribute to axonal regeneration and functional recovery after SCI. Another scRNA-seq study showed the dynamic changes and molecular characteristics of microglia within 38 days after SCI, providing additional evidence for strategies targeting microglia to promote neurological function repair (26). The current study identified the clusters of macrophages (*Cx3cr1*, *Csf1r*, *Cst3*) and microglia (*Trem2*, *C1qa*, *Fcrls*) and found that *B2m* and *Itgb5* were mainly located in microglia, while *Vav1* was mainly located in macrophages.

Drug discovery is the process of identifying potential new drugs from existing molecular databases and is a necessary part of the human pathway to treating disease. There are two key components involved in drug discovery: the protein (target) and the small molecule (ligand), which also known as protein-ligand interaction. In the present study, decitabine was shown to act as a ligand to inhibit the activity of B2m, Itgb5, and Vav1 proteins. Among them, decitabine exerts its pharmacological effects mainly through polar covalent bonds with GLU-524, ARG-54 and ARG550 of the VAV1 protein, with SER-534, CYS-489, GLY-492, GLU-502 of the Itgb5 protein and with ARG-12, ARG-97 and TRP-95 of the Itgb5 protein. Of course, the simulated

docking results need further validation by liquid chromatography and mass spectrometry.

Whether neurons and axons can regenerate after SCI depend not only on their original growth ability, but also on the neurovascular microenvironment and epigenetic changes, which is mainly embodied in DNA methylation and histone acetylation (27). Among these, DNA methylation affects many aspects of neural stem cell maintenance and proliferation, neuronal differentiation and maturation, and synaptogenesis (28). Decitabine is a demethylating drug that can inhibit DNA methyltransferase, reduce DNA methylation, and inhibit tumor cell proliferation, and it has been the primary drug for elderly AML patients (29). Decitabine can also reduce the proliferation and vitality of tumor cells in malignant meningioma and glioblastoma (30, 31). Interestingly, a recent study showed that decitabine can improve white matter lesions caused by chronic cerebral hypoperfusion (32). To our best knowledge, this study is the first to report that decitabine may promote the recovery of neural function after SCI by promoting the transformation of proinflammatory macrophages/microglia to anti-inflammatory macrophages/microglia.

However, this study also has some limitations. First, in the Bulk RNA-seq analyses, although data were preprocessed using the "sva" package, batch effect of different datasets should also be addressed. Meanwhile, deconvolution of scRNA-seq to further discover the consistency of immune cells with bulk RNA seq is our follow-up research work. Second, although no obvious side effects were observed within 6 weeks, the mice injected with small doses of decitabine died in succession at 8 weeks. Therefore, the injection dose and safety of decitabine need to be further evaluated in *in vivo* and *in vitro* experiments. Thirdly, restricted by the fact that Autodock is limited to the docking of a single receptor ligand, there was a possibility that decitabine may bind to genes other than the hub gene in macrophages/microglia for pharmacological effects. Lastly, hub gene knockdown to clarify the role of hub genes (B2m, Itgb5, and Vav1) in SCI was a topic that we will explore in the future.

In conclusion, the current study identified the changes in immune cell clusters and immune hub genes after SCI using a combination of Bulk RNA-seq and scRNA-seq and discovered the drugs that can regulate macrophage/microglia polarization to improve neural function. The exploration of the immune microenvironment after SCI and the identification of immune hub genes may provide additional scientific evidence for developing more effective treatment modalities targeting the microglia in SCI.

Data availability statement

The original contributions presented in the study are included in the article/Supplementary Material. Further inquiries can be directed to the corresponding authors.

Ethics statement

The animal study was reviewed and approved by the Intramural Animal Use and Care Committee of the Fourth Military Medical University.

Author contributions

QZ, BY and YZ: manuscript preparation, data analysis, and the research conception. YT and SY: Animal experiment and qRT-PCR. YC and HW: manuscript revision. All authors contributed to the article and approved the submitted version.

Funding

This work was supported by the Construction and application of big data self-evolution remote diagnosis and treatment system in ICU for severe neurological diseases (Grant No.2022ZDLSF04-01).

Conflict of interest

The authors declare that the research was conducted in the absence of any commercial or financial relationships that could be construed as a potential conflict of interest.

Publisher's note

All claims expressed in this article are solely those of the authors and do not necessarily represent those of their affiliated organizations, or those of the publisher, the editors and the reviewers. Any product that may be evaluated in this article, or claim that may be made by its manufacturer, is not guaranteed or endorsed by the publisher.

References

1. Lindsay SL, McCanney GA, Willison AG, Barnett SC. Multi-target approaches to CNS repair: Olfactory mucosa-derived cells and heparan sulfates. *Nat Rev Neurol* (2020) 16(4):229–40. doi: 10.1038/s41582-020-0311-0

2. Donovan J, Kirshblum S. Clinical trials in traumatic spinal cord injury. *Neurotherapeutics* (2018) 15(3):654–68. doi: 10.1007/s13311-018-0632-5

3. Huang H, Young W, Skaper S, Chen L, Moviglia G, Saberi H, et al. Clinical neurorestorative therapeutic guidelines for spinal cord injury (IANR/CANR version 2019). *J Orthop Translat* (2020) 20:14–24. doi: 10.1016/j.jot.2019.10.006

4. Ahuja CS, Wilson JR, Nori S, Kotter MRN, Druschel C, Curt A, et al. Traumatic spinal cord injury. *Nat Rev Dis Primers* (2017) 3:17018. doi: 10.1038/nrdp.2017.18

5. Alexander JK, Popovich PG. Neuroinflammation in spinal cord injury: Therapeutic targets for neuroprotection and regeneration. *Prog Brain Res* (2009) 175:125–37. doi: 10.1016/s0079-6123(09)17508-8

6. Ma D, Zhao Y, Huang L, Xiao Z, Chen B, Shi Y, et al. A novel hydrogel-based treatment for complete transection spinal cord injury repair is driven by microglia/macrophages repopulation. *Biomaterials* (2020) 237:119830. doi: 10.1016/j.biomaterials.2020.119830

7. Al Mamun A, Monalisa I, Tul Kubra K, Akter A, Akter J, Sarker T, et al. Advances in immunotherapy for the treatment of spinal cord injury. *Immunobiology* (2021) 226 (1):152033. doi: 10.1016/j.imbio.2020.152033

8. Fang YP, Qin ZH, Zhang Y, Ning B. Implications of microglial heterogeneity in spinal cord injury progression and therapy. *Exp Neurol* (2023) 359:114239. doi: 10.1016/j.expneurol.2022.114239

9. Milich LM, Choi JS, Ryan C, Cerqueira SR, Benavides S, Yahn SL, et al. Single-cell analysis of the cellular heterogeneity and interactions in the injured mouse spinal cord. *J Exp Med* (2021) 218(8):e20210040. doi: 10.1084/jem.20210040

10. Guo L, Lv J, Huang YF, Hao DJ, Liu JJ. Bioinformatics analyses of differentially expressed genes associated with spinal cord injury: A microarray-based analysis in a mouse model. *Neural Regener Res* (2019) 14(7):1262–70. doi: 10.4103/1673-5374.251335

11. Wu J, Renn CL, Faden AI, Dorsey SG. TrkB.T1 contributes to neuropathic pain after spinal cord injury through regulation of cell cycle pathways. *J Neurosci* (2013) 33 (30):12447–63. doi: 10.1523/jneurosci.0846-13.2013

12. Hou J, Bi H, Ge Q, Teng H, Wan G, Yu B, et al. Heterogeneity analysis of astrocytes following spinal cord injury at single-cell resolution. *FASEB J* (2022) 36(8):e22442. doi: 10.1096/fj.202200463R

13. Yu B, Tian Y, Zhang Y, Lv B, Li J, Gong S. Experimental verification and validation of immune biomarkers based on chromatin regulators in ischemic stroke. *Front Genet* (2022) 13:992847. doi: 10.3389/fgene.2022.992847

14. Hosseini SM, Sharafkhah A, Koohi-Hosseinabadi O, Semsar-Kazerooni M. Transplantation of neural stem cells cultured in alginate scaffold for spinal cord injury in rats. *Asian Spine J* (2016) 10(4):611–8. doi: 10.4184/asj.2016.10.4.611

15. Basso DM, Beattie MS, Bresnahan JC. Graded histological and locomotor outcomes after spinal cord contusion using the NYU weight-drop device versus transection. *Exp Neurol* (1996) 139(2):244–56. doi: 10.1006/exnr.1996.0098

16. Flack JA, Sharma KD, Xie JY. Delving into the recent advancements of spinal cord injury treatment: a review of recent progress. *Neural Regener Res* (2022) 17(2):283–91. doi: 10.4103/1673-5374.317961

17. Feng Y, Peng Y, Jie J, Yang Y, Yang P. The immune microenvironment and tissue engineering strategies for spinal cord regeneration. *Front Cell Neurosci* (2022) 16:969002. doi: 10.3389/fncel.2022.969002

18. Wang J, Xu L, Lin W, Yao Y, Li H, Shen G, et al. Single-cell transcriptome analysis reveals the immune heterogeneity and the repopulation of microglia by Hif1α in mice after spinal cord injury. *Cell Death Dis* (2022) 13(5):432. doi: 10.1038/s41419-022-04864-z

19. Chio JCT, Xu KJ, Popovich P, David S, Fehlings MG. Neuroimmunological therapies for treating spinal cord injury: Evidence and future perspectives. *Exp Neurol* (2021) 341:113704. doi: 10.1016/j.expneurol.2021.113704

20. Gensel JC, Zhang B. Macrophage activation and its role in repair and pathology after spinal cord injury. *Brain Res* (2015) 1619:1–11. doi: 10.1016/j.brainres.2014.12.045

21. Cartarozzi LP, Perez M, Kirchhoff F, Oliveira ALR. Role of MHC-I expression on spinal motoneuron survival and glial reactions following ventral root crush in mice. *Cells* (2019) 8(5):483. doi: 10.3390/cells8050483

22. Du N, Li H, Sun C, He B, Yang T, Song H, et al. Adult astrocytes from reptiles are resistant to proinflammatory activation via sustaining Vav1 expression. *J Biol Chem* (2021) 296:100527. doi: 10.1016/j.jbc.2021.100527

23. Liu D, Liu S, Fang Y, Liu L, Hu K. Comprehensive analysis of the expression and prognosis for ITGBs: Identification of ITGB5 as a biomarker of poor prognosis and correlated with immune infiltrates in gastric cancer. *Front Cell Dev Biol* (2021) 9:816230. doi: 10.3389/fcell.2021.816230

24. Qi F, Li Q, Lu X, Chen Z. Bioinformatics analysis of high-throughput data to validate potential novel biomarkers and small molecule drugs for glioblastoma multiforme. *J Int Med Res* (2020) 48(7):300060520924541. doi: 10.1177/0300060520924541

25. Hellenbrand DJ, Quinn CM, Piper ZJ, Morehouse CN, Fixel JA, Hanna AS. Inflammation after spinal cord injury: a review of the critical timeline of signaling cues and cellular infiltration. *J Neuroinflamm* (2021) 18(1):284. doi: 10.1186/s12974-021-02337-2

26. Li C, Wu Z, Zhou L, Shao J, Hu X, Xu W, et al. Temporal and spatial cellular and molecular pathological alterations with single-cell resolution in the adult spinal cord after injury. *Signal Transduct Target Ther* (2022) 7(1):65. doi: 10.1038/s41392-022-00885-4

27. Kameda T, Imamura T, Nakashima K. Epigenetic regulation of neural stem cell differentiation towards spinal cord regeneration. *Cell Tissue Res* (2018) 371(1):189–99. doi: 10.1007/s00441-017-2656-2

28. Shi G, Zhou X, Wang X, Zhang X, Zhang P, Feng S. Signatures of altered DNA methylation gene expression after central and peripheral nerve injury. *J Cell Physiol* (2020) 235(6):5171–81. doi: 10.1002/jcp.29393

29. Dhillon S. Decitabine/Cedazuridine: First approval. *Drugs* (2020) 80(13):1373–8. doi: 10.1007/s40265-020-01389-7

30. Riccadonna C, Yacoub Maroun C, Vuillefroy de Silly R, Boehler M, Calvo Tardón M, Jueliger S, et al. Decitabine treatment of glioma-initiating cells enhances immune recognition and killing. *PloS One* (2016) 11(8):e0162105. doi: 10.1371/journal.pone.0162105

31. Stögbauer L, Thomas C, Wagner A, Warneke N, Bunk EC, Grauer O, et al. Efficacy of decitabine in malignant meningioma cells: Relation to promoter demethylation of distinct tumor suppressor and oncogenes and independence from TERT. *J Neurosurg* (2020) 135(3):845–54. doi: 10.3171/2020.7.Jns193097

32. Wang YH, Cheng C, Zuo XZ, Cheng WC, Chen XY, Dong KY, et al. Inhibition of A2AR gene methylation alleviates white matter lesions in chronic cerebral hypoperfusion rats. *Eur Rev Med Pharmacol Sci* (2022) 26(8):2702–11. doi: 10.26355/eurrev_202204_28600

frontiers | Frontiers in Immunology

TYPE Review
PUBLISHED 23 January 2023
DOI 10.3389/fimmu.2023.1051606

Check for updates

OPEN ACCESS

EDITED BY
Guangzhi Ning,
Tianjin Medical University General Hospital, China

REVIEWED BY
Peng Li,
Southern Medical University, China
Weidong Zhang,
First Affiliated Hospital of Soochow University, China
Zhonghai Li,
First Affiliated Hospital of Dalian Medical University, China
Ming Yang,
Department of Orthopedics, Southwest Hospital, Army Medical University Chongqing, China, in collaboration with reviewer ZL

*CORRESPONDENCE
Changfeng Fu
fucf@jlu.edu.cn

SPECIALTY SECTION
This article was submitted to Multiple Sclerosis and Neuroimmunology, a section of the journal Frontiers in Immunology

RECEIVED 23 September 2022
ACCEPTED 03 January 2023
PUBLISHED 23 January 2023

CITATION
Xia Y, Wang H, Yang R, Hou Y, Li Y, Zhu J and Fu C (2023) Biomaterials delivery strategies to repair degenerated intervertebral discs by regulating the inflammatory microenvironment. *Front. Immunol.* 14:1051606. doi: 10.3389/fimmu.2023.1051606

COPYRIGHT
© 2023 Xia, Wang, Yang, Hou, Li, Zhu and Fu. This is an open-access article distributed under the terms of the Creative Commons Attribution License (CC BY). The use, distribution or reproduction in other forums is permitted, provided the original author(s) and the copyright owner(s) are credited and that the original publication in this journal is cited, in accordance with accepted academic practice. No use, distribution or reproduction is permitted which does not comply with these terms.

Biomaterials delivery strategies to repair degenerated intervertebral discs by regulating the inflammatory microenvironment

Yuanliang Xia[1], Hengyi Wang[1], Ruohan Yang[2], Yulin Hou[3], Yuehong Li[1], Jianshu Zhu[1] and Changfeng Fu[1]*

[1]Department of Spine Surgery, The First Hospital of Jilin University, Changchun, China, [2]Cancer Center, The First Hospital of Jilin University, Changchun, China, [3]Department of Cardiology, Guangyuan Central Hospital, Guangyuan, China

Intervertebral disc degeneration (IVDD) is one of the leading causes of lower back pain. Although IVDD cannot directly cause death, it can cause pain, psychological burdens, and economic burdens to patients. Current conservative treatments for IVDD can relieve pain but cannot reverse the disease. Patients who cannot tolerate pain usually resort to a strategy of surgical resection of the degenerated disc. However, the surgical removal of IVDD can affect the stability of adjacent discs. Furthermore, the probability of the reherniation of the intervertebral disc (IVD) after surgery is as high as 21.2%. Strategies based on tissue engineering to deliver stem cells for the regeneration of nucleus purposes (NP) and annulus fibrosus (AF) have been extensively studied. The developed biomaterials not only locally withstand the pressure of the IVD but also lay the foundation for the survival of stem cells. However, the structure of IVDs does not provide sufficient nutrients for delivered stem cells. The role of immune mechanisms in IVDD has recently become clear. In IVDD, the IVD that was originally in immune privilege prevents the attack of immune cells (mainly effector T cells and macrophages) and aggravates the disease. Immune regulatory and inflammatory factors released by effector T cells, macrophages, and the IVD further aggravate IVDD. Reversing IVDD by regulating the inflammatory microenvironment is a potential approach for the treatment of the disease. However, the biological factors modulating the inflammatory microenvironment easily degrade *in vivo*. It makes it possible for different biomaterials to modulate the inflammatory microenvironment to repair IVDD. In this review, we have discussed the structures of IVDs and the immune mechanisms underlying IVDD. We have described the immune mechanisms elicited by different biological factors, including tumor necrosis factors, interleukins, transforming growth factors, hypoxia-inducible factors, and reactive oxygen species in IVDs. Finally, we have discussed the biomaterials used to modulate the inflammatory microenvironment to repair IVDD and their development.

KEYWORDS

intervertebral disc degeneration, lower back pain, nucleus pulposus, annulus fibrosus, biomaterials

1 Introduction

Intervertebral disc degeneration (IVDD) is a common clinical form of spinal degeneration. Inflammation, oxidative stress, and mechanical stimulation may lead to an imbalance of the anabolic and catabolic processes in the extracellular matrix (ECM) of intervertebral discs (IVDs) and loss of nucleus pulposus (NP), leading to IVD dysfunction and structural damage (1, 2). IVDD leads to the partial or complete rupture of annulus fibrosus (AF). The NP protrudes backward from the ruptures, irritating or compressing the nerve root and causing low back and leg pain (3). IVDD is one of the leading causes of chronic low back pain (LBP) in patients (4). Clinically, approximately 40% of LBP cases are due to discogenic causes (5). Although IVDD does not have a fatal impact on patients in the short term, it is a significant cause of disability and socioeconomic stress (6). In the U.S. alone, for example, indirect and direct costs of LBP costs over $100 billion (7).

IVDs are the fundamental motor units of the spine. They have high compressive and tensile strengths, which can maintain the axial pressure of the spine and ensure the axial flexibility of the body (8). IVDD is an abnormal, cell-mediated response to progressive structural damage (9). The decreased height of the degenerative IVDs changes the stress-bearing spine segment and accelerates the degeneration of other adjacent segments. The late stage of IVDD causes the chronic instability of spinal segments, which seriously affects the quality of life of patients (10). The prevalence of IVDD is rising owing to risk factors such as aging, obesity, chronic stress, and smoking (7). Currently, the leading conservative treatment methods for IVDD are anti-inflammatory analgesia and physical therapy (11). Conservative treatments can only delay degeneration, slow down the rate of IVD degradation, and temporarily relieve pain, but cannot reverse IVDD (12). Patients with advanced IVDD can undergo surgical decompression and disc replacement (13). However, surgical resections of IVDs can still lead to re-protrusion. In a 2015 meta-analysis, the reherniation rate after lumbar disc herniation was found to be as high as 21.2% (14). Surgical treatments aim for symptomatic relief but increase the pressure and risk of injury to discs adjacent to the affected IVD (15).

Current regenerative IVD technologies based on tissue engineering have achieved encouraging results (16). For example, biomaterials for the repair of NP and AF have regenerated IVDs in animals by carrying mesenchymal stem cells (MSCs) like bone marrow-derived mesenchymal stem cells (BMSCs), adipose-derived mesenchymal stem cells (ADSCs) and induced pluripotent stem cells (iPSCs) (17–23). Cartilage endplate-derived stem cells (CESCs), annulus fibrosus-derived stem cells (AFSCs), and nucleus pulposus-derived stem cells (NPSCs) can also replace the IVD (21, 24–26). IVDD can also secrete Stromal cell-derived factor-1α (SDF-1α) to induce the chemotaxis of NPSCs to the NPs center for *in situ* regeneration (27). IVD regeneration is mainly achieved by inducing the differentiation of MSCs into NPCs or AFCs (28–30). Although MSCs have achieved good results in bone and cartilage regeneration, similar effects cannot currently be exerted in IVDD, even if the MSCs were delivered to IVDs, due to the lack of vascular systems in the discs (31). This is because MSCs cannot absorb sufficient nutrients during IVDD. The harsh environment of IVDD is unsuitable for NPSCs and MSCs to proliferate and repair NPs. Although current cell transplantation technologies can regenerate IVDs, cell transplantation strategies remain insufficient, and the regeneration of IVDs cannot be completed in a time-efficient manner (32).

Studies have shown that when IVDs degenerate, NP that initially maintained immune tolerance become targets of immune system attacks (33, 34). T cells, macrophages, and inflammatory factors like interleukin (IL)-1β, tumor necrosis factor (TNF)-α) are recruited around NP. The inflammatory response caused by IL-1β, TNF-α, and reactive oxygen species (ROS) further amplifies the inflammatory response locally and accelerates IVDD (35). Impaired AF and prominent NP cause IVD to lose its physical barrier, and IVD is fully exposed to the immune system. While removing cellular debris and foreign bodies, T cells and macrophages destroy normal AF and NP, further exacerbating damage to IVD. Macrophages are divided into two types according to their role: M1 type and M2 type. M1 macrophages are pro-inflammatory cells, and M2 macrophages are anti-inflammatory cells. While M1 macrophages have the effect of phagocytosing necrotic matter in the early stages of inflammation, excessive inflammation can exacerbate the progression of IVDD. M2 macrophages are mainly manifested as promoting tissue repair (33). Therefore, the inhibition of IVDD by regulating the inflammatory microenvironment is feasible. However, biological factors that regulate immunity (such as growth and inflammatory factors and chemokines) are easily degraded *in vivo* and cannot meet the long-term requirements for IVDD repair (5, 36). Furthermore, IVDs do not have a vascular system and cannot transport biological factors through systemic administration. A feasible way to repair IVDD is to inject biological factors into IVDs by designing biomaterials. Biomaterials based on chitosan and alginate have good biocompatibility and can not only treat IVDD by regulating the inflammatory microenvironment but also by carrying immune regulators (34, 37). In this review, we have discussed the structures of IVDs, the immune mechanisms of IVDD, and the effects of inflammatory immune factors such as IL-1β and TNF-α on IVDD. Finally, we have discussed the various biomaterials that regulate IVDD repair in the inflammatory microenvironment (Figure 1; Table 1) and their development.

2 Intervertebral discs and their mechanisms in inflammatory-immunity

IVDs are the connecting parts and are the most fundamental functional units of the spine. IVDs consist of three tissue types: the central gelatinous NP, surrounding AF tissue, and upper and lower cartilage endplates (CEPs). The IVD cartilaginous tissue in the spine acts as a shock absorber, assists in the movement of vertebral bones, and holds the vertebrae together to coordinate the direction of the spine (57). The IVD has been identified as an immune privilege organ (34). As the IVD aging process or traumatic injury occurs, immune and inflammatory cells infiltrate the IVDs. These cells and cytokines produce pro-inflammatory substances while clearing necrotic cells, leading to disturbances in the inflammatory microenvironment and

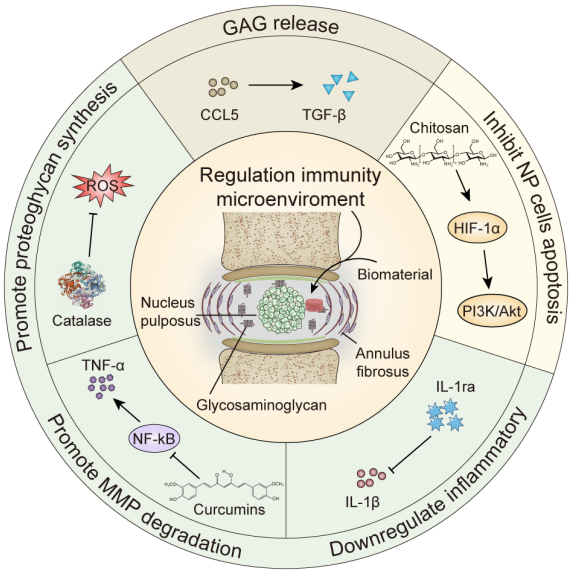


FIGURE 1
Biomaterials regulate cytokine repair of intervertebral disc degeneration. GAG, glycosaminoglycan; MMP, matrix metalloproteinase; HIF-1α, hypoxia inducible factor-1α; IL-1ra, Interleukin -1 receptor antagonist; TNF, tumor necrosis factor; ROS, reactive oxygen species.

aggravating IVDD (58). Therefore, understanding the connection between the structure of IVDs and the immune system is crucial in elucidating the mechanisms of IVDD.

2.1 Nucleus pulposus

NP consists of water, type II collagen, chondrocyte-like cells, and proteoglycans. These structures make NP elastic to resist pressure on the spine and transmit the pressure to AF and surrounding CEPs (59). The absence of nerve cells or blood vessels within NP allows NP to become an immune-privileged organ (33). Recently, an increasing number of studies have shown that maintaining immune privilege requires using various molecular biology techniques. For example, NP can express the Fas ligand (FasL) to induce the apoptosis of T cells and macrophages to maintain their immune tolerance (60). In addition, FasL expressed by NP can also lead to the apoptosis of vascular endothelial cells. AF and CEPs tightly surround NP to isolate NP from the host immune system (34). These main mechanisms make normal NP immune to attacks by the immune system and contribute significantly to maintaining IVD stability.

As IVDD progresses, AF ruptures, and NP protrudes, so the barrier between the IVD and the immune system is broken. The damage exposes the NP that was originally immune-privileged to the

TABLE 1 Biomaterials regulate the inflammatory microenvironment to repair degenerated intervertebral discs.

Regulator	Biomaterial	Production Method	Therapeutic components	Target	Result	Reference
TGF	Fibrin hydrogels	Fibrinogen	CCL5	AF	Fibrin hydrogels release CCL5 for the chemotaxis homing effect of AF cells, but do not promote AF cell repair in sheep.	(38)
TGF	pullulan microbeads	Fitc-pullulan was dissolved in 20 mL of distilled water under magnetic stirring and lyophilized after the addition of a cross-linking agent. Pullulan microbeads (PMBs) and 500 u of LCCL5 and TGF-β1 were magnetically stirred for 24 h.	CCL-5 TGF-β1	ECM	PMBs were loaded with CCL5/TGF-β1/GDF-5 continuously and sustainably released growth factors and maintained their biological activities *in vitro*. Increased distance that ASCs can migrate to NP.	(39)
TGF	Collagen-Polyurethane scaffold	Polyurethane (PU) was dissolved in N,N-dimethylformamide solution, and the PU film was formed after evaporating the solvent. Type I collagen fibers were used as cell carriers to encapsulate AF cells and TGF-β1 on PU membranes to make collagen-PU scaffolds.	AF cells TGF-β1	AF ECM	The TGF-β1 treatment of collagen hydrogels further promotes cell proliferation and matrix production in AF cells *in vitro*.	(40)
	chitosan (CH)-based scaffold	Mixing chitosan with porcine gelatin at a ratio of 3:2 can further increase the biological	Link	ECM	LN increased GAG production in degenerative media to the same level as that of TGF-β. The addition of 1% gelatin to the CH hydrogel further increased GAG production *in vitro*.	(41)

(Continued)

TABLE 1 Continued

Regulator	Biomaterial	Production Method	Therapeutic components	Target	Result	Reference
		response of encapsulated cells by adding gelatin and Link N (a peptide present in IVDs).				
	TGF-β3@PDA NPs	PDA NP were prepared through chemical oxidative polymerization using dopamine (DA) and tris-(hydroxymethyl)-aminomethane (Tris). TGF-β3 was loaded onto the surface of PDA nanoparticles in a covalent binding manner.	TGF-β3	AF NP	The released GFs could induce the differentiation of BSMCs into myeloid and annulus-like cells and maintain high activity. Finally, *in vivo* experiments confirmed that the reconstituted IVD scaffolds exhibited region-specific stromal phenotypes with histological and immunological features.	(42)
	Genipin Fibrin Gel	Genipin and fibrinogen in a humidified incubator for 3–4 h for polymerization and cross-linking.	TGF-β3	ECM	Fibrin increases integrin binding sites and prevents partially encapsulated cells from undergoing apoptosis, allowing encapsulated cells to increase ECM synthesis *in vitro*.	(43)
	gelatin-hyaluronic acid methacrylate (GelHA) hydrogel	Methacrylic anhydride (MA) was added to the gelatin solution and allowed to react for 1 h. The resulting solution was dialyzed for 3 days and lyophilized. Photoinitiators and integrins were added, and photocrosslinking was performed under UV light irradiation for 2 min.	integrin	ECM	The combination of photocrosslinked GelHA hydrogel and ASC can enable ASC to undergo NP-like differentiation and enhance the efficacy of ASC for IVD repair by activating the integrin αvβ6-TGF-β1 pathway *in vitro*.	(44)
IL-α	HA-pNIPAM	Gelatin was combined with EGCG, mixed with water, and stirred at 40°C for 4–6 h. Poly-N-isopropylacrylamide was directly grafted onto HA. Gelatin was directly applied to (HA-pNIPAM).	EGCG	ECM	EGCG microparticles combined with a suitable carrier can modulate the activity/release of EGCG in the IVD *in vitro*.	(45)
IL	HMw-HA Gel	HMw sodium hyaluronate was dissolved in 1 mL of distilled water and mixed with PGE-amine to induce cross-linking to obtain spherical hydrogels.	–	ECM	The hydrogels inhibited the expression of the inflammatory receptors IL-1R1 and MyD88, downregulated NGF and BDNF gene expression, and upregulated CD44 receptor expression *in vitro*.	(46)
IL	PLGA Microspheres	After mixing IL-1ra with 1 mL of 75:25 PLGA and sonicating the mixture, 1% polyvinyl alcohol (PVA) magnetic stir bar was added and mixed for 3 h.	IL-1ra	NP	IL-1ra delivered from PLGA microspheres effectively attenuated IL-1β-mediated inflammatory changes in engineered NP constructs *in vitro*.	(47)

(Continued)

TABLE 1 Continued

Regulator	Biomaterial	Production Method	Therapeutic components	Target	Result	Reference
IL	Chitosan/Poly-γ-glutamic acid nanoparticles	Chitosan/Poly-γ-glutamic acid was mixed at a molar ratio of 1:1.5 to prepare nanoparticles by the co-coagulation method. Diclofenac (Df) was added to the nanoparticles and stirred at a constant speed.	Df	ECM	The intradiscal injection of Ch/Df/γ-PGA NPs reduced pro-inflammatory mediators, downregulated MMP 1 and 3 expression, and upregulated Col II and Agg production in a pro-inflammatory/degenerative IVD organ culture model *in vitro*.	(48)
TNF	ELP-curcumin conjugates	Elastin-like polypeptide (ELP) is a thermoresponsive biopolymer composed of Val-Pro-Gly Xaa-Gly pentapeptide repeating units. Curcumin is chemically modified and coupled with ELP.	Curcumin	ECM	The ELP-curcumin conjugate rapidly forms a depot after physiological administration and slowly releases bioactive curcumin in the perineural space to treat neuroinflammation *in vitro*.	(49)
	pNIPAAM MgFe-LDH Gel	N-isopropylacrylamide forms a pNIPAAM polymer *via* free radical polymerization. Polymers with MgFe layered double hydroxide (LDH) nanoparticles and CXB were dissolved in water.	CXB	ECM	The controlled release of CXB from this hydrogel resulted in the inhibition of PGE 2 in a mice model of spontaneous IVD degeneration.	(50)
HIF	Small leucine-rich proteoglycans	–	–	ECM	Biglycan can bind and (TGF-β) to activate the MAPK pathway to enhance HIF-1α translation *in vitro*.	(51)
	Chitosan-alginate gel scaffold	Chitosan was dissolved in acetic acid, and after filtering the solution, the pH was adjusted to 8.5 with 0.1 mol/L NaOH. The sterile alginate solution was then mixed with the chitosan solution at a ratio of 1:1.	ADSC	NP ECM	ADSCs grew well in the C/A gel scaffolds, differentiated into NP-like cells under certain induction conditions, produced the sameECM as NP cells, and were promoted under hypoxia *in vitro*.	(52)
	Nanofibrous spongy microspheres	Development of poly (L-lactic acid) grafted poly(hydroxyethyl methacrylate) (PLLA-g-PHEMA) nanoparticles using the phase separation method. miR-199a was encapsulated in nanoparticles using the double emulsion technique.	miR-199a	NP	Sustained release of *in situ* anti-miR-199a inhibits miR-199a, which in turn enhances HIF-1α and Sox-9 activity, thereby inhibiting calcification and promoting NP regeneration in mice.	(53)
	Polymer capsule	Calcium carbonate was used as a sacrificial template to fabricate catalase-loaded polymer capsules functionalized with an outer layer of tannic	Catalase	ECM	ROS-responsive polymer capsules reduce the potential for oxidative stress and downregulate MMP expression in the ECM.	(54)

(Continued)

TABLE 1 Continued

Regulator	Biomaterial	Production Method	Therapeutic components	Target	Result	Reference
		acid (TA) by a layer-by-layer approach.				
ROS	Rapamycin hydrogel	The ROS-labile linker was synthesized *via* the quaternization reaction of tetramethylpropane-1,3-diamine with an excess of 4-(bromomethyl) phenylboronic acid. Cross-linking of the ROS-labile linker with poly(vinyl alcohol) (PVA) to form ROS-scavenging hydrogels for loading rapamycin.	Rapamycin	ECM	ROS-responsive hydrogel scaffolds and rapamycin can reduce ROS levels and promote macrophage polarization to M2 type *in vitro*.	(55)
	Alginate scaffold	The sodium alginate solution was diluted with sterile saline, then the Perfluorotributylamine emulsion was added and sonicated.	–	NP ECM	Perfluorotributylamine -enriched alginate scaffolds promote NP cell survival and proliferation *in vitro*. Furthermore, Perfluorotributylamine can modulate ECM expression to generate disc-like tissue grafts in mice.	(56)

GAG, glycosaminoglycan; MMP, matrix metalloproteinase; HIF-1α, hypoxia inducible factor-1α; IL-1ra, Interleukin -1 receptor antagonist; TNF, tumor necrosis factor; ROS, reactive oxygen species; ECM, extracellular matrix; CCL-5, chemokine (C–C motif) ligand; ELP, elastin-like polypeptide; CXB, celecoxib; NGF, nerve growth factors.

immune system so that they become targets for immune system attacks (33). Nerve root compression and the autoimmune response to NP are the critical causes of radicular pain in the late stage of IVDD (58). A large number of macrophages, T cells, B cells, and natural killer (NK) cells and cytokines (such as fibroblast growth factors, IL family members, and TNFs) are recruited around nerve roots, causing nerve root immune stress pain (13, 34, 61). The infiltration of inflammatory cells removes necrotic cells. At the same time, excessive inflammatory cells also remove non-necrotic cells, which aggravates the destruction of IVD by the immune system (62). Studies have shown that macrophages are the inflammatory cells that infiltrate IVDs and are associated with IVDD progression (63). This is due to the upregulation and activation of p38 in IVDD. The activation of p38 in NP induces macrophage polarization and the expression of the catabolic enzyme matrix metalloproteinase-13 (MMP-13). Overexpressed MMPs destroy the ECM, thereby aggravating the degenerative process (63). The difference in macrophage phenotypes between degenerated and normal IVDs may be a novel target for therapies.

2.2 Annulus fibrosus

AF is highly fibrotic tissue that surrounds the exterior of the NP. AF mainly contains type I collagen produced by fibroblasts and contain type II collagen produced by fibrochondrocytes (64). This unique structure provides AF with good mechanical properties. AF tightly protect NP in the inner layer and provides a foundation for maintaining the structure of IVD (34). There are various stem cells present around AF. These stem cells contribute to maintaining the turnover of AF (65). With increasing age, the numbers of stem cells gradually decrease and become insufficient to repair damaged AF promptly, which is the main reason for the impaired healing of AF (66). After AF is damaged, T cells and macrophages are activated to clear the damaged tissue and debris. Intercellular adhesion molecule 1 (ICAM1) is an inducible surface glycoprotein that induces the adhesion, migration, and invasion of lymphocytes to sites of degeneration during immune responses (67). Studies have shown that chemokine ligand CCL-2 can differentiate monocytes into macrophages and that macrophage infiltration is a significant cause of IVDD-induced radicular pain (68). Although T cells and macrophages are recruited to clear damaged AF, T cells and macrophages also aggravate AF damage (66). This balance is difficult to grasp, but modulating it to tilt it in the desired direction may be a new target for IVDD immunotherapy.

2.3 Cartilage endplates

CEPs are thin layers of hyaline cartilage that separate IVDs from the upper and lower vertebral bodies. IVDs, composed of CEPs, NP, and AF, protect the bones of the vertebral body from mechanical damage and maintain the normal physiological movement of the spine. Unlike NP and AF, CEPs have a vascular system. The nutrient metabolism of IVDs is mainly dependent on the vascular system within CEPs (69). CEPs are composed of hyaluronic acid (HA), type II collagen, and PECM secreted by chondrocytes (70). The ECM is rich in stem cells, which are advantageous not only in osteogenesis and chondrogenesis (71) but also in replacing AF and NP. Studies have shown that HIF-1α is highly expressed in NP owing to hypoxia (72). HIF-1α induces the differentiation of cartilage endplate stem cells (ECSCs) into NP (73, 74). CEP-derived exosomes (N-Exos)

reduce apoptosis of CEP by activating the phosphoinositide 3 kinase/protein kinase B (PI3K/AKT) signaling pathway (74). The mechanisms play an essential role in maintaining the structure of IVDs.

IVDD is associated with inflammation, immune cell infiltration, and neovascularization (2). These processes facilitate tissue repair in normal tissues. In the inflammatory microenvironment of IVDD, however, they exacerbate pain (75). Although the mechanisms by which T cells and macrophages are involved in the progression of IVDD are unclear, the passage of the disease may be due to the immune privilege of IVDs (62). The involvement of inflammatory factors and cytokines (such as IL-6, IL-1β, VEGF, and TNF-α) in the degeneration process can aggravate degeneration and cause pain (13). Therefore, reducing radicular pain and reversing the progression of IVDD by modulating the inflammatory microenvironment may be an effective treatment for IVDD.

3 Regulation of the inflammatory microenvironment

Protruding NP-secreted cytokines can worsen radicular pain and IVDD (33). Since there are no immune cell populations in the early stages of IVDD, the clearance of necrotic cells cannot be completed in a timely manner (13). Cells with phagocyte function are beneficial early in injury. Therefore, we hypothesize that infiltrating cells may perform specialized tasks in the healing processes of IVDs, whereas local phagocytosis-related cells fail to manifest at sufficient levels or at the right time (76). Therefore, the artificial intervention of cytokine release and induction of T cells and macrophages may be potential therapeutic strategies for IVDD.

3.1 Promotes the upregulation of anti-inflammatory factors

Transforming growth factor-β (TGF-β) is a multifunctional cytokine closely related to cell differentiation, apoptosis, and the maintenance of cell stability (77, 78). Many cells in the body, such as epithelial cells, tumor cells, immune cells, and stromal fibroblasts, can differentiate into inactive TGF-β complexes, which proteolytically leak TGF-β entities (79). There are three main isoforms of TGF-β (TGF-β1, -β2, and -β3) that cause different physiological responses after binding to their corresponding receptors (80). TGF-β receptors have many co-receptors in addition to the type I and II superfamily receptors (81). These receptors are widely present on the surfaces of body tissues and cells, making the body responses caused by TGF-β diverse (81). For example, TGF-β is a potent immunosuppressant and is closely related to the escape of cancer cells from immune system attacks (82). Studies have shown that TGF-β1 increases the contractility of myofibroblasts during wound healing, inhibits proteolytic enzymes in the ECM, and plays a crucial role in tissue remodeling (83). TGF-β1 further blocks IVDD by inhibiting the expression of chemokine (C–C motif) ligand 4 (CCL4) through extracellular signal-regulated kinase signaling (84). The inhibition of CCL4 by TGF-β1 occurs time- and dose-dependent. TGF-β1 can further inhibit the expression of IL-1β and TNF-α, thereby inhibiting the inflammatory response of IVDD (85, 86). The resolution of inflammation may therefore relieve the radicular pain caused by disc degeneration (87).

Systemic CCL5 is associated with discogenic back pain and moderate/severe IVDD. CCL5 can therefore be considered a biomarker for the diagnosis and monitoring of IVDD (88). Studies have confirmed that prominent NP can release CCL5 to induce MSCs to migrate into degenerated IVDs and promote their regeneration (89). Therefore, it is plausible that targeting CCL5 in IVDD could benefit disc repair. Zhou et al. used fibrin gel to target CCL5 around degenerated IVDs for their regeneration (38). CCL5 within fibrin gel is released around NF in a dose-dependent manner. Although CCL5 has a chemotaxis-homing effect on AF *in vitro* experiments, it does not promote IVDD regeneration in sheep IVDD models. This may have been because fibrin gel does not effectively encourage the movement of cell (38). In another study, Frapin et al. labeled pullulan with fluorescein isothiocyanate isomer I (FITC) (39). FITC-pullulan was stirred with NaOH solution and sodium trimetaphosphate to make pullulan microbeads (PMBs) carrying CCL5 to the degeneration sites. The PMBs adsorbed CCL5 and released 99% of it around the IVDs sustainably within 21 days. A significant increase in the migration distance of PMB-induced ADSCs to NPs and the number of ADSCs was observed on day 21 *in vitro* (39).

Since CCL5 cannot effectively induce TGF-β, the direct regulation of TGF-β may be beneficial to induce AF cells to differentiate and repair IVDs. Zhi et al. dissolved a prepared polyurethane (PU) fiber scaffold in an N, N-dimethylformamide solution and evaporated the solvent to form a PU film (40). The synthesis methods of the materials are shown in Table 1. Type I collagen fibers was used as cell carriers to encapsulate AF cells pretreated with TGF-β1 on PU membranes to create collagen-PU scaffolds. The advantage of PU scaffold is the continuous release of TGF and type I collagen to maintain the AF phenotype. *In vitro* experiments, the gene and protein expressions of AF cells were enhanced after induction by TGF-β1. It seems to indicate that AF cells pretreated with TGF-β1 may be a suitable cell source for the repair of AF ruptures (40). However, PU scaffolds have low porosity and are insufficient to carry a sufficient amount of TGF-β to maintain long-term effects. In addition, no animal experiments have proven this claim. Lerouge et al. mixed chitosan and porcine gelatin at a ratio of 3:2 to prepare chitosan hydrogels for loading NP cells (41). The peptide Link N (a peptide present in IVDs) outside the IVDs was further encapsulated in the hydrogels. The addition of Link polypeptide increased the NP encapsulation rate in hydrogels and increased NP deposition in a degenerative environment. Compared to the control group, the chitosan hydrogels induced more glycosaminoglycan (GAG) release from NP cells at 14 days *in vitro*. The increase in the number of GAGs was caused by the enhancement of NP cell activity. This increase in GAG release was nearly identical to that induced by TGF-β. This indicates that both induced AF and NP can repair IVDs. However, this is limited to early IVDD (90). In addition, most of these studies were conducted *in vitro*. It is, therefore, not yet known whether the effects *in vivo* are similar.

Connective tissue growth factor (CTGF) plays an essential role in extracellular matrix synthesis, especially in IVD (91). CTGF injections have been shown to promote the increased synthesis of human NP

cells and induce decreased anti-inflammatory cytokines (92).Sun et al. fabricated PDA-NP scaffolds with dopamine and polycaprolactone (PCL) using 3D printing technology (Figure 2) (42). The synthesis methods of the materials are shown in Table 1. TGF-β3 and CTGF were loaded onto the surface of PDA-NP through covalent binding, forming a 3D-printed scaffold that could release dual growth factors for the reconstruction of NP and AF. CTGF is a cysteine-rich stromal cell protein involved in cell proliferation, differentiation, and connective tissue differentiation (93). PCL, which is widely used in 3D printing, was selected as the mechanical support for IVD scaffolds because of its good biodegradability and biocompatibility (94). PDA NPs have a diameter of 324.2 ± 13.9 nm. The loading efficiencies of CTGF and TGF-β3 for PDA NPs were 70.04 ± 0.94% and 72.34 ± 1.06%, respectively. PDA-NP released CTGF and TGF-β3 slowly and continuously (Figure 2B) and induced bone marrow stromal cells to differentiate into fibrocartilage-like cells (main components in the area around AF) and hyaline chondroid cells (main components in the area around NP). After 3 months of *in vivo* experiments, it was found that PDA-NP could effectively promote the expression of type I collagen, aggrecan (Figure 2C), and GAG in the AF and NP regions without causing apparent inflammation (Figure 2D) (42). However, not all fibrin types are good cellular carriers. For example, genipin-crosslinked fibrin (FibGen) is a viscous, high-modulus biomaterial that matches the properties of AF and exhibits low risk of hernias (95). FibGen is cytotoxic and induces the apoptosis of AF cells. In one study, the acute cytotoxicity of FibGen was reduced by modifying the binding sites of integrins to FibGen (43). The synthesis methods of the materials are shown in Table 1. The advantage of FibGen hydrogel is that the addition of integrins reverses apoptosis and increases TGF-β encapsulation (44, 96). The improved FibGen hydrogel carried TGF-β3 to repair AF *in vitro*. However, the toxicity of FibGen to normal AF still needs to be noted.

Although biomaterials loaded with TGF-β have achieved the ability to promote the reconstitution of NP and AF *in vivo*, this has

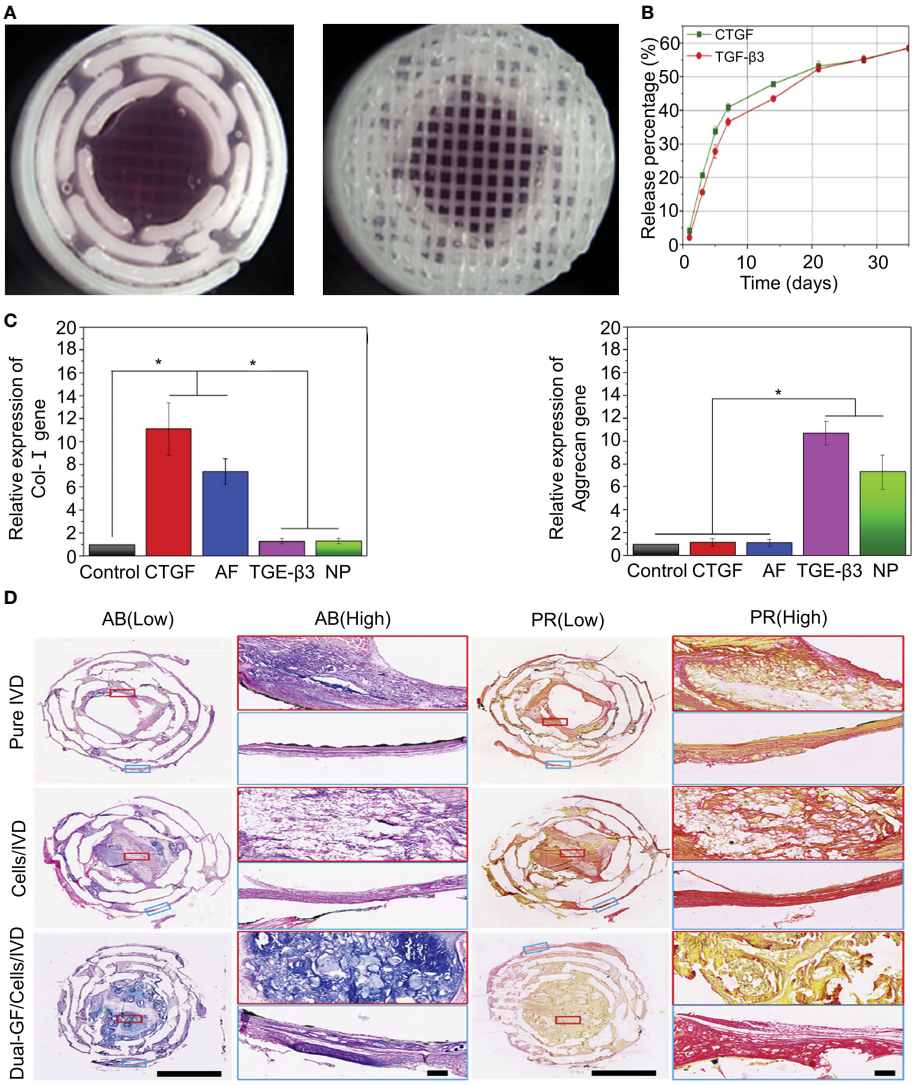


FIGURE 2
(A) Stereomicroscope images of the intermediate and surface structures of the 3D-printed scaffolds. **(B)** Release behavior of CTGF and TGF-β3 in the IVD scaffolds. **(C)** Expression of the type I collagen and aggrecan genes after inducing differentiation in different groups. **(D)** Histological staining of the intermediate layers of three IVD scaffolds with AB and PR dyes. Magnified images at low and high magnification. AB and PR dyes specifically stained GAG (blue) and type I collagen (red), respectively. Reproduced with permission from (42). *Indicates significant difference at a 99 %confidence level.

only been verified in mice and not in large animals. Furthermore, TGF-β induces the differentiation of ADSCs into AF and NP cells only at the early stage of degeneration. As we have learned, IVDD is challenging to detect in the early stages, and most patients are diagnosed in the late stage when they have radicular pain. Therefore, whether TGF-β can reverse advanced IVDD remains unknown.

3.2 Inhibits the expression of inflammatory factors

3.2.1 Interleukins inhibits

IL-1β is the most widely studied inflammatory factor in IVDD and is associated with inflammatory radiculopathy (13). IL-1β accelerates IVDD mainly by inducing the expression of MMPs in the ECM (35, 97). This process primarily depends on wingless-related integration site (Wnt)/β-catenin signaling (98). Studies have shown that the expression of Wnt1 and β-catenin in the NP of patients with lumbar disc herniation is significantly higher than that in regular patients. The activation of Wnt signaling induces senescence in NPC cells. Furthermore, the activation of Wnt/β-catenin signaling induces MMP expression, leading to increased ECM breakdown and IDD progression (99). Studies have confirmed that inhibiting Wnt/β-catenin signaling slows IVDD (100). As inflammatory factors can induce accelerated IVDD, the downregulation of local inflammation may restore IVDD.

Epigallocatechin 3-gallate (EGCG) exhibits anti-inflammatory, anti-catabolic, and antioxidant activities in IVD cells (101). EGCG interferes with the pro-inflammatory IL-1β cascade by reducing the activity of IRAK1–NF-κB/JNK/p38 signaling (101). However, oral EGCG does not increase intra-IVD EGCG concentrations, and high doses of EGCG increase hepatotoxicity and nephrotoxicity (102). Loepfe et al. used electrospray technology to encapsulate EGCG in porcine gelatin to produce gelatin microparticles (45). Electrospraying is a mild electrohydrodynamic encapsulation method that produces solid particles without needing high temperatures or toxic solvents. The average diameter of the gelatin microparticles was 661 ± 120 nm. The drug loading of gelatin microparticles reached 5.42 wt% and sustained the release of EGCG (80%) within 7 days. *In vitro* experiments confirmed that the gelatin microparticles significantly inhibited the expression of IL-1β. However, it has not been confirmed whether the gelatin microparticles have anti-inflammatory effects in the IVDD environment *in vivo*. A recent study further showed that IL-1β induces the mRNA expression of nerve growth factors (NGFs) and brain-derived neurotrophic factors (BDNFs) in degenerative NP cells (103). These neurotrophic factors have been shown to induce neural growth in IVDs (104). A normal IVD has no nerve tissue, and neuropathic pain occurs when neurotrophic factors induce nerve ingrowth into the IVD. Pandit et al. cross-linked high molecular weight (HMw)HA and 1-ethyl-3-(3-(dimethylamino)propyl) carbodiimide (EDC) to develop the cross-linked HA hydrogel system (Figure 3) (46). The synthesis methods of the materials are shown in Table 1. This study confirmed that the cross-linked HA hydrogel system with different doses of HA did not cause NP cell death *in vivo* (Figure 3B). The cross-linked HA hydrogel system could bind to the CD44 receptor on the surface of NPc and interfere with the binding of the CD44 receptor to IL-1β. After blocking the binding of IL-1β to CD44, the downregulation of NGF and BNGF mRNA expression provided a protective mechanism for inflammation-related pain (Figure 3C). However, the cross-linked HA hydrogel system only relieved neuropathic pain. It did not treat the underlying degeneration or restore the natural function of IVDs. This phenomenon may be caused by HA competing with IL-1β for its receptors. But this effect is weak enough to inhibit IL-1β completely. To increase the long-term inhibitory effect on IL1-β, Smith et al. mixed poly(lactic-co-glycolic acid) (PLGA) and IL-1 receptor antagonist (IL-1ra) to produce PLGA microparticles (47). The synthesis methods of the materials are shown in Table 1. *In vitro* experiments showed that PLGA microparticles could release IL-1ra continuously for 35 days. However, *in vivo* experiments demonstrated that PLGA microparticles effectively inhibited IL-1β for 7 days and that the effect of IL-1ra beyond 7 days was to reduce GAG loss. This difference is not due to insufficient IL-1ra but to a lower pH at the release site due to PLGA degradation. Therefore, the degradation properties of biomaterials are essential, and we must develop biomaterials that are more suitable for substance delivery.

Chitosan is a natural, biocompatibile, and biodegradable polysaccharide that is mainly used in drug delivery systems and tissue engineering (105). The chitosan surface polarizes macrophages into the M2 phenotype without causing significant T cell proliferation. Goncalves et al. prepared nanoparticles using a combination of chitosan and poly γ-glutamic acid (γ-PGA) for the coacervation method (48). Diclofenac (Df) was added to the nanoparticles to form Ch/Df/γ-PGA NP. The diameter of the nanoparticles was 175 ± 32 nm. The Df reduces the local inflammatory response and the production of pro-inflammatory cytokines (IL-1β and IL-6) by inhibiting the cyclooxygenase (COX)-2 pathway. In addition, down-regulation of MMPs expression in ECM was detected 7 days after NP injection, and IVDD was remodeled *in vitro*. The Ch/Df/γ-PGA NP has promising prospects for development. However, animal experiments were not performed in this study, and it is not yet known whether Ch/Df/γ-PGA NP was advantageous in IVD anti-inflammatory activity and the remodeling of IVDD.

Acid-sensing ion channels (ASICs) are expressed in the nervous system and are mainly activated by extracellular acid regulation (106). ASIC3 is mainly expressed in the peripheral nervous system and, to a lesser extent, in the central nervous system (CNS) (107). Hyperactivation of ASIC-3 induces the expression of proinflammatory cytokines in the NPs. APETx2 is an antagonist of ASIC3. Blocking ASIC3 reduces local inflammation and reduces inflammatory pain (107). Bian et al. designed a "peptide-cell-hydrogel" GelMA microsphere for the control of intervertebral disc inflammation (108) (Figure 4A). The carboxyl on the microsphere surface was activated by EDC/NHS, followed by being covalently linked to the amino residue on the APETx2 to form APETx2-GelMA microsphere (GA) (Figure 4B). NP cells were premixed with GA to make a "peptide-cell-hydrogel" GelMA microsphere (GNA). The hydrogel has an elastic modulus of 25.23 ± 2.58 kPa, which can protect NP cells from shear damage. Detected at week 8 after GNA infusion into degenerate discs in mice, GNA downregulated ASIC-3 expression, decreased peripheral IL-1β expression, increased proliferative activity, and enhanced ECM deposition

10.3389/fimmu.2023.1051606

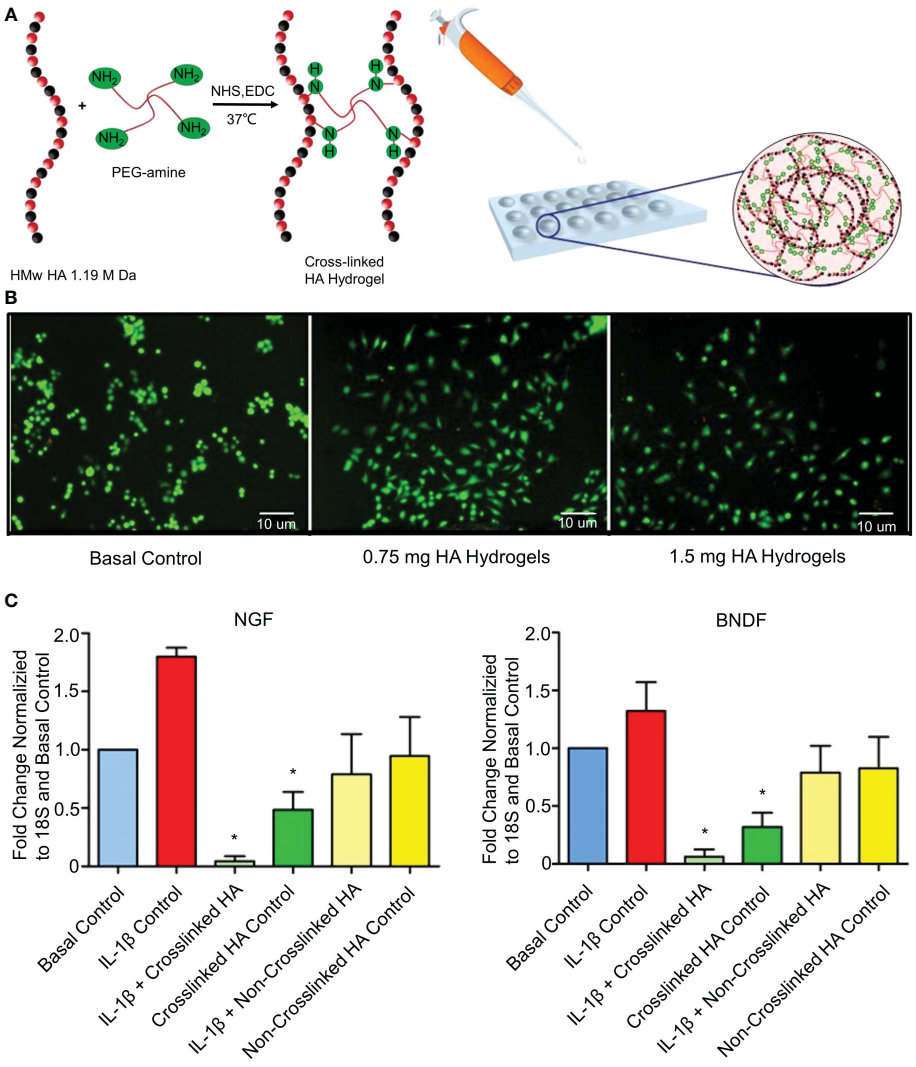


FIGURE 3
(A) Schematic diagram of the synthesis of the cross-linked HA hydrogel system. **(B)** Stained NP cell morphology by the LIVE/DEAD assay after 3 days of culture in the presence of hydrogels containing different doses of HA. Live cells are green (calcein staining) and dead cells are red (ethidium bromide staining). **(C)** Fold changes of NGF and BNDF downregulated in IL-1β-induced inflammation and normal NP cells treated with cross-linked HA hydrogels for 7 days. Reproduced with permission from (46). *Indicates significant difference at a 99 %confidence level.

IL-17 is a crucial characteristic cytokine of T-helper 17 (Th17) cells. Th17 is the primary source of IL-17. The innate immune system can further secrete IL-17 (109). IL-17 is associated with inflammation, and increasing evidence has shown that IL-17 is involved in the occurrence and progression of IVDD (110–112). There is no IL-17 in normal AF and NP, and elevations of IL-17 can be detected in degenerative structures (113). Importantly, the expression of IL-17 in IVD tissues has been found to increase with the severity of IVDD. Therefore, IL-17 levels may be associated with the extent of IVDD (112). IVDD exposure to TNF-α stimulates the production of IL-17, which promotes the degradation of the ECM mainly through the IL-17A receptor-nuclear factor kappa B (NF-κB) pathway (114). IL-17A receptors are mainly distributed on the surfaces of NP cells; therefore, the inhibition of IL-17A receptors can attenuate ECM degradation and delay IVDD. This approach has not been reported so far, but we speculate it may be a new target for slowing IVDD.

Biomaterials for the treatment of IL-regulated IVDD have also been reported. However, the studies were primarily performed *in vitro* with cellular experiments to verify its role in IVDD. There are a few reports of 3D-printed biomaterials that simulate IVDD in mice, and this scaffold has been confirmed to have good support and regulation. However, this phenomenon has not been previously reported in large animals. The developed nanoparticles are anti-inflammatory to IVDD and promote ECM regeneration *in vitro*. However, most of these nanoparticles require local injections. The high pressure inside NP makes NP cells unable to withstand the pressure of the nanoparticle injection. Therefore, our future research direction is not only toward finding new targets but also toward developing new biomaterials to repair IVDD.

3.2.2 Tumor necrosis factors

Similar to IL-1β, TNF-α is a pro-inflammatory cytokine that belongs to the TNF ligand superfamily (115). TNF-α can trigger inflammatory responses *in vivo* and induce the expression of IL-1β, IL-6, IL-8, and IL-17 (116). IL-17 has been linked to the severity of IVDD (112). Prominent NP can release CCL5 to induce MSC

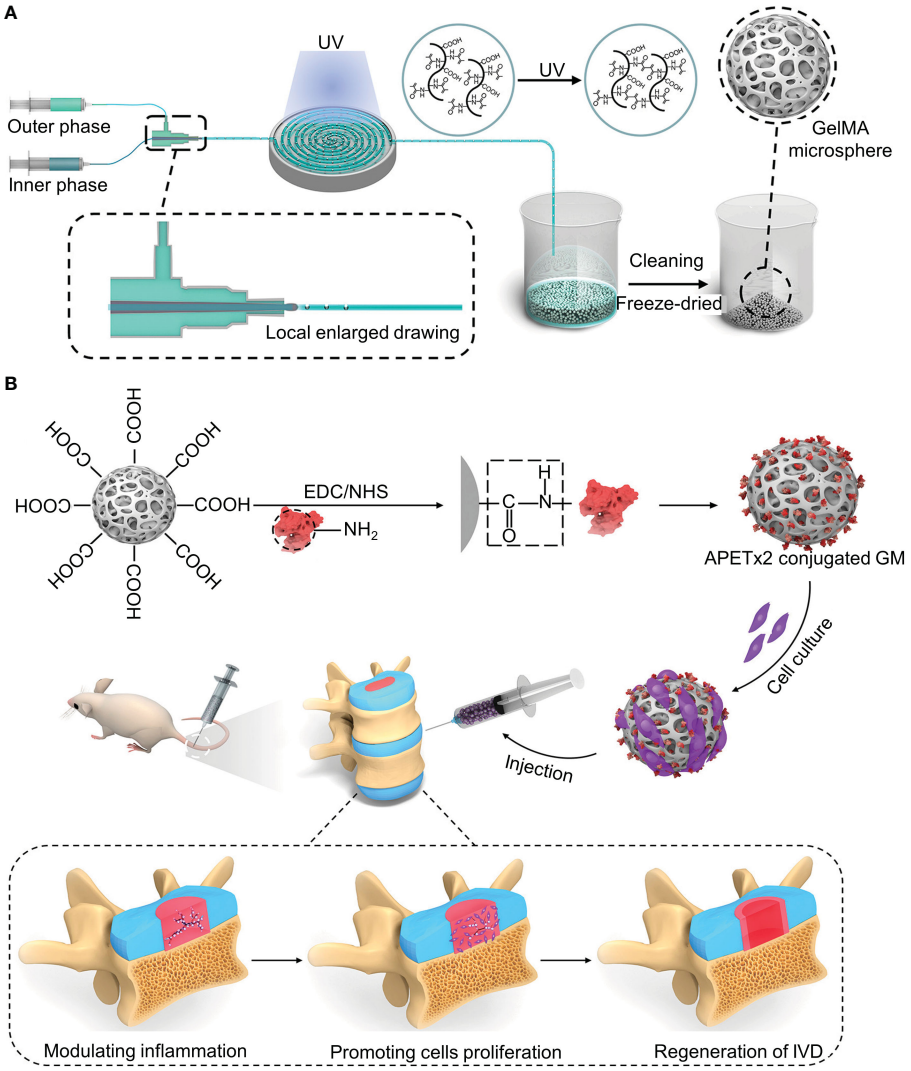


FIGURE 4
(A) Schematic diagram of the synthesis of the GelMA microsphere. **(B)** The carboxyl on the microsphere surface was activated by EDC/NHS, followed by being covalently linked to the amino residue on the APETx2 to form APETx2-GelMA microsphere (GA). Reproduced with permission from (108).

migration into IVDD to promote IVD regeneration (89). However, studies have shown that TNF-α can recruit more inflammatory factors by inducing CCL5 differentiation (117). In addition to promoting inflammatory cells, TNF-α can increase MMP expression through the NF-κB/MAPK signaling pathway to degrade the ECM (118). Recently, it has been shown that the secretion of TNF-α by degenerated IVDs induces senescence in NP cells that induce senescence in healthy cells by inhibiting Stat3 phosphorylation through paracrine effects (119). Similar to IL-1β, TNF-α can accelerate IVDD. Therefore, the inhibition of TNF-α may delay neuropathic pain.

Curcumin is derived from the rhizomes of natural herbs and has anticancer, antibacterial, and anti-inflammatory properties (120). Studies have shown that curcumin inhibits TNF-induced NF-κB activation and downregulates the release of pro-inflammatory factors (121). However, the low solubility of curcumin and its poor absorption into systemic circulation limit its clinical applications (122). Setton et al. modified curcumin with carbamate and coupled it with an elastin-like polypeptide (ELP) to obtain a biodegradable ELP-curcumin conjugate (49). The synthesis methods of the materials are shown in Table 1. ELP-curcumin conjugates have a high drug load, rapidly releasing curcumin *in vitro* and maintaining its biological activity. In an *in vitro* study, curcumin was continuously removed from the conjugate. After 96 h, 55% of the loaded curcumin had been released. The curcumin content around the nerve was detected at 48 h, and the amount of curcumin released in the conjugate was five times that of free curcumin. This suggests that the conjugate could reduce the adverse factors of the poor systemic absorption of curcumin and effectively deliver curcumin to the periphery of nerves to alleviate peripheral inflammatory responses. Further studies have shown that TNF-α can upregulate the expression of prostaglandin E 2 (PGE2) in NP cells. PGE2 inhibits proteoglycan synthesis, thereby degrading the ECM (123). Willems et al. loaded celecoxib (CXB) into a poly-N-isopropylacrylamide (pNIPAAM) polymer (Figure 5) (50). The synthesis methods of the materials are shown in Table 1. CXB is a COX-2 inhibitor that can specifically

10.3389/fimmu.2023.1051606

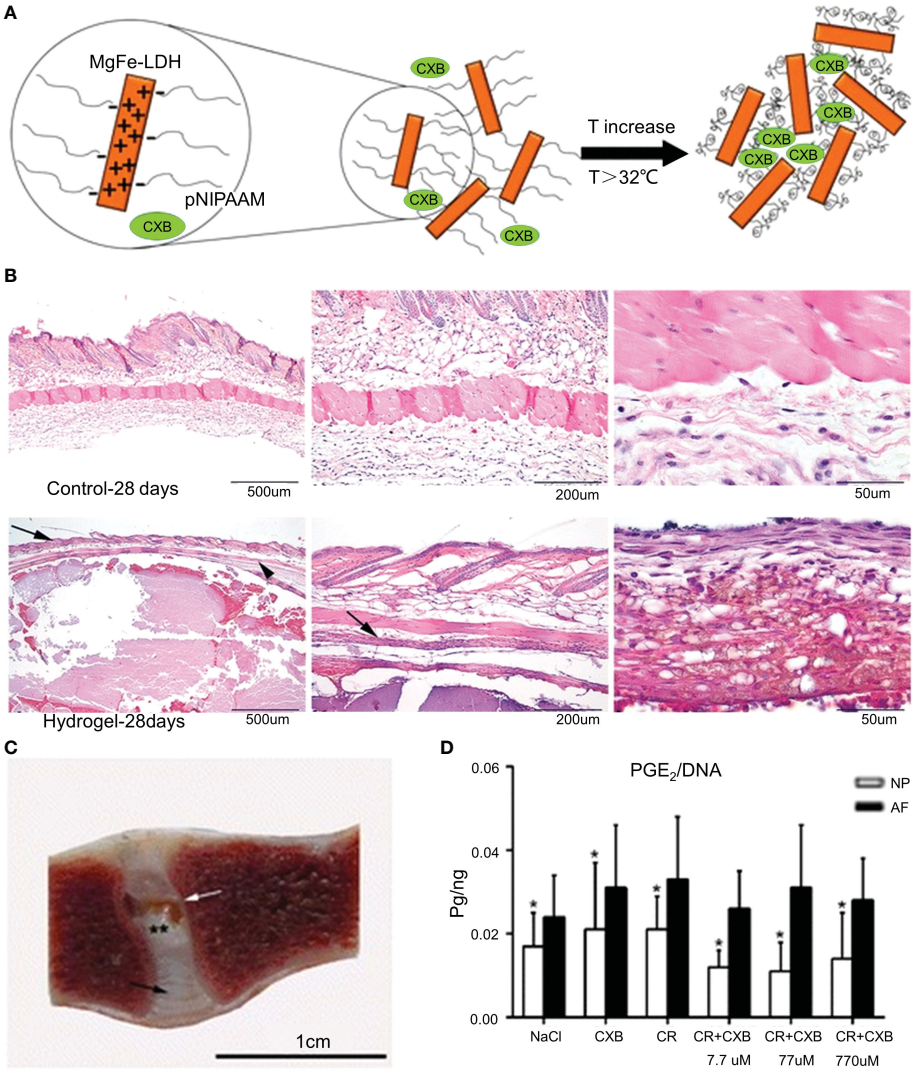


FIGURE 5
(A) Schematic diagram of the synthesis of the pNIPAAM hydrogel. **(B)** Histological staining (hematoxylin and eosin staining) of the hydrogel and control group after 28 days in mice. The epidermis and flesh lipid membranes are indicated by the arrows. **(C)** One month after the intradiscal injections, the pNIPAAM hydrogel (white arrow) was visible in the NP. **(D)** The DNA level in PGE 2NP was significantly lower than that in AF in all treatments. Reproduced with permission from (50). *Indicates significant difference at a 99 % confidence level P ≤ 0.05. **Indicates significant difference at a 99 % confidence level P ≤ 0.01.

block the production of PGE2. CXB-containing hydrogels effectively released CXB and continuously inhibited PGE2 (52%) *in vitro*. Twenty-eight days after the mice were injected with the hydrogel, the pNIPAAM polymer formed a denser fibrous structure than the blank control group (Figure 5B). Reductions in spinal reflexes were detected on the day after the infusion of the CXB-filled hydrogels into dogs. The hydrogel with CXB spontaneously formed a solid at 37°C without leakage after the injection (Figure 5C). The pNIPAAM polymer significantly reduced PGE2 in NP compared to AP (Figure 5D). This was consistent with the results of previous studies (123). Interestingly, this was one of the few *in vivo* experiments conducted in large animals to demonstrate the efficacy of hydrogels. However, similar to IL, the reduction of inflammatory responses by inhibiting TNF-α to modulate the microenvironment remains limited to early IVDD. There have been no reports relating to late IVDD.

3.3 Oxidative stress correlated factors

3.3.1 Hypoxia-inducible factors

HIF is a transcription factor expressed in cells in response to hypoxia. HIF-1 consists of a constitutively expressed subunit, HIF-1β, and another subunit, HIF-1α, which is regulated by cellular O concentration (124). HIFs have strong anti-apoptotic effects and are involved in regulating cellular responses to oxidative stress (125). NP cells have been reported to express HIF-1α to maintain cellular energy and ECM metabolism independent of oxygen tension (126). Endoplasmic reticulum oxidative stress in IVDD can accelerate IVDD progression, and HIF can reduce endoplasmic reticulum oxidative stress in IVDD (127). Studies have shown that the knockout of the HIF-1α gene in mouse NP cells results in massive death and the loss of HIF-1α results in reduced collagen II and proteoglycan protein expression in IVDs (128, 129).

Therefore, HIF-1α is expressed by NP cells and has a protective effect on IVDs.

Cells with degenerated NP or AF have multi-differentiation potential and can be stimulated to repair IVDs (130). However, NP cell-derived disc progenitor cells (DPCs) are sensitive to hypoxia and fail to upregulate HIF to undergo apoptosis under hypoxia (125). Huang et al. used small leucine-rich proteoglycans (SLRPs) and biglycan to provide growth substrates for DPCs (51). SLRPs can bind and regulate TGF-β to activate the MAPK pathway, and TGF-β can enhance HIF-1α expression through TGF-β receptor (ALK5) kinase activity. It has been further confirmed that IVDD can be repaired by adjusting HIF *in vitro*. However, there are currently no studies showing the effects on animals. Chitosan itself can reduce the apoptosis of NP owing to oxidative stress (131, 132). Studies have shown that the enhancement of the PI3K/Akt pathway by chitosan protects cells against apoptosis (131). Zhang et al. mixed chitosan and alginate at a ratio of 1:1. The mixture was phacoemulsified to obtain a C/A gel scaffold (52). Alginate is also a safe biodegradable polysaccharide material with biocompatibility, solubility, porosity, and tunability of viscosity and concentration (133). The C/A gel scaffold has a porosity of 80.57%, which can effectively load ADSCs and provide a good framework for their growth. Morphological changes can occur during gel scaffold degradation, such as shrinkage, increased transparency, and 3D morphology. The advantage of the C/A gel scaffold is that it can provide ADSCs with a hypoxic environment similar to NP cells during *in vitro* degradations. This hypoxic environment favors the differentiation of ADSCs into NPs. After 21 days of culture *in vitro*, the C/A gel scaffold induced a significantly higher mRNA expression of HIF-1α than the normoxia-induced group. It increased the number of type II collagen fibers in the ECM. C/A gel scaffolds can generate the same functional ECM as standard NP, providing a basis for the active recovery of IVDD.

Calcification is frequently associated with IVDD, a condition of osteophyte growth at the peripheries of endplates, and vertebral margins (125). This is mainly due to the deposition of calcium-containing substances in the ECM outside the IVD. Studies have shown that HIF-1α can inhibit the secretion of inorganic pyrophosphate by NP and reduce the calcification of IVDs (134). Calcification can aggravate IVDD. miR-199a is an endogenous small non-coding RNA that directly targets HIF-1α and downregulates HIF-1α expression (135). Thus, anti-miR-199a delivery specifically inhibited endogenous miR-199a and enhanced Hif-1α expression to inhibit the calcification of IVDs. Feng Ganjun et al. developed poly (L-lactic acid) graft poly(hydroxyethyl methacrylate) (PLLA-g-PHEMA) nanoparticles using a phase separation method (53). The synthesis methods of the materials are shown in Table 1. The diameter of the nanoparticles was between 30 and 60 μm. Nanoparticles as non-viral vectors for miRNA delivery can efficiently deliver miRNAs into cells and bone marrow MSCs (BMMSCs) together in the ECM. BMMSCs promote the regeneration of aging NP. The detection of nanoparticles at week 12 in mice reduced calcification of ECM and enhanced HIF-1α-induced BMMSCs to promote mouse NP cell regeneration.

3.3.2 Reactive oxygen species

In addition to inflammatory cells, oxidative stress caused by high levels of ROS is a hallmark of chronic inflammation (136). Oxidative stress damages vital cellular structures, leading to apoptosis and senescence (54). The exposure of NP to ROS releases IL-1β, triggering a cascade of reactions that exacerbate IVD damage (137). High levels of ROS also inhibited HIF-α expression. ROS is regulated by glutathione, superoxide dismutase, and catalase (138). Therefore, blocking ROS production may be beneficial for the repair of IVDD. An ROS-labile linker was synthesized *via* the quaternization reaction of N1,N1,N3,N3-tetramethylpropane-1,3-diamine with an excess of 4-(bromomethyl) phenylboronic acid (Figure 6) (55). The synthesis methods of the materials are shown in Table 1. The ROS-labile linker was cross-linked with vinyl alcohol (PVA) to form a ROS-scavenging hydrogel for loading rapamycin. In a ROS-rich environment, the ROS-scavenging hydrogel was degraded by the consumption of ROS to release rapamycin. Rapamycin has immunosuppressive effects and induces apoptosis. Rapamycin hydrogel clears ROS and promotes macrophage polarization to M2, reducing inflammatory responses *in vitro*. At week 12 of the *in vivo* IVDD model, rapamycin hydrogels downregulated MMP-13 in the ECM and upregulated type II collagen (Figure 6B).

Pandit et al. prepared calcium carbonate, poly (allylamine hydrochloride) (PAH), and tannic acid (TA) into polymer capsules using a layer-by-layer approach (54). TA is a natural polyphenol that has shown a considerable capacity to scavenge a wide variety of free radicals and pro-oxidant molecules owing to its redox properties (139). Calcium carbonate was used as the core of the polymer capsule to load catalase. TA accelerated the release of catalase while scavenging ROS on the surface. The TA-functionalized polymer capsules promoted the release of hydrogen peroxide more effectively than the non-TA-functionalized capsules. The study confirmed that the encapsulation rate of hydrogen peroxide in the polymer capsule was 97.8%, which was five times higher than that of physical adsorption. Compared with 67% of oxidative stress-positive NP cells in the blank group, this double ROS-scavenging polymer capsule reduced oxidative stress-positive NP cells to 3% *in vitro*. In addition, polymer capsules can downregulate the expression of MMPs in the ECM. Although the polymer capsules exhibited the ability to induce the regeneration of IVDs *in vitro*, it has not been verified whether a similar effect occurs *in vivo*.

IVDs are non-neurovascular structures, and the growth of NP cells is adapted to the hypoxic state. However, studies have demonstrated that hypoxia in NP cells may exacerbate IVDD (140, 141). A particular concentration of oxygen appears to be beneficial to NP cells. Perfluorotributylamine (PFTBA) belongs to the perfluorocarbon family with high oxygen solubility and can modulate the oxygen tension of IVDs (142). Zhen et al. used PFTBA to prepare scaffolds to load alginate. Alginate, a widely used scaffold for the regeneration of IVDs, has shown better ECM deposition than other materials (56). The synthesis methods of the materials are shown in Table 1. The PFTBA concentration in the scaffolds was proportional to the oxygen concentration in the ECM. This study confirmed that the addition of PFTBA (2.5–10%) under hypoxic conditions significantly reduced the rate of cell death in NP cells *in vitro*. When simulating IVDD in mice, it was found that 2.5% of the PFTBA scaffolds induced more type II collagen and proteoglycans in the ECM at 6 weeks compared with other concentrations of the PFTBA scaffolds. Another advantage of the PFTBA-alginate scaffolds was that their stability did not change as

10.3389/fimmu.2023.1051606

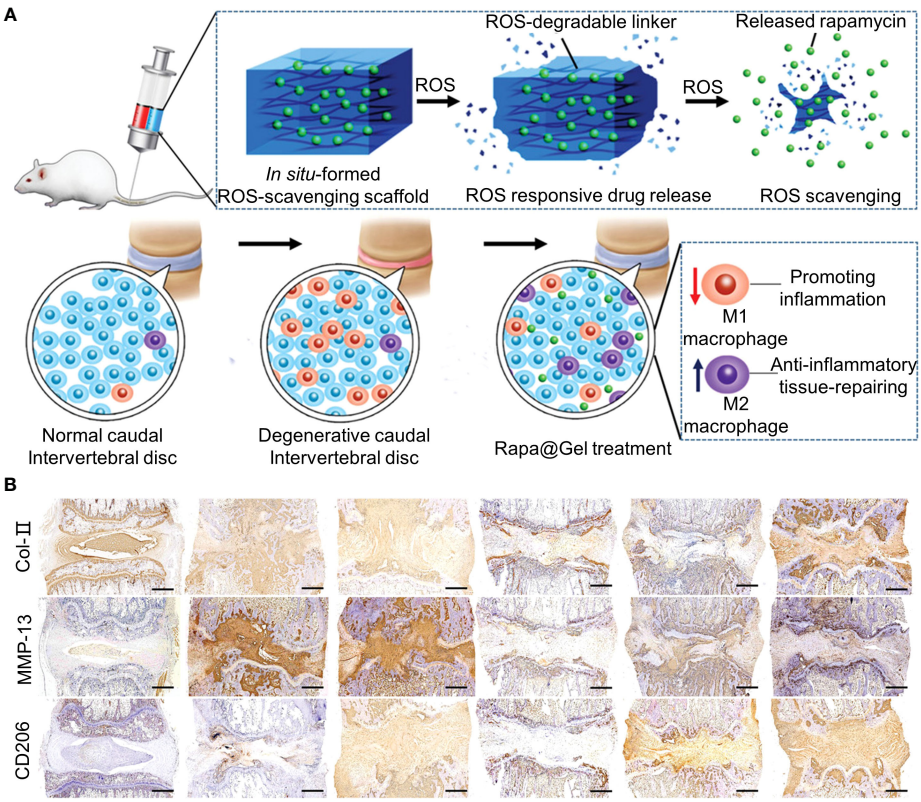


FIGURE 6
(A) Schematic representation of Rapa-loaded ROS-responsive hydrogels. **(B)** Immunohistochemical staining for collagen type II (COL2), matrix metalloproteinase 13 (MMP13), and CD206 at week 12. Immunohistochemical staining showed that COL2 expression was upregulated, MMP13 expression was downregulated, and CD206 expression was upregulated in the rapamycin-treated group compared with the degenerative control group. Reproduced with permission from (55).

PFTBA degraded. However, the study did not measure the oxygen levels *in vivo*. Furthermore, IVDD in mice results from spontaneous terminal calcification, the mechanism of which remains unclear. Therefore, it is necessary to investigate further whether regulating the oxygen content of NP cells in animals is beneficial for the repair of IVDD.

4 Discussion

Normal IVDs are immune-privileged tissue structures. Degeneration occurs when IVDs are stimulated by inflammation, oxidative stress, and stress. IVDD recruits T cells and macrophages to clear necrotic tissues and cellular debris. Furthermore, the average NP and AF cells of IVDD become targets of immune system attacks, thereby aggravating IVDD. We found that repairing IVDD by modulating the inflammatory microenvironment is a viable therapeutic modality. However, owing to the lack of vascular structures in IVDs, the biological factors that regulate immunity cannot effectively reach the sites of IVDD. In addition, the lack of blood vessels in IVDs means that natural characteristics cannot obtain the nutrients they need to repair degenerated IVDs. Therefore, spontaneous repair of IVDD seems impossible. In recent years, biomaterials that regulate the inflammatory microenvironment to improve IVDD have been reported. For example, chitosan, curcumin, and alginate can protect NP cells and the ECM and act in gels to carry biological regulators to repair IVDD. Engineered nano scaffolds can also delay IVDD while preserving the survival of bioregulators by delivering them around IVDs. These biomaterials have shown advantages in inducing stem cell differentiation and reducing the inflammatory cascade induced by IL-1β and TNF-α. Still, they have also downregulated the inflammatory response by scavenging ROS in the ECM. The biomaterials can also reduce MMP expression and provide a favorable environment for IVD repair. These advantages indicate that regulating the inflammatory microenvironment by biomaterials to repair IVDD may be helpful in clinical treatments.

Although it seems possible that biomaterials regulate inflammation-immune environment repair IVDD, there are two significant problems worth noting. First, most of the studies on IVDD were performed under conditions that mimicked IVDD *in vitro*. In line with the studies conducted on mice and dogs, biomaterials can adapt to *in vivo* stress and histocompatibility and play a positive role in the repair of IVDs. However, there are few studies on regulating IVDD repair in the inflammatory microenvironment *in vivo*. Further validation is needed to confirm the strategies involving biomaterials to modulate the inflammatory microenvironment *in vivo*, especially in large animals. Second, the use of biomaterials in regulating the inflammatory microenvironment to repair IVDD is only significant in the early stage of the disease. However, most cases of IVDD are challenging to detect early on when the patients are asymptomatic. However, it is unknown whether

biomaterials modulate the inflammatory microenvironment to repair IVDD in patients with advanced IVDD.

Author contributions

All authors read and approved the final manuscript. YX wrote the initial manuscript. CF and YX contributed new ideas. HW created the figures. YL and RY created Table 1. YH and JZ made the english language editing. YX, YL, and RY revised the manuscript and approved the final version.

Funding

This work was supported by the National Natural Science Foundation of China (Grant Nos. 82071391), the "13th Five-Y ear" Science and Technology Research Planning Project of Jilin Province (Grant No. JLKHJJKH20190042KJ), and the Achievement Transformation Fund of the First Hospital of Jilin University (Grant No. JDYYZH-2102052).

Acknowledgments

We would like to express our appreciation to everyone who was involved in the drafting and preparation of the manuscript. We would like to thank Editage (www.editage.cn) for English language editing.

Conflict of interest

The authors declare that the research was conducted in the absence of any commercial or financial relationships that could be construed as a potential conflict of interest.

Publisher's note

All claims expressed in this article are solely those of the authors and do not necessarily represent those of their affiliated organizations, or those of the publisher, the editors and the reviewers. Any product that may be evaluated in this article, or claim that may be made by its manufacturer, is not guaranteed or endorsed by the publisher.

References

1. Zhang G-Z, Liu M-Q, Chen H-W, Wu Z-L, Gao Y-C, Ma Z-J, et al. NF-κB signalling pathways in nucleus pulposus cell function and intervertebral disc degeneration. *Cell Prolif* (2021) 54:e13057–7. doi: 10.1111/cpr.13057

2. Krut Z, Pelled G, Gazit D, Gazit Z. Stem cells and exosomes: New therapies for intervertebral disc degeneration. *Cells* (2021) 10:2241. doi: 10.3390/cells10092241

3. Adams MA, Lama P, Zehra U, Dolan P. Why do some intervertebral discs degenerate, when others (in the same spine) do not? *Clin Anat* (2015) 28:195–204. doi: 10.1002/ca.22404

4. Samartzis D, Karppinen J, Chan D, Luk KD, Cheung KM. The association of lumbar intervertebral disc degeneration on magnetic resonance imaging with body mass index in overweight and obese adults: a population-based study. *Arthritis rheumatism* (2012) 64:1488–96. doi: 10.1002/art.33462

5. Kamali A, Ziadlou R, Lang G, Pfannkuche J, Cui S, Li Z, et al. Small molecule-based treatment approaches for intervertebral disc degeneration: Current options and future directions. *Theranostics* (2021) 11:27–47. doi: 10.7150/thno.48987

6. Ashinsky B, Smith HE, Mauck RL, Gullbrand SE. Intervertebral disc degeneration and regeneration: a motion segment perspective. *Eur Cell Mater* (2021) 41:370–80. doi: 10.22203/eCM.v041a24

7. Kirnaz S, Capadona C, Wong T, Goldberg JL, Medary B, Sommer F, et al. Fundamentals of intervertebral disc degeneration. *World Neurosurg* (2022) 157:264–73. doi: 10.1016/j.wneu.2021.09.066

8. Chao-yang G, Peng C, Hai-hong Z. Roles of NLRP3 inflammasome in intervertebral disc degeneration. *Osteoarthritis Cartilage* (2021) 29:793–801. doi: 10.1016/j.joca.2021.02.204

9. Adams MA, Roughley PJ. What is intervertebral disc degeneration, and what causes it? *Spine* (2006) 31:2151–61. doi: 10.1097/01.brs.0000231761.73859.2c

10. Kos N, Gradisnik L, Velnar T. A brief review of the degenerative intervertebral disc disease. *Med Arch* (2019) 73:421–4. doi: 10.5455/medarh.2019.73.421-424

11. Yan C, Wang X, Xiang C, Wang Y, Pu C, Chen L, et al. Applications of functionalized hydrogels in the regeneration of the intervertebral disc. *BioMed Res Int* (2021) 2021:2818624–2818624. doi: 10.1155/2021/2818624

12. Mirza SK, Deyo RA. Systematic review of randomized trials comparing lumbar fusion surgery to nonoperative care for treatment of chronic back pain. *Spine* (2007) 32:816–23. doi: 10.1097/01.brs.0000259225.37454.38

13. Risbud MV, Shapiro IM. Role of cytokines in intervertebral disc degeneration: pain and disc content. *Nat Rev Rheumatol* (2014) 10:44–56. doi: 10.1038/nrrheum.2013.160

14. Ran J, Hu Y, Zheng Z, Zhu T, Zheng H, Jing Y, et al. Comparison of discectomy versus sequestrectomy in lumbar disc herniation: a meta-analysis of comparative studies. *PloS One* (2015) 10:e0121816. doi: 10.1371/journal.pone.0121816

15. Wang F, Cai F, Shi R, Wang XH, Wu XT. Aging and age related stresses: a senescence mechanism of intervertebral disc degeneration. *Osteoarthritis Cartilage* (2016) 24:398–408. doi: 10.1016/j.joca.2015.09.019

16. Huang YC, Hu Y, Li Z, Luk KDK. Biomaterials for intervertebral disc regeneration: Current status and looming challenges. *J Tissue Eng regenerative Med* (2018) 12:2188–202. doi: 10.1002/term.2750

17. Fiordalisi M, Silva AJ, Barbosa M, Gonçalves R, Caldeira J. Decellularized scaffolds for intervertebral disc regeneration. *Trends Biotechnol* (2020) 38:947–51. doi: 10.1016/j.tibtech.2020.05.002

18. De Pieri A, Byerley AM, Musumeci CR, Salemizadehparizi F, Vanderhorst MA, Wuertz-Kozak K. Electrospinning and 3D bioprinting for intervertebral disc tissue engineering. *JOR Spine* (2020) 3:e1117. doi: 10.1002/jsp2.1117

19. Xu H, Sun M, Wang C, Xia K, Xiao S, Wang Y, et al. GDF5-GelMA injectable microspheres laden with adipose-derived stem cells for disc degeneration repair. *Biofabrication* (2020) 13(1):015010. doi: 10.1088/1758-5090/abc4d3

20. Kim MJ, Lee JH, Kim JS, Kim HY, Lee HC, Byun JH, et al. Intervertebral disc regeneration using stem Cell/Growth factor-loaded porous particles with a leaf-stacked structure. *Biomacromolecules* (2020) 21:4795–805. doi: 10.1021/acs.biomac.0c00992

21. Kamatani T, Hagizawa H, Yarimitsu S, Morioka M, Koyamatsu S, Sugimoto M, et al. Human iPS cell-derived cartilaginous tissue spatially and functionally replaces nucleus pulposus. *Biomaterials* (2022) 284:121491. doi: 10.1016/j.biomaterials.2022.121491

22. Zhang J, Zhang W, Sun T, Wang J, Li Y, Liu J, et al. The influence of intervertebral disc microenvironment on the biological behavior of engrafted mesenchymal stem cells. *Stem Cells Int* (2022) 2022:8671482. doi: 10.1155/2022/8671482

23. Zhang W, Sun T, Li Y, Yang M, Zhao Y, Liu J, et al. Application of stem cells in the repair of intervertebral disc degeneration. *Stem Cell Res Ther* (2022) 13:70. doi: 10.1186/s13287-022-02745-y

24. Baldia M, Mani S, Walter N, Kumar S, Srivastava A, Prabhu K. Bone marrow-derived mesenchymal stem cells augment regeneration of intervertebral disc in a reproducible and validated mouse intervertebral disc degeneration model. *Neurol India* (2021) 69:1565–70. doi: 10.4103/0028-3886.333531

25. Wang C, Li Z, Zhang K, Zhang C. Self-assembling peptides with hBMP7 biological activity promote the differentiation of ADSCs into nucleus pulposus-like cells. *J Orthop Surg Res* (2022) 17:197. doi: 10.1186/s13018-022-03102-8

26. Wang H, Zhou Y, Huang B, Liu LT, Liu MH, Wang J, et al. Utilization of stem cells in alginate for nucleus pulposus tissue engineering. *Tissue engineering. Part A* (2014) 20:908–20. doi: 10.1089/ten.TEA.2012.0703

27. Ying J, Han Z, Pei S, Su L, Ruan D. Effects of stromal cell-derived factor-1α secreted in degenerative intervertebral disc on activation and recruitment of nucleus pulposus-derived stem cells. *Stem Cells Int* (2019) 2019:9147835. doi: 10.1155/2019/9147835

28. Richardson SM, Kalamegam G, Pushparaj PN, Matta C, Memic A, Khademhosseini A, et al. Mesenchymal stem cells in regenerative medicine: Focus on articular cartilage and intervertebral disc regeneration. *Methods* (2016) 99:69–80. doi: 10.1016/j.ymeth.2015.09.015

29. Kraus P, Samanta A, Lufkin S, Lufkin T. Stem cells in intervertebral disc regeneration-more talk than action? *Biocell: Off J Sociedades Latinoamericanas Microscopia Electronica … et al.* (2021) 46:893–8.

30. Esquijarosa Hechavarria M, Richard SA. Edifying the focal factors influencing mesenchymal stem cells by the microenvironment of intervertebral disc degeneration in low back pain. *Pain Res Manage* (2022) 2022:6235400. doi: 10.1155/2022/6235400

31. Stergar J, Gradisnik L, Velnar T, Maver U. Intervertebral disc tissue engineering: A brief review. *Bosn J Basic Med Sci* (2019) 19:130–7. doi: 10.17305/bjbms.2019.3778

32. Zhang XB, Chen XY, Qi J, Zhou HY, Zhao XB, Hu YC, et al. New hope for intervertebral disc degeneration: bone marrow mesenchymal stem cells and exosomes derived from bone marrow mesenchymal stem cell transplantation. *Curr Gene Ther* (2022) 22(4):291–302. doi: 10.2174/1566523221666211012092855

33. Ye F, Lyu FJ, Wang H, Zheng Z. The involvement of immune system in intervertebral disc herniation and degeneration. *JOR Spine* (2022) 5:e1196. doi: 10.1002/jsp2.1196

34. Sun Z, Liu B, Luo ZJ. The immune privilege of the intervertebral disc: Implications for intervertebral disc degeneration treatment. *Int J Med Sci* (2020) 17:685–92. doi: 10.7150/ijms.42238

35. Wang J, Markova D, Anderson DG, Zheng Z, Shapiro IM, Risbud MV. TNF-α and IL-1β promote a disintegrin-like and metalloprotease with thrombospondin type I motif-5-mediated aggrecan degradation through syndecan-4 in intervertebral disc*. *J Biol Chem* (2011) 286:39738–49. doi: 10.1074/jbc.M111.264549

36. Bowles RD, Setton LA. Biomaterials for intervertebral disc regeneration and repair. *Biomaterials* (2017) 129:54–67. doi: 10.1016/j.biomaterials.2017.03.013

37. Whitaker R, Hernaez-Estrada B, Hernandez RM, Santos-Vizcaino E, Spiller KL. Immunomodulatory biomaterials for tissue repair. *Chem Rev* (2021) 121:11305–35. doi: 10.1021/acs.chemrev.0c00895

38. Zhou Z, Zeiter S, Schmid T, Sakai D, Iatridis JC, Zhou G, et al. Effect of the CCL5-releasing fibrin gel for intervertebral disc regeneration. *Cartilage* (2020) 11:169–80. doi: 10.1177/1947603518764263

39. Frapin L, Clouet J, Chédeville C, Moraru C, Samarut E, Henry N, et al. Controlled release of biological factors for endogenous progenitor cell migration and intervertebral disc extracellular matrix remodelling. *Biomaterials* (2020) 253:120107. doi: 10.1016/j.biomaterials.2020.120107

40. Du J, Long RG, Nakai T, Sakai D, Benneker LM, Zhou G, et al. Functional cell phenotype induction with TGF-β1 and collagen-polyurethane scaffold for annulus fibrosus rupture repair. *Eur Cell Mater* (2020) 39:1–17. doi: 10.22203/eCM.v039a01

41. Adoungotchodo A, Epure LM, Mwale F, Lerouge S. Chitosan-based hydrogels supplemented with gelatine and link n enhance extracellular matrix deposition by encapsulated cells in a degenerative intervertebral disc environment. *Eur Cell Mater* (2021) 41:471–84. doi: 10.22203/eCM.v041a30

42. Sun B, Lian M, Han Y, Mo X, Jiang W, Qiao Z, et al. A 3D-bioprinted dual growth factor-releasing intervertebral disc scaffold induces nucleus pulposus and annulus fibrosus reconstruction. *Bioactive materials* (2021) 6:179–90. doi: 10.1016/j.bioactmat.2020.06.022

43. Panebianco CJ, DiStefano TJ, Mui B, Hom WW, Iatridis JC. Crosslinker concentration controls TGFβ-3 release and annulus fibrosus cell apoptosis in genipin-crosslinked fibrin hydrogels. *Eur Cell Mater* (2020) 39:211–26. doi: 10.22203/eCM.v039a14

44. Chen P, Ning L, Qiu P, Mo J, Mei S, Xia C, et al. Photo-crosslinked gelatin-hyaluronic acid methacrylate hydrogel-committed nucleus pulposus-like differentiation of adipose stromal cells for intervertebral disc repair. *J Tissue Eng regenerative Med* (2019) 13:682–93. doi: 10.1002/term.2841

45. Loepfe M, Duss A, Zafeiropoulou K-A, Björgvinsdóttir O, D'Este M, Eglin D, et al. Electrospray-based microencapsulation of epigallocatechin 3-gallate for local delivery into the intervertebral disc. *Pharmaceutics* (2019) 11:435. doi: 10.3390/pharmaceutics11090435

46. Isa ILM, Srivastava A, Tiernan D, Owens P, Rooney P, Dockery P, et al. Hyaluronic acid based hydrogels attenuate inflammatory receptors and neurotrophins in interleukin-1β induced inflammation model of nucleus pulposus cells. *Biomacromolecules* (2015) 16:1714–25. doi: 10.1021/acs.biomac.5b00168

47. Gorth DJ, Mauck RL, Chiaro JA, Mohanraj B, Hebela NM, Dodge GR, et al. IL-1ra delivered from poly(lactic-co-glycolic acid) microspheres attenuates IL-1β-mediated degradation of nucleus pulposus in vitro. *Arthritis Res Ther* (2012) 14:R179–9. doi: 10.1186/ar3932

48. Teixeira GQ, Leite Pereira C, Castro F, Ferreira JR, Gomez-Lazaro M, Aguiar P, et al. Anti-inflammatory Chitosan/Poly-γ-glutamic acid nanoparticles control inflammation while remodeling extracellular matrix in degenerated intervertebral disc. *Acta biomaterialia* (2016) 42:168–79. doi: 10.1016/j.actbio.2016.06.013

49. Sinclair SM, Bhattacharyya J, McDaniel JR, Gooden DM, Gopalaswamy R, Chilkoti A, et al. A genetically engineered thermally responsive sustained release curcumin depot to treat neuroinflammation. *J Controlled release: Off J Controlled Release Soc* (2013) 171:38–47. doi: 10.1016/j.jconrel.2013.06.032

50. Willems N, Yang H-Y, Langelaan MLP, Tellegen AR, Grinwis GCM, Kranenburg H-JC, et al. Biocompatibility and intradiscal application of a thermoreversible celecoxib-loaded poly-n-isopropylacrylamide MgFe-layered double hydroxide hydrogel in a canine model. *Arthritis Res Ther* (2015) 17:214–4. doi: 10.1186/s13075-015-0727-x

51. Huang S, Leung VYL, Long D, Chan D, Lu WW, Cheung KMC, et al. Coupling of small leucine-rich proteoglycans to hypoxic survival of a progenitor cell-like subpopulation in rhesus macaque intervertebral disc. *Biomaterials* (2013) 34:6548–58. doi: 10.1016/j.biomaterials.2013.05.027

52. Zhang Z, Li F, Tian H, Guan K, Zhao G, Shan J, et al. Differentiation of adipose-derived stem cells toward nucleus pulposus-like cells induced by hypoxia and a three-dimensional chitosan-alginate gel scaffoldin vitro. *Chin Med J* (2014) 127. doi: 10.3760/cma.j.issn.0366-6999.20130584

53. Feng G, Zhang Z, Dang M, Rambhia KJ, Ma PX. Nanofibrous spongy microspheres to deliver rabbit mesenchymal stem cells and anti-miR-199a to regenerate nucleus pulposus and prevent calcification. *Biomaterials* (2020) 256:120213–3. doi: 10.1016/j.biomaterials.2020.120213

54. Larrañaga A, Isa ILM, Patil V, Thamboo S, Lomora M, Fernández-Yague MA, et al. Antioxidant functionalized polymer capsules to prevent oxidative stress. *Acta biomaterialia* (2018) 67:21–31. doi: 10.1016/j.actbio.2017.12.014

55. Bai J, Zhang Y, Fan Q, Xu J, Shan H, Gao X, et al. Reactive oxygen species-scavenging scaffold with rapamycin for treatment of intervertebral disk degeneration. *Adv Healthc Mater* (2020) 9:e1901186. doi: 10.1002/adhm.201901186

56. Sun Z, Luo B, Liu Z, Huang L, Liu B, Ma T, et al. Effect of perfluorotributylamine-enriched alginate on nucleus pulposus cell: Implications for intervertebral disc regeneration. *Biomaterials* (2016) 82:34–47. doi: 10.1016/j.biomaterials.2015.12.013

57. Dowdell J, Erwin M, Choma T, Vaccaro A, Iatridis J, Cho SK. Intervertebral disk degeneration and repair. *Neurosurgery* (2017) 80:S46–54. doi: 10.1093/neuros/nyw078

58. Kokubo Y, Uchida K, Kobayashi S, Yayama T, Sato R, Nakajima H, et al. Herniated and spondylotic intervertebral discs of the human cervical spine: histological and immunohistological findings in 500 en bloc surgical samples. *Lab Invest J neurosurgery. Spine* (2008) 9:285–95. doi: 10.3171/SPI/2008/9/9/285

59. Nedresky D, Reddy V, Singh G. Anatomy, back, nucleus pulposus. In: *StatPearls*. Treasure Island (FL: StatPearls Publishing LLC. (2021).

60. Wang HQ, Yu XD, Liu ZH, Cheng X, Samartzis D, Jia LT, et al. Deregulated miR-155 promotes fas-mediated apoptosis in human intervertebral disc degeneration by targeting FADD and caspase-3. *J Pathol* (2011) 225:232–42. doi: 10.1002/path.2931

61. Francisco V, Pino J, González-Gay M, Lago F, Karppinen J, Tervonen O, et al. A new immunometabolic perspective of intervertebral disc degeneration. *Nat Rev Rheumatol* (2022) 18:47–60. doi: 10.1038/s41584-021-00713-z

62. Wiet MG, Piscioneri A, Khan SN, Ballinger MN, Hoyland JA, Purmessur D. Mast cell-intervertebral disc cell interactions regulate inflammation, catabolism and angiogenesis in discogenic back pain. *Sci Rep* (2017) 7:12492–2. doi: 10.1038/s41598-017-12666-z

63. Yang C, Cao P, Gao Y, Wu M, Lin Y, Tian Y, et al. Differential expression of p38 MAPK α, β, γ, δ isoforms in nucleus pulposus modulates macrophage polarization in intervertebral disc degeneration. *Sci Rep* (2016) 6:22182–2. doi: 10.1038/srep22182

64. Eyre DR, Muir H. Types I and II collagens in intervertebral disc. interchanging radial distributions in annulus fibrosus. *Biochem J* (1976) 157:267–70. doi: 10.1042/bj1570267

65. Sugimoto Y, Takimoto A, Akiyama H, Kist R, Scherer G, Nakamura T, et al. Scx +/Sox9+ progenitors contribute to the establishment of the junction between cartilage and tendon/ligament. *Dev (Cambridge England)* (2013) 140:2280–8. doi: 10.1242/dev.096354

66. Torre OM, Mroz V, Bartelstein MK, Huang AH, Iatridis JC. Annulus fibrosus cell phenotypes in homeostasis and injury: implications for regenerative strategies. *Ann New York Acad Sci* (2019) 1442:61–78. doi: 10.1111/nyas.13964

67. Huang B-R, Bau D-T, Chen T-S, Chuang IC, Tsai C-F, Chang P-C, et al. Pro-inflammatory stimuli influence expression of intercellular adhesion molecule 1 in human anulus fibrosus cells through FAK/ERK/GSK3 and PKCδ signaling pathways. *Int J Mol Sci* (2018) 20:77. doi: 10.3390/ijms20010077

68. Karli P, Martlé V, Bossens K, Summerfield A, Doherr MG, Turner P, et al. Dominance of chemokine ligand 2 and matrix metalloproteinase-2 and -9 and suppression of pro-inflammatory cytokines in the epidural compartment after intervertebral disc extrusion in a canine model. *Spine journal: Off J North Am Spine Soc* (2014) 14:2976–84. doi: 10.1016/j.spinee.2014.05.021

69. Holm S, Maroudas A, Urban JP, Selstam G, Nachemson A. Nutrition of the intervertebral disc: solute transport and metabolism. *Connective Tissue Res* (1981) 8:101–19. doi: 10.3109/03008208109152130

70. Sophia Fox AJ, Bedi A, Rodeo SA. The basic science of articular cartilage: structure, composition, and function. *Sports Health* (2009) 1:461–8. doi: 10.1177/1941738109350438

71. Liu L-T, Huang B, Li C-Q, Zhuang Y, Wang J, Zhou Y. Characteristics of stem cells derived from the degenerated human intervertebral disc cartilage endplate. *PloS One* (2011) 6:e26285–5. doi: 10.1371/journal.pone.0026285

72. Risbud MV, Guttapalli A, Stokes DG, Hawkins D, Danielson KG, Schaer TP, et al. Nucleus pulposus cells express HIF-1 alpha under normoxic culture conditions: a metabolic adaptation to the intervertebral disc microenvironment. *J Cell Biochem* (2006) 98:152–9. doi: 10.1002/jcb.20765

73. Luo L, Gong J, Zhang H, Qin J, Li C, Zhang J, et al. Cartilage endplate stem cells transdifferentiate into nucleus pulposus cells *via* autocrine exosomes. *Front Cell Dev Biol* (2021) 9:648201. doi: 10.3389/fcell.2021.648201

74. Luo L, Jian X, Sun H, Qin J, Wang Y, Zhang J, et al. Cartilage endplate stem cells inhibit intervertebral disc degeneration by releasing exosomes to nucleus pulposus cells to activate akt/autophagy. *Stem Cells (Dayton Ohio)* (2021) 39:467–81. doi: 10.1002/stem.3322

75. Freemont AJ, Peacock TE, Goupille P, Hoyland JA, O'Brien J, Jayson MI. Nerve ingrowth into diseased intervertebral disc in chronic back pain. *Lancet (London England)* (1997) 350:178–81. doi: 10.1016/S0140-6736(97)02135-1

76. Sun Z, Zhang M, Zhao X-H, Liu Z-H, Gao Y, Samartzis D, et al. Immune cascades in human intervertebral disc: the pros and cons. *Int J Clin Exp Pathol* (2013) 6:1009–14.

77. Chen S, Lei L, Li Z, Chen F, Huang Y, Jiang G, et al. Grem1 accelerates nucleus pulposus cell apoptosis and intervertebral disc degeneration by inhibiting TGF-β-mediated Smad2/3 phosphorylation. *Exp Mol Med* (2022) 54(4):518–30. doi: 10.1038/s12276-022-00753-9

78. Wang J, Xu Z, Wang Z, Du G, Lun L. TGF-beta signaling in cancer radiotherapy. *Cytokine* (2021) 148:155709. doi: 10.1016/j.cyto.2021.155709

79. Aubert A, Mercier-Gouy P, Aguero S, Berthier L, Liot S, Prigent L, et al. Latent TGF-β activation is a hallmark of the tenascin family. *Front Immunol* (2021) 12:613438–8. doi: 10.3389/fimmu.2021.613438

80. Gough NR, Xiang X, Mishra L. TGF-β signaling in liver, pancreas, and gastrointestinal diseases and cancer. *Gastroenterology* (2021) 161:434–452.e15. doi: 10.1053/j.gastro.2021.04.064

81. Pawlak JB, Blobe GC. TGF-β superfamily co-receptors in cancer. *Dev dynamics: an Off Publ Am Assoc Anatomists* (2022) 251:137–63. doi: 10.1002/dvdy.338

82. Zhao H, Wu L, Yan G, Chen Y, Zhou M, Wu Y, et al. Inflammation and tumor progression: signaling pathways and targeted intervention. *Signal transduction targeted Ther* (2021) 6:263. doi: 10.1038/s41392-021-00658-5

83. Tomasek JJ, Gabbiani G, Hinz B, Chaponnier C, Brown RA. Myofibroblasts and mechano-regulation of connective tissue remodelling. *Nat Rev Mol Cell Biol* (2002) 3:349–63. doi: 10.1038/nrm809

84. Zhang J, Li Z, Chen F, Liu H, Wang H, Li X, et al. TGF-β1 suppresses CCL3/4 expression through the ERK signaling pathway and inhibits intervertebral disc degeneration and inflammation-related pain in a rat model. *Exp Mol Med* (2017) 49: e379–9. doi: 10.1038/emm.2017.136

85. Li W, Liu T, Wu L, Chen C, Jia Z, Bai X, et al. Blocking the function of inflammatory cytokines and mediators by using IL-10 and TGF-β: a potential biological immunotherapy for intervertebral disc degeneration in a beagle model. *Int J Mol Sci* (2014) 15:17270–83. doi: 10.3390/ijms151017270

86. Yang H, Cao C, Wu C, Yuan C, Gu Q, Shi Q, et al. TGF-βl suppresses inflammation in cell therapy for intervertebral disc degeneration. *Sci Rep* (2015) 5:13254–4. doi: 10.1038/srep13254

87. Liu C, Li P, Ao X, Lian Z, Liu J, Li C, et al. Clusterin negatively modulates mechanical stress-mediated ligamentum flavum hypertrophy through TGF-β1 signaling. *Exp Mol Med* (2022) 54:1549–62. doi: 10.1038/s12276-022-00849-2

88. Grad S, Bow C, Karppinen J, Luk KD, Cheung KM, Alini M, et al. Systemic blood plasma CCL5 and CXCL6: Potential biomarkers for human lumbar disc degeneration. *Eur Cell Mater* (2016) 31:1–10. doi: 10.22203/eCM.v031a01

89. Haro H, Shinomiya K, Komori H, Okawa A, Saito I, Miyasaka N, et al. Upregulated expression of chemokines in herniated nucleus pulposus resorption. *Spine* (1996) 21:1647–52. doi: 10.1097/00007632-199607150-00006

90. Hegewald AA, Cluzel J, Krüger JP, Endres M, Kaps C, Thomé C. Effects of initial boost with TGF-beta 1 and grade of intervertebral disc degeneration on 3D culture of human annulus fibrosus cells. *J Orthop Surg Res* (2014) 9:73–3. doi: 10.1186/s13018-014-0073-8

91. Tran CM, Shapiro IM, Risbud MV. Molecular regulation of CCN2 in the intervertebral disc: lessons learned from other connective tissues. *Matrix biol: J Int Soc Matrix Biol* (2013) 32:298–306. doi: 10.1016/j.matbio.2013.03.006

92. Matta A, Karim MZ, Gerami H, Jun P, Funabashi M, Kawchuk G, et al. NTG-101: A novel molecular therapy that halts the progression of degenerative disc disease. *Sci Rep* (2018) 8:16809–9. doi: 10.1038/s41598-018-35011-4

93. Ramazani Y, Knops N, Elmonem MA, Nguyen TQ, Arcolino FO, . van den Heuvel L, et al. Connective tissue growth factor (CTGF) from basics to clinics. *Matrix biol: J Int Soc Matrix Biol* (2018) 68-69:44–66. doi: 10.1016/j.matbio.2018.03.007

94. Chia HN, Wu BM. Recent advances in 3D printing of biomaterials. *J Biol Eng* (2015) 9:4–4. doi: 10.1186/s13036-015-0001-4

95. Likhitpanichkul M, Dreischarf M, Illien-Junger S, Walter BA, Nukaga T, Long RG, et al. Fibrin-genipin adhesive hydrogel for annulus fibrosus repair: performance evaluation with large animal organ culture, *in situ* biomechanics, and *in vivo* degradation tests. *Eur Cell Mater* (2014) 28:25–38. doi: 10.22203/eCM.v028a03

96. Baffi MO, Slattery E, Sohn P, Moses HL, Chytil A, Serra R. Conditional deletion of the TGF-β type II receptor in Col2a expressing cells results in defects in the axial skeleton without alterations in chondrocyte differentiation or embryonic development of long bones. *Dev Biol* (2004) 276:124–42. doi: 10.1016/j.ydbio.2004.08.027

97. Zhang W, Yang M, Sun T, Zhang J, Zhao Y, Li J, et al. Can manganese dioxide microspheres be used as intermediaries to alleviate intervertebral disc degeneration with strengthening drugs? *Front bioengineering Biotechnol* (2022) 10:866290. doi: 10.3389/fbioe.2022.866290

98. Xie H, Jing Y, Xia J, Wang X, You C, Yan J. Aquaporin 3 protects against lumbar intervertebral disc degeneration *via* the wnt/β-catenin pathway. *Int J Mol Med* (2016) 37:859–64. doi: 10.3892/ijmm.2016.2470

99. Hiyama A, Sakai D, Risbud MV, Tanaka M, Arai F, Abe K, et al. Enhancement of intervertebral disc cell senescence by WNT/β-catenin signaling–induced matrix metalloproteinase expression. *Arthritis Rheumatism* (2010) 62:3036–47. doi: 10.1002/art.27599

100. Wang X, Wang B, Zou M, Li J, Lü G, Zhang Q, et al. CircSEMA4B targets miR-431 modulating IL-1β-induced degradative changes in nucleus pulposus cells in intervertebral disc degeneration *via* wnt pathway. *Biochim Biophys Acta (BBA) - Mol Basis Dis* (2018) 1864:3754–68. doi: 10.1016/j.bbadis.2018.08.033

101. Krupkova O, Hlavna M, Amir Tahmasseb J, Zvick J, Kunz D, Ito K, et al. An inflammatory nucleus pulposus tissue culture model to test molecular regenerative therapies: Validation with epigallocatechin 3-gallate. *Int J Mol Sci* (2016) 17:1640. doi: 10.3390/ijms17101640

102. Krupkova O, Ferguson SJ, Wuertz-Kozak K. Stability of (–)-epigallocatechin gallate and its activity in liquid formulations and delivery systems. *J Nutr Biochem* (2016) 37:1–12. doi: 10.1016/j.jnutbio.2016.01.002

103. Lee JM, Song JY, Baek M, Jung H-Y, Kang H, Han IB, et al. Interleukin-1β induces angiogenesis and innervation in human intervertebral disc degeneration. *J Orthopaedic Res* (2011) 29:265–9. doi: 10.1002/jor.21210

104. Gingras M, Bergeron J, Déry J, Durham HD, Berthod F. *In vitro* development of a tissue-engineered model of peripheral nerve regeneration to study neurite growth. *FASEB journal: Off Publ Fed Am Societies Exp Biol* (2003) 17:2124–6. doi: 10.1096/fj.02-1180fje

105. Kim IY, Seo SJ, Moon HS, Yoo MK, Park IY, Kim BC, et al. Chitosan and its derivatives for tissue engineering applications. *Biotechnol Adv* (2008) 26:1–21. doi: 10.1016/j.biotechadv.2007.07.009

106. Short B. How stomatin stops ASIC3 gating. *J Gen Physiol 152* (2020) 152(3): e202012574. doi: 10.1085/jgp.202012574

107. Yen L-T, Hsieh C-L, Hsu H-C, Lin Y-W. Preventing the induction of acid saline-induced fibromyalgia pain in mice by electroacupuncture or APETx2 injection. *Acupunct Med* (2020) 38:188–93. doi: 10.1136/acupmed-2017-011457

108. Bian J, Cai F, Chen H, Tang Z, Xi K, Tang J, et al. Modulation of local overactive inflammation *via* injectable hydrogel microspheres. *Nano Lett* (2021) 21:2690–8. doi: 10.1021/acs.nanolett.0c04713

109. Cua DJ, Tato CM. Innate IL-17-producing cells: the sentinels of the immune system. *Nat Rev Immunol* (2010) 10:479–89. doi: 10.1038/nri2800

110. Tan JH, Li ZP, Liu LL, Liu H, Xue JB. IL-17 in intervertebral disc degeneration: Mechanistic insights and therapeutic implications. *Cell Biol Int* (2022) 46:535–47. doi: 10.1002/cbin.11767

111. Wang S, Wei J, Fan Y, Ding H, Tian H, Zhou X, et al. Progranulin is positively associated with intervertebral disc degeneration by interaction with IL-10 and IL-17 through TNF pathways. *Inflammation* (2018) 41:1852–63. doi: 10.1007/s10753-018-0828-1

112. Banimostafavi ES, Fakhar M, Abediankenari S, Alizadeh-Navaei R, Mehdipour K, Omrani-Nava V, et al. Determining serum levels of IL-10 and IL-17 in patients with low back pain caused by lumbar disc degeneration. *Infect Disord Drug Targets* (2021) 21: e270421185135. doi: 10.2174/1871526520666200820093924

113. Jiang H, Deng Y, Wang T, Ma J, Li P, Tian P, et al. Interleukin-23 may contribute to the pathogenesis of lumbar disc herniation through the IL-23/IL-17 pathway. *J Orthop Surg Res* (2016) 11:12. doi: 10.1186/s13018-016-0343-8

114. Suyama K, Sakai D, Watanabe M. The role of IL-17-Mediated inflammatory processes in the pathogenesis of intervertebral disc degeneration and herniation: A comprehensive review. *Front Cell Dev Biol* (2022) 10:857164–4. doi: 10.3389/fcell.2022.857164

115. Bazzoni F, Beutler B. The tumor necrosis factor ligand and receptor families. *New Engl J Med* (1996) 334:1717–25. doi: 10.1056/NEJM199606273342607

116. Kepler CK, Markova DZ, Hilibrand AS, Vaccaro AR, Risbud MV, Albert TJ, et al. Substance p stimulates production of inflammatory cytokines in human disc cells. *Spine* (2013) 38:E1291–9. doi: 10.1097/BRS.0b013e3182a42bc2

117. Gruber HE, Hoelscher GL, Ingram JA, Bethea S, Norton HJ, Hanley EN. Production and expression of RANTES (CCL5) by human disc cells and modulation by IL-1-β and TNF-α in 3D culture. *Exp Mol Pathol* (2014) 96:133–8. doi: 10.1016/j.yexmp.2014.01.002

118. Wang Y, Che M, Xin J, Zheng Z, Li J, Zhang S. The role of IL-1β and TNF-α in intervertebral disc degeneration. *Biomed Pharmacother* (2020) 131:110660. doi: 10.1016/j.biopha.2020.110660

119. Ashraf S, Santerre P, Kandel R. Induced senescence of healthy nucleus pulposus cells is mediated by paracrine signaling from TNF-α–activated cells. *FASEB J* (2021) 35: e21795. doi: 10.1096/fj.202002201R

120. Anand P, Thomas SG, Kunnumakkara AB, Sundaram C, Harikumar KB, Sung B, et al. Biological activities of curcumin and its analogues (Congeners) made by man and mother nature. *Biochem Pharmacol* (2008) 76:1590–611. doi: 10.1016/j.bcp.2008.08.008

121. Singh S, Aggarwal BB. Activation of transcription factor NF-kappa b is suppressed by curcumin (diferuloylmethane) [corrected]. *J Biol Chem* (1995) 270:24995–5000. doi: 10.1074/jbc.270.42.24995

122. Anand P, Kunnumakkara AB, Newman RA, Aggarwal BB. Bioavailability of curcumin: problems and promises. *Mol pharmaceutics* (2007) 4:807–18. doi: 10.1021/mp700113r

123. Séguin CA, Pilliar RM, Roughley PJ, Kandel RA. Tumor necrosis factorα modulates matrix production and catabolism in nucleus pulposus tissue. *Spine 30* (2005) 30(17):1940–8. doi: 10.1097/01.brs.0000176188.40263.f9

124. Semenza GL. HIF-1: mediator of physiological and pathophysiological responses to hypoxia. *J Appl Physiol (Bethesda Md.: 1985)* (2000) 88:1474–80. doi: 10.1152/jappl.2000.88.4.1474

125. Guehring T, Wilde G, Sumner M, Grünhagen T, Karney GB, Tirlapur UK, et al. Notochordal intervertebral disc cells: Sensitivity to nutrient deprivation. *Arthritis Rheumatism* (2009) 60:1026–34. doi: 10.1002/art.24407

126. Tran CM, Fujita N, Huang B-L, Ong JR, Lyons KM, Shapiro IM, et al. Hypoxia-inducible factor (HIF)-1α and CCN2 form a regulatory circuit in hypoxic nucleus

pulposus cells: CCN2 suppresses HIF-1α level and transcriptional activity. *J Biol Chem* (2013) 288:12654–66. doi: 10.1074/jbc.M112.448860

127. Novais EJ, Choi H, Madhu V, Suyama K, Anjo SI, Manadas B, et al. Hypoxia and hypoxia-inducible factor-1α regulate endoplasmic reticulum stress in nucleus pulposus cells: Implications of endoplasmic reticulum stress for extracellular matrix secretion. *Am J Pathol* (2021) 191:487–502. doi: 10.1016/j.ajpath.2020.11.012

128. Meng X, Zhuang L, Wang J, Liu Z, Wang Y, Xiao D, et al. Hypoxia-inducible factor (HIF)-1alpha knockout accelerates intervertebral disc degeneration in mice. *Int J Clin Exp Pathol* (2018) 11:548–57.

129. Zheng J, Chang L, Bao X, Zhang X, Li C, Deng L. TRIM21 drives intervertebral disc degeneration induced by oxidative stress *via* mediating HIF-1α degradation. *Biochem Biophys Res Commun* (2021) 555:46–53. doi: 10.1016/j.bbrc.2021.03.088

130. Blanco JF, Graciani IF, Sanchez-Guijo FM, Muntión S, Hernandez-Campo P, Santamaria C, et al. Isolation and characterization of mesenchymal stromal cells from human degenerated nucleus pulposus: Comparison with bone marrow mesenchymal stromal cells from the same subjects. *Spine* (2010) 35:2259–65. doi: 10.1097/BRS.0b013e3181cb8828

131. Jia P, Yu L, Tao C, Dai G, Zhang Z, Liu S. Chitosan oligosaccharides protect nucleus pulposus cells from hydrogen peroxide-induced apoptosis in a rat experimental model. *Biomed Pharmacother* (2017) 93:807–15. doi: 10.1016/j.biopha.2017.06.101

132. He B, Tao H, Liu S, Wei A. Protective effect of carboxymethylated chitosan on hydrogen peroxide-induced apoptosis in nucleus pulposus cells. *Mol Med Rep* (2015) 11:1629–38. doi: 10.3892/mmr.2014.2942

133. Rastogi P, Kandasubramanian B. Review of alginate-based hydrogel bioprinting for application in tissue engineering. *Biofabrication* (2019) 11:042001. doi: 10.1088/1758-5090/ab331e

134. Skubutyte R, Markova D, Freeman TA, Anderson DG, Dion AS, Williams CJ, et al. Hypoxia-inducible factor regulation of ANK expression in nucleus pulposus cells: possible implications in controlling dystrophic mineralization in the intervertebral disc. *Arthritis rheumatism* (2010) 62:2707–15. doi: 10.1002/art.27558

135. Chen X, Gu S, Chen BF, Shen WL, Yin Z, Xu GW, et al. Nanoparticle delivery of stable miR-199a-5p agomir improves the osteogenesis of human mesenchymal stem cells *via* the HIF1a pathway. *Biomaterials* (2015) 53:239–50. doi: 10.1016/j.biomaterials.2015.02.071

136. Marchand F, Perretti M, McMahon SB. Role of the immune system in chronic pain. *Nat Rev Neurosci* (2005) 6:521–32. doi: 10.1038/nrn1700

137. Zhao Y, Qiu C, Wang W, Peng J, Cheng X, Shangguan Y, et al. Cortistatin protects against intervertebral disc degeneration through targeting mitochondrial ROS-dependent NLRP3 inflammasome activation. *Theranostics* (2020) 10:7015–33. doi: 10.7150/thno.45359

138. Rhee SG. Redox signaling: hydrogen peroxide as intracellular messenger. *Exp Mol Med* (1999) 31:53–9. doi: 10.1038/emm.1999.9

139. Lopes GKB, Schulman HM, Hermes-Lima M. Polyphenol tannic acid inhibits hydroxyl radical formation from fenton reaction by complexing ferrous ions1This study is dedicated to the memory of botany professor luiz F.G. labouriau (1921–1996). *Biochim Biophys Acta (BBA) - Gen Subj* (1999) 1472:142–52. doi: 10.1016/S0304-4165(99)00117-8

140. Ogawa T, Matsuzaki H, Uei H, Nakajima S, Tokuhashi Y, Esumi M. Alteration of gene expression in intervertebral disc degeneration of passive cigarette- smoking rats: Separate quantitation in separated nucleus pulposus and annulus fibrosus. *Pathobiology* (2005) 72:146–51. doi: 10.1159/000084118

141. Lee DC, Adams CS, Albert TJ, Shapiro IM, Evans SM, Koch CJ. *In situ* oxygen utilization in the rat intervertebral disc. *J Anat* (2007) 210:294–303. doi: 10.1111/j.1469-7580.2007.00692.x

142. Lowe KC, Davey MR, Power JB. Perfluorochemicals: their applications and benefits to cell culture. *Trends Biotechnol* (1998) 16:272–7. doi: 10.1016/S0167-7799(98)01205-0

frontiers | Frontiers in Immunology

TYPE Review
PUBLISHED 02 February 2023
DOI 10.3389/fimmu.2022.1047550

Check for updates

OPEN ACCESS

EDITED BY
Bo Li,
Sun Yat-sen Memorial Hospital, Sun Yat-sen University, China

REVIEWED BY
Dayun Feng,
Fourth Military Medical University, China
Sterling B. Ortega,
University of North Texas Health Science Center, United States

*CORRESPONDENCE
Jinwen Ge
001267@hnucm.edu.cn

SPECIALTY SECTION
This article was submitted to Multiple Sclerosis and Neuroimmunology, a section of the journal Frontiers in Immunology

RECEIVED 18 September 2022
ACCEPTED 05 December 2022
PUBLISHED 02 February 2023

CITATION
Zeng J, Bao T, Yang K, Zhu X, Wang S, Xiang W, Ge A, Zeng L and Ge J (2023) The mechanism of microglia-mediated immune inflammation in ischemic stroke and the role of natural botanical components in regulating microglia: A review.
Front. Immunol. 13:1047550.
doi: 10.3389/fimmu.2022.1047550

COPYRIGHT
© 2023 Zeng, Bao, Yang, Zhu, Wang, Xiang, Ge, Zeng and Ge. This is an open-access article distributed under the terms of the Creative Commons Attribution License (CC BY). The use, distribution or reproduction in other forums is permitted, provided the original author(s) and the copyright owner(s) are credited and that the original publication in this journal is cited, in accordance with accepted academic practice. No use, distribution or reproduction is permitted which does not comply with these terms.

The mechanism of microglia-mediated immune inflammation in ischemic stroke and the role of natural botanical components in regulating microglia: A review

Jinsong Zeng[1], Tingting Bao[2], Kailin Yang[3], Xiaofei Zhu[4], Shanshan Wang[3], Wang Xiang[5], Anqi Ge[1], Liuting Zeng[3] and Jinwen Ge[3,6]*

[1]The First Hospital of Hunan University of Chinese Medicine, Changsha, Hunan, China, [2]Institute of Metabolic Diseases, Guang'anmen Hospital, China Academy of Chinese Medical Sciences, Beijing, China, [3]Key Laboratory of Hunan Province for Integrated Traditional Chinese and Western Medicine on Prevention and Treatment of Cardio-Cerebral Diseases, Hunan University of Chinese Medicine, Changsha, China, [4]Fudan University, Shanghai, China, [5]Department of Rheumatology, The First People's Hospital Changde City, Changde, Hunan, China, [6]Hunan Academy of Chinese Medicine, Changsha, Hunan, China

Ischemic stroke (IS) is one of the most fatal diseases. Neuroimmunity, inflammation, and oxidative stress play important roles in various complex mechanisms of IS. In particular, the early proinflammatory response resulting from the overactivation of resident microglia and the infiltration of circulating monocytes and macrophages in the brain after cerebral ischemia leads to secondary brain injury. Microglia are innate immune cells in the brain that constantly monitor the brain microenvironment under normal conditions. Once ischemia occurs, microglia are activated to produce dual effects of neurotoxicity and neuroprotection, and the balance of the two effects determines the fate of damaged neurons. The activation of microglia is defined as the classical activation (M1 type) or alternative activation (M2 type). M1 type microglia secrete pro-inflammatory cytokines and neurotoxic mediators to exacerbate neuronal damage, while M2 type microglia promote a repairing anti-inflammatory response. Fine regulation of M1/M2 microglial activation to minimize damage and maximize protection has important therapeutic value. This review focuses on the interaction between M1/M2 microglia and other immune cells involved in the regulation of IS phenotypic characteristics, and the mechanism of natural plant components regulating microglia after IS, providing novel candidate drugs for regulating microglial balance and IS drug development.

KEYWORDS

ischemic stroke, microglia/macrophages, neuroimmune inflammation, natural botanical components, botanicals

1 Introduction

Ischemic stroke (IS) is one of the common cerebrovascular diseases, which seriously affects national health due to its high morbidity and lethality (1). It is characterized by the pathological changes of the cerebral arteries or the carotid arteries that innervate the brain, causing cerebral blood circulation disorders, which in turn lead to acute or subacute brain damage. It often causes patients to have varying degrees of language, motor and sensory dysfunction (2). Among them, focal rapid-onset cerebral ischemia-hypoxia (or hemispherical in the case of coma) persists for more than 24 hours or results in death (3). IS constitutes 87% of strokes, including cryptogenic, lacunar and thromboembolic strokes (4). The risk factors for IS include age, smoking, diabetes, high blood pressure and obesity (5). The pathological mechanism is that ischemia and hypoxia in the brain can lead to a series of events including calcium overload, excitatory amino acid neurotoxicity, free radical generation, activation of apoptotic genes, and immune inflammation (6). In fact, recent studies have found that the inflammatory response plays a dual key role in neuroprotection and neurotoxicity in IS (6). Activation of resident cells, such as microglia, astrocytes and endothelial cells promotes both brain regeneration and recovery. It also recruits immune cells that express inflammatory mediators, leading to blood-brain barrier (BBB) disruption, neuronal death, brain edema, and hemorrhagic transformation (6). In this case, clinical treatment options for acute ischemic stroke remain limited. Intravenous injection of tissue-type plasminogen activator (t-PA) restores cerebral perfusion through thrombolysis, which to a certain extent rescues dying cells in the ischemic penumbra (7). However, the treatment time window of 3-4.5 hours is too narrow for practical use of thrombolytics in most parts of the world. Once the therapeutic window is exceeded, the benefits of t-PA are outweighed by its risks, with a dramatic increase in the chance of hemorrhagic transformation (8). Meanwhile, the choice of medical devices for intra-arterial thrombectomy can be used as an alternative to clinical thrombolysis, but it may also cause other complications, so it has great limitations (9). The current study shows that the regulation of immune cells after stroke is the key to regulating inflammation and repairing vascular neural units after stroke (10). As the main body of neuroimmune inflammation in the brain after stroke, microglia play functions such as immune recruitment, regulation, inflammation, phagocytosis, and vascular repair, which in turn become the key to the development of stroke drugs (11). This review focuses on the interaction between classical activation (M1 type) or alternative activation (M2 type) microglia and other immune cells involved in the regulation of IS phenotypic characteristics. Meanwhile, Our previous studies have found that natural compounds and multi-component herbs may treat IS by regulating microglia (12–16); other teams also explored the mechanism by which natural plant active ingredients regulate microglia after IS (17). Therefore, this review also summarizes the natural plant compounds that regulate M1/M2 microglia after IS, in order to provide candidate or lead compounds for the development of drugs that regulate neuroimmune inflammation after IS.

2 Pathological mechanisms of immune inflammation in IS

2.1 Pathological mechanism of IS

Following an ischemic attack, a series of events involving the central nervous system (CNS) is triggered (18). The pathogenesis of IS begins in the blood vessels, in part due to arterial occlusion leading to hypoxia, reactive oxidative species production, and changes in shear stress on the luminal wall (19, 20). During hypoxia, shear stress on the vascular endothelium due to changes in rheology and blood flow stagnation causes activation of platelets, the complement system and the coagulation cascade, resulting in endothelial cell destruction and microvascular occlusion (21). The combined effect of oxidative stress, inflammatory mediators (such as IL-1β, TNF-α), down-regulated endothelin, and up-regulated leukocyte- or vascular-derived proteases increases BBB permeability (22). Endothelial cell-derived prostaglandins and chemoattractants also promote leukocyte entry into the infarct site (22). The increased surface affinity of leukocytes, the activation of integrin molecules and the up-regulated expression of corresponding ligands on endothelial cells further promote the infiltration of neutrophils, macrophages and other leukocytes. Activated leukocytes produce reactive oxidative species, proteolytic enzymes, cytokines, platelet-activating factor, which promote vasoconstriction, platelet aggregation and further neurotoxicity (19). In the perivascular space, activated macrophages secrete numerous pro-inflammatory cytokines, leading to the release of histamine, proteases and TNF-α, and further reducing the integrity of the BBB (18).

While all of the above processes occur in the vascular and perivascular spaces, ischemia can also affect the brain parenchyma. Following the impact of ischemia, a series of interrelated cytoplasmic and nuclear events, including bioenergetic exhaustion, excitotoxicity, Ca2+ overload, oxidative stress, and inflammatory responses, begin to occur at the damaged site, culminating in neuronal cell death (20). Excitotoxicity and Ca2+ overload are the main factors leading to the early stage of ischemic cell death (23). Glutamate overload results in prolonged activation of AMPA and NMDA ionotropic receptor subtypes, resulting in an enhanced influx of calcium, sodium and water to neurons (23). A large influx of calcium activates protease, lipase and nuclease-mediated catabolic

processes (24). Increased calcium influx from glutamate receptor hyperactivation, Ca2+ release from mitochondria, and failure of Ca2+ efflux mechanisms are known to explain the irreversible accumulation of intracellular Ca2+ following excitotoxic stimulation. Meanwhile, oxidative and nitrosative stress are also potent mediators of ischemic injury. Under normal physiological conditions, there is a balance between the production and decomposition of reactive oxygen species (ROS), but IS disrupts this balance and leads to an increase in its production (25). The metabolic activity of ROS and reactive nitrogen species is rapid, and the antioxidant defense capacity of the brain is limited, so the brain is sensitive to damage caused by oxidative and nitrosative stress (26). Damage-associated molecular patterns (DAMPs) released by dying neurons contribute to a new phase of the inflammatory response (27, 28). Among them, heat shock proteins, high mobility group-binding protein 1 (HMGB1), mitochondria-derived N-formyl peptides and peroxidases, activate brain-native immune cells through pattern recognition receptors (29–31). DAMPs lead to an inflammatory environment by stimulating immune cells to produce cytokines, chemokines, adhesion molecules and many immune effector molecules (32–34).

2.2 Key events and pathways of immune biological modules involved in the IS pathological progression

After the occurrence of IS, the immune system starts rapidly, participates in all aspects of the occurrence, development and prognosis of stroke, and plays a corresponding role in different stages of stroke (35). Intracerebral inflammation after IS is not limited to the surrounding ischemic foci, but spreads to the whole brain and persists for a long time, continuously affecting the pathophysiological changes of brain tissue after stroke (36). Therefore, understanding the changes and roles of immune responses in different stages of stroke has important guiding significance for further research on neuroprotection and neuroreparation in stroke. Previous studies have shown that in the early stage of IS, various inflammatory cells and factors are involved in the development of inflammation in the brain and aggravate secondary brain injury (21, 37). In the subacute phase, brain injury can remodel the immune system, turning immune system function from activation to suppression, but it leads to an increase in post-stroke infections (21, 38). Moreover, the spread of neuroinflammation in the whole brain after IS can lead to delayed brain tissue changes (39).

2.2.1 Immune activation after IS

After the occurrence of IS, with the occurrence of intravascular hypoxia and changes in hemodynamics, platelets, coagulation and complement systems are activated, and the inflammatory response first occurs in the blood vessels (40). The oxidative stress response and activated complement system caused by hypoxia directly damage the local vascular system, leading to necrosis and dissociation of vascular endothelial cells, destruction of BBB integrity, and exposure of antigens under the vascular endothelium (41). Immune cells in the blood adhere to the vessel wall and upregulate the expression of adhesion factors and chemokines. Innate immune cells such as neutrophils, monocytes, and macrophages are activated, migrate to ischemic sites under the action of chemokines and extravasate into the extravascular space through the damaged BBB (42). Subsequently, macrophages in the ischemic brain tissue are activated to further release inflammatory factors and aggravate the chemotaxis and extravasation of innate immune cells (43). Meanwhile, immune cells such as neutrophils and mast cells at the site of ischemic injury release intracellular MMPs, destroy vascular basement membrane and tight junction proteins, accelerate the destruction of BBB, and lead to an increase in cerebral infarct size (44). Neurons are extremely sensitive to ischemia, hence, ischemia leads to rapid neuronal necrosis. Necrotic neurons release endogenous factors, called DAMPs. DAMPs increase the release of chemokines from immune cells through Toll-like receptors (TLRs) on the surface of immune cells such as microglia, macrophages, dendritic-like cells, and exuding neutrophils (45). This further promotes the chemotaxis of immune cells, activates and amplifies the innate immune response, accelerates vascular destruction and cell death, and ultimately forms a vicious cycle of vascular damage, inflammation, and neuronal death (46). The adaptive immune response is the second phase of the immune response after ischemic stroke, which arises from BBB disruption. Normally immune-isolated central nervous system antigens can contact antigen-presenting cells (APCs) in peripheral blood to induce autoimmune responses. DAMPs can promote the interaction between APCs and receptors to activate adaptive immune responses, which are mediated by effector T cells (47). Effector T cells play a role in the adaptive immune response by recruiting to ischemic areas, traversing the injured BBB, releasing inflammatory cytokines such as interferon gamma (IFN-γ) in the brain parenchyma, and ultimately leading to delayed neurotoxicity (39, 48). The immune response after IS is a self-limiting pathophysiological process that gradually subsides under the combined action of regulatory T cells and B cells, preparing for the structural and functional reconstruction of the later brain injury site. In the process of inflammation resolution, regulatory T cells play a role through IL-10 and transforming growth factor-β (TGF-β) secreted by macrophages in the local tissues, inhibiting helper T cells to further induce inflammation, thereby promoting the repair of residual neurons (49, 50).

2.2.2 Immunosuppression after IS

After IS, while the immune system is activated, immunosuppression will occur at the same time. The systemic immune function is down-regulated within a few hours after

cerebral ischemia, the cellular immunity is suppressed, the number of various immune cells such as monocytes, T lymphocytes, B lymphocytes and natural killer cells is decreased, apoptosis is increased, or cell dysfunction occurs (51). Meanwhile, a variety of inflammatory factors, including IL-10, IL-1β, TNF-α, IL-6, etc. are inhibited. This immunosuppressive state is known as stroke-induced immunosuppressive syndrome (SIDS) (52). Its occurrence is related to the activation of the hypothalamic-pituitary-adrenal axis and the sympathetic nervous system caused by stress, and the secretion of adrenocortical hormones and catecholamines increases and plays an immunosuppressive effect (53). Immune activation and immunosuppression after IS are a contradictory unity. The former removes necrotic tissue through inflammatory response to create conditions for nerve repair, and it can also cause secondary nerve damage due to an excessive inflammatory response. The latter can reduce the destruction of neurons by the immune system and play a neuroprotective role, but excessive immunosuppression inevitably increases the chance of infection and worsens clinical prognosis (54).

3 Mechanisms of microglia/macrophages in IS

3.1 Physiological functions of microglia

Microglia account for approximately 10% of the CNS and are traditionally thought to function as immunocompetent cells of the brain and spinal cord, and undertake sensory functions of injury and infection in tissues (55). Microglia is derived from the primitive c-kit(+) erythroid precursor in the yolk sac, migrates into the brain during early embryonic development before the formation of the BBB, and remains there until the BBB is formed (56). Notably, this is a population of self-maintaining and renewing cells, and peripheral macrophages only contribute to this population in disease states, i.e. when the BBB is damaged (57). Initial studies generally believed that under normal physiological conditions, the microglia in the brain were branched with multiple slender protrusions and were in a resting state. However, recent studies have shown that the microglia never really rests, and the branched microglia constantly patrols the brain, using its motor branch as a sentinel to investigate and scan its nearby microenvironment to detect changes in brain homeostasis (58). Once a threat is identified, microglia rapidly activate to an amoeba-like phenotype with large cell bodies (59). Activated microglia can eliminate cellular debris through phagocytosis on the one hand, and produce a wide range of signaling molecules, including cytokines, neurotransmitters, and extracellular matrix proteins, to regulate neuronal and synaptic activity and their functional plasticity (58). Furthermore, when microglia are involved in the degradation of internalized targets in the phagosome, it may become a major source of ROS. If these internalization targets are too large and not properly processed inside the phagosome, it will result in the release of toxic molecules, including ROS, from the surrounding microglia (60). The normal phagocytosis process is accompanied by the release of several anti-inflammatory cytokines, growth factors and neurotrophic factors, and reduced release of pro-inflammatory cytokines (61). As immune effector cells in the CNS, microglia are continuously active. They monitor the brain microenvironment in real time through the elongation and retraction of branches, modulate neural circuits through specific interactions with neuronal synapses (59, 62), participate in pruning synapses and clear apoptotic cells in time to maintain CNS homeostasis (63–65). They play an important role in most known CNS diseases. A study has monitored the interaction between neurons and fluorescently labeled microglia in transgenic mice by intravital two-photon microscopy imaging (66). They found that microglia made direct contact with neuronal synapses during imaging every 5 minutes for 1 hour. Microglia can rapidly change their phenotype in active response to perturbation of CNS homeostasis and are often activated based on changes in their morphology or cell surface antigen expression (67–69).

3.2 Activation and differentiation of microglia/macrophages regulate immune inflammation

3.2.1 Activation of microglia/macrophages after IS

M2-type microglia mainly regulate the repair of brain injury after IS. It mainly promotes the survival and recovery of injured neurons by secreting brain-derived neurotrophic factors, insulin secretion factors and transforming growth factors, and at the same time enhances the ability of neurons to withstand stimulation and damage (70, 71). It produces cytokines IL-10, TGF-β, IL-4, IL-13, IGF-1, etc., which cooperate with the clearance of infiltrating neutrophils, thereby preventing neuronal damage caused by cytotoxic substances (72, 73). Unlike M2-type microglia, which inhibit inflammation, M1-type microglia will produce a large number of pro-inflammatory cytokines IFN-γ, IL-1β, TNF-α, IL-6, etc. to activate the inflammatory cascade, and promote the activation of T and B lymphocytes to regulate immune responses. It can also increase the release of vasoactive factors, causing vasoconstriction and aggravating ischemic cerebral edema (74). M1 type acts on the extracellular matrix through the production of ROS and NO production as well as proteolytic enzymes (MMP9, MMP3), resulting in the decomposition of BBB (39, 75). M1 type also generates reactive oxygen species through nicotinamide adenine dinucleotide phosphate (NADPH) oxidase, which further aggravates the damage of cerebral ischemia (76, 77). Therefore,

regulating the homeostasis of M1/M2 type may become an important strategy for the treatment of IS.

3.2.2 Activation and differentiation of M1/M2 type microglia/macrophages

As the first line of defense of the immune system in the brain, microglia are rapidly activated within minutes of the acute phase of ischemic stroke, peak around day 2/3 of activation, and persist for several weeks after the onset of IS (78). At the core of ischemic injury, microglia activation is essentially triggered by excitotoxic signals generated during the ischemic cascade. In the peri-infarct region, the activation of microglia is associated with several innate immune receptors that can be activated by DAMP stimulation (79). For example, purinergic receptors, especially P2X7 and P2Y12, regulate microglial activation and mediate neurotoxicity, and similarly, pharmacological inhibition of P2X7 and P2Y12 reduces brain damage in experimental stroke models (80). Several other innate immune receptors involved in microglial activation include TLR, CD36 scavenger receptor, and receptor for advanced glycation end products (RAGE) (81). In addition to morphological changes, activated microglia also showed altered gene expression patterns, polarizing toward functionally distinct phenotypes: "classically activated" M1 and "alternatively activated" M2.

At present, the main signal pathways that contribute to the polarization of M1/M2 microglia are as follows: (1) IFN-γ secreted by helper T cells 1 (Th1) induces the transformation of microglia into M1 phenotype by activating JAK1/JAK2 and STAT (82). (2) Another pathway to induce M1 activation is triggered by lipopolysaccharide (LPS) or DAMP stimulation of TLR4. Subsequently, an "activation complex" composed of myeloid differentiation factor 88 (Myd88), nuclear factor-KB (NF-KB), p65, p38 and interferon regulatory factor 3 (IRF3) is formed (83). This complex in turn regulates the expression of inflammatory mediators of M1-inducible nitric oxide synthase (iNOS), CD16, CD32, etc. and cell surface markers-histocompatibility complex (MHC-II), CD86, etc. Microglial polarization of the M1 phenotype is characterized by high expression of IL-12, high expression of IL-23 and low expression of IL-10 (84). M2-type microglial replacement activation is usually induced by IL4 or IL-10 and IL-13, and is usually characterized by high expression of IL-12, high expression of IL-23b, and low expression of IL-10. To activate M2-type microglia, IL4 or IL-13 binds to IL4Rx or IL-13Ra1 to activate transcription factors, such as STAT6, peroxisome proliferator-activated receptor gamma (PPARγ), Jumonji domain-containing protein 3 (Jmjd3), and IRF4, respectively. This subsequently causes M2-type microglia to release cytokines such as IL-10, transforming growth factor B (TGFβ), IL-1 receptor agonists, CD302, CD163 and other inflammatory mediators such as platelet-derived growth factor (PDGF), fibronectin 1 and arginase 1 (Arg1), etc. (84).

3.2.3 Activation of microglia and activation, recruitment and polarization of blood-derived macrophages after IS

After IS, intracerebral microglia are rapidly activated within minutes of injury (85), while disruption of BBB integrity allows macrophages to infiltrate the injury site (86, 87). Cerebral ischemia results in dramatic changes in the morphology, density, and function of branched microglia, including processes such as cell body enlargement, debranching, and cell wall thickening. It eventually becomes "amebic", produces inflammatory proteins, and undergoes changes in proliferation, migration, and phagocytosis (88). Because microglia and blood-migrating macrophages are morphologically indistinguishable and perform similar functions, they are represented as microglia/macrophages in many studies. The current single-cell transcriptomic sequencing also found that the two have similar phenotypes (89). Activated microglia/macrophages have been found to produce a variety of mediators, including iNOS (90), inflammatory cytokines (such as TNF-α, IL-1β, TGF-β, IL-10) (86), nerve growth and trophic factors (such as IGF-1, bFGF, PDGF, BDNF) (91).

Many surface receptors involved in regulating the activation and function of microglia/macrophages have been found: (1) TLRs: TLRs represent a series of pattern-recognition transmembrane receptors that recognize relevant molecular patterns on the surface of pathogens. It is an essential component of the innate immune response of microglia and induces microglia to produce neurotoxic factors that contribute to the microglia response to neuronal damage (92, 93). Studies have found that stimulation of TLR2 and TLR4 activates microglia, produces pro-inflammatory cytokines, and exacerbates brain damage after focal cerebral ischemia (94–99). Knockdown of TLR2 or TLR4 reduces the production of TNF-α, iNOS and cyclooxygenase-2 (COX-2), contributing to smaller cerebral infarct volume (100, 101). (2) Purinergic receptors: Purinergic receptors consist of P1 adenosine receptors and P2ATP receptors (102). Among P1 adenosine receptors, A2A receptors are upregulated in microglia after focal cerebral ischemia and are involved in the control of microglial proliferation and BDNF release induced by LPS stimulation (103). The use of A2A receptor antagonists attenuates ischemia-induced brain damage (104). P2ATP receptors are composed of P2X and P2Y receptors, each containing distinct subunit subtypes (105, 106). Among them, the P2X7 receptor mediates microglia activation after ischemic stroke (107, 108). P2X7 receptor activation induces microglia to release proinflammatory cytokines such as TNF-α, IL-1β, NO, CXCL2 and CCL (109, 110). In addition, P2Y12 is another purinoceptor expressed on microglia, and P2Y12 is down-regulated upon activation of microglia. The accumulation of microglia in the infarcted area was reduced after knockout of the

P2Y12 receptor, while attenuating neuronal death following cerebral ischemia in mice (80). (3) CCR2: CCR2 is present in almost all immune cells and highly inflammatory mononuclear MPs (111). However, under normal conditions, CCR2 is poorly expressed in brain microglia (102, 112). CCR2 and its ligand monocyte chemoattractant protein-1 (MCP-1) are upregulated in microglia and migrating macrophages after ischemic stroke (113). Activation of CCR2 enhances cerebral inflammatory responses and significantly increases the volume of cerebral infarcts (114). Deletion of CCR2 in mice reduces blood immune cell recruitment, but does not affect microglia activation after transient MCAO (115). Thus, CCR2 appears to be critical for blood immune cell recruitment, but has little effect on microglia activation after focal cerebral ischemia. (4) Receptor for advanced glycation end products (RAGE): RAGE is another receptor that mediates the activation of microglia/macrophages and plays an important role in the inflammatory response of many diseases (116, 117). In IS patients, RAGE is upregulated in brain and plasma (117, 118). *In vitro* studies have shown that the interaction between RAGE and its ligand high mobility group box 1 (HMGB1) is critical for neuronal death induced by microglia activation (119).

3.2.4 Molecular mechanisms of signaling pathway transduction of M1 and M2 polarization under IS

Microglia/macrophages are activated and polarized upon an ischemic injury, and the degree of polarization changes with pathophysiological conditions (102, 120, 121). Different phenotypes of microglia/macrophages can differentially regulate dying cells after brain injury, possibly aggravating neuronal death or promoting damaged tissue repair (122, 123). Among them, iNOS, IL-1β, IL-6, TNF-α, etc. can be used as molecular markers of M1-type microglia/macrophages. IL-10, IL-4, TGF-β, CD206, Ym1, etc. can be used as molecular markers of M2-type microglia/macrophages. Studies on the progression of IS over time found that on day 1, the M2 phenotype marker Ym1 was highly upregulated in border regions, which induces an M2-type response that provides a protective function for the damaged brain; on day 7, it performs a phagocytic function (124). Further studies showed that M1/M2 microglia participate in different stages of IS. Among them, M2 type mainly appeared in the early stage of cerebral ischemia, appeared 1 to 3 days after ischemia, rose to the highest peak in 3 to 5 days, and returned to the low level before injury on the 14th day. Then it gradually transformed into M1 type on the 3rd day, and maintained a high level for 14 days after ischemia (31). In addition, microglia/macrophages are susceptible to ischemia-induced injury, which may be related to the purinoceptors P2X4 and P2X7, resulting in reduced numbers and suppressed activity of microglia/macrophages in the ischemic core (125, 126). Thus, low levels of microglia/macrophages in the ischemic core and high proportions of M1 and M2 phenotype cells in the peri-infarct area may contribute to the pathological process of ischemic injury.

The signaling molecules associated with M1 phenotype polarization mainly include the following: (1) NF-κB: NF-κB is a traditional transcription factor that is activated by LPS and regulates the expression of most M1 phenotype marker genes. Substantial evidence suggests that the NF-κB signaling cascade adversely affects cerebral ischemia because of its role in regulating pro-inflammatory mediators, including IL-1, IL-2, IL-6, IL-12, TNF-α, iNOS and cyclooxygenase-2 (COX-2) (127, 128). In addition, NF-κB regulates the expression and activation of MMPs, leading to leakage of the BBB and exacerbating the inflammatory response (129, 130). (2) Notch signaling: Notch signaling in response to LPS activation enhances IFN-γ production by co-recruiting p50 and c-Rel (131, 132). Notch signaling exacerbates ischemic brain injury by prolonging NF-κB activation with concomitant persistent inflammation and enhancing microglia/macrophage-induced neurotoxicity (131, 133). (3) Signal transducers and activators of transcription (STAT1 and STAT3): STAT1 and STAT3 can increase the expression of NF-κB/p65 (134). Inhibition of the activation of STAT1 and STAT3 attenuates the inflammatory response induced by cerebral ischemia while improving infarct volume (135, 136). (4) Glycogen synthase kinase-3β (GSK-3β): Cerebral ischemia-induced dephosphorylation and activation of GSK-3β reduces cAMP response element-binding protein (CREB) activity while enhancing NF-κB signaling to initiate pro-inflammatory capacity (137, 138). (5) Prostaglandin E2 (PGE2): PGE2 is the main product of cyclooxygenase and prostaglandin E synthase, and is considered to be a typical pro-inflammatory mediator in the brain. PGE2 activates its downstream signaling pathways through the G protein-coupled E-prostaglandin (EP) receptors EP1-EP4 (139). The EP1 receptor is expressed in microglia, and EP1 deletion inhibits microglial activity and phagocytosis. Although EP2 is expressed in neurons and not in microglia, loss of EP2 results in increased activation of M1-type microglia, suggesting that EP2 mediates the interaction between neurons and microglia (140, 141). (6) mTORC1: mTORC1 is a protein complex downstream of the PI3K-AKt pathway, and is one of the participants in the dysregulation after ischemia and OGD. Maria J et al. (142) showed that blocking mTORC1 can reduce lesion size, improve motor function, significantly reduce the production of pro-inflammatory cytokines and chemokines, and reduce the number of M1-type microglia. Thus, mTORC1 blockade attenuates behavioral deficits and post-stroke inflammation after MCAO by preventing the polarization of microglia towards the M1 type. (7) Related microRNAs: Recent studies have also identified the role of microRNAs (miRNAs) in microglial polarization (143). Current studies have shown that miRNAs involved in the positive regulation of microglial activation and M1 transformation after IS include: miR-689, miR-124, miR-155, miRNAlet-7c-5p, miRNA-200b, MiR-377,

etc. These may be related to pro-inflammatory pathways and M1-type polarization (144, 145).

The signaling molecules associated with M2 phenotype polarization mainly include the following: (1) Peroxisome proliferator-activated receptor γ (PPARγ): In the inflammatory response, PPARγ can inhibit the inflammatory response by competitively inhibiting the inflammatory signaling pathway and the generation of inflammatory mediators. Among them, the crosstalk between Notch and NF-κB signaling pathway can inhibit the expression of PPARγ, which will decrease the expression of PPARγ after stroke, thereby aggravating the inflammatory response (146, 147). (2) cAMP response element binding protein (CREB): CREB cooperates with C/EBPβ and amplifies the expression of M2 phenotype-specific genes such as IL-10 and Arg1, promoting tissue repair (148), while the expression of M1 phenotype genes encoding pro-inflammatory molecules is also regulated by C/EBPβ (149). The dual role of C/EBPβ in regulating gene expression of M1 and M2 phenotypes may result from the competition between CREB and NF-κB for binding to C/EBP (148, 150). (3) Interferon regulatory factor-3 (IRF-3): In response to TLR activation, PI3K/Akt signaling initiates phosphorylated IRF-3. Activated IRF-3 translocates into the nucleus and drives polarization of the M2 phenotype by interacting with CREB-binding protein (CBP) (151, 152). (4) Related microRNAs: Current studies have shown that miR-124, miR-711, miR-145, miRNA203 and miRNA27a, which are involved in the positive regulation of microglial activation and M2 transformation after ischemic stroke, may be involved in the regulation of anti-inflammatory pathways and M2-type polarization (144, 145). Among them, miR-146a can not only inhibit the LPS-induced M1-type polarization of microglia, but also promote the M2-type polarization of microglia (145).

3.3 Regulation of cellular interactions between microglia/macrophages, neurons, and other immune-inflammatory cells after IS

3.3.1 The effect of the interactive regulation of microglia/macrophages and neurons on brain injury after IS

After IS, a large number of nerve cells die due to reduced blood flow and insufficient supply of glucose and oxygen. Dying neuronal cells release injury-associated ligands and excitotoxic glutamate to promote microglia/macrophage activation (153), thereby exacerbating neuronal damage (154). However, ischemia-induced neuronal injury can release IL-4, which can enhance the expression of IL-4 receptors in microglia/macrophages and promote microglia/macrophage polarization to the M2 phenotype. IL-4-activated PPARγ enhances the phagocytosis of apoptotic neurons by microglia/macrophages (155). The release of glutamate enables neurons to secrete soluble fractalkine (sFKN), which enhances the ability of microglia/macrophages to clear neuronal debris (156). These studies suggest that damaged neurons can promote microglia/macrophage protection to help neurons survive ischemic conditions (154, 157–159). Microglia/macrophages play a beneficial role in tissue remodeling and regeneration after IS by eliminating dead or dying neurons (160). A study of the infiltration of microglia and macrophages in the brain of chimeric mice found that microglia in the brain could phagocytose neuronal debris as early as day 1, and reached a peak on day 2, while infiltrating macrophages began to clear neuronal debris on day 4 after MCAO. They found that microglia in the brain are more sensitive and important in defense against ischemia by eliminating dead neurons (115).

3.3.2 The effect of interaction between microglia/macrophages and astrocytes on brain injury after IS

Microglia and astrocytes play important roles in the innate immune environment of the brain. In two-photon microscopy-based time-lapse imaging recordings, it was found that microglia directly contact astrocytes by extending their branches toward the astrocytes (161). When the brain microenvironment is disrupted, microglia/macrophages and astrocytes play important roles in various pathological states such as IS (162–164). Among them, modulators such as IL-1β, TNF-α, TGF-β, adenosine, ATP and glutamate contribute to functional communication between microglia/macrophages and astrocytes (165–168), which is critical for immune responses in the brain (163). In the CNS, astrocytes mainly secrete cytokines such as IL-6, IL-1β, and IL-10. In addition, astrocytes secrete many chemokines, such as CCL2, CXCL1, CXCL10, and CXCL12, etc., and several chemokines have been found to be involved in microglial activation and polarization, as well as M1 and M2 phenotype switching. *In vitro* studies found that CCL2 released by primary astrocytes contributed to the polarization of M1-type microglia. The proinflammatory mediator lysophosphatidylcholine (LPC) produced by neurons and astrocytes after IS stimulates microglia/macrophages to upregulate the mRNA expression of Mcp-1 and Ccr2, which is involved in mediating the inflammatory response after cerebral ischemia (113). Therefore, there is a complex communication between microglia/macrophages and astrocytes.

3.3.3 The effect of the interaction between microglia/macrophages and T cells on brain injury after IS

After cerebral ischemia, T cells activate and infiltrate into brain tissue, release cytokines and ROS, and induce brain injury by inducing early inflammatory response (169). However, some T cell subtypes have protective effects on brain cells in the early stage of cerebral ischemia. Existing evidence shows that T cells also play an important role in the repair and regeneration of

brain tissue in the late stage of stroke (170). T cells include a variety of functional subsets, mainly pro-inflammatory Th1 and Th17 subsets and anti-inflammatory Th2 and Treg subsets. Different T cell subsets play different roles in ischemic brain injury (171). Among them, Th1 can secrete pro-inflammatory cytokines IL-2, IL-12, INF-γ and TNF-α, and play an important role in IS; while Th2 can exert neuroprotective effects by secreting anti-inflammatory cytokines IL-4, IL-10, IL-5 and IL-13 (172). Th17 mainly secretes IL-17, which can promote the occurrence of inflammation (172). IL-10 secreted by Treg is also an important brain protective mediator, which exerts neuroprotective effects mainly by inhibiting the secretion of pro-inflammatory cytokines TNF-α and INF-γ. Treg inhibits secondary infarct enlargement by inhibiting the production of pro-inflammatory cytokines, regulating lymphocyte activation and/or human invasion of ischemic brain tissue (172, 173). After IS, activated microglia and secreted cytokines promote the differentiation of T cells into different functional subsets (6). Among them, M1-type microglia promote the proliferation and differentiation of Th1, while M2-type microglia induce the production of Treg with strong inhibitory function. The interaction between them exerts pro-inflammatory and anti-inflammatory effects, respectively, after stroke, thereby inhibiting the occurrence of the disease or promoting the recovery of the disease (174). Immunofluorescence double-staining of IS brain tissue found that there was a certain interaction between microglia and T cells, indicating that T cells also had a certain regulatory effect on the mutual transformation of M1/M2 microglia (175, 176).

(1) Interaction between M1-type microglia and Th1/Th17: After ischemia, M1-type microglia can produce pro-inflammatory cytokines leading to BBB disruption (177). Both Th1 and M1 microglia can produce pro-inflammatory cytokines, and iNOS is closely related to inflammatory cells. Cerebral ischemia can induce the up-regulation of iNOS mRNA and protein expression in inflammatory cells, enhance iNOS activity, and promote the production of NO, which can further generate peroxynitrite, thereby aggravating brain damage (178, 179). Studies have shown that Th1 can produce IFN-γ and promote the transformation of microglia into M1 type, thereby aggravating secondary ischemic injury (180). In addition, M1-type microglia can induce Th1 to secrete pro-inflammatory cytokines IL-12 and TNF-α (181–183), and the chemokines (CXCL9, CXCL10) they express can mobilize Th1 to participate in the inflammatory response. Therefore, Th1 and M1-type microglia interact after cerebral ischemia, and can simultaneously promote inflammatory response and aggravate brain injury. IL-17 secreted by Th17 is a powerful pro-inflammatory cytokine that induces the expression of other pro-inflammatory cytokines (such as IL-6 and TNF-α), chemokines, and MMPs, causing inflammatory cell infiltration and tissue destruction. Meanwhile, M1-type microglia induce Th17 differentiation by secreting IL6 and IL-23, which together promote immune response (181–183). Therefore, M1-type microglia and Th17 act as pro-inflammatory effects of brain injury after cerebral ischemia.

(2) Interaction between M2-type microglia and Th2/Treg: After cerebral ischemia, the expression of inflammatory mediators is up-regulated, which induces the accumulation of microglia to the injured area and breaks the dynamic balance between M1 and M2 types. The anti-inflammatory cytokines IL4 and IL-10 secreted by Th2 can further promote the polarization of microglia to M2 type (184, 185). This indicates that there is an interaction between M2-type microglia and Th2 cells, which together play an anti-inflammatory role after cerebral ischemia (186). After cerebral ischemia, Treg inhibits the activation of microglia and reduces the inflammatory response in the brain by secreting IL-10 and TGF-β (187). In addition, Treg cell-derived osteopontin acts through integrin receptors on microglia to enhance the repair activity of microglia, thereby promoting oligodendrogliosis and white matter repair (188). Treg can induce the polarization of microglia to M2 type through the IL-10/GSK3 β/PTEN signaling pathway, thereby reducing the inflammatory injury caused by cerebral hemorrhage (189–191). Treg regulates the expression of other cytokines and inhibits the activation of microglia by releasing IL-10 in the late stage of cerebral infarction. In addition, studies on amyotrophic lateral sclerosis show that Treg can promote the transformation of microglia to M2 type. This suggests that Treg can change its effect from neurotoxicity to neuroprotection without changing the number of microglia (189). After cerebral ischemia, Treg can reduce infarct volume and improve neurological function by reducing T cell infiltration, reducing microglia/monocyte activation, or promoting M2-type polarization of microglia (187). The key inflammatory responses after ischemic stroke are summarized in Figure 1.

4 Modulatory effects of natural botanical components on microglia-mediated immune inflammation in IS

4.1 Natural botanical component monomer

4.1.1 Polyphenols and phenols

(1) Gastrodin: Gastrodin is an organic compound extracted from the dried roots of *Gastrodia elata* Bl (192). Gastrodin has a good sedative and sleeping effect on neurasthenia, insomnia, headache symptoms have eased. *Gastrodia elata* Bl. Is able to treat pain, dizziness, limb numbness, and convulsions. Clinically, *Gastrodia elata* Bl. is generally used to treat vertebrobasilar insufficiency, vestibular neuritis and vertigo (193). Gastrodin is one of the main effective monomer components of *Gastrodia elata* Bl. It is currently widely used in clinical applications, and can exert neuroprotective effects in neurological diseases through multiple

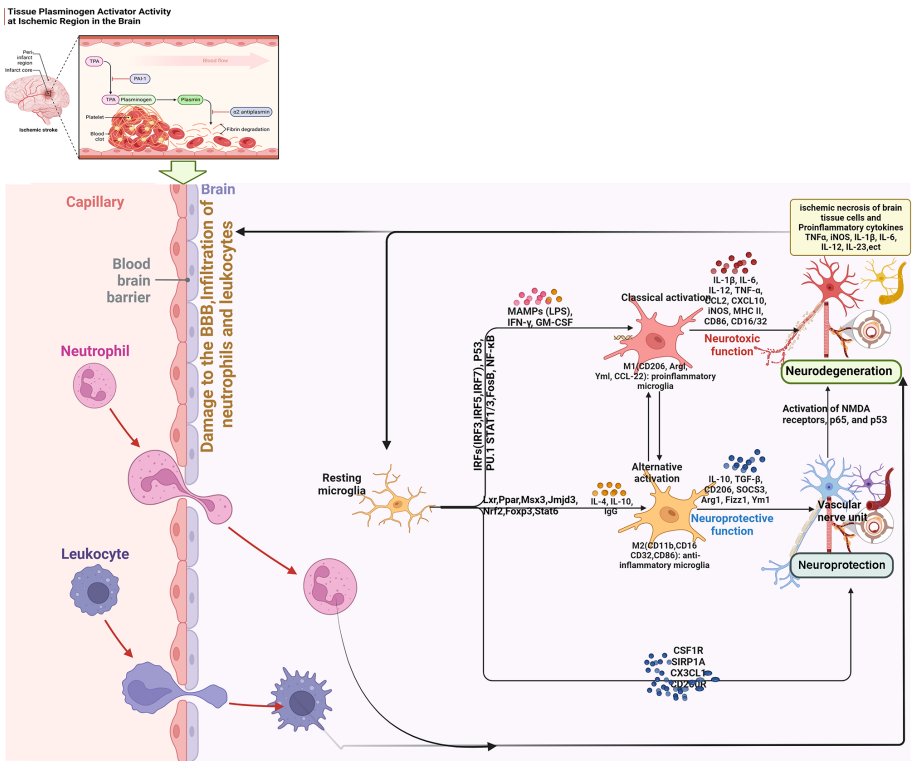


FIGURE 1
Summary of key inflammatory responses after ischemic stroke (BBB, blood brain barrier; IRF, interferon regulatory factor; STAT, signal transducer and activator of transcription; NF-κB, nuclear factor-κB; IFN, Interferon; NMDA, N-methyl-D-aspartate receptor; MAMPs, Metabolism-related molecular patterns; LPS, Lipopolysaccharide; GM-CSF, granulocyte-macrophage colony stimulating factor).

pathways such as anti-oxidative stress, anti-neuroinflammatory response, regulation of neurotransmitters, regulation of neural remodeling, anti-apoptosis and anti-autophagy. The study found that gastrodin pretreatment can significantly improve the neurological function of MCAO rats after 72h of reperfusion, and reduce the volume of cerebral infarction and BBB permeability. Gastrodin at 100 mg/kg *in vivo* and 40 μmol/L *in vitro* can inhibit microglia MMP2, MMP9 and AQP4, and increase ZO-1 expression, thereby exerting its protective effect on ischemia-reperfusion injury in MCAO and OGD/R models. In addition, OGD/R and MCAO can significantly increase the expression of SOX4 in microglia *in vitro* and *in vivo*, and pretreatment with gastrodin can inhibit the trend of increasing SOX4. Overexpression of SOX4 could reverse the effects of gastrodin on MMP2, MMP9, AQP4, and ZO-1 in OGD/R microglia, suggesting that gastrodin could regulate MMP2, MMP9, AQP4, and ZO-1 through SOX4 to exert neuroprotective effects (194).

(2) Malibatol A: Malibatol A is a natural resveratrol oligomer purified from the leaves of serrata with antioxidant activity. Yang et al. (195) found that Malibatol A improved mitochondrial dysfunction induced by middle cerebral artery occlusion. Pan et al. (196) found that Malibatol A significantly reduced the infarct size of mice with MCAO and improve neurological function. Weng et al. (197) found that Malibatol A can attenuate OGD/R-induced BV2 cell damage and promote M2 microglial polarization, which may be related to the inhibition of mammalian Ste20-like kinase 1 phosphorylation.

(3) Resveratrol: Resveratrol, a non-flavonoid polyphenolic organic compound, is an antitoxin produced by many plants when stimulated, with a chemical formula of C14H12O3. It can be synthesized in grape leaves and grape skins and is a bioactive component in wine and grape juice (198). *In vitro* and animal experiments have shown that resveratrol has anti-oxidation, anti-inflammatory, inhibition of platelet formation, blood clot adhesion to the vascular wall, anti-cancer and cardiovascular protection (199–201). Resveratrol reduces glial cell activation and prevents delayed neuronal cell death in MCAO rats (202). In addition, resveratrol may protect cranial nerves by reducing the production of inflammatory mediators such as IL-1β, TNF-α and ROS in the ischemic cortex, possibly mediated by attenuating the activation of microglia (203).

(4) 6-Shogaol: 6-shogaol, an active substance isolated from ginger, has a variety of biological activities, including anticancer, anti-inflammatory and antioxidant. For example, 6-shogaol reduced diethylnitrosamine (DEN)-mediated

elevation of serum aspartate aminotransferase and alanine aminotransferase and DEN-induced hepatic lipid peroxidation. The induction of Nrf2 and HO-1 by 6-shogaol was also confirmed in mice. 6-shogaol also restores the decreased activity of DEN and the protein expression of liver antioxidant enzymes such as superoxide dismutase, glutathione peroxidase and catalase in mice (204–206). 6-Shogaol also reduces inflammatory biomarkers levels in LPS-activated microglia and neuroinflammation in the brain. It also attenuates iNOS, NO, COX-2, PGE2, TNF-α and IL-1β production by downregulating MAPK (p38, JNK and ERK)/NF-κB signaling. The inhibition of microglial activation and inflammatory mediators by 6-Shogaol contributes to its neuroprotective effect (207).

(5) 6-Paradoll: 6-Paradoll reduces tMCAO-induced cerebral infarction, neurological deficit, and the inflammatory cascade in the ischemic brain, which is mainly mediated by inhibition of microglia/macrophage activation (208).

(6) Honokiol: Honokiol is derived from the bark, root bark and branches of *Magnolia officinalis* Rehd. et Wils. or *M. officinalis* Rehd. et Wils. var. biloba Rehd. et Wils (209). Honokiol has obvious and long-lasting central muscle relaxation, central nervous system inhibition, anti-inflammatory, antibacterial, anti-pathogenic microorganisms, anti-ulcer, antioxidant, anti-aging, anti-tumor, cholesterol-lowering and other pharmacological effects. It is used to treat acute enteritis, bacterial or amoebic dysentery, chronic gastritis, etc. (210, 211). Honokiol inhibits inflammatory biomarkers in the ischemic brain, including NF-κB transcriptional activation, NO, and TNF-α production (212), which are mainly produced by activated glial cells and infiltrating macrophages.

(7) Indole-3-propionic acid: Indole-3-propionic acid treatment not only inhibited glial (astrocyte and microglia) activation in the ischemic brain, but also reduced lipid peroxidation, neuronal DNA damage. Its neuroprotective efficacy is mainly related to the fight against glial cell activation (213).

(8) Paeonol: Paeonol is a monomer extracted from the dried roots of Paeonia suffruticosa Andr. or Cynanchum paniculatum (Bge.) Kitag., which has various pharmacological effects (214). Paeonol has the effect of treating cardiovascular and cerebrovascular diseases, such as lipid-lowering and anti-atherosclerosis, vasodilation and blood pressure lowering, anti-arrhythmia, anti-cerebral ischemia-reperfusion injury and neuroprotection. It also has anti-hepatic injury and liver fibrosis, anti-inflammatory, antibacterial activity, anti-inflammatory activity, antioxidant activity and anti-tumor activity (215–217). Paeonol also decreased IL-1β immunoreactive cell numbers and microglia/macrophage activation in the ischemic brain (218).

(9) Epigallocatechin gallate: Epigallocatechin gallate is a component extracted from green tea. It is the main active and water-soluble component of green tea and is a component of catechins (219). Catechins are mainly divided into four categories: epicatechin, epigallocatechin, epicatechin gallate, epigallocatechin gallate (220). Epigallocatechin gallate has the activity of protecting dopaminergic neurons, inhibiting inflammation, inhibiting oxidative stress, anti-oxidation, protecting nervous system, anti-tumor and protecting cardiovascular and cerebrovascular (221, 222). Epigallocatechin gallate reduces infarct volume by reducing microglia/macrophage activation (223).

(10) Theaflavins: Theaflavins generally refers to tea yellow pigment, is a golden yellow pigment in black tea, is the product of tea fermentation. In biochemistry, tea yellow pigment is a class of polyphenols hydroxyl benzophenone structure of the material, with inhibition of inflammation, anti-oxidative stress and the neuroprotective effect (224–226). Theaflavins reduce infarct and edema volume by reducing microglial inflammatory mediators such as COX-2, iNOS, and ICAM-1 in the damaged brain (227).

(11) Propofol: Propofol reduces infarct volume and improves neurological function by reducing microglia/macrophage CD68 and Emr1 levels and inhibiting proinflammatory cytokines including TNF-α, IL-6, and IL-1β. Inhibition of microglial proinflammatory cytokine production during propofol-mediated MCAO contributes to neuroprotection against IS (228).

(12) Probucol: The neuroprotective effect of probucol is related to its anti-inflammatory effect in microglia. It downregulates NF-κB, MAPKs and AP-1 signaling pathways in LPS-activated microglia to reduce inflammatory mediators such as NO, PGE2, IL-1β and IL-6. It also reduces iNOS, COX-2, IL-1 and IL-6 in the brains of MCAO mice (229).

4.1.2 Anthraquinones

(1) Emodin: Emodin, an active ingredient extracted from the *Rheum palmatum* L., has a wide range of pharmacological properties, including anticancer, hepatoprotective, anti-inflammatory, antioxidant and antibacterial activities (230). Previous studies have shown that (231, 232) emodin has neuroprotective effects, antagonizes CIRI, and prevents the formation of atherosclerotic plaques. However, its neuroprotective mechanism remains unclear. Cai et al. found that emodin may play a role in brain protection by inhibiting the activation of microglia and the release of inflammatory factors mediated by the TLR4/NF-κB pathway (233).

(2) Chrysophanol: Zhang et al. found that Iba-1 positive cells in the cerebral ischemic penumbra of MCAO model rats increased significantly, and were amoeba-shaped or round; the neurological deficit score, the percentage of cerebral infarction and the relative expression of Notch-1, TNF-α and ICAM-1 proteins in the ischemic penumbra were significantly increased (234). However, after chrysophanol intervention, Iba-1-positive cells in the cerebral ischemic penumbra were reduced; the neurological deficit score, the percentage of cerebral infarction and the relative expression of Notch-1, TNF-α and ICAM-1 proteins in the ischemic penumbra were significantly decreased (234). This suggests that chrysophanol has a certain cerebral

protective effect on cerebral ischemia injury model rats, and can reduce its nerve damage, and its mechanism may be related to the inhibition of Notch signaling pathway-mediated activation of microglia and the expression of inflammatory factors. In addition, some studies have used a neuroinflammation model of LPS-induced microglial activation, and found that chrysophanol can inhibit LPS-induced microglial inflammatory response and promote the transformation of microglial M1 type to M2 type. The mechanism may be related to down-regulation of TLR4/NF-κB signaling pathway (235).

4.1.3 Terpenes and alkaloids

(1) Astragaloside IV: Astragaloside IV is an organic compound with a chemical formula of C41H68O14. It is a white crystalline powder and is extracted from the herbal medicine *Astragali radix*. The main active ingredients in *Astragali radix* are astragalus polysaccharides, astragalussaponins and isoflavones. Astragaloside IV is mainly used as a quality control standard to evaluate the quality of *Astragali radix* (236, 237). Studies have shown that astragaloside IV can reduce cerebral infarct volume, down-regulate the M1-type microglia/macrophage markers CD86, iNOS, TNF-α, IL-1β and IL-6 mRNA, and up-regulate the M2-type microglia/macrophage markers CD206, Arg-1, YM1/2, IL-10 and TGF-β mRNAs. Astragaloside IV can also reduce the number of CD16/32+/Iba1+ cells and increase the number of CD206+/Iba1+ cells in the ischemic area of the brain. This suggests that astragaloside IV has a protective effect on cerebral ischemia injury in rats, which may be related to promoting the transformation of microglia/macrophages from M1 type to M2 type and inhibiting the inflammatory response (238). In addition, studies have shown that astragaloside IV can inhibit IFN-γ-induced activation of microglia. This is related to inhibiting the activation of STAT1/IκB/NF-κB signaling pathway, reducing the gene expression of IL-1β, TNF-α and iNOS in microglia under inflammatory state, thereby reducing the production of NO and TNF-α (239).

(2) Cycloastragenol: Cycloastragenol is directly extracted from the dried roots of Astragalus membranaceus (Fisch.) Bge.var.mongholicus (Bge.) Hsiao or Astragalus membranaceus (Fisch.) Bge., or obtained by hydrolysis of Astragaloside IV (240, 241). It has oral safety, a wide range of pharmacological effects, anti-oxidation, anti-inflammatory, anti-aging, anti-apoptosis and cardiovascular protection (242, 243). Li et al. found that Cycloastragenol dose-dependently reduced cerebral infarct volume, significantly ameliorated functional deficits, and prevented neuronal cell loss in MCAO mice. Meanwhile, Cycloastragenol significantly reduced the activity of MMP9, prevented the degradation of tight junctions, and subsequently ameliorated the disruption of the BBB. Furthermore, Cycloastragenol significantly upregulated the expression of SIRT1 in the ischemic brain, but did not directly activate its enzymatic activity. Concomitant with SIRT1 upregulation, Cycloastragenol reduces p53 acetylation and Bax to Bcl-2 ratio in the ischemic brain. Cycloastragenol also inhibits NF-κB p65 nuclear translocation. In summary, Cycloastragenol inhibits the expression of proinflammatory cytokines including TNF-α and IL-1β mRNA and inhibits the activation of microglia and astrocytes in the ischemic brain (243).

(3) Triptolide: Tripterygium is derived from the root bark of the traditional Chinese medicine Tripterygium wilfordii, which has anti-inflammatory, antioxidant and anti-cancer effects. Triptolide has been used in the treatment of various diseases, such as tumors [colorectal cancer (244), hepatocellular carcinoma (245)], autoimmune-related diseases [rheumatoid arthritis (246)], obesity (247), etc. Triptolide exerts anti-inflammatory and neuroprotective effects on cerebral ischemia rats through the nuclear factor-KB signaling pathway (248). Jiang et al. found that triptolide reduced neuronal apoptosis and inflammatory factor expression in rats with cerebral ischemia through IL-33/growth-stimulating expression gene 2 protein-mediated polarization of M2 microglia, thereby reducing cerebral infarct volume (249).

(4) Artesunate: Artesunate is a derivative of artemisinin with high water solubility and can pass through the BBB for the treatment of cerebral and other types of severe malaria (250). Artesunate can also maintain a high concentration in the nervous system, showing high efficiency and low toxicity (251–254). Studies have shown that artesunate may exert multiple functions, including anti-inflammatory, immunomodulatory, BBB protection, antibacterial and antitumor effects (253, 254). Studies have shown that the anti-inflammatory effects of artesunate are mediated by NF-κB and inflammatory cytokine inhibition. Lai et al. found that artesunate could alleviate liver fibrosis and inflammation by inhibiting the LPS/TLR4/NF-κB pathway (255). Okorji and Olajide found that artesunate reduced proinflammatory cytokine production by inhibiting the p38 MAPK-NF-κB signaling pathway in activated BV2 microglia (256). Artesunate also exerts a protective effect in CIRI and inhibits the expression of TNF-α and IL-1β (257). Liu et al. found that artesunate significantly improved neurological deficit score and infarct volume, and improved inflammation by reducing neutrophil infiltration, inhibiting microglial activation, and downregulating the expression of TNF-α and IL-1β. In addition, artesunate inhibits nuclear translocation of NF-κB and inhibits protein α proteolysis. In summary, artesunate may protect against inflammatory injury by reducing neutrophil infiltration and microglial activation, inhibiting inflammatory cytokines and inhibiting NF-κB pathway. Therefore, artesunate is a potential IS treatment drug (258).

(5) Neo-Minophagen C: Glycyrrhizin is derived from the glycosides of *Glycyrrhizae radix et rhizoma*, among which Neo-Minophagen C has anti-inflammatory effect, immunomodulatory effect, inhibitory effect on experimental liver cell injury, inhibition of virus proliferation and inactivation of virus (259, 260). Neo-Minophagen C reduces

infarct volume and improves motor function and neurological deficits. The neuroprotective effect of Neo-Minophagen C is mediated by reducing neutrophil infiltration and microglial activation after ischemia. Neo-Minophagen C reduces inflammatory mediators and pro-inflammatory cytokines in LPS-activated microglia. Inhibition of microglial activation and inflammatory mediators contributes to the neuroprotective effect of neophage C after cerebral ischemia (261).

(6) Hyperforin: Hyperforin, as an active ingredient of Hypericum perforatum L, is used to alleviate mild to moderate depression and has a significant antidepressant effect (262). Further studies have shown that hyperforin has good anti-inflammatory, anti-tumor and neuroprotective effects (263, 264). Hyperforin reduces infarct size and improves nerve damage by inhibiting inflammatory microglial activation and promoting microglial polarization towards an anti-inflammatory M2 phenotype in the peri-infarct striatum (265).

(7) Ilexonin A: Ilexonin A is a water-soluble compound, 3-succinyl-18-dehydroursolic acid disodium salt, prepared by succinylation of 18-dehydroursolic acid isolated from the rhizome or root bark of Ilex pubescens Hook.et Arn (266). Ilexonin A is an antithrombotic drug whose chemical structure is different from the currently known antiplatelet aggregation drugs. Ilexonin A is effective in the treatment of ischemic cerebrovascular disease, coronary heart disease, central retinal choroiditis, peripheral vascular disease, etc., especially for the treatment of acute ischemic cerebrovascular disease (267, 268). Meanwhile, Ilexonin A reduces inflammatory microglial activation in the ischemic brain. Its neuroprotective effects may be related to neuronal regeneration, inhibition of microglial activation and increased angiogenesis (269).

(8) Huperzine A: Huperzine A is an alkaloid extracted from *Huperzinaserrata (Thumb.)* Trev. It is a potent cholinesterase reversible inhibitor. Its characteristics are similar to neostigmine, but the duration of action is longer than the latter (270, 271). Huperzine A can effectively prevent brain neurasthenia in middle-aged and elderly people, restore brain nerve function, and activate brain nerve transmission substances (272). Huperzine A may inhibit NF-κB activity and pro-inflammatory mediator production in the cerebral cortex and striatum of MCAO rats. It reduces neurological deficits and glial cell activation after ischemic injury mainly through its anti-inflammatory effect in the post-ischemic brain (232). Huperzine A can also down-regulate MAPK signaling, especially JNK and p38, to reduce the level of the inflammatory factor TNF-α. Huperzine A exerts neuroprotection against 2-VO-induced cognitive impairment by promoting an anti-inflammatory response in the brain (273).

(9) Berberine: Berberine, a quaternary ammonium alkaloid isolated from COPTIDIS RHIZOMA, is the main active ingredient in COPTIDIS RHIZOMA for antimicrobial activity. Studies have shown that berberine regulates immune and inflammatory mechanisms (274, 275). Berberine also improves ischemia-induced short-term memory impairment by reducing neuronal apoptosis, microglial activation and oxidative stress. Berberine exerts neuroprotective effects against ischemic injury by increasing the activation of the PI3K/Akt pathway through its phosphorylation in the hippocampus of ischemic gerbils (276).

(10) Sinomenine: Sinomenine is the main active ingredient isolated from *Sinomenium acutum* (Thunb.) Rehd.et Wils (277), which is a kind of morpholine alkaloids, molecular formula is C19H23NO4. It has anti-inflammatory, antihypertensive, analgesic, anti-arrhythmic and other pharmacological activities, and also plays an important role in the treatment of chronic nephritis, anti-oxidation, anti-tumor, detoxification and so on (278, 279). Sinomenine also reduces glial cell activation by inhibiting the NLRP3-ASC-Caspase-1 inflammasome in mixed glial cultures exposed to OGD as well as in MCAO mice. Sinomenine also reduces OGD-induced K phosphorylation in A macrophages *in vitro*. The inhibition of NLRP3 and A-macrophage K activation in activated glial cells by sinomenine is a key cellular mechanism for its neuroprotective effect against stroke (280).

4.1.4 Flavonoids

(1) Icariin: Icariin is the main active ingredient of *Epimedii folium*, which is an 8-prenyl flavonoid glycoside compound (281). Icariin can increase cardiovascular and cerebrovascular blood flow, inhibit inflammation, resist oxidative stress, regulate immunity, promote hematopoietic function, immune function and bone metabolism, and also has the effects of tonifying kidney and strengthening yang, anti-aging and so on (282–284). Tang et al. found that after icariin treatment, the neurological function score and cerebral infarction rate of MCAO model rats were improved, the activation of Iba1 and TLR4 in microglia decreased, the NF-κB p65 protein level decreased, and the content of inflammatory factors IL-1α and TNF-α decreased significantly. This suggests that icariin may play a role in brain protection by regulating the activation of microglia, inhibiting the activation of TLR4 and its downstream NF-κB signaling pathway, and reducing the expression of related inflammatory factors IL-1α and TNF-α (285).

(2) Eupatilin: Eupatilin, a lipophilic flavonoid isolated from ARTEMISIAE ARGYI FOLIUM, is a PPARα agonist with anti-apoptotic, anti-oxidant and anti-inflammatory effects (286–288). Eupatilin may inhibit pro-inflammatory mediators including nitrite, PGE2, TNF-α and IL-6 in activated microglia *in vitro* and *in vivo* to combat focal cerebral ischemia. In the post-ischemic brain of mice challenged with tMCAO, eupatin significantly improved neurological function and reduced cerebral infarction. It also significantly reduced Iba1-immunopositive cells, microglia/macrophage proliferation, NF-κB signaling, IKKα/β phosphorylation, IκBα phosphorylation, and IκBα degradation in the tMCAO-attacked brain. This suggests its powerful effect on counteracting the inflammatory response of microglia/macrophages in the ischemic brain (289).

(3) Heptamethoxyflavonoids: Heptamethoxyflavone protects neuronal cells from ischemia-induced injury by increasing BDNF production, CaMK II phosphorylation, and reducing microglia/macrophage activation (290).
(4) Wogonin: Wogonin is a flavonoid extracted from the root of *Scutellaria baicalensis* Georgi (291). Wogonin has attracted attention because of its various pharmacological activities, including antioxidant activity, anti-inflammatory, immune regulation, and cardiovascular protection. It also has neuroprotective effects during cerebral ischemia (292, 293). Wogonin reduces LPS-induced microglial activation by attenuating the production of inflammatory biomarkers, including iNOS, nitrite, IL-1β, TNF-α and NF-κB in microglia. Furthermore, wogonin treatment down-regulated hippocampal neuronal death by reducing inflammatory mediators such as iNOS and TNF-α after systemic ischemia. It also inhibited the level of microglia-specific isolectin B4 staining, suggesting its role in inhibiting microglial activation (294).
(5) Puerarin: Puerarin is the main active ingredient extracted from Pueraria lobata (Willd.) Ohwi (295). It has the effect of protecting cardiovascular and cerebrovascular and nerve cells, and can dilate blood vessels, lower blood pressure, lower blood sugar, anti-tumor, improve immunity, anti-oxidation, anti-inflammatory and regulate bone metabolism (296–298). Puerarin also reduces ischemia-induced COX-2 expression and reduces cerebral infarction in MCAO rats by inhibiting microglia and astrocyte activation (299).
(6) Quercetin: Quercetin is a naturally occurring phytochemical with good biological activity. It mainly exists in vegetables, fruits, tea and wine in the form of glycosides and has a healthy effect (300, 301). The anti-diabetic, anti-hypertensive, anti-Alzheimer's disease, anti-arthritis, anti-influenza virus, anti-microbial infection, anti-aging, autophagy and cardiovascular protective effects of quercetin have been extensively studied (302–304). Quercetin may reduce neuroinflammation and apoptosis by reducing the expression of iNOS and caspase-3, which is associated with hippocampal neuroprotection after systemic ischemia in rats (299).
(7) Fisetin: Fisetin is a compound extracted from natural plants with pharmacological effects against different pathological processes (305). The concentration of Fisetin in food is 2 ~ 160μg/g. The content of Fisetin in strawberry, apple and persimmon is high, and fisetin is also abundant in various legume trees and shrubs (306). Studies have shown that Fisetin has a certain therapeutic effect on neurological abnormalities, cardiovascular disease, diabetes, obesity, lung disease, immune disease, cancer and other inflammatory diseases (307, 308). Fisetin may reduce the infiltration of macrophages and dendritic cells into the ischemic hemisphere and reduces immune cell activation in the brain, as evidenced by decreased TNF-α levels. Fisetin significantly downregulates inflammation in LPS-activated microglia and macrophages by reducing NF-κB signaling and reducing TNF-α production. This anti-inflammatory effect of Fisetin is associated with reduced neurotoxicity and neuroprotection by activated microglia and macrophages following ischemic injury (309).
(8) Breviscapine: Breviscapine is the extract of *Erigeron breviscapus* (Vant.) Hand.-Mazz. It is composed of flavonoids, lignans, coumarins, terpenoids, phytosterols and other chemical components (310). Modern pharmacological studies have shown that Breviscapine has a wide range of pharmacological effects, including anti-oxidation, anti-fibrosis, anti-inflammatory, anti-aging, anti-platelet aggregation, reducing blood lipids, increasing blood flow, improving microcirculation, preventing and treating tumors, and anti-brain injury. At present, Breviscapine has been widely used in the treatment of diabetes, cerebral insufficiency, sequelae caused by a cerebral hemorrhage, hyperviscosity, cerebral thrombosis, nephropathy, liver disease, Alzheimer's disease and other complex diseases (311–313). Breviscapine reduces microglial activation by inhibiting inflammatory biomarkers (such as ROS, NO, and iNOS) in LPS-activated microglia. It also inhibited pro-inflammatory cytokines, especially TNF-α, in the rat brain after ischemia (314). Breviscapine reduces levels of NF-κB, MCP-1 and Notch-1 signaling *in vitro* and *in vivo* in animal models of ischemia. It also reduced microglial migration and adhesion. Breviscapine also inhibits the inflammatory microglia/macrophage phenotype through the Notch pathway and contributes to neuroprotection against ischemia/stroke (315).
(9) Chrysin: Chrysin is a flavonoid found in plant species such as *Oroxylum indicum* (L.) Vent. It is mainly used for intervention in the treatment of hyperlipidemia, cardiovascular and cerebrovascular diseases, anxiety, inflammation, gout, cancer, muscle enhancement, etc. (316–318). Chrysin may reduce the number of activated glial cells, production of pro-inflammatory cytokines, iNOS, COX-2, and NF-κB signaling in the brain after ischemia. Through this anti-inflammatory mechanism, chrysin reduces infarct size and improves neurological deficits (319).
(10) Epicatechin: Epicatechin is a natural plant flavanol compound, chemical formula C15H14O6, with epigallocatechin, catechin gallate, epicatechin gallate, epigallocatechin gallate collectively referred to as catechin compounds (320, 321). Epicatechin and other flavonoids have the effects of anti-oxidation, scavenging free radicals, enhancing metabolism, regulating immunity and anti-tumor (322, 323). Epicatechin reduces oxidative stress by activating the antioxidant Nrf2 pathway, thereby increasing neuronal viability against OGD-mediated injury. In MCAO, epicatechin down-regulates motor dysfunction by down-regulating microglia/macrophage activation (324).

4.1.5 Glycosides

(1) Salidroside: Salidroside is a phenylpropanol glycoside extracted from Rhodiola rosea L., which has good anti-inflammatory and antioxidant effects (325). Han et al. (326) found that salidroside can reduce the size of cerebral infarction

in IS rats and improve neurological function and histological changes in rats, which may involve the activation of Nrtf2 pathway and its endogenous antioxidant system. Liu et al. (327) found that in the IS mouse model, salidroside decreased the expression of M1-type markers, increased the expression of M2-type markers, and induced the transformation of microglia from M1 phenotype to M2 phenotype. Salidroside can also inhibit LPS-induced BV2 microglia inflammatory response, mainly by activating PI3K/Akt signaling pathway, promoting Akt phosphorylation, inhibiting NF-κB p50 nuclear transcription, and then inhibiting cytokines. In addition, in a model of neuroinflammation after spinal cord injury, Li et al. found that salidroside can restore motor function in rats, increase the M2/M1 polarization ratio in the spinal cord, reduce the expression of Bax, NF-κB, iNOS and COX-2 mRNA, increase the expression of Bcl-2, p-AMPK, and reduce the expression of p-mTOR.

(2) Forsythin: Forsythin is the dried fruit of *Forsythia suspensa* (Thunb.) Vahl (328, 329). Modern pharmacological studies have shown that Forsythia suspense has antibacterial, anti-inflammatory, antiviral, hepatoprotective, anti-tumor, immune regulation and antioxidant effects (328). Studies have found that *Forsythia suspensa* (Thunb.) Vahl and its constituents have significant effects in improving neurodegenerative diseases and other neuroprotection in the elderly (330). Meanwhile, forsythin may protect neuronal cells in the CA1 region of the hippocampus after ischemia by attenuating glial activation. Forsythin also reduces the levels of pro-inflammatory cytokines such as IL-1β and TNF-α (331).

(3) Ginsenosides: Ginsenoside is a steroid compound, also known as triterpenoid saponins, which mainly exists in *Panax* L (332). The experimental results showed that Ginsenoside inhibited the formation of lipid peroxide in the brain and liver, reduced the content of lipofuscin in the cerebral cortex and liver, and also increased the content of superoxide dismutase and catalase in the blood (333, 334). In addition, some monomer saponins in Ginsenoside such as rb1, rb2, rd, rc, re, rg1, rg2, rh1, etc.can reduce the content of free radicals in the body to varying degrees. Ginsenoside can delay neuronal senescence and reduce memory impairment in the elderly, and has a stable membrane structure and increased protein synthesis, thereby improving the memory ability of the elderly (332, 335). The inhibitory effect of ginsenoside Rd on inflammation was demonstrated by reducing microglial activation and inflammatory biomarkers, including iNOS and COX-2, to exert neuroprotective effects against transient focal ischemia (336). Ginsenoside Rb1 improves neurological deficit and reduces infarct size by reducing microglia activation. Ginsenoside Rb1 treatment reduces the mRNA levels of proinflammatory cytokines such as IL-6, TNF-α by downregulating NF-κB-mediated transcription in the ischemic brain. This suggests that its neuroprotective efficacy is exerted by down-regulating the inflammatory response of activated glia (337).

(4) Kaempferol glycosides: Kaempferol is a flavonoid compound mainly derived from the rhizome of *Kaempferol galanga* L, which is widely found in various fruits, vegetables and beverages (338, 339). It has been widely concerned because of its anti-cancer, anti-cancer, anti-inflammatory, antioxidant, antibacterial, antiviral and other effects (340–342). Kaempferol glycosides, kaempferol-3-O-rutinoside and kaempferol-3-O-glucoside significantly reduced infarct volume, neurological deficits, neuronal and axonal damage in the brains of tMCAO-injured rats. Furthermore, these glycosides inhibit inflammation by reducing transcription mediated by GFAP, OX-42, phosphorylated STAT3, and NF-κB. These glycosides also inhibit macrophage O, iNOS, TNF-α, IL-1β, ICAM-1 and MMP-9 production for neuroprotective effects (343).

(5) Paeoniflorin: Paeoniflorin is derived from the roots of *Paeonia albiflora* Pall, *P. suffersticosa* Andr and *P. delarayi* Franch, and its content is high in *P. lactiflora* (344). Its pharmacological effects of paeoniflorin has significant analgesic, sedative, anticonvulsant effect, antithrombotic effect, anti-platelet aggregation, anti-hyperlipidemia effect, etc. (345, 346). Paeoniflorin ameliorates learning and memory impairment by reducing morphological and structural changes in the CA1 region of brain injury in rats with cerebral hypoperfusion. This neuroprotective efficacy was associated with reductions in inflammatory mediators (eg, NO) and proinflammatory cytokines (eg, IL-1β, TNF-α, and IL-6), and increases in anti-inflammatory cytokines (IL-10 and TGF-β1). Thus, down-regulation of the pro-inflammatory phenotype and increased anti-inflammatory phenotype of activated microglia/macrophages are associated with the neuroprotective efficacy of paeoniflorin (347).

4.1.6 Others

(1) Fingolimod (FTY720): FTY720 is a high affinity agonist for sphingosine 1-phosphate (S1P) receptors and was developed from a sphingosine analogue extracted from *Ophiocordyceps sinensis* (Berk.) G.H. Sung, J.M.Sung, Hywel-Jones & Spatafora as a lead compound; it is approved by the US Food and Drug Administration for the treatment of relapsing-remitting multiple sclerosis (348). Among the four S1P receptor subtypes targeted by FTY720, the current study found that S1P1 and S1P3 are associated with cerebral ischemia (349). The therapeutic mechanism of FTY720 for ischemic stroke is not fully understood. Li et al. (350) found that FTY720 can activate the mammalian target of rapamycin/p70S6 signaling pathway and inhibit neuronal autophagy activity. Many scholars believe that (351, 352), the beneficial effect of FTY720 on IS has nothing to do with direct neuronal protection, but is anti-inflammatory and vascular protection by reducing the invasion of brain lymphocytes. Gaire et al. (349) found that FTY720 inhibits S1P3, thereby inhibiting the transformation of microglia to M1 type. Qin et al. (352) found that FTY720 activates signal

transducer and activator of transcription 3 and promotes the polarization of microglia from M1 to M2.

(2) 3-N-butylphthalide (NBP): NBP is a compound isolated from celery seeds, and there are three types of derivatives: L-NBP, D-NBP and DL-NBP (353). L-NBP has been approved for use in China. Among the three derivatives, L-NBP has the strongest biological effect and the best safety (353). NBP has neuroprotective effects on ischemic stroke animal models by inhibiting oxidative damage, neuronal apoptosis and glial cell activation, increasing the level of circulating endothelial progenitor cells (354, 355). Li et al. (356) observed that L-NBP could enhance the M2 polarization of microglia in animal models of cerebral ischemia and inhibit the M1 polarization.

(3) Danshenol bornanyl ester: Danshenol bornanyl ester is a new compound with anti-cerebral ischemia effect, which is designed and synthesized based on the active ingredient of Salvia miltiorrhiza Bge.and the effective structural fragment of borneol by using the principle of modern drug design (357, 358). Danshenol bornanyl ester significantly inhibits NF-κB activity, inhibits the production of pro-inflammatory mediators, and simultaneously promotes the expression of M2 mediators in LPS-stimulated BV2 cells and mouse primary microglia. Danshenol bornanyl ester also exhibits antioxidant activity by enhancing Nrf2 nuclear accumulation and transcriptional activity, increasing HO-1 and NQO1 expression, and inhibiting LPS-induced ROS production in BV2 cells. The aforementioned anti-neuroinflammatory and antioxidant effects could be reversed by Nrf2 knockdown. In addition, Danshenol bornanyl ester improves disease behavior in mice with neuroinflammation induced by systemic LPS administration, significantly reduces infarct volume in rats with transient MCAO (tMCAO), and improves sensorimotor and cognitive function. Danshenol bornanyl ester also restores microglia morphological changes and alters M1/M2 polarization (359).

(4) Arctigenin: Arctigenin is a lignan compound from Arctium lappa L., which can effectively inhibit the release of inflammatory factors. It inhibits the proliferation, migration and angiogenesis of human umbilical vein endothelial cells (HUVECs) induced by high glucose, and plays a protective and anti-oxidative stress role in HUVECs injury (360–362). Arctigenin reduces the activation of microglia by reducing the release of TNF-α and IL-1β in rats with ischemic injury. This anti-inflammatory effect of arctigenin contributes to its neuroprotective effect (363).

(5) Sesamin: Sesamin mainly comes from the roots of *Acanthopanax sessiliflorus* (Rupr.et Maxim.) Seem., the seeds or seed oil of *Sesamum indicum* DC., and the wood of *Paulownia tomentosa* (Thunb.) Steud. Its main pharmacological effects are inhibition of inflammation and anti-oxidative stress (364, 365). Current research found that sesamin may inhibit oxidative stress and reduces cleaved-caspase-3 activation, lipid peroxidation and increases GSH activity. It also inhibited inflammatory mediators such as peroxynitrite, iNOS, COX-2, Iba1, Nox-2 in the brains of MCAO-challenged mice to exert their neuroprotective effects (366).

(6) Edaravone: Edaravone ameliorates cognitive decline and delays neuronal death after focal cerebral ischemia by inhibiting inflammatory biomarkers including iNOS, NO, ROS, IL-1β and TNF-α production. In addition, inhibition of inflammation, oxidative stress, and astrocyte activation are thought to be relevant mechanisms for the neuroprotective effect of edaravone against ischemic injury (314, 367).

(7) Tetramethylpyrazine (Ligustrazine): Ligustrazine is an alkyl pyrazine extracted from *Ligusticum wallichii* (368). It has potential anti-neural and anti-inflammatory activity in rats, can protect vascular endothelial cells, reduce capillary permeability, reduce vascular resistance in anesthetized dogs, and increase blood flow in brain, cerebral arteries and lower limbs (369, 370). Ligustrazine can also reduce the damage of neurons and microvascular endothelial cells and improve neurological signs. It has a short-term improvement effect on complete cerebral ischemia, and has a certain degree of promoting cerebral resuscitation, antagonizing systemic circulation and pulmonary blood pressure after cerebral ischemia (371). Ligustrazine has a strong inhibitory effect on rabbit platelet aggregation induced by ADP, collagen and thrombin *in vitro*, and inhibits the production of platelet malondialdehyde. Its mechanism is to inhibit the phosphorylation of phosphatidylinositol 4-phosphate (PIP) kinase and 20K protein in platelets (87). Ligustrazine can also reduce whole blood viscosity, red blood cell and platelet electrophoresis speed up, reduce fibrinogen, inhibit thrombosis (372). In regulating microglia, ligustrazine can reduce the activation of microglia/macrophages, lymphocyte infiltration and the production of inflammatory mediators in the brain after ischemia. It also reduces inflammatory responses and increases antioxidant/anti-inflammatory responses in microglia/macrophages and post-ischemic neurons *via* Nrf2/HO-1 (373).

(8) Cannabidiol: Cannabidiol is an ingredient extracted from *Cannabis sativa* L (374, 375). At present, its main pharmacological effects are analgesic and anti-inflammatory, inhibition of nerve growth factor-induced mast cell degranulation and neutrophil aggregation to inhibit allergic inflammation, and thus mediate immunosuppression (376, 377). Cannabidiol inhibits hippocampal neurodegeneration, cognitive and memory impairment, glial responses, and white matter damage against BCCAO. It also induces BDNF production in the hippocampus, promoting neurogenesis and dendritic reorganization in BCCAO mice (378).

(9) Ligustolide: Ligustolide is the main active ingredient in the volatile oil of Angelica sinensis (379). The current pharmacological Ligustolide can inhibit the proliferation of vascular smooth muscle cells and cell cycle progression, and inhibit vasoconstriction (380). It also increases vasodilation, antithrombotic and serotoninergic activity, and reduces

platelet aggregation (381, 382). Currently, Ligustolide is widely used in the research and treatment of cardiovascular and cerebrovascular diseases and ischemic brain injury (383). Ligustolide can inhibit neuroinflammation and oxidative stress on CIRI damage (384) and reduces cerebral infarct volume and improves neurological function. Ligustolide-induced neuroprotection was accompanied by amelioration of neuropathological changes, decreased activation of microglia and macrophages, infiltration of neutrophils and lymphocytes, and downregulation of inflammatory mediators. This anti-inflammatory effect is controlled by the ERK/NF-κB signaling axis in the ischemic brain. Ligustolide-mediated inhibition of TLR4/Prx6 signaling induces neuroprotection against ischemic stroke (384).

4.2 Herb Extracts

4.2.1 Salvia Polyphenolic Acid

Salvia Polyphenolic Acid is an active ingredient extracted from *Salvia miltiorrhiza* Bge. Its main function is to improve the viscous state of blood, with blood circulation, blood stasis, and good clinical tolerance (385, 386). Current studies have shown that its mechanism of action is to inhibit the inflammatory response of endothelial cells, improve energy metabolism, promote vascular endothelial cell migration, and improve ischemia-reperfusion injury (380, 387, 388). Studies have shown that salvianolic acid can reduce the inflammatory factors (such as ICAM-1, IL-1β, IL-18 and TNF-α) in the cerebral cortex of the rat brain MCAO/R model, and reduce the apoptosis of cortical neurons. Salvianolic acid can alleviate the cell damage of oxygen glucose deprivation/reoxygenation (OGD/R)-treated neurons alone and co-cultured with microglia, improve cell viability, and reduce the rate of apoptosis, suggesting that salvianolic acid may reduce the cytotoxicity of microglia to neurons. Salvianolic acid can reduce the expression of NLRP3 in microglia after cerebral ischemia-reperfusion injury (CIRI) in rats, and inhibit the expression of pro-inflammatory factors such as IL-1β and IL-18 in the brain. It can also inhibit the cleavage of the pyroptosis-related protein GSDMD in microglia after CIRI, and reduce the expression of NLRP3, ASC, caspase1, and IL-1β mRNA in microglia. Salvianolic acid can also reduce the number of Iba1 and P2X7 double-labeled microglia in the MCAO/R model rat cerebral cortex, and can reduce the expression of P2X7 protein and mRNA in microglia (194).

4.2.2 Panax notoginseng saponins

Panax notoginseng saponins are the main active ingredients of *Panax notoginseng* (Burkill) F. H. Chen ex C. H., mainly containing ginsenoside Rb1, ginsenoside Rg1, notoginsenoside R1 and other components (389). It can inhibit platelet aggregation in rabbits caused by ADP, and can also dilate cerebral vessels and increase cerebral blood flow (390, 391). Current studies have shown that Panax notoginseng saponins have a wide range of functions in the central nervous system, cardiovascular system, blood system, immune system, anti-fibrosis, anti-aging, anti-tumor, etc. (392–394). Jia et al. found that Panax notoginseng saponins can improve cerebral blood flow, neurological deficits, tissue morphology, and neuronal damage. It can also promote the expression of CD206/Iba-1 in M2-type microglia, and up-regulate the expression of CD206, TGF-β and IL-10 protein; inhibit the expression of CD16/Iba-1 in M1 type microglia cells and down-regulate the expressions of IL-1β, IL-6, TNF-α and iNOS protein. This suggests that Panax notoginseng saponins may promote the transition from M1-type polarization to M2-type in microglia (395).

4.2.3 Omega-3 polyunsaturated fatty acids (n-3 PUFA)

n-3 PUFA is one of the members of the PUFA family, mainly derived from deep-sea fish and some plants, among which eicosapentaenoic acid and docosahexaenoic acid are most involved in the regulation of human physiology. n-3 PUFAs play a role in the prevention and treatment of ischemic stroke (396, 397) can promote neurogenesis, increase peri-infarct vascular formation, improve glial scarring after cerebral ischemia, reduce mitochondrial dysfunction, reduce neuroinflammation, etc. (398, 399). Jiang et al. (400) found that n-3 PUFAs can switch the phenotype of microglia from M1 to M2 in mice with cerebral ischemia, which helps to improve white matter integrity and sensorimotor recovery.

4.2.4 Notoginseng leaf triterpenes

Notoginseng leaf triterpenes, as a valuable drug, have been found to have neuroprotective effects. It can reduce the expression of HMGB1, inhibit the inflammation caused by HMGB1, and inhibit the activation of microglia (IBA1) in hippocampus and cortex, thereby reducing the concentration of inflammatory cytokines including VCAM-1, MMP-9 and MMP-2 and ICAM-1 of IS in a dose-dependent manner. In addition, it can inhibit the activation of MAPKs and NF-κB, thereby ameliorating the neuropathological changes induced by CIRI (401).

4.2.5 Fructus Gardenia Extracts

Fructus Gardenia is a TCM with various pharmacological effects, such as anti-inflammatory, antidepressant, improving cognition and ischemic brain injury. GJ-4 is a natural extract from Fructus Gardenia, GJ-4 can significantly improve memory impairment, cerebral infarction and neurological deficit in MCAO/R-induced vascular dementia (VD) rats. Further studies showed that GJ-4 attenuated VD-induced neuronal damage. In addition, GJ-4 can protect the synapses of VD rats by up-regulating the expression of synaptophysin, postsynaptic density 95 protein (PSD95) and down-regulating the expression of N-methyl-D-aspartate receptor 1 (NMDAR1). Subsequent

investigations into the underlying mechanism found that GJ-4 could inhibit neuroinflammatory responses, supported by inhibiting microglia activation and reducing the expression of inflammatory proteins, ultimately exerting neuroprotective effects on VD (402).

The structures of those components are shown in Figure 2. The effects of natural botanical components on microglia/macrophages after cerebral ischemia are summarized in Table 1 and Figure 3.

5 Prospect

Microglia play a biphasic regulatory role in ischemic stroke. After IS, microglia were activated, migrated, and exerted pro-inflammatory and anti-inflammatory effects through M1/M2 phenotype polarization, respectively, and at the same time played a protective role by inhibiting M1 phenotype polarization or promoting M2 phenotype polarization. However, the research on induced cell polarization is limited to animal experiments and *in vitro* experiments, and the potential mechanism still needs further research. Apoptosis after IS involves many complex signaling pathways. Regulating the programmed death of neurons in the ischemic penumbra can save dying neurons to the greatest extent and promote the recovery of neural function. In addition, activation of SIPRs, TLRs, NLRPs, PPARs, and P2X7R may be the potential mechanisms for regulating microglia after IS, however, the mechanisms need to be further studied.

Natural plant compounds may have great potential as therapeutic agents to reduce pro-inflammatory responses after cerebral ischemia. As can be seen from the foregoing, most of the current studies describe M1/M2 polarization, but most studies show a mixed signature of M1 or M2 microglial/macrophage phenotypes after cerebral ischemia. An urgent need to address is the need to define the M1 or M2 microglia/macrophage phenotype in experiments with these natural compounds. Furthermore, the markers currently used to differentiate M1 and M2 phenotypes are not microglia or macrophage specific. Therefore, technologies that can separate M1 from M2 microglia/macrophages (such as microfluidics and single-cell transcriptomics to identify novel microglia-specific biomarkers) are needed in the future.

The limitation of this review is that this review focuses on the detailed mechanisms of microglia/macrophages in IS and the mechanisms of natural compound intervention, but lacks a summary of other immune cells such as T cells, B cells, and neutrophils in IS. Since immune cells such as T cells and B cells also play an important role in the pathophysiological process of IS, it is recommended to review the mechanism of these immune cells in IS in the future (39, 169, 172).

In summary, it can be seen that not only single-component natural botanical components can exert a therapeutic effect on IS by regulating microglia, but multi-component natural botanical components also show potential synergistic effects in regulating

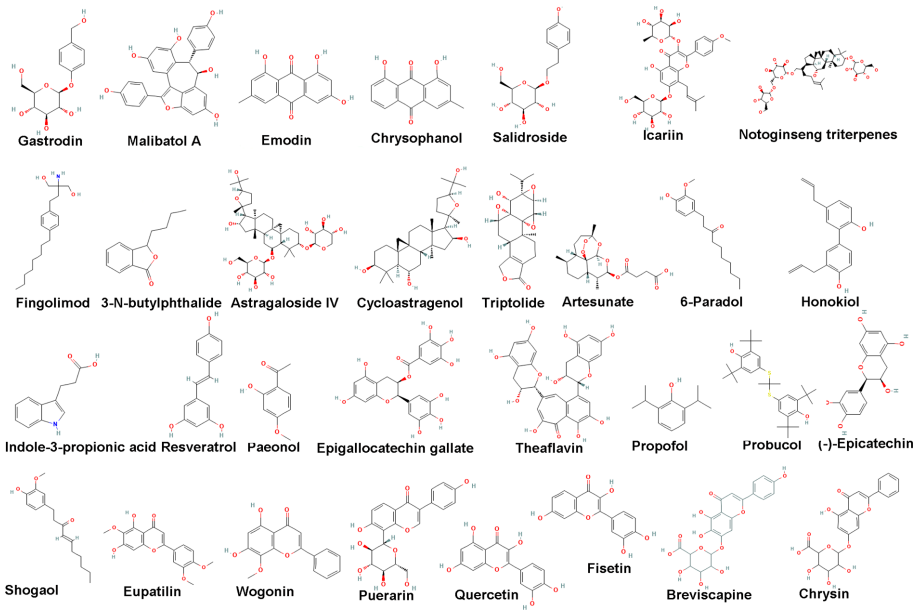


FIGURE 2
The structure of main natural botanical components.

10.3389/fimmu.2022.1047550

TABLE 1 Summary of the role of natural botanical components on IS.

Natural botanical component	Effects	Ischemia type	Category	Reference
Gastrodin	The volume of cerebral infarction and BBB permeability ↓; MMP2, MMP9, AQP4, IL-1β, COX-2 and iNOS↓; ZO-1↑	MCAO/R and OGD/R	Polyphenols and Phenols	(194)
Malibatol A	Promoting M2 microglial polarization	OGD/R	Polyphenols and Phenols	(195–197)
Emodin	MMP-9, TLR4, NF-κB, TNF-α, ICAM-1 ↓	MCAO	Anthraquinones	(230–233)
Chrysophanol	Notch-1, TNF-α and ICAM-1 protein ↓; Iba-1 positive cells↓; promoting the transformation of microglial M1 type to M2 type	MCAO	Anthraquinones	(234, 235)
Salidroside	CD16, CD32, CD11b, iNOS↓; CD206, Arg-1, TGF-β, Ym-1/2 ↑	MCAO	Glycosides	(326, 327)
Icariin	the activation of Iba1 and TLR4 in microglia ↓NF-κB p65 protein ↓; IL-1α and TNF-α ↓	MCAO	Flavonoids	(285)
Salvia Polyphenolic Acid	ICAM-1, IL-1β, IL-18, TNF-α, NLRP3, GSDMD, ASC, CASP1↓; Iba1/P2X7 double-labeled microglia↓	MCAO/R and OGD/R	Polyphenols and Phenols	(194)
Panax notoginseng saponins	CD206, TGF-β and IL-10↑;IL-1β, IL-6, TNF-α and iNOS↓;Promoting the expression of CD206/Iba-1 in M2-type microglia; Inhibiting the expression of CD16/Iba-1 in M1 type microglia cells	MCAO/R	Glycosides	(395)
Notoginseng leaf triterpenes	ICAM-1, VCAM-1, MMP-9, MMP-2, HMGB1 ↓	MCAO/R	Terpenes and Alkaloids	(401)
Omega-3 polyunsaturated fatty acid	Promoting the phenotype of microglia from M1 to M2.	MCAO	Lipids	(398–400)
Fingolimod	promoting the polarization of microglia from M1 to M2	Bilateral carotid artery stenosis	Other	(349–352, 403)
3-N-butylphthalide	Inhibiting oxidative damage, neuronal apoptosis and glial cell activation, increasing the level of circulating endothelial progenitor cells; promoting the M2-type polarization of microglia, inhibiting the M1-type polarization	IS patients; MCAO animal	Other	(356)
Danshenol bornanyl ester	HO-1 and NQO1↑; NF-κB ↓ Altering M1/M2 polarization	MCAO/R	Other	(359)
Astragaloside IV	M1-type microglia/macrophage markers CD86, iNOS, TNF-α, IL-1β and IL-6 mRNA ↓; M2-type microglia/macrophage markers CD206, Arg-1, YM1/2, IL-10 and TGF-β mRNAs ↑; the number of CD16/32+/Iba1+ cells↓; the number of CD206+/Iba1+ cells ↑; IL-1β, TNF-α and iNOS↓	MCAO	Terpenes and Alkaloids	(238, 239)
Cycloastragenol	SIRT1↑; p53, Bax/Bax ratio ↓;TNF-α and IL-1β mRNA↓; Inhibiting NF-κB p65 nuclear translocation; Inhibiting the activation of microglia and astrocytes	MCAO	Terpenes and Alkaloids	(243)
Triptolide	IL-1β, IL-6, TNF-α, IL-33, IL-10 ↓; promoting the M2-type polarization	IS paitents; MCAO/R and OGD/R animal	Terpenes and Alkaloids	(248, 249)
Artesunate	TNF-α and IL-1β ↓; Inhibiting microglial activation	MCAO	Terpenes and Alkaloids	(255–258)
6-Paradol	Iba1 ↓; TNF-α and iNOS↓; Inhibiting microglia/macrophages	MCAO/R	Polyphenols and Phenols	(208)
Honokiol	NF-κB, NO, and TNF-α↓; Inhibiting the M1 phenotypes	2 vessel occlusion/ reperfusing	Polyphenols and Phenols	(212)
Indole-3-propionic acid	Iba1 ↓; Inhibiting microglia; Inhibiting the M1 phenotypes	2 vessel occlusion/ reperfusing	Polyphenols and Phenols	(213)

(Continued)

TABLE 1 Continued

Natural botanical component	Effects	Ischemia type	Category	Reference
Resveratrol	Iba1 ↓; IL-1β and TNF-α↓Inhibiting microglia; Inhibiting the M1 phenotypes	MCAO/R; Bilateral common carotid artery occlusion	Polyphenols and Phenols	(202, 203)
Paeonol	IL-1β↓; Inhibiting microglia; Inhibiting the M1 phenotypes	MCAO/R	Polyphenols and Phenols	(218)
Epigallocatechin gallate	iNOS↓; Inhibiting the M1 phenotypes	MCAO/R	Polyphenols and Phenols	(223)
Theaflavin	COX-2, iNOS↓; Inhibiting the M1 phenotypes	MCAO/R	Polyphenols and Phenols	(227)
Propofol	IL-1β, IL-6, TNF-α↓Inhibiting microglia; Inhibiting the M1 phenotypes	MCAO/R	Polyphenols and Phenols	(314)
Probucol	COX-2, IL-1β, IL-7, iNOS↓; Inhibiting the M1 phenotypes	MCAO/R	Polyphenols and Phenols	(229)
6-Shogaol	Iba1 ↓; Inhibiting microglia	2 vessel occlusion/ reperfusing	Polyphenols and Phenols	(207)
Eupatilin	Iba1 ↓; Inhibiting microglia; Inhibiting the M1 phenotypes	MCAO/R	Flavonoids	(289)
Heptamethoxyflavonoids	BDNF↑;Iba1 ↓; Inhibiting microglia; Promoting the M2 phenotypes	2 vessel occlusion	Flavonoids	(290)
Wogonin	TNF-α, iNOS↓; Inhibiting microglia; Inhibiting the M1 phenotypes	MCAO	Flavonoids	(294)
Puerarin	COX-2↓; Inhibiting microglia; Inhibiting the M1 phenotypes	4 vessel occlusion	Flavonoids	(299)
Quercetin	iNOS↓; Inhibiting the M1 phenotypes	Bilateral common carotid artery occlusion	Flavonoids	(299)
Fisetin	TNF-α↓; Inhibiting the M1 phenotypes	MCAO/R	Flavonoids	(309)
Breviscapine	TNF-α, NF-κB, Notch-1, MCP-1, Hes-1 and iNOS↓; Inhibiting microglia; Inhibiting the M1 phenotypes	MCAO	Flavonoids	(314, 315)
Chrysin	Iba1, iNOS, COX-2, CD68, IL-1β, IL-6, IL-12, IL-1α, IL-17a, IFN-γ, and TNF-α ↓; Ym-1↑; Inhibiting microglia; Inhibiting the M1 phenotypes	MCAO/R	Flavonoids	(319)
Epicatechin	Iba1 ↓; Inhibiting the M1 phenotypes	MCAO	Flavonoids	(324)

microglia. This suggests that the combination of natural botanical components to treat multiple inflammatory models (including macrophages and microglia) is a promising direction, and we can see that the combination of natural botanical components will be more effective to achieve the desired therapeutic effect.

6 Conclusion

Intervention of natural botanical components and their derivatives in microglia-mediated neuroinflammation in IS is a promising research direction. In the absence of effective neuroprotective drugs, we should pay more attention to the mechanisms of natural botanical components in regulating microglia-mediated neuroinflammatory diseases such as IS. Future research directions are suggested as follows: (1) Differentiate between microglia and macrophages through new techniques (such as single-cell transcriptomics and its derivatives) to more accurately determine the regulatory effects of natural compounds. (2) A more standardized and stable IS model is needed to determine the effects of drugs. (3) Using spatiotemporal omics to map the dynamic continuity state of microglia in natural botanical components intervening in IS. (4) Validate the long-term brain-protective effects of natural botanical components and the mechanisms regulating microglia in rodent and mammalian IS

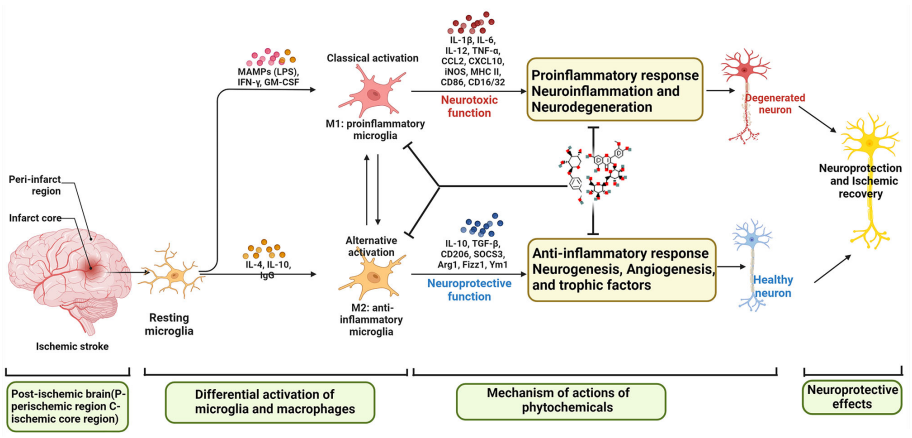


FIGURE 3
Effects of Natural botanical components on microglia/macrophages after cerebral ischemia (MAMPs, Metabolism-related molecular patterns; LPS, Lipopolysaccharide; GM-CSF, granulocyte-macrophage colony stimulating factor; IL, interleukin; TGF, transforming growth factor).

models. (5) Pay attention to the pharmacokinetics, pharmacodynamics, and toxicological properties of natural botanical components. (6) Explore the synergistic effect of natural botanical components in inhibiting neuroinflammation. (7) If all results are favorable, the next step is to conduct clinical trials of potential phytochemicals to investigate their neuroprotective effects on cerebral ischemia/stroke (For example, the team is currently conducting a clinical trial of Naotai Fang in the treatment of cerebral small vessel disease: ChiCTR1900024524).

Author contributions

TB, and JZ are responsible for the study concept and design. TB, JZ, KY, SW, WX, XZ, AG, LZ, JG are responsible for the data collection, data analysis and interpretation; JZ and KY drafted the paper; JG supervised the study; all authors participated in the analysis and interpretation of data and approved the final paper.

Funding

This work is supported by the National Natural Science Foundation of China (81774174), the National Key Research and Development Project of China (No. 2018YFC1704904), National Natural Science Foundation of Hunan Province, China (2020JJ5424 and 2020JJ5442), Hunan University of Chinese Medicine "Double First-Class" Discipline Open Fund Project of Integrated Traditional Chinese and Western Medicine (2020ZXYJH08 and 2020ZXYJH09), Hunan Provincial Department of Education Youth Fund Project (21B0386).

Conflict of interest

The authors declare that the research was conducted in the absence of any commercial or financial relationships that could be construed as a potential conflict of interest.

Publisher's note

All claims expressed in this article are solely those of the authors and do not necessarily represent those of their affiliated organizations, or those of the publisher, the editors and the reviewers. Any product that may be evaluated in this article, or claim that may be made by its manufacturer, is not guaranteed or endorsed by the publisher.

References

1. Feske SK. Ischemic stroke. *Am J Med* (2021) 134(12):1457–64. doi: 10.1016/j.amjmed.2021.07.027

2. Herpich F, Rincon F. Management of acute ischemic stroke. *Crit Care Med* (2020) 48(11):1654–63. doi: 10.1097/CCM.0000000000004597

3. Putaala J. Ischemic stroke in young adults. *Continuum (MinneapMinn)* (2020) 26(2):386–414. doi: 10.1212/CON.0000000000000833

4. Mendelson SJ, Prabhakaran S. Diagnosis and management of transient ischemic attack and acute ischemic stroke: A review. *JAMA* (2021) 325 (11):1088–98. doi: 10.1001/jama.2020.26867

5. GBD 2019 Stroke Collaborators. Global, regional, and national burden of stroke and its risk factors, 1990-2019: a systematic analysis for the global burden of disease study 2019. *Lancet Neurol* (2021) 20(10):795–820. doi: 10.1016/S1474-4422(21)00252-0

6. Xu S, Lu J, Shao A, Zhang JH, Zhang J. Glial cells: Role of the immune response in ischemic stroke. *Front Immunol* (2020) 11:294. doi: 10.3389/fimmu.2020.00294

7. Kim JS. tPA helpers in the treatment of acute ischemic stroke: Are they ready for clinical use? *J Stroke* (2019) 21(2):160–74. doi: 10.5853/jos.2019.00584

8. Hollist M, Morgan L, Cabatbat R, Au K, Kirmani MF, Kirmani BF. Acute stroke management: Overview and recent updates. *Aging Dis* (2021) 12(4):1000–9. doi: 10.14336/AD.2021.0311

9. Paul S, Candelario-Jalil E. Emerging neuroprotective strategies for the treatment of ischemic stroke: An overview of clinical and preclinical studies. *Exp Neurol* (2021) 335:113518. doi: 10.1016/j.expneurol.2020.113518

10. Qin C, Zhou LQ, Ma XT, Hu ZW, Yang S, Chen M, et al. Dual functions of microglia in ischemic stroke. *Neurosci Bull* (2019) 35(5):921–33. doi: 10.1007/s12264-019-00388-3

11. Li LZ, Huang YY, Yang ZH, Zhang SJ, Han ZP, Luo YM. Potential microglia-based interventions for stroke. *CNS NeurosciTher* (2020) 26(3):288–96. doi: 10.1111/cns.13291

12. Jiang J, Bai Q, He C, Li Z, Song Z, Cheng S, et al. Dihuang-Yinzi Decoction Contained Serum Suppresses LPS-induced BV2 Cells Inflammatory Response Through PPARγ/NF-κB Signaling Pathway. *World Sci Technology-China Modernization Med* (2021) 23(05):1610–6. doi: 10.11842/wst.20210104003

13. Zhang X, Lei C, Liu Y, Ge J, Meng P, Zhangyu, et al. The regulatory effect of naotaifang II drug-containing serum on LPS-induced microglial polarization. *J Beijing Univ Traditional Chin Med* (2020) 43(05):408–13. doi: CNKI:SUN:JZYB.0.2020-05-010

14. Zuo L. The effect of annao pingchong recipe on inflammatory response after cerebral hemorrhage from the P2X7R/NLRP3 pathway[D]. *Hunan Univ Traditional Chin Med* (2020). doi: 10.27138/d.cnki.ghuzc.2020.000171

15. He C, Yu W, Yang M, Li Z, Xia X, Li P, et al. Baicalin inhibits lipopolysaccharide/interferon γ-induced inflammatory response in BV2 cells *via* TREM2/TLR4/NF-κB signaling pathway. *China J Traditional Chin Med* (2022) 47(06):1603–10. doi: 10.19540/j.cnki.cjcmm.20211103.401

16. Wang XJ, Hu R, Huang QY, Peng QH, Yu J. Gynostemma glycosides protect retinal ganglion cells in rats with chronic high intraocular pressure by regulating the STAT3/JAK2 signaling pathway and inhibiting astrocyte and microglia activation. *Evid Based Complement Alternat Med* (2022) 2022:9963754. doi: 10.1155/2022/9963754.P

17. Chen M, Lai X, Wang X, Ying J, Zhang L, Zhou B, et al. Long non-coding RNAs and circular RNAs: Insights into microglia and astrocyte mediated neurological diseases. *Front Mol Neurosci* (2021) 14:745066. doi: 10.3389/fnmol.2021.745066

18. Di Napoli M, Elkind MS, Godoy DA, Singh P, Papa F, Popa-Wagner A. Role of c-reactive protein in cerebrovascular disease: a critical review. *Expert Rev Cardiovasc Ther* (2011) 9(12):1565–84. doi: 10.1586/erc.11.159

19. Kissa K, Herbomel P. Blood stem cells emerge from aortic endothelium by ael type of cell transition. *Nature* (2010) 464(7285):112–5. doi: 10.1038/nature08761

20. Lichanska AM, Browne CM, Henkel GW, Murphy KM, Ostrowski MC, McKercher SR, et al. Differentiation of the mononuclear phagocyte system during mouse embryogenesis: the role of transcription factor PU. *1 Blood* (1999) 94(1):127–38. doi: 10.1182/blood.V94.1.127.413k07_127_138

21. Iadecola C, Anrather J. The immunology of stroke: from mechanisms to translation. *Nat Med* (2011) 17(7):796–808. doi: 10.1038/nm.2399

22. Endres M, Moro MA, Nolte CH, Dames C, Buckwalter MS, Meisel A. Immune pathways in etiology, acute phase, and chronic sequelae of ischemic stroke. *Circ Res* (2022) 130(8):1167–86. doi: 10.1161/CIRCRESAHA.121.319994

23. Liu R, Song P, Gu X, Liang W, Sun W, Hua Q, et al. Comprehensive landscape of immune infiltration and aberrant pathway activation in ischemic stroke. *Front Immunol* (2022) 12:766724. doi: 10.3389/fimmu.2021.766724

24. Ankarcrona M, Dypbukt JM, Bonfoco E, Zhivotovsky B, Orrenius S, Lipton SA, et al. Glutamate-induced neuronal death: a succession of necrosis or apoptosis depending on mitochondrial function. *Neuron* (1995) 15(4):961–73. doi: 10.1016/0896-6273(95)90186-8

25. Rana AK, Singh D. Targeting glycogen synthase kinase-3 for oxidative stress and neuroinflammation: Opportunities, challenges and future directions for cerebral stroke management. *Neuropharmacology* (2018) 139:124–36. doi: 10.1016/j.neuropharm.2018.07.006

26. Adibhatla RM, Hatcher JF. Lipid oxidation and peroxidation in CNS health and disease: from molecular mechanisms to therapeutic opportunities. *Antioxid Redox Signal* (2010) 12(1):125–69. doi: 10.1089/ars.2009.2668

27. Gomez Perdiguero E, Geissmann F. Myb-independent macrophages: a family of cells that develops with their tissue of residence and is involved in its homeostasis. *Cold Spring Harb Symp Quant Biol* (2013) 78:91–100. doi: 10.1101/sqb.2013.78.020032

28. Gomez Perdiguero E, Schulz C, Geissmann F. Development and homeostasis of "resident" myeloid cells: the case of the microglia. *Glia* (2013) 61(1):112–20. doi: 10.1002/glia.22393

29. Zeyu Z, Yuanjian F, Cameron L, Sheng C. The role of immune inflammation in aneurysmal subarachnoid hemorrhage. *Exp Neurol* (2021) 336:113535. doi: 10.1016/j.expneurol.2020.113535

30. Garcia-Bonilla L, Iadecola C. Peroxiredoxin sets the brain on fire after stroke. *Nat Med* (2012) 18(6):858–9. doi: 10.1038/nm.2797

31. Petrovic-Djergovic D, Goonewardena SN, Pinsky DJ. Inflammatory disequilibrium in stroke. *Circ Res* (2016) 119(1):142–58. doi: 10.1161/CIRCRESAHA.116.308022

32. Sánchez KE, Rosenberg GA. Shared inflammatory pathology of stroke and COVID-19. *Int J Mol Sci* (2022) 23(9):5150. doi: 10.3390/ijms23095150

33. DeLong JH, Ohashi SN, O'Connor KC, Sansing LH. Inflammatory responses after ischemic stroke. *Semin Immunopathol* (2022) 44 (5):625–48. doi: 10.1007/s00281-022-00943-7

34. Guo J, Wang J, Sun W, Liu X. The advances of post-stroke depression: 2021 update. *J Neurol* (2022) 269(3):1236–49. doi: 10.1007/s00415-021-10597-4

35. Levard D, Buendia I, Lanquetin A, Glavan M, Vivien D, Rubio M. Filling the gaps on stroke research: Focus on inflammation and immunity. *Brain Behav Immun* (2021) 91:649–67. doi: 10.1016/j.bbi.2020.09.025

36. Iadecola C, Buckwalter MS, Anrather J. Immune responses to stroke: mechanisms, modulation, and therapeutic potential. *J Clin Invest* (2020) 130(6):2777–88. doi: 10.1172/JCI135530

37. Jayaraj RL, Azimullah S, Beiram R, Jalal FY, Rosenberg GA. Neuroinflammation: friend and foe for ischemic stroke. *J Neuroinflamm* (2019) 16(1):142. doi: 10.1186/s12974-019-1516-2

38. Stanzione R, Forte M, Cotugno M, Bianchi F, Marchitti S, Rubattu S. Role of DAMPs and of leukocytes infiltration in ischemic stroke: Insights from animal models and translation to the human disease. *Cell Mol Neurobiol* (2022) 42(3):545–56. doi: 10.1007/s10571-020-00966-4

39. Qiu YM, Zhang CL, Chen AQ, Wang HL, Zhou YF, Li YN, et al. Immune cells in the BBB disruption after acute ischemic stroke: Targets for immune therapy? *Front Immunol* (2021) 12:678744. doi: 10.3389/fimmu.2021.678744

40. Shi K, Tian DC, Li ZG, Ducruet AF, Lawton MT, Shi FD. Global brain inflammation in stroke. *Lancet Neurol* (2019) 18(11):1058–66. doi: 10.1016/S1474-4422(19)30078-X

41. Orellana-Urzúa S, Rojas I, Líbano L, Rodrigo R. Pathophysiology of ischemic stroke: Role of oxidative stress. *Curr Pharm Des* (2020) 26(34):4246–60. doi: 10.2174/1381612826666200708133912

42. Maida CD, Norrito RL, Daidone M, Tuttolomondo A, Pinto A. Neuroinflammatory mechanisms in ischemic stroke: Focus on cardioembolic stroke, background, and therapeutic approaches. *Int J Mol Sci* (2020) 21(18):6454. doi: 10.3390/ijms21186454

43. Lambertsen KL, Finsen B, Clausen BH. Post-stroke inflammation-target or tool for therapy? *Acta Neuropathol* (2019) 137(5):693–714. doi: 10.1007/s00401-018-1930-z

44. Mashaqi S, Mansour HM, Alameddin H, Combs D, Patel S, Estep L, et al. Matrix metalloproteinase-9 as a messenger in the cross talk between obstructive sleep apnea and comorbid systemic hypertension, cardiac remodeling, and ischemic stroke: a literature review. *J Clin Sleep Med* (2021) 17(3):567–91. doi: 10.5664/jcsm.8928

45. Wang M, Pan W, Xu Y, Zhang J, Wan J, Jiang H. Microglia-mediated neuroinflammation: A potential target for the treatment of cardiovascular diseases. *J Inflammation Res* (2022) 15:3083–94. doi: 10.2147/JIR.S350109

46. Couch C, Mallah K, Borucki DM, Bonilha HS, Tomlinson S. State of the science in inflammation and stroke recovery: A systematic review. *Ann Phys Rehabil Med* (2022) 65(2):101546. doi: 10.1016/j.rehab.2021.101546

47. Wicks EE, Ran KR, Kim JE, Xu R, Lee RP, Jackson CM. The translational potential of microglia and monocyte-derived macrophages in ischemic stroke. *Front Immunol* (2022) 13:897022. doi: 10.3389/fimmu.2022.897022

48. Muhammad S, Chaudhry SR, Kahlert UD, Niemelä M, Hänggi D. Brain immune interactions-novel emerging options to treat acute ischemic brain injury. *Cells* (2021) 10(9):2429. doi: 10.3390/cells10092429

49. An C, Shi Y, Li P, Hu X, Gan Y, Stetler RA, et al. Molecular dialogs between the ischemic brain and the peripheral immune system: dualistic roles in injury and repair. *Prog Neurobiol* (2014) 115:6–24. doi: 10.1016/j.pneurobio.2013.12.002

50. Ziv Y, Ron N, Butovsky O, Landa G, Sudai E, Greenberg N, et al. Immune cells contribute to the maintenance of neurogenesis and spatial learning abilities in adulthood. *Nat Neurosci* (2006) 9(2):268–75. doi: 10.1038/nn1629

51. Hug A, Dalpke A, Wieczorek N, Giese T, Lorenz A, Auffarth G, et al. Infarct volume is a major determiner of post-stroke immune cell function and susceptibility to infection. *Stroke* (2009) 40(10):3226–32. doi: 10.1161/STROKEAHA.109.557967

52. Meisel C, Schwab JM, Prass K, Meisel A, Dirnagl U. Central nervous system injury-induced immune deficiency syndrome. *Nat Rev Neurosci* (2005) 6(10):775–86. doi: 10.1038/nrn1765

53. Chen C, Ai QD, Chu SF, Zhang Z, Chen NH. NK cells in cerebral ischemia. *BioMed Pharmacother* (2019) 109:547–54. doi: 10.1016/j.biopha.2018.10.103

54. Shim R, Wong CH. Ischemia, immunosuppression and infection–tackling the predicaments of post-stroke complications. *Int J Mol Sci* (2016) 17(1):64. doi: 10.3390/ijms17010064

55. Shi AC, Rohlwink U, Scafidi S, Kannan S. Microglial metabolism after pediatric traumatic brain injury - overlooked bystanders or active participants? *Front Neurol* (2021) 11:626999. doi: 10.3389/fneur.2020.626999

56. Zhou R, Qian S, Cho WCS, Zhou J, Jin C, Zhong Y, et al. Microbiota-microglia connections in age-related cognitionline. *Aging Cell* (2022) 21(5):e13599. doi: 10.1111/acel.13599

57. Leng F, Edison P. Neuroinflammation and microglial activation in Alzheimer disease: where do we go from here? *Nat Rev Neurol* (2021) 17 (3):157–72. doi: 10.1038/s41582-020-00435-y

58. Borst K, Dumas AA, Prinz M. Microglia: Immune and non-immune functions. *Immunity* (2021) 54(10):2194–208. doi: 10.1016/j.immuni.2021.09.014

59. Cserép C, Pósfai B, Dénes Á. Shaping neuronal fate: Functional heterogeneity of direct microglia-neuron interactions. *Neuron* (2021) 109 (2):222–40. doi: 10.1016/j.neuron.2020.11.007

60. Wink DA, Hines HB, Cheng RY, Switzer CH, Flores-Santana W, Vitek MP, et al. Nitric oxide and redox mechanisms in the immune response. *J Leukoc Biol* (2011) 89(6):873–91. doi: 10.1189/jlb.1010550

61. Lukens JR, Eyo UB. Microglia and neurodevelopmental disorders. *Annu Rev Neurosci* (2022) 45:425–45. doi: 10.1146/annurev-neuro-110920-023056

62. Andoh M, Koyama R. Microglia regulate synaptic development and plasticity. *Dev Neurobiol* (2021) 81(5):568–90. doi: 10.1002/dneu.22814

63. Woodburn SC, Bollinger JL, Wohleb ES. The semantics of microglia activation: neuroinflammation, homeostasis, and stress. *J Neuroinflamm* (2021) 18(1):258. doi: 10.1186/s12974-021-02309-6

64. Marinelli S, Basilico B, Marrone MC, Ragozzino D. Microglia-neuron crosstalk: Signaling mechanism and control of synaptic transmission. *Semin Cell Dev Biol* (2019) 94:138–51. doi: 10.1016/j.semcdb.2019.05.017

65. Verkhratsky A, Sun D, Tanaka J. Snapshot of microglial physiological functions. *Neurochem Int* (2021) 144:104960. doi: 10.1016/j.neuint.2021.104960

66. Wake H, Moorhouse AJ, Jinno S, Kohsaka S, Nabekura J. Resting microglia directly monitor the functional state of synapses *in vivo* and determine the fate of ischemic terminals. *J Neurosci* (2009) 29(13):3974–80. doi: 10.1523/JNEUROSCI.4363-08.2009

67. Andoh M, Koyama R. Assessing microglial dynamics by live imaging. *Front Immunol* (2021) 12:617564. doi: 10.3389/fimmu.2021.617564

68. Guo S, Wang H, Yin Y. Microglia polarization from M1 to M2 in neurodegenerative diseases. *Front Aging Neurosci* (2022) 14:815347. doi: 10.3389/fnagi.2022.815347

69. Zhang L, Cao Y, Zhang X, Gu X, Mao Y, Peng B. The origin and repopulation of microglia. *Dev Neurobiol* (2022) 82(1):112–24. doi: 10.1002/dneu.22862

70. Orihuela R, McPherson CA, Harry GJ. Microglial M1/M2 polarization and metabolic states. *Br J Pharmacol* (2016) 173(4):649–65. doi: 10.1111/bph.13139

71. Ma D, Feng L, Deng F, Feng JC. Overview of experimental and clinical findings regarding the neuroprotective effects of cerebral ischemic postconditioning. *BioMed Res Int* (2017) 2017:6891645. doi: 10.1155/2017/6891645

72. Saxena S, Kruys V, Vamecq J, Maze M. The role of microglia in perioperative neuroinflammation and neurocognitive disorders. *Front Aging Neurosci* (2021) 13:671499. doi: 10.3389/fnagi.2021.671499

73. Kanazawa M, Ninomiya I, Hatakeyama M, Takahashi T, Shimohata T. Microglia and Monocytes/Macrophages polarization revealel therapeutic mechanism against stroke. *Int J Mol Sci* (2017) 18(10):2135. doi: 10.3390/ijms18102135

74. Lanza M, Casili G, Campolo M, Paterniti I, Colarossi C, Mare M, et al. Immunomodulatory effect of microglia-released cytokines in gliomas. *Brain Sci* (2021) 11(4):466. doi: 10.3390/brainsci11040466

75. Tian DS, Li CY, Qin C, Murugan M, Wu LJ, Liu JL. Deficiency in the voltage-gated proton channel Hv1 increases M2 polarization of microglia and attenuates brain damage from photothrombotic ischemic stroke. *J Neurochem* (2016) 139(1):96–105. doi: 10.1111/jnc.13751

76. Hur J, Lee P, Kim MJ, Kim Y, Cho YW. Ischemia-activated microglia induces neuronal injury *via* activation of gp91phox NADPH oxidase. *Biochem Biophys Res Commun* (2010) 391(3):1526–30. doi: 10.1016/j.bbrc.2009.12.114

77. Li QQ, Li JY, Zhou M, Qin ZH, Sheng R. Targeting neuroinflammation to treat cerebral ischemia - the role of TIGAR/NADPH axis. *Neurochem Int* (2021) 148:105081. doi: 10.1016/j.neuint.2021.105081

78. Candelario-Jalil E, Dijkhuizen RM, Magnus T. Neuroinflammation, stroke, blood-brain barrier dysfunction, and imaging modalities. *Stroke* (2022) 53 (5):1473–86. doi: 10.1161/STROKEAHA.122.036946

79. Kwon HS, Koh SH. Neuroinflammation in neurodegenerative disorders: the roles of microglia and astrocytes. *Transl Neurodegener* (2020) 9(1):42. doi: 10.1186/s40035-020-00221-2

80. Webster CM, Hokari M, McManus A, Tang XN, Ma H, Kacimi R, et al. Microglial P2Y12 deficiency/inhibition protects against brain ischemia. *PloS One* (2013) 8(8):e70927. doi: 10.1371/journal.pone.0070927

81. Kawabori M, Kacimi R, Kauppinen T, Calosing C, Kim JY, Hsieh CL, et al. Triggering receptor expressed on myeloid cells 2 (TREM2) deficiency attenuates phagocytic activities of microglia and exacerbates ischemic damage in experimental stroke. *J Neurosci* (2015) 35(8):3384–96. doi: 10.1523/JNEUROSCI.2620-14.2015

82. Roesch S, Rapp C, Dettling S, Herold-Mende C. When immune cells turn bad-Tumor-Associated Microglia/Macrophages in glioma. *Int J Mol Sci* (2018) 19 (2):436. doi: 10.3390/ijms19020436

83. Chu F, Shi M, Zheng C, Shen D, Zhu J, Zheng X, et al. The roles of macrophages and microglia in multiple sclerosis and experimental autoimmune encephalomyelitis. *J Neuroimmunol* (2018) 318:1–7. doi: 10.1016/j.jneuroim.2018.02.015.E

84. Dos Santos IRC, Dias MNC, Gomes-Leal W. Microglial activation and adult neurogenesis after brain stroke. *Neural Regener Res* (2021) 16(3):456–9. doi: 10.4103/1673-5374.291383

85. Mahmood A, Miron VE. Microglia as therapeutic targets for central nervous system remyelination. *Curr Opin Pharmacol* (2022) 63:102188. doi: 10.1016/j.coph.2022.102188

86. Lin X, Wang H, Chen J, Zhao P, Wen M, Bingwa LA, et al. Nonhuman primate models of ischemic stroke and neurological evaluation after stroke. *J Neurosci Methods* (2022) 376:109611. doi: 10.1016/j.jneumeth.2022.109611

87. Zhu T, Wang L, Feng Y, Sun G, Sun X. Classical active ingredients and extracts of Chinese herbal medicines: Pharmacokinetics, pharmacodynamics, and molecular mechanisms for ischemic stroke. *Oxid Med Cell Longev* (2021) 2021:8868941. doi: 10.1155/2021/8868941

88. Holste KG, Xia F, Ye F, Keep RF, Xi G. Mechanisms of neuroinflammation in hydrocephalus after intraventricular hemorrhage: a review. *Fluids Barriers CNS* (2022) 19(1):28. doi: 10.1186/s12987-022-00324-0

89. Shi X, Luo L, Wang J, Shen H, Li Y, Mamtilahun M, et al. Stroke subtype-dependent synapse elimination by reactive gliosis in mice. *Nat Commun* (2021) 12 (1):6943. doi: 10.1038/s41467-021-27248-x

90. Dhillon SK, Gunn ER, Lear BA, King VJ, Lear CA, Wassink G, et al. Cerebral oxygenation and metabolism after hypoxia-ischemia. *Front Pediatr* (2022) 10:925951. doi: 10.3389/fped.2022.925951

91. Zhang Q, Jia M, Wang Y, Wang Q, Wu J. Cell death mechanisms in cerebral ischemia-reperfusion injury. *Neurochem Res* (2022) 47(12):3525–42. doi: 10.1007/s11064-022-03697-8

92. Wang Z, Weaver DF. Microglia and microglial-based receptors in the pathogenesis and treatment of alzheimer's disease. *Int Immunopharmacol* (2022) 110:109070. doi: 10.1016/j.intimp.2022.109070

93. Shi Y, Holtzman DM. Interplay between innate immunity and Alzheimer disease: APOE and TREM2 in the spotlight. *Nat Rev Immunol* (2018) 18(12):759–72. doi: 10.1038/s41577-018-0051-1

94. Caso JR, Pradillo JM, Hurtado O, Lorenzo P, Moro MA, Lizasoain I. Toll-like receptor 4 is involved in brain damage and inflammation after experimental stroke. *Circulation* (2007) 115(12):1599–608. doi: 10.1161/CIRCULATIONAHA.106.603431

95. Kilic U, Kilic E, Matter CM, Bassetti CL, Hermann DM. TLR-4 deficiency protects against focal cerebral ischemia and axotomy-induced neurodegeneration. *Neurobiol Dis* (2008) 31(1):33–40. doi: 10.1016/j.nbd.2008.03.002

96. Lehnardt S, Lehmann S, Kaul D, Tschimmel K, Hoffmann O, Cho S, et al. Toll-like receptor 2 mediates CNS injury in focal cerebral ischemia. *J Neuroimmunol* (2007) 190(1-2):28–33. doi: 10.1016/j.jneuroim.2007.07.023

97. Lehnardt S, Massillon L, Follett P, Jensen FE, Ratan R, Rosenberg PA, et al. Activation of innate immunity in the CNS triggers neurodegeneration through a toll-like receptor 4-dependent pathway. *Proc Natl Acad Sci U S A* (2003) 100 (14):8514–9. doi: 10.1073/pnas.1432609100

98. Rosenberger K, Derkow K, Dembny P, Krüger C, Schott E, Lehnardt S. The impact of single and pairwise toll-like receptor activation on neuroinflammation and neurodegeneration. *J Neuroinflamm* (2014) 20:11:166. doi: 10.1186/s12974-014-0166-7

99. Ngwa C, Al Mamun A, Qi S, Sharmeen R, Xu Y, Liu F. Regulation of microglial activation in stroke in aged mice: a translational study. *Aging (Albany NY)* (2022) 14(15):6047–65. doi: 10.18632/aging.204216

100. Pradillo JM, Fernández-López D, García-Yébenes I, Sobrado M, Hurtado O, Moro MA, et al. Toll-like receptor 4 is involved in neuroprotection afforded by ischemic preconditioning. *J Neurochem* (2009) 109(1):287–94. doi: 10.1111/j.1471-4159.2009.05972.x

101. Tang SC, Arumugam TV, Xu X, Cheng A, Mughal MR, Jo DG, et al. Pivotal role for neuronal toll-like receptors in ischemic brain injury and functional deficits. *Proc Natl Acad Sci U S A* (2007) 104(34):13798–803. doi: 10.1073/pnas.0702553104

102. Hu X, Liou AK, Leak RK, Xu M, An C, Suenaga J, et al. Neurobiology of microglial action in CNS injuries: receptor-mediated signaling mechanisms and functional roles. *Prog Neurobiol* (2014) 119-120:60–84. doi: 10.1016/j.pneurobio.2014.06.002

103. Trincavelli ML, Melani A, Guidi S, Cuboni S, Cipriani S, Pedata F, et al. Regulation of A(2A) adenosine receptor expression and functioning following permanent focal ischemia in rat brain. *J Neurochem* (2008) 104(2):479–90. doi: 10.1111/j.1471-4159.2007.04990.x

104. Rivera-Oliver M, Díaz-Ríos M. Using caffeine and other adenosine receptor antagonists and agonists as therapeutic tools against neurodegenerative diseases: a review. *Life Sci* (2014) 101(1-2):1–9. doi: 10.1016/j.lfs.2014.01.083

105. Abbracchio MP, Burnstock G, Verkhratsky A, Zimmermann H. Purinergic signalling in the nervous system: an overview. *Trends Neurosci* (2009) 32(1):19–29. doi: 10.1016/j.tins.2008.10.001

106. Burnstock G. Purinergic signalling and disorders of the central nervous system. *Nat Rev Drug Discovery* (2008) 7(7):575–90. doi: 10.1038/nrd2605

107. Burnstock G. Physiology and pathophysiology of purinergic neurotransmission. *Physiol Rev* (2007) 87(2):659–797. doi: 10.1152/physrev.00043.2006

108. Cavaliere F, Florenzano F, Amadio S, Fusco FR, Viscomi MT, D'Ambrosi N, et al. Up-regulation of P2X2, P2X4 receptor and ischemic cell death: prevention by P2 antagonists. *Neuroscience* (2003) 120(1):85–98. doi: 10.1016/s0306-4522(03)00228-8

109. Gendron FP, Chalimoniuk M, Strosznajder J, Shen S, González FA, Weisman GA, et al. P2X7 nucleotide receptor activation enhances IFN gamma-induced type II nitric oxide synthase activity in BV-2 microglial cells. *J Neurochem* (2003) 87(2):344–52. doi: 10.1046/j.1471-4159.2003.01995.x

110. Shiratori M, Tozaki-Saitoh H, Yoshitake M, Tsuda M, Inoue K. P2X7 receptor activation induces CXCL2 production in microglia through NFAT and PKC/MAPK pathways. *J Neurochem* (2010) 114(3):810–9. doi: 10.1111/j.1471-4159.2010.06809.x

111. Ajami B, Bennett JL, Krieger C, McNagny KM, Rossi FM. Infiltrating monocytes trigger EAE progression, but do not contribute to the resident microglia pool. *Nat Neurosci* (2011) 14(9):1142–9. doi: 10.1038/nn.2887

112. Savarin-Vuaillat C, Ransohoff RM. Chemokines and chemokine receptors in neurological disease: raise, retain, or reduce? *Neurotherapeutics* (2007) 4(4):590–601. doi: 10.1016/j.nurt.2007.07.004

113. Inose Y, Kato Y, Kitagawa K, Uchiyama S, Shibata N. Activated microglia in ischemic stroke penumbra upregulate MCP-1 and CCR2 expression in response to lysophosphatidylcholine derived from adjacent neurons and astrocytes. *Neuropathology* (2015) 35(3):209–23. doi: 10.1111/neup.12182

114. Dimitrijevic OB, Stamatovic SM, Keep RF, Andjelkovic AV. Absence of the chemokine receptor CCR2 protects against cerebral ischemia/reperfusion injury in mice. *Stroke* (2007) 38(4):1345–53. doi: 10.1161/01.STR.0000259709.16654.8f

115. Schilling M, Strecker JK, Ringelstein EB, Schäbitz WR, Kiefer R. The role of CC chemokine receptor 2 on microglia activation and blood-borne cell recruitment after transient focal cerebral ischemia in mice. *Brain Res* (2009) 1289:79–84. doi: 10.1016/j.brainres.2009.06.054

116. Lue LF, Walker DG, Brachova L, Beach TG, Rogers J, Schmidt AM, et al. Involvement of microglial receptor for advanced glycation endproducts (RAGE) in alzheimer's disease: identification of a cellular activation mechanism. *Exp Neurol* (2001) 171(1):29–45. doi: 10.1006/exnr.2001.7732

117. Zhai DX, Kong QF, Xu WS, Bai SS, Peng HS, Zhao K, et al. RAGE expression is up-regulated in human cerebral ischemia and pMCAO rats. *Neurosci Lett* (2008) 445(1):117–21. doi: 10.1016/j.neulet.2008.08.077

118. Menini T, Ikeda H, Kimura S, Gugliucci A. Circulating soluble RAGE increase after a cerebrovascular event. *Clin Chem Lab Med* (2014) 52(1):109–16. doi: 10.1515/cclm-2012-0813

119. Muhammad S, Barakat W, Stoyanov S, Murikinati S, Yang H, Tracey KJ, et al. The HMGB1 receptor RAGE mediates ischemic brain damage. *J Neurosci* (2008) 28(46):12023–31. doi: 10.1523/JNEUROSCI.2435-08.2008

120. Hu X, Li P, Guo Y, Wang H, Leak RK, Chen S, et al. Microglia/macrophage polarization dynamics revealel mechanism of injury expansion after focal cerebral ischemia. *Stroke* (2012) 43(11):3063–70. doi: 10.1161/STROKEAHA.112.659656

121. Norden DM, Godbout JP. Review: microglia of the aged brain: primed to be activated and resistant to regulation. *Neuropathol Appl Neurobiol* (2013) 39 (1):19–34. doi: 10.1111/j.1365-2990.2012.01306.x

122. O'Neill LA, Hardie DG. Metabolism of inflammation limited by AMPK and pseudo-starvation. *Nature* (2013) ;493(7432):346–55. doi: 10.1038/nature11862

123. Salvany S, Casanovas A, Piedrafita L, Tarabal O, Hernández S, Calderó J, et al. Microglial recruitment and mechanisms involved in the disruption of afferent synaptic terminals on spinal cord motor neurons after acute peripheral nerve injury. *Glia* (2021) 69(5):1216–40. doi: 10.1002/glia.23959

124. Perego C, Fumagalli S, De Simoni MG. Temporal pattern of expression and colocalization of microglia/macrophage phenotypekers following brain ischemic injury in mice. *J Neuroinflamm* (2011) 8:174. doi: 10.1186/1742-2094-8-174

125. Denes A, Vidyasagar R, Feng J, Narvainen J, McColl BW, Kauppinen RA, et al. Proliferating resident microglia after focal cerebral ischaemia in mice. *J Cereb Blood Flow Metab* (2007) 27(12):1941–53. doi: 10.1038/sj.jcbfm.9600495

126. Vázquez-Villoldo N, Domercq M, Martín A, Llop J, Gómez-Vallejo V, Matute C. P2X4 receptors control the fate and survival of activated microglia. *Glia* (2014) 62(2):171–84. doi: 10.1002/glia.22596

127. Barnabei L, Laplantine E, Mbongo W, Rieux-Laucat F, Weil R. NF-κB: At the borders of autoimmunity and inflammation. *Front Immunol* (2021) 12:716469. doi: 10.3389/fimmu.2021.716469

128. Cheng QJ, Ohta S, Sheu KM, Spreafico R, Adelaja A, Taylor B, et al. NF-κB dynamics determine the stimulus specificity of epigenomic reprogramming in macrophages. *Science* (2021) 372(6548):1349–53. doi: 10.1126/science.abc0269.5

129. Lenglet S, Montecucco F, Mach F. Role of matrix metalloproteinases in animal models of ischemic stroke. *Curr Vasc Pharmacol* (2015) 13(2):161–6. doi: 10.2174/1570161113116660161

130. Kim SR, Jung YR, An HJ, Kim DH, Jang EJ, Choi YJ, et al. Anti-wrinkle and anti-inflammatory effects of active garlic components and the inhibition of MMPs *via* NF-κB signaling. *PloS One* (2013) 8(9):e73877. doi: 10.1371/journal.pone.0073877

131. Shin HM, Minter LM, Cho OH, Gottipati S, Fauq AH, Golde TE, et al. Notch1ments NF-kappaB activity by facilitating its nuclear retention. *EMBO J* (2006) 25(1):129–38. doi: 10.1038/sj.emboj.7600902

132. Jha NK, Chen WC, Kumar S, Dubey R, Tsai LW, Kar R, et al. Molecular mechanisms of developmental pathways in neurological disorders: a pharmacological and therapeutic review. *Open Biol* (2022) 12(3):210289. doi: 10.1098/rsob.210289

133. Wei Z, Chigurupati S, Arumugam TV, Jo DG, Li H, Chan SL. Notch activation enhances the microglia-mediated inflammatory response associated with focal cerebral ischemia. *Stroke* (2011) 42(9):2589–94. doi: 10.1161/STROKEAHA.111.614834

134. Qin H, Holdbrooks AT, Liu Y, Reynolds SL, Yanagisawa LL, Benveniste EN. SOCS3 deficiency promotes M1 macrophage polarization and inflammation. *J Immunol* (2012) 189(7):3439–48. doi: 10.4049/jimmunol.1201168

135. Takeda H, Yamaguchi T, Yano H, Tanaka J. Microglial metabolic disturbances and neuroinflammation in cerebral infarction. *J Pharmacol Sci* (2021) 145(1):130–9. doi: 10.1016/j.jphs.2020.11.007

136. Lai CS, Lee JH, Ho CT, Liu CB, Wang JM, Wang YJ, et al. Rosmanol potently inhibits lipopolysaccharide-induced iNOS and COX-2 expression through downregulating MAPK, NF-kappaB, STAT3 and C/EBP signaling pathways. *J Agric Food Chem* (2009) 57(22):10990–8. doi: 10.1021/jf9025713

137. Jover-Mengual T, Miyawaki T, Latuszek A, Alborch E, Zukin RS, Etgen AM. Acute estradiol protects CA1 neurons from ischemia-induced apoptotic cell death *via* the PI3K/Akt pathway. *Brain Res* (2010) 1321:1–12. doi: 10.1016/j.brainres.2010.01.046

138. Hu X, Chen J, Wang L, Ivashkiv LB. Crosstalk among jak-STAT, toll-like receptor, and ITAM-dependent pathways in macrophage activation. *J Leukoc Biol* (2007) 82(2):237–43. doi: 10.1189/jlb.1206763

139. Barić A, Dobrivojević Radmilović M. Microglia and bradykinin cross talk in poststroke cognitive impairment in diabetes. *Am J Physiol Cell Physiol* (2021) 320(4):C613–8. doi: 10.1152/ajpcell.00402.2020

140. Hosoi T, Oba T, Ozawa K. ER stress-mediated regulation of immune function under glucose-deprived condition in glial cells: up- and down-regulation of PGE2 + IFNγ-induced IL-6 and iNOS expressions. *BiochemBiophys Res Commun* (2013) 441(2):525–8. doi: 10.1016/j.bbrc.2013.10.109

141. Hosoi T, Honda M, Oba T, Ozawa K. ER stress upregulated PGE_2/IFNγ-induced IL-6 expression and down-regulated iNOS expression in glial cells. *Sci Rep* (2013) 3:3388. doi: 10.1038/srep03388

142. Li D, Wang C, Yao Y, Chen L, Liu G, Zhang R, et al. mTORC1 pathway disruption ameliorates brain inflammation following stroke *via* a shift in microglia phenotype from M1 type to M2 type. *FASEB J* (2016) 30(10):3388–99. doi: 10.1096/fj.201600495R

143. Lukiw WJ, Pogue AI. Vesicular transport of encapsulated microRNA between glial and neuronal cells. *Int J Mol Sci* (2020) 21(14):5078. doi: 10.3390/ijms21145078

144. Vasudeva K, Munshi A. miRNA dysregulation in ischaemic stroke: Focus on diagnosis, prognosis, therapeutic and protective biomarkers. *Eur J Neurosci* (2020) 52(6):3610–27. doi: 10.1111/ejn.14695

145. Wang SW, Liu Z, Shi ZS. Non-coding RNA in acute ischemic stroke: Mechanisms, biomarkers and therapeutic targets. *Cell Transplant* (2018) 27 (12):1763–77. doi: 10.1177/0963689718806818

146. Maniati E, Bossard M, Cook N, Candido JB, Emami-Shahri N, Nedospasov SA, et al. Crosstalk between the canonical NF-κB and notch signaling pathways inhibits pparγ expression and promotes pancreatic cancer progression in mice. *J Clin Invest* (2011) 121(12):4685–99. doi: 10.1172/JCI45797

147. Zhao Y, Patzer A, Herdegen T, Gohlke P, Culman J. Activation of cerebral peroxisome proliferator-activated receptors gamma promotes neuroprotection by attenuation of neuronal cyclooxygenase-2 overexpression after focal cerebral ischemia in rats. *FASEB J* (2006) 20(8):1162–75. doi: 10.1096/fj.05-5007com

148. Ruffell D, Mourkioti F, Gambardella A, Kirstetter P, Lopez RG, Rosenthal N, et al. A CREB-C/EBPbeta cascade induces M2 macrophage-specific gene expression and promotes muscle injury repair. *Proc Natl Acad Sci U.S.A.* (2009) 106(41):17475–80. doi: 10.1073/pnas.0908641106

149. Gorgoni B, Maritano D, Marthyn P, Righi M, Poli V. C/EBP beta gene inactivation causes both impaired and enhanced gene expression and inverse regulation of IL-12 p40 and p35 mRNAs in macrophages. *J Immunol* (2002) 168 (8):4055–62. doi: 10.4049/jimmunol.168.8.4055

150. Stein B, Cogswell PC, Baldwin ASJr. Functional and physical associations between NF-kappa b and C/EBP family members: a rel domain-bZIP interaction. *Mol Cell Biol* (1993) 13(7):3964–74. doi: 10.1128/mcb.13.7.3964-3974.1993

151. Chistiakov DA, Myasoedova VA, Revin VV, Orekhov AN, Bobryshev YV. The impact of interferon-regulatory factors to macrophage differentiation and polarization into M1 and M2. *Immunobiology* (2018) 223(1):101–11. doi: 10.1016/j.imbio.2017.10.005

152. Qin BY, Liu C, Srinath H, Lam SS, Correia JJ, Derynck R, et al. Crystal structure of IRF-3 in complex with CBP. *Structure* (2005) 13(9):1269–77. doi: 10.1016/j.str.2005.06.011

153. Zhao SC, Ma LS, Chu ZH, Xu H, Wu WQ, Liu F. Regulation of microglial activation in stroke. *Acta Pharmacol Sin* (2017) 38(4):445–58. doi: 10.1038/aps.2016.162

154. Neher JJ, Emmrich JV, Fricker M, Mander PK, Théry C, Brown GC. Phagocytosis executes delayed neuronal death after focal brain ischemia. *Proc Natl Acad Sci U S A* (2013) 110(43):E4098–107. doi: 10.1073/pnas.1308679110

155. Zhao X, Wang H, Sun G, Zhang J, Edwards NJ, Aronowski J. Neuronal interleukin-4 as a modulator of microglial pathways and ischemic brain damage. *J Neurosci* (2015) 35(32):11281–91. doi: 10.1523/JNEUROSCI.1685-15.2015

156. Noda M, Doi Y, Liang J, Kawanokuchi J, Sonobe Y, Takeuchi H, et al. Fractalkine attenuates excito-neurotoxicity *via* microglial clearance of damaged neurons and antioxidant enzyme heme oxygenase-1 expression. *J Biol Chem* (2016) 291(27):14388. doi: 10.1074/jbc.A110.169839

157. Dénes A, Ferenczi S, Halász J, Környei Z, Kovács KJ. Role of CX3CR1 (fractalkine receptor) in brain damage and inflammation induced by focal cerebral ischemia in mouse. *J Cereb Blood Flow Metab* (2008) 28(10):1707–21. doi: 10.1038/jcbfm.2008.64

158. Franco EC, Cardoso MM, Gouvêia A, Pereira A, Gomes-Leal W. Modulation of microglial activation enhances neuroprotection and functional recovery derived from bonerow mononuclear cell transplantation after cortical ischemia. *Neurosci Res* (2012) 73(2):122–32. doi: 10.1016/j.neures.2012.03.006

159. Wu LJ, Wu G, Akhavan Sharif MR, Baker A, Jia Y, Fahey FH, et al. The voltage-gated proton channel Hv1 enhances brain damage from ischemic stroke. *Nat Neurosci* (2012) 15(4):565–73. doi: 10.1038/nn.3059

160. Brown GC, Neher JJ. Microglial phagocytosis of live neurons. *Nat Rev Neurosci* (2014) 15(4):209–16. doi: 10.1038/nrn3710

161. Nimmerjahn A, Kirchhoff F, Helmchen F. Resting microglial cells are highly dynamic surveillants of brain parenchyma *in vivo*. *Science* (2005) 308 (5726):1314–8. doi: 10.1126/science.1110647

162. Parajuli B, Koizumi S. Strategies for manipulating microglia to determine their role in the healthy and diseased brain. *Neurochem Res* (2022) 9:1–11. doi: 10.1007/s11064-022-03742-6

163. Ransohoff RM, Brown MA. Innate immunity in the central nervous system. *J Clin Invest* (2012) 122(4):1164–71. doi: 10.1172/JCI58644

164. Young AP, Denovan-Wright EM. The dynamic role of microglia and the endocannabinoid system in neuroinflammation. *Front Pharmacol* (2022) 12:806417. doi: 10.3389/fphar.2021.806417

165. Araki T, Ikegaya Y, Koyama R. The effects of microglia- and astrocyte-derived factors on neurogenesis in health and disease. *Eur J Neurosci* (2021) 54 (5):5880–901. doi: 10.1111/ejn.14969

166. Pascual O, Ben Achour S, Rostaing P, Triller A, Bessis A. Microglia activation triggers astrocyte-mediated modulation of excitatory neurotransmission. *Proc Natl Acad Sci U S A* (2012) 109(4):E197–205. doi: 10.1073/pnas.1111098109

167. Rouach N, Avignone E, Même W, Koulakoff A, Venance L, Blomstrand F, et al. Gapctions and connexin expression in the normal and pathological central nervous system. *Biol Cell* (2002) 94(7-8):457–75. doi: 10.1016/s0248-4900(02)00016-3

168. ouach N, Calvo CF, Glowinski J, Giaume C. Brain macrophages inhibit gapctional communication and downregulate connexin 43 expression in cultured astrocytes. *Eur J Neurosci* (2002) 15(2):403–7. doi: 10.1046/j.0953-816x.2001.01868.x

169. Zhang D, Ren J, Luo Y, He Q, Zhao R, Chang J, et al. T Cell response in ischemic stroke: From mechanisms to translational insights. *Front Immunol* (2021) 12:707972. doi: 10.3389/fimmu.2021.707972

170. Selvaraj UM, Stowe AM. Long-term T cell responses in the brain after an ischemic stroke. *Discovery Med* (2017) 24(134):323–33.

171. Gill D, Veltkamp R. Dynamics of T cell responses after stroke. *CurrOpinPharmacol* (2016) 26:26–32. doi: 10.1016/j.coph.2015.09.009

172. Wu Y, Li J, Shou J, Zhang W, Chen C. Diverse functions and mechanisms of regulatory T cell in ischemic stroke. *Exp Neurol* (2021) 343:113782. doi: 10.1016/j.expneurol.2021.113782

173. Chen S, Wu H, Klebe D, Hong Y, Zhang J, Tang J. Regulatory T cell in stroke: a new paradigm for immune regulation. *Clin Dev Immunol* (2013) 2013:689827. doi: 10.1155/2013/689827

174. Arya AK, Hu B. Brain-gut axis after stroke. *Brain Circ* (2018) 4(4):165–73. doi: 10.4103/bc.bc_32_18

175. Meng H. *Neuronal soluble FasL mediates M1-type microglia after ischemic stroke [3 (plasma cell polarization and mechanism[D]*. Nanjing: Nanjing University (2016).

176. Li Q. *Tregs attenuates inflammatory injury in cerebral hemorrhage through IL-10/STAT3-induced M2-type polarization of microglia [D]*. Chongqing: Chongqing Medical University (2018).

177. Wang S, Zhang H, Xu Y. Crosstalk between microglia and T cells contributes to brain damage and recovery after ischemic stroke. *Neurol Res* (2016) 38(6):495–503. doi: 10.1080/01616412.2016.1188473

178. Coughlan T, Gibson C, Murphy S. Modulatory effects of progesterone on inducible nitric oxide synthase expression *in vivo* and *in vitro*. *J Neurochem* (2005) 93(4):932–42. doi: 10.1111/j.1471-4159.2005.03068.x

179. Park EM, Cho S, Frys KA, Glickstein SB, Zhou P, Anrather J, et al. Inducible nitric oxide synthase contributes to gender differences in ischemic brain injury. *J Cereb Blood Flow Metab* (2006) 26(3):392–401. doi: 10.1038/sj.jcbfm.9600194

180. Liesz A, Zhou W, Na SY, Hämmerling GJ, Garbi N, Karcher S, et al. Boosting regulatory T cells limits neuroinflammation in permanent cortical stroke. *J Neurosci* (2013) 33(44):17350–62. doi: 10.1523/JNEUROSCI.4901-12.2013

181. Kleinschnitz C, Kraft P, Dreykluft A, Hagedorn I, Göbel K, Schuhmann MK, et al. Regulatory T cells are strong promoters of acute ischemic stroke in mice by inducing dysfunction of the cerebral microvasculature. *Blood* (2013) 121 (4):679–91. doi: 10.1182/blood-2012-04-426734

182. Sakaguchi S, Ono M, Setoguchi R, Yagi H, Hori S, Fehervari Z, et al. Foxp3 + CD25+ CD4+ natural regulatory T cells in dominant self-tolerance and autoimmune disease. *Immunol Rev* (2006) 212:8–27. doi: 10.1111/j.0105-2896.2006.00427.x

183. Ren X, Akiyoshi K, Vandenbark AA, Hurn PD, Offner H. CD4+FoxP3+ regulatory T-cells in cerebral ischemic stroke. *Metab Brain Dis* (2011) 26(1):87–90. doi: 10.1007/s11011-010-9226-6

184. Zouggari Y, Ait-Oufella H, Waeckel L, Vilar J, Loinard C, Cochain C, et al. Regulatory T cells modulate postischemic neovascularization. *Circulation* (2009) 6;120(14):1415–25. doi: 10.1161/CIRCULATIONAHA.109.875583

185. Michels M, Sonai B, Dal-Pizzol F. Polarization of microglia and its role in bacterialsis. *J Neuroimmunol* (2017) 303:90–8. doi: 10.1016/j.jneuroim.2016.12.015

186. Savage ND, de Boer T, Walburg KV, Joosten SA, van Meijgaarden K, Geluk A, et al. Human anti-inflammatory macrophages induce Foxp3+ GITR+ CD25+ regulatory T cells, which suppress *via* membrane-bound TGFbeta-1. *J Immunol* (2008) 181(3):2220–6. doi: 10.4049/jimmunol.181.3.2220

187. Passaro AP, Lebos AL, Yao Y, Stice SL. Immune response in neurological pathology: Emerging role of central and peripheral immune crosstalk. *Front Immunol* (2021) 12:676621. doi: 10.3389/fimmu.2021.676621

188. Shi L, Sun Z, Su W, Xu F, Xie D, Zhang Q, et al. Treg cell-derived osteopontin promotes microglia-mediated white matter repair after ischemic stroke. *Immunity* (2021) 54(7):1527–1542.e8. doi: 10.1016/j.immuni.2021.04.022

189. Rashid ChehrehBargh S, Tafakhori A, Masoumi F, Rahmani F, Ahmadi M, Namdar A, et al. Evaluation of regulatory T lymphocytes and IL2Ra and FOXP3 gene expression in peripheral mononuclear cells from patients with amyotrophic lateral sclerosis. *Ir J Med Sci* (2018) 187(4):1065–71. doi: 10.1007/s11845-018-1793-2

190. Li Q, Zhang W, Tan Y, Zhao G, Zhang X, Zhang P, et al. Tregs attenuate the inflammatory injury of cerebral hemorrhage through IL-10/STAT3-induced M2-type polarization of microglia. *J Third Military Med Univ* (2018) 40(16):1461–8. doi: 10.16016/j.1000-5404.201802129

191. Zhou K. Treg cells reduce inflammatory injury in cerebral hemorrhage by regulating microglia/macrophage polarization through IL-10/GSK3β/PTEN signaling. *Third Military Med Univ* (2016).

192. Liu Y, Gao J, Peng M, Meng H, Ma H, Cai P, et al. A review on central nervous system effects of gastrodin. *Front Pharmacol* (2018) 9:24. doi: 10.3389/fphar.2018.00024

193. Deng C, Chen H, Meng Z, Meng S. Gastrodin and vascular dementia: Advances and current perspectives. *Evid Based Complement Alternat Med* (2022) 2022:2563934. doi: 10.1155/2022/2563934

194. Ma D. Salvia polyphenolic acid attenuates experimental cerebral ischemia-reperfusion injury through microglia P2X7/NLRP3/GSDMD pathway [D]. *Liaoning Univ Traditional Chin Med* (2021). doi: 10.27213/d.cnki.glnzc.2021.000034

195. Yang W, Chen X, Pan J, Ge H, Yin K, Wu Z, et al. Malibatol a protects against brain injury through reversing mitochondrial dysfunction in experimental stroke. *Neurochem Int* (2015) 80:33–40. doi: 10.1016/j.neuint.2014.11.003

196. Pan J, Jin JL, Ge HM, Yin KL, Chen X, Han LJ, et al. Malibatol a regulates microglia M1/M2 polarization in experimental stroke in a PPARγ-dependent manner. *J Neuroinflamm* (2015) 14:12:51. doi: 10.1186/s12974-015-0270-3

197. Weng L, Wu Z, Zheng W, Meng H, Han L, Wang S, et al. Malibatol a enhances alternative activation of microglia by inhibiting phosphorylation of mammalian Ste20-like kinase1 in OGD-BV-2 cells. *Neurol Res* (2016) 38(4):342–8. doi: 10.1080/01616412.2016.1174423

198. Meng T, Xiao D, Muhammed A, Deng J, Chen L, He J. Anti-inflammatory action and mechanisms of resveratrol. *Molecules* (2021) 26(1):229. doi: 10.3390/molecules26010229

199. Pignet AL, Schellnegger M, Hecker A, Kohlhauser M, Kotzbeck P, Kamolz LP. Resveratrol-induced signal transduction in wound healing. *Int J Mol Sci* (2021) 22(23):12614. doi: 10.3390/ijms222312614

200. Zhou DD, Luo M, Huang SY, Saimaiti A, Shang A, Gan RY, et al. Effects and mechanisms of resveratrol on aging and age-related diseases. *Oxid Med Cell Longev* (2021) 2021:9932218. doi: 10.1155/2021/9932218

201. Parsamanesh N, Asghari A, Sardari S, Tasbandi A, Jamialahmadi T, Xu S, et al. Resveratrol and endothelial function: A literature review. *Pharmacol Res* (2021) 170:105725. doi: 10.1016/j.phrs.2021.105725

202. Wang Q, Xu J, Rottinghaus GE, Simonyi A, Lubahn D, Sun GY, et al. Resveratrol protects against global cerebral ischemic injury in gerbils. *Brain Res* (2002) 958(2):439–47. doi: 10.1016/s0006-8993(02)03543-6

203. Shin JA, Lee H, Lim YK, Koh Y, Choi JH, Park EM. Therapeutic effects of resveratrol during acute periods following experimental ischemic stroke. *J Neuroimmunol* (2010) 227(1-2):93–100. doi: 10.1016/j.jneuroim.2010.06.017

204. Bischoff-Kont I, Fürst R. Benefits of ginger and its constituent 6-shogaol in inhibiting inflammatory processes. *Pharm (Basel)* (2021) 14(6):571. doi: 10.3390/ph14060571

205. Ooi SL, Campbell R, Pak SC, Golombick T, Manoharan A, Ramakrishna R, et al. Is 6-shogaol an effective phytochemical for patients with lower-risk myelodysplastic syndrome? a narrative review. *Integr Cancer Ther* (2021) 20:15347354211065038. doi: 10.1177/15347354211065038

206. Kou X, Wang X, Ji R, Liu L, Qiao Y, Lou Z, et al. Occurrence, biological activity and metabolism of 6-shogaol. *Food Funct* (2018) 9(3):1310–27. doi: 10.1039/c7fo01354j

207. Ha SK, Moon E, Ju MS, Kim DH, Ryu JH, Oh MS, et al. 6-shogaol, a ginger product, modulates neuroinflammation: a new approach to neuroprotection. *Neuropharmacology* (2012) 63(2):211–23. doi: 10.1016/j.neuropharm.2012.03.016

208. Gaire BP, Kwon OW, Park SH, Chun KH, Kim SY, Shin DY, et al. Neuroprotective effect of 6-paradol in focal cerebral ischemia involves the attenuation of neuroinflammatory responses in activated microglia. *PloS One* (2015) 10(3):e0120203. doi: 10.1371/journal.pone.0120203

209. Sarrica A, Kirika N, Romeo M, Salmona M, Diomede L. Safety and toxicology of magnolol and honokiol. *Planta Med* (2018) 84(16):1151–64. doi: 10.1055/a-0642-1966

210. Rauf A, Olatunde A, Imran M, Alhumaydhi FA, Aljohani ASM, Khan SA, et al. Honokiol: A review of its pharmacological potential and therapeutic insights. *Phytomedicine* (2021) 90:153647. doi: 10.1016/j.phymed.2021.153647

211. Rauf A, Patel S, Imran M, Maalik A, Arshad MU, Saeed F, et al. Honokiol: An anticancer lignan. *BioMed Pharmacother* (2018) 107:555–62. doi: 10.1016/j.biopha.2018.08.054

212. Zhang P, Liu X, Zhu Y, Chen S, Zhou D, Wang Y. Honokiol inhibits the inflammatory reaction during cerebral ischemia reperfusion by suppressing NF-κB activation and cytokine production of glial cells. *Neurosci Lett* (2013) 8:534:123–7. doi: 10.1016/j.neulet.2012.11.052

213. Hwang IK, Yoo KY, Li H, Park OK, Lee CH, Choi JH, et al. Indole-3-propionic acid attenuates neuronal damage and oxidative stress in the ischemic hippocampus. *J Neurosci Res* (2009) 87(9):2126–37. doi: 10.1002/jnr.22030

214. Zhang L, Li DC, Liu LF. Paeonol: pharmacological effects and mechanisms of action. *Int Immunopharmacol* (2019) 72:413–21. doi: 10.1016/j.intimp.2019.04.033

215. Wang J, Wu G, Chu H, Wu Z, Sun J. Paeonol derivatives and pharmacological activities: A review of recent progress. *Mini Rev Med Chem* (2020) 20(6):466–82. doi: 10.2174/1389557519666191015204223

216. Wu M, Yu Z, Li X, Zhang X, Wang S, Yang S, et al. Paeonol for the treatment of atherosclerotic cardiovascular disease: A pharmacological and mechanistic overview. *Front Cardiovasc Med* (2021) 8:690116. doi: 10.3389/fcvm.2021.690116

217. Vellasamy S, Murugan D, Abas R, Alias A, Seng WY, Woon CK. Biological activities of paeonol in cardiovascular diseases: A review. *Molecules* (2021) 26(16):4976. doi: 10.3390/molecules26164976

218. Hsieh CL, Cheng CY, Tsai TH, Lin IH, Liu CH, Chiang SY, et al. Paeonol reduced cerebral infarction involving the superoxide anion and microglia activation in ischemia-reperfusion injured rats. *J Ethnopharmacol* (2006) 106(2):208–15. doi: 10.1016/j.jep.2005.12.027

219. Chu C, Deng J, Man Y, Qu Y. Green tea extracts epigallocatechin-3-gallate for different treatments. *BioMed Res Int* (2017) 2017:5615647. doi: 10.1155/2017/5615647

220. Cione E, La Torre C, Cannataro R, Caroleo MC, Plastina P, Gallelli L. Quercetin, epigallocatechin gallate, curcumin, and resveratrol: From dietary sources to human MicroRNA modulation. *Molecules* (2019) 25(1):63. doi: 10.3390/molecules25010063

221. Singh BN, Shankar S, Srivastava RK. Green tea catechin, epigallocatechin-3-gallate (EGCG): mechanisms, perspectives and clinical applications. *Biochem Pharmacol* (2011) 82(12):1807–21. doi: 10.1016/j.bcp.2011.07.093

222. Pervin M, Unno K, Takagaki A, Isemura M, Nakamura Y. Function of green tea catechins in the brain: Epigallocatechin gallate and its metabolites. *Int J Mol Sci* (2019) 20(15):3630. doi: 10.3390/ijms20153630

223. Sutherland BA, Shaw OM, Clarkson AN, Jackson DN, Sammut IA, Appleton I. Neuroprotective effects of (-)-epigallocatechin gallate following hypoxia-ischemia-induced brain damage:el mechanisms of action. *FASEB J* (2005) 19(2):258–60. doi: 10.1096/fj.04-2806fje

224. Shan Z, Nisar MF, Li M, Zhang C, Wan CC. Theaflavin chemistry and its health benefits. *Oxid Med Cell Longev* (2021) 2021:6256618. doi: 10.1155/2021/6256618

225. Cai Q, Ji S, Li M, Zheng S, Zhou X, Guo H, et al. Theaflavin-regulated imd condensates control drosophila intestinal homeostasis and aging. *iScience* (2021) 24(3):102150. doi: 10.1016/j.isci.2021.102150

226. Khan N, Mukhtar H. Tea polyphenols in promotion of human health. *Nutrients* (2018) 11(1):39. doi: 10.3390/nu11010039

227. Cai F, Li CR, Wu JL, Chen JG, Liu C, Min Q, et al. Theaflavin ameliorates cerebral ischemia-reperfusion injury in rats through its anti-inflammatory effect and modulation of STAT-1. *Mediators Inflamm* (2006) 2006(5):30490. doi: 10.1155/MI/2006/30490

228. Zhou R, Yang Z, Tang X, Tan Y, Wu X, Liu F. Propofol protects against focal cerebral ischemia *via* inhibition of microglia-mediated proinflammatory cytokines in a rat model of experimental stroke. *PloS One* (2013) 8(12):e82729. doi: 10.1371/journal.pone.0082729

229. Jung YS, Park JH, Kim H, Kim SY, Hwang JY, Hong KW, et al. Probucol inhibits LPS-induced microglia activation and ameliorates brain ischemic injury in normal and hyperlipidemic mice. *Acta Pharmacol Sin* (2016) 37(8):1031–44. doi: 10.1038/aps.2016.51

230. Xiong XY, Liu L, Yang QW. Refocusing neuroprotection in cerebral reperfusion era: New challenges and strategies. *Front Neurol* (2018) 9:249. doi: 10.3389/fneur.2018.00249

231. Jickling GC, Liu D, Stamova B, Ander BP, Zhan X, Lu A, et al. Hemorrhagic transformation after ischemic stroke in animals and humans. *J Cereb Blood Flow Metab* (2014) 34(2):185–99. doi: 10.1038/jcbfm.2013.203

232. Wang ZF, Wang J, Zhang HY, Tang XC. Huperzine a exhibits anti-inflammatory and neuroprotective effects in a rat model of transient focal cerebral ischemia. *J Neurochem* (2008) 106(4):1594–603. doi: 10.1111/j.1471-4159.2008.05504.x

233. Cai Y, He Q, Hu F, Guo Q, Li Y. The effect of emodin on the activation of microglia and the expression of inflammatory factors after cerebral ischemia. *Shizhen Traditional Chin Med* (2021) 32(03):574–7. doi: 10.3969/j.issn.1008-0805.2021.03.17.

234. Zhang Y, Cai Y, Hu F, Guo Q, Li Y, He Q. Effects of chrysophanol on the activation of microglia and the expression of inflammatory factors in rats with cerebral ischemia injury. *Chin Pharm* (2020) 31(23):2858–63. doi: 10.6039/j.issn.1001-0408.2020.23.08

235. Guo Q, He Q, Hu F, Cai Y, Li Y. Chrysophanol regulates inflammatory response of microglia through TLR4/NF-kB signaling pathway. *Med Inf* (2020) 33(19):51–54+58. doi: 10.3969/j.issn.1006-1959.2020.19.016

236. Zhang J, Wu C, Gao L, Du G, Qin X. Astragaloside IV derived from astragalus membranaceus: A research review on the pharmacological effects. *Adv Pharmacol* (2020) 87:89–112. doi: 10.1016/bs.apha.2019.08.002

237. Xia ML, Xie XH, Ding JH, Du RH, Hu G. Astragaloside IV inhibits astrocyte senescence: implication in parkinson's disease. *J Neuroinflamm* (2020) 17 (1):105. doi: 10.1186/s12974-020-01791-8

238. Zheng X, Gan H, Li L, Hu X, Fang Y, Chu L. Astragaloside IV inhibits inflammatory response after cerebral ischemia in rats by promoting the M2-type polarization of microglia/macrophages. *Zhejiang J Univ (Medical Edition)* (2020) 49(06):679–86. doi: 10.3785/j.issn.1008-9292.2020.12.02

239. He Y, Shi H, Liu H, Wu H, Zhang B, Wu X, et al. Astragaloside IV regulates STAT1/IκB/NF-κB signaling pathway and inhibits γ-interferon-induced BV-2 cell activation. *China J Traditional Chin Med* (2015) 40(01):124–8. doi: 10.4268/cjcmm20150124

240. Yu Y, Zhou L, Yang Y, Liu Y. Cycloastragenol: An exciting novel candidate for age-associated diseases. *Exp Ther Med* (2018) 16(3):2175–82. doi: 10.3892/etm.2018.6501

241. Shen CY, Jiang JG, Yang L, Wang DW, Zhu W. Anti-ageing active ingredients from herbs and nutraceuticals used in traditional Chinese medicine: pharmacological mechanisms and implications for drug discovery. *Br J Pharmacol* (2017) 174(11):1395–425. doi: 10.1111/bph.13631

242. Li M, Han B, Zhao H, Xu C, Xu D, Sieniawska E, et al. Biological active ingredients of astragali radix and its mechanisms in treating cardiovascular and cerebrovascular diseases. *Phytomedicine* (2022) 98:153918. doi: 10.1016/j.phymed.2021.153918

243. Li M, Li SC, Dou BK, Zou YX, Han HZ, Liu DX, et al. Cycloastragenol upregulates SIRT1 expression, attenuates apoptosis and suppresses neuroinflammation after brain ischemia. *Acta Pharmacol Sin* (2020) 41(8):1025–32. doi: 10.1038/s41401-020-0386-6

244. Barker EC, Kim BG, Yoon JH, Tochtrop GP, Letterio JJ, Choi SH. Potent suppression of both spontaneous and carcinogen-induced colitis-associated colorectal cancer in mice by dietary celastrol supplementation. *Carcinogenesis* (2018) 39(1):36–46. doi: 10.1093/carcin/bgx115

245. Ren B, Liu H, Gao H, Liu S, Zhang Z, Fribley AM, et al. Celastrol induces apoptosis in hepatocellular carcinoma cells *via* targeting ER-stress/UPR. *Oncotarget* (2017) 8(54):93039–50. doi: 10.18632/oncotarget.21750

246. Astry B, Venkatesha SH, Laurence A, Christensen-Quick A, Garzino-Demo A, Frieman MB, et al. Celastrol, a Chinese herbal compound, controls autoimmune inflammation by altering the balance of pathogenic and regulatory T cells in the target organ. *Clin Immunol* (2015) 157(2):228–38. doi: 10.1016/j.clim.2015.01.011

247. Luo D, Guo Y, Cheng Y, Zhao J, Wang Y, Rong J. Natural product celastrol suppressed macrophage M1 polarization against inflammation in diet-induced obese mice *via* regulating Nrf2/HO-1, MAP kinase and NF-κB pathways. *Aging (Albany NY)* (2017) 9(10):2069–82. doi: 10.18632/aging.101302

248. Bai S, Hu Z, Yang Y, Yin Y, Li W, Wu L, et al. Anti-inflammatory and neuroprotective effects of triptolide *via* the NF-κB signaling pathway in a rat MCAO model. *Anat Rec (Hoboken)* (2016) 299(2):256–66. doi: 10.1002/ar.23293

249. Jiang M, Liu X, Zhang D, Wang Y, Hu X, Xu F, et al. Celastrol treatment protects against acute ischemic stroke-induced brain injury by promoting an IL-33/ST2 axis-mediated microglia/macrophage M2 polarization. *J Neuroinflamm* (2018) 15(1):78. doi: 10.1186/s12974-018-1124-6

250. Lalloo DG, Shingadia D, Bell DJ, Beeching NJ, Whitty CJM, Chiodini PL. PHE advisory committee on malaria prevention in UK travellers. UK malaria treatment guidelines 2016. *J Infect* (2016) 72(6):635–49. doi: 10.1016/j.jinf.2016.02.001

251. Zuo S, Ge H, Li Q. Artesunate protected blood-brain barrier *via* sphingosine 1 phosphate receptor 1/phosphatidylinositol 3 kinase pathway after subarachnoid hemorrhage in rats. *Mol Neurobiol* (2017) 54:1213–28. doi: 10.1007/s12035-016-9732-6

252. Clemmer L, Martins YC, Zanini GM, Frangos JA, Carvalho LJ. Artemether and artesunate show the highest efficacies in rescuing mice with late-stage cerebral malaria and rapidlyrease leukocyte accumulation in the brain. *Antimicrob Agents Chemother* (2011) 55(4):1383–90. doi: 10.1128/AAC.01277-10

253. Ho WE, Peh HY, Chan TK, Wong WS. Artemisinins: pharmacological actions beyond anti-malarial. *Pharmacol Ther* (2014) 142(1):126–39. doi: 10.1016/j.pharmthera.2013.12.001

254. Zuo S, Li Q, Liu X, Feng H, Chen Y. The potential therapeutic effects of artesunate on stroke and other central nervous system diseases. *BioMed Res Int* (2016) 2016:1489050. doi: 10.1155/2016/1489050

255. Lai L, Chen Y, Tian X, Li X, Zhang X, Lei J, et al. Artesunate alleviates hepatic fibrosis induced by multiple pathogenic factors and inflammation through the inhibition of LPS/TLR4/NF-κB signaling pathway in rats. *Eur J Pharmacol* (2015) 15;765:234–41. doi: 10.1016/j.ejphar.2015.08.040

256. Okorji UP, Olajide OA. A semi-synthetic derivative of artemisinin, artesunate inhibits prostaglandin E2 production in LPS/IFNγ-activated BV2 microglia. *Bioorg Med Chem* (2014) 22:4726–34. doi: 10.1016/j.bmc.2014.07.007

257. Lu H, Wang B, Cui N, Zhang Y. Artesunate suppresses oxidative and inflammatory processes by activating Nrf2 and ROS dependent p38 MAPK and protects against cerebral ischemia reperfusion injury. *Mol Med Rep* (2018) 17:6639–46. doi: 10.3892/mmr.2018.8666

258. Liu Y, Dang W, Zhang S, Wang L, Zhang X. Artesunate attenuates inflammatory injury and inhibits the NF-κB pathway in a mouse model of cerebral ischemia. *J Int Med Res* (2021) 49(11):3000605211053549. doi: 10.1177/03000605211053549

259. Bailly C, Vergoten G. Glycyrrhizin: An alternative drug for the treatment of COVID-19 infection and the associated respiratory syndrome? *Pharmacol Ther* (2020) 214:107618. doi: 10.1016/j.pharmthera.2020.107618

260. Al-Kamel H, Grundmann O. Glycyrrhizin as a potential treatment for the novel coronavirus (COVID-19). *Mini Rev Med Chem* (2021) 21(16):2204–8. doi: 10.2174/1389557521666210210160237

261. Kim SW, Lim CM, Lee HK, Lee JK. The use of stronger neo-minophagen c, a glycyrrhizin-containing preparation, in robust neuroprotection in the postischemic brain. *Anat Cell Biol* (2011) 44(4):304–13. doi: 10.5115/acb.2011.44.4.304

262. Gaid M, Biedermann E, Füller J, Haas P, Behrends S, Krull R, et al. Biotechnological production of hyperforin for pharmaceutical formulation. *Eur J Pharm Biopharm* (2018) 126:10–26. doi: 10.1016/j.ejpb.2017.03.024

263. Billard C, Merhi F, Bauvois B. Mechanistic insights into the antileukemic activity of hyperforin. *Curr Cancer Drug Targets* (2013) 13(1):1–10. doi: 10.2174/156800913804486601

264. Chrubasik-Hausmann S, Vlachojannis J, McLachlan AJ. Understanding drug interactions with St john's wort (Hypericum perforatum l.): impact of hyperforin content. *J Pharm Pharmacol* (2019) 71(1):129–38. doi: 10.1111/jphp.12858

265. Ma L, Pan X, Zhou F, Liu K, Wang L. Hyperforin protects against acute cerebral ischemic injury through inhibition of interleukin-17A-mediated microglial activation. *Brain Res* (2018) 1678:254–61. doi: 10.1016/j.brainres.2017.08.023

266. Xu AL, Zheng GY, Wang ZJ, Chen XD, Jiang Q. Neuroprotective effects of ilexonin a following transient focal cerebral ischemia in rats. *Mol Med Rep* (2016) 13(4):2957–66. doi: 10.3892/mmr.2016.4921

267. Xu AL, Zheng GY, Ye HY, Chen XD, Jiang Q. Characterization of astrocytes and microglial cells in the hippocampal CA1 region after transient focal cerebral ischemia in rats treated with ilexonin a. *Neural Regener Res* (2020) 15 (1):78–85. doi: 10.4103/1673-5374.264465

268. Zhang BQ, Zheng GY, Han Y, Chen XD, Jiang Q. Ilexonin a promotes neuronal proliferation and regeneration *via* activation of the canonical wnt signaling pathway after cerebral ischemia reperfusion in rats. *Evid Based Complement Alternat Med* (2016) 2016:9753189. doi: 10.1155/2016/9753189

269. Asgharzade S, Khorrami MB, Forouzanfar F. Neuroprotective effect of herniarin following transient focal cerebral ischemia in rats. *Metab Brain Dis* (2021) 36(8):2505–10. doi: 10.1007/s11011-021-00841-1

270. Friedli MJ, Inestrosa NC. Huperzine a and its neuroprotective molecular signaling in alzheimer's disease. *Molecules* (2021) 26(21):6531. doi: 10.3390/molecules26216531

271. Shukla M, Wongchitrat P, Govitrapong P. A synopsis of multitarget potential therapeutic effects of huperzine a in diverse pathologies-emphasis on alzheimer's disease pathogenesis. *Neurochem Res* (2022) 47(5):1166–82. doi: 10.1007/s11064-022-03530-2

272. Li X, Li W, Tian P, Tan T. Delineating biosynthesis of huperzine a, a plant-derived medicine for the treatment of alzheimer's disease. *Biotechnol Adv* (2022) 60:108026. doi: 10.1016/j.biotechadv.2022.108026

273. Wang J, Zhang HY, Tang XC. Huperzine a improves chronic inflammation and cognitiveline in rats with cerebral hypoperfusion. *J Neurosci Res* (2010) 88 (4):807–15. doi: 10.1002/jnr.22237

274. Baska A, Leis K, Gałązka P. Berberine in the treatment of diabetes mellitus: A review. *Endocr Metab Immune Disord Drug Targets* (2021) 21(8):1379–86. doi: 10.2174/1568026620666210221144405

275. Xu X, Yi H, Wu J, Kuang T, Zhang J, Li Q, et al. Therapeutic effect of berberine on metabolic diseases: Both pharmacological data and clinical evidence. *BioMed Pharmacother* (2021) 133:110984. doi: 10.1016/j.biopha.2020.110984

276. Kim M, Shin MS, Lee JM, Cho HS, Kim CJ, Kim YJ, et al. Inhibitory effects of isoquinoline alkaloid berberine on ischemia-induced apoptosis *via* activation of phosphoinositide 3-Kinase/Protein kinase b signaling pathway. *Int Neurourol J* (2014) 18(3):115–25. doi: 10.5213/inj.2014.18.3.115

277. Jiang W, Fan W, Gao T, Li T, Yin Z, Guo H, et al. Analgesic mechanism of sinomenine against chronic pain. *Pain Res Manage* (2020) 2020:1876862. doi: 10.1155/2020/1876862

278. Zhang MW, Wang XH, Shi J, Yu JG. Sinomenine in cardio-cerebrovascular diseases: Potential therapeutic effects and pharmacological evidences. *Front Cardiovasc Med* (2021) 8:749113. doi: 10.3389/fcvm.2021.749113

279. Tang J, Raza A, Chen J, Xu H. A systematic review on the sinomenine derivatives. *Mini Rev Med Chem* (2018) 18(11):906–17. doi: 10.2174/1389557517666171123212557

280. Qiu J, Wang M, Zhang J, Cai Q, Lu D, Li Y, et al. The neuroprotection of sinomenine against ischemic stroke in mice by suppressing NLRP3 inflammasome *via* AMPK signaling. *Int Immunopharmacol* (2016) 40:492–500. doi: 10.1016/j.intimp.2016.09.024

281. He C, Wang Z, Shi J. Pharmacological effects of icariin. *Adv Pharmacol* (2020) 87:179–203. doi: 10.1016/bs.apha.2019.10.004

282. Wang S, Ma J, Zeng Y, Zhou G, Wang Y, Zhou W, et al. Icariin, an up-and-Coming bioactive compound against neurological diseases: Network pharmacology-based study and literature review. *Drug Des Devel Ther* (2021) 15:3619–41. doi: 10.2147/DDDT.S310686

283. Wang Z, Wang D, Yang D, Zhen W, Zhang J, Peng S. The effect of icariin on bone metabolism and its potential clinical application. *Osteoporos Int* (2018) 29 (3):535–44. doi: 10.1007/s00198-017-4255-1

284. Wang M, Gao H, Li W, Wu B. Icariin and its metabolites regulate lipid metabolism: From effects to molecular mechanisms. *BioMed Pharmacother* (2020) 131:110675. doi: 10.1016/j.biopha.2020.110675

285. Tang B, Zhang Y, Wu Y, Liu Y, Liu M, Hu W. The effect of icariin on neuroprotection and microglial TLR4/NF-κB pathway in cerebral ischemia-reperfusion rats]. *Chin J Exp Prescriptions* (2020) 26(22):47–52. doi: 10.13422/j.cnki.syfjx.20201865

286. Park SJ, Choi H, Kim JH, Kim CS. Antifibrotic effects of eupatilin on TGF-β1-treated human vocal fold fibroblasts. *PloS One* (2021) 16(3):e0249041. doi: 10.1371/journal.pone.0249041

287. Wu Z, Zou B, Zhang X, Peng X. Eupatilin regulates proliferation and cell cycle of cervical cancer by regulating hedgehog signalling pathway. *Cell Biochem Funct* (2020) 38(4):428–35. doi: 10.1002/cbf.3493

288. Cinar AK, Ozal SA, Serttas R, Erdogan S. Eupatilin attenuates TGF-β2-induced proliferation and epithelial-mesenchymal transition of retinal pigment epithelial cells. *Cutan Ocul Toxicol* (2021) 40(2):103–14. doi: 10.1080/15569527.2021.1902343

289. Sapkota A, Gaire BP, Cho KS, Jeon SJ, Kwon OW, Jang DS, et al. Eupatilin exerts neuroprotective effects in mice with transient focal cerebral ischemia by reducing microglial activation. *PloS One* (2017) 12(2):e0171479. doi: 10.1371/journal.pone.0171479

290. Okuyama S, Morita M, Miyoshi K, Nishigawa Y, Kaji M, Sawamoto A, et al. Heptamethoxyflavone, a citrus flavonoid, on protection against memory impairment and neuronal cell death in a global cerebral ischemia mouse model. *Neurochem Int* (2014) 70:30–8. doi: 10.1016/j.neuint.2014.03.008

291. Khan S, Kamal MA. Can wogonin be used in controlling diabetic cardiomyopathy? *Curr Pharm Des* (2019) 25(19):2171–7. doi: 10.2174/1381612825666190708173108

292. Sharifi-Rad J, Herrera-Bravo J, Salazar LA, Shaheen S, Abdulmajid Ayatollahi S, Kobarfard F, et al. The therapeutic potential of wogonin observed in preclinical studies. *Evid Based Complement Alternat Med* (2021) 2021:9935451. doi: 10.1155/2021/9935451

293. Huynh DL, Ngau TH, Nguyen NH, Tran GB, Nguyen CT. Potential therapeutic and pharmacological effects of wogonin: an updated review. *Mol Biol Rep* (2020) 47(12):9779–89. doi: 10.1007/s11033-020-05972-9

294. Lee H, Kim YO, Kim H, Kim SY, Noh HS, Kang SS, et al. Flavonoid wogonin from medicinal herb is neuroprotective by inhibiting inflammatory activation of microglia. *FASEB J* (2003) 17(13):1943–4. doi: 10.1096/fj.03-0057fje

295. Zhou YX, Zhang H, Peng C. Puerarin: a review of pharmacological effects. *Phytother Res* (2014) 28(7):961–75. doi: 10.1002/ptr.5083

296. Zhang L. Pharmacokinetics and drug delivery systems for puerarin, a bioactive flavone from traditional Chinese medicine. *Drug Deliv* (2019) 26(1):860–9. doi: 10.1080/10717544.2019.1660732

297. Kulczyński B, Gramza-Michałowska A, Sulibурska J, Sidor A. Puerarin-an isoflavone with beneficial effects on bone health. *Front Biosci (Landmark Ed)* (2021) 26(12):1653–67. doi: 10.52586/5058

298. Zhou YX, Zhang H, Peng C. Effects of puerarin on the prevention and treatment of cardiovascular diseases. *Front Pharmacol* (2021) 12:771793. doi: 10.3389/fphar.2021.771793

299. Lim DW, Lee C, Kim IH, Kim YT. Anti-inflammatory effects of total isoflavones from pueraria lobata on cerebral ischemia in rats. *Molecules* (2013) 18 (9):10404–12. doi: 10.3390/molecules180910404

300. Derosa G, Maffioli P, D'Angelo A, Di Pierro F. A role for quercetin in coronavirus disease 2019 (COVID-19). *Phytother Res* (2021) 35(3):1230–6. doi: 10.1002/ptr.6887

301. Singh P, Arif Y, Bajguz A, Hayat S. The role of quercetin in plants. *Plant Physiol Biochem* (2021) 166:10–9. doi: 10.1016/j.plaphy.2021.05.023

302. Hosseini A, Razavi BM, Banach M, Hosseinzadeh H. Quercetin and metabolic syndrome: A review. *Phytother Res* (2021) 35(10):5352–64. doi: 10.1002/ptr.7144

303. Shen P, Lin W, Deng X, Ba X, Han L, Chen Z, et al. Potential implications of quercetin in autoimmune diseases. *Front Immunol* (2021) 12:689044. doi: 10.3389/fimmu.2021.689044

304. Pierro F DI, Khan A, Bertuccioli A, Maffioli P, Derosa G, Khan S, et al. Quercetin phytosome® as a potential candidate for managing COVID-19. *Minerva Gastroenterol (Torino)* (2021) 67(2):190–5. doi: 10.23736/S2724-5985.20.02771-3

305. Imran M, Saeed F, Gilani SA, Shariati MA, Imran A, Afzaal M, et al. Fisetin: An anticancer perspective. *Food Sci Nutr* (2020) 9(1):3–16. doi: 10.1002/fsn3.1872

306. Kirkland JL, Tchkonia T. Senolytic drugs: from discovery to translation. *J Intern Med* (2020) 288(5):518–36. doi: 10.1111/joim.13141

307. Farooqi AA, Naureen H, Zahid R, Youssef L, Attar R, Xu B. Cancer chemopreventive role of fisetin: Regulation of cell signaling pathways in different cancers. *Pharmacol Res* (2021) 172:105784. doi: 10.1016/j.phrs.2021.105784

308. Kubina R, Krzykawski K, Kabała-Dzik A, Wojtyczka RD, Chodurek E, Dziedzic A. Fisetin, a potent anticancer flavonol exhibiting cytotoxic activity against neoplastic malignant cells and cancerous conditions: A scoping, comprehensive review. *Nutrients* (2022) 14(13):2604. doi: 10.3390/nu14132604

309. Gelderblom M, Leypoldt F, Lewerenz J, Birkenmayer G, Orozco D, Ludewig P, et al. Theflavonoid fisetin attenuates postischemic immune cell infiltration, activation andinfarct size after transient cerebral middle artery occlusion in mice. *J Cereb.Blood Flow Metab* (2012) 32(5):835–43. doi: 10.1038/jcbfm.2011.189

310. Wen L, He T, Yu A, Sun S, Li X, Wei J, et al. Breviscapine: A review on its phytochemistry, pharmacokinetics and therapeutic effects. *Am J Chin Med* (2021) 49(6):1369–97. doi: 10.1142/S0192415X21500646

311. Ma Y, Li H, Guan S. Enhancement of the oral bioavailability of breviscapine by nanoemulsions drug delivery system. *Drug Dev Ind Pharm* (2015) 41(2):177–82. doi: 10.3109/03639045.2014.947510

312. Wu L, Liu M, Fang Z. Combined therapy of hypertensive nephropathy with breviscapine injection and antihypertensive drugs: A systematic review and a meta-analysis. *Evid Based Complement Alternat Med* (2018) 2018:2958717. doi: 10.1155/2018/2958717

313. Long Y, Yang Q, Xiang Y, Zhang Y, Wan J, Liu S, et al. Nose to brain drug delivery - a promising strategy for active components from herbal medicine for treating cerebral ischemia reperfusion. *Pharmacol Res* (2020) 159:104795. doi: 10.1016/j.phrs.2020.104795

314. Yuan Y, Zha H, Rangarajan P, Ling EA, Wu C. Anti-inflammatory effects of edaravone and scutellarin in activated microglia in experimentally induced ischemia injury in rats and in BV-2 microglia. *BMC Neurosci* (2014) 22:15:125. doi: 10.1186/s12868-014-0125-3

315. Yuan Y, Rangarajan P, Kan EM, Wu Y, Wu C, Ling EA. Scutellarin regulates the notch pathway and affects the migration and morphological transformation of activated microglia in experimentally induced cerebral ischemia in rats and in activated BV-2 microglia. *J Neuroinflamm* (2015) 20:12:11. doi: 10.1186/s12974-014-0226-z

316. Naz S, Imran M, Rauf A, Orhan IE, Shariati MA, Iahtisham-Ul-Haq, et al. Chrysin: Pharmacological and therapeutic properties. *Life Sci* (2019) 235:116797. doi: 10.1016/j.lfs.2019.116797

317. Mani R, Natesan V. Chrysin: Sources, beneficial pharmacological activities, and molecular mechanism of action. *Phytochemistry* (2018) 145:187–96. doi: 10.1016/j.phytochem.2017.09.016

318. Stompor-Gorący M, Bajek-Bil A, Machaczka M. Chrysin: Perspectives on contemporary status and future possibilities as pro-health agent. *Nutrients* (2021) 13(6):2038. doi: 10.3390/nu13062038

319. Yao Y, Chen L, Xiao J, Wang C, Jiang W, Zhang R, et al. Chrysin protectsagainst focal cerebral ischemia/reperfusion injury in mice through attenuation ofoxidative stress and inflammation. *Int J Mol Sci* (2014) 15 (11):20913–26. doi: 10.3390/ijms151120913

320. Daussin FN, Heyman E, Burelle Y. Effects of (-)-epicatechin on mitochondria. *Nutr Rev* (2021) 79(1):25–41. doi: 10.1093/nutrit/nuaa094

321. Cremonini E, Iglesias DE, Kang J, Lombardo GE, Mostofinejad Z, Wang Z, et al. (-)-Epicatechin and the comorbidities of obesity. *Arch Biochem Biophys* (2020) 690:108505. doi: 10.1016/j.abb.2020.108505

322. Si H, Lai CQ, Liu D. Dietary epicatechin, a novel anti-aging bioactive small molecule. *Curr Med Chem* (2021) 28(1):3–18. doi: 10.2174/0929867327666191230104958

323. Qu Z, Liu A, Li P, Liu C, Xiao W, Huang J, et al. Advances in physiological functions and mechanisms of (-)-epicatechin. *Crit Rev Food Sci Nutr* (2021) 61 (2):211–33. doi: 10.1080/10408398.2020.1723057

324. Leonardo CC, Agrawal M, Singh N, Moore JR, Biswal S, Dore S. Oraladministration of the flavanol (-)-epicatechin bolsters endogenous

protectionagainst focal ischemia through the Nrf2 cytoprotective pathway. *Eur J Neurosci* (2013) 38(11):3659–68. doi: 10.1111/ejn.12362

325. Zhang X, Xie L, Long J, Xie Q, Zheng Y, Liu K, et al. Salidroside: A review of its recent advances in synthetic pathways and pharmacological properties. *Chem Biol Interact* (2021) 339:109268. doi: 10.1016/j.cbi.2020.109268

326. Han J, Xiao Q, Lin YH, Zheng ZZ, He ZD, Hu J, et al. Neuroprotective effects of salidroside on focal cerebral ischemia/reperfusion injury involve the nuclear erythroid 2-related factor 2 pathway. *Neural Regener Res* (2015) 10 (12):1989–96. doi: 10.4103/1673-5374.172317

327. Liu X, Wen S, Yan F, Liu K, Liu L, Wang L, et al. Salidroside provides neuroprotection by modulating microglial polarization after cerebral ischemia. *J Neuroinflamm* (2018) 15(1):39. doi: 10.1186/s12974-018-1081-0

328. Pan LL, Yang Y, Hui M, Wang S, Li CY, Zhang H, et al. Sulfation predominates the pharmacokinetics, metabolism, and excretion of forsythin in humans: major enzymes and transporters identified. *Acta Pharmacol Sin* (2021) 42 (2):311–22. doi: 10.1038/s41401-020-0481-8

329. Han Z, Guo J, Meng F, Liao H, Deng Y, Huang Y, et al. Genetic toxicology and safety pharmacological evaluation of forsythin. *Evid Based Complement Alternat Med* (2021) 2021:6610793. doi: 10.1155/2021/6610793

330. Yuan WJ, Zhang SP, He ZY, He YX, He SQ, Liu LJ, et al. Comparative transcriptome analyses identify genes involved into the biosynthesis of forsythin and forsythoside a in forsythia suspensa. *Funct Integr Genomics* (2022) 22(5):731–41. doi: 10.1007/s10142-022-00887-z

331. Kim JM, Kim S, Kim DH, Lee CH, Park SJ, Jung JW, et al. Neuroprotective effect of forsythiaside against transient cerebral global ischemia in gerbil. *Eur J Pharmacol* (2011) 660(2-3):326–33. doi: 10.1016/j.ejphar.2011.03.051

332. Yin X, Hu H, Shen X, Li X, Pei J, Xu J. Ginseng omics for ginsenoside biosynthesis. *Curr Pharm Biotechnol* (2021) 22(5):570–8. doi: 10.2174/1389201021666200807113723

333. Nakhjavani M, Smith E, Townsend AR, Price TJ, Hardingham JE. Anti-angiogenic properties of ginsenoside Rg3. *Molecules* (2020) 25(21):4905. doi: 10.3390/molecules25214905

334. Lee HW, Lee MS, Kim TH, Alraek T, Zaslawski C, Kim JW, et al. Ginseng for erectile dysfunction. *Cochrane Database Syst Rev* (2021) 4(4):CD012654. doi: 10.1002/14651858.CD012654.pub2

335. Guo M, Shao S, Wang D, Zhao D, Wang M. Recent progress in polysaccharides from panax ginseng c. a. Meyer. *Food Funct* (2021) 12(2):494–518. doi: 10.1039/d0fo01896a

336. Ye R, Yang Q, Kong X, Han J, Zhang X, Zhang Y, et al. Ginsenoside Rd attenuates early oxidative damage and sequential inflammatory response after transient focal ischemia in rats. *Neurochem Int* (2011) 58(3):391–8. doi: 10.1016/j.neuint.2010.12.015

337. Zhu J, Jiang Y, Wu L, Lu T, Xu G, Liu X. Suppression of local inflammation contributes to the neuroprotective effect of ginsenoside Rb1 in rats with cerebral ischemia. *Neuroscience* (2012) 202:342–51. doi: 10.1016/j.neuroscience.2011.11.070

338. Yuan Y, Zhai Y, Chen J, Xu X, Wang H. Kaempferol ameliorates oxygen-glucose Deprivation/Reoxygenation-induced neuronal ferroptosis by activating Nrf2/SLC7A11/GPX4 axis. *Biomolecules* (2021) 11(7):923. doi: 10.3390/biom11070923

339. Imran M, Salehi B, Sharifi-Rad J, Aslam Gondal T, Saeed F, Imran A, et al. Kaempferol: A key emphasis to its anticancer potential. *Molecules* (2019) 24 (12):2277. doi: 10.3390/molecules24122277

340. Dabeek WM, Marra MV. Dietary quercetin and kaempferol: Bioavailability and potential cardiovascular-related bioactivity in humans. *Nutrients* (2019) 11 (10):2288. doi: 10.3390/nu11102288

341. Calderón-Montaño JM, Burgos-Morón E, Pérez-Guerrero C, López-Lázaro M. A review on the dietary flavonoid kaempferol. *Mini Rev Med Chem* (2011) 11 (4):298–344. doi: 10.2174/138955711795305335

342. Devi KP, Malar DS, Nabavi SF, Sureda A, Xiao J, Nabavi SM, et al. Kaempferol and inflammation: From chemistry to medicine. *Pharmacol Res* (2015) 99:1–10. doi: 10.1016/j.phrs.2015.05.002

343. Yu L, Chen C, Wang LF, Kuang X, Liu K, Zhang H, et al. Neuroprotective effect of kaempferol glycosides against brain injury and neuroinflammation by inhibiting the activation of NF-kappaB and STAT3 in transient focal stroke. *PloS One* (2013) 8(2):e55839. doi: 10.1371/journal.pone.0055839

344. Zhang L, Wei W. Anti-inflammatory and immunoregulatory effects of paeoniflorin and total glucosides of paeony. *Pharmacol Ther* (2020) 207:107452. doi: 10.1016/j.pharmthera.2019.107452

345. Ji Y, Dou YN, Zhao QW, Zhang JZ, Yang Y, Wang T, et al. Paeoniflorin suppresses TGF-β mediated epithelial-mesenchymal transition in pulmonary fibrosis through a smad-dependent pathway. *Acta Pharmacol Sin* (2016) 37 (6):794–804. doi: 10.1038/aps.2016.36

346. Wang XL, Feng ST, Wang YT, Chen NH, Wang ZZ, Zhang Y. Paeoniflorin: A neuroprotective monoterpenoid glycoside with promising anti-depressive properties. *Phytomedicine* (2021) 90:153669. doi: 10.1016/j.phymed.2021.153669

347. Luo XQ, Li A, Yang X, Xiao X, Hu R, Wang TW, et al. Paeoniflorin exerts neuroprotective effects by modulating the M1/M2 subset polarization of microglia/macrophages in the hippocampal CA1 region of vascular dementia rats *via* cannabinoid receptor 2. *Chin Med* (2018) 13:14. doi: 10.1186/s13020-018-0173-1

348. Cohen JA, Chun J. Mechanisms of fingolimod's eficacy and adverse effects in multiple sclerosis. *Ann Neurol* (2011) 69(5):759–77. doi: 10.1186/s12974-018-1323-1

349. Gaire BP, Song MR, Choi JW. Sphingosine 1-phosphate receptor subtype 3 (S1P3)contributes to brain injury after transient focal cerebral ischemia *via* modulating microglial activation and their M1 polarization. *J Neuroinflamm* (2018) 15(1):284. doi: 10.1186/s12974-018-1323-1

350. Li X, Wang MH, Qin C. Fingolimod suppresses neuronal autophagy through the mTOR/p70S6K pathway and alleviates ischemic brain damage in mice. *PloS One* (2017) 12(11):e0188748. doi: 10.1371/journal.pone.0188748

351. Kraft P, Gob E, Gobel K. FTY720 ameliorates acute ischemic stroke in mice by reducing thrombo-inflammation but not by direct neuroprotection. *Stroke* (2013) 44(11):3202–10. doi: 10.1161/STROKEAHA.113.002880

352. Campos F, Qin T, Castillo J. Fingolimod reduces hemorrhagic transformation associated with delayed tissue plasminogen activator treatment in a mouse thromboembolic model. *Stroke* (2013) 44(2):505–11. doi: 10.1161/STROKEAHA.112.679043

353. Ali AI, Jing GY. Areview of recent advances in neuroprotective potential of 3-n-butylphthalide and its derivatives. *BioMed Res Int* (2016) 2016:1–9. doi: 10.1155/2016/5012341

354. Zhao H, Yun W, Zhang Q, et al. Mobilization of circulating endothelial progenitor cells by DL-3-N-butylphthalide in acute ischemic stroke patients. *J StrokeCerebrovasc Dis* (2016) 25(4):.752–760. doi: 10.1016/j.jstrokecerebrovasdis.2015.11.018

355. Hu J, Wen Q, Wu Y, Li B, Gao P. The effect of butylphthalide on the brain edema, blood-brain barrier of rats after focal cerebral infarction and the expression of Rho A. *Cell Biochem Biophys* (2014) 69(2):363–8. doi: 10.1007/s12013-013-9808-0

356. Li F, Ma Q, Zhao H, Wang R, Tao Z, Fan Z, et al. L-3-n-Butylphthalide reduces ischemic stroke injury and increases M2 microglial polarization. *Metab Brain Dis* (2018) 33(6):1995–2003. doi: 10.1007/s11011-018-0307-2

357. Han D. Danshensu borneol improves pressure-induced heart failure through the mTOR / β-TrcP / Nrf2 pathway [d]. *Zhengzhou Univ* (2021). doi: 10.27466/d.cnki.gzzdu.2021.000719

358. Zhang Z. Brain targeting effect of danshensu borneol ester and its effect on p-glycoprotein on blood-brain barrier [d]. *Hefei Univ Technol* (2017).

359. Liao S, Wu J, Liu R, Wang S, Luo J, Yang Y, et al. Ael compound DBZ ameliorates neuroinflammation in LPS-stimulated microglia and ischemic stroke rats: Role of Akt(Ser473)/GSK3β(Ser9)-mediated Nrf2 activation. *Redox Biol* (2020) 36:101644. doi: 10.1016/j.redox.2020.101644

360. Shabgah AG, Suksatan W, Achmad MH, Bokov DO, Abdelbasset WK, Ezzatifar F, et al. Arctigenin, an anti-tumor agent; a cutting-edge topic and up-to-the-minute approach in cancer treatment. *Eur J Pharmacol* (2021) 909:174419. doi: 10.1016/j.ejphar.2021.174419

361. He Y, Fan Q, Cai T, Huang W, Xie X, Wen Y, et al. Molecular mechanisms of the action of arctigenin in cancer. *BioMed Pharmacother* (2018) 108:403–7. doi: 10.1016/j.biopha.2018.08.158

362. Gao Q, Yang M, Zuo Z. Overview of the anti-inflammatory effects, pharmacokinetic properties and clinical efficacies of arctigenin and arctiin from arctium lappa l. *Acta Pharmacol Sin* (2018) 39(5):787–801. doi: 10.1038/aps.2018.32

363. Fan T, Jiang WL, Zhu J, Feng Zhang Y. Arctigenin protects focal cerebral ischemia-reperfusion rats through inhibiting neuroinflammation. *Biol Pharm Bull* (2012) 35(11):2004–9. doi: 10.1248/bpb.b12-00463

364. Mottaghi S, Abbaszadeh H. A comprehensive mechanistic insight into the dietary and estrogenic lignans, arctigenin and sesamin as potential anticarcinogenic and anticancer agents. current status, challenges, and future perspectives. *Crit Rev Food Sci Nutr* (2022) 62(26):7301–18. doi: 10.1080/10408398.2021.1913568

365. Anju VT, Busi S, Ranganathan S, Ampasala DR, Kumar S, Suchiang K, et al. Sesamin and sesamolin rescues caenorhabditis elegans from pseudomonas aeruginosa infection through the attenuation of quorum sensing regulated virulence factors. *Microb Pathog* (2021) 155:104912. doi: 10.1016/j.micpath.2021.104912

366. Ahmad S, Elsherbiny NM, Haque R, Khan MB, Ishrat T, Shah ZA, et al. Sesamin attenuates neurotoxicity in mouse model of ischemic brain stroke. *Neurotoxicology* (2014) 45:100–10. doi: 10.1016/j.neuro.2014.10.002

367. Jiao L, Zhang J, Li Z, Liu H, Chen Y, Xu S. Edaravone alleviates delayed neuronal death and long-dated cognitive dysfunction of hippocampus after transient focal ischemia in wistar rat brains. *Neuroscience* (2011) 19:182:177–83. doi: 10.1016/j.neuroscience.2011.01.017

368. Gao HJ, Liu PF, Li PW, Huang ZY, Yu FB, Lei T, et al. Ligustrazine monomer against cerebral ischemia/reperfusion injury. *Neural Regener Res* (2015) 10(5):832–40. doi: 10.4103/1673-5374.156991

369. Shao H, He X, Zhang L, Du S, Yi X, Cui X, et al. Efficacy of ligustrazine injection as adjunctive therapy in treating acute cerebral infarction: A systematic review and meta-analysis. *Front Pharmacol* (2021) 12:761722. doi: 10.3389/fphar.2021.761722

370. Zheng Q, Huang YY, Zhu PC, Tong Q, Bao XY, Zhang QH, et al. Ligustrazine exerts cardioprotection in animal models of myocardial Ischemia/Reperfusion injury: Preclinical evidence and possible mechanisms. *Front Pharmacol* (2018) 9:729. doi: 10.3389/fphar.2018.00729

371. Ni X, Ni X, Liu S, Guo X. Medium- and long-term efficacy of ligustrazine plus conventional medication on ischemic stroke: a systematic review and meta-analysis. *J Tradit Chin Med* (2013) 33(6):715–20. doi: 10.1016/s0254-6272(14)60002-9

372. Lin J, Wang Q, Zhou S, Xu S, Yao K. Tetramethylpyrazine: A review on its mechanisms and functions. *BioMed Pharmacother* (2022) 150:113005. doi: 10.1016/j.biopha.2022.113005

373. Kao TK, Chang CY, Ou YC, Chen WY, Kuan YH, Pan HC, et al. Tetramethylpyrazine reduces cellular inflammatory response following permanent focal cerebral ischemia in rats. *Exp Neurol* (2013) 247:188–201. doi: 10.1016/j.expneurol.2013.04.010

374. Britch SC, Babalonis S, Walsh SL. Cannabidiol: pharmacology and therapeutic targets. *Psychopharmacol (Berl)* (2021) 238(1):9–28. doi: 10.1007/s00213-020-05712-8

375. von Wrede R, Helmstaedter C, Surges R. Cannabidiol in the treatment of epilepsy. *Clin Drug Investig* (2021) 41(3):211–20. doi: 10.1007/s40261-021-01003-y

376. Gaston TE, Martin RC, Szaflarski JP. Cannabidiol (CBD) and cognition in epilepsy. *Epilepsy Behav* (2021) 124:108316. doi: 10.1016/j.yebeh.2021.108316

377. Batalla A, Bos J, Postma A, Bossong MG. The impact of cannabidiol on human brain function: A systematic review. *Front Pharmacol* (2021) 11:618184. doi: 10.3389/fphar.2020.618184

378. Mori MA, Meyer E, Soares LM, Milani H, Guimarães FS, de Oliveira RMW. Cannabidiol reduces neuroinflammation and promotes neuroplasticity and functional recovery after brain ischemia. *Prog Neuropsychopharmacol Biol Psychiatry* (2017) 3:75:94–105. doi: 10.1016/j.pnpbp.2016.11.005

379. Xie Q, Zhang L, Xie L, Zheng Y, Liu K, Tang H, et al. Z-ligustilide: A review of its pharmacokinetics and pharmacology. *Phytother Res* (2020) 34(8):1966–91. doi: 10.1002/ptr.6662

380. Zhang Q, Liu J, Duan H, Li R, Peng W, Wu C. Activation of Nrf2/HO-1 signaling: An important molecular mechanism of herbal medicine in the treatment of atherosclerosis *via* the protection of vascular endothelial cells from oxidative stress. *J Adv Res* (2021) 34:43–63. doi: 10.1016/j.jare.2021.06.023

381. Tasneem S, Liu B, Li B, Choudhary MI, Wang W. Molecular pharmacology of inflammation: Medicinal plants as anti-inflammatory agents. *Pharmacol Res* (2019) 139:126–40. doi: 10.1016/j.phrs.2018.11.001

382. Prud'homme GJ, Kurt M, Wang Q. Pathobiology of the klotho antiaging protein and therapeutic considerations. *Front Aging* (2022) 3:931331. doi: 10.3389/fragi.2022.931331

383. Ghosh N, Ghosh R, Bhat ZA, Mandal V, Bachar SC, Nima ND, et al. Advances in herbal medicine for treatment of ischemic brain injury. *Nat Prod Commun* (2014) 9(7):1045–55. doi: 10.1177/1934578X1400900739

384. Kuang X, Wang LF, Yu L, Li YJ, Wang YN, He Q, et al. Ligustilide ameliorates neuroinflammation and brain injury in focal cerebral ischemia/reperfusion rats: involvement of inhibition of TLR4/peroxiredoxin 6 signaling. *Free Radic Biol Med* (2014) 71:165–75. doi: 10.1016/j.freeradbiomed.2014.03.028

385. Ma L, Tang L, Yi Q. Salvianolic acids: Potential source of natural drugs for the treatment of fibrosis disease and cancer. *Front Pharmacol* (2019) 10:97. doi: 10.3389/fphar.2019.00097

386. Du G, Song J, Du L, Zhang L, Qiang G, Wang S, et al. Chemical and pharmacological research on the polyphenol acids isolated from danshen: A review of salvianolic acids. *Adv Pharmacol* (2020) 87:1–41. doi: 10.1016/bs.apha.2019.12.004

387. Han R, Huang H, Xia W, Liu J, Luo H, Tang J, et al. Perspectives for forkhead box transcription factors in diabetic cardiomyopathy: Their therapeutic potential and possible effects of salvianolic acids. *Front Cardiovasc Med* (2022) 9:951597. doi: 10.3389/fcvm.2022.951597

388. Xu H, Wang E, Chen F, Xiao J, Wang M. Neuroprotective phytochemicals in experimental ischemic stroke: Mechanisms and potential clinical applications. *Oxid Med Cell Longev* (2021) 2021:6687386. doi: 10.1155/2021/6687386

389. Liu H, Lu X, Hu Y, Fan X. Chemical constituents of panax ginseng and panax notoginseng explain why they differ in therapeutic efficacy. *Pharmacol Res* (2020) 161:105263. doi: 10.1016/j.phrs.2020.105263

390. Zhang X, Zhang B, Zhang C, Sun G, Sun X. Effect of panax notoginseng saponins and major anti-obesity components on weight loss. *Front Pharmacol* (2021) 11:601751. doi: 10.3389/fphar.2020.601751

391. Ji C, Zhang Q, Shi R, Li J, Wang X, Wu Z, et al. Determination of the authenticity and origin of panax notoginseng: A review. *J AOAC Int* (2022) 105(6):1708–18. doi: 10.1093/jaoacint/qsac081

392. Wang R, Wang M, Zhou J, Wu D, Ye J, Sun G, et al. Saponins in Chinese herbal medicine exerts protection in myocardial ischemia-reperfusion injury: Possible mechanism and target analysis. *Front Pharmacol* (2021) 11:570867. doi: 10.3389/fphar.2020.570867

393. Li Y, Guo Q, Huang J, Wang Z. Antidepressant active ingredients from Chinese traditional herb panax notoginseng: A pharmacological mechanism review. *Front Pharmacol* (2022) 13:922337. doi: 10.3389/fphar.2022.922337

394. Tan MM, Chen MH, Han F, Wang JW, Tu YX. Role of bioactive constituents of panax notoginseng in the modulation of tumorigenesis: A potential review for the treatment of cancer. *Front Pharmacol* (2021) 12:738914. doi: 10.3389/fphar.2021.738914

395. Jia Z, Chen H, Zhao L, Yuan Q, Yin M, Wang S, et al. Salvia polyphenolic acid combined with panax notoginseng saponins can regulate the polarization of M1/M2 type microglia on cerebral ischemia-regeneration in rats. influence of perfusion injury. *Tianjin Traditional Chin Med* (2020) 37(07):824–30. doi: 10.11656/j.issn.1672-1519.2020.07.26

396. Zhang M, Wang S, Mao L. Omega-3 fatty acids protect the brain against ischemic injury by activating Nrf2 and upregulating heme oxygenase 1. *JNeurosci* (2014) 34(5):1903–15. doi: 10.1523/JNEUROSCI.4043-13.2014

397. Yang B, Ren XL, Huang H, Guo XJ, Ma AG, Li D, et al. Circulating long-chain n-3 polyunsaturated fatty acid and incidence of stroke:a meta-analysis of prospective cohort studies. *Oncotarget* (2017) 8(48):83781–91. doi: 10.18632/oncotarget.19530

398. Cai M, Zhang W, Weng Z, Stetler RA, Jiang X, Shi Y, et al. Promoting neurovascular recovery in aged mice after ischemic stroke -prophylactic effect of omega.3 polyunsaturated fatty acids. *Aging Dis* (2017) 8(5):531–45.

399. Berressem D, Koch K, Franke N, Klein J, Eckert GP. Intravenous treatment with a longchain omega-3 lipid emulsion provides neuroprotection in a murine model of ischemic stroke:a pilot study. *PloS One* (2016) 11(11):e0167329.

400. Jiang X, Pu H, Hu X, Wei Z, Hong D, Zhang W, et al. A post-stroke therapeutic regimen with omega-3 polyunsaturated fatty acids that promotes white matter integrity and beneficial microglial responses after cerebral ischemia. *Transl Stroke Res* (2016) 7(6):548–61. doi: 10.1007/s12975-016-0502-6

401. Xie W, Zhu T, Dong X, Nan F, Meng X, Zhou P, et al. HMGB1-triggered triggered inflammation inhibition of notoginseng leaf triterpenes against cerebral ischemia and reperfusion injury *via* MAPK and NF-κB signaling pathways. *Biomolecules* (2019) 9(10):512. doi: 10.3390/biom9100512

402. Liu H, Zhang Z, Zang C, Wang L, Yang H, Sheng C, et al. GJ-4 ameliorates memory impairment in focal cerebral ischemia/reperfusion of rats *via* inhibiting JAK2/STAT1-mediated neuroinflammation. *J Ethnopharmacol* (2021) 267:113491. doi: 10.1016/j.jep.2020.113491

403. Qin C, Fan WH, Liu Q. Fingolimod protects against ischemic white matter damage by modulating microglia toward M2 polarization *via* STAT3 pathway. *Stroke* (2017) 48(12):3336–46. doi: 10.1161/STROKEAHA.117.018505

frontiers | Frontiers in Immunology

TYPE Original Research
PUBLISHED 08 February 2023
DOI 10.3389/fimmu.2022.1095657

Check for updates

OPEN ACCESS

EDITED BY
Bo Li,
Department of Orthopedics, Sun Yat-sen University, China

REVIEWED BY
Shen He,
Shanghai Mental Health Center, China
Huimei Wang,
Fudan University, China

*CORRESPONDENCE
Ping Zheng
jojo_ras@126.com

†These authors have contributed equally to this work

‡These authors share senior authorship

SPECIALTY SECTION
This article was submitted to Multiple Sclerosis and Neuroimmunology, a section of the journal Frontiers in Immunology

RECEIVED 11 November 2022
ACCEPTED 23 December 2022
PUBLISHED 08 February 2023

CITATION
Zheng P, Zhang N, Ren D, Yu C, Zhao B, Bai Q, Zhang Y and Sun W (2023) Integrated single-cell multiomics reveals novel immune candidate markers for post-traumatic coagulopathy. *Front. Immunol.* 13:1095657. doi: 10.3389/fimmu.2022.1095657

Integrated single-cell multiomics reveals novel immune candidate markers for post-traumatic coagulopathy

Ping Zheng[1,2*†], Ning Zhang[3†], Dabin Ren[1], Cong Yu[1], Bin Zhao[4], Qingke Bai[5], Yisong Zhang[1‡] and Wanju Sun[6‡]

[1]Department of Neurosurgery, Shanghai Pudong New area People's Hospital, Shanghai, China, [2]Key Laboratory, Shanghai Pudong New area People's Hospital, Shanghai, China, [3]Department of Neurosurgery, Shanghai Fengxian Hospital, Shanghai, China, [4]Department of Neurosurgery, Second Hospital affiliated to Anhui Medical University, Shanghai, China, [5]Department of Neurology, Shanghai Pudong New area People's Hospital, Shanghai, China, [6]Department of Emergency Medicine, Shanghai Pudong New area People's Hospital, Shanghai, China

Introduction: Post-traumatic coagulopathy (PTC) is a critical pathology in traumatic brain injury (TBI), however, its potential mechanism is not clear. To explore this in peripheral samples, we integrated single cell RNA-sequencing and T cell repertoire (TCR)-sequencing across a cohort of patients with TBI.

Methods: Clinical samples from patients with more brain severity demonstrated overexpression of T cell receptor–encoding genes and less TCR diversity.

Results: By mapping TCR clonality, we found patients with PTC have less TCR clones, and the TCR clones are mainly distributed in cytotoxic effector CD8+T cell. In addition, the counts of CD8+ T cell and natural killer (NK) cells are associated with the coagulation parameter by WGCNA, and the granzyme and lectin-like receptor profiles are also decreased in the peripheral blood from TBI patients, suggesting that reduced peripheral CD8+ clonality and cytotoxic profiles may be involved in PTC after TBI.

Conclusion: Our work systematically revealed the critical immune status in PTC patients at the single-cell level.

KEYWORDS

single-cell, multi-omics, RNA-seq, TCR-seq, post-traumatic coagulopathy

1 Introduction

Post-traumatic coagulopathy (PTC) is one of the critical pathophysiologies in a traumatic brain injury (TBI) population (1). Recent statistics show that approximately two-thirds of severe TBI patients have abnormal coagulation function on admission (2), and we previously show that coagulopathy and initial head computer tomography (CT) signs could be independent risk factors for progressive hemorrhagic injury (PHI) including epidural, subdural hematoma, brain contusion, subarachnoid hemorrhage, cranial fracture, and plasma D-dimer level (3, 4). The mechanisms of PTC include platelet dysfunction, endogenous anticoagulation, endothelial activation, abnormal fibrinogen (Fg), neuroinflammation, and hyperfibrinolysis (2, 5–7); however, up to now, the exact mechanism is unclear.

The key role of peripheral blood in TBI has been identified in our study and in other studies, and several biomarkers in peripheral blood mononuclear cells (PBMCs) are related to neurodegenerative diseases (8). In this study, we collected PBMCs from 12 TBI patients and four healthy controls for single-cell RNA sequencing (scRNA-seq) and TCR sequencing. The clonal expansion of CD8+ T cells in TBI and PTC progression was identified in TBI and PTC, which were further validated using fluorescence-activated cell sorting (FACS). Our finding might be useful for the development of immune cell-targeted therapy in PTC.

2 Experimental section

2.1 Participants

Four normal individuals and 12 TBI patients (4 with mild TBI, 4 with moderate TBI, and 4 with severe TBI) were enrolled. PBMCs from 11 TBI patients were further collected for validated FACS and correlation analysis with the patients' GCS scores with randomization. The inclusion criteria are as follows: a clinical diagnosis of TBI, an age range of 18–60 years, and no previous history of brain, liver, or hematologic disorders. Patients were excluded if they met the following criteria: active systemic infection or multiple injury, use of immunosuppressants, and other serious coagulopathy not related to trauma.

The consent form was obtained from patients' family members. Patients' characteristics are summarized in Tables S1 and S2. There were no subjects dropped out from the study. No female patients were on progestin. This project was approved by the Ethics Committee of Shanghai Pudong New Area People's Hospital (approval number 2021-K02) and was conducted in accordance with the Declaration of Helsinki.

2.2 Head CT imaging

The diagnosis of PHI was previously reported(3,4).

2.3 Post-traumatic coagulopathy definition

The coagulation parameters include the prothrombin time (PT), international normalized ratio (INR), activated partial thromboplasting time (APTT), Fg, and platelet count (Plt). The PTC is defined as abnormal value of PT, INR, APTT, Fg, or Plt(3,4). Detailed information of coagulation parameters on these patients is shown in Table S3.

2.4 Microarray information

The Agilent Human lncRNA Microarray 2019 (4*180k, Design ID:086188) was used here. The RNA extraction and quantification method was previously reported.

2.5 ScRNA-seq method and TCR-seq

The exact procedure for scRNA-seq and TCR-seq for PBMCs could be obtained from the 10X website. Fresh blood samples from 12 TBI patients (Se1–4, Mo1–4, and Mi1–4) and four age-matched healthy controls (Co1–4) were collected and PBMCs were isolated with the assay. Single-cell 5′ and TCR V(D)J libraries were constructed according to the 10X Chromium Immune Profiling protocol. Briefly, CD3+ T cells (isolated with FACS) were loaded onto Chromium Controller (10X Genomics, USA) with a V(D)J Kit. Each single-cell 5' and V(D)J library was sequenced with the Illumina Novaseq 6000.

2.6 Cell quality control

We carried out data quality control. We captured cells with less than 10% of mitochondrial genes, with the total number of genes ranging from 200 to 6,000 and were expressed in at least three cells. Doublets were removed with the DoubletFinder package with a doublet rate <5%. The number of highly

variable genes was set at 3,000. These two samples were integrated through SCT correction. Then, both the tSNE and uMAP methods were used to reduce the dimension of data.

2.7 Fluorescence-activated cell sorting

PBMCs from 11 TBI patients were isolated by FACS to further validate the results of scRNA-seq. The exact procedure was previously reported (9).

2.8 Cell–cell interaction

Using scRNA-seq data, taking the gene expression data of cell subsets as the research object, with the help of the ligand–receptor database, the ligand and receptor information in cells can be obtained using cellphoneDB (10), and the signal communication relationship between cells can be obtained, to elucidate the complexity, diversity, and dynamics of cell-to-cell communication in a wide range of biological processes.

2.9 RNA velocity assessment

RNA velocity is the testing rate of change in the abundance of mRNA molecules in a cell (11). Previous studies have demonstrated that RNA velocity can be estimated from unspliced and spliced mRNA abundance, which can predict the future state of individual cells on a timescale of hours (11). RNA velocity can reveal the dynamics of single-cell gene expression on timescales that match developmental, regeneration, and response processes in humans and other mammals. We employed the velocyto algorithm to estimate changes in RNA abundance over time by calculating the ratio of intracellular mRNA before and after splicing, and infer the next possible differentiation direction of cells.

2.10 Weighted co-expression network analysis

Weighted co-expression network analysis (WGCNA) is a computational method to describe co-expressed genes between different groups. It can identify marker genes based on the non-orientation analysis between the gene set and phenotypes. Here, WGCNA was used to locate the gene modules related to coagulation dysfunction in TBI.

2.11 Statistical analysis

Statistical analysis was performed using GraphPad Prism software (v8.1, GraphPad Software Inc., San Diego, CA, USA). The data were analyzed by those who were blinded to patients' grouping. No power analysis was required as we had four subjects in each group. The correlation among the number of T cells, the expression levels of genes, and GCS scores (the severity of TBI) was analyzed using the Pearson correlation. Any difference with a p-value < 0.05 was considered significant. The exact method for analysis was mentioned in essential parts.

3 Results

3.1 Single-cell transcriptional landscape of PBMCs from TBI patients

The schematic plot of the study is graphed in Figure S1. Head CT scans showed progressive brain contusions in PTC patients (Figures S2A, B) compared to nPTC individual (Figures S2C, D). The chipset results for peripheral blood of TBI patients showed that the hallmark of coagulation was among the enriched pathways (Figures S2E, F). The KEGG analysis also showed that coagulation cascades were activated in TBI, while the antigen processing and presentation were deactivated in TBI (Figure S2G). This leads us to investigate the role of immune system in coagulation after TBI. When we investigated the coagulation parameter and immune profiles, we found the increased expression of CD8+ T cells in PBMCs of patients with more severe brain injury (Figure S2H) and the increased count of CD8+ T cells was positively associated with the increased Fg value; meanwhile, the counts of NK cells had a negative correlation with the PT and INR value.

To explore the peripheral immune status in TBI, we collected PBMCs from TBI patients for scRNA-seq based on 10x Genomics. Cells were subjected to t-distributed stochastic neighbor embedding (t-SNE) analysis, and 15 clusters in four groups were obtained (Figure 1A). The cell annotation identifies eight clusters, namely, T cells, monocytes, NK cells, B cells, pre-B cells, neutrophils, macrophages, and platelets (Figure 1B). About 1,300 highly variable genes were identified in 16 samples, and less genes (982) were found in mi2 (a sample from a mild TBI patient) (Table S2). The pairwise correlation between intergroup variability ranges from 0.8101 to 0.9496 (Figure 1C).

Through the clustering analysis, the top 10 cell markers in each cluster were analyzed in two dimensions with Monocle2 (Figure 1D). Then, the quantification data showed high densities

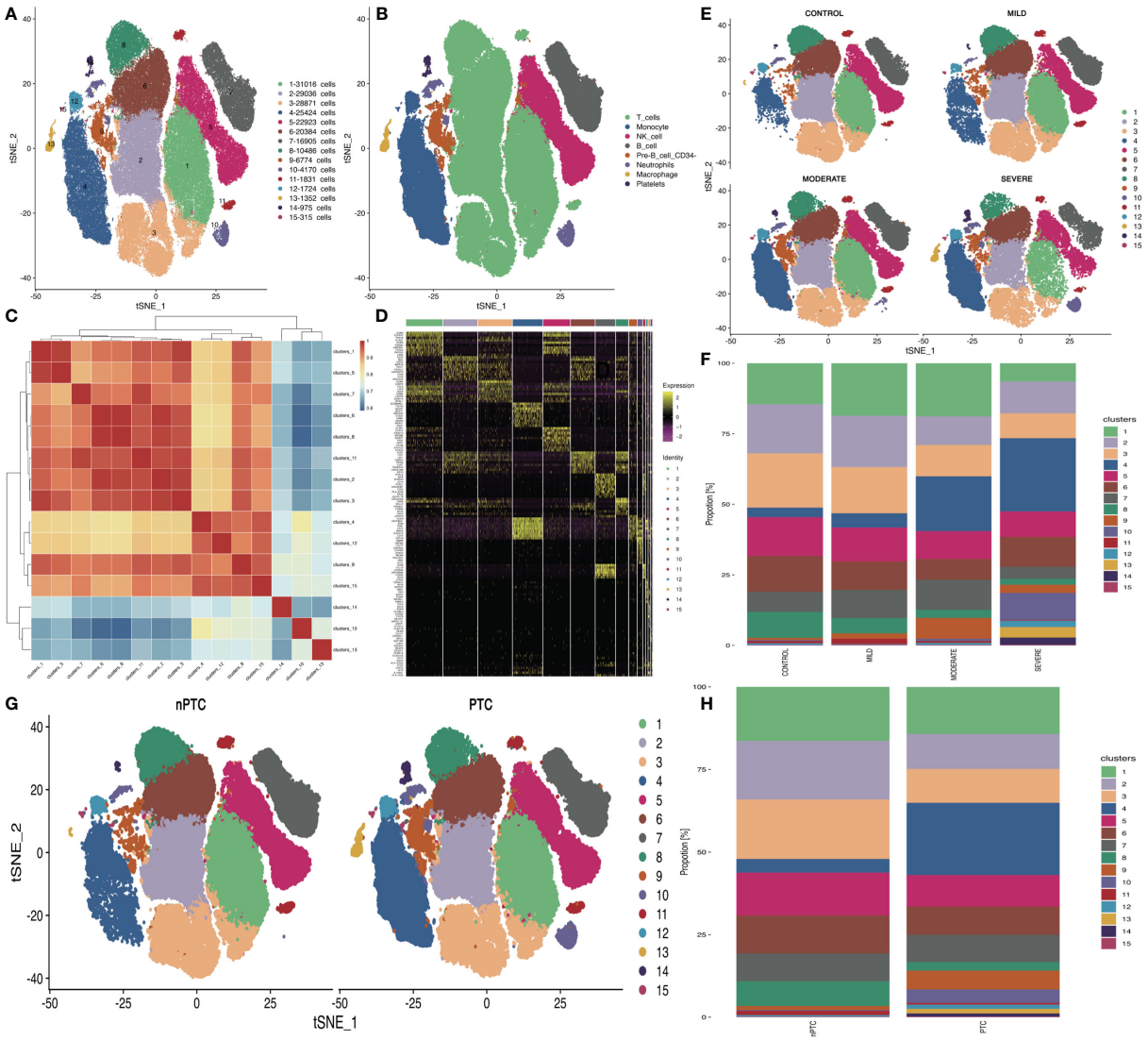


FIGURE 1
The differences in cell subsets of PBMCs in TBI patients. **(A)** t-SNE plot shows the 15 cell subsets in all PBMC samples from 12 TBI patients and 4 healthy controls. **(B)** Cell annotations in eight clusters. **(C)** Correlations of 15 cell subsets are analyzed with Pearson method for the mean expression of genes between each cluster to investigate the similarity between each cell cluster. The *X*- and *Y*-axis is each cell cluster. The red color indicates the higher correlation similarity, while the blue color suggests the lower correlation. **(D)** Top 10 cell markers in each cluster. **(E)** The t-SNE distribution of 15 cell subsets in different TBI groups. **(F)** The bar plot of 15 cell subsets' distribution in different TBI groups. **(G)** The t-SNE distribution of 15 cell subsets' distribution in nPTC and PTC groups. **(H)** The bar plot of 15 cell subsets in nPTC and PTC groups.

of T cells and NK cells in each sample (Figures 1E, F). In the PBMCs of PTC patients, the percentage of T and NK cells was obviously reduced compared with those of nPTC groups as well (Figures 1G, H).

The differentially expressed genes (DEGs) between different TBI groups and the control are listed in Figures S3A–C. The DEGs between PTC and nPTC groups are listed in Figure S3D. Next, KEGG analysis of DEGs identified by scRNA-seq was mainly enriched in the immune system, infectious disease, and signal transduction (Figures S3E–G). The similar enriched pathways were identified between the PTC and the nPTC group (Figure S3H). Then, the bubble plot shows that the upregulated genes identified by scRNA-seq were mainly involved in ko04620: Toll-like receptor signaling pathway; ko04612: antigen processing and presentation; and ko04610: complement and coagulation cascades (Figures S3I, J).

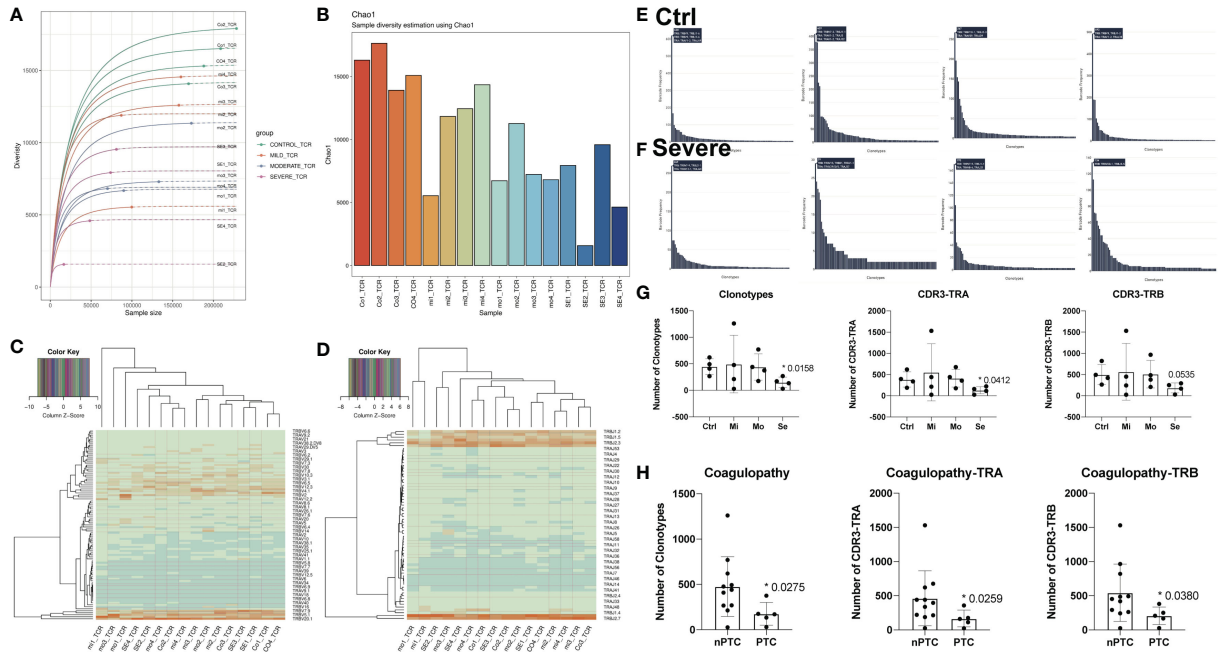


FIGURE 2
The differences of T-cell clonity in TBI patients. **(A)** Clonotype richness of TCR in different samples. **(B)** Chao1 index of TCR in different samples. **(C, D)** The relative expression of V and J genes in different groups. **(E, F)** The number of clonotypes of TCR genes in the control and severe group. **(G)** The quantification of clonotypes CD3-TRA and CD3-TRB in different TBI groups. **(H)** The quantification of clonotypes CD3-TRA and CD3-TRB between nPTC and PTC group.

3.2 Decreased TCR diversity in PBMCs from TBI patients

To further accurately identify the peripheral immune function in TBI, we performed TCR-seq for collected PBMCs from TBI patients based on 10x Genomics again. The dilution curve of the sample list in Figure 2A shows the dependence between clonotype diversity and clonotype size. In theory, if the sequencing depth is large enough, ideally, the curve will eventually tend to be horizontal. Here, we can directly show the difference in clonotype richness between samples and can also find that the diversity of TCR repertoire was largely reduced with the severity of TBI. Again, the Chao1 index also decreased in the severe TBI group, indicating that severe TBI disrupts the diversity of T cells (Figure 2B). Furthermore, TCR V–J gene combinations were conserved in the TBI groups and the control group (Figure S4), and the relative expression of V genes (Figure 2C) and J genes (Figure 2D) in different groups was also conserved. These results suggested that TCR genes were conserved among groups. As the diversity of T cells decreased in TBI, we further investigated the number of clonotypes of TCR genes and found that it was obviously decreased in the severe TBI groups (Figures 2E, F) regarding the number of clonotypes, number of CDR3-TRA, and number of CDR3-TRB (Figure 2G). The difference also occurred between nPTC and PTC groups (Figure 2H). This indicates that CDR3 genes might be a biomarker for TBI and also involved in PTC.

3.3 Expanded CD8+ T cells in TBI patients

Therefore, we further looked at the distribution of different CDR3 lengths and found that the CDR3 length increased in the severe TBI group and the distribution of CDR3 length shows a symmetry style in the control group while it demonstrates a bias distribution (Figure S5). These findings indicate that the severe TBI group might have T-cell expansion, which leads us to further explore the leading role of CD4+ T and CD8+ T cells in TBI.

We first looked at the subpopulations of CD4+ T cells of PBMC in TBI patients and identified four clusters: Naïve CD4 T, Treg, Effector_memory CD4 T, and cytotoxic effector CD4 T (Figure 3A). There are very few TCR clones in CD4+ T cells, and they are sparsely distributed in cytotoxic effector CD4 T (Figure 3B). Next, the t-SNE map shows the different

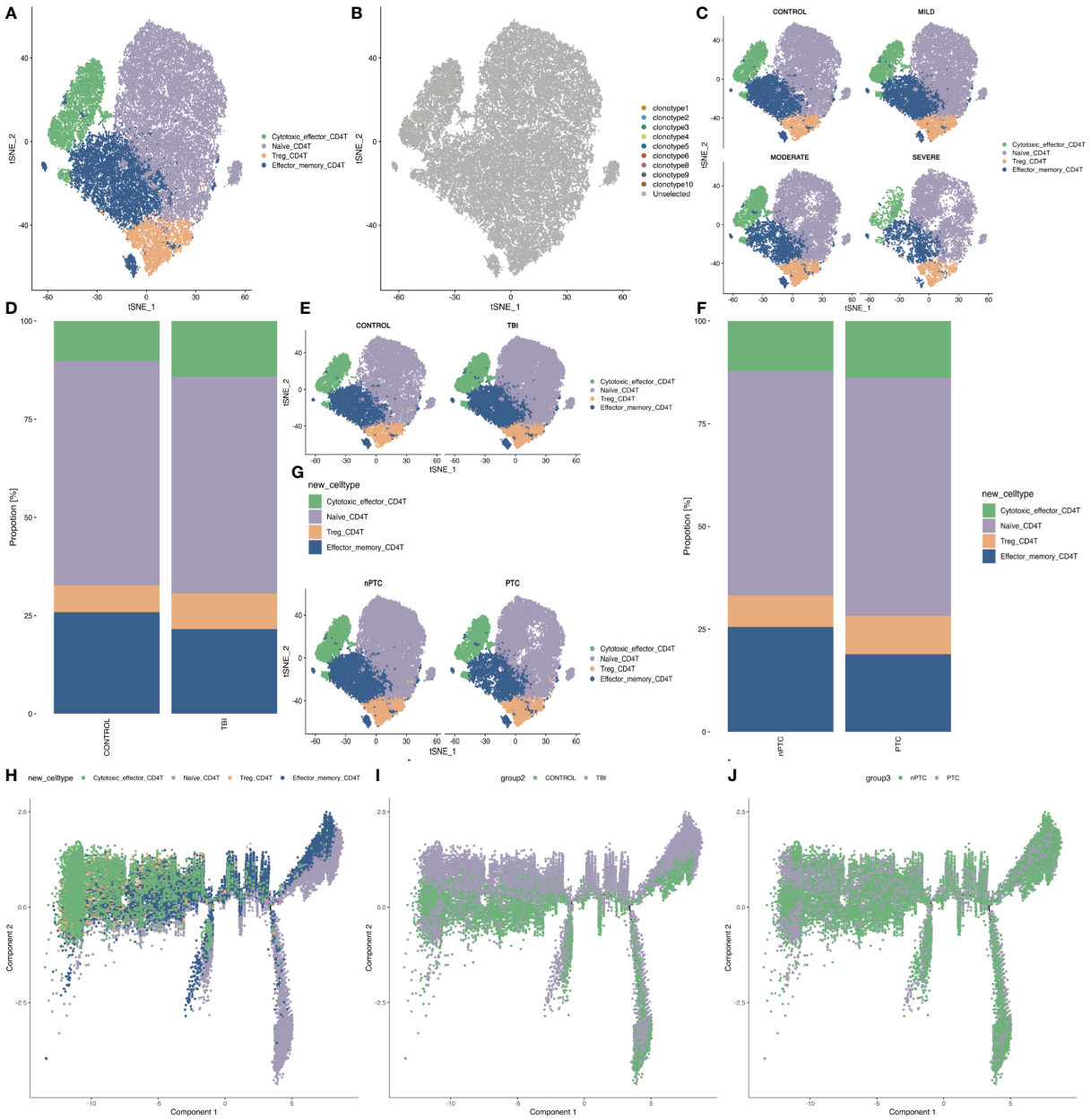


FIGURE 3
The subpopulations of CD4+ T cells of PBMCs in TBI patients. **(A)** The four clusters of CD4+ cells in t-SNE map. **(B)** The TCR clone in each CD4 + cell cluster. **(C)** The t-SNE map shows the different distribution of four clusters in control, mild, moderate, and severe TBI. **(D, E)** t-SNE map shows the four CD4+ cell subsets between TBI and control and quantification of the proportion of cells in each group. **(F, G)** t-SNE map shows the four CD4+ cell subsets between nPTC and PTC groups and quantification of the proportion of cells in each group. **(H–J)** Pseudo-time analysis for CD4 subsets between control vs. TBI and nPTC vs. PTC group.

distribution of these clusters in control and TBI groups. We found that the number of effector_memory CD4 T cells decreased with the severity of TBI (Figures 3C–E). In addition, the number of effector_memory CD4 T cells was also reduced in the PTC group compared to the nPTC group (Figures 3F, G). Pseudo-time analysis for CD4 subsets shows that the Naïve CD4 T and effector_memory CD4 T cells are mainly distributed in control and nPTC groups, while the cytotoxic_effector CD4 T and Tregs are dominant in TBI and PTC groups, which also have a trend from Naïve CD4 T to cytotoxic_effector CD4 T and

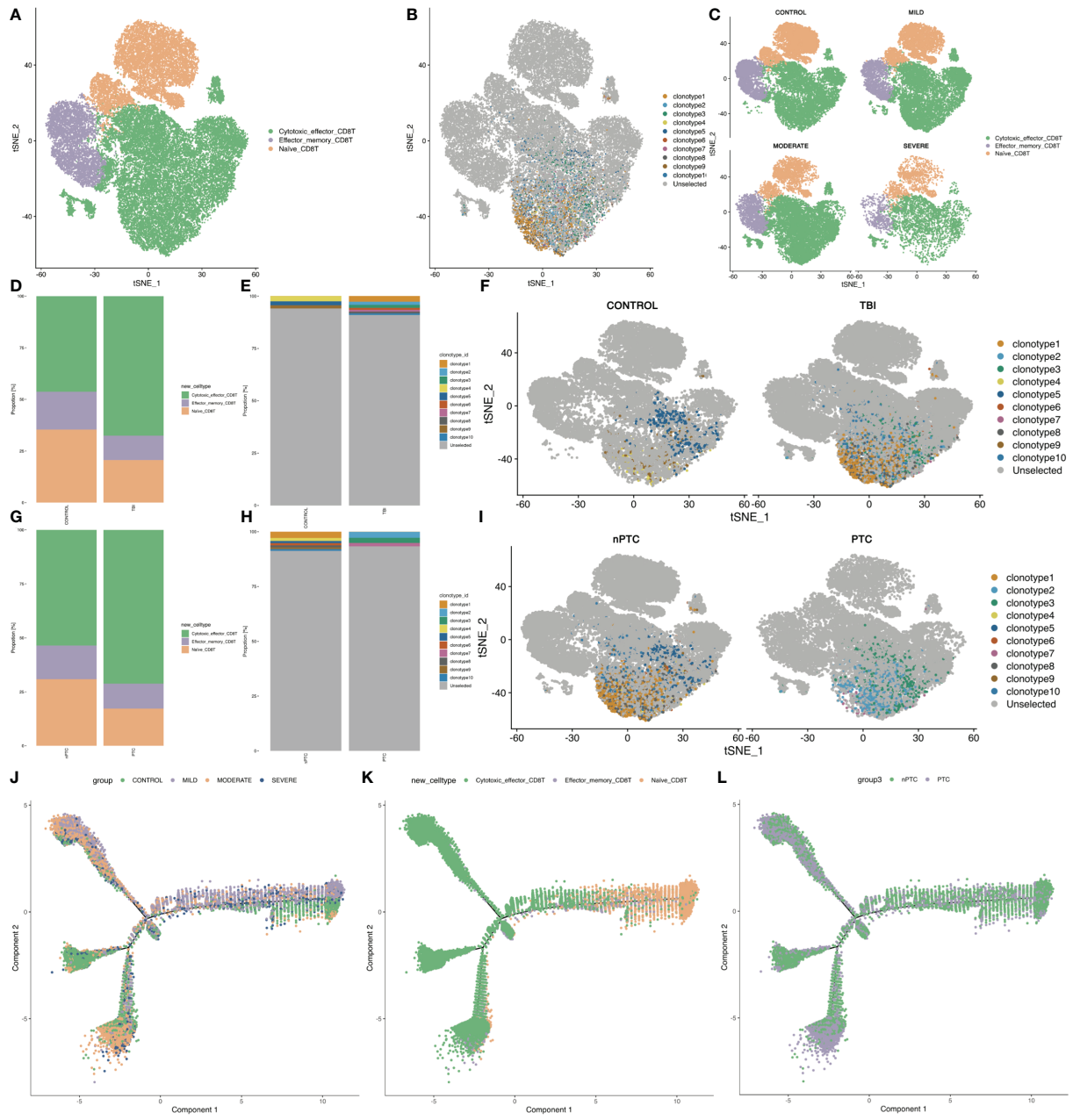


FIGURE 4
The subpopulations of CD8+ T cells and CD8 T clone of PBMCs in TBI patients. **(A)** The three clusters of CD8+ cells in the t-SNE map. **(B)** The TCR clone in each CD8+ cell cluster. **(C)** The t-SNE map shows the different distributions of three clusters in control, mild, moderate, and severe TBI. **(D–F)** t-SNE map shows the clone expansion between TBI and control and quantification of the proportion of TCR clonotype in each group. **(G–I)** t-SNE map shows the clone expansion between nPTC and PTC groups; and quantification of the proportion of TCR clonotype in each group. **(J–L)** Pseudo-time analysis for CD8 subsets between control vs. TBI and nPTC vs. PTC group.

Tregs (Figures 3H–J). The molecular markers of cytotoxic_effector CD4 T, Naïve CD4 T, Treg_CD4 T, and Effector_memory_CD4 T are listed in Figures S6A–E.

Next, we investigated the subpopulations of CD8+ T cells of PBMC in TBI patients and identified three clusters: Naïve CD8 T, Effector_memory CD8 T, and Cytotoxic effector CD8 T (Figure 4A). The TCR clone is mainly distributed in cytotoxic effector CD8 T (Figure 4B). Next, the t-SNE map shows the different distribution of these clusters in control and TBI groups. We found that the quantity of cytotoxic effector CD8 T cells

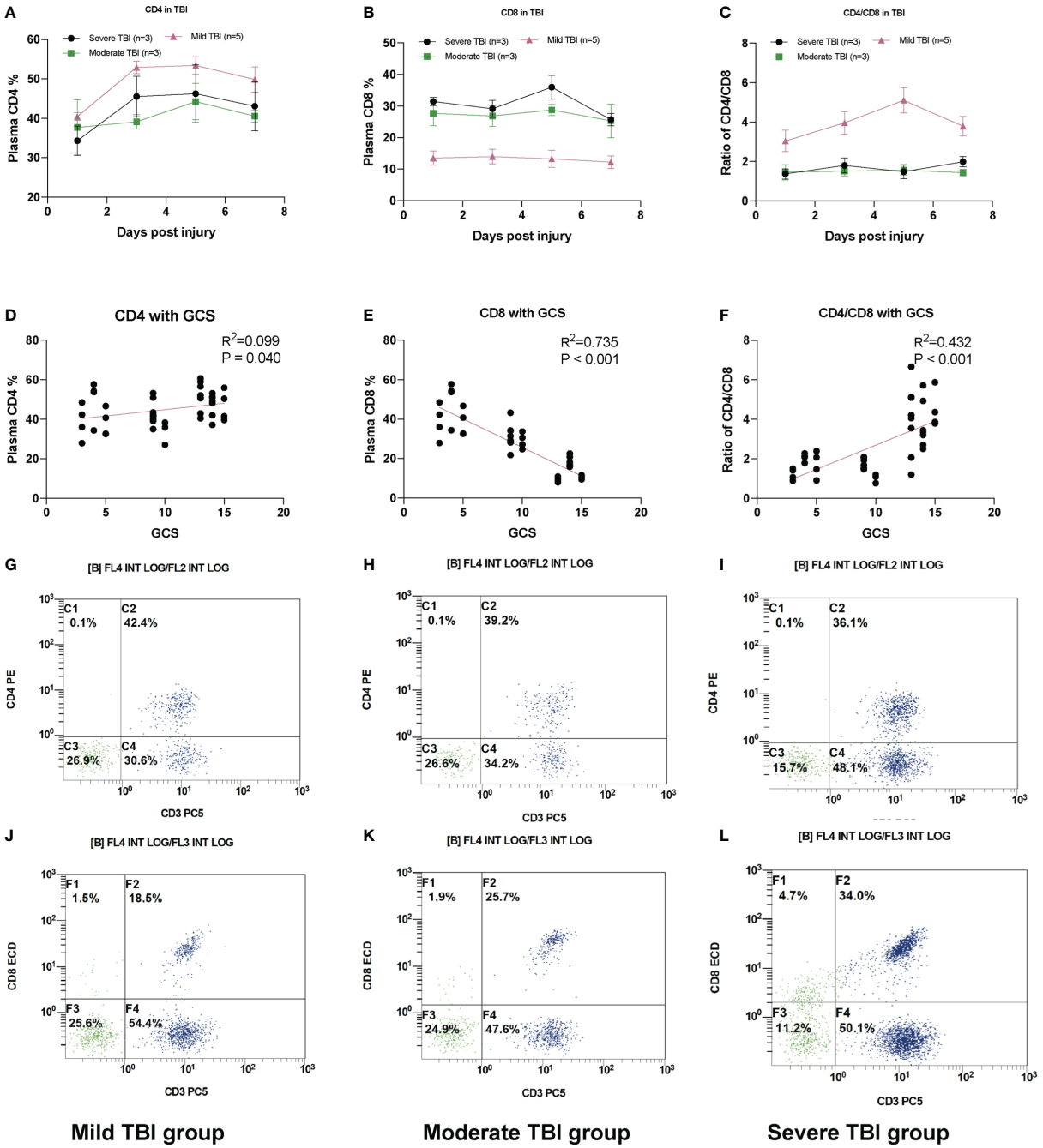


FIGURE 5
Plasma CD8+ T-cell increases in TBI. **(A)** The relative plasma CD4 percentage (reflected by CD3+ CD4+) in TBI groups. **(B)** The relative plasma CD8 percentage (reflected by CD3+ CD8+) in TBI groups. **(C)** The ratio of CD4/CD8 in TBI groups. **(D)** The scatter plot of plasma CD4 T% with GCS. **(E)** The scatter plot of plasma CD8 T% with GCS. **(F)** The scatter plot of CD4/CD8 with GCS. **(G)** The representative FACS image of CD4 (reflected by CD3+ CD4+) in severe TBI groups. **(H)** Moderate TBI and **(I)** mild TBI. The representative FACS image of CD8 (reflected by CD3+ CD8+) in **(J)** mild TBI groups. **(K)** Moderate TBI and **(L)** severe TBI. *N* = 3–5 in each group.

increased with the severity of TBI (Figures 4C–F). In addition, the clonotypes of cytotoxic effector CD8 T cells were also increased in the PTC group compared to the nPTC group, and the dominant clonotypes shifted between these two groups as well (Figures 4G–I). Pseudo-time analysis for CD8 subsets shows that the Naïve CD8 T and effector_memory CD8 T cells are mainly distributed in control and nPTC groups, while the cytotoxic_effector CD8 T is dominant in TBI and PTC groups, which also have a trend from Naïve CD8 T to cytotoxic_effector CD8 T (Figures 4J–L). The molecular markers of

10.3389/fimmu.2022.1095657

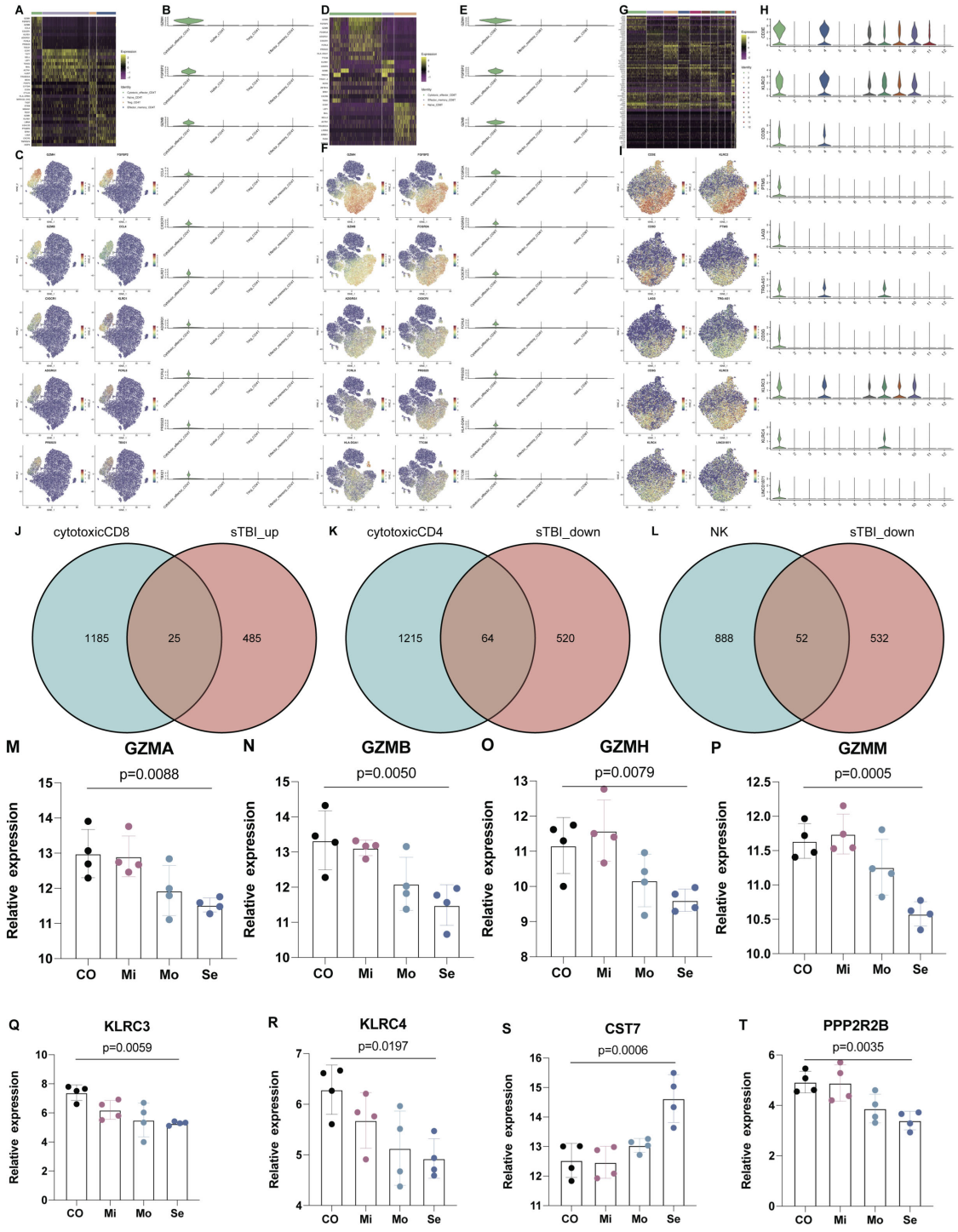


FIGURE 6
The marker genes for subtypes of CD4, CD8, and NK cells. **(A)** Heatmap shows the DEGs in Naïve CD4 T, Treg, Effector_memory CD4 T, and cytotoxic effector CD4 T. **(B, C)** Marker genes for cytotoxic effector CD4 T. **(D)** Heatmap shows the DEGs in Naïve CD8 T, Effector_memory CD8 T and Cytotoxic effector CD8 T. **(E, F)** Marker genes for cytotoxic effector CD8 T. **(G)** Heatmap shows the DEGs in NK cell subsets. **(H, I)** Marker genes for NK cell subsets. **(J–L)** Intersected marker genes of brain injury in cytotoxic CD8+, CD4+, and NK cells. **(M–P)** The expression of cytotoxic markers (granzyme **A, B, H, M**) in peripheral blood of TBI patients. **(Q, R)** The expression of c-type lectin receptors in peripheral blood of TBI patients. **(S)** The expression of CST7 as a marker of cytotoxic CD8 T cells. **(T)** The expression of PPP2R2B as a marker of NK cells. *n* = 4 in each group and one-way ANOVA is applied.

cytotoxic_effector CD8T, Effector_memory_CD8 T, and Naïve CD8T are listed in Figures S7A–D. These findings indicate the clonal expansion of CD8 T cells in the TBI, which might be involved in the PTC.

3.4 Cell–cell interaction in TBI patients

As the number of TCR clonity in TBI decreased, we further investigated the cell–cell interaction in the scRNA-seq data and found the cell–cell connection reduced in both TBI (Figure S8) and PTC compared to the control and nPTC groups (Figure S9); in particular, the interaction between T cells and other cell types decreased obviously in the PTC group (Figures S9C, E). Consistently, the RNA velocity map showed that the T-cell subset differentiation was also decreased in the TBI group compared to the control group (Figures S8G, H). The decreased differentiation ability of T cells also occurred in the PTC group compared to the nPTC group (Figures S9G, H).

3.5 Validation of immune cell proportion in peripheral blood by FACS

The immune system impairment has been previously reported in severe infection and neurodegenerative disease, both indicating the inverted ratio of CD4 T/CD8 T cells. Here, we also found this trend from our scRNA-seq results and further validated in our FACS analysis (Figure 5) and previous report (12). The plasma percentage of CD4+ T cells and ratio of CD4/CD8 decreased with the severity of TBI, while the ratio of CD8+ T cells increased. Both the CD4 expression and CD4/CD8 ratio show a positive correlation with the GCS score, while the CD8 expression has a negative correlation with the GCS score (Figures 5A–G). The representative FACS images of CD4 and CD8 in mild, moderate, and severe TBI groups are demonstrated in Figures 5H–M.

3.6 The cytotoxic profiles decrease in PTC groups

In addition, marker genes in cytotoxic CD8+ T, CD4+ T, and NK cells were also identified in PTC (Figure 6). The marker genes for different subsets of cytotoxic CD4+ T, CD8+ T, and NK cells were identified in Figures 6A–I for cytotoxic_effector CD4 T, cytotoxic_effector CD8 T, and NK cells. Furthermore, the intersecting marker genes of these subsets are listed (Figures 6J–L), and the cytotoxic profile of both cells that was validated in the plasma chipset data from 12 TBI patients and four healthy controls shows that the expression of cytotoxic markers (granzymes A, B, H, and M) and c-type lectin receptors (Figures 6M–P) and a representative NK cell marker (PPP2R2B) was also reduced with more severity in TBI (Figures 6Q–T), while the expression of a representative marker for cytotoxic CD8 T cells, CST7, increased with the severity of TBI (Figure 6S).

4 Discussion

In this study, differentially expressed cell subpopulations were screened in PBMCs of TBI patients by scRNA-seq analysis; CD8+ T cells represented a crucial cell subset in the progression of TBI, as verified through FACS in TBI patients. The mechanism of PTC has been a challenging undertaking. Coagulation characterization with peripheral blood has been regarded as the standard diagnosis for PTC, but this method is a traditional clinical test, which has limited extensibility in terms of treatment target.

Immune cells, particularly lymphocytes, may be involved in the pathogenesis of PTC. The scRNA-seq results in this work provide a detailed view of PBMCs in normal and TBI patients, in which the top eight cell subsets were T cells, monocytes, NK cells, B cells, pre-B cells, neutrophils, macrophages, and platelets, and the cell difference in each cluster can be clearly seen (Figure 1D). Furthermore, while studying signaling pathways, KEGG analysis revealed that the upregulated genes in PBMCs were mainly enriched in the following pathways: antigen processing, presentation, and coagulation, while the similar enriched pathways were identified between the PTC and nPTC group: Toll-like receptor signaling pathway, antigen processing and presentation, and complement and coagulation cascades.

In addition, cytotoxic profiling genes in CD8+ T, CD4+ T, and NK cells were identified as marker genes (Figure 6). The cytotoxic profile of all these cells was validated in the plasma chipset data from 12 TBI patients and four healthy controls and shows that the expression of cytotoxic markers (granzymes A, B, H, and M) and c-type lectin receptors is reduced with more severity in TBI (Figures 6J–O). Immediately, the investigation value of CD8+ T cells in TBI stands out from other cell subsets. Afterward, the results were continuously expanded in 11 TBI patients through FACS, and CD8+ T cells were found to be specifically increased in PBMCs of severe TBI patients compared to mild TBI groups, and the increased number of CD8+ T cells was closely associated with TBI severity. A similar study showed that the percentage of CD8+ T cells in the lymphocyte subsets of TBI were increased compared with healthy people (12), which was consistent with our study.

To verify the role of CD8+ T cells in TBI progression, we further exploited TCR-seq for collected PBMCs from TBI patients based on 10x Genomics. First, we found that the diversity of the TCR repertoire was largely reduced with the severity of TBI. Correspondingly, the number of clonotypes of TCR genes, specifically the number of CDR3-TRA and CDR3-TRB, was also decreased in the severe TBI groups. This indicates that CDR3 genes might be a biomarker for TBI and also involved

in PTC. However, when we further looked at the distribution of different CDR3 lengths, we found that the CDR3 length increased in the severe TBI group. In particular, we found that the amount of effector_memory CD4+ T cells decreased and the number of cytotoxic effector CD8+ T cells increased with the severity of TBI. In addition, the clonotypes of cytotoxic effector CD8+ T cells were also increased in the PTC group compared to the nPTC group. These findings indicate the clonal expansion of CD8+ T cells in TBI, which might be involved in the PTC. Functionally, the cell–cell interaction was also reduced in both TBI and PTC compared to the control and nPTC group; in particular, the interaction between T cells and other cell types decreased obviously in the PTC group. This is consistent with the RNA velocity map showing the reduced T-cell subset differentiation in TBI and PTC groups. Furthermore, the cytotoxic profiles in PBMC obviously decreased in the TBI and PTC groups, which is consistent with previous studies (13). All these findings suggest that CD8+ T cells might be involved in the PTC.

Traditionally, it would be difficult to link peripheral immune status to coagulation function. Consistent with our observation, one cellular therapy study of 100 patients with hematologic malignancies have coagulation disorders after chimeric antigen receptor (CAR)-T cell therapy, which demonstrated that imbalanced T-cell subsets may initiate the coagulopathy characterized by prolonged PT, APTT, INR, D-dimer, and decreased Fg (14). Meanwhile, patients accepting CD19 CAR-T cell therapy also demonstrate impaired coagulation function with severe cytokine release syndrome (15, 16). In addition, Johnsrud et al. also proposed that CAR-T cell therapy may trigger neurotoxicity as well (16). Accordingly, expanded CD8 T cells with reduced clonal diversity were identified in the early stage of TBI and might be involved in the mechanisms of PTC. Recently, immunity, endothelial injury, and complement-induced coagulopathy in COVID-19 have been the topic of many investigations, some of which consistently revealed that peripheral CD8+ T cells from patients with COVID-19 express high levels of exhaustion markers, including programmed cell death protein 1 (PD1) and T-cell immunoglobulin mucin-3 (TIM3) (17). However, the cytotoxic activity of $CD8^+$ T cells in COVID-19 remains elusive, which are assessed in three ongoing clinical trials (17). Cytotoxic $CD8^+$ T cells in TBI mice were mostly infiltrated in the injured brain, which initiate the neuro-immune response after TBI, and these infiltrated T cells were effector resident memory T cells (18), while whether these cytotoxic cells resident in the injured mouse brain had a conserved phenotype in human patients needs to be validated in a spatial transcriptomics study.

Regarding the marker genes for cytotoxic immune cells, we found that the expression of CST7 increased in the peripheral blood while the expression of PPP2R2B and cytotoxic profiling decreased. CST7 has been previously reported to increase in Alzheimer's disease (AD) and as a cytotoxic marker for cytotoxic CD8 T cells in colorectal cancer with a hypomethylation status. We have previously shown that PPP2R2B as a subunit of protein phosphatase 2A had a decreased expression in brain injury animals (TBI model and three epilepsy models) (19, 20). Th17 cells are thought to drive the cytotoxicity of CD8+ T cells in brain insults (21), and increasing levels of IL-17 associated with worse neurological outcomes were found in the peripheral blood through 3 days after onset in stroke patients (22). Activated CD8+ T cells are proven to cause long-term neurological dysfunction in TBI mice (23), and depletion of CD8+ T but not B cells promotes neurological recovery following TBI. Interestingly, a current study from Xiong et al. reported that depletion of B cells is able to reduce the Aβ burden and cognitive impairment in AD mice (24). Although TBI is an independent risk factor for AD, these studies suggest that the heterogeneity of CNS and CD8+ T cells is also a biomarker in AD (13). Although these studies did not mention the source of infiltrated CD8+ T cells in TBI and B cells in AD, it could be predicted that these cells were from the peripheral system. In addition, almost no current studies have linked the immune cells with the coagulation function in brain insults. Based on our findings, it could also be proposed that the expanded peripheral CD8+ T cells might be involved in the progress of PTC. However, the exact role of cytotoxic CD8+ T cells and the neuro-immune interaction needs to be further confirmed in spatial transcriptomic and *in vivo* studies.

Meanwhile, we also showed that the peripheral CD4+ T cells decreased in TBI and correlated with the GCS score as well. To validate this, we first performed WGCNA for the chipset data and identified two modules (MEred and MEturquoise), which are positively and negatively correlated with the GCS score, coagulation dysfunction (Dysf), and Fg value (Figure S10A, B). The TOM graph shows that the most interacting modules were MSred and MEturquoise (Figure S10C) and the Fg value is mostly correlated with the MSred module (Figure S10D). Then, we selected genes from both modules to carry out pathway enrichment analysis and found that the turquoise module was mostly enriched in the T-cell receptor complex, T-cell activation, and lymphocyte differentiation, while the red module was dominantly enriched in neutrophil activation and neutrophil degranulation, which suggests a link between T cells and neutrophils (Figures S10E, F). To confirm this, we selected the CD4-related genes in the MEred module and listed both genes (from node in red and to node in blue color, Figure S10G). To explore the link between CD4 T cells and neutrophils, we crossed the CD4 nodes, CD4 gene marker, and neutrophil marker and found that only one gene was intersected, named MGST1, as a CD4 node and neutrophil marker, which is not a CD4 T-cell marker (Figure S10H). The mRNA expression of MGST1 in

human plasma was increased in the severe TBI group compared to the controls (Figure S10I, $p = 0.0161$). MGST1 (microsomal glutathione S-transferase 1) is considered to be an antioxidant molecule and has a neuroprotective role in suppressing ferroptosis *via* binding to ALOX5 (25). To validate this, we applied the cell–cell interaction study, and the interaction between ALOX5 and ALOX5AP was only found in the PTC group, but not in the control group (Figures S10J, K). In addition, we validated MGST1 as a marker gene for the neutrophil subgroup. From the tSNE analysis, we found that most subsets of neutrophils increased in TBI and PTC compared to the control group (Figures S11A, B). MGST1 is a marker gene for subset 8 (Figure S11C) and the expression of MGST1 was further validated (Figures S11D, E). This might indicate that the interaction between CD4 T cells and neutrophils is involved in the coagulation dysfunction in TBI and needs to be validated in laboratory experiments.

Collectively, a toxic expansion in CD8+ T cells was found to be associated with PTC development. This study only investigated potential biomarkers of PTC progression without a solid experimental validation; however, several immune markers here could be potential targets to reverse the PTC following TBI.

Data availability statement

The data presented in the study are deposited in the GEO repository, accession number GSE223245 (https://www.ncbi.nlm.nih.gov/geo/query/acc.cgi?acc=GSE223245). The datasets supporting the conclusions of this article are included within the article and Supplemental Information. The intersected marker genes for cytotoxic CD8+T, CD4+ T and NK cells are listed as Supple Intersected Markergenes.xlsx. The images with high-resolution were uploaded in the Jianguoyun as: https://www.jianguoyun.com/p/DSqdGXIQu7igCxjYge0EIAA.

Ethics statement

The studies involving human participants were reviewed and approved by the Ethics Committee of Shanghai Pudong New area People's Hospital (approval number 2021-K02). The patients/participants provided their written informed consent to participate in this study.

Author contributions

PZ and BZ participated in the study design. PZ, NZ, and DR collected PBMC samples and did data analyses. CY, QB, and YZ performed the clinical data analyses. PZ and WS wrote the manuscript. All the authors read and approved the final manuscript.

Funding

We acknowledge the funding from The Featured Clinical Discipline Project of Shanghai Pudong (PWYst2018-01) and the Key Discipline Group Construction Project of Shanghai Pudong (PWZxq2017-02).

Conflict of interest

The authors declare that the research was conducted in the absence of any commercial or financial relationships that could be construed as a potential conflict of interest.

Publisher's note

All claims expressed in this article are solely those of the authors and do not necessarily represent those of their affiliated organizations, or those of the publisher, the editors and the reviewers. Any product that may be evaluated in this article, or claim that may be made by its manufacturer, is not guaranteed or endorsed by the publisher.

Supplementary material

The Supplementary Material for this article can be found online at: https://www.frontiersin.org/articles/10.3389/fimmu.2022.1095657/full#supplementary-material

References

1. Maegele M, Schöchl H, Menovsky T, Maréchal H, Marklund N, Buki A, et al. Coagulopathy and haemorrhagic progression in traumatic brain injury: Advances in mechanisms, diagnosis, and management. *Lancet Neurol* (2017) 16:630–47. doi: 10.1016/s1474-4422(17)30197-7

2. Böhm JK, Güting H, Thorn S, Schäfer N, Rambach V, Schöchl H, et al. Global characterisation of coagulopathy in isolated traumatic brain injury (iTBI): A CENTER-TBI analysis. *Neurocrit Care* (2021) 35:184–96. doi: 10.1007/s12028-020-01151-7

3. Tong W-S, Zheng P, Xu J-F, Guo Y-J, Zeng J-S, Yang W-J, et al. Early CT signs of progressive hemorrhagic injury following acute traumatic brain injury. *Neuroradiology* (2011) 53:305–9. doi: 10.1007/s00234-010-0659-8

4. Tong W-S, Zheng P, Zeng J-S, Guo Y-J, Yang W-J, Li G-Y, et al. Prognosis analysis and risk factors related to progressive intracranial haemorrhage in patients with acute traumatic brain injury. *Brain Injury* (2012) 26:1136–42. doi: 10.3109/02699052.2012.666437

5. Innerhofer P, Fries D, Mittermayr M, Innerhofer N, von Langen D, Hell T, et al. Reversal of trauma-induced coagulopathy using first-line coagulation factor concentrates or fresh frozen plasma (RETIC): A single-centre, parallel-group, open-label, randomised trial. *Lancet Haematol* (2017) 4:e258–71. doi: 10.1016/s2352-3026(17)30077-7

6. Duque P, Calvo A, Lockie C, Schöchl H. Pathophysiology of trauma-induced coagulopathy. *Transfus Med Rev* (2021) 35:80–6. doi: 10.1016/j.tmrv.2021.07.004

7. Moore EE, Moore HB, Kornblith LZ, Neal MD, Hoffman M, Mutch NJ , et al. Trauma-induced coagulopathy. *Nat Rev Dis Primers* (2021) 7:29. doi: 10.1038/s41572-021-00270-5

8. Reale M, Carrarini C, Russo M, Dono F, Ferri L, Pietro MD, et al. Muscarinic receptors expression in the peripheral blood cells differentiate dementia with lewy bodies from alzheimer's disease. *J Alzheimer's Dis* (2022) 85:323–30. doi: 10.3233/jad-215285

9. Zheng P, Shu L, Ren D, Kuang Z, Zhang Y, Wan J. circHtra1/miR-3960/GRB10 axis promotes neuronal loss and immune deficiency in traumatic brain injury. *Oxid Med Cell Longev* (2022) 2022:3522492. doi: 10.1155/2022/3522492

10. Vento-Tormo R, Efremova M, Botting RA, Turco MY, Vento-Tormo M, Meyer KB, et al. Single-cell reconstruction of the early maternal–fetal interface in humans. *Nature* (2018) 563:347–53. doi: 10.1038/s41586-018-0698-6

11. Manno GL, Soldatov R, Zeisel A, Braun E, Hochgerner H, Petukhov V, et al. RNA Velocity of single cells. *Nature* (2018) 560:494–8. doi: 10.1038/s41586-018-0414-6

12. Miao Y, Zhang M, Nie Y, Zhao W, Huang B, Jiang Z, et al. Changes in T lymphocyte subsets after severe traumatic brain injury. *Neural Regener Res* (2007) 2:126–8. doi: 10.1016/s1673-5374(07)60028-0

13. Gate D, Saligrama N, Leventhal O, Yang AC, Unger MS, Middeldorp J, et al. Clonally expanded CD8 T cells patrol the cerebrospinal fluid in alzheimer's disease. *Nature* (2020) 577:399–404. doi: 10.1038/s41586-019-1895-7

14. Wang Y, Qi K, Cheng H, Cao J, Shi M, Qiao J, et al. Coagulation disorders after chimeric antigen receptor T cell therapy: Analysis of 100 patients with relapsed and refractory hematologic malignancies. *Biol Blood Marrow Tr* (2020) 26:865–75. doi: 10.1016/j.bbmt.2019.11.027

15. Hay KA, Hanafi L-A, Li D, Gust J, Liles WC, Wurfel MM, et al. Kinetics and biomarkers of severe cytokine release syndrome after CD19 chimeric antigen receptor–modified T-cell therapy. *Blood* (2017) 130:2295–306. doi: 10.1182/blood-2017-06-793141

16. Johnsrud A, Craig J, Baird J, Spiegel J, Muffly L, Zehnder J, et al. Incidence and risk factors associated with bleeding and thrombosis following chimeric antigen receptor T-cell therapy. *Blood Adv* (2021) 5:4465–75. doi: 10.1182/bloodadvances.2021004716

17. Perico L, Benigni A, Casiraghi F, Ng LFP, Renia L, Remuzzi G. Immunity, endothelial injury and complement-induced coagulopathy in COVID-19. *Nat Rev Nephrol* (2020) 17:1–19. doi: 10.1038/s41581-020-00357-4

18. Wojciechowski S, Virenque A, Vihma M, Galbardi B, Rooney EJ, Keuters MH, et al. Developmental dysfunction of the central nervous system lymphatics modulates the adaptive neuro-immune response in the perilesional cortex in a mouse model of traumatic brain injury. *Front Immunol* (2021) 11:559810. doi: 10.3389/fimmu.2020.559810

19. Shultz SR, Wright DK, Zheng P, Stuchbery R, Liu S-J, Sashindranath M, et al. Sodium selenate reduces hyperphosphorylated tau and improves outcomes after traumatic brain injury. *Brain* (2015) 138:1297–313. doi: 10.1093/brain/awv053

20. Liu S, Zheng P, Wright DK, Dezsi G, Braine E, Nguyen T, et al. Sodium selenate retards epileptogenesis in acquired epilepsy models reversing changes in protein phosphatase 2A and hyperphosphorylated tau. *Brain* (2016) 139:1919–38. doi: 10.1093/brain/aww116

21. Braun M, Vaibhav K, Saad N, Fatima S, Brann DW, Vender JR, et al. Activation of myeloid TLR4 mediates T lymphocyte polarization after traumatic brain injury. *J Immunol* (2017) 198:3615–26. doi: 10.4049/jimmunol.1601948

22. Selvaraj UM, Stowe AM. Long-term T cell responses in the brain after an ischemic stroke. *Discov Med* (2017) 24:323–33.

23. Daglas M, Draxler DF, Ho H, McCutcheon F, Galle A, Au AE, et al. Activated CD8+ T cells cause long-term neurological impairment after traumatic brain injury in mice. *Cell Rep* (2019) 29:1178–1191.e6. doi: 10.1016/j.celrep.2019.09.046

24. Xiong L-L, Xue L-L, Du R-L, Niu R-Z, Chen L, Chen J, et al. Single-cell RNA sequencing reveals b cell–related molecular biomarkers for alzheimer's disease. *Exp Mol Med* (2021) 53:1888–901. doi: 10.1038/s12276-021-00714-8

25. Kuang F, Liu J, Xie Y, Tang D, Kang R. MGST1 is a redox-sensitive repressor of ferroptosis in pancreatic cancer cells. *Cell Chem Biol* (2021) 28:765–775.e5. doi: 10.1016/j.chembiol.2021.01.006

COPYRIGHT

© 2023 Zheng, Zhang, Ren, Yu, Zhao, Bai, Zhang and Sun. This is an open-access article distributed under the terms of the Creative Commons Attribution License (CC BY). The use, distribution or reproduction in other forums is permitted, provided the original author(s) and the copyright owner(s) are credited and that the original publication in this journal is cited, in accordance with accepted academic practice. No use, distribution or reproduction is permitted which does not comply with these terms.

frontiers | Frontiers in Immunology

TYPE Original Research
PUBLISHED 09 March 2023
DOI 10.3389/fimmu.2023.1120894

Check for updates

OPEN ACCESS

EDITED BY
Bo Li,
Department of Orthopedics, Sun Yat-sen University, China

REVIEWED BY
Amanda Piquet,
University of Colorado Anschutz Medical Campus, United States
Luis Rafael Moscote-Salazar,
Latinamerican Council of Neurocritical Care (CLaNi), Colombia

*CORRESPONDENCE
Yimin Chen
drymchen@126.com
Zhanhang Wang
kedafu2005@sina.com
Yaqin Li
liyaqin@sysush.com

†These authors have contributed equally to this work

SPECIALTY SECTION
This article was submitted to Multiple Sclerosis and Neuroimmunology, a section of the journal Frontiers in Immunology

RECEIVED 10 December 2022
ACCEPTED 20 February 2023
PUBLISHED 09 March 2023

CITATION
Kuang Z, Baizabal-Carvallo JF, Mofatteh M, Xie S, Pan M, Ye J, Zhou L, Yang S, Wang Z, Chen Y and Li Y (2023) Meningoencephalitis associated with GAD65 autoimmunity. *Front. Immunol.* 14:1120894. doi: 10.3389/fimmu.2023.1120894

COPYRIGHT
© 2023 Kuang, Baizabal-Carvallo, Mofatteh, Xie, Pan, Ye, Zhou, Yang, Wang, Chen and Li. This is an open-access article distributed under the terms of the Creative Commons Attribution License (CC BY). The use, distribution or reproduction in other forums is permitted, provided the original author(s) and the copyright owner(s) are credited and that the original publication in this journal is cited, in accordance with accepted academic practice. No use, distribution or reproduction is permitted which does not comply with these terms.

Meningoencephalitis associated with GAD65 autoimmunity

Zuying Kuang[1†], José Fidel Baizabal-Carvallo[2,3†], Mohammad Mofatteh[4], Sifen Xie[1], Mengqiu Pan[1], Jinlong Ye[1], Lihua Zhou[1], Shuiquang Yang[5], Zhanhang Wang[1*], Yimin Chen[5*] and Yaqin Li[6*]

[1]Department of Neurology, GuangDong 999 Brain Hospital, Guangzhou, China, [2]Parkinson's Disease Center and Movement Disorders Clinic, Department of Neurology, Baylor College of Medicine, Houston, TX, United States, [3]Department of Sciences and Engineering, University of Guanajuato, León, Mexico, [4]School of Medicine, Dentistry and Biomedical Sciences, Queen's University Belfast, Belfast, United Kingdom, [5]Department of Neurology, Foshan Sanshui District People's Hospital, Foshan, Guangdong, China, [6]Department of Neurology, The Seventh Affiliated Hospital, Sun Yat-sen University, Shenzhen, Guangdong, China

Background: Encephalitis has been recognized in patients with autoimmunity related to the 65-kDa isoform of glutamic acid decarboxylase (GAD65) antibodies; however, patients with meningoencephalitis associated with those antibodies have been rarely identified in the medical literature. We aimed to define the frequency, clinical features, response to therapy, and functional outcomes of patients with meningoencephalitis associated with GAD antibodies.

Methods: We retrospectively studied consecutive patients attending a tertiary care center for evaluation of an autoimmune neurological disorder from January 2018 to June 2022. The modified Rankin Scale (mRS) was used to assess the functional outcome at the last follow-up.

Results: We evaluated 482 patients with confirmed autoimmune encephalitis during the study period. Four among the 25 patients with encephalitis related to GAD65 antibodies were identified. One patient was excluded owing to the coexistence of NMDAR antibodies. Three male patients aged 36, 24, and 16 years had an acute (n = 1) or subacute (n = 2) onset of confusion, psychosis, cognitive symptoms, seizures, or tremor. No patient had fever or clinical signs of meningeal irritation. Mild pleocytosis (<100 leukocytes/106) was identified in two patients, whereas one patient had normal CSF. Following immunotherapy with corticosteroids (n = 3) or intravenous immunoglobulin (n = 1), significant improvement was observed in all three cases, achieving a good outcome (mRS 1) in all cases.

Conclusion: Meningoencephalitis is an uncommon presentation of GAD65 autoimmunity. Patients present with signs of encephalitis but with meningeal enhancement and have good outcomes.

KEYWORDS

anti-glutamic acid decarboxylase, antibodies, encephalitis, autoimmunity, GAD65, meningoencephalitis

Introduction

The knowledge of autoimmunity related to the 65-kDa isoform of glutamic acid decarboxylase (GAD65), the enzyme that converts the excitatory glutamate to inhibitory gamma-aminobutyric acid (GABA), has markedly evolved in recent decades (1). Cerebellar ataxia, epilepsy, and stiff-person syndrome were clinical syndromes initially linked to the presence of these antibodies (Abs) (2, 3). However, in these cases, conspicuous brain or spinal cord inflammation is usually absent in neuroimaging studies. More recently, a small proportion of patients with GAD65 autoimmunity have been described with clinical and radiological signs of brain inflammation that may affect the limbic and/or extralimbic cortices (4). Parenchymal inflammation in such cases is believed to originate from an autoimmune cellular response, rather than a direct effect of GAD65 Abs.

Aseptic meningitis is characterized by the lack of an identifiable bacterial cause in cerebrospinal fluid (CSF) cultures (5). Viruses are the most common cause of aseptic meningitis (6). Among them, enteroviruses and varicella zoster virus are the most common (6). Selected patients with inflammatory or autoimmune diseases, including Still disease, systemic lupus erythematosus (SLE), sarcoidosis, Behçet's disease, Sjögren's syndrome, and periodic fever syndrome, have been identified with aseptic meningitis secondary to the underlying systemic disorder (5–10). In contrast, meningeal enhancement has been identified in patients with paraneoplastic or autoimmune encephalitis, specifically anti-*N*-methyl-D-aspartate receptor (NMDAR) encephalitis (11, 12). However, neuroimaging findings consistent with meningeal enhancement are rarely seen in patients with GAD65 autoimmunity.

In this study, we aimed to retrospectively characterize the frequency, clinical findings, response to therapy, and functional outcomes in patients with meningoencephalitis associated with GAD Abs. As patients with GAD65 encephalitis frequently present with inflammatory CSF, possibly reflecting meningeal inflammation, but without contrast enhancement on MRI, hence, we defined "meningoencephalitis" by the presence of patchy or diffuse contrast enhancement in the leptomeninges, supporting an inflammatory process disrupting the blood–brain barrier in these sites, with or without clinical or neuroimaging findings of brain parenchyma inflammation.

Methods

We retrospectively studied consecutive patients referred for evaluation at the Department of Neurology and Immunology of the GuangDong 999 Brain Hospital in Guangdong Province in the People's Republic of China, a tertiary care center for autoimmune neurological disorders from January 2018 to June 2022. Patients were enrolled if they had clinical and neuroimaging features of acute or subacute encephalitis attributed primarily to anti-GAD65 autoimmunity, owing to the presence of serum anti-GAD65 Abs and/or positive anti-GAD65 Abs in the CSF (13).

General assessment and follow-up

All patients underwent general and neurological examinations to assess for rheumatological or systemic inflammatory causes of meningitis. History of medication, illicit drug consumption, or poisoning was determined. Blood count, glucose, kidney, and liver function tests were performed to assess for evidence of metabolic derangement. The outcome was defined according to the modified Rankin Scale (mRS) determined at the last date of follow-up. The mRS scores were categorized as follows: 0, no symptoms; 1, total independence despite symptoms; 2, unable to carry all previous activities but look after own affairs; 3, requiring some help but able to walk without assistance; 4, unable to walk without assistance; 5, bedridden; and 6, death. A favorable outcome was defined as an mRS score between 0 and 2, while a poor outcome was defined as an mRS score of 3-5 at the last follow-up.

Antibody screening

We used commercially available cell-based assay or radioimmunoassay to check for anti-GAD65 Abs. Antibody screening ruled out anti-glial fibrillary acidic protein (GFAP), anti-NMDAR, anti-LGI1, anti-CASPR2, anti-$GABA_B$, anti-$GABA_A$, anti-GlyR, anti-AMPA, anti-DPPX, anti-DRD2, anti-IgLON5, anti-mGlutR1, anti-mGlutR5, anti-MOG, and anti-Neurexin-3.

Infectious disease screening

All patients underwent extensive diagnostic tests to rule out infectious causes. A lumbar puncture was performed in four patients and CSF was collected. Opening pressure was measured in all cases in the lateral decubitus position, with the legs and neck in a neutral position. Intracranial hypertension was considered in case the opening pressure was above 200 mmH_2O, whereas intracranial hypotension was considered in case the opening pressure was below 60 mmH_2O (14, 15). CSF samples were extensively assessed for white blood cells (WBC), proteins, and glucose levels using bacterial cultures and Gram stain. Acid-fast staining and India ink/cryptococcal antigen preparation were done in order to detect tuberculosis or *Cryptococcus neoformans*, respectively (16). Polymerase chain reaction was carried out in the CSF to assess for the presence of viral causes of meningitis. Hepatitis B (HBV), hepatitis C (HCV), and human immunodeficiency virus (HIV) type 1 and 2 serology were carried out in these patients.

Results

Among the 482 patients evaluated with confirmed autoimmune encephalitis during the study period, there were 25 patients with encephalitis associated with positive anti-GAD65 Abs. Four (16%)

of such patients had meningeal enhancement identified in the brain MRI. However, one patient, a 9-year-old girl with subacute headache and positive serum GAD65 Abs, was excluded from the study, owing to the presence of anti-NMDAR Abs in the CSF. The remaining three were all male patients, of Chinese origin, and between 16 and 36 years of age (Table 1). Extensive diagnostic studies ruled out metabolic, infectious, or drug-induced meningitis in all cases.

Case 1

A 36-year-old male patient presented for evaluation of a 3-month history of behavioral changes and poor sleep. There was no history of fever or seizures. The patient presented with episodes of odd behavior, restlessness, irritability, aggressiveness, and agitation. There were sporadic visual hallucinations. Neurological examination was remarkable for fluctuating mental confusion with disorientation and bilateral upper limb resting tremor. There was no focal paralysis. Nuchal rigidity and Kernig's and Brudzinski's signs were all negative. Brain MRI showed diffuse leptomeningeal enhancement with scattered non-enhancing hyperintensities in the white matter (Figures 1A, B). EEG showed diffuse slow waves in the bilateral frontal lobes and bilateral centrotemporal regions, mostly on the right side. Lumbar puncture revealed an opening pressure of 150 mmH_2O, and the CSF showed elevated WBC, 39 × 10^6/L (normal ≤5 × 10^6/L); lymphocytes, 74%; proteins, 0.28 g/L (normal: 0.15-0.45 g/L); and glucose, 3.4 mmol/L (range: 2.5-4 mmol/L). The patient had positive GAD65 Abs in the serum 1:10, but these Abs were negative in the CSF. Investigations for infectious causes were all negative. During the evaluation, the patient was diagnosed with type 2 diabetes mellitus with glycosylated hemoglobin (HbA1c) (8.6%) and received treatment with oral repaglinide and metformin. Treatment with progressively higher doses of risperidone did not provide benefit. However, marked clinical improvement was observed following treatment with oral methylprednisolone 40 mg per day for 2 weeks followed by progressively decreasing doses of 4 mg every week. The patient achieved an mRS score of 0 at the 16-month follow-up, after the onset of symptoms.

Case 2

A 24-year-old male patient came for evaluation of sudden onset of abnormal behavior and headache that started a few hours before the presentation. There was no history of a triggering event including poisoning or drug consumption. The patient and family denied fever or seizures. The clinical picture was characterized by severe, generalized, throbbing headache plus abnormal behavior with episodes of irritability, motor and language perseverance, disorientation, poor concentration, altered memory, and judgment. There were delusional thoughts, and the patient complained of being electrocuted, although no historical or clinical evidence of such an event was identified. Ritualistic behavior such as repetitive knocking on the wall was also present. There was evidence of insomnia and moderate anxiety. The neurological examination did not show a focal deficit; meningeal and cerebellar signs were negative. Cranial nerves were normal. Brain MRI showed extensive meningeal enhancement with a thickening of the tentorium more prominent on the right side. Brain parenchyma did not show abnormal hyperintensities or

TABLE 1 Summary of clinical and demographic features of GAD65 patients with meningeal enhancement.

Age/sex (Author)	Clinical manifestations	MRI	EEG	Therapy	Response to therapy
36/M (This report)	Behavioral changes, confusion, poor sleep, visual hallucinations	Diffuse leptomeningeal enhancement	Slow waves in bilateral frontal lobes and centrotemporal regions	Risperidone MTP 40 mg/day with progressive dose reduction	Complete recovery (mRS: 0) at 16 months
24/M (This report)	Behavioral changes, severe throbbing headache, delusional thoughts, cognitive disturbances, motor/language perseverance, insomnia	Diffuse leptomeningeal enhancement, thickening of the tentorium	Diffuse slow waves; epileptiform discharges in the bilateral frontal lobes and right temporal lobe	Olanzapine IVIg 20 g/day for 5 days MTP 40 mg/day with progressive dose reduction	Prominent recovery (mRS: 1) at 12 months
16/M (This report)	Sleepiness, fatigue, insomnia	Scattered line-like enhancement in intracranial sulci	N/A	IVIg 25 g/day for 5 days MTP 500 mg/day for 5 days, followed by prednisone with progressive dose reduction	Complete recovery (mRS: 0) at 10 months
21/F (Triplett 2018)	Seizures, coma	Leptomeningeal enhancement; bilateral frontal, insular, and temporal hyperintensities	Generalized slowing, left frontal epileptic activity	Antiepileptics; cyclophosphamide, rituximab, IVIg, MTP, mycophenolate mofetil, prednisone	Mild improvement
44/F (Salari 2022)	Cognitive symptoms and mental confusion	Hydrocephalus, meningeal enhancement[a]	N/A	MTP	Good recovery

F, female; IVIg, intravenous immunoglobulin; M, male; MTP, methylprednisolone; mRS, modified Rankin Scale; N/A, not available.
[a] Not observed in published neuroimaging.

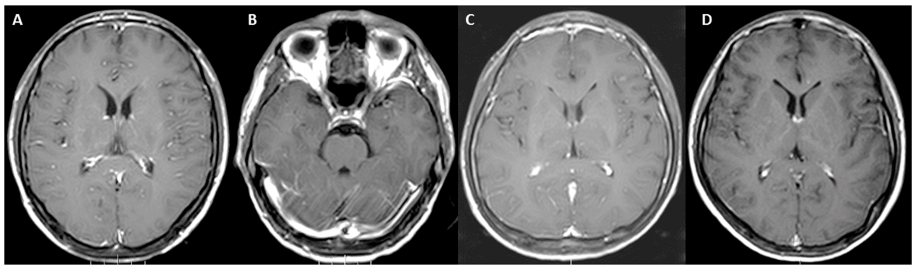


FIGURE 1
Contrast -enhanced brain MRIs of **(A, B)** case 1 show diffuse enhancement of the leptomeninges without abnormalities in the brain parenchyma. **(C)** Case 2 and **(D)** case 3 also show conspicuous and scattered enhancement, respectively of the leptomeninges.

contrast enhancement (Figure 1C). EEG showed diffuse slow waves; epileptiform discharges were identified in the bilateral frontal lobes and right temporal lobe. Lumbar puncture revealed an opening pressure of 120 mmH_2O, and cell count, proteins, and glucose levels were all normal in the CSF. Anti-GAD65 Abs were positive in the serum (1:30) and cerebrospinal fluid (1:10). The patient initially received variable doses of oral olanzapine with partial improvement. This was followed by a course of intravenous immunoglobulin (IVIg) 20 g per day for 5 days (total: 100 g) plus oral methylprednisolone 40 mg per day for 2 weeks followed by progressively decreasing doses of 4 mg every week. The patient achieved an mRS of 1 at the 12-month follow-up, after the onset of symptoms with a sporadic headache.

Case 3

A 16-year-old male patient presented for evaluation of a 20-day history of severe daytime sleepiness. There were no apparent precipitating events, and no recent history of fever, psychosis, mental confusion, behavioral changes, or seizures was recorded. The patient showed an increased propensity to fall asleep, poor responsiveness during episodes of sleeping, generalized fatigue, and night insomnia with sleep fragmentation. The neurological examination was consistent with normal cranial nerves. Muscle strength and tendinous reflexes were also normal. Babinski sign was negative, and there were no signs of meningeal irritation. Brain MRI showed a scattered line-like enhancement in the intracranial sulci. The right tentorium was thickened and showed contrast enhancement (Figure 1D). The lumbar puncture showed an opening pressure of 100 mmH_2O, and the CSF showed elevated WBC, 18 × 10^6/L (normal ≤5 × 10^6/L); lymphocytes, 70%; mildly elevated proteins, 1.14 g/L (normal: 0.15-0.45 g/L); and glucose, 3.2 mmol/L (range: 2.5-4 mmol/L). Anti-GAD65 Abs were positive in the serum (1:10), confirmed with radioimmunoassay with >2,000 U/ml, and in the cerebrospinal fluid (1:10). The patient received treatment with IVIg 25 g/day for 5 days and methylprednisolone 500 mg per day for 5 days followed by oral prednisone with progressively decreasing doses. The patient achieved an mRS score of 0 at the 10-month follow-up, after the onset of symptoms.

Discussion

In this study, we reported three patients with clinical–radiological findings consistent with meningoencephalitis. All three were male patients, despite the higher frequency of GAD65 autoimmunity in women (4). Reports of meningeal involvement defined as contrast enhancement in the leptomeninges in patients with GAD65 autoimmunity are very scarce. A 44-year- old female patient has been reported under the diagnosis of "meningoencephalitis" associated with GAD65 Abs, 1 month after receiving remdesivir for COVID-19 infection (Table 1). The CT scan showed hydrocephalus and some meningeal enhancement; however, it is unclear whether the findings were related to COVID-19 infection (17). On the other hand, Triplett and colleagues reported on a 21-year-old female patient with seizures and progressively decreased level of consciousness with MR showing leptomeningeal enhancement aside from prominent hyperintense lesions involving both frontal lobes (18). The patient showed clinical worsening despite the use of first-line immunosuppressive drugs but responded to cyclophosphamide and rituximab (18).

The question is whether our patients actually had a neurological disorder secondary to GAD65 Abs, as they had a relatively low titer of Abs. Case 3 had >2,000 U/ml in the serum by RIA. This is consistent with GAD65 Abs titers that are considered high according to Saiz and colleagues (13). It is possible that GAD65 Abs 1:10 reported in commercially available cell-based assay are consistent with titers over 2,000 U/ml by RIA. Low titers of GAD65 Abs have been detected in up to 1% of the general population and 5% with various neurological disorders (19); therefore, these Abs may coincide and be confused as the cause of a specific neurological disorder. For example, patients with some forms of viral meningitis (i.e., related to the enterovirus) or rheumatic disorders may have meningeal enhancement with a benign clinical course and response to corticosteroids. The suspected autoimmune basis in our patients is supported by the lack of identification of specific infectious agents, despite extensive evaluation, the absence of recent history of poisoning or drug consumption, and no identification of metabolic or rheumatic diseases in the follow-up. Moreover, there is emerging evidence that low titers of GAD65 Abs may be related to some neurological syndromes, such as cerebellar ataxia (3).

The pathological role of GAD65 Abs has been questioned, mostly as the target antigen is intracellular. In contrast, the role of cellular autoimmunity has been highlighted. There are few pathological reports in patients with GAD65 autoimmunity showing microglial proliferation and mild infiltration of $CD8^+$ cytotoxic T cells in the anterior horn cells of the spinal cord in a patient with stiff-person syndrome (20). On the other hand, in a pathological study of three cases with limbic encephalitis related to GAD65 encephalitis, parenchymal infiltration of $CD3^+$ T cells was low but higher than that of the controls, with intermediate infiltration of $CD8^+$ T cells between patients with autoimmunity related to onconeural and surface antigen Abs (21). Apposition of GrB^+ lymphocytes to single neurons and CD107a, a lysosomal-associated membrane protein-1, both markers of cytotoxic cell attack, were identified in a single patient with limbic encephalitis associated with GAD Abs (21). These findings were coupled with the loss of neural tissue but glial preservation, suggesting that a cytotoxic rather than a humoral response underlies the pathogenesis in these patients. Moreover, the ratio of CD8/CD3 in the perivascular space of blood vessels is lower than in the parenchyma, supporting the $CD8^+$ T-cell migration into the brain parenchyma (21). We speculate that a local cellular inflammatory response in the leptomeninges may occur disrupting the blood–brain barrier leading to contrast enhancement. This is supported by the presence of $CD3^+$ T cells in the leptomeninges in a patient with GAD65 meningoencephalitis (18).

Meningeal enhancement has been found in patients with anti-NMDAR encephalitis, which is the prototype of autoimmune encephalitis. In these patients, an abnormal MRI is observed in less than 50% of cases (11). However, among patients with abnormal MRIs, medial temporal and frontal hyperintensities in T2W and FLAIR sequences along with leptomeningeal enhancement are the most common findings (11). Evidence from cytokine dynamics suggests that patients with anti-NMDAR encephalitis have an early chemoattractant immune response despite the paucity of cellular T- and B-cell response identified in the brain parenchyma in most of these patients (22). Minimal inflammatory infiltrates in the leptomeninges have been identified in patients with anti-NMDAR encephalitis (23). It is unclear why patients with GAD65 encephalitis uncommonly present with meningeal enhancement. Similar to anti-NMDAR encephalitis, patients with GAD65 encephalitis may show a paucity of inflammatory T-cell infiltrates in the leptomeninges that appears during a specific time window during the evolution; however, further studies are required to confirm these findings.

None of our patients had positive anti-GFAP Abs; patients with autoimmunity associated with these Abs have a median age at onset of 44 years and are most commonly women (54%) (24). Perivascular radial enhancement perpendicular to the ventricles is one characteristic, and it has been detected in about half of the cases in some series; meningeal enhancement is also a distinctive feature (25). Patients with anti-GFAP Abs usually have a high number of cells in the CSF ($>50 \times 10^6$/L), which contrasts with the paucity of inflammatory response found in the CSF of patients with GAD65 autoimmunity. Moreover, a third of cases may have an underlying neoplasm (24), contrasting with the apparent low occurrence of cancer in patients with GAD65 autoimmunity.

The main limitation of our study is the lack of pathological specimens in order to assess the presence of lymphocyte infiltration in the meninges. However, justification of leptomeningeal biopsy may be questionable in a patient with aseptic meningitis showing rapid recovery with anti-inflammatory therapies. In this regard, the identification of CSF cytokines can be helpful in understanding the immunological dynamics of T and B cells, which may yield the type of immunological response in these patients.

Conclusion

In summary, a clinical picture characterized by the presence of signs of encephalitis combined with meningeal enhancement in the brain MRI but lack of fever and/or signs of meningeal irritation may be observed in patients with otherwise positive GAD65 Abs. These patients showed a rapid response to immunotherapy with a favorable outcome. Further studies should clarify the role of GAD65 autoimmunity in meningeal inflammation.

Data availability statement

The original contributions presented in the study are included in the article/supplementary material. Further inquiries can be directed to the corresponding authors.

Ethics statement

The studies involving human participants were reviewed and approved by the Guangdong999 Brain Hospital Institute Review Board. Written informed consent for participation was not required for this study in accordance with the national legislation and the institutional requirements. Written informed consent was not obtained from the individual(s) for the publication of any potentially identifiable images or data included in this article.

Author contributions

YC, JB-C, ZK, ZW, and YL designed the study and drafted the manuscript. All authors reviewed and approved the final manuscript.

Funding

This work was supported by grants from the Bureau of Science and Technology of Guangzhou Municipality (Grant No. 202201011583) and the National Natural Science Foundation of China (Grant No. 81901160).

Acknowledgments

The authors thank all their colleagues for the data collection and the patients for their contribution to this study.

Conflict of interest

The authors declare that the research was conducted in the absence of any commercial or financial relationships that could be construed as a potential conflict of interest.

Publisher's note

All claims expressed in this article are solely those of the authors and do not necessarily represent those of their affiliated organizations, or those of the publisher, the editors and the reviewers. Any product that may be evaluated in this article, or claim that may be made by its manufacturer, is not guaranteed or endorsed by the publisher.

References

1. Ali F, Rowley M, Jayakrishnan B, Teuber S, Gershwin ME, Mackay IR. Stiff-person syndrome (SPS) and anti-GAD-related CNS degenerations: Protean additions to the autoimmune central neuropathies. *J Autoimmun* (2011) 37(2):79–87. doi: 10.1016/j.jaut.2011.05.005

2. Solimena M, Folli F, Denis-Donini S, Comi GC, Pozza G, De Camilli P, et al. Autoantibodies to glutamic acid decarboxylase in a patient with stiff-man syndrome, epilepsy, and type I diabetes mellitus. *N Engl J Med* (1988) 318(16):1012–20. doi: 10.1056/NEJM198804213181602

3. Baizabal-Carvallo JF, Alonso-Juarez M. Cerebellar disease associated with anti-glutamic acid decarboxylase antibodies: review. *J Neural Transmission.* (2017) 124 (10):1171–82. doi: 10.1007/s00702-017-1754-3

4. Baizabal-Carvallo JF. The neurological syndromes associated with glutamic acid decarboxylase antibodies. *J Autoimmun* (2019) 101:35–47. doi: 10.1016/j.jaut.2019.04.007

5. Kaur H, Betances EM, Perera TB. Aseptic meningitis. In: *StatPearls*. Treasure Island (FL: StatPearls Publishing (2022).

6. Han SH, Choi HY, Kim JM, Park KR, Youn YC, Shin HW. Etiology of aseptic meningitis and clinical characteristics in immune-competent adults. *J Med Virol* (2016) 88(1):175–9. doi: 10.1002/jmv.24316

7. Bożek M, Konopko M, Wierzba-Bobrowicz T, Witkowski G, Makowicz G, Sienkiewicz-Jarosz H. Autoimmune meningitis and encephalitis in adult-onset still disease - case report. *Neurol Neurochir Pol* (2017) 51(5):421–6. doi: 10.1016/j.pjnns.2017.06.006

8. Baizabal-Carvallo JF, Delgadillo-Márquez G, Estañol B, García-Ramos G. Clinical characteristics and outcomes of the meningitides in systemic lupus erythematosus. *Eur Neurol* (2009) 61(3):143–8. doi: 10.1159/000186504

9. Cheok LH, Lee WWH, Cheng WM, Cheong YK, Teh CL. Aseptic meningitis as initial manifestation of systemic lupus erythematosus: Case series. *Lupus* (2022) 31 (3):373–7. doi: 10.1177/09612033221078213

10. Novroski AR, Baldwin KJ. Chronic autoimmune meningoencephalitis and periodic fever syndrome treated with anakinra. *Case Rep Neurol* (2017) 9(1):91–7. doi: 10.1159/000472147

11. Bacchi S, Franke K, Wewegama D, Needham E, Patel S, Menon D. Magnetic resonance imaging and positron emission tomography in anti-NMDA receptor encephalitis: A systematic review. *J Clin Neurosci* (2018) 52:54–9. doi: 10.1016/j.jocn.2018.03.026

12. Douma B, Ben Younes T, Benrhouma H, Miladi Z, Zamali I, Rouissi A, et al. Autoimmune encephalitis in Tunisia: Report of a pediatric cohort. *J Immunol Res* (2021) 2021:6666117. doi: 10.1155/2021/6666117

13. Saiz A, Blanco Y, Sabater L, González F, Bataller L, Casamitjana R, et al. Spectrum of neurological syndromes associated with glutamic acid decarboxylase antibodies: diagnostic clues for this association. *Brain* (2008) 131(10):2553–63. doi: 10.1093/brain/awn183

14. Khurana RK. Intracranial hypotension. *Semin Neurol* (1996) 16(1):5–10. doi: 10.1055/s-2008-1040953

15. Shahan B, Choi EY, Nieves G. Cerebrospinal fluid analysis. *Am Fam Physician.* (2021) 103(7):422–8.

16. Greenlee JE. Approach to diagnosis of meningitis. *Cerebrospinal fluid evaluation. Infect Dis Clin North Am* (1990) 4(4):583–98. doi: 10.1016/S0891-5520(20)30367-6

17. Salari M, Harofteh B, Etemadifar M. Autoimmune meningoencephalitis associated with anti-glutamic acid decarboxylase antibody following covid-19 infection: A case report. (2022). doi: 10.22541/au.165086648.83240713/v1

18. Triplett J, Vijayan S, MacDonald A, Lawn N, McLean-Tooke A, Bynevelt M, et al. Fulminant anti-GAD antibody encephalitis presenting with status epilepticus requiring aggressive immunosuppression. *J Neuroimmunol.* (2018) 323:119–24. doi: 10.1016/j.jneuroim.2018.06.013

19. Meinck HM, Faber L, Morgenthaler N, Seissler J, Maile S, Butler M, et al. Antibodies against glutamic acid decarboxylase: Prevalence in neurological diseases. *J Neurol Neurosurg Psychiatry* (2001) 71(1):100–3. doi: 10.1136/jnnp.71.1.100

20. Holmøy T, Skorstad G, Røste LS, Scheie D, Alvik K. Stiff person syndrome associated with lower motor neuron disease and infiltration of cytotoxic T cells in the spinal cord. *Clin Neurol Neurosurg* (2009) 111(8):708–12. doi: 10.1016/j.clineuro.2009.06.005

21. Bien CG, Vincent A, Barnett MH, Becker AJ, Blümcke I, Graus F, et al. Immunopathology of autoantibody-associated encephalitides: Clues for pathogenesis. *Brain* (2012) 135(Pt 5):1622–38. doi: 10.1093/brain/aws082

22. Liba Z, Kayserova J, Elisak M, Marusic P, Nohejlova H, Hanzalova J, et al. Anti-N-methyl-D-aspartate receptor encephalitis: the clinical course in light of the chemokine and cytokine levels in cerebrospinal fluid. *J Neuroinflammation.* (2016) 13(1):55. doi: 10.1186/s12974-016-0507-9

23. Tüzün E, Zhou L, Baehring JM, Bannykh S, Rosenfeld MR, Dalmau J. Evidence for antibody-mediated pathogenesis in anti-NMDAR encephalitis associated with ovarian teratoma. *Acta Neuropathol.* (2009) 118(6):737–43. doi: 10.1007/s00401-009-0582-4

24. Flanagan EP, Hinson SR, Lennon VA, Fang B, Aksamit AJ, Morris PP, et al. Glial fibrillary acidic protein immunoglobulin G as biomarker of autoimmune astrocytopathy: Analysis of 102 patients. *Ann Neurol* (2017) 81(2):298–309. doi: 10.1002/ana.24881

25. Shan F, Long Y, Qiu W. Autoimmune glial fibrillary acidic protein astrocytopathy: A review of the literature. *Front Immunol* (2018) 9:2802. doi: 10.3389/fimmu.2018.02802

frontiers | Frontiers in Immunology

TYPE Original Research
PUBLISHED 05 April 2023
DOI 10.3389/fimmu.2023.1105432

Check for updates

OPEN ACCESS

EDITED BY
Guangzhi Ning,
Tianjin Medical University General Hospital, China

REVIEWED BY
Nunzio Vicario,
University of Catania, Italy
C Jane Reeson Welsh,
Texas A&M University, United States
Andrew J. Steelman,
University of Illinois at Urbana-Champaign, United States

*CORRESPONDENCE
Wolfgang Baumgärtner
wolfgang.baumgaertner@tiho-hannover.de

SPECIALTY SECTION
This article was submitted to Multiple Sclerosis and Neuroimmunology, a section of the journal Frontiers in Immunology

RECEIVED 22 November 2022
ACCEPTED 20 March 2023
PUBLISHED 05 April 2023

CITATION
Hülskötter K, Lühder F, Leitzen E, Flügel A and Baumgärtner W (2023) CD28-signaling can be partially compensated in CD28-knockout mice but is essential for virus elimination in a murine model of multiple sclerosis. *Front. Immunol.* 14:1105432. doi: 10.3389/fimmu.2023.1105432

COPYRIGHT
© 2023 Hülskötter, Lühder, Leitzen, Flügel and Baumgärtner. This is an open-access article distributed under the terms of the Creative Commons Attribution License (CC BY). The use, distribution or reproduction in other forums is permitted, provided the original author(s) and the copyright owner(s) are credited and that the original publication in this journal is cited, in accordance with accepted academic practice. No use, distribution or reproduction is permitted which does not comply with these terms.

CD28-signaling can be partially compensated in CD28-knockout mice but is essential for virus elimination in a murine model of multiple sclerosis

Kirsten Hülskötter[1], Fred Lühder[2], Eva Leitzen[1], Alexander Flügel[2] and Wolfgang Baumgärtner[1]*

[1]Department of Pathology, University of Veterinary Medicine Hannover, Foundation, Hannover, Germany, [2]Institute for Neuroimmunology and Multiple Sclerosis Research (IMSF), University Medical Center Goettingen, Goettingen, Germany

The intracerebral infection of mice with Theiler's murine encephalomyelitis virus (TMEV) represents a well-established animal model for multiple sclerosis (MS). Because CD28 is the main co-stimulatory molecule for the activation of T cells, we wanted to investigate its impact on the course of the virus infection as well as on a potential development of autoimmunity as seen in susceptible mouse strains for TMEV. In the present study, 5 weeks old mice on a C57BL/6 background with conventional or tamoxifen-induced, conditional CD28-knockout were infected intracerebrally with TMEV-BeAn. In the acute phase at 14 days post TMEV-infection (dpi), both CD28-knockout strains showed virus spread within the central nervous system (CNS) as an uncommon finding in C57BL/6 mice, accompanied by histopathological changes such as reduced microglial activation. In addition, the conditional, tamoxifen-induced CD28-knockout was associated with acute clinical deterioration and weight loss, which limited the observation period for this mouse strain to 14 dpi. In the chronic phase (42 and 147 dpi) of TMEV-infection, surprisingly only 33% of conventional CD28-knockout mice showed chronic TMEV-infection with loss of motor function concomitant with increased spinal cord inflammation, characterized by T- and B cell infiltration, microglial activation and astrogliosis at 33-42 dpi. Therefore, the clinical outcome largely depends on the time point of the CD28-knockout during development of the immune system. Whereas a fatal clinical outcome can already be observed in the early phase during TMEV-infection for conditional, tamoxifen-induced CD28-knockout mice, only one third of conventional CD28-knockout mice develop clinical symptoms later, accompanied by ongoing inflammation and an inability to clear the virus. However, the development of autoimmunity could not be observed in this C57BL/6 TMEV model irrespective of the time point of CD28 deletion.

KEYWORDS

conventional CD28-knockout, conditional CD28-knockout, multiple sclerosis (MS) disease, Theiler's murine encephalomyelitis virus (TMEV), immunology & infectious diseases, neuroimmunology and neuropathology

1 Introduction

The intracerebral inoculation with Theiler's murine encephalomyelitis virus (TMEV) is a widely used, infectious model for neuro-inflammatory and -degenerative diseases like multiple sclerosis (MS) or epilepsy in humans (1). Susceptibility and outcome of a TMEV-infection in mice is genetically defined by the host (2). Infection of the central nervous system (CNS) is also influenced by the virus strain and as importantly, disease progression and virus spread within the nervous tissue from the cerebrum to the spinal cord is associated with changes in cell tropism (2–5). TMEV shows a strong tropism to neurons during the acute phase, which is followed by a predominant infection of glial cells and macrophages in the chronic phase of infection after three to four weeks (2–8). Briefly, the acute phase of the TMEV-infection is related to a direct virus-mediated effect predominantly on neurons and characterized by a transient encephalitis that lasts about two to three weeks after intracerebral infection in most mouse strains (1, 9). In resistant C57BL/6 mice the acute phase of TMEV-infection is restricted to the brain, especially the hippocampus, and these animals are able to eliminate the virus from the CNS within about two weeks (9). In susceptible mouse strains with an insufficient anti-viral immune response, like SJL mice, the acute phase is followed by a chronic phase, characterized by virus spread into the spinal cord and persistent TMEV-infection with concomitant development of a progressive demyelinating disease (TMEV-IDD), resembling progressive MS (1, 9). The alterations seen in the chronic phase are caused by immune-mediated tissue damage and infection of glial cells and macrophages (2–8). Thus, the division into an acute and chronic phase is not only based on the pathomorphological changes in the CNS, but also characterized by a changing cell tropism of the virus and underlying pathogenetic mechanisms (2–5).The clearance of a pathogen is critically dependent on a functioning immune system. For a virus infection, especially cytotoxic $CD8^+$ T cells and NK cells are significantly involved, but the function of these cells is also embedded in the general context of a healthy immune system, involving antigen-presenting cells of the myeloid lineage as important cells for T cell activation and also T-helper cells for assisting the $CD8^+$ cytotoxic response. The co-stimulatory molecule CD28 is considered the most important accessory molecule for the activation of naïve T cells (10–13). CD28 is first expressed on T cells during the β-selection in the thymus (14, 15) and keeps up its regulatory functions until the exhaustion of the T cell (16). When the CD28-mediated co-stimulatory signal is missing, T cells are unable to be fully activated and to differentiate and are becoming anergic instead. Beside its function in activation and differentiation of effector T cells, CD28 is also found to be critically involved in the maintenance of regulatory T cells (17–19). In 1993, a conventional CD28-knockout mouse was published missing the co-stimulatory molecule in all cells through all stages of life (20). These mice have some defects in germinal center reactions and antibody class switch recombination, but in principle are still able to mount cytotoxic T cell responses to certain viruses (20). Additionally, they exhibit a normal susceptibility to Leishmania major and are able to mount Th1 and Th2 responses (21). However, knockout of CD28 or blockade of CD28 with specific antibodies prevents the development of autoimmunity such as experimental autoimmune encephalitis (EAE) in rodents (22–24), and rhesus monkeys (25) or collagen-induced arthritis (26). The caveat in using conventional CD28-knockout mice is that adaptation mechanisms could have taken place where either other co-stimulatory receptors take over the function of CD28 or a different T cell repertoire with a different overall affinity/avidity of the T cell receptor (TCR) is selected in the thymus, changing the sensitivity of effector T cells for the requirement of co-stimulation during activation/differentiation. To overcome this problem, conditional CD28-knockout mice have been generated in which CD28 can be deleted pharmaceutically (27). These mice show normal expression of CD28 until administration of the inductive agent, like tamoxifen for activation of a modified estrogen receptor-coupled cre-recombinase (cre). This enables to define the exact time point of loss of CD28 expression in these mice without the problems of aberrant T cell selection in the thymus.

For human autoimmune diseases, aberrations of CD28-expression appears to influence the risk for MS relapses (28) as well as severity of Crohn's disease (29). In addition, it was hypothesized that if a chronic virus infection of the CNS is involved in the disease pathology, as recently proposed for MS (30, 31), a downregulation of the immune response might be disadvantageous for the host. However, beside the "molecular mimicry" hypothesis (32) for the involvement of pathogens in the pathogenesis of autoimmune diseases, it is currently unknown how pathogens could contribute to their development.

In the present study we investigated how mice with a constitutive ($CD28^{-/-}$; further named CD28KO) or conditional deletion of CD28 ($CD28^{-/flox}$ $Cre^{+/-}$; further named Cre) are able to deal with a TMEV-infection in comparison to controls without Cre-expression ($CD28^{-/flox}$ $Cre^{-/-}$; further named B6) and to controls without tamoxifen administration. It could be shown that the CD28 knockout renders genetically resistant mice susceptible for chronic TMEV-infection reflected by persistent virus presence, modified immune responses and histopathological changes within the CNS.

2 Materials and methods

2.1 Mice and housing

Conditional CD28-knockout mice with cre-expression ($CD28^{-/flox}$ $Cre^{+/-}$; Cre) and without cre-expression ($CD28^{-/flox}$ $Cre^{-/-}$; B6) (27) as well mice with a conventional CD28 knockout ($CD28^{-/-}$; CD28KO) (20) on a C57BL/6 background were bred at the central animal facility of the Institute for Multiple Sclerosis Research (IMSF), University of Göttingen. The study took place in the Department for Pathology of the University of Veterinary Medicine Hannover, where the mice were housed in individual ventilated cages (IVC) with ad libitum access to water and food (ssniff Spezialdiäten GmbH, DE- 59494 Soest, cat. V1534-000). All experiments were performed in accordance with German law and approved by the Lower Saxony State Office for Consumer Protection and Food Safety as the responsible authority

(Niedersächsisches Landesamt für Verbraucherschutz- und Lebensmittelsicherheit (LAVES), Oldenburg, Germany; permission number: -17/2418).

2.2 Induction of CD28-knockout

The knockout of CD28 was induced in Cre-expressing FEC2/FLCK CD28KO mice ($CD28^{-/flox}$ $Cre^{+/-}$) by three oral gavages of tamoxifen (3 mg tamoxifen/100µl rapeseed oil) at 5, 7 and 9 dpi, using a flexible 20 G feeding tube (Instech, cat. FTP-20-38-50) as described before (4).

2.3 TMEV-infection

All mice of the study were infected intracerebrally at the age of five weeks with 20µl of a TMEV-BeAn-1-TiHo cell culture supernatant of $2.7x10^7$ plaque-forming units (PFU)/ml (infective dose of $5.4x10^5$ PFU) under injection-anesthesia as described before (33).

2.4 Study design

2.4.1 Acute phase of infection

To study the acute phase of TMEV-infection, mice with conventional innate (CD28KO) and tamoxifen-induced, conditional knockout (Cre-Tam) of CD28 were infected intracerebrally at the age of five weeks. The conditional knockout was induced 5 days post infection (dpi) in Cre-Tam mice by oral gavages of tamoxifen at 5, 7 and 9 dpi. Clinical scoring and motor tests (RotaRod) were performed weekly. The mice were sacrificed at 14 dpi. Control animals without CD28 knockout were treated accordingly.

As controls for the wild type-phenotype mice with loxP-flanked exons 2 and 3 of CD28 (flox) without expression of cre-recombinase ($CD28^{-/flox}$ $Cre^{-/-}$, further named: B6) were used (27). Additionally, $CD28^{-/flox}$ $Cre^{-/-}$ animals without tamoxifen application (nT) were involved in this study, since tamoxifen is known to influence the immune response after TMEV-infection (4, 34).

The genotypes, number of animals and information about infection, Tam application and necropsy are presented in Table 1.

2.4.2 Chronic phase of infection

For investigations on the chronic TMEV-infection, only mice with conventional innate CD28-knockout (CD28KO) were used. Due to detrimental effects of the induced conditional CD28-knockout on the clinical score of the Cre-Tam mice, these animals were not included in the long-term studies for animal welfare reasons. Of the mice with conventional CD28-knockout (CD28KO) planned for necropsy at 42 dpi (n=6) and 147 dpi (n=6, data not shown), one third (n= 4 out of 12) developed motoric deficiencies starting at 21-33 dpi. These four mice were thus evaluated separately as 'responders' (CD28KO-R). Two of the four CD28KO-R mice developed hind limb paresis and were immediately euthanized for humane reasons at 33 (n=1) or 35 dpi (n=1), respectively. Two of the four CD28KO-R mice showed only mild to moderate clinical signs and thus reached the scheduled necropsy date at 42 dpi (n=2). The CD28KO-R group was thus composed of n=4 animals euthanized at 33 (n=1), 35 (n=1) and 42 dpi (n=2). These were compared to the CD28KO mice without clinical signs (n=4) and controls without tamoxifen application (B6-nT, n=6), all sacrificed at 42 dpi. Remaining CD28KO mice that did not show clinical signs until 42 dpi (n=4) as well as further B6-nT control mice (n=7) did not develop any clinical signs until 147 dpi (endpoint of investigation). At 147 dpi, there was no difference in clinical as well as histological data between these animals (data not shown). The genotypes, number of animals and information about infection, Tam application and necropsy are presented in Table 2.

2.5 Clinical scoring, RotaRod®

Mice were visually inspected daily; clinical scoring (appearance [0-3], activity [0-3], gait [0-4]) and RotaRod®-testing for motor skills were performed weekly as described (4). The intervals of clinical scoring were increased according to the animals' clinical signs as described before (4).

TABLE 1 Overview of conditional and conventional CD28-knockout mice investigated in the early phase of TMEV-infection at 14 dpi, including the group names, genetic background, age at TMEV-infection, days of oral tamoxifen application, number of animals, information about CD28 knockout status and/or induction, day of necropsy after TMEV infection.

Group name	Genetic background	Age at TMEV infection	Tamoxifen application (dpi)	Number of animals	CD28 KO	Necropsy (dpi)
B6-nT	$CD28^{-/flox}$ $Cre^{-/-}$	5 weeks	None	6	No	14 dpi
B6-Tam	$CD28^{-/flox}$ $Cre^{-/-}$	5 weeks	5, 7 and 9 dpi	10	No	14 dpi
CD28KO	$CD28^{-/-}$	5 weeks	None	6	Yes	14 dpi
Cre-Tam	$CD28^{-/flox}$ $Cre^{+/-}$	5 weeks	5, 7 and 9 dpi	17	Yes	14 dpi

B6, mice without Cre expression (conditional CD28-knockout cannot be induced by tamoxifen); Cre, mice with cre-recombinase expression (conditional CD28-knockout can be induced by tamoxifen); CD28KO, mice with conventional; innate CD28-knockout; nT, mice without Cre expression and without tamoxifen application; Tam, oral tamoxifen application 5; 7 and 9 days post infection; TMEV, Theiler's murine encephalomyelitis virus; dpi, days post TMEV infection.

TABLE 2 Overview of conventional CD28-knockout mice in the investigation on the chronic phase of TMEV-infection at 33-42 dpi, including the group names, genetic background, age at TMEV-infection, days of oral tamoxifen application, number of animals, information about CD28 knockout status, day of necropsy after TMEV infection.

Group name	Genetic background	Age at TMEV infection	Tamoxifen application	Number of animals	CD28 KO	Necropsy (dpi)
B6-nT	$CD28^{-/flox}$ $Cre^{-/-}$	5 weeks	None	6	No	42 dpi
CD28KO	$CD28^{-/-}$	5 weeks	None	4	Yes	42 dpi
CD28KO-R	$CD28^{-/-}$	5 weeks	None	4	Yes	33,35 and 42 dpi
B6-nT	$CD28^{-/flox}$ $Cre^{-/-}$	5 weeks	None	7	No	147 dpi
CD28KO	$CD28^{-/-}$	5 weeks	None	4	Yes	147 dpi

B6-nT, mice without Cre expression and without tamoxifen application; CD28KO, mice with conventional innate CD28-knockout without motoric deficiencies; CD28KO-R, mice with conventional innate CD28-knockout and motor deficiencies (responders); TMEV, Theiler's murine encephalomyelitis virus; wpp. weeks post-partum; dpi, days post TMEV infection.

2.6 Necropsy

Animals were sacrificed at 14 (n=39), 42 (n=12) or 147 (n= 11, data not shown) days post infection (dpi). Mice with CD28 knockout that reached the pre-defined termination criteria (weight loss ≥ 20%, high clinical scores, paralysis of limbs) were euthanized for humane reasons at 14 (Cre-Tam), 33 (n=1) and 35 (n=1) dpi (CD28KO-R). After euthanasia, mice were perfused with phosphate buffered saline (PBS) at a flow rate of 3.75 ml/min through the left ventricle. Brain, spinal cord, thymus, spleen, and intestine were removed and fixed in 4% formaldehyde solution followed by paraffin embedding.

2.7 Histology and immunohistochemistry – staining and scoring

For histology and immunohistochemistry, the formalin-fixed, paraffin-embedded (FFPE) tissue was cut to 2 µm thick sections and mounted on glass slides (Thermo Scientific, Superfrost® Plus, cat. J1800AMNZ). Hematoxylin-eosin (HE) stained sagittal sections of the brain were divided into 10 regions (as seen in Supplementary Figure S1) and scores (0-3) for hyper-cellularity, perivascular infiltration, meningeal infiltration, vacuolization, and neuronal/axonal damage (4, 35) were added up. The scores (0-3) for hyper-cellularity in the white matter, the grey matter, perivascular infiltration, vacuolization and meningeal infiltration from three spinal cord segments (cervical, thoracic, and lumbar) each divided into 6 regions (left/right, dorsal, middle and ventral) were added up for every animal.

Immunohistochemistry was performed applying the avidin-biotin complex (ABC)-method with 3,3'-diaminobenzidine (DAB)-labelling as described before (36). The pretreatment and concentrations of primary antibodies are presented in Table 3 below:

For morphometry and figures, stained sections were scanned with extended focal image (EFI) on an Olympus Slide Scanner VS200. Tissue detection was done by thresholding (CellSens, ImageJ). Positive stained areas and cell counts were obtained according to the requirements by manual counting on glass slides (TMEV, CD45R, Caspase 3, beta amyloid precursor protein [beta-APP], S100A10) or applying a neural network (CD3 [Olympus cellSens imaging software VS200]) trained on respective tissue to detect the cell numbers per area. Brain and spinal cord sections with glial markers (ionized calcium-binding adapter molecule 1 [Iba-1] and glial fibrillary acidic protein [GFAP]) were digitalized (VS200) followed by thresholding and automatic detection of the percentage of positive areas (ImageJ, QuPath) to account for changes in cell volumes during the inflammatory response. The cell numbers and positive areas were evaluated on one sagittal brain section (including all 10 regions as defined above) or three spinal cord sections (cervical, thoracic, lumbar) combined into one evaluated area, respectively.

2.8 Figures, graphs and statistics

Photographs for the figures were obtained from scanned slides (VS200) and edited with GIMP 2.10.32 (GNU Image Manipulation Program). Graphs were created with Graphpad Prism (Graphpad Software Inc.) and show scatter plots (one dot per animal) with median (black bar) and 95% confidence intervals (black error bars). Statistical analyses were conducted using SPSS for Windows TM v. 27 (IBM® SPSS® Statistics, SPSS Inc., Chicago, IL, United States). Data were analyzed for normal distribution using the Shapiro–Wilk test. Significant differences between the groups were investigated *via* Kruskal–Wallis tests followed by Dunn–Bonferroni *post hoc* testing with correction of significance levels for multiple testing. Corrected p-values of ≤ 0.05 were recognized as statistically significant and indicated by an asterisk (*) within the graphs. Figures of multiple panels were generated with GIMP and Inkscape 1.2 (Inkscape Community).

3 Results

3.1 Conditional and conventional CD28-knockout mice are unable to eliminate the virus during the acute phase (14 dpi) of a TMEV-infection

Mice with tamoxifen-induced, conditional knockout of CD28 (Cre-Tam) showed a marked loss of body weight between 7 and 14 dpi (Figure 1A). Additionally, only Cre-Tam mice showed significantly increased clinical scores (Figure 1B) but without measurable effects on their RotaRod performance (Figure 1C) at 14 dpi.

10.3389/fimmu.2023.1105432

TABLE 3 List of antibodies for immunohistochemistry.

Abbre-viation	Primary antibody	Company, #cat-no.	Concentration of primary antibody	Pretreatment	Blocking	Secondary antibody (1:200)	Company, cat-no#2
Beta-APP	Anti-APP A4 Mouse mAb, clone 22C11	Merck, #MAB348	1:2000	20 min. microwave, citrate buffer (pH 6)	Goat-serum	Biotinylated-goat-anti-mouse IgG	Vector, #BA9200
Caspase 3	Anti-cleaved caspase 3 (Asp175) Rabbit pAb	Cell Signaling, #9661	1:200	20 min. microwave, citrate buffer (pH 6)	Goat-serum	Biotinylated-goat-anti-rabbit IgG	Vector, #BA1000
CD3	Anti-human CD3 Rabbit pAb	Dako, #A0452	1:250	20 min. microwave, citrate buffer (pH 6)	Goat-serum	Biotinylated-goat-anti-rabbit IgG	Vector, #BA1000
CD45R	Biotinylated-anti mouse CD45R/B220 Rat mAb	BD Pharmin-gen, #553085	1:1000	20 min. microwave, citrate buffer (pH 6)	None	None	None
GFAP	Anti-cow GFAP Rabbit pAb	Agilent, #Z033429-2	1:1000	None	Goat-serum	Biotinylated-goat-anti-rabbit IgG	Vector, #BA1000
Iba-1	Anti-Iba1 Rabbit pAb	Wako, #019-19741	1:500	None	Goat-serum	Biotinylated-goat-anti-rabbit IgG	Vector, #BA1000
S100A10	Anti- S100A10 Rabbit mAb	Bio Techne, #Ab JF0987	1:100	None	Goat-serum	Biotinylated-goat-anti-rabbit IgG	Vector, #BA1000
TCF-1	Anti-TCF1/TCF7 (CD63D9) Rabbit mAb	Cell Signaling, #2203	1:1000	20 min. microwave, citrate buffer (pH 6)	Goat-serum +1% BSA +0,1% Triton X	Biotinylated-goat-anti-rabbit IgG	Vector, #BA1000
TMEV	Anti-TMEV Rabbit pAb	(30)	1:2000	None	Goat-serum	Biotinylated-goat-anti-rabbit IgG	Vector, #BA1000

APP, amyloid precursor protein (marker for axonal damage); caspase 3 (marker for apoptotic cells), CD3 (T cell marker), CD45R (B cell marker), GFAP, glial fibrillary acidic protein (astrocyte marker); Iba-1, ionized calcium-binding adapter molecule 1 (marker for macrophages and microglia); S100A10 (marker for neurotrophic astrocytes); TCF, T cell factor (naïve T cell marker); TMEV, Theiler's murine encephalomyelitis virus; mAb, monoclonal antibody; pAb, polyclonal antibody.

Histopathological examination of the brain and spinal cord revealed that the sum score in HE-stained brain sections is significantly lower in Cre-Tam mice compared to the B6-Tam controls without CD28 deletion (Figures 2A, B). Inflammation within the spinal cord was most apparent within the lumbar region of all mouse strains (Figure 2A). Concerning the virus clearance, there were also differences between the groups. Whereas B6 mice without tamoxifen administration (B6-nT) completely cleared the virus by 14 dpi as expected (Figure 2C, upper left), mice with tamoxifen application (B6-Tam) still show virus antigen within the brain at 14 dpi (Figure 2C, upper right), as reported before (28). Virus persistence was also seen in both mouse strains in which CD28 had been deleted (Figures 2C, D). Remaining TMEV-antigen was detected preferably within the hippocampus of mice without CD28 knockout but tamoxifen application (B6-Tam), while in both mouse strains with CD28-knockout (CD28KO, Cre-Tam), the antigen was more likely to be spread over more brain regions, except for the olfactory bulb, forebrain, and cerebellum (Supplementary Figure S1). Highest numbers of TMEV-antigen positive cells were detected within the cerebral cortex, hippocampus and thalamus of both CD28-knockout strains (Supplementary Figure S1). Furthermore, only in mice with CD28-knockout (Cre-Tam, CD28KO), an unexpected virus spread into the spinal cord was seen (Figure 2D).

Immunohistochemical assessment of the local immune response by counting infiltrating immune cells into the CNS revealed significant differences in the T- and B cell response as well as microglial activation. It was observed that mice with conditional, tamoxifen-induced CD28-knockout mice (Cre-Tam, Figure 3A, lower right) showed increased T cell infiltration into the brain (Figure 3B). The T cell infiltration in B6-nT mice without tamoxifen application (Figure 3A, upper left) and animals with conventional CD28-knockout (Figure 3A, lower left) were at similarly low levels, despite the presence of TMEV-antigen in the CNS in the CD28KO mice. Within the spinal cord, there were no significant differences in T cell infiltration between the groups at 14 dpi (Figure 3B). The number of B cells in B6-nT mice without tamoxifen application (Figure 3C, upper left) and mice with conventional CD28-knockout (Figure 3C, lower left) were, as seen for T cell infiltration, at comparable levels (Figure 3D). Contrary to T cells, the B cell infiltration showed the opposite trend with non-significantly reduced B cell numbers in tamoxifen-treated B6-Tam mice (Figure 3C, upper right) and significantly reduced B cell numbers in Cre-Tam mice with conditional CD28 knockout (Figure 3C, lower right) in both the

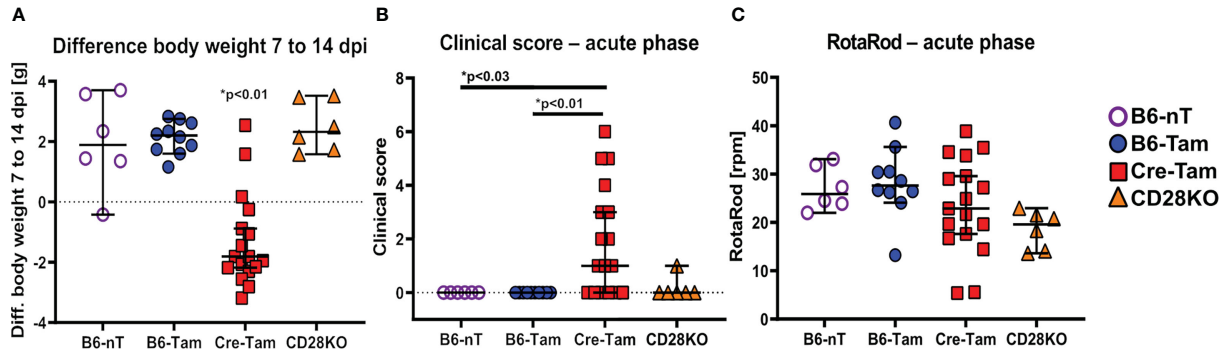


FIGURE 1
(A-C) Assessment of general parameters and clinical score during the acute phase of a Theiler's murine encephalomyelitis virus (TMEV)-infection at 14 days post infection (dpi). **(A)** Mice with tamoxifen-induced CD28-knockout (Cre-Tam, n=17) show a significant loss of the body weight within the second week of infection (7 to 14 dpi). **(B)** At 14 dpi, the clinical score of Cre-Tam mice (n=17) is significantly increased compared to B6-nT (n=6) and B6-Tam (n=10) controls. **(C)** RotaRod-performance was similar and lacked significant differences between the groups at 14 dpi. Graphs show scatter plots (one dot per animal) with median (black bar) and 95% confidence intervals (black error bars). Statistically significant p-values are depicted within the graphs (Kruskal-Wallis test followed by Dunn-Bonferroni *post-hoc* test and significance level correction for multiple testing).

brain and the spinal cord (Figure 3D). Prominent reactive microgliosis was seen in the brain of B6-nT and B6-Tam mice without CD28-knockout (Figure 3E, upper left and upper right). Within the brain, microglial activation was significantly reduced in Cre-Tam and CD28KO mice with knockout of CD28 (Figures 3E, F). Within the spinal cord, there was no significant difference between mice with or without CD28-knockout (Figure 3F).

The number of apoptotic cells (caspase 3 positive cells) within the brain and spinal cord was not elevated in CD28-knockout mice compared to the controls at 14 dpi (Supplementary Figure S2). In addition, there was no increase in axonal damage (beta APP positive axons) within the spinal cord of CD28-knockout mice in the early phase of TMEV-infection at 14 dpi (Supplementary Figure S2).

The summarized results of the clinical and histopathological findings in intracerebrally TMEV-infected mice reveal that mice lacking CD28-expression (Cre-Tam, CD28KO) show virus persistence and spreading of virus within the brain as well as into the spinal cord at 14 dpi. This is correlated with significantly less microglial activation, despite presence of virus antigen within the CNS. T- and B cell infiltration seem to be influenced by tamoxifen administration and CD28-knockout in a mutually enhancing manner. The influence of tamoxifen on the number of infiltrating lymphocytes can be seen in the direct comparison with B6-nT controls, but only reaches statistical significance in Cre-Tam mice with CD28-knockout, that show significantly increased T cell infiltration and decreased B-cell infiltration.

3.2 Conventional CD28-knockout mice partially develop a clinical phenotype during the chronic phase (21-42 dpi) of a TMEV-infection

Because TMEV has not been cleared yet at 14 dpi, it was interesting to follow up the fate of the mice also in the chronic stage of TMEV infection. In susceptible SJL mice, the chronic phase is characterized by progressive clinical signs and loss of myelin caused by different immunopathologies of this model (1). Since the CD28KO mice were unable to clear the virus within 2 weeks after infection, a longer period was studied to see whether CD28-deficiency results in a similar fate on the otherwise resistant C57BL/6 background. Due to the detrimental effects of the tamoxifen-induced conditional CD28-knockout in the early phase of TMEV-infection (weight loss, clinical signs), Cre-Tam mice were not included in this part of the study for animal welfare reasons. Mice with a conventional CD28-knockout (CD28KO) either showed no clinical signs, similar to the control animals (B6-nT) or developed motoric deficiencies at 21 (n=1), 32 (n=1) and 33 (n=2) days post TMEV-infection. Mice that developed these clinical signs were thus evaluated separately as 'responders' (CD28KO-R, n= 4 out of 12). At the end of experiment, the four responders with conventional CD28-knockout had a lower body weight (Figure 4A) and showed increased clinical scores (Figure 4B). The high clinical scores in CD28KO-R mice were mainly determined by hind limb paresis (score 4) of two mice at 33 (n=1) and 35 dpi (n=1). Mice with hind limb paresis were euthanized immediately for humane reasons and thus not put on the RotaRod. Accordingly, the presented data (Figure 4C) show the last RotaRod performance on 28 dpi of mice prior to the hind limb paresis and 42 dpi of the mice with mild gait abnormalities. It can be seen, that anyways, the motor skills of the CD28KO-R mice are non-significantly reduced compared to the non-responder CD28KO mice (Figure 4C).

Histopathological examination at 42 dpi revealed that B6-nT control animals without knockout (Figure 5A, upper left) as well as conventional CD28KO mice without gait abnormalities (Figure 5A, upper right) showed no, or only minor inflammation characterized by single parenchymal and perivascular infiltrations of immune cells within the brain and spinal cord (Figure 5B). In contrast, inflammation was still visible within the spinal cord of the CD28KO-R mice and most prominent in the lumbar segment (Figures 5A, B). The B6-nT controls (Figure 5C, upper left) and

10.3389/fimmu.2023.1105432

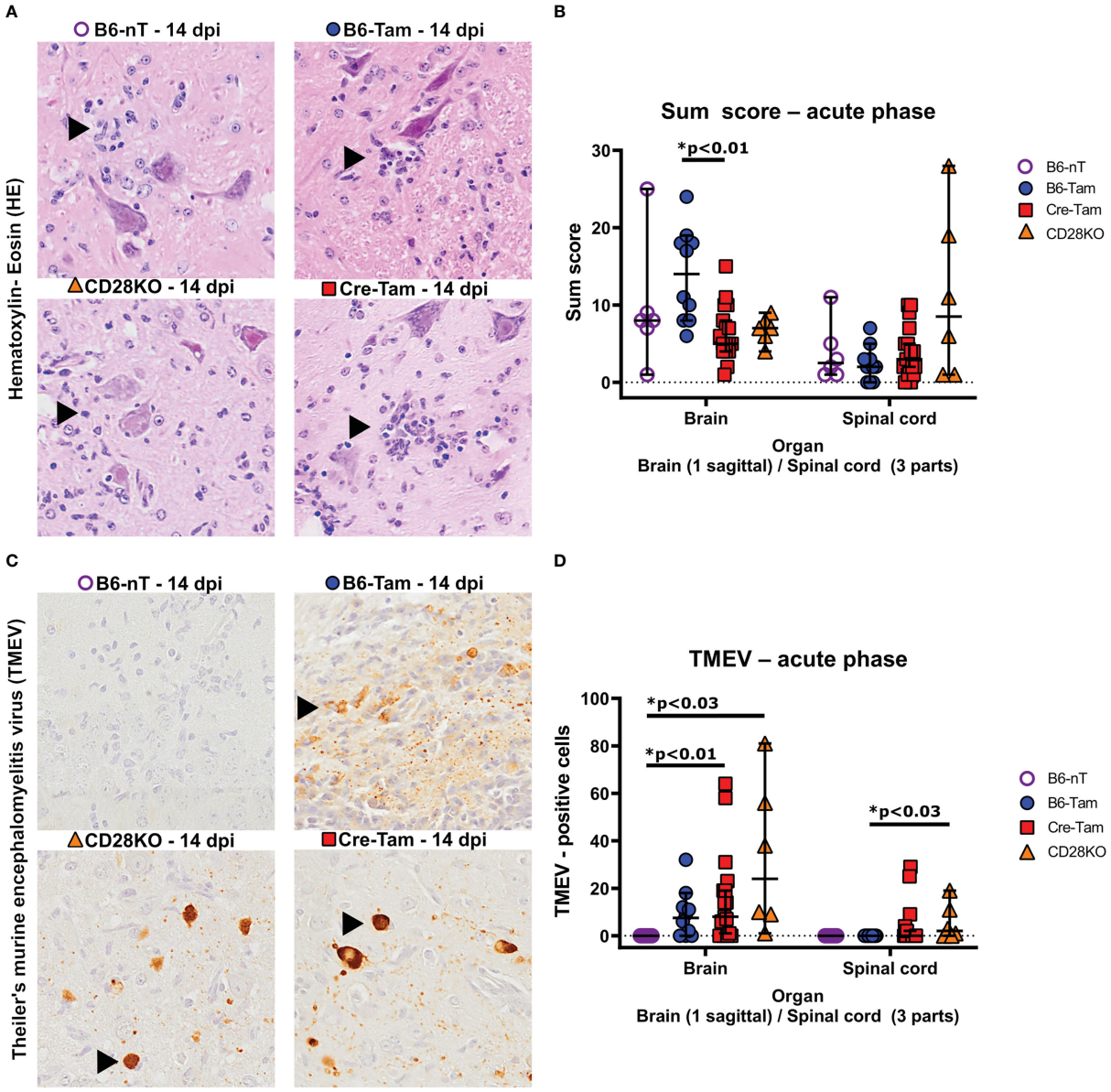


FIGURE 2
(A, B) Semi-quantitative scores of the brains and spinal cords of TMEV-infected B6-nT mice (no CD28-knockout, no tamoxifen application, n=6), B6-Tam mice (no CD28-knockout, tamoxifen application, n=10), CD28KO mice (CD28-knockout, no tamoxifen application, n=6) and Cre-Tam mice (CD28-knockout, tamoxifen application, n=17) using hematoxylin-eosin (HE) stained sections in the acute phase at 14 days post infection (dpi). **(A)** Representative pictures showing inflammatory infiltrates (arrowheads) within the lumbar spinal cords in Theiler's murine encephalomyelitis virus (TMEV) infected mice at 14 dpi. **(B)** Summarized graphical presentation of semi-quantitative scores obtained in 10 brain regions and 6 spinal cord regions at 14 dpi, showing significantly lower scores within the brains of CD28-knockout (Cre-Tam) mice compared to B6-Tam controls and similar scores within the spinal cord. **(C, D)** Immunohistochemical detection of TMEV-antigen within the brains and spinal cords of TMEV-infected mice at 14 dpi. **(C)** Representative pictures showing no TMEV-antigen in B6-nT mice (upper left) and persisting TMEV-antigen within the hippocampus (B6-Tam, upper right) and cerebral cortex (CD28KO, lower left; Cre-Tam, lower right) at 14 dpi. **(D)** In contrast to B6-nT-control animals, mice with tamoxifen application (B6-Tam) as well as mice with CD28-knockout (Cre-Tam, CD28KO) showed virus antigen in the brain at 14 dpi. Virus spread into the spinal cord was only detected in mice with CD28-knockout (Cre-Tam, CD28KO) and reached statistically significance between CD28KO mice and B6-Tam controls. Graphs show scatter plots (one dot per animal) with median (black bar) and 95% confidence intervals (black error bars). Statistically significant p-values are depicted within the graphs (Kruskal-Wallis test followed by Dunn-Bonferroni *post-hoc* test and significance level correction for multiple testing).

clinically unaffected CD28KO mice (Figure 5C, upper right),except for one mouse with very low titer, were able to eliminate TMEV from the brain and spinal cord (Figure 5D) at 42 dpi. Conversely, TMEV-antigen was still detectable within the brain (Figure 5C, lower left) of 3 and spinal cords of 2 out of 4 CD28KO-R mice, respectively (Figure 5D).

The low sum score of the CNS of B6-nT control animals and non-responder CD28KO mice, were affirmed by low numbers of

10.3389/fimmu.2023.1105432

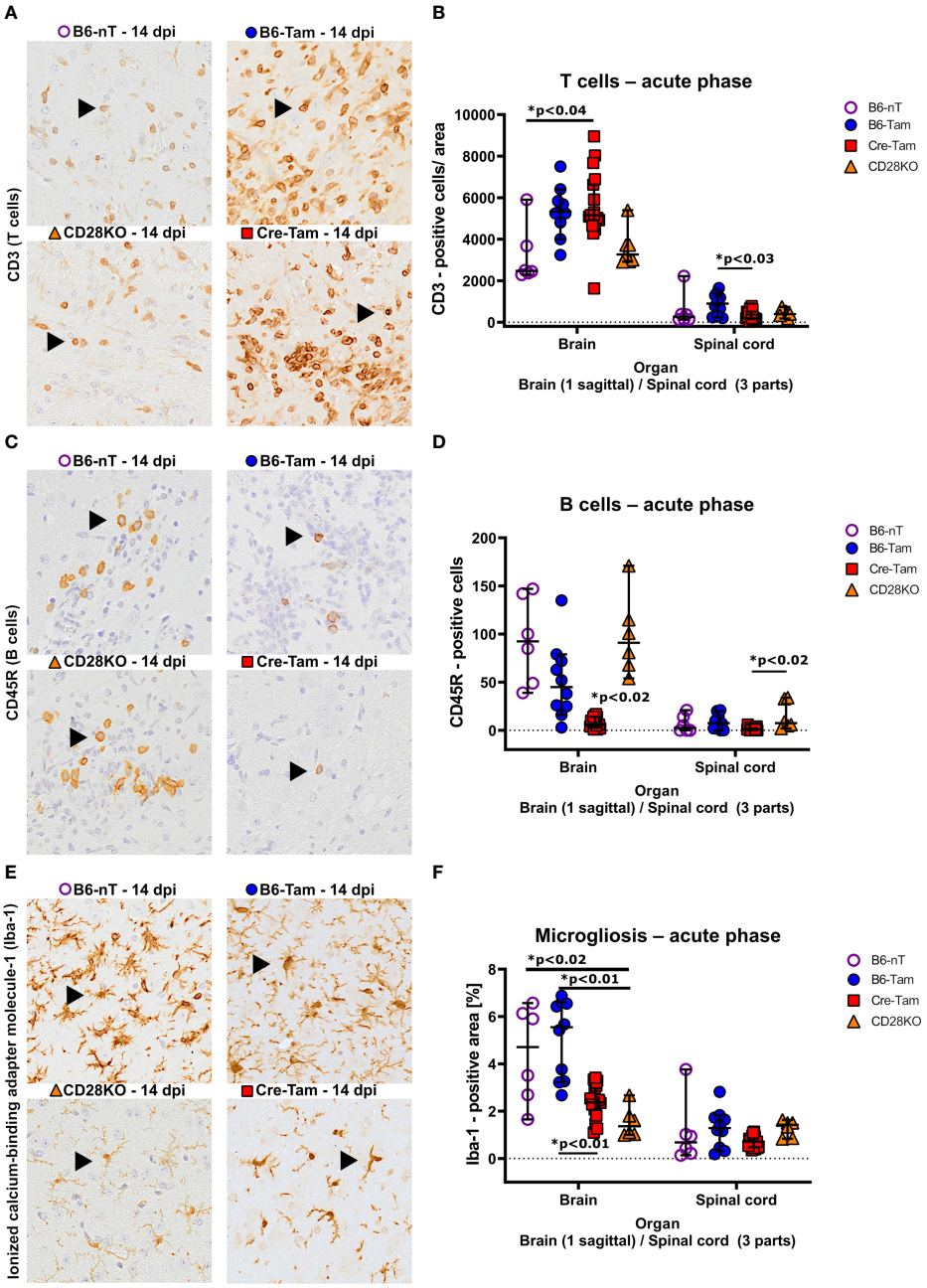


FIGURE 3
(A, B) Immunohistochemical detection of CD3-positive T cell infiltration into the brain and spinal cord of Theiler's murine encephalomyelitis virus (TMEV)-infected B6-nT mice (no CD28-knockout, no tamoxifen application, n=6), B6-Tam mice (no CD28-knockout, tamoxifen application, n=10), CD28KO mice (CD28-knockout, no tamoxifen application, n=6) and Cre-Tam mice (CD28-knockout, tamoxifen application, n=17) in the acute phase at 14 days post infection (dpi). **(A)** Representative pictures showing moderate T cell infiltration (arrowheads) into the thalamus of B6-nT (upper left) and CD28KO mice (lower left) in contrast to high numbers of infiltrating T cells in B6-Tam (upper right) and Cre-Tam mice (lower right) at 14 dpi. **(B)** Quantitative evaluation of T cells per area (0.5 cm^2 brain, 0.07cm^2 spinal cord) reveals increased infiltration into the brain of Cre-Tam compared to B6-nT controls and spinal cord of B6-Tam mice, compared to Cre-Tam mice. **(C, D)** Infiltration of CD45R-positive B cells into the brain and spinal cord of TMEV-infected mice at 14 dpi. **(C)** Representative pictures showing moderate infiltration of B cells (arrowheads) into the hippocampus of TMEV-infected B6-nT (upper left) and CD28KO mice (lower left) in contrast to low numbers of infiltrating B cells in B6-Tam (upper right) and Cre-Tam mice (lower right) at 14 dpi. **(C)** Quantitative analysis shows significantly decreased B cell infiltration in the brain of Cre-Tam mice compared to all other groups. Within the spinal cord, B cell numbers are significantly lower in Cre-Tam mice, compared to CD28KO mice at 14 dpi. **(E, F)** Analysis of microgliosis within the brain and spinal cord of TMEV-infected mice at 14 dpi. **(E)** Representative pictures of activated, ionized calcium-binding adapter molecule-1 (Iba-1)-positive microglia/macrophages within the thalamus, showing increased cell numbers and ramification in B6-nT (upper left) and B6-Tam mice (upper right) in contrast to lower cell numbers with only few cell processes in CD28KO (lower left) and Cre-Tam mice (lower right) at 14 dpi. **(F)** A detailed analysis of Iba-1 positive areas reveals significantly decreased microgliosis within the brain of CD28-knockout mice (Cre-Tam, CD28KO) compared to controls (B6-nT, B6-Tam) at 14 dpi. Within the spinal cord, there is no difference at 14 dpi concerning microgliosis. Graphs show scatter plots (one dot per animal) with median (black bar) and 95% confidence intervals (black error bars). Statistically significant p-values are depicted within the graphs (Kruskal-Wallis test followed by Dunn-Bonferroni *post-hoc* test and significance level correction for multiple testing).

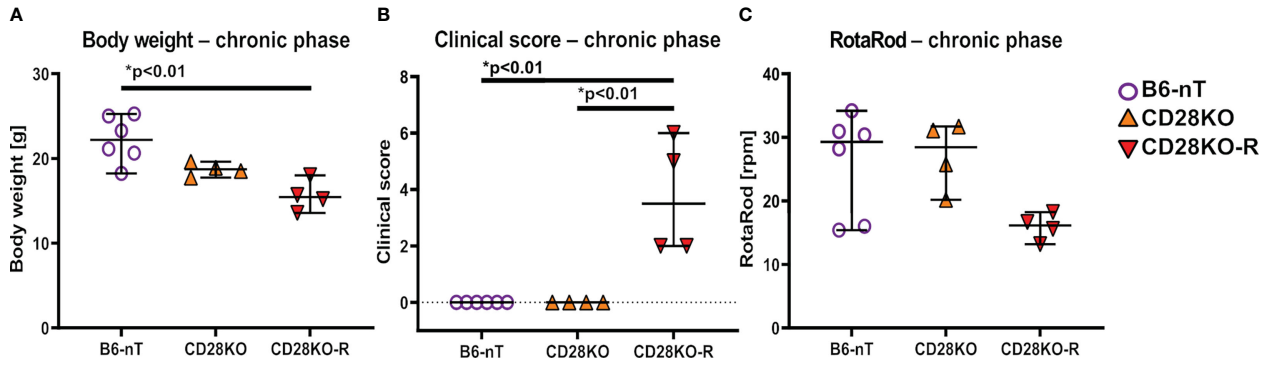


FIGURE 4
(A–C) Assessment of general parameters and clinical score during the chronic phase of Theiler's murine encephalomyelitis virus (TMEV)-infection. TMEV-infected conventional CD28-knockout mice with clinical signs in the chronic phase, termed 'responder CD28KO' mice, (CD28KO-R, n=4) were euthanized at 33 (n=1), 35 (n=1) and 42 dpi (n=2) and compared to CD28-knockout mice without clinical signs (CD28KO, n=4) and control mice without knockout (B6-nT, n= 6) that were sacrificed on 42 dpi. **(A)** CD28KO-R mice show a significantly lower body weight at the end of experiment, compared to B6-nT controls. **(B)** B6-nT and CD28KO mice do not show a clinical score at 42 dpi. The clinical scores of CD28KO-R mice (n=4) are elevated significantly at the end of experiment at 33, 35 and 42 dpi, respectively. **(C)** RotaRod performance tests show a mildly reduced performance of CD28KO-R mice compared to CD28KO mice, that however reaches no statistical significance (p= 0.104). Graphs show scatter plots (one dot per animal) with median (black bar) and 95% confidence intervals (black error bars). Statistically significant p-values are depicted within the graphs (Kruskal-Wallis test followed by Dunn-Bonferroni *post-hoc* test and significance level correction for multiple testing).

infiltrating T cells (Figures 6A, B) and B cells (Figures 6C, D). This was in contrast to the ongoing T cell (Figures 6A, B) and B cell (Figures 6C, D) infiltration in CD28KO-R mice.

Compared to the B6-nT controls (Figures 7A–D, upper left) the astroglial and microglial response in the brain was mildly but not significantly elevated in CD28KO mice without clinic (Figures 7A–D, upper right). CD28KO-R mice showed significantly increased density of astrocytes (astrogliosis) within the brain and spinal cord (Figures 7A, B) as well as a high density of hypertrophic/hyper-ramified microglia (Figures 7C, D). These data indicate an ineffective and delayed immune response against TMEV-infection in clinically affected CD28KO-R mice.

Concomitant to the chronic TMEV-infection and ongoing inflammation within the CNS of CD28KO-R mice, the responders also show increased numbers of apoptotic cells (Figures 8A, B) and damaged axons within the spinal cord (Figures 8C, D). The number of neurotrophic S100A10-positive astrocytes in the spinal cord was not affected (Figures 8E, F). Prominent loss of myelin was not seen in luxol-fast-blue (LFB)-stained sections of the spinal cord in any of the mice (data not shown). When following the remaining B6-nT control animals (n=7) and conventional CD28KO animals (n=4) up to 147 dpi, no development of clinical signs or histopathological abnormalities were observed (data not shown).

In summary, in the chronic phase after TMEV-infection, the deletion of CD28 results in variable outcome. Control mice (as expected) and two third of conventional CD28KO mice are able to resolve the virus infection without development of clinical symptoms and histopathological abnormalities. In contrast, one third of CD28KO mice are susceptible for a chronic TMEV-infection with an inefficient inflammatory response and concomitant loss of lower motor neurons within inflamed spinal cord regions as well as increased apoptosis and axonal damage.

4 Discussion

The deletion of the co-stimulatory molecule CD28 has considerable impact in the TMEV-model at different time points after virus inoculation as determined by clinical evaluation, functional testing and pathohistological analysis. In the early phase at 14 dpi, both conventional and conditional deletion of CD28 resulted in impaired viral clearance with spread of TMEV within the brain and into the spinal cord, the latter being a rather uncommon finding in C57BL/6 mice. Furthermore, despite more abundant T cell infiltration, the microglial activation was reduced in both mouse strains, which correlated with the inability for the clearance of the virus. The chronic phase of TMEV-infection was only investigated in conventional CD28KO mice, due to animal welfare reasons. Two third of the animals did not develop clinical symptoms and showed no histopathological abnormalities when investigated at 42 or 147 dpi, pointing to a rather delayed then abolished immune response and eventual clearance of the virus. However, one third of the CD28KO mice developed clinical symptoms with loss of motor function in the chronic phase (CD28KO-R), indicating that these mice could not clear the virus with fatal consequences. The clinical signs seen between 21-42 dpi were associated with virus persistence and increased inflammation within the CNS of CD28KO-R mice, characterized by increased T- and B cell infiltration, microglial activation and astrogliosis at 33-42 dpi.

In summary, loss of CD28 in any case resulted in an impaired anti-viral immune response reflected by abnormal histopathology and accompanied by the development of clinical symptoms already in the early phase in the case of conditional deletion of CD28 and in one third of the mice in the case of permanent deletion of CD28 in the chronic phase of the disease.

4.1 CD28 and controlling a virus infection in the CNS – immune cell homeostasis

The infection of C57BL/6 mice with low virulent TMEV is known to cause acute and chronic seizures and is thus used as a

10.3389/fimmu.2023.1105432

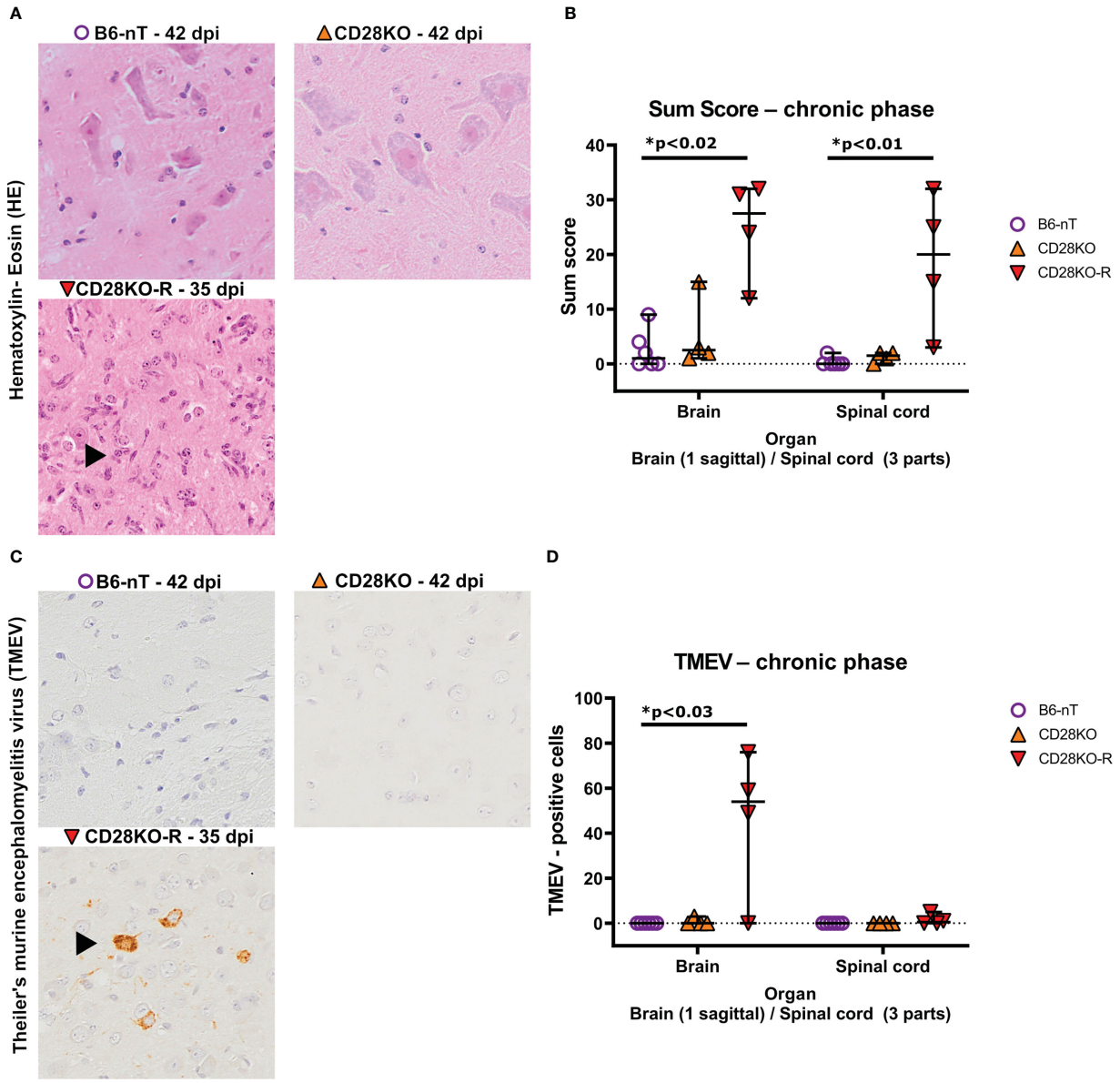


FIGURE 5
(A, B) Semi-quantitative scoring of brain and spinal cord on hematoxylin-eosin (HE) stained sections in the chronic phase at 33, 35 or 42 days post infection (dpi), respectively. Theiler's murine encephalomyelitis virus (TMEV)-infected CD28-knockout mice with clinical signs in the chronic phase, termed 'responder CD28KO' mice, (CD28KO-R, n=4) were euthanized at 33 (n=1), 35 (n=1) and 42 dpi (n=2) and compared to CD28-knockout mice without clinical signs (CD28KO, n=4) and control mice without knockout (B6-nT, n= 6) that were sacrificed on 42 dpi. **(A)** Representative pictures of lumbar spinal cord of TMEV-infected mice showing lack of inflammatory changes in B6-nT (upper left) and CD28KO mice without clinical signs (upper right) in contrast to ongoing inflammation (arrowhead) in the spinal cord of a CD28KO-R mouse at 35 dpi (lower left). **(B)** Semi-quantitative scores representing the total sum obtained by added scores of 10 different brain- or 6 spinal cord regions, respectively, showed significantly increased scores in the brain and spinal cord of CD28KO-R mice compared to B6-nT controls in the chronic phase of TMEV-infection.
(C, D) Immunohistochemical analysis of TMEV-antigen within the brain and spinal cords of mice in the chronic phase of TMEV-infection.
(C) Representative pictures lack TMEV-antigen in B6-nT control mice (upper left) and CD28KO mice without clinical signs (upper right) in contrast to persisting TMEV-antigen within the cerebral cortex of a CD28KO-R mouse at 35 dpi (lower left). **(D)** Quantitative analysis revealed TMEV-persistence within the brain and spinal cord of CD28KO-R mice. Graphs show scatter plots (one dot per animal) with median (black bar) and 95% confidence intervals (black error bars). Statistically significant p-values are depicted within the graphs (Kruskal-Wallis test followed by Dunn-Bonferroni *post-hoc* test and significance level correction for multiple testing).

model for human temporal lobe epilepsy (37). However, the occurrence and frequency of seizures depends on the virus strain (38). About 50%-75% of mice intracerebrally infected with the Daniel's strain of TMEV (TMEV-DA) develop seizures, depending on the applied detection method and initial virus dose (39–41). For the TMEV-BeAn-strain the percentage differs between 0-40% (39, 41). It was seen that seizure development does not correlate with neuropathological changes (39). In the present experiment the variant BeAn-1-TiHo was used, which is not suspected to cause seizures in C57BL/6 mice (41). Concomitantly, no apparent seizures were observed after TMEV-BeAn-infection in the present study. However, it cannot be excluded that seizures might have occurred

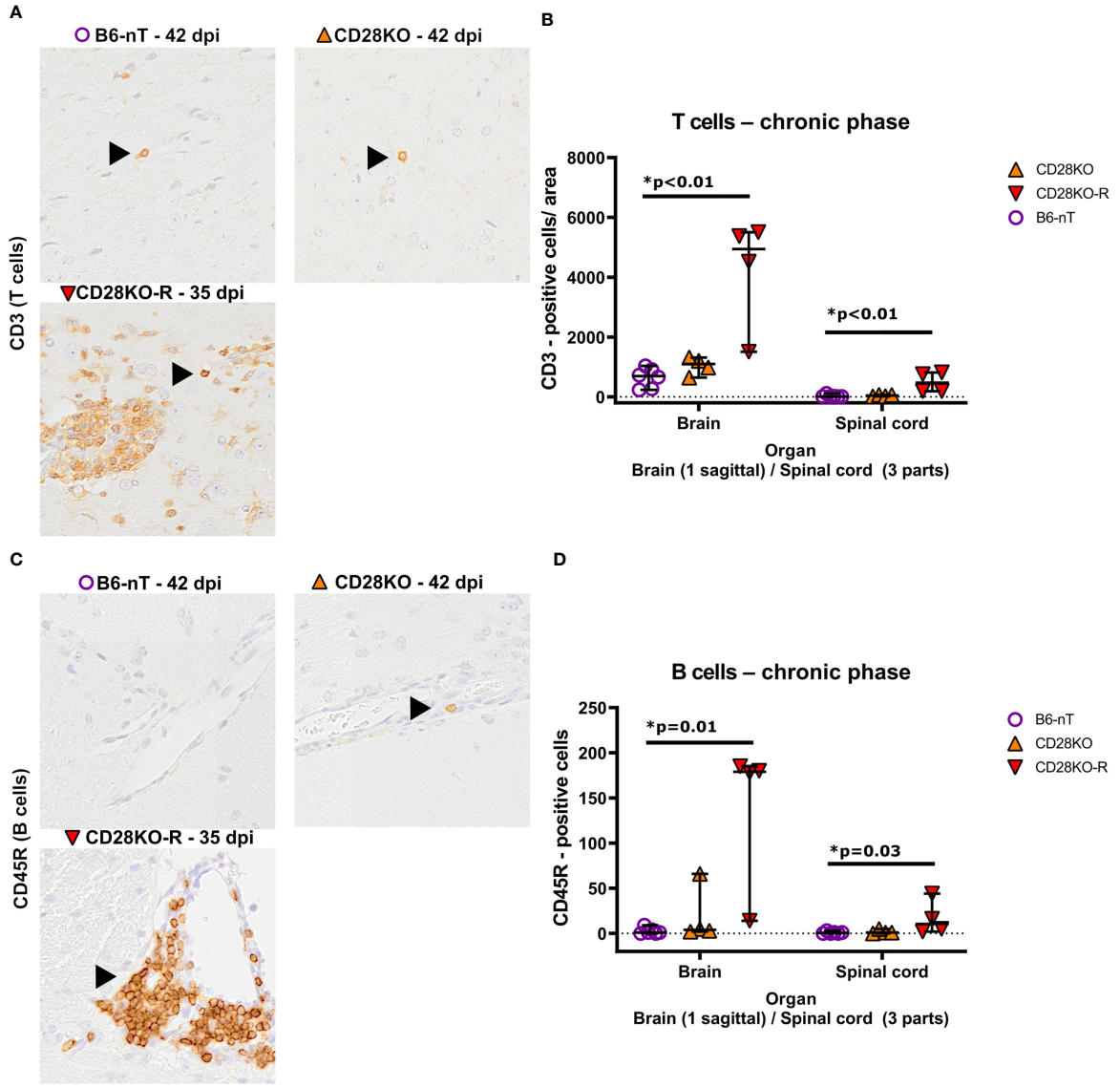


FIGURE 6
(A, B) Immunohistochemical analysis of CD3-positive T cell infiltration into the brain and spinal cord of Theiler's murine encephalomyelitis virus (TMEV)-infected mice in the chronic phase at 33, 35 and 42 days post infection (dpi), respectively. TMEV-infected conventional CD28-knockout mice with clinical signs in the chronic phase, termed 'responder CD28KO' mice, (CD28KO-R, n=4) were euthanized at 33 (n=1), 35 (n=1) and 42 dpi (n=2) and compared to CD28-knockout mice without clinical signs (CD28KO, n=4) and control mice without knockout (B6-nT, n= 6) that were sacrificed on 42 dpi. **(A)** Representative pictures showing single CD3-positive T cells within the hypothalamus (B6-nT, upper left)) and thalamus (CD28KO, upper right) in contrast to increased T cell infiltration into the thalamus of a TMEV-infected CD28KO-R mouse (lower left) at 35 and 42 dpi, respectively. **(B)** Quantitative evaluation of T cells per area (0.5 cm^2 brain, 0.07cm^2 spinal cord) shows, compared to B6-nT controls at 42 dpi, a significantly increased T cell infiltration into the brain and spinal cord of CD28KO-R mice at 33, 35 and 42 dpi, respectively. **(C-D)** Immunohistochemical analysis of CD45R-positive B cell infiltration into the brain and spinal cord of TMEV-infected mice in the chronic phase at 33, 35 and 42 dpi, respectively. **(C)** Representative pictures of CD45R-positive B cells (arrowheads) within the hypothalamus, showing no B cells in a B6-nT (upper left) or single perivascular B cells in a CD28KO mouse (upper right), in contrast to increased perivascular infiltration in a CD28KO-R mouse at 35 dpi (lower left). **(B)** Quantitative analysis of B cell infiltration shows significantly increased numbers of B cells within the brain and spinal cord of CD28KO-R mice at 33, 35 and 42 dpi, compared to B6-nT controls at 42 dpi. Graphs show scatter plots (one dot per animal) with median (black bar) and 95% confidence intervals (black error bars). Statistically significant p-values are depicted within the graphs (Kruskal-Wallis test followed by Dunn-Bonferroni *post-hoc* test and significance level correction for multiple testing).

apart from the general examinations, since no specific scoring (Racine score) or continuous monitoring *via* video-electroencephalogram (VEEG) were applied.

One of the hallmarks after CD28 loss – both conventional and conditional - is the unexpected virus spread within the brain as well as into the spinal cord of mice with a C57BL/6 background (Figures 2C, D). In general, C57BL/6 mice are considered to be resistant to a chronic TMEV-infection and are able to eliminate the virus within 2 weeks after intracranial infection (9). Although it was previously already shown that the tamoxifen application is associated with delayed virus elimination (34), the tamoxifen treated mice without CD28 knockout (B6-Tam) did not show

10.3389/fimmu.2023.1105432

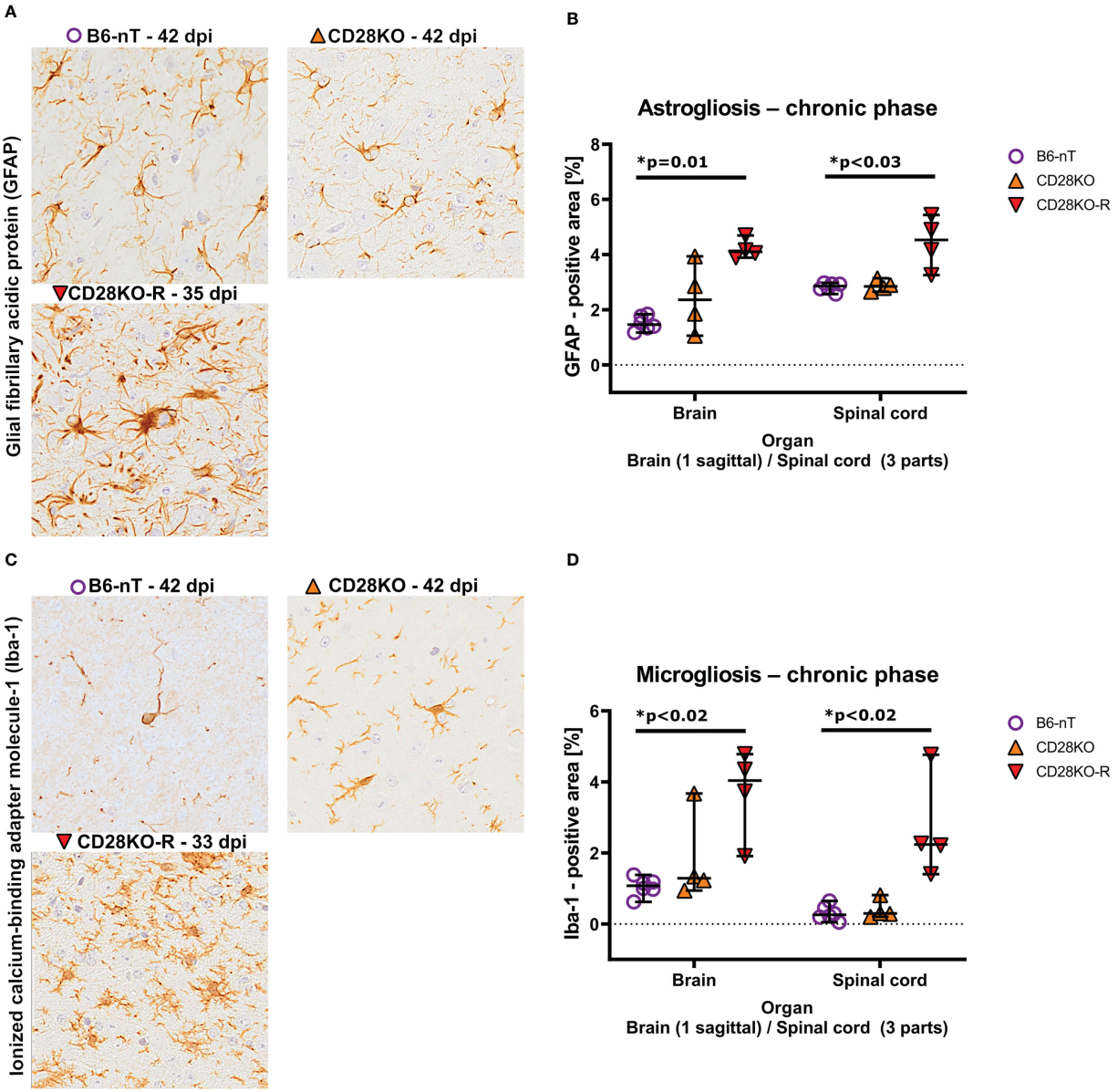


FIGURE 7
(A, B) Immunohistochemical analysis of glial fibrillary acidic protein (GFAP)-positive astroglia (astrogliosis) within the brain and spinal cord of Theiler's murine encephalomyelitis virus (TMEV)-infected mice in the chronic phase at 33, 35 and 42 days post infection (dpi), respectively. TMEV-infected conventional CD28-knockout mice with clinical signs in the chronic phase, termed 'responder CD28KO' mice, (CD28KO-R, n=4) were euthanized at 33 (n=1), 35 (n=1) and 42 dpi (n=2) and compared to CD28-knockout mice without clinical signs (CD28KO, n=4) and control mice without knockout (B6-nT, n= 6) that were sacrificed on 42 dpi. **(A)** Representative pictures of GFAP-positive astroglia (arrowheads) within the thalamus of TMEV-infected mice, showing moderate numbers of astroglia with few processes in the brains of B6-nT (upper left) and CD28KO mice (upper right) at 42 dpi in contrast to increased cell size and number of processes in a CD28KO-R mouse (lower left) at 35 dpi. **(B)** Quantitative analysis of GFAP-positive area revealed significantly increased astrogliosis within the brain and spinal cord of CD28KO-R mice compared to B6-nT controls in the chronic phase. **(C, D)** Analysis of activated, ionized calcium-binding adapter molecule-1 (Iba-1)-positive microglia within the brain and spinal cord of TMEV-infected mice at 33, 35 and 42 dpi, respectively. **(C)** Representative pictures of Iba-1-psotive microglia/macrophages (arrowheads) within the thalamus of TMEV-infected mice at 33 and 42 dpi showing low cell numbers and few processes in B6-nT (upper left) and CD28KO mice (upper right) at 42 dpi, in contrast to increased ramification of microglia within a CD28KO-R mouse (lower left) at 33 dpi. **(D)** Quantitative analysis of Iba-1-positive area revealed significantly increased microgliosis within the brain and spinal cord of CD28KO-R mice compared to B6-nT controls. Graphs show scatter plots (one dot per animal) with median (black bar) and 95% confidence intervals (black error bars). Statistically significant p-values are depicted within the graphs (Kruskal-Wallis test followed by Dunn-Bonferroni *post-hoc* test and significance level correction for multiple testing).

virus spread into the spinal cord, or elevated clinical scores. In both CD28-knockout strains, microglial activation and change of morphology as reaction to the acute TMEV-infection in the brain were reduced.

Brain-resident microglia and infiltrating monocytes as part of the innate immune response play a pivotal role in the acute, as well as in the chronic phase of a TMEV-infection (42). On the one hand, these cell types contribute to local damage, scarring and

10.3389/fimmu.2023.1105432

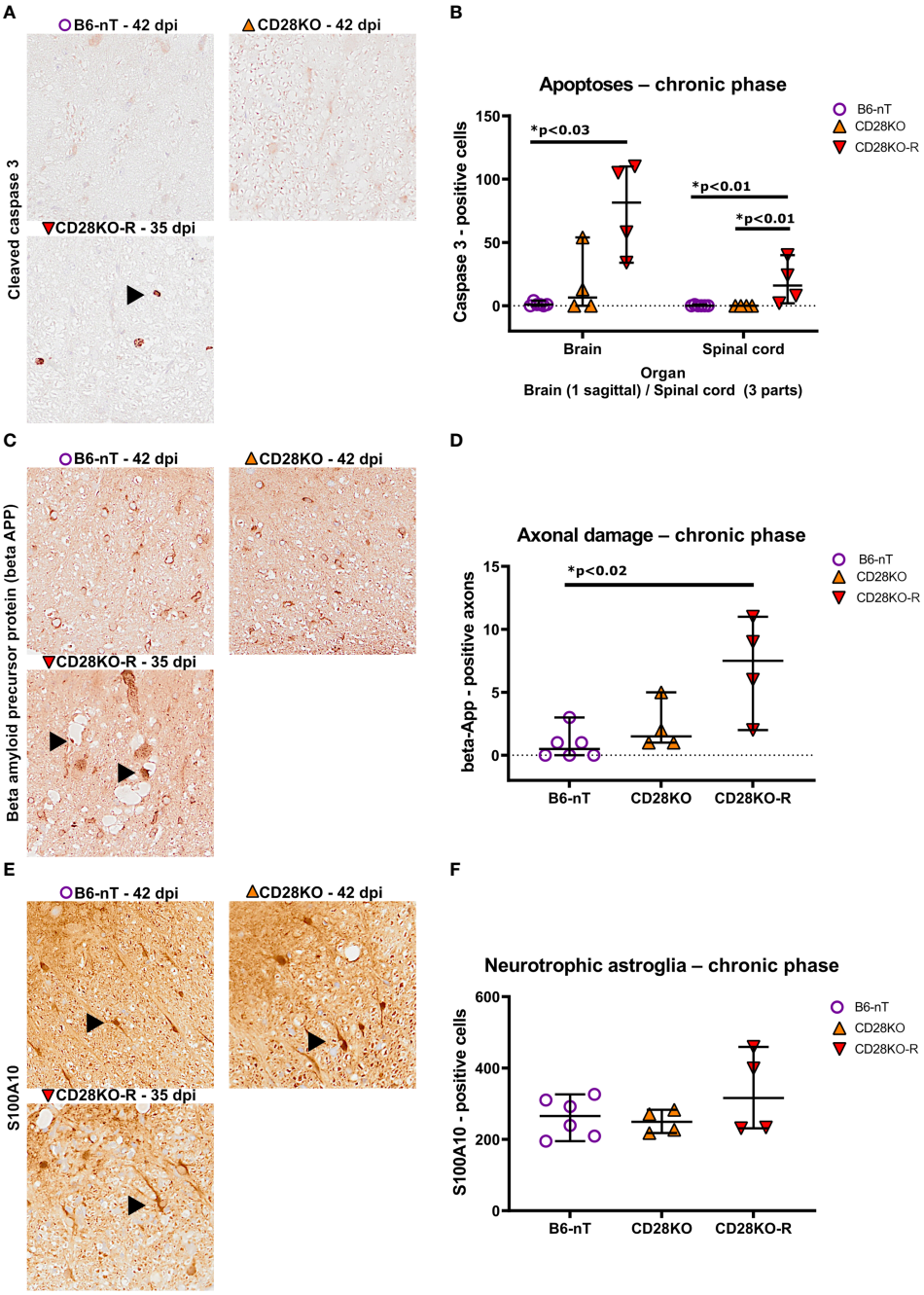


FIGURE 8
(A, B) Immunohistochemical analysis of cleaved caspase 3-positive, apoptotic cells within the brain and spinal cord of Theiler's murine encephalomyelitis virus (TMEV)-infected mice in the chronic phase at 33, 35 and 42 days post infection (dpi), respectively. TMEV-infected conventional CD28-knockout mice with clinical signs in the chronic phase termed 'responder CD28KO' mice (CD28KO-R, n=4), were euthanized at 33 (n=1), 35 (n=1) and 42 dpi (n=2) and compared to CD28-knockout mice without clinical signs (CD28KO, n=4) and control mice without knockout (B6-nT, n= 6) that were sacrificed on 42 dpi. **(A)** Representative pictures of the lumbar spinal cord show no apoptoses in B6-nT (upper left) and CD28KO mice (upper right) at 42 dpi in contrast to low numbers of apoptotic cells (arrowhead) in a CD28KO-R mouse (lower left) at 35 dpi. **(B)** Quantitative analysis of cleaved caspase 3-positive cells revealed significantly increased numbers of apoptoses within the brain and spinal cord of CD28KO-R mice compared to B6-nT controls. **(C, D)** Immunohistochemical analysis of beta amyloid precursor protein (beta-APP)-positive, damaged axons within the spinal cord of TMEV-infected mice at 33, 35 and 42 dpi. **(C)** Representative pictures show no damaged axons in B6-nT (upper left) and CD28KO mice (upper right) at 42 dpi, in contrast to the CD28KO-R mouse (lower left) showing small and enlarged beta-APP-positive axons (arrowheads) within dilated myelin sheets in the lumbar spinal cord at 35 dpi. **(D)** Quantitative analysis of beta-APP-positive axons revealed significantly increased axonal damage within the spinal cord of CD28KO-R mice compared to B6-nT controls. **(E, F)** Immunohistochemical analysis of S100A10-positive, neurotrophic astroglia within the spinal cord of TMEV-infected mice in the chronic phase at 33, 35 and 42 dpi, respectively. **(E)** Representative pictures show S100A10-positive astroglia (arrowheads) within the spinal cord of all TMEV-infected mice in the chronic phase of TMEV-infection. **(F)** Quantitative analysis revealed no significant difference between the groups regarding the number of neurotrophic astroglia in the chronic phase. Graphs show scatter plots (one dot per animal) with median (black bar) and 95% confidence intervals (black error bars). Statistically significant p-values are depicted within the graphs (Kruskal-Wallis test followed by Dunn-Bonferroni *post-hoc* test and significance level correction for multiple.

development of seizures in C57BL/6 mice (42). Further, microglia are susceptible for TMEV-infection and the major host cells during the chronic TMEV-BeAn infection as seen in SJL mice (43). On the other hand, a clearing of TMEV from the CNS is impossible for C57BL/6 mice after depletion of microglia (44). Similarly, the presented data indicate a link between reduced microglial activation (Figures 3E, F) and delayed virus elimination and virus spread within the CNS in mice lacking CD28 (Figures 2C, D). The molecular background of this correlation will be subject of further studies.

For infiltration of cells of the adaptive immune response (T- and B cells), the situation is different. As described in other studies on the immune system (45), conventional TMEV-infected CD28KO mice had similar levels of infiltrating T- and B cells into the brain and spinal cord as their B6-nT controls. Conversely, Cre-Tam mice with an induced knockout showed increased T-cell infiltration and almost a total lack of B cell infiltration into the TMEV-infected brain. Furthermore, it was shown that the tamoxifen application alone (B6-Tam) has a similar effect, but to a lesser extent. Thus, it seems that the tamoxifen application and the delayed anti-viral immune response is the main reason for the changed T- and B-cell infiltration, and that the actual deletion of CD28 is somehow reinforcing these effects, whereas the pure lack of CD28 from the beginning has no influence of T- and B cell infiltration. Based on these data, it also seems that T- and B cell infiltration is uncoupled from microglial activation after TMEV-infection and also from the development of neurological symptoms.

CD28 is important during the antigen presentation from myeloid cells, for instance dendritic cells (DC), but also decisive in the communication between T- and B cells (46). Antigens binding to the B cell-receptor (BCR) are processed and presented on MHC-II with concomitant expression of CD80/CD86 (B7-1/B7-2) as ligands for CD28 on the T cell (46, 47). Activated T cells secrete interleukins to further stimulate B cells, however, the interaction of CD28 with the B7 molecules itself poses a direct co-stimulatory signal for B cells (48). The presented data show, that the activation and expansion of B cells is almost completely aborted in mice with induced CD28 knockout, which is likely due to a loss of communication between the B- and T cells as well as loss of CD28/B7 mediated co-stimulation of B cells (48). The similarity in T- and B cell reaction of mice with conventional CD28 knockout in this study indicates an alternative route of activation in these mice. Although CD28 is a main molecule for the activation of naïve T cells, it is by far not the only one (49). Upregulation of other co-stimulatory molecules may have compensated the lack of CD28-signaling in the thymus of CD28KO mice with conventional CD28-knockout (45, 49, 50).

Tamoxifen as a selective estrogen receptor modulator (SERM) is known to influence the immune response under therapeutic as well as in experimental conditions (4, 34, 51–53). Although tamoxifen is designed to act on human estrogen receptors (hER) it also influences murine immune cells and has estrogen-like (agonistic) as well as antagonistic properties, depending on the expression of ER-subtypes (4, 34, 51–57). Since tamoxifen is a SERM and not a specific ER-inhibitor, and it also modulates cell responses through estrogen-independent mechanisms, reported effects on the immune response on a cellular level are divergent and highly depend on the applied method (51, 58). In the CNS, tamoxifen has mostly neuroprotective and anti-inflammatory properties, increases proliferation and differentiation of oligodendrocyte progenitor cells (OPC), decreases production of pro-inflammatory cytokines like TNF-alpha, IL-12 and IL-1 by micro- and astroglia, as well as reduces astrogliosis under non-infectious conditions (59, 60). Under infectious conditions, these effects might affect the initial immune response to be less efficient, resulting in a delayed virus elimination as seen in tamoxifen treated animals in the present study. The ongoing presence of TMEV-antigen is however suspected to stimulate the immune response in these animals, possibly covering an initially anti-inflammatory effect until 14 dpi. Further, tamoxifen is known to negatively influence the activation and maturation of B cells (54). The B cell response after a virus infection is dependent on factors of the virus itself, such as pathogenicity and cell tropism, as well as the accessibility and presentation of virus peptides and a pro- or anti-inflammatory microenvironment (61, 62). Although ER-β-mediated effects of tamoxifen are suspected to have negative effects on B cells (63), the molecular mechanism behind the reduced B cell response remains unclear for the present study and demands further investigation.

Despite differences in T- and B cell infiltration into the CNS of TMEV-infected mice with conventional and induced CD28-knockout, the virus elimination in these mice was equally impaired. The weak microglial activation in the early phase of TMEV-infection in both types of CD28-knockout mice indicates a disruption of an activation pathway, which could not be quickly overcome by other routes of co-stimulation and is somewhat independent of the B- and T cell infiltration. A comparable stimulatory function of B7-signaling on microglia (64), similar to B cells (48), might be a factor that should be addressed in future studies.

Since the cre-expression of these mice is not controlled by a cell-specific promotor, but rather expressed in all cells after tamoxifen application, a CD28 knockout in all cells is expected in the Cre-Tam mice. The variable significant difference in T- and B cell infiltrations of Cre-Tam mice compared to the TMEV-infected mice without CD28-knockout, as well as the decreased microglial reaction during the acute phase of TMEV-infection supports this assumption of a CD28-knockoutin the infiltrating immune cells.

The role of a CD28-knockout for $CD4^+$ and $CD8^+$ T cells separately represent an interesting topic for future studies in this model. The outcome and special contributions of MHC-I molecule H-$2D^b$ (65, 66), the early anti-viral $CD8^+$T cell response to a TMEV-infection, the reaction of $CD4^+$ T helper and effector cells as well as regulatory T cells (Tregs) (67, 68) could not be differentiated in the present study, utilizing a generalized CD28-knockout. A cell specific promotor for the cre-expression might aid to shed light on the contribution of different immune cell subsets to the observed neuropathologies in the present study (69). It would further be of interest to implement this model in mice on a susceptible SJL-background to investigate the effect of a CD28-knockout on demyelination (TMEV-IDD) (1).

4.2 Chronic infection of mice with conventional CD28-knockout

Due to the acute clinical and pathomorphological impairments of conditional CD28-knockout at 14 dpi, this mouse strain could

not be included in long-term studies. Therefore, the chronic TMEV-infection was only investigated in mice with conventional CD28-knockout (CD28KO).

A surprising finding here was the heterogeneity in the long-term clinical outcome of the intracerebral TMEV-infection in CD28KO mice. Two thirds of CD28KO mice were, just like the B6-nT control animals, clinically unaffected until 42 dpi or even 147 dpi (data not shown). 33% of the animals showed progressive impairments of motor function (CD28KO-R, 'responders'), starting around 21-33 dpi, leading up to hind-limb paresis in 2 of 4 affected animals.

Analysis of body weight, clinical score and RotaRod-performance test of the CD28KO-R did not reveal changes in the acute phase of TMEV-infection that would signal that these animals would develop clinical signs during the chronic phase. From 14 dpi until 42 dpi, the median RotaRod-performance of CD28KO-R mice is reduced compared to the other groups, followed by first clinical signs in some mice at 21 dpi and a lower median body weight from 28 until 42 dpi (Supplementary Figure S3).

Histologically, the responder-mice (CD28KO-R) were affected by ongoing virus spread and CNS-inflammation, indicating that the virus could not be cleared due to an inefficient immune response. However, in contrast to susceptible SJL mice (4), the myelitis of CD28KO-R mice was not associated with prominent demyelination, but inflammation and possible damage of lower motor neurons in the ventral horns. Thus, autoimmunity did not develop in the absence of CD28 in C57BL/6 mice, even when the virus could not be cleared similar to SJL mice. The marked difference to the early phase for the CD28-knockout mice was the increased microglial and astroglial activation at 33-42 dpi, combined with high numbers of infiltrating lymphocytes. However, despite this inflammatory response and microglial activation, the CD28KO-R mice were not able to eliminate the virus. It would be interesting to investigate the trigger(s) that differentiate mice able versus unable to clear the virus on the long run.

CD28 signaling is not only important for T cell activation and priming but also plays an important role for effector T cells (70). In $CD28^{flox/flox}$ $Ox40^{cre/+}$ mice where CD28 expression is lost after T cell priming following an influenza A infection, it was shown that T follicular helper cells (Tfh) need CD28 for survival, and T helper (Th1) require CD28-signaling for expansion after activation (70). These findings corroborate studies that showed a decreased germinal center formation and isotype switching in CD28-deficient C57BL/6 mice (20, 71). Conversely, it was shown that stimulation of the CD28-receptor on human and murine Th1 cells induces IFN-γ secretion (72). In microglia and astrocytes, IFN-γ and other Th1 effectors regulate gene expression associated with neuroinflammation (73), indicating that a loss of CD28-sinaling might have an anti-inflammatory effect. Further, the interaction of CD28 with the B7-ligands not only stimulates cytokine production in T cells but also triggers auto- and paracrine IL-6 and IFN-γ-secretion by dendritic cells (DC) (74). This bidirectional signaling of CD28 and B7 molecules has yet to be shown for microglia, as a possible factor for initially decreased microgliosis in TMEV-infected, CD28-knockout mice. However, in the present study it was seen, that a chronic TMEV-infection of CD28KO mice is associated with ongoing neuroinflammation, characterized by T- and B cell infiltration as well as astro- and microgliosis. In the early phase of TMEV-infection, the T- and B cell response of CD28KO mice does not differ significantly from the B6-nT controls. This indicates a CD28-independent activation pathway in lymphocytes of conventional CD28KO mice, and might indicate a disturbed interaction of lymphocytes and microglia in the early phase of TMEV-infection, as reported for DCs (74). The glial reaction in the late phase of TMEV-infection is likely reflective of the pro-inflammatory microenvironment, sustained by activated T and B cells in response to virus persistence.

Besides CD28, T cells own a large variety of co-stimulatory and co-inhibitory receptors whose expression depends on the cell's environment and activation status (49). Hence, despite their narrow genetic diversity, also inbred mice own individual expression panels of TCRs and co-receptors (20). In absence of CD28, individual expression of co-receptors could explain the heterogeneity in virus persistence and clinic seen in mice with a lack of CD28 (75).

5 Summary and conclusions

In summary, the absence of CD28 in T cells severely impacts the immune response against Theiler`s murine encephalomyelitis virus (TMEV)-infection, but significant differences are also seen depending on the time point of the deletion during the development of the immune system. CD28KO mice with a conventional CD28-knockout appear to develop early and individual compensatory mechanisms to overcome the lack of CD28 co-stimulation in the thymus as well as peripheral T- and B cells. Therefore, they do not develop clinical signs in the early phase of the infection. However, nevertheless these alternative pathways are inefficient under infectious conditions as indicated by delayed virus clearance accompanied by histopathological abnormalities in the early phase and the inability to finally clear the virus in one third of the mice in the chronic phase. This phenotype is much more pronounced in Cre-Tam mice with a tamoxifen-induced, conditional knockout of CD28. In these mice, viral spread within the brain and into the spinal cord was also observed in the early phase of the disease. Additionally, they show reactive T cell infiltration into the TMEV-infected brain, and develop clinical signs accompanied by a significantly reduced body weight already in this stage. Therefore, the immune system obviously has more problems to deal with virus infections when CD28 is suddenly lost without the possibility that adaptive mechanisms take place. However, the persistent virus infection within the CNS in these CD28-deficient C57BL/6 mice does not lead to autoimmunity as seen in susceptible mouse strains such as SJL, leading to the conclusion that other factors besides virus persistence may contribute to this phenotype.

Data availability statement

The original contributions presented in the study are included in the article/Supplementary Material. Further inquiries can be directed to the corresponding author.

Ethics statement

The animal study was reviewed and approved by Lower Saxony State Office for Consumer Protection and Food Safety (LAVES), 26029 Oldenburg, Germany.

Author contributions

KH: planning and execution of animal experiment, laboratory work, analysis, manuscript preparation, figures, statistics; FL: planning of experiment, generation of genetically engineered mice, writing and revision of the manuscript; EL: statistics, manuscript editing; AF: planning of experiment, revision of the manuscript; WB: planning of experiment, revision of the manuscript, corresponding author. All authors contributed to the article and approved the submitted version.

Funding

The authors did not receive project-associated funding for this investigation. This Open Access publication was funded by the Deutsche Forschungsgemeinschaft (DFG, German Research Foundation) - 491094227 "Open Access Publication Funding" and the University of Veterinary Medicine Hannover, Foundation.

Acknowledgments

The authors would like to thank Angelika Mönnich, Caroline Schütz, Julia Baskas, Jana-Svea Harre, Danuta Waschke and Petra Grünig for their technical support.

Conflict of interest

The authors declare that the research was conducted in the absence of any commercial or financial relationships that could be construed as a potential conflict of interest.

Publisher's note

All claims expressed in this article are solely those of the authors and do not necessarily represent those of their affiliated organizations, or those of the publisher, the editors and the reviewers. Any product that may be evaluated in this article, or claim that may be made by its manufacturer, is not guaranteed or endorsed by the publisher.

Supplementary material

The Supplementary Material for this article can be found online at: https://www.frontiersin.org/articles/10.3389/fimmu.2023.1105432/full#supplementary-material

References

1. Gerhauser I, Hansmann F, Ciurkiewicz M, Löscher W, Beineke A. Facets of theiler's murine encephalomyelitis virus-induced diseases: An update. *Int J Mol Sci* (2019) 20(2):448. doi: 10.3390/ijms20020448

2. Lawley KS, Rech RR, Perez Gomez AA, Hopkins L, Han G, Amstalden K, et al. Viral clearance and neuroinflammation in acute TMEV infection vary by host genetic background. *Int J Mol Sci* (2022) 23(18):10482. doi: 10.3390/ijms231810482

3. Brinkmeyer-Langford CL, Rech R, Amstalden K, Kochan KJ, Hillhouse AE, Young C, et al. Host genetic background influences diverse neurological responses to viral infection in mice. *Sci Rep* (2017) 7(1):12194–. doi: 10.1038/s41598-017-12477-2

4. Hülskötter K, Jin W, Allnoch L, Hansmann F, Schmidtke D, Rohn K, et al. Double-edged effects of tamoxifen-in-oil-gavage on an infectious murine model for multiple sclerosis. *Brain Pathol* (2021) 31(6):e12994. doi: 10.1111/bpa.12994

5. Zhang J, Lipton HL, Perelson AS, Dahari H. Modeling the acute and chronic phases of theiler murine encephalomyelitis virus infection. *J virology* (2013) 87 (7):4052–9. doi: 10.1128/JVI.03395-12

6. Lipton HL, Twaddle G, Jelachich ML. The predominant virus antigen burden is present in macrophages in theiler's murine encephalomyelitis virus-induced demyelinating disease. *J Virology* (1995) 69(4):2525–33. doi: 10.1128/jvi.69.4.2525-2533.1995

7. Aubert C, Brahic M. Early infection of the central nervous system by the GDVII and DA strains of theiler's virus. *J Virology* (1995) 69(5):3197–200. doi: 10.1128/jvi.69.5.3197-3200.1995

8. Zheng L, Calenoff MA, Dal Canto MC. Astrocytes, not microglia, are the main cells responsible for viral persistence in theiler's murine encephalomyelitis virus infection leading to demyelination. *J Neuroimmunology* (2001) 118(2):256–67. doi: 10.1016/S0165-5728(01)00338-1

9. Oleszak EL, Chang JR, Friedman H, Katsetos CD, Platsoucas CD. Theiler's virus infection: A model for multiple sclerosis. *Clin Microbiol Rev* (2004) 17(1):174–207. doi: 10.1128/CMR.17.1.174-207.2004

10. June CH, Ledbetter JA, Linsley PS, Thompson CB. Role of the CD28 receptor in T-cell activation. *Immunol Today* (1990) 11(6):211–6. doi: 10.1016/0167-5699(90)90085-N

11. Hünig T, Lühder F, Elflein K, Gogishvili T, Fröhlich M, Guler R, et al. CD28 and IL-4: two heavyweights controlling the balance between immunity and inflammation. *Med Microbiol Immunol* (2010) 199(3):239–46. doi: 10.1007/s00430-010-0156-z

12. Holdorf AD, Kanagawa O, Shaw AS. CD28 and T cell co-stimulation. *Rev Immunogenet* (2000) 2(2):175–84.

13. Keir ME, Sharpe AH. The B7/CD28 costimulatory family in autoimmunity. *Immunol Rev* (2005) 204(1):128–43. doi: 10.1111/j.0105-2896.2005.00242.x

14. Teague TK, Tan C, Marino JH, Davis BK, Taylor AA, Huey RW, et al. CD28 expression redefines thymocyte development during the pre-T to DP transition. *Int Immunol* (2010) 22(5):387–97. doi: 10.1093/intimm/dxq020

15. Mitnacht R, Tacke M, Hunig T. Expression of cell interaction molecules by immature rat thymocytes during passage through the CD4+8+ compartment: Developmental regulation and induction by T cell receptor engagement of CD2, CD5, CD28, CD11a, CD44 and CD53. *Eur J Immunol* (1995) 25(2):328–32. doi: 10.1002/eji.1830250204

16. Zhao Y, Shao Q, Peng G. Exhaustion and senescence: two crucial dysfunctional states of T cells in the tumor microenvironment. *Cell Mol Immunol* (2020) 17(1):27–35. doi: 10.1038/s41423-019-0344-8

17. Salomon B, Lenschow DJ, Rhee L, Ashourian N, Singh B, Sharpe A, et al. B7/CD28 costimulation is essential for the homeostasis of the CD4+CD25+ immunoregulatory T cells that control autoimmune diabetes. *Immunity.* (2000) 12 (4):431–40. doi: 10.1016/S1074-7613(00)80195-8

18. Gogishvili T, Luhder F, Goebbels S, Beer-Hammer S, Pfeffer K, Hunig T. Cell-intrinsic and -extrinsic control of treg-cell homeostasis and function revealed by induced CD28 deletion. *Eur J Immunol* (2013) 43(1):188–93. doi: 10.1002/eji.201242824

19. Mikami N, Sakaguchi S. CD28 signals the differential control of regulatory T cells and effector T cells. *Eur J Immunol* (2014) 44(4):955–7. doi: 10.1002/eji.201444513

20. Shahinian A, Pfeffer K, Lee KP, Kundig TM, Kishihara K, Wakeham A, et al. Differential T cell costimulatory requirements in CD28-deficient mice. *Science.* (1993) 261(5121):609–12. doi: 10.1126/science.7688139

21. Brown DR, Green JM, Moskowitz NH, Davis M, Thompson CB, Reiner SL. Limited role of CD28-mediated signals in T helper subset differentiation. *J Exp Med* (1996) 184(3):803–10. doi: 10.1084/jem.184.3.803

22. Chitnis T, Najafian N, Abdallah KA, Dong V, Yagita H, Sayegh MH, et al. CD28-independent induction of experimental autoimmune encephalomyelitis. *J Clin Invest* (2001) 107(5):575–83. doi: 10.1172/JCI11220

23. Oliveira-dos-Santos AJ, Ho A, Tada Y, Lafaille JJ, Tonegawa S, Mak TW, et al. CD28 costimulation is crucial for the development of spontaneous autoimmune encephalomyelitis. *J Immunol* (1999) 162(8):4490–5. doi: 10.4049/jimmunol.162.8.4490

24. Perrin PJ, June CH, Maldonado JH, Ratts RB, Racke MK. Blockade of CD28 during *in vitro* activation of encephalitogenic T cells or after disease onset ameliorates experimental autoimmune encephalomyelitis. *J Immunol* (1999) 163(3):1704–10. doi: 10.4049/jimmunol.163.3.1704

25. Haanstra KG, Dijkman K, Bashir N, Bauer J, Mary C, Poirier N, et al. Selective blockade of CD28-mediated T cell costimulation protects rhesus monkeys against acute fatal experimental autoimmune encephalomyelitis. *J Immunol* (2015) 194(4):1454–66. doi: 10.4049/jimmunol.1402563

26. Tada Y, Nagasawa K, Ho A, Morito F, Ushiyama O, Suzuki N, et al. CD28-deficient mice are highly resistant to collagen-induced arthritis. *J Immunol* (1999) 162 (1):203–8. doi: 10.4049/jimmunol.162.1.203

27. Gogishvili T, Luhder F, Kirstein F, Nieuwenhuizen NE, Goebbels S, Beer-Hammer S, et al. Interruption of CD28-mediated costimulation during allergen challenge protects mice from allergic airway disease. *J Allergy Clin Immunol* (2012) 130(6):1394–403 e4. doi: 10.1016/j.jaci.2012.08.049

28. Wagner M, Sobczynski M, Karabon L, Bilinska M, Pokryszko-Dragan A, Pawlak-Adamska E, et al. Polymorphisms in CD28, CTLA-4, CD80 and CD86 genes may influence the risk of multiple sclerosis and its age of onset. *J Neuroimmunol* (2015) 288:79–86. doi: 10.1016/j.jneuroim.2015.09.004

29. Dai S-x, Gu H-x, Lin Q-y, Wu Y-k, Wang X-y, Huang S-z, et al. Decreased CD8 +CD28+/CD8+CD28– T cell ratio can sensitively predict poor outcome for patients with complicated crohn disease. *Medicine* (2017) 96(26):e7247. doi: 10.1097/MD.0000000000007247

30. Guan Y, Jakimovski D, Ramanathan M, Weinstock-Guttman B, Zivadinov R. The role of Epstein-Barr virus in multiple sclerosis: From molecular pathophysiology to *in vivo* imaging. *Neural regeneration Res* (2019) 14(3):373–86. doi: 10.4103/1673-5374.245462

31. Dobson R, Giovannoni G. Multiple sclerosis – a review. *Eur J Neurol* (2019) 26 (1):27–40. doi: 10.1111/ene.13819

32. Rojas M, Restrepo-Jiménez P, Monsalve DM, Pacheco Y, Acosta-Ampudia Y, Ramírez-Santana C, et al. Molecular mimicry and autoimmunity. *J Autoimmun* (2018) 95:100–23. doi: 10.1016/j.jaut.2018.10.012

33. Kummerfeld M, Seehusen F, Klein S, Ulrich R, Kreutzer R, Gerhauser I, et al. Periventricular demyelination and axonal pathology is associated with subependymal virus spread in a murine model for multiple sclerosis. *Intervirology.* (2012) 55(6):401. doi: 10.1159/000336563

34. Hülskötter K, Lühder F, Flügel A, Herder V, Baumgärtner W. Tamoxifen application is associated with transiently increased loss of hippocampal neurons following virus infection. *Int J Mol Sci* (2021) 22(16):8486. doi: 10.3390/ijms22168486

35. Ulrich R, Kalkuhl A, Deschl U, Baumgärtner W. Machine learning approach identifies new pathways associated with demyelination in a viral model of multiple sclerosis. *J Cell Mol Med* (2010) 14(1-2):434–48. doi: 10.1111/j.1582-4934.2008.00646.x

36. Kummerfeld M, Meens J, Haas L, Baumgärtner W, Beineke A. Generation and characterization of a polyclonal antibody for the detection of theiler's murine encephalomyelitis virus by light and electron microscopy. *J virological Methods* (2009) 160(1):185–8. doi: 10.1016/j.jviromet.2009.04.030

37. Batot G, Metcalf CS, Bell LA, Pauletti A, Wilcox KS, Bröer S. A model for epilepsy of infectious etiology using theiler's murine encephalomyelitis virus. *J visualized experiments JoVE* (2022) 184. doi: 10.3791/63673-v

38. Bröer S, Hage E, Käufer C, Gerhauser I, Anjum M, Li L, et al. Viral mouse models of multiple sclerosis and epilepsy: Marked differences in neuropathogenesis following infection with two naturally occurring variants of theiler's virus BeAn strain. *Neurobiol Dis* (2017) 99:121–32. doi: 10.1016/j.nbd.2016.12.020

39. Libbey JE, Kennett NJ, Wilcox KS, White HS, Fujinami RS. Lack of correlation of central nervous system inflammation and neuropathology with the development of seizures following acute virus infection. *J Virology* (2011) 85(16):8149–57. doi: 10.1128/JVI.00730-11

40. Stewart K-AA, Wilcox KS, Fujinami RS, White HS. Development of postinfection epilepsy after theiler's virus infection of C57BL/6 mice. *J neuropathology Exp neurology* (2010) 69(12):1210–9. doi: 10.1097/NEN.0b013e3181ffc420

41. Bröer S, Käufer C, Haist V, Li L, Gerhauser I, Anjum M, et al. Brain inflammation, neurodegeneration and seizure development following picornavirus infection markedly differ among virus and mouse strains and substrains. *Exp Neurol* (2016) 279:57–74. doi: 10.1016/j.expneurol.2016.02.011

42. Howe CL, LaFrance-Corey RG, Overlee BL, Johnson RK, Clarkson BDS, Goddery EN. Inflammatory monocytes and microglia play independent roles in inflammatory ictogenesis. *J Neuroinflamm* (2022) 19(1):22. doi: 10.1186/s12974-022-02394-1

43. Kumnok J, Ulrich R, Wewetzer K, Rohn K, Hansmann F, Baumgärtner W, et al. Differential transcription of matrix-metalloproteinase genes in primary mouse astrocytes and microglia infected with theiler's murine encephalomyelitis virus. *J Neurovirology* (2008) 14(3):205–17. doi: 10.1080/13550280802008305

44. Sanchez JMS, DePaula-Silva AB, Doty DJ, Hanak TJ, Truong A, Libbey JE, et al. The CSF1R-microglia axis has protective host-specific roles during neurotropic picornavirus infection. *Front Immunol* (2021) 12:621090. doi: 10.3389/fimmu.2021.621090

45. Uri A. Differential requirement for CD28 co-stimulation on donor T cell subsets in mouse models of acute graft versus host disease and graft versus tumour effect unterschiedlicher einfluss der CD28 kostimulation auf donor-T zell-populationen in mausmodellen der akuten graft-versus-Host disease und des graft-versus-Tumor effekts. (2019). doi: 10.25972/OPUS-16586

46. Linsley PS, Brady W, Grosmaire L, Aruffo A, Damle NK, Ledbetter JA. Binding of the b cell activation antigen B7 to CD28 costimulates T cell proliferation and interleukin 2 mRNA accumulation. *J Exp Med* (1991) 173(3):721–30. doi: 10.1084/jem.173.3.721

47. Chen X, Jensen PE. The role of b lymphocytes as antigen-presenting cells. *Arch Immunol Ther Exp (Warsz)* (2008) 56(2):77. doi: 10.1007/s00005-008-0014-5

48. Rau FC, Dieter J, Luo Z, Priest SO, Baumgarth N. B7-1/2 (CD80/CD86) direct signaling to b cells enhances IgG secretion. *J Immunol* (2009) 183(12):7661–71. doi: 10.4049/jimmunol.0803783

49. Chen L, Flies DB. Molecular mechanisms of T cell co-stimulation and co-inhibition. *Nat Rev Immunol* (2013) 13(4):227–42. doi: 10.1038/nri3405

50. Heinly CS, Sempowski GD, Lee DM, Patel DD, McDermott PM, Scearce RM, et al. Comparison of thymocyte development and cytokine production in CD7-deficient, CD28-deficient and CD7/CD28 double-deficient mice. *Int Immunol* (2001) 13(2):157–66. doi: 10.1093/intimm/13.2.157

51. Behjati S, Frank MH. The effects of tamoxifen on immunity. *Curr Med Chem* (2009) 16(24):3076–80. doi: 10.2174/092986709788803042

52. Bebo BFJr., Dehghani B, Foster S, Kurniawan A, Lopez FJ, Sherman LS. Treatment with selective estrogen receptor modulators regulates myelin specific T-cells and suppresses experimental autoimmune encephalomyelitis. *Glia.* (2009) 57 (7):777–90. doi: 10.1002/glia.20805

53. Elloso MM, Phiel K, Henderson RA, Harris HA, Adelman SJ. Suppression of experimental autoimmune encephalomyelitis using estrogen receptor-selective ligands. *J Endocrinol* (2005) 185(2):243–52. doi: 10.1677/joe.1.06063

54. Peeva E, Venkatesh J, Diamond B. Tamoxifen blocks estrogen-induced b cell maturation but not survival. *J Immunol* (2005) 175(3):1415–23. doi: 10.4049/jimmunol.175.3.1415

55. Gallo MA, Kaufman D. Antagonistic and agonistic effects of tamoxifen: significance in human cancer. *Semin Oncol* (1997) 24(1 Suppl 1):S1–71-s1-80.

56. Sakamoto T, Eguchi H, Omoto Y, Ayabe T, Mori H, Hayashi S. Estrogen receptor-mediated effects of tamoxifen on human endometrial cancer cells. *Mol Cell Endocrinol* (2002) 192(1-2):93–104. doi: 10.1016/S0303-7207(02)00086-2

57. Wang Z, Kyo S, Maida Y, Takakura M, Tanaka M, Yatabe N, et al. Tamoxifen regulates human telomerase reverse transcriptase (hTERT) gene expression differently in breast and endometrial cancer cells. *Oncogene.* (2002) 21(22):3517–24. doi: 10.1038/sj.onc.1205463

58. Amitabha R, Monica F. Immunomodulatory effects of anti-estrogenic drugs. *Acta Pharmaceutica* (2012) 62(2):141–55. doi: 10.2478/v10007-012-0012-3

59. Baez-Jurado E, Rincón-Benavides MA, Hidalgo-Lanussa O, Guio-Vega G, Ashraf GM, Sahebkar A, et al. Molecular mechanisms involved in the protective actions of selective estrogen receptor modulators in brain cells. *Front Neuroendocrinol* (2019) 52:44–64. doi: 10.1016/j.yfrne.2018.09.001

60. Barreto GE, Santos-Galindo M, Garcia-Segura LM. Selective estrogen receptor modulators regulate reactive microglia after penetrating brain injury. *Front Aging Neurosci* (2014) 6:132. doi: 10.3389/fnagi.2014.00132

61. Hope JL, Bradley LM. Lessons in antiviral immunity. *Science.* (2021) 371 (6528):464–5. doi: 10.1126/science.abf6446

62. Nothelfer K, Sansonetti PJ, Phalipon A. Pathogen manipulation of b cells: The best defence is a good offence. *Nat Rev Microbiol* (2015) 13(3):173–84. doi: 10.1038/nrmicro3415

63. Langendonk M, de Jong MRW, Smit N, Seiler J, Reitsma B, Ammatuna E, et al. Identification of the estrogen receptor beta as a possible new tamoxifen-sensitive target in diffuse large b-cell lymphoma. *Blood Cancer J* (2022) 12(3):36. doi: 10.1038/s41408-022-00631-7

64. Bhatia S, Edidin M, Almo SC, Nathenson SG. B7-1 and B7-2: Similar costimulatory ligands with different biochemical, oligomeric and signaling properties. *Immunol Lett* (2006) 104(1):70–5. doi: 10.1016/j.imlet.2005.11.019

65. Tritz ZP, Orozco RC, Malo CS, Ayasoufi K, Fain CE, Khadka RH, et al. Conditional silencing of h-2D(b) class I molecule expression modulates the protective and pathogenic kinetics of virus-Antigen-Specific CD8 T cell responses during theiler's virus infection. *J Immunol (Baltimore Md 1950)* (2020) 205(5):1228–38. doi: 10.4049/jimmunol.2000340

66. Huseby Kelcher AM, Atanga PA, Gamez JD, Cumba Garcia LM, Teclaw SJ, Pavelko KD, et al. Brain atrophy in picornavirus-infected FVB mice is dependent on the h-2D(b) class I molecule. *FASEB J* (2017) 31(6):2267–75. doi: 10.1096/fj.201601055R

67. Murray PD, Pavelko KD, Leibowitz J, Lin X, Rodriguez M. CD4(+) and CD8(+) T cells make discrete contributions to demyelination and neurologic disease in a viral model of multiple sclerosis. *J Virology* (1998) 72(9):7320–9. doi: 10.1128/JVI.72.9.7320-7329.1998

68. Kang HS, Hou W, Kim BS. Rapid expansion of virus-specific CD4+ T cell types in the CNS of susceptible mice infected with theiler's virus. *Int J Mol Sci* (2020) 21 (20):7719. doi: 10.3390/ijms21030771

69. Kim H, Kim M, Im S-K, Fang S. Mouse cre-LoxP system: General principles to determine tissue-specific roles of target genes. *Lab Anim Res* (2018) 34(4):147–59. doi: 10.5625/lar.2018.34.4.147

70. Linterman MA, Denton AE, Divekar DP, Zvetkova I, Kane L, Ferreira C, et al. CD28 expression is required after T cell priming for helper T cell responses and protective immunity to infection. *eLife* (2014) 3:e03180. doi: 10.7554/eLife.03180

71. Ferguson SE, Han S, Kelsoe G, Thompson CB. CD28 is required for germinal center formation. *J Immunol* (1996) 156(12):4576–81. doi: 10.4049/jimmunol.156.12.4576

72. Haack S, Baiker S, Schlegel J, Sauer M, Sparwasser T, Langenhorst D, et al. Superagonistic CD28 stimulation induces IFN-γ release from mouse T helper 1 cells *in vitro* and in vivo. *Eur J Immunol* (2021) 51(3):738–41. doi: 10.1002/eji.202048803

73. Prajeeth CK, Dittrich-Breiholz O, Talbot SR, Robert PA, Huehn J, Stangel M. IFN-γ producing Th1 cells induce different transcriptional profiles in microglia and astrocytes. *Front Cell Neurosci* (2018) 12. doi: 10.3389/fncel.2018.00352

74. Orabona C, Grohmann U, Belladonna ML, Fallarino F, Vacca C, Bianchi R, et al. CD28 induces immunostimulatory signals in dendritic cells *via* CD80 and CD86. *Nat Immunol* (2004) 5(11):1134–42. doi: 10.1038/ni1124

75. Montufar-Solis D, Garza T, Klein JR. T-Cell activation in the intestinal mucosa. *Immunol Rev* (2007) 215:189–201. doi: 10.1111/j.1600-065X.2006.00471.x

Frontiers in Immunology

Explores novel approaches and diagnoses to treat immune disorders.

The official journal of the International Union of Immunological Societies (IUIS) and the most cited in its field, leading the way for research across basic, translational and clinical immunology.

Discover the latest Research Topics

See more →



Frontiers

Avenue du Tribunal-Fédéral 34
1005 Lausanne, Switzerland
frontiersin.org

Contact us

+41 (0)21 510 17 00
frontiersin.org/about/contact